Expanding the Scope of Visible Light Chemistry — Research and Development of Photocatalyzed *N*-centered Radical Reactions.

Dissertation

Zur Erlangung des Doktorgrades der Naturwissenschaften

Dr. rer. nat.

an der Fakultät für Chemie und Pharmazie

Der Universität Regensburg

vorgelegt von

Lukas Traub

Aus Neu-Ulm

Im Jahre 2020

Diese Arbeit wurde angeleitet von: Prof. Dr. Oliver Reiser

Promotionsgesuch eingereicht am: 16.07.2020

Promotionskolloquium am: 07.09.2020

Prüfungsausschuss: Vorsitz: Prof. Alexander Breder

                    1. Gutachter: Prof. Oliver Reiser

                    2. Gutachter: Prof. Kirsten Zeitler

                    3. Gutachter: Prof. Frank-Michael Matysik

Der experimentelle Teil der vorliegenden Arbeit wurde in der Zeit zwischen November 2016 und Februar 2020 unter der Leitung von Prof. Dr. Oliver Reiser am Lehrstuhl für Organische Chemie der Universität Regensburg angefertigt.

Meiner Freundin Johanna

und meiner Familie

"The story so far:

In the beginning the Universe was created. This has made a lot of people very angry and been widely regarded as a bad move."

-Douglas Adams, "The Restaurant at the End of the Universe"

Table of Contents

1. Introduction

1.1 Basics of Photocatalysis

The research area of photocatalysis enjoyed continued interest and tremendous developments in recent years.[1–6] Despite this, many are not familiar with the chemistry exploiting the properties of visible light. In this chapter a brief overview over the basics of photochemistry will be presented.

Most organic molecules are not able to absorb light in the visible spectrum, for a lack of a chromophore in their structure. While common functional groups like phenyl groups and unsaturated bonds can absorb light in the near UV spectrum (200-400 nm), working with light of such wavelengths requires precautions and special glassware. Additionally, reactions with UV light suffer from low selectivity and several undesired side reactions.[7]

This problem has been overcome by the development of photocatalysts.[8] Photocatalysts transform the energy of a photon into chemical energy *via* an absorption process and are capable of transferring that energy to an acceptor molecule, activating it in the process (Scheme 1). Note, that no regeneration step is required for solely energy transfer processes.
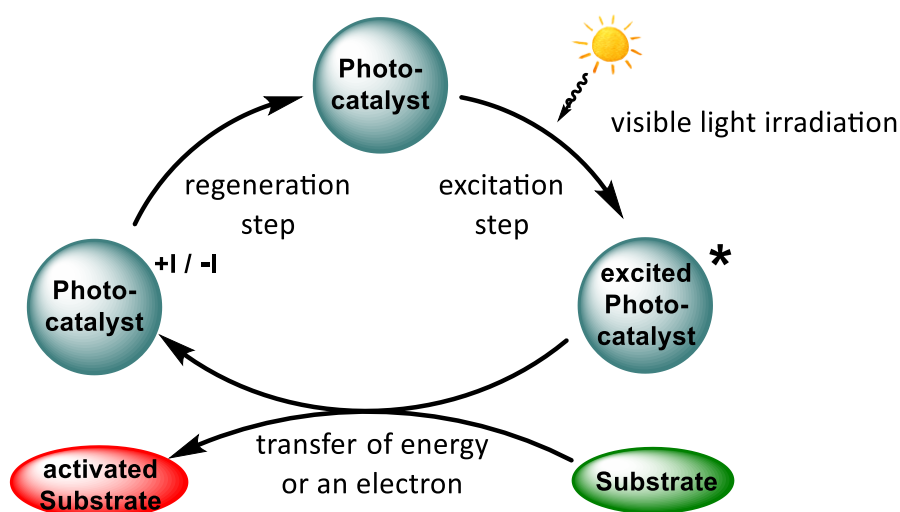
Scheme 1: Working principle of photocatalysis.

Introduction

Both excitation processes and the transfer of an absorbed photon's energy to a suitable substrate follow certain intricacies, the understanding of which is crucial for successful photocatalyst and reaction design. While the basic underlying mechanisms involved can differ in between certain classes of photocatalysts, noble metal complexes are one of the most commonly used photocatalysts and will serve as suitable example for the following considerations.

The transformation of physical energy in form of a photon to chemical energy is exemplified in an simplified molecular orbital depiction of the photocatalyst $[Ir(ppy)_3]$ (**1**) (Scheme 2). Through absorption of a photon by the Iridium **1**, an electron is elevated from the ground state t_{2g} orbital to the π^* orbital, which is located on the ligand backbone of the complex in an MLCT process (MLCT = Metal to Ligand Charge Transfer). This generates a short-lived singlet state that rapidly undergoes inter system crossing (ISC) to the long-lived triplet state **2** (lifetime τ = 1900 ns).[2] This can be visualized by a charge separation between the metal core and the ligand shell in the excited Iridium complex **2**. Both the oxidation-, as well as the reduction potential are increased in comparison to ground state **1**.
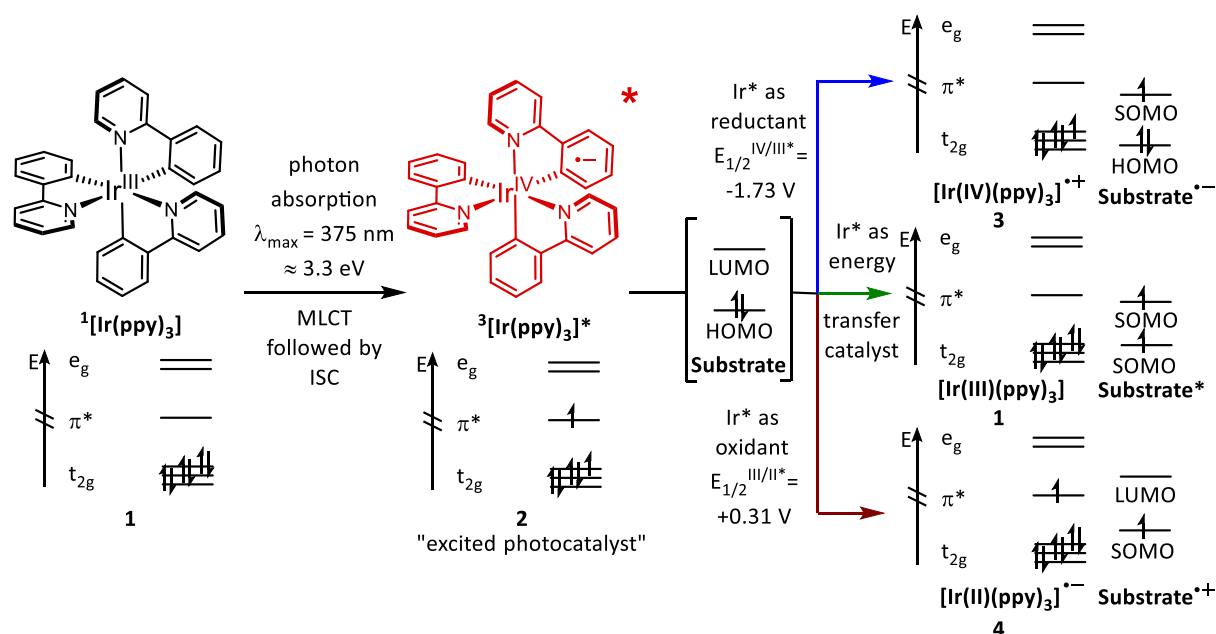
Scheme 2: Simplified depiction of the photophysical processes involved in substrate activation.

Upon collision of a substrate molecule with complex **2**, several different electronic processes can take place, among them the three main product yielding mechanisms in photochemistry. Acting as a reductant, a substrate is reduced by the donation of an electron into the previously

empty LUMO orbital of the substrate, yielding the *de facto* oxidized Ir(IV) complex **3** (**Scheme 2,** upper (blue) pathway). Acting as an oxidant, a substrate is oxidized by the removal of an electron from its HOMO orbital, yielding the *de facto* reduced Ir(II) complex **4** (**Scheme 2,** lower (red) pathway). In contrast to these photo redox pathways, an energy transfer (ET) mechanism directly transfers energy to the substrate by exciting an electron in the HOMO orbital into an Lumo oribtal, turning both into triplet SOMO orbitals, while the catalyst itself returns to its ground state (**Scheme 2**, middle (green) pathway). Organic substrate in a triplet state can undergo a plethora of valuable and useful reactions.[9]

$E_{1/2}^{IV/III*} = -1.73\ V$ **A** $[Ir(ppy)_3]^*$ **2** **D** $E_{1/2}^{III*/II} = +0.31\ V$

$A^{\bullet-}$ $D^{\bullet+}$

$[Ir(IV)(ppy)_3]^{\bullet+}$ **3** ET *hν* relax-ation $[Ir(II)(ppy)_3]^{\bullet-}$ **4**

D **A**

oxidative quenching $E_{1/2}^{IV/III} = +0.77\ V$ $[Ir(ppy)_3]$ **1** $E_{1/2}^{III/II} = -2.19\ V$ reductive quenching

$D^{\bullet+}$ $A^{\bullet-}$
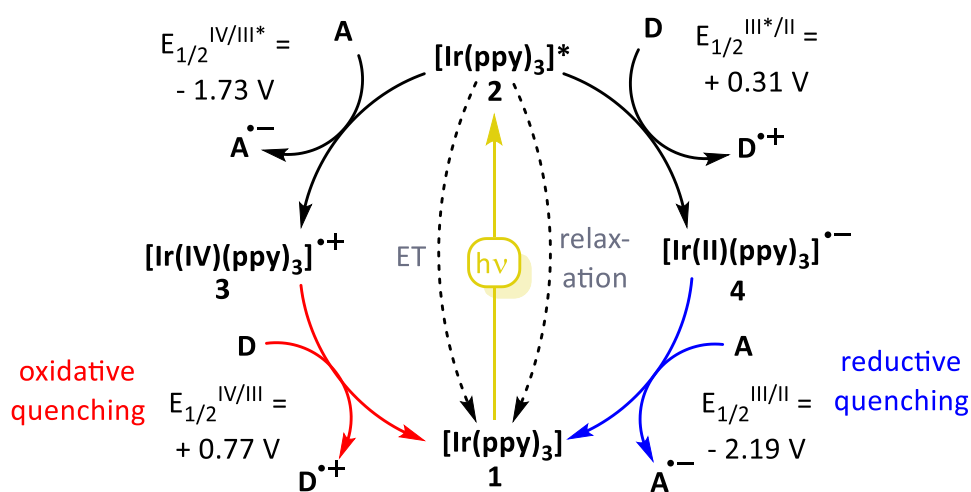
Scheme 3: Photoredox pathways visualized on the example of [Ir(ppy)₃].

For both photoredox pathways the catalytic cycle is not finished, since neither of them has returned to the neutral ground state **2**. For the oxidized complex **3**, Donor **D** quenches the active complex through donating an electron and being oxidized itself, thus regenerating catalyst **1** and giving access to the donor radical cation (Scheme 3, oxidative cycle). Similarly, for the reduced complex **4**, an Acceptor **A** will quench the active complex by accepting an electron and thus being reduced itself, regenerating the catalyst **1** in the process and yielding the acceptor radical anion (Scheme 3,reductive quenching cycle). The excited charge-separated catalyst **2** can also return to its ground state **1** through an energy transfer to a suitable substrate like molecular oxygen, or through relaxation processes. Non-radiative relaxation, in which energy is converted into molecular vibrations and dissipated by collisions with other molecules, and phosphorescence, in which a red-shifted – compared to absorption - photon is emitted from the complex, are the two main unproductive pathways reducing photocatalytic efficiency.

1.2 The diverse reactivity of nitrogen-centered radicals

The formation of carbon-nitrogen bonds remains a field of considerable interest, since they are an integral part of the basic structures of most pharmaceuticals, agrochemicals, food additives and organic materials.[10] Generally, common methods to form C-N bonds exploit nitrogen's nucleophilicity after deprotonation by strong bases or metal-couplings such as the Ullman- or Buchwald-Hartwig cross-coupling reaction.[11] However, such methods have often been limited by their need for elevated temperatures, prefunctionalized substrates or their lacking functional group tolerance in the past.[12] In recent years, a rising number of radical approaches have emerged towards selective bond-formations as the mechanisms behind catalyzed radical reactions are increasingly explored.[4,5] Curiously, the highly reactive nitrogen-centered radicals have been relatively under-utilized as powerful synthetic tool in comparison to their carbon radical counterparts.[13] Despite this, nitrogen radicals offer great opportunities towards the formation of carbon-nitrogen bonds.

1.2.1 Generation of nitrogen-centered radicals

A possible reason as to why nitrogen-centered radicals have found only limited application in industrial settings is the lack of convenient routes to access these highly reactive radicals. In recent years, this problem has been somewhat alleviated by the progress of photoredox chemistry as convenient way to generate these radicals.[14] This chapter will focus on selected examples on how to generate various highly reactive nitrogen radicals utilizing both thermal as well as photochemical approaches. The reactivity of such radicals will be discussed in chapter 1.2.2.

1.2.1.1 Thermal initiation and UV methods

In general, methods generating nitrogen radicals involve the scission of a weak N-X bond, whereas X can be any good leaving group such as halogen-, nitrogen-, oxygen-, or sulfur-based moieties. To achieve this scission, stoichiometric amounts of reducing agents such as low-valent transition metals facilitate an heterolytic cleavage of this bond, leaving a nitrogen radical. Alternatively, labile N-X bonds can be cleaved by irradiation with UV-light or radical initiators inducing an homolytic cleavage of the N-X bond.

N-halo bonds:

(a) Löffler, 1909:
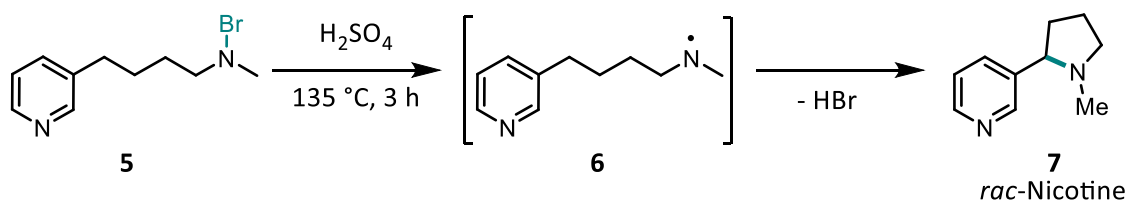
(b) Barton, 1965
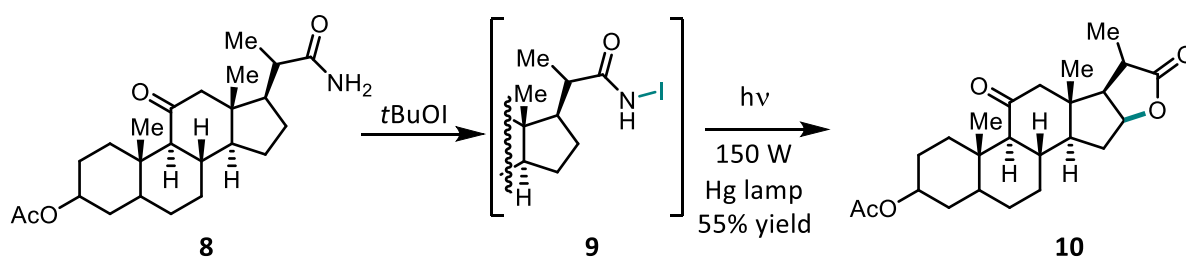
Scheme 4: Selected examples for the generation of nitrogen-centered radicals by cleavage of weak *N*-halo bonds by the groups of Löffler[15] and Barton[16].

The first known example for the utilization of nitrogen radicals in organic synthesis was demonstrated by Hofmann in a reaction that is nowadays known as the Hofmann-Löffler-Freytag reaction in 1885.[17] This reaction utilizes the lability of *N*-halogen bonds under thermal and acidic conditions. Herein, secondary amines are brominated and subsequently cleaved to achieve the formation of *N*-methylated pyrrolidines. C. Löffler elegantly demonstrated the synthetic potential of this reaction for the synthesis of racemic Nicotine **7** *via* secondary amine radical **6** (Scheme 4, a).[15] The group of Barton further developed this reaction towards the formation of lactones from amides under milder conditions, while generating the necessary *N*-halo reagents (*e.g.* **9**) *in situ* from an *tert*-butyl hypoiodite reagent. This N-I bond was readily cleaved by UV-light irradiation. Illustrating the synthetic applicability, the lactonization of a challenging pregnane derivative **10** in 55% yield was demonstrated (Scheme 4, b).[16] While *N*-chloro bonds are also accessible to this reaction, the usage of *N*-fluoro bonds as nitrogen radical precursor has not been reported thus far.

Additionally, wide range of nitrogen-radical precursors besides *N*-halo compounds have been explored.[13] The group of Kaim reported on the ability of 1-aminobenzotriazoles to act as iminyl radical precursor after condensation with a suitable ketone. Imine derivative **11** could be transformed into 2*H*-Indole **13** in good yields by a radical reaction using tributyltin hydride in an 5-exo-trig cyclization, albeit with low diastereoselectivity (Scheme 5, a).[18] This is

especially notable, since benzotriazole can be recycled into 1-aminobenzotriazole and subsequently be reused as nitrogen-radical precursor. However, the use of stoichiometric amounts of organotin reagents keeps this from being a "green" reaction protocol. Other methods included azide groups,[19] dihydropyridines,[20] triazenes[21] or thiocarbazoles[22] as suitable precursors for nitrogen-centered radicals under similar conditions.

(a) N-N bonds: Kaim, 1996:
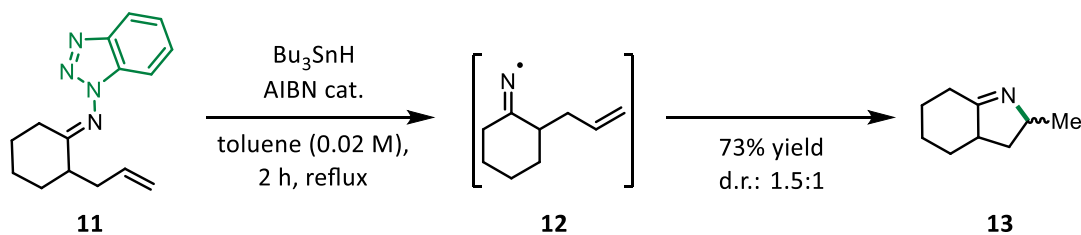
(b) N-O bonds: Rodriguez, 2006:
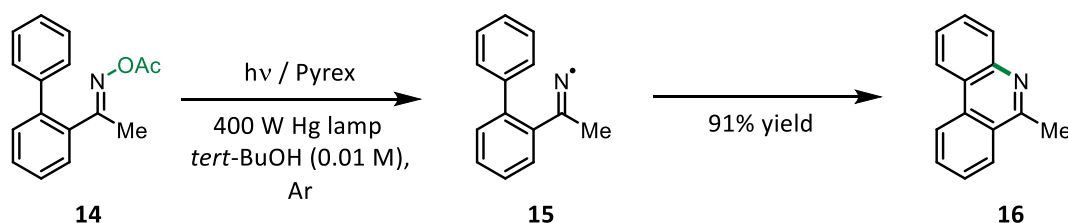
(c) N-S bonds: Marmon, 1994:
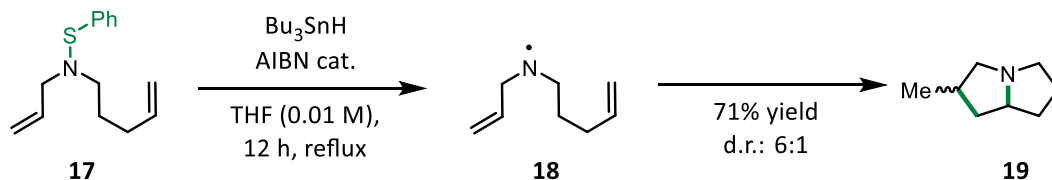
Scheme 5: Selected examples for the generation of nitrogen-centered radicals by cleavage of weak (a) N-N bonds,[18] (b) N-O bonds[23] and (c) N-S bonds.[24]

The group of Rodriguez demonstrated that readily *N*-Acetyl oxime **14** can give access to highly reactive iminyl radical **15** by UV-light irradiation. Yields for condensation to biphenyl moieties were good, however divergence from this structural motive led to a significant decrease in reaction yields (Scheme 5, b).[23] Purely thermal decomposition of oxime compounds is also possible, giving rise to iminyl-radicals at 90 °C in *tert*-butyl benzene solvents.[25] Many variations of different oxime esters to give access to nitrogen-centered radicals exist, including methods with a preliminary Barton decarboxylation.[26]

Similar to N-N and N-O bonds, the scission of N-S bonds is achievable through treatment with an organotin compound. Marmon and co-workers demonstrated a radical cascade 5-exo-trig

cyclization with a secondary amine radical **18** generated after cleavage of a sulfenamine group in **17** (Scheme 5, c).[24,27] Additionally, sulfonamides[28] and *N*-Xanthyl[29] derivates were also established as viable precursor moieties. While such methods accessing a wide variety of nitrogen compounds are certainly useful, their common disadvantage is the necessity for UV light, organotin compounds, stoichiometric reductants or other harsh reaction conditions that hamper their synthetic applicability and restrict them to mostly intramolecular reactions.

1.2.1.2 Photocatalytic methods

Visible-light photocatalysis has not only found great success in the field of carbon-centered radicals, it has also greatly improved on the accessibility of *N*-centered radicals for organic synthesis. In general, photocatalytic methods to generate reactive nitrogen radicals employ the same precursor molecules as the previously described thermal methods, being weak N-X, N-N, N-O and N-S bonds. However, photon coupled electron transfer (PCET) processes towards the activation of amides add unfunctionalized N-H amide bonds to the pool of potential *N*-radical precursors.[30]

(a) N-X bonds: Lee, 2014:
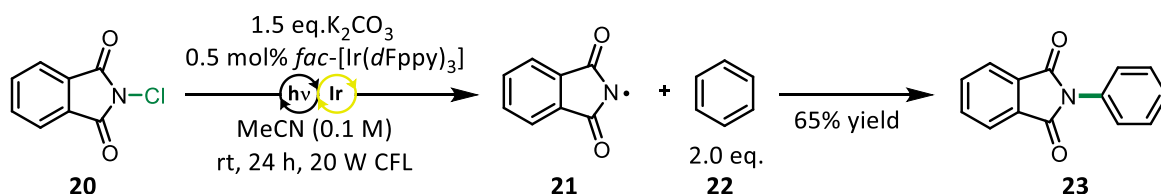
(b) N-N bonds: Akita, 2015:
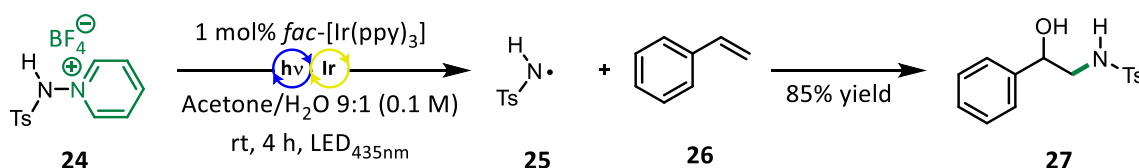
Scheme 6: Selected examples for the photocatalytic generation of nitrogen-centered radicals by cleavage of weak (a) N-halo bonds[31] or (b) N-N bonds.[32]

The group of Lee demonstrated that easily available and bench-stable chlorinated phthalimides can give access to nitrogen radicals in combination with an Iridium catalyst and visible light irradiation (Scheme 6, a).[31] The electrophilic amidyl radicals **21** created hereby were employed in an direct amidation of various arenes **22** in good yields, however with low

regioselectivities. While N-halogen compounds besides N-Cl containing molecules also form nitrogen-centered radicals, their low stability and tendency for the homolytic cleavage of the N-X bond makes it difficult to distinguish between catalyzed and radical-chain processes. Akita and co-workers demonstrated the feasibility of pyridinium tetrafluoroborate salts **24** as electron acceptors, leading to tosylamide radicals **25** after heterolytic scission of a pyridine molecule (Scheme 6, b).[32] Such radicals were shown to be active in ATRA-type hydroxy-aminations when reacted with styrenes **26**. While the Akita group obtained such precursors from unsubstituted *N*-aminopyridinium salts, Studer and co-workers demonstrated pyrylium salts as a convenient method to obtain pyridinium precursors from primary amines, hydrazines or amides.[33] Furthermore, saturated and unsaturated azides remain viable precursors for various nitrogen-centered radicals.[34,35]
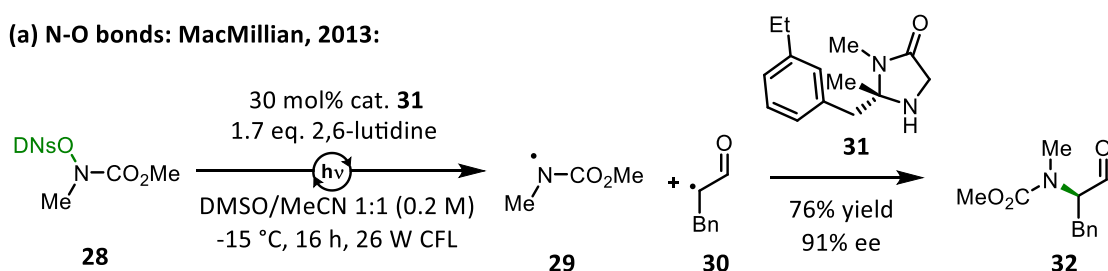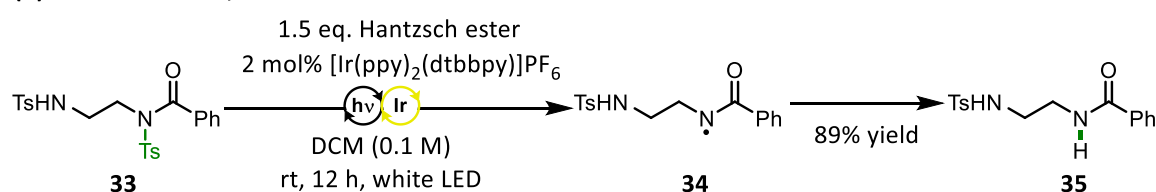

Scheme 7: Selected examples for the photocatalytic generation of nitrogen-centered radicals by cleavage of weak (a) N-O bonds or (b) N-S bonds.

Next to the previously established oxime chemistry,[36] other weak N-O bonds have found their place in photoredox catalyzed nitrogen radical chemistry. In an impressive display of enantioselective asymmetric aminocatalysis, MacMillan and co-workers accessed amide radicals **29** by cleavage of a photolabile dinitrophenylsulfonyloxy (DNsO) group in precursor **28**. This radical was used for the α-amination of various aldehydes **30** in good yields and enantioselectivities (Scheme 7,a).[37] The group of Sanford demonstrated the formation of phthalimide radicals similar to Lee et al. (Scheme 6, a), albeit with scission of an *N*-alkoxy bond.[38] In contrast to thermal methodologies, to the best of our knowledge, sulfenamines have not been reported as suitable nitrogen-radical precursors. However, the group of Xiao

reported on the generation of amidyl radicals from tosylamides **33** (Scheme 7, b).[39] The generated amide radicals **34** were subsequently quenched by an hydrogen atom donor, effectively resulting in an highly chemo-selective de-tosylation protocol.
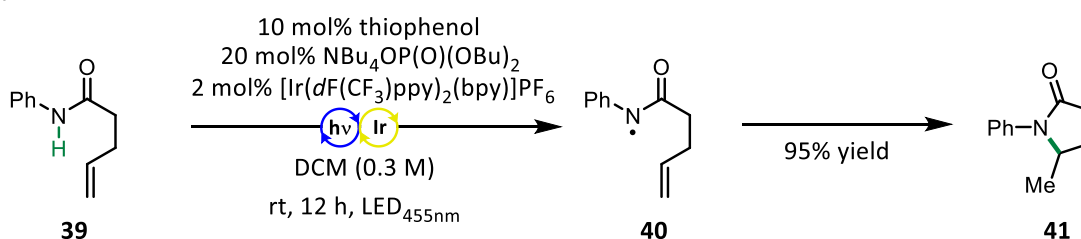
(a) direct oxidation: Chen and Xiao, 2014:
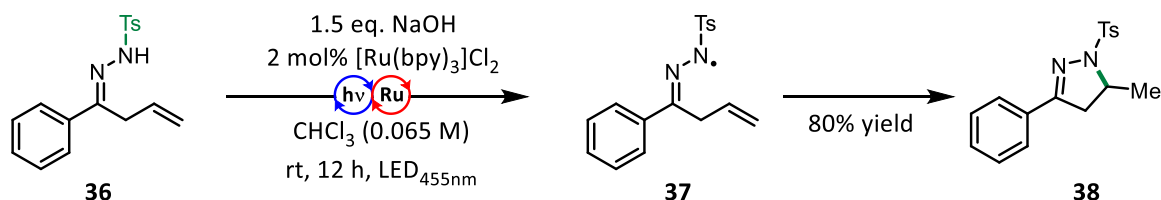
(b) PCET: Knowles, 2014:
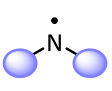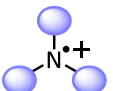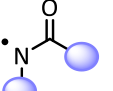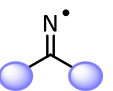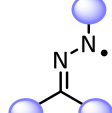
Scheme 8: Selected examples for the photocatalytic generation of nitrogen-centered radicals from N-H bonds by (a) direct photocatalytic oxidation (b) PCET processes.

An alternative and favorable strategy is the use of unfunctionalized N-H bonds to directly access nitrogen-centered radicals. However, due to the high bond strength of amine and amide bonds this is rarely possible by direct oxidation.[40] An exception to this are hydrazinium compounds, which can be directly oxidized by common photocatalysts giving access to hydrazonyl radicals after deprotonation. Highlighting this principle, the group of Xiao and Chen realized a hydroamination of β,γ-unsaturated hydrazones **36** by an ruthenium photocatalyst in good yields (Scheme 8, a).[41] While arylated amides are not accessible to direct oxidation processes, PCET processes are an elegant way to directly access amidyl radicals. The Knowles group successfully applied this process in an intramolecular hydroamination with excellent yields after generating the necessary amidyl radicals **40** directly from the corresponding amide N-H bond **39** in conjuncture with a phosphate base. The final hydrogen atom transfer of this reaction towards **41** was mediated by thiophenol (Scheme 8, b).[42] Overall, the direct transformation of N-H bonds into highly reactive radical intermediates might be the most elegant and synthetically interesting method, however it is limited by the scope of substrates available for these reactions.

1.2.2 Reactivity of nitrogen-centered radicals

Having elaborated on various methods for the generation of *N*-centered radicals on the previous chapters, this chapter will take a closer look at the varied reactivities of different configurations of nitrogen radicals. Based on their *N*-hybridization and substitution patterns, nitrogen radicals can be assigned to different classes. Each class of *N*-centered radical displays distinct reactivities depending on the electron density at the nitrogen center, the orbital in which the radical is located and whether the radical is dislocated in a π-system (Scheme 9, a).[36] In this chapter, five different distinct classes and their reactivities will be elaborated: Aminyl-. Aminium-. Amidyl-, Iminyl- and Hydrazonyl-radicals.

(a) classification of nitrogen-centered radicals:

Structure					
Name	aminyl	aminium	amidyl	iminyl	hydrazonyl
Configuration	π	π	π	σ	π
Philicity	nucleophilic	electrophilic	electrophilic	ambiphilic	electrophilic

(b) reactions of nitrogen-centered radicals:

[I] 5-exo-cyclization

[II] addition to π-systems

[III] radical-radical couplings

[IV] 1,5-HAT processes

[V] Norrish type-I fragmentations
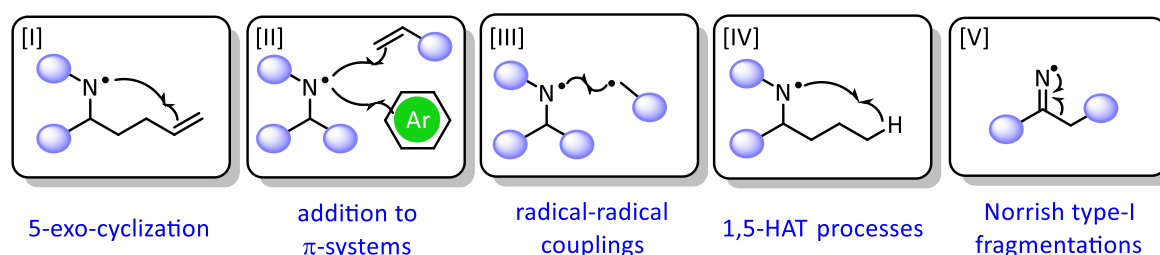
Scheme 9: (a) General classification of different nitrogen radicals. (b) reactions of nitrogen-centered radicals.

The main reaction pathways performed by nitrogen radicals are: displayed in Scheme 9:b (I) intramolecular 5-exo-cyclizations to unsaturated moieties, (II) additions to π-systems (*i.e.* aromatic systems or olefins), (III) radical-radical couplings with carbon- or other nitrogen-centered radicals, (IV) Hydrogen atom transfer (HAT) processes (mainly 1,5-HATs) and (V) Norrish-type-I reactions, leading to fragmentary products. Not all reaction pathways are available to every class of nitrogen-centered radicals and depending on their philicity and stabilization (or lack of thereof) of relevant transition states, certain mechanisms will be

favored over others. Knowing about the reactivities of each radical in question is elemental to designing an appropriate reaction pathway.

1.2.2.1 Aminyl radicals

The nucleophilic π-configured aminyl radicals are generally not accessed by PCET-type processes, but from precursor molecules such as *N*-chloro compounds. Illustrating the potential of aminyl radicals towards non-directed aminations of aromatic compounds, the group of Wang described the amination of benzoxazoles by *N*-chloromorpholine (Scheme 10 ,a).[43] In this work, the key SET steps were performed by an iridium catalyst under blue light irradiation. The labile *N*-Chloro precursors could also be generated in situ from **43**, giving access to substituted benzoxazoles **44** in good yields. Meanwhile, the group of Zanardi demonstrated that aminyl radicals generated from saturated azides **48** by indium chemistry are able to partake in condensations to C_{sp}-centers by reacting them with cyano groups to obtain the corresponding ring-closure products **49** in excellent yields (Scheme 10 ,b).[44]
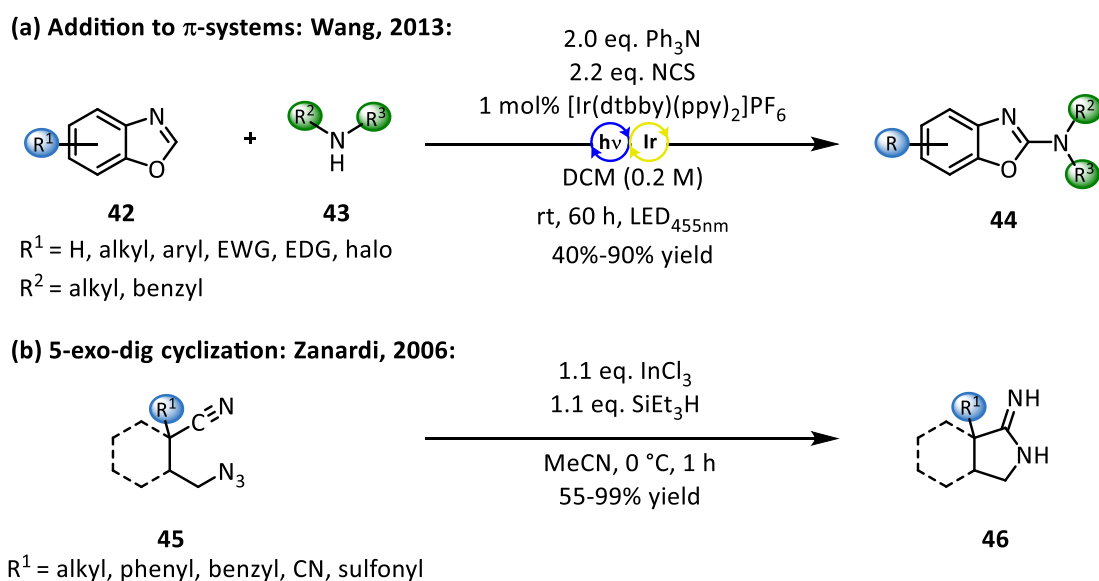
Scheme 10: Reactivities of aminyl radicals as demonstrated by the groups of Wang[43] and Zanardi.[44]

Wan and co-workers demonstrated an effective radical-radical coupling between acyl- and aminyl radicals. In this case, aminyl radicals were created from formamides after CO extrusion initiated by *tert*-butylperoxide (Scheme 11).[45] Various formamides **46** and aldehydes **45** were compatible with this protocol, leading to different amides **47** in good to excellent yields. The mechanisms of this reactions exploit the ability of *tert*-butylperoxide radicals – generated

from the peroxide and iodide − to abstract an hydrogen atom from aldehyde **47** and **48** moieties. This results in aminyl radical **50** after carbon monoxide extrusion and acyl radical **51**, which subsequently recombine to give rise to amide **49**.

Radical-radical coupling: Wan, 2012:

20 mol% Bu$_4$NI
5.8 eq. 70% tBuOOH

1,1,2-trichloroethan (0.25 M)
90 °C, 24 h
45-94% yield
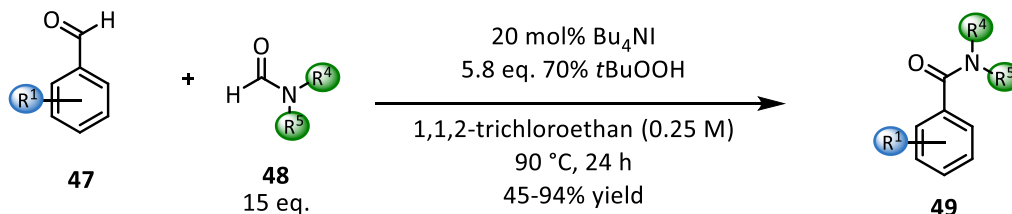
R^1 = alkyl, aryl, EWG, EDG, halo
R^2 = alkyl, aryl, benzyl

Mechanism radical-radical coupling:
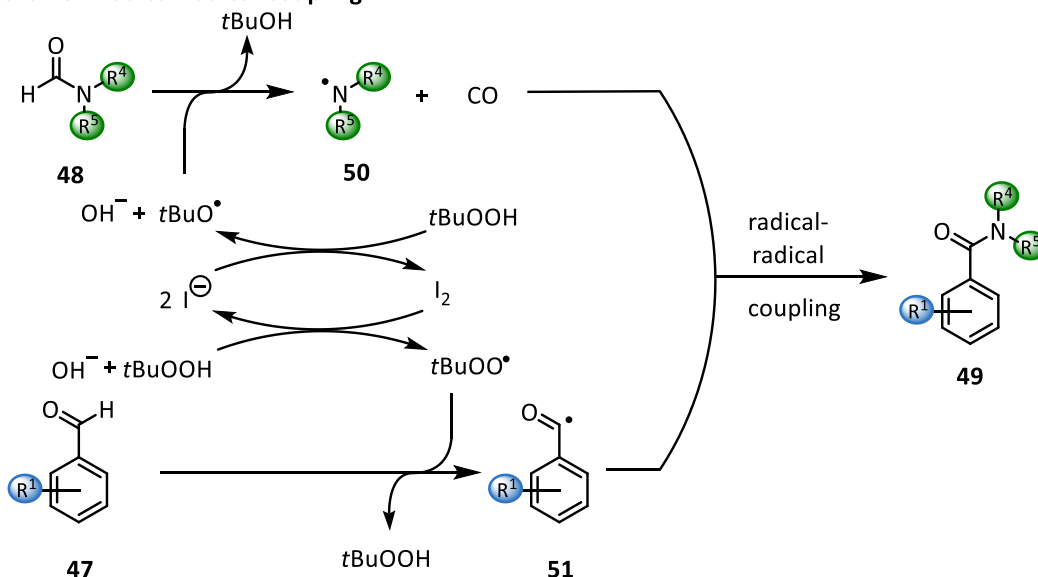
Scheme 11: Radical-radical coupling reaction of aminyl radicals, demonstrated by Wan and co-workers.[45]

Since the direct oxidation of amines leads to aminium radicals, other precursor molecules are required to give rise to aminyl radicals. However, the use of deprotonated amines to directly access aminyl radicals *in situ* is demonstrated by the group of Furusaki *via* anodic oxidation.[46] Furusaki and co-workers used these radicals for a 5-exo-trig cyclization to obtain pyrrolidine products in moderate yields. Other 5-exo-trig cyclizations have been depicted in Scheme 5 by Marmon et al. Interpreting the available literature reports, aminyl radicals seem to favor condensations to C$_{sp}^2$- and C$_{sp}$-centers and radical-radical couplings, while also able to partake in 5-exo-trig cyclizations.

1.2.2.2 Aminium radicals

Aminium radicals **53** can be obtained by direct oxidation of their corresponding amines **52** and have access to an additional mechanistic pathway: the 1,2-radical shift, or α-amino oxidation. However, this mechanism directly leads to carbon-centered radicals **54** or iminium ions **55** that dictate the subsequent reaction pathway and will not be elaborated in this chapter. Similar to aminyl radicals aminium radicals are π-radicals, however their philicity is inversed.[47]
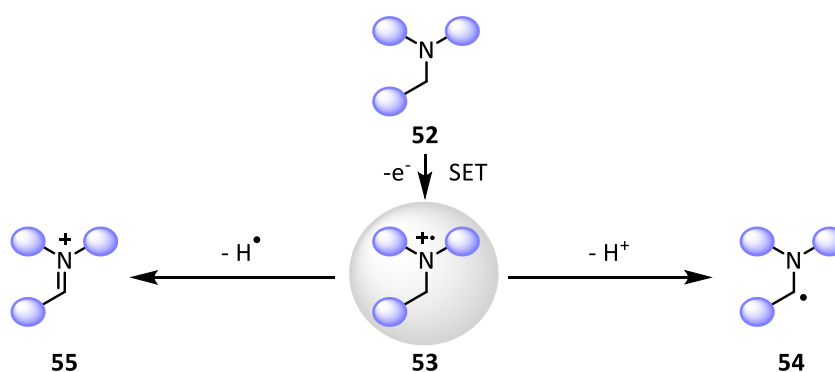
Scheme 12: Direct oxidation of amines leading to α-amino oxidation products.

The group of Leonori disclosed, that aminium radicals are far more efficient for adding to aromatic systems than aminyl radicals, which was initially reported by Wang and co-workers.[43] In their initial report, Leonori *et al.* used amines with electron deficient N-O bonds as precurso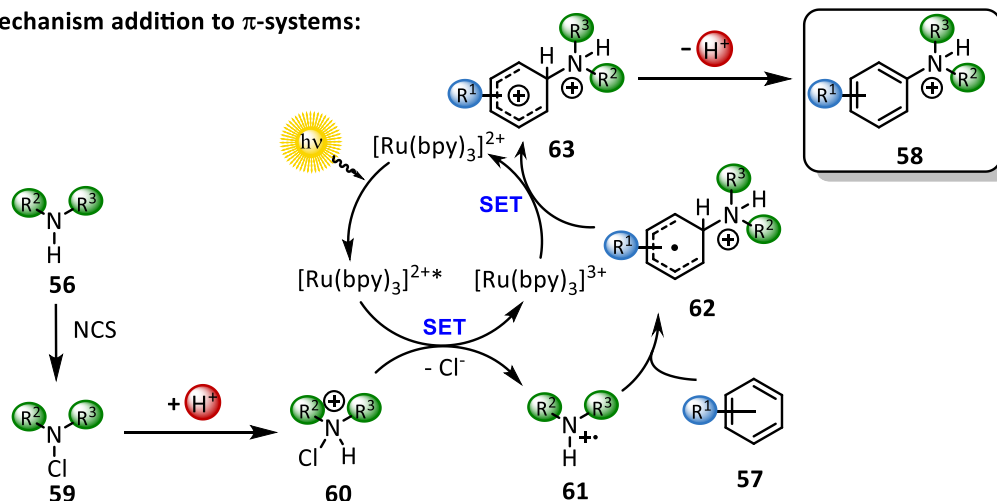r material. After protonation of this amine, an SET from an excited photocatalyst was possible, leading to the desired aminium radical, which in turn was able to add to various aromatic moieties.[48] In an impressive display of the versatility of this reaction, the group improved on this method by using *in situ* generated *N*-chloro compounds in conjuncture with perchloric acid as protonating agent to achieve an highly efficient amination protocol that tolerated almost all substitution patterns on the aromatic core **57**. A great variety of products in excellent yields highlighted this method as an viable alternative to established Buchwald-Hartwig and Ullman coupling reactions (Scheme 13).[49] The necessary aminium radical **61** is hereby generated after an SET from the photocatalyst to the protonated *N*-chloro compound **60**. After an electrophilic attack the resulting radical **62** is oxidized by the photocatalyst, closing the catalytic cycle and yielding **58** after re-aromatization of **63**.

Addition to π-systems: Leonori, 2019:

R^1 = alkyl, aryl, EWG, EDG, halo, silyl, boronyl
R^2 = R^3 = H, alkyl
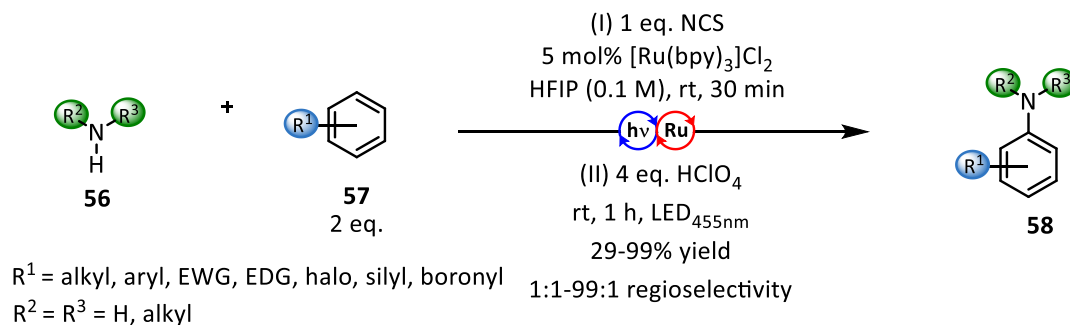
Mechanism addition to π-systems:

Scheme 13: Amination of aromatic systems by aminium radicals.[49]

5-exo-trig cyclizations of aminium radicals have been successfully demonstrated by the Zheng and Knowles group.[50,51] Electron-rich *N*-arylated compounds **64** are oxidizable by an iridium photocatalyst, subsequently leading an aminium radical which reacted in a 5-exo-trig cyclization. After reduction of the resulting benzylic radical by the photocatalyst, the Knowles group obtained pyrrolidines **65** in good to excellent yields in an overall redox neutral reaction (Scheme 13, a).

(a) 5-exo-trig cyclization: Knowles, 2014:

R^1 = alkyl, aryl, EDG, halo
R^2 = alkyl, EDG, EWG, halo
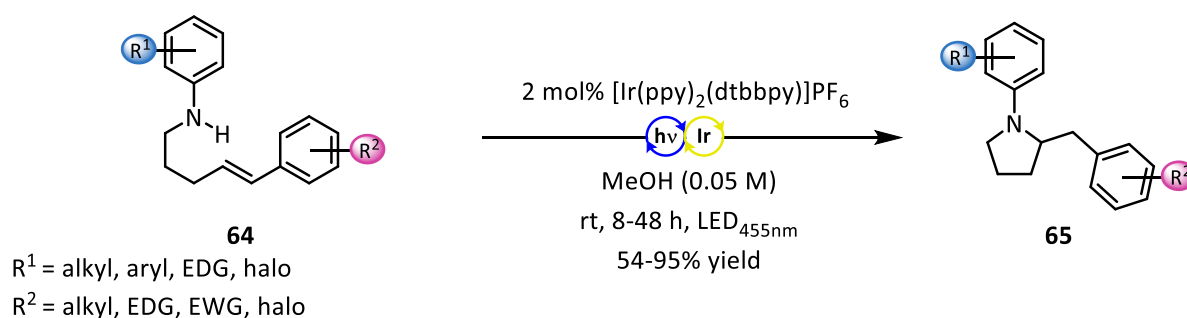
(b) Norrish type-I: Zheng, 2012:

R^1 = alkyl, aryl, EDG, EWG, halo
R^2 = alkyl
R^3 = aryl, EDG, halo
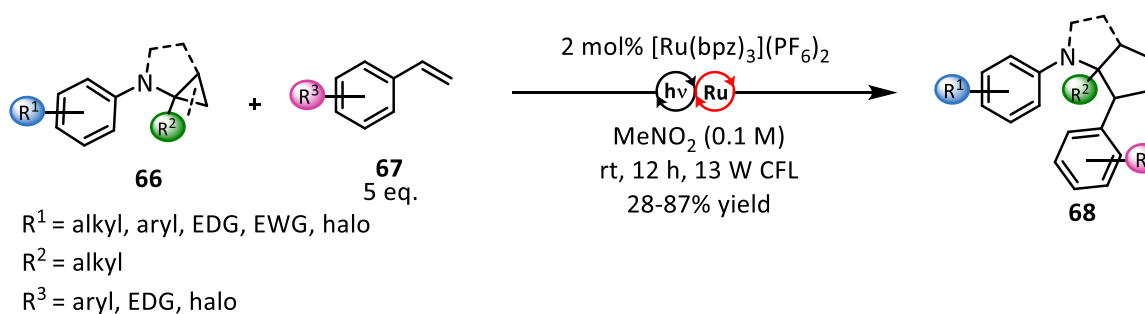
Scheme 14: Reactivities of aminium radicals as demonstrated by the groups of Knowles[51] and Zheng.[52]

Zheng an co-workers extended this to the synthesis of indoles, by performing this reaction under oxidizing conditions by the presence of molecular oxygen. The same group also demonstrated the ability of aminium radicals to react *via* a Norrish type-I mechanism.[52] Oxidation of secondary and cyclic tertiary amines with an α-cyclopropane substitution **66** led to ring-opening reactions of the external cyclopropane bond, leading to the formation of a primary radical. After a formal [3+2] cycloaddition to styrenes **67** and reduction of the resulting radical intermediate, a ring expansion of the initial cyclopropane moiety to product **68** was observed (Scheme 14, b). Summing up, while aminium radicals perform similar reactions to aminyl radicals, their increased electrophilicity makes them more effective and versatile for additions to C_{sp}^2 systems. However, that increased electrophilicity also favors Norrish type-I and 1,2-radical shift reactions that need to be considered when designing a reaction with aminium radicals.
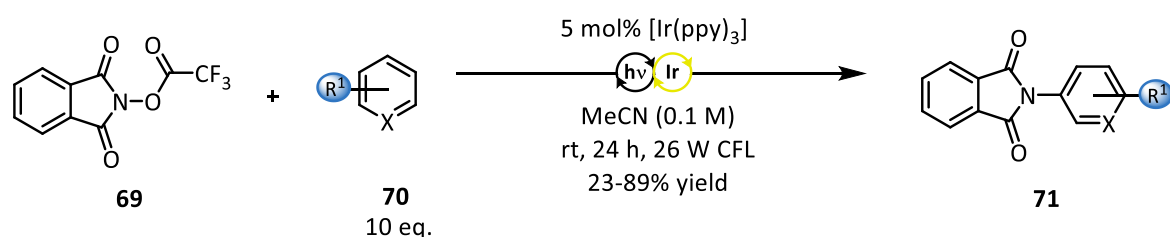
1.2.2.3 Amidyl radicals

The class of electrophilic amidyl π-radicals is not purely limited to amides, but also contain neutral radicals originating from *N*-sulfonylated amines, phtalimides and carbamyl groups.[53,54] Similar to aminium radicals, amidyl radicals are of a highly electrophilic character that contrast the nucleophilic character of polar C-N bond formation.[55] However, compared to aminium radicals, amidyl radicals favor inter- and intramolecular HAT processes that make efficient reaction design challenging.[56]

Consequently, amide radicals are a very versatile class of radicals that have found numerous applications in organic synthesis. The most common reaction reported in literature is the addition of amidyl radicals to unsaturated systems and 5-exo-trig cyclizations, aromatic amidations and ATRA type reactions have all been reported. The group of Sanford illustrated the ability of phtalimidyl radicals, generated from **69**, to add to aromatic systems in intermolecular reactions. The group was successful in amidating a number of benzene derivatives and heterocycles **70** in moderate to good yields, albeit with only moderate regioselectivity (Scheme 15, a).[38] Building on this initial report, Leonori and co-workers managed to expand the scope to more general amides and more substrates in good yields.[53,57] Shortly afterwards, Yu and co-workers demonstrated that in the presence of styrene derivatives **73**, products from ATRA-type halo-aminations **74** are obtainable in good yields (Scheme 15, b).[58] Similarly, intramolecular ATRA-type amino-hydroxylations by amidyl radicals have been realized by Lu et al.[59]

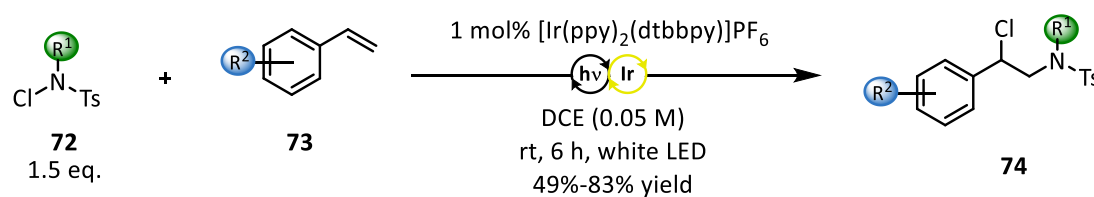**(a) Addition to π-systems: Sanford, 2014:**

R^1 = alkyl, aryl: EDG, halo

X = C, N

(b) Haloamination: Yu, 2016:

R^1 = alkyl

R^2 = alkyl, aryl: EDG, halo

Scheme 15: Intermolecular reactivities of amidyl radicals as demonstrated by the groups of Sandford[38] and Yu.[58]

In general, intramolecular reactions of amidyl radicals are favored over intermolecular reactions are favored and have been more thoroughly explored. The Knowles group highlighted the ability of PCET processes to access amidyl radicals from **75**, reacting them in 5-exo-trig cyclizations (Scheme 16, a). This hydroamidation was applicable to a significant number of substrates to give excellent yields and good diastereoselectivites for products **77** in most cases.[42]

In a follow-up report the group was successful in intercepting the intermediary primary radicals formed during cyclization with various olefinic acceptors, further increasing the synthetic applicability for the synthesis of various lactams.[60] Subsequent literature reports also establish the use of weak N-O bonds[53] and electrochemistry[61] to be compatible with this hydro-amination reaction.

When no suitable olefinic bonds are available, the highly reactive amidyl radicals will site selectively abstract a C$_{sp}^3$-H atom in a 1,5-HAT process. This is reminiscent of the original Hoffman-Löffler-Freytag reaction and enables the site selective catalytic functionalization of inert aliphatic chains. Yu and co-workers applied this principle for the synthesis of pyrrolidines *via* 1,5-HAT from a benzylic group in moderate to good yields.[62] The groups of Rovis and

Introduction

Knowles demonstrated the ability to functionalize C_{sp3}-H bond in 5-position of an electron poor amide **78** (Scheme 16, b). In this mechanism, a PCET process facilitated by an iridium photocatalyst and K_3PO_4 gives rise to amidyl radical **81**. This *in situ* generated radical partakes in a 1,5-HAT reaction towards carbon-centered radical **82**. This intermediate can subsequently be intercepted by various electron-poor olefins **79**. Simultaneously, this highlights the inability of amide radicals **81** to directly react with electron-poor unactivated alkenes.[63,64]
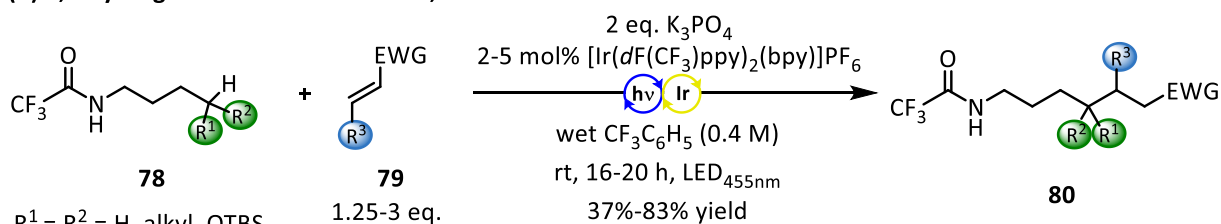
(a) 5-exo-trig cyclization: Knowles, 2015:
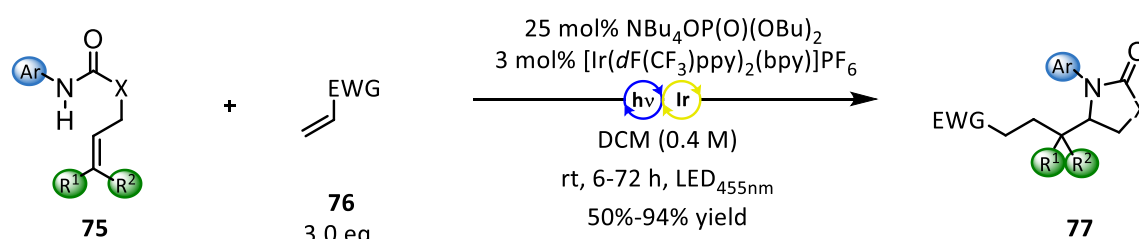
$R^1 = R^2 = H$, Me, alkyl
X = C, O, NMe, NPh, S
Ar = alkyl, aryl: halo, EWG, EDG
EWG = CO_2Me, COMe, CHO, CN, Pyridyl
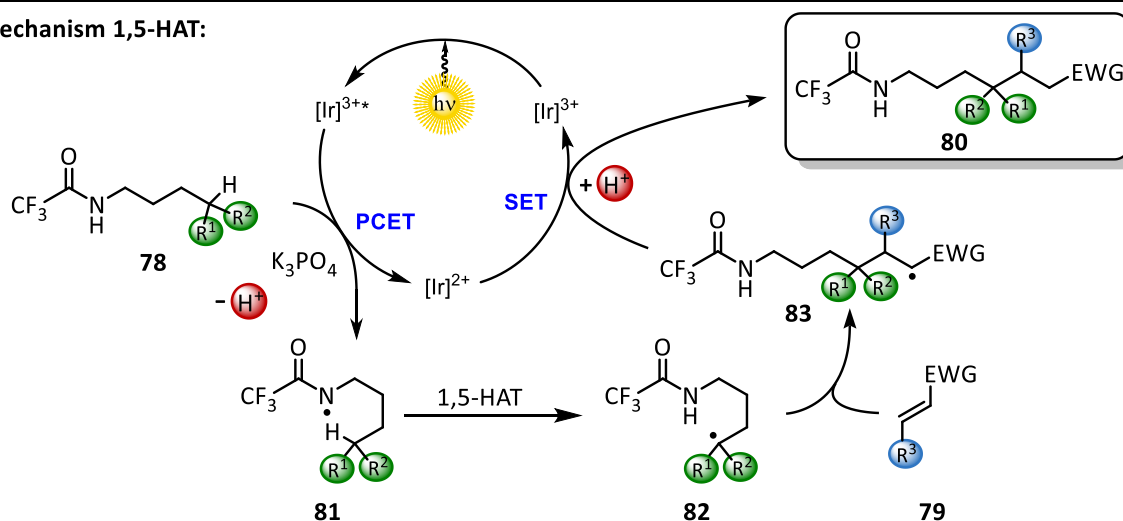
(b) 1,5-hydrogen atom transfer: Rovis, 2016:

$R^1 = R^2 = H$, alkyl, OTBS
$R^3 = H$, Me, CO_2Me
EWG = CO_2R, $CONMe_2$, COR

Mechanism 1,5-HAT:

Scheme 16: Intramolecular reactivities of amidyl radicals.
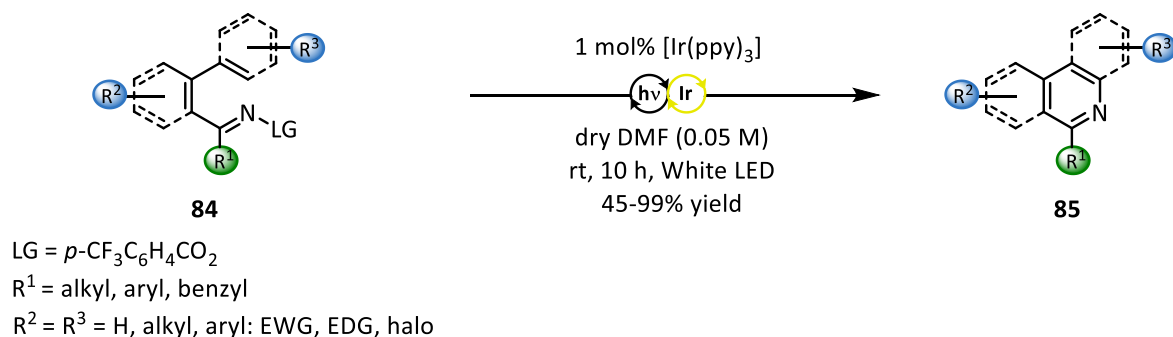
In this report the Knowles group also highlighted the ability of amidyl radicals to be used in an intermolecular HAT catalyst system. Radical-radical couplings of amidyl radicals were highlighted by the Macmillan group in 2013 with their enantioselective α-amination of aldehydes.[37] This reaction has already been described in chapter 1.2.1.2. The reactions shown in this chapter outline the versatile, but challenging nature of highly reactive amidyl radicals and their applications in organic chemistry.

1.2.2.4 Iminyl radicals

Generally, iminyl radicals are most easily accessed by the scission of an N-O bond in oxime derivatives by SET catalysis.[36] Alternatively, unsaturated azides lead to iminyl radicals after reaction with an radical imitator and nitrogen extrusion.[65] In contrast to their other *N*-centered radical counterparts, iminyl radicals are σ-radicals localized on an sp^2-hybridized nitrogen atom and display an ambiphilic character.[66] Despite their reactivity, to the best of our knowledge no intermolecular reactions by iminyl radicals have been reported so far.

(a) Addition to π-systems: Yu, 2015:

LG = *p*-CF$_3$C$_6$H$_4$CO$_2$
R^1 = alkyl, aryl, benzyl
R^2 = R^3 = H, alkyl, aryl: EWG, EDG, halo

(b) 5-exo-trig cyclization: Studer, 2017:

EWG = CO$_2$R, CONR$_2$, PO(OR)$_2$, SO$_2$Ph, COR
R^1 = alkyl, aryl, EWG, EDG, halo
R^2 = R^3 =H, Me, CO$_2$Me, Ph
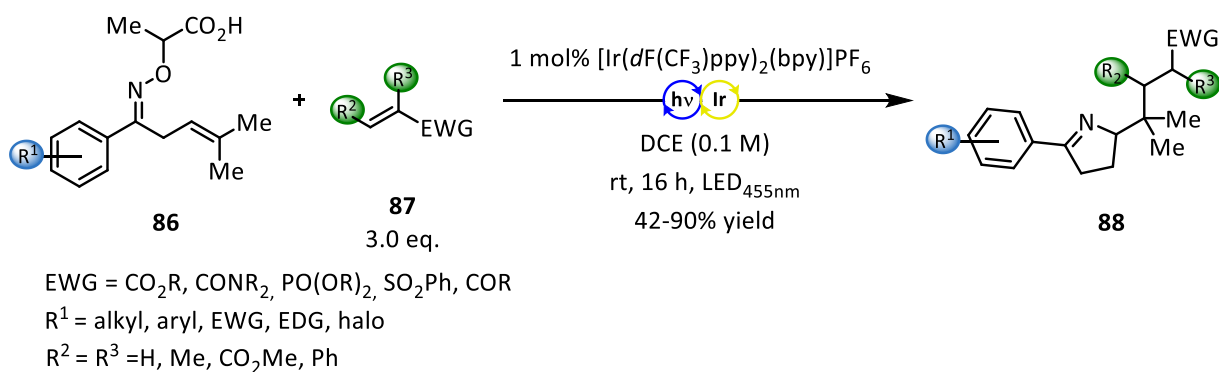
Scheme 17: Reactivities of iminyl radicals as demonstrated by the groups of Yu[67] and Studer.[68,69]

Introduction

The group of Yu demonstrated the synthesis of a significant scope of pyridine, quinoline and phenanthridine derivatives **85** by addition of iminyl radicals to π-systems in good to excellent yields (Scheme 17, a).[67] For this purpose, the group utilized iridium photoredox catalysis to generate *N*-centered iminyl radicals from oxime precursors in a redox-neutral reaction, and demonstrated the synthetic applicability of their method with the synthesis of the noravicine alkaloid. An effective demonstration of 5-exo-trig cyclizations by iminyl radicals were simultaneously developed by the groups of Studer and Leonori.[68,69] Contrasting the previous report of the Yu group, in this reaction the iminyl radicals were generated by an oxidative quenching cycle from **86**. While Studer and co-workers realized carboiminations by subsequent condensation of the *in situ* generated carbon radicals to electron poor olefins (Scheme 17, b), the group of Leonori highlighted the ability of iminyl radicals towards intramolecular halo-amination reactions. The same group also extended this method to 5-exo-dig cyclizations[70] and demonstrated the potential for ATRA-type cyclizations by iminyl radical precursors when suitable leaving groups are chosen.[71]

(a) radical-radical coupling: Chiba, 2013:
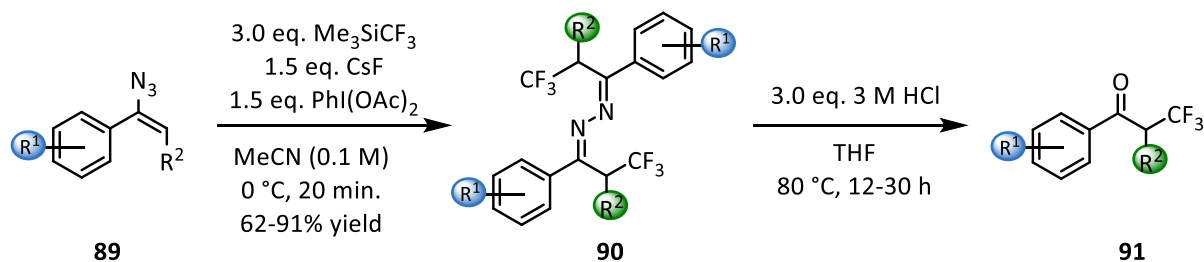
R^1 = alkyl, aryl, EWG, EDG, halo

R^2 = H, alkyl

(b) Norrish type-I: Xiao, 2017:
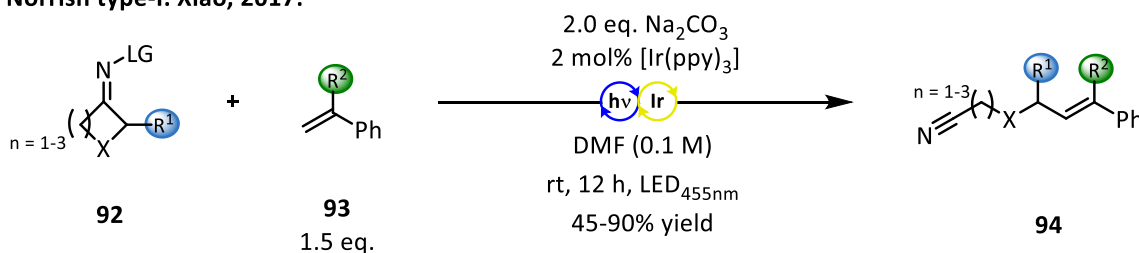
LG = p-CF$_3$C$_6$H$_4$CO$_2$, X = C, N, O

R^1 = Me, Ph, allyl, benzyl

R^2 = alkyl, aryl, OTMS

Mechanism Norrish type-I:
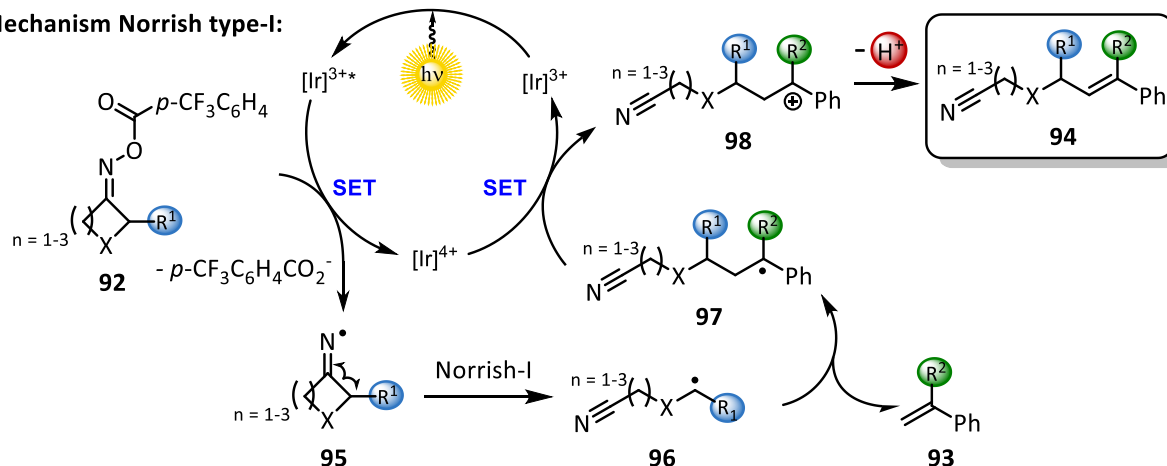
Scheme 18: Reactivities of iminyl radicals as demonstrated by the groups of Chiba[72] and Xiao.[73]

1,5-HAT reactions by highly reactive iminyl radicals are a powerful synthetic tool in organic chemistry. A closer look into this reaction is taken in chapter 3.1. When no suitable intramolecular reaction partner is available, iminyl radicals will dimerize through radical-radical coupling mechanisms. The group of Chiba illustrated how α-trifluoromethyl ketones **91** can be obtained in good yields after hydrolyzation of iminyl dimers **90**. Hereby, iminyl radicals were obtained after nitrogen extrusion caused by radical condensation of trifluoromethyl radicals to unsaturated azides **89** (Scheme 18, a).[72] The group of Liu improved this method

by removing the need of a stoichiometric oxidant through the use of an organic photoredox catalyst.[74]

When attached to three- or four-membered carbocycles, iminyl radicals will favor a Norrish-I reaction pathway. W.-J. Xiao *et al.* demonstrated this reaction pathway for the addition of cyc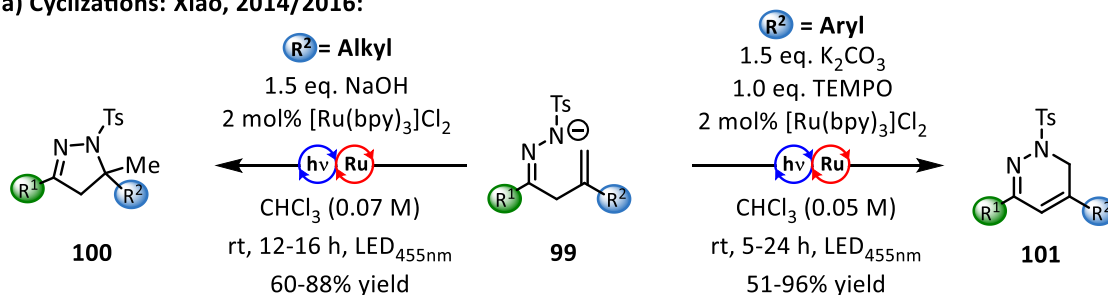lobutanone derived oxime esters to unsaturated bonds after ring opening.[73,75,76] The Xiao group proved, that up to six-membered carbocycles **92** are eligible for Norrish-I type ring opening reactions after activation by iridium photocatalysis. Hereby, resulting carbon-centered radicals **96** were trapped by diarylstyrenes **93**, α-substituted styrenes and α-aryl silyl enol ethers to give the corresponding products **94** in good to very good yields after oxidation by the photocatalyst (Scheme 18, b). Considering the number of available reports on the reactivities of iminyl radicals, it is no wonder that the highly reactive ambiphilic iminyl radicals can be considered the most versatile class of nitrogen-centered radical. However, this versatility and reactivity comes at the cost of reaction control and side product formation, which can be problematic when handling iminyl radicals outside of optimal parameters and limits them to intramolecular reactions.

1.2.2.5 Hydrazonyl radicals

Despite containing a weak N-N bond similar to other precursors, the latter is not cleaved to access hydrazonyl radicals, but direct oxidation of a deprotonated hydrazonyl moiety is employed. The resulting electrophilic radicals are conjugated over the π-system, which stabilizes the N-N bond. However, the group of Han and co-workers demonstrated that attaching a trifluoro- or a trichloroacetyl group to the hydrazonyl moiety turns the resulting radical into a σ-radical after oxidation by TEMPO.[77] Furthermore, the group highlighted that both nitrogen atoms can be the reactive nitrogen to partake in 5-exo-trig cyclizations. To the best of our knowledge, the only reaction mechanisms reported for hydrazonyl radicals are intramolecular cyclizations and 1,5-HAT processes.

(a) Cyclizations: Xiao, 2014/2016:

R^2= Alkyl
1.5 eq. NaOH
2 mol% [Ru(bpy)$_3$]Cl$_2$

CHCl$_3$ (0.07 M)
rt, 12-16 h, LED$_{455nm}$
60-88% yield

R^2 = Aryl
1.5 eq. K$_2$CO$_3$
1.0 eq. TEMPO
2 mol% [Ru(bpy)$_3$]Cl$_2$

CHCl$_3$ (0.05 M)
rt, 5-24 h, LED$_{455nm}$
51-96% yield

100 **99** **101**

R^1 = alkyl, aryl: EWG, EDG, halo

(b) 1,5-HAT: Chiba, 2013:

3.0 eq. TEMPO
2.0 eq. K$_2$CO$_3$

DMF (0.06 M)
130 °C, 12-60 h
70-90% yield

102 **103**

R^1 = alkyl, aryl
R^2 = Me, aryl
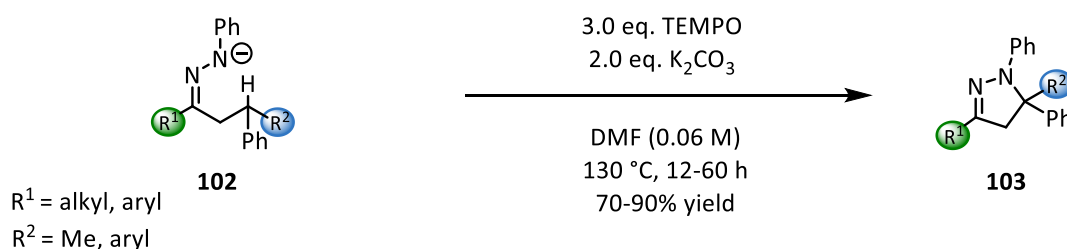
Scheme 19: Reactivities of hydrazonyl radicals.

Xiao and co-workers illustrated photoredox chemistry as valuable synthetic tool towards the synthesis of pyrazoles in moderate to good yields. Tosyl-protected hydrazones were deprotonated by sodium hydroxide, which enabled the substrate **99** to be oxidized by a ruthenium photocatalyst upon irradiation, resulting in a 5-exo-trig cyclization towards **100**.[41] In a subsequent report, the group elaborated on the tunability of this cyclization: By installing an aryl group on the unsaturated bond of **99**, 6-endo-trig cyclizations could be favored over 5-exo-trig cyclizations (Scheme 19, a), leading to product **101**.[78] Additionally, the possibility for the resulting carbon-centered radical to take part in radical cascades was demonstrated.

The groups of Belmont and König expanded the available scope of available cyclizations for tosyl-protected hydrazones to 5-exo-dig mechanisms. In this reaction, a highly reactive vinyl radical is generated *in situ* after a radical attack on the triple bond by a photocatalytically generated hydrazonyl radical. This vinyl radical attacks the tosyl protecting group leading to a Smiles rearrangement, ultimately yielding benzhydrylphtalazines in good yields.[79] A similar radical cascade was demonstrated by the group of Xiao and co-workers.[80] In this report a cobalt catalyst was used as terminal oxidant in conjunction with photoredox catalysis. Similar to the work by the König's group, the *in situ* generated carbon-centered radical attacked the

tosyl protecting group. Hereby, the cobalt catalyst fulfilled the essential role of re-aromatization, which was not possible without the cobalt catalyst.

Only one occasion of 1,5-HAT processes by hydrazonyl radicals has been reported so far: The group of Chiba described, that hydrazonyl radicals generated from **102** and over-stoichiometric amounts of TEMPO, lead to 1,5-HAT processes which, after subsequent oxidation of the resulting carbon-centered radical result in pyrazoles **103** in good yields (Scheme 19, b).[81] Hereby, the same mechanism was reported for unsubstituted oximes. It is surprising that despite the ease of *in situ* access to hydrazonyl radicals, no reports of other mechanisms or intermolecular examples of this versatile and interesting group have been reported so far.

2 Nitrogen radicals in ATRA reactions: A holistic picture for three distinct ATRA mechanisms.

2.1 Introduction

In recent years, photoredox catalysis evolved into an important tool for the activation and functionalization of various substrates.[1,2,82,83] Hereby, vicinal difunctionalizations of unsaturated hydrocarbons by atom transfer radical addition (ATRA) reactions are of special interest, since they enable easy access to a plethora of valuable heterofunctionalized products.[84,85]
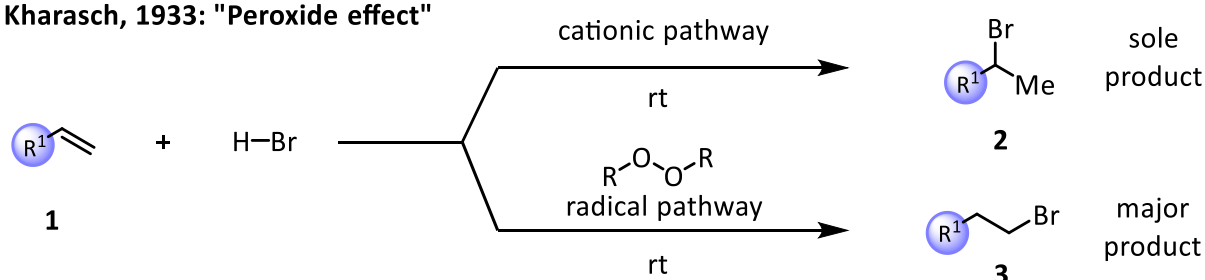

Scheme 20: Kharasch*s initial report on peroxides influencing the chemo-selectivity of halogen additions to alkenes: The "peroxide effect".

Three distinct mechanistic pathways for mediated ATRA reactions are discussed in the literature.[84,86,87] Seminal work of Kharasch[88] on the addition of hydrogen halides across alkene double bonds **1** (Scheme 20) demonstrates that a radical-chain mechanism – initiated by the UV-light or radical induced homolysis of peroxides – can be operating for such transformations. Expanding this approach from hydrogen halides to the more general addition of organohalide compounds **4** to unsaturated bonds **1**, the generation of the initial carbon-centered radical **6** needs to be considered (Scheme 21, b). Next to UV-light irradiation or radical initiation, such radicals can also be formed upon reduction of **4** *via* photoelectron transfer (PET) from a redox active metal complex (Scheme 21, b). The carbon-centered radical

6 subsequently adds to alkene **1** to give rise to radical **7**, which can attack the initial organohalide **4**, ultimately yielding product **5** and another radical **6** in a chain propagation step. However, radical **7** also opens up the possibility for an alternate pathway - coined photoredox cycle - that calls for the oxidation of **7** to cation **8** with concurrent regeneration of the metal complex in order to close the catalytic cycle. Hereby, the combination of cation **8** and a halide then leads to the ATRA product **5** (Scheme 21, c).
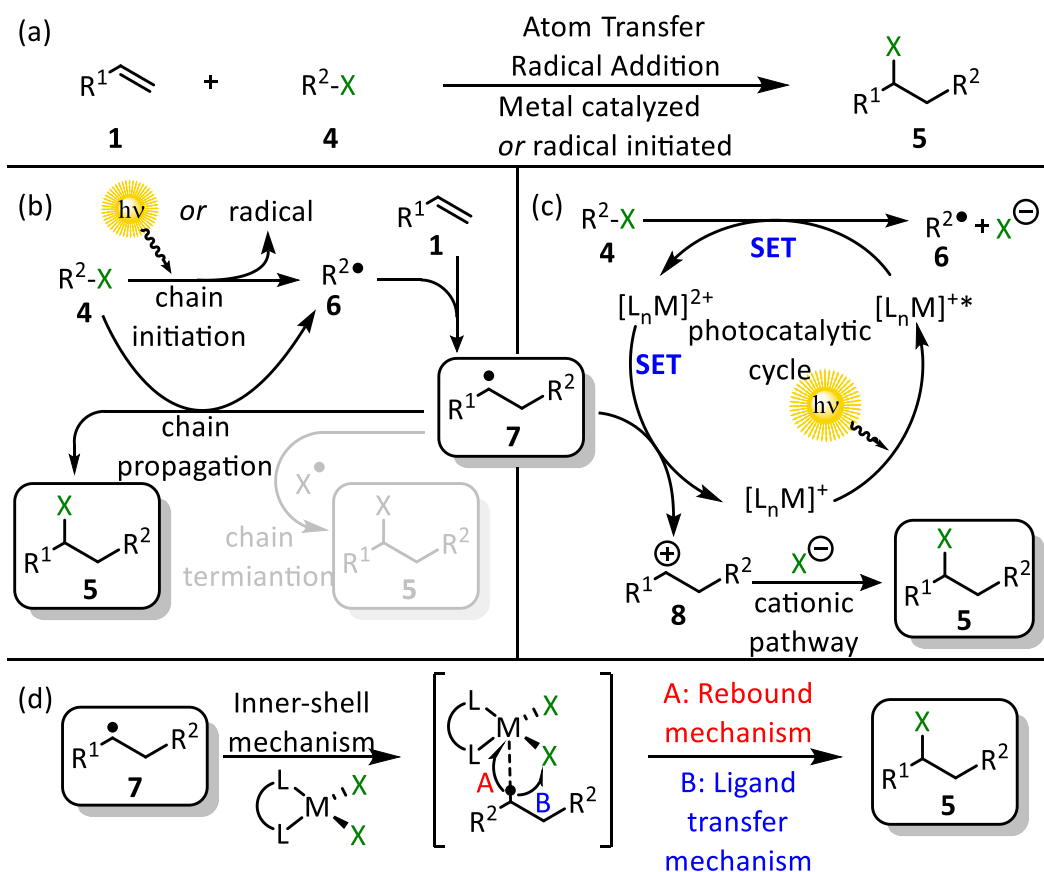

Scheme 21: (a) Generalized ATRA reaction (b) ATRA mechanism for radical-chain reactions. (c) ATRA mechanism for photoredox reactions. (d) ATRA mechanism for Inner-shell processes

As a third possibility, interaction of the transient radical **7** with the photocatalyst in an inner-shell mechanism was suggested (Scheme 21, d), either by directly abstracting a ligand ("ligand transfer") or by adding to the metal center followed by reductive elimination to form the final product **5** ("rebound mechanism").

Evidence towards this mechanistic proposal came from ATRA reactions catalyzed by Cu(I)-based photocatalysts,[89] given that such processes can proceed with different chemo-selectivity compared to iridium- and ruthenium photocatalysts.[90,91] Moreover, it can be

rendered asymmetric, making an intricate interaction of substrate and catalyst essential for obtaining products enantioselectively (Scheme 22).[92,93]
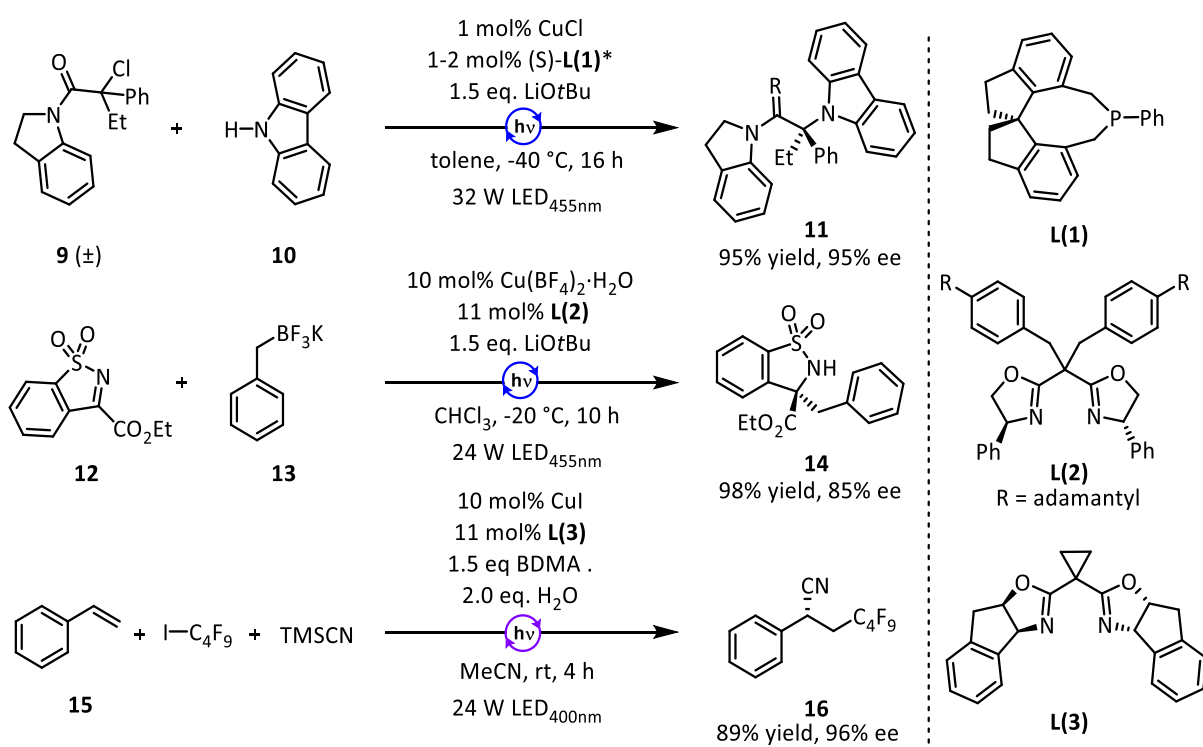

Scheme 22: Selected examples for asymmetric copper catalyzed photoredox reactions.

The validity of a photoredox catalytic cycle has been argued by "on/off experiments", which claim that the ATRA process is shut down/turned back on by off/on cycles of the light source.[94] However, Yoon and coworkers refuted in an insightful study that such "on/off experiments" can be taken as unambiguous evidence for the presence of a photocatalytic cycle in ATRA reactions, considering the fast rates of radical-chain processes.[95]

Taking the chloroamination of styrenes as a representative example, in this study we offer a holistic picture demonstrating that all three mechanistic proposals are valid, but depend on the catalyst used and the electronic properties of the alkene employed, which ultimately decides the success or the failure of such transformations.
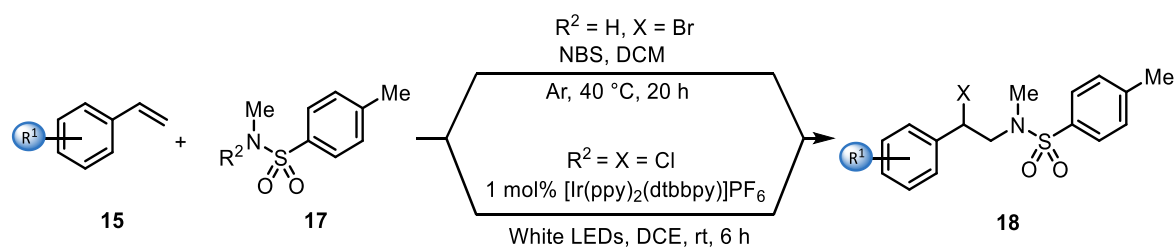
Scheme 23: Halo-aminations driven by thermal or photochemical conditions.

Halo-aminations of styrene have been demonstrated both under photochemical and thermal conditions.[8-11] Y.-Y. Yeung and coworkers demonstrated how to control the Markovnikov or anti-Markovnikov chemo-selectivity of thermal bromo-aminations by suppressing or encouraging a radical-chain mechanism in favor of a bromonium intermediate (Scheme 23, upper). In contrast to this, S. Yu and coworkers achieved the more challenging reaction between electron rich styrenes **15** and *N*-chlorosulfonamides **17a** by utilizing visible light conditions employing [Ir(ppy)$_2$(dtbbpy)]PF$_6$ (**[Ir]**, ppy = 2-phenylpyridine, dtbbpy = 4,4-di-*tert*-butyl-2,2´-bipyridine) as the photocatalyst (Scheme 23, lower). The reaction is proposed to proceed *via* a photoredox cycle according to which the oxidation of radical **7** to the cation **8** ultimately takes place to allow the combination with the halide anion towards the final product **5** (Scheme 21, b).[58] Highlighting the potential for enantioselective difunctionalizations of alkenes, thermal intra- and intermolecular additions of various *N*-Halo compounds to alkenes have been realized by chiral metal complexes, chiral phosphoric acids and chiral hydrogen bond donors.[96] However, to the best of our knowledge, no enantioselective photochemical halo-aminations have been reported so far.

The intermolecular radical halo-amination of alkenes (Scheme 21, a) with *N*-halo sulfonamides represents a useful transformation for the synthesis of biologically important compounds, since sulfonamides have found special applications for pharmaceuticals.[97]

Ar = *p*-OMe-Ph

[Cu(dap)$_2$]Cl (**[Cu]**)　　　　[Ir(ppy)$_2$(dtbbpy)]PF$_6$ (**[Ir]**)　　　　[Ru(bpy)$_3$]Cl$_3$
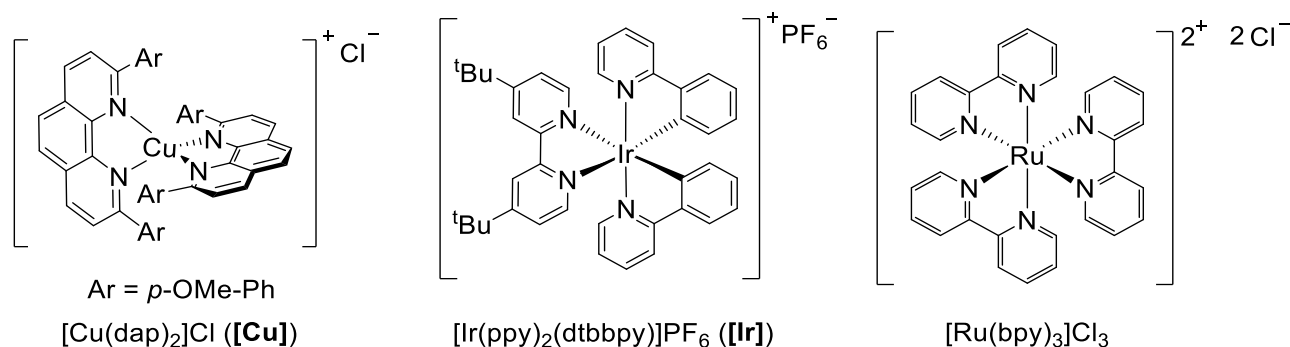
Figure 1: Common metal-based photoredox catalysts.

Furthermore, this work leads towards further distinguishing copper-based photocatalysts as a bifunctional class of catalysts, separate from previously established Ir- and Ru-based photocatalysts (*e.g.* Figure 1).[89] Herein demonstrated is coppers' ability to interact with carbon-centered radicals in inner-shell mechanisms, thereby directly influencing the mechanistic pathway and in some cases product formation. Additionally, the use of green (530 nm) *vs.* blue (455 nm) light in conjunction with copper catalysts has been proven to be beneficial for reaction outcomes in cases where traditionally difficult ATRA reagents had to be used.[90,98] This work represents another example in which coppers ability to facilitate reactions with green light results in more benign reaction conditions, avoiding free radical-chain reactions.

2.2 Reaction screening

On the outset we sought to prove that different ATRA mechanisms are at work for this reaction, dependent on the electronic properties of the substrate and catalyst involved. Our studies into ATRA mechanisms with nitrogen radicals began by investigating the chloroamination of *para*-methylstyrene **15a**. Using [Ir(ppy)$_2$(dtbbpy)](PF$_6$) (**[Ir]**) as catalyst, the halo-amination product **18a** was obtained in 57% yield. While the group of S. Yu previously reported an isolated yield of 83% for those reaction conditions,[62] we were unable to reproduce the reported yields using our internal irradiation setup. Comparable to this, [Cu(dap)$_2$]Cl (**[Cu]**) was able to afford **18a** in 66% yield. (Table 1, entry 1-3).

Nitrogen radicals in ATRA reactions: A holistic picture for three distinct ATRA mechanisms.

Table 1: Reaction screening for the chloroamination of 4-methylstyrene.
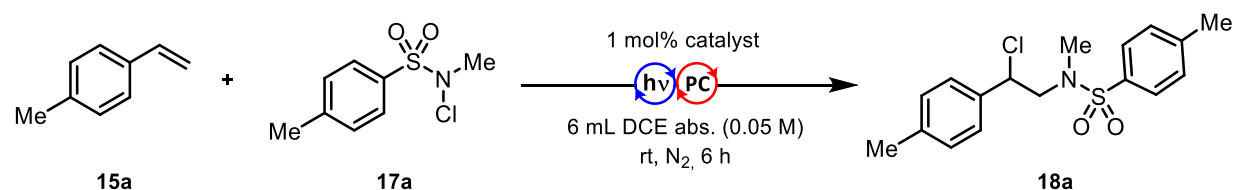
Entry[a]	λ [nm]	catalyst	Yield [%]
1	455	[Ir(ppy)$_2$(dtbbpy)](PF$_6$)	57
2	455	[Cu(dap)$_2$]Cl	66
3	455	no	85
4[c]	455	no, 1 bar O$_2$	n.r.
5[b]	455	CuCl$_2$ 5 mol%	22
6	dark	[Cu(dap)$_2$]Cl	4[d]
7	dark	no	n.r.
8	dark	No, 80 °C	10[d]
9	dark	AIBN[e], 80 °C	88[d]

(a) Reaction conditions: 0.3 mmol **15a**, 0.45 mmol **17a**, DCE abs. 6 mL (0.05 M). Reactions were irradiated using a 3W blue LED$_{455nm}$ for 6 h at room temperature. (b) Prepared by L. Traub. Other reactions were prepared by C. Lankes. (c) Reaction time: 4 h. (d) Determined by ^{1}H-NMR using 2-nitropropane as internal standard. (e) 1 mol% AIBN, dark.

Surprisingly, a control experiment in absence of catalyst resulted in an increase in reaction yield to 85% (entry 3). This result was attributed to a radical-chain reaction mechanism, although the lack of coloration of the reaction solution pointed towards very weak absorption in the visible region of light. This claim was validated by inhibition of the reaction by persistent radicals in the form of molecular oxygen or CuCl$_2$ (entry 4 & 5). Furthermore, the need for irradiation was demonstrated by two dark reactions, both in presence and absence of a photocatalyst (entry 6 & 7). Heating the reaction mixture to 80 °C was not sufficient to facilitate a radical-chain reaction on its own, however, upon addition of 1 mol% AIBN as radical starter **18a** was obtained in excellent yields.
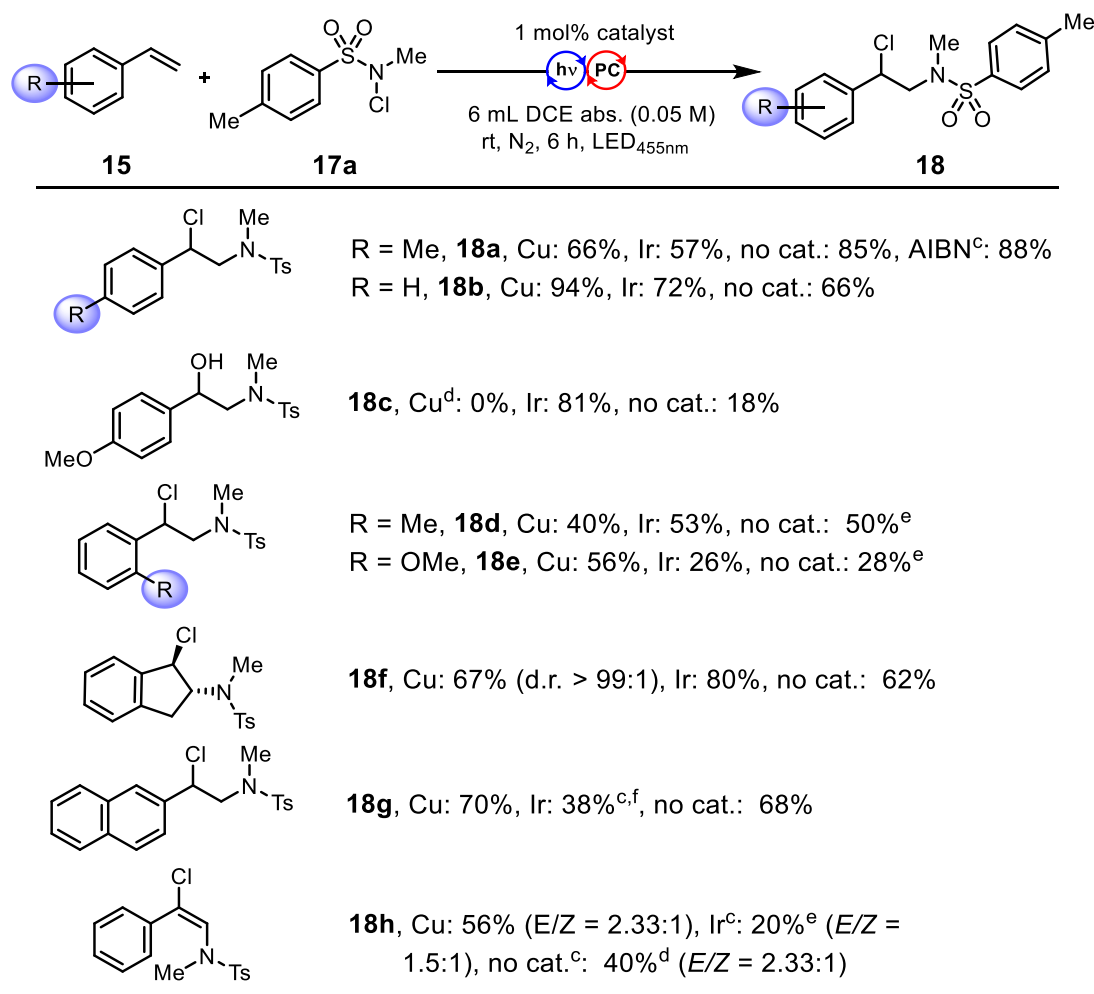
2.3 Substrate Scope

Intrigued by those initial results, we set out to further investigate the differences between radical-chain and photocatalyzed reactions. Styrene derivatives are a popular class of unsaturated compounds for ATRA reactions, due to the tunability of their electronic properties. Varying substitutions patterns influence the stability of the benzylic radicals formed upon radical addition to the unsaturated moiety.

2.3.1 Electron-rich Styrenes

Having chosen a suitable class of substrate for mechanistic investigations, we began by investigating styrene. Hereby, **[Cu]** outperformed **[Ir]** and the radical-chain reaction. Notably, while yields for both metal-based catalysts rose in comparison to **18a** (Table 1), the yield for the radica-chain reaction decreased (Figure 2). The very electron rich 4-methoxystyrene **15c** resulted in a product mixture which was determined to be unstable towards hydrolyzation. The expected chloro-substituted product was not be observed, and only product **18c** was obtained in case of **[Ir]** and no catalyst. **[Cu]** only afforded a complex reaction mixture in this case.

R = Me, **18a**, Cu: 66%, Ir: 57%, no cat.: 85%, AIBN[c]: 88%
R = H, **18b**, Cu: 94%, Ir: 72%, no cat.: 66%

18c, Cu[d]: 0%, Ir: 81%, no cat.: 18%

R = Me, **18d**, Cu: 40%, Ir: 53%, no cat.: 50%[e]
R = OMe, **18e**, Cu: 56%, Ir: 26%, no cat.: 28%[e]

18f, Cu: 67% (d.r. > 99:1), Ir: 80%, no cat.: 62%

18g, Cu: 70%, Ir: 38%[c,f], no cat.: 68%

18h, Cu: 56% (E/Z = 2.33:1), Ir[c]: 20%[e] (E/Z = 1.5:1), no cat.[c]: 40%[d] (E/Z = 2.33:1)

(a) Reaction conditions: 0.3 mmol **15**, 0.45 mmol **17a**, DCE abs. 6 mL (0.05 M). Reactions were irradiated using a 3W blue LED$_{455nm}$ for 6 h at room temperature. (b) Reactions were irradiated using a 3 W green LED (530 nm) (c) 1 mol% AIBN, 80 °C, dark. (c) Prepared by L. Traub. Other reactions were prepared by C. Lankes. (d) Polymerization of starting material. (e) Determined by ^{1}H-NMR using 2-nitropropane as internal standard. (f) In agreement with ^{1}H-NMR yield (39%).

Figure 2: Substrate Scope for electron-rich alkenes.

Regarding *ortho*-substitution of the styrene core, the +I-effect of the methyl group in **15d** caused yield to decline to 40% for **[Cu]**. **[Ir]** outperformed copper in this example (53%), achieving a yield close to that for the uncatalyzed reaction (50%). In contrast to this, the electron rich *ortho*-methoxystyrene **15e** gave best yields with **[Cu]** (56%), while **[Ir]** (26%) and the radical-chain reaction (28%) only resulted in poor yields. Inden derivative **18f** was obtained diastereoselectively in all reactions, with **[Ir]** giving the best isolated yield with 80% in this photoredox pathway. **[Cu]** and the radical-chain reaction achieved similarly good results with 67% and 62% yield respectively. The reaction towards naphthalene derivative **18g** produced similarly good yields for **[Cu]** and no catalyst (70% and 68%), while **[Ir]** displayed a significantly lower yield due to side reactions (38%). Pleasingly, the chloroamination of phenylacetylene

15h was successful with copper catalysis, resulting in product **18h** (56%) with the *Z*-diastereomer favored in a 2.33:1 d.r. While the uncatalyzed reaction afforded lower yields in the same d.r. (40%), **[Ir]** displayed a drop in diastereoselectivity and yield (20%). However, as demonstrated by Liu and coworkers, the pure (*E*)-product **18h** is obtainable by a thermal reaction using a different copper catalyst.[99] The initial assumption that energy transfer processes from the photocatalyst trigger isomerization reactions was disproven by a control reaction with no catalyst resulting in the same d.r. as the copper catalyzed reaction. No tests with pure (*E*)-**18h** and blue light irradiation were performed to see if 455 nm light irradiation triggers the isomerization event. In conclusion, electron-rich styrenes led to mixed results. Each of the three mechanisms at work here – radical-chain, outer- and inner-shell photoredox mechanism - were able to achieve the best yields depending on the substrate. In general, variations in yield were high In between different substrates.

2.3.2 Electron-deficient Styrenes

Having established a scope of electron-rich substrates, our attention turned to electron poor styrenes. Pleasingly, in all cases **[Cu]** achieved the best yields, ranging between 60%-98% yield. Strong electron withdrawing groups (**18i-18l**, Figure 3) in *para*-position led to a breakdown of the radical-chain mechanism. This was confirmed by two AIBN experiments at 80 °C (1 mol%) with *para*-cyano **15i** and the *para*-nitro styrene **15j** which led to comparable yields to reactions with only irradiations at 455 nm. **[Ir]** catalysis resulted in low to mediocre yields for the desired products **18i/18l** (26-54%), while **[Cu]** led to excellent yields in all cases (85-98%).

15   **17a**   **18**

R = CN, **18i**, Cu: 96%, Ir: 26%, no cat.:7%[b], AIBN[c]: 16%[b]
R = NO$_2$, **18j**, Cu: 98% Ir: 34%, no cat.: 2%, AIBN[c]: 6%[b]
R = CO$_2$Me, **18k**, Cu[d]: 95%, Ir[d]: 45%, no cat.[d]: 20%
R = CF$_3$, **18l**, Cu[e]: 85%, Ir[d]: 54%, no cat.[d]: 0%
R = F, **18m**, Cu: 80%, Ir: 61%, no cat.[d]: 16%
R = Cl, **18n**, Cu: 88%, Ir: 50%, no cat.: 44%
R = Br, **18o**, Cu: 81%, Ir: 37%, no cat.[d]: 23%

R = Cl, **18p**, Cu: 86%, Ir: 38%, no cat.: 30%[b], AIBN[c]: 40%[b]
R = OMe, **18q**, Cu: 96%, Ir: 52%, no cat.[d]: 0%

18r, Cu[d]: 83%, Ir[d]: 15%, no cat.[d]: 30%

18s, Cu: 60%, Ir: 19%, no cat.: 0%

18t, Cu: 35%, Ir: 41%[b], no cat.[d]: 0%

(a) Reaction conditions: 0.3 mmol 5**1**, 0.45 mmol **17a**, DCE abs. 6 mL (0.05 M). Reactions were irradiated using a 3W blue LED$_{455nm}$ for 6 h at room temperature. (b) Determined by ^{1}H-NMR using 2-nitropropane as internal standard. (c) 1 mol% AIBN, 80 °C, dark. (d) Prepared by L. Traub. Other reactions were prepared by C. Lankes. (e) Reactions were irradiated using a 3 W green LED (530 nm).

Figure 3: Substrate Scope for electron poor styrenes

Halogen substitution in *para*-position (**18m**- **18o**) resulted in very good yields for **[Cu]** catalysis (80-88%). Interestingly, yields for **[Ir]** increased again in comparison to strong electron withdrawing groups to good yields (37-61%). This trend repeated itself in radical-chain reactions, giving access to product **18m**-**18o** in low yields (16-44%).

While *meta*-chloro substitution **18p** led to very good yields for **[Cu]** (86%), yields for **[Ir]** and the radical-chain mechanism were comparable (38% and 30% respectively). This result was confirmed by an experiment with 1 mol% AIBN at 80 °C, which even surpassed the yield obtained with **[Ir]** (40%). This continued the tendency of AIBN experiments giving slightly

higher yields than experiments that rely solely on 455 nm irradiation. In contrast to **18p**, while *meta*-methoxy substituted derivative **18q** still produced almost quantitative yields with **[Cu]**, a significant difference in yields between **[Ir]** (52%) and radical-chain reactions (0%) was observed.

A heterocyclic ortho-vinyl pyridine **15r** afforded the desired product **18r** in 83% yield in a **[Cu]** catalyzed reaction. Noble metal photocatalysis and the uncatalyzed reaction only achieved low yields for this example. An extremely electron-poor pentafluoro styrene **15s** was still convertible by **[Cu]** to give rise to product **18s** in 60% yield. While radical-chain chemistry with this compound was no longer possible, **[Ir]** managed to give access to **18s** in 19% yield. In an effort to broaden the substrate scope from styrenes to more general alkenes, 1-octene was investigated as ideal substrate. **[Cu]** & **[Ir]** afforded product **18t** in 35% and 41% yield respectively. Radical-chain mechanisms failed to give rise to any isolatable product. With a sufficient scope of styrenes investigated for the three postulated mechanistic pathways, we set out to visualize the results in a more readily apparent way.

2.3.3 Visualization of Reaction Trends

Across the substrate scope a distinct difference in yields in-between applied catalysts is apparent, while the magnitude of these differences is dependent on the electronic properties of the substrate. Because such trends seem random at first glance, a quantifiable method of tracking these dependencies was desired. The Hammett substitution constant σ correlates the electronic properties of a substituent or substitution pattern in *para*- or *meta*-position to a numerical value. Hereby, electron donating substituents are negative, while electron withdrawing groups are given positive numerical values. These values are calculated by inserting kinetic rate constants and equilibrium constants in the Hammett equation.[100] These catalogued σ-values were plotted against the yields of each reaction (Figure 4).
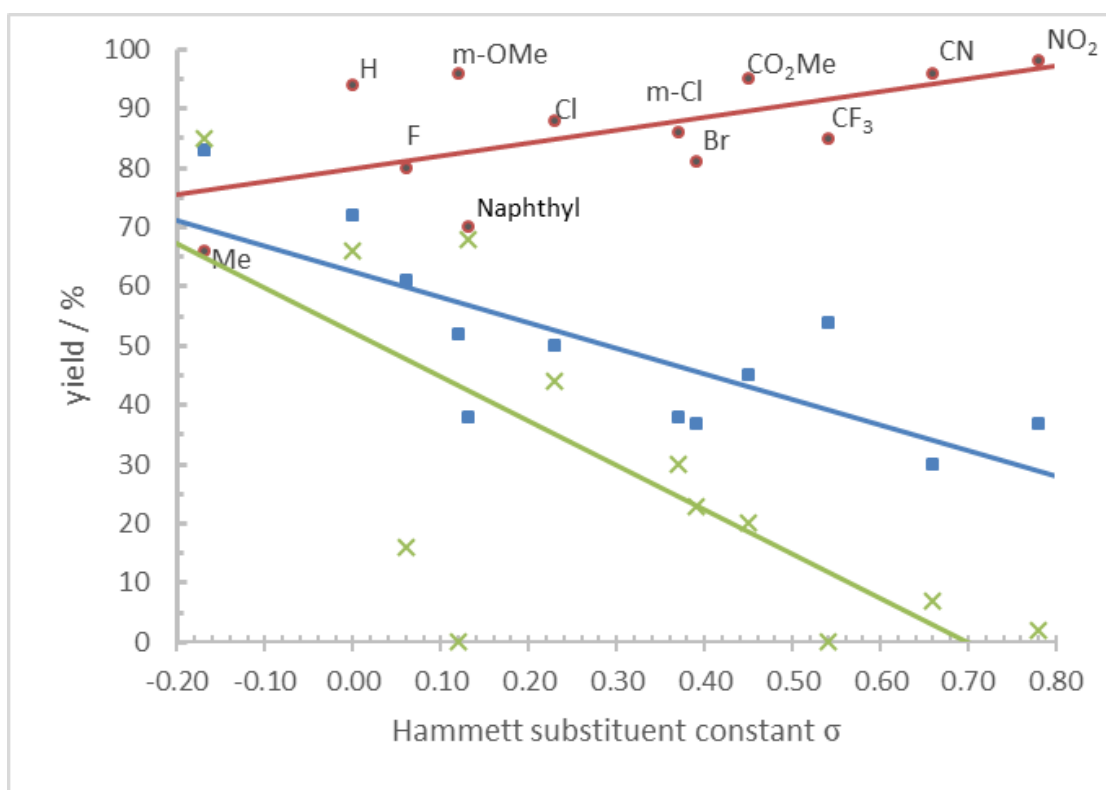
Figure 4: Visualization of electronic trends for each catalyst by plotting product yield against the corresponding Hammett substituent constant σ in a linear regression. Red corresponds to copper, blue to iridium and green to results with no catalyst. Substituents without a prefix are *para*-substituted.

This plot illustrates the different trends for each mechanism in dependence of the electronic properties of each substrate in a linear regression. While yields for reactions using **[Cu]** as catalyst (red line) increase the more electron withdrawing the substitution pattern becomes, both **[Ir]** (blue line) as catalyst and radical-chain mechanism (green line) fall of significantly with a rising Hammett constant σ. It is worth noting, that while the results for copper catalyzed ATRA reactions, as well as those for iridium catalysis, displayed low deviation from their trend-lines (visualized by straight lines in Figure 4), the results for the radical-chain mechanism had high deviancy. Overall, radical-chain reactions also had the biggest variations in yield during reproduction experiments *i.e.* their outcomes differed the most when experiments were repeated under the same conditions. This was rationalized by the high impact of secondary factors (*e.g.* batch of solvent, LED or quality of styrene used) on this reaction with a low concentration of active radicals driving the reaction. Overall **[Cu]** was demonstrated to be the most suitable catalyst for ATRA reactions by *N*-halo compounds, since every experiment but *para*-methyl styrene afforded a higher yield than either **[Ir]**- or radical-chain mechanisms.

2.3.4 Unsuccessful Substrates

During the span of this work, several attempts to further broaden the substrate scope for chloroaminations by ATRA mechanisms towards including more meaningful examples and other non-styrene unsaturated compounds have been made. However, the scope of chloroaminations by photocatalysis remains mostly limited to styrene derivatives **15**.
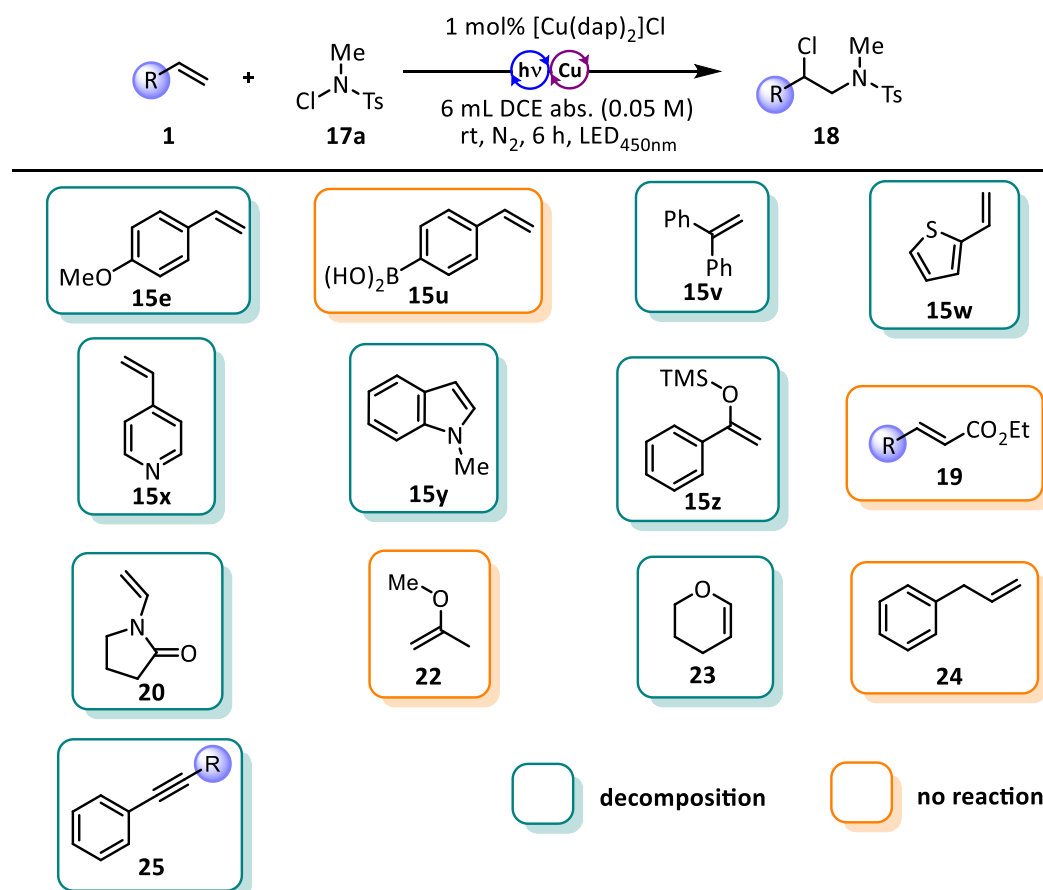
(a) Reaction conditions: 0.3 mmol **1**, 0.45 mmol **17a**, DCE abs. 6 mL (0.05 M). Reactions were irradiated using a 3W blue LED$_{455nm}$ for 6 h at room temperature.

Figure 5: Unsuccessful unsaturated compounds for the copper catalyzed chloroamination.

Para-methoxy styrene **15e** decomposed during the reaction, and **[Ir]** catalysis was only able to afford the hydrolyzed product **18c**. 4-Vinylphenylbornic acid **15u** as substrate for Suzuki couplings lead to quenching of the generated *N*-centered radicals to their corresponding N-H compounds with all three mechanisms. In a similar manner, α,β-unsaturated compounds (*e.g.* acrylic esters and cinnamates) failed to give product in significant amount. α-Aryl substituted styrene **15v**, vinyl amide **20**, and various heterocyclic compounds (**15w** to **15y**) resulted in

polymerization of the unsaturated starting materials. Analogous to this, vinyl ethers (**22** to **23**) did not yield their desired products. Notably, allylbenzene **24** led to no productive coupling between nitrogen-centered radical and alkene, while the un-activated alkene 1-octene **15t** was previously successful. Internal alkynes **25** led to complex mixtures in case of phenyl and methyl substitution.

2.3.4.1 Unactivated alkenes

Previous reports on copper photocatalyzed ATRA reactions of alkenes have elaborated on the difficulties of derivatizing such substrates *via* ATRA reactions. Reiser and co-workers demonstrated, that during the chlorosulfonylation of alkenes and alkynes a base is necessary to avoid catalyst poisoning during the reaction. However, the presence of a base was also necessary for the derivatization of 1-octene, which worked in our case, albeit with mediocre yields. This conundrum warranted further investigation into the chloroamination of allylbenzene.

Table 2: Screening for the chloroamination of allylbenzene.
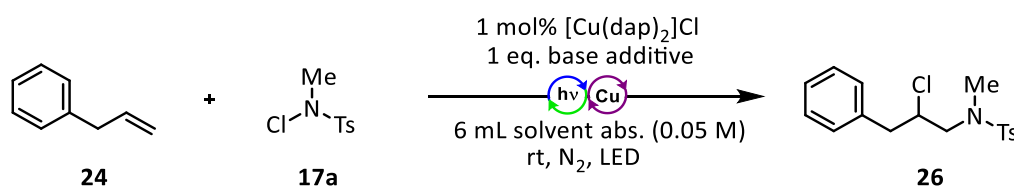
Entry	λ [nm]	solvent	time [h]	base	^{1}H-NMR yield
1	455	DCE	6	---	7%
2	455	DCE	34	---	7%
3	455	DCE	6	$NaHCO_3$	18%
4	455	DCE	34	$NaHCO_3$	19%
5	530	DCE	48	Na_2CO_3	20%
6	455	MeCN	48	---	20%
7	455	MeCN	6	$NaHCO_3$	12%
8	455	MeCN	48	$NaHCO_3$	9%
9	530	MeCN	48	$NaHCO_3$	22%
10	**530**	**MeCN**	**48**	**Na_2CO_3**	**30%**
11	530	*i*PrOH	6	Na_2CO_3	no rxn.[b]

(a) Reaction conditions: 0.3 mmol **24**, 0.45 mmol **17a**, DCE/MeCN abs. 6 mL (0.05 M). Reactions were irradiated using a 3 W LED at room temperature. (b) **2** completely decomposed to NHMeTs.

Nitrogen radicals in ATRA reactions: A holistic picture for three distinct ATRA mechanisms.

The effects of irradiation source, solvents, reaction time and base additive were investigated (Table 2). While prolonging reaction time seemed to have no significant effect on ^{1}H-NMR yield (entry 1 -4, 7 & 8), the addition of $NaHCO_3$ or Na_2CO_3 to DCE increased the yield to 18-20%. Switching between 455 nm to 530 nm irradiation had no obvious effect on reaction yield. For acetonitrile as solvent, adding a carbonate base while irradiating at 455 nm had a negative effect on the reaction yield. This problem could be avoided by using 530 nm irradiation, which led to the most optimal result of 30% yield. However, *iso*-propanol as solvent resulted in an immediate quenching of all nitrogen-centered radicals and quantitative formation of *N,4*-dimethylbenzenesulfonamide.

In conclusion, the screening towards the chloroamination of allylbenzene was unsuccessful. Two theories were formed to explain this: The possibility of creating a highly stabilized benzylic radical in an allylic position might be detrimental for this reaction, or the electronic properties of the *in situ* generated amidyl radical were unsuitable for condensation to unactivated alkenes. These two hypotheses were tested by using neohexene **27**, an unactivated, unsaturated compound without any allylic C-H bonds. Additionally, two more electronically distinguished *N*-halo compounds were tested in comparison to *N*-chloro-*N,4*-dimethylbenzenesulfonamide **17a**: The more electron-rich *N*-chloro piperidine **c** and the more electron-poor *N*-chloro saccharin **17b**.

	NCl reagent	result
	NClSaccharin **17b**	21% **28**
	NClPiperidin **17c**	decomposition
	NClSaccharin **17b**	decomposition
	NClPiperidin **17c**	decomposition
	NClMeTs **17a**	no reaction
	NClPiperidin **17c**	decomposition
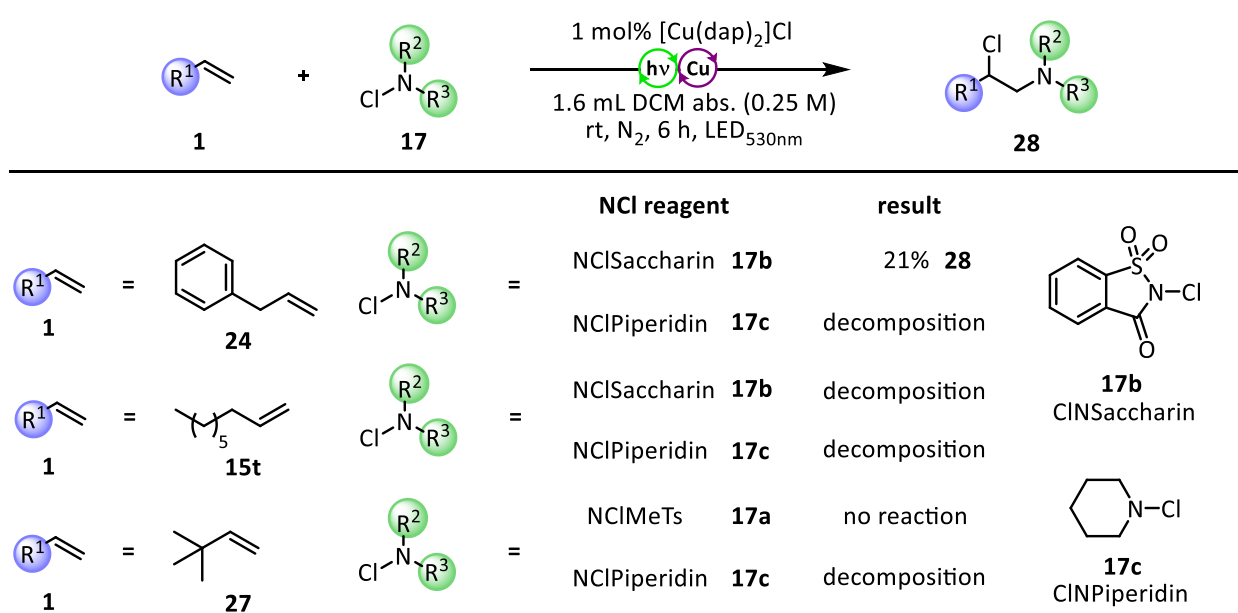
(a) Reaction conditions: 0.8 mmol alkene, 0.4 mmol **17**, DCM abs. 1.6 mL (0.25 M). Reactions were irradiated using a 3 W green LED$_{530nm}$ for 16 h at room temperature.

Figure 6: Screening of various alkenes and nitrogen radical precursors.

In all reactions with the more electron-rich *N*-chloro piperidine **17c** a decomposition of the reaction mixture was observed. Generally, only electron-poor *N*-chloro reagents are stable enough for storage, and **17c** already decomposed upon prolonged storage (several hours) at room temperature. An inversion in reactivity for allylbenzene **24** and 1-octene **15t** towards ATRA with *N*-chloro saccharin **17b** in comparison to *N*-chloro-*N,4*-dimethylbenzenesulfonamide **17a** was observed. While product **28** could be successfully isolated in 21% yield, no product from 1-octene was observed. A test reaction between neohexene **27** and *N*-chloro-*N,4*-dimethylbenzenesulfonamide **17a** only led to the re-isolation of decomposed starting material.

Concluding, the copper photocatalyzed ATRA reaction between common *N*-chloro compounds and unactivated alkenes was deemed unfeasible. Whether this is due to catalyst poisoning during the reaction, or due to a more fundamental problem with this reaction remains unknown at this point.

2.4 Upscaling and Applications

To increase the applicability and demonstrate the synthetic usefulness of this reaction, several derivatizations of the obtained product were performed. This included up-scaling of the initial reaction to demonstrate scalability and to gain access to sufficient amount of material for derivatizations.

2.4.1 Upscaling
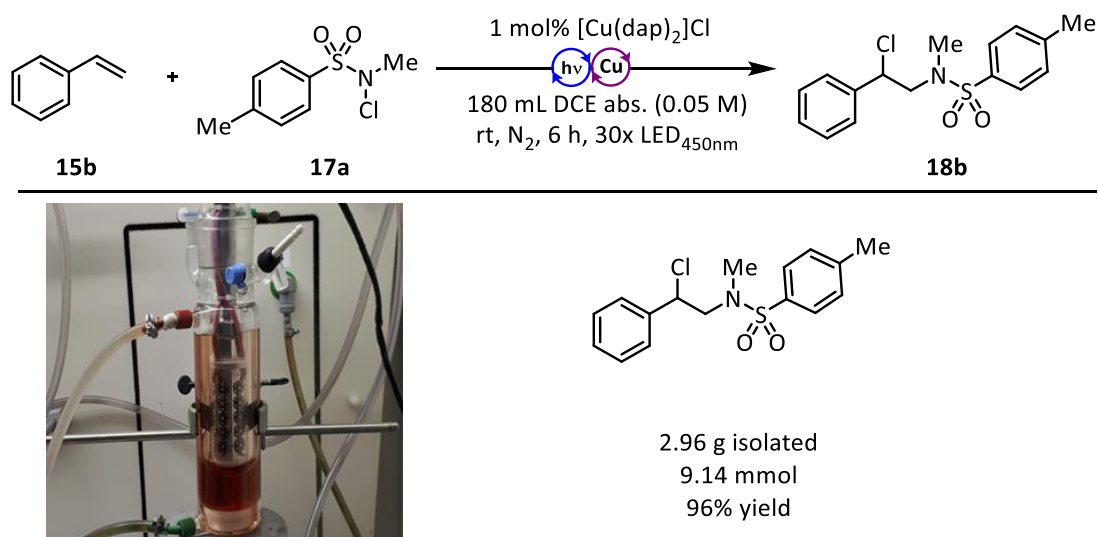
Figure 7: Reaction setup for a multi-gram scale batch reaction.

A batch irradiation reaction setup was chosen for this reaction. The total amount of solvent in the reactor amounted to 190 mL. Irradiation was achieved by thirty 455 nm 3 W LEDs in a water-cooled glass finger. The outer mantle of the reaction vessel was also water-cooled, providing reaction temperature at room temperature despite the 90 W of irradiation power. A glass connector bridge (not visible) from the bottom to the top of the vessel ensured vertical convection of the reaction mixture by a disc magnetic stirrer. Product **18b** could be isolated in 96% yield after chromatography, marking a minuscule increase in yield by 2% compared to the small-scale reaction setup.

2.4.2 Derivatization and Applications

Having synthesized a sufficient amount of starting material, investigations into derivatization reactions for product **18b** began. Three reactions were tested: Elimination towards vinylic amides, formation of a Grignard reagent and subsequent coupling to an electrophile thereafter as well as the reaction with a Grignard reagent *via* a Kumada coupling.
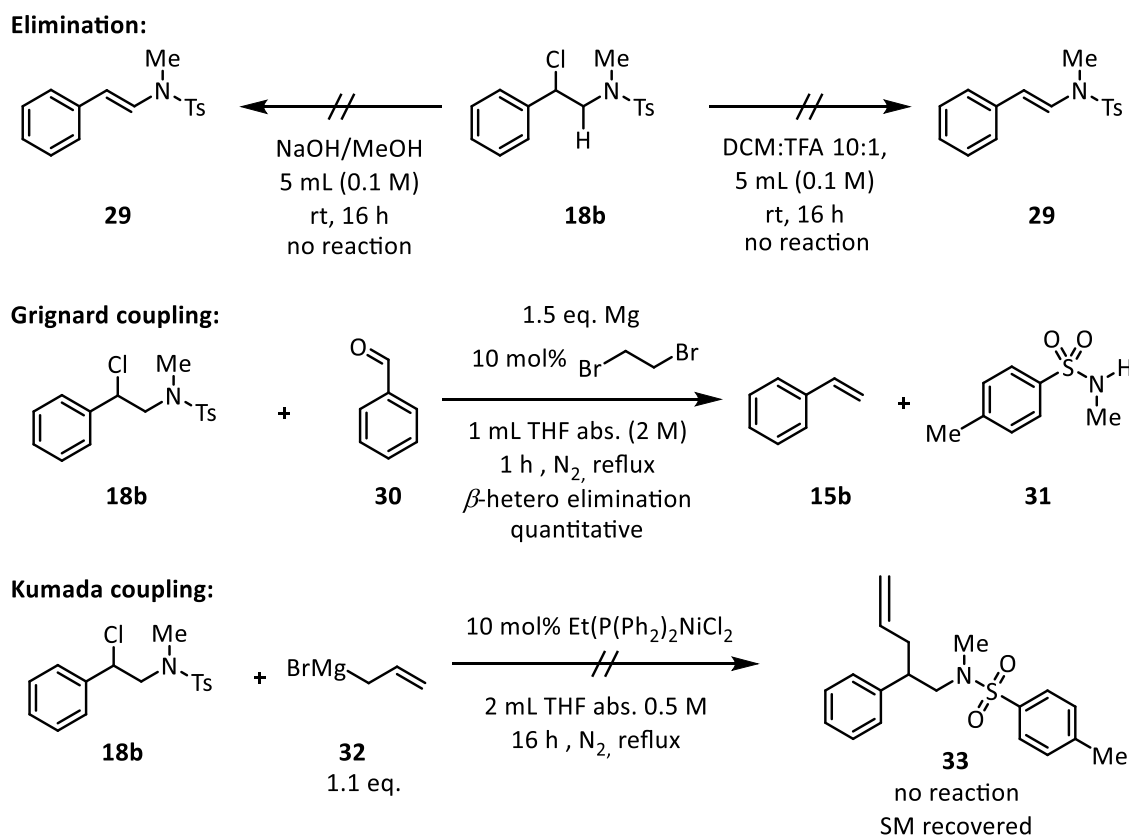
Scheme 24: Derivatization attempts using chloroamination product **18b**.

Contrary to our initial expectations, elimination of the benzylic chlorine atom was not possible (Scheme 24). Neither strongly acidic, nor strongly basic reaction conditions at room temperature led to elimination. In all cases, the vast majority of **18b** was re-isolated after the reaction. In a similar vein, most tests conducted towards Grignard reactions of **18b** led to no reaction with benzaldehyde **30**. However, once reaction conditions were forcing enough to facilitate the formation of a Grignard reagent *β*-hetero elimination occurred, ultimately yielding styrene **15b** and *N,4*-dimethylbenzenesulfonamide **31** in quantitative amounts. Therefore, this was effectively the *retro*-reaction of the chloroamination. Using a Ni(II) catalyst for oxidative insertion into the benzylic C-Cl bond followed by a transmetallation from a

Grignard reagent – a Kumada coupling – did not give access to the desired product **33**. After refluxing overnight with the Nickel catalyst, most of the starting material **18b** was re-isolated after chromatography. Surprisingly, the benzylic C-Cl bond of **18b** proved to be much more stable than initially anticipated. Turning our attention to different ways of derivatization, we studied modifications to the photocatalytic protocol in order to achieve derivatizations without the need of an extra reaction step (Scheme 25).
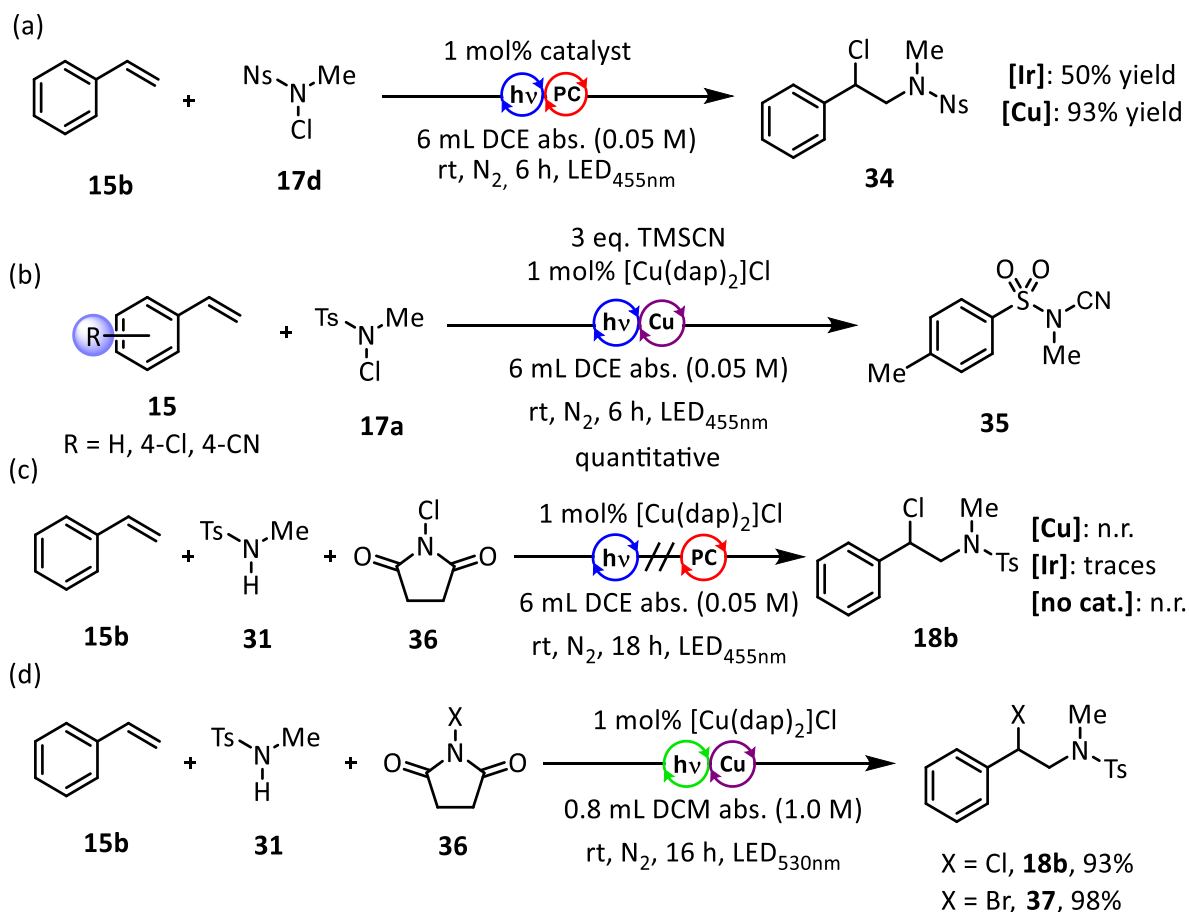
(a-c) Reaction conditions: 0.3 mmol **15b**, 0.45 mmol **17**, DCE abs. 6 mL (0.05 M). Reactions were irradiated using a 3W blue LED$_{455nm}$ for 6 h at room temperature. (a) was prepared by C. Lankes (d) Reaction conditions: 1.6 mmol **15d**, 0.8 mmol **31**, 0.9 mmol **36**, DCM abs. 0.8 mL (1 M). Reactions were irradiated using a 3 W green LED$_{530nm}$ for 16 h at room temperature.

Scheme 25: Halo-amination with a Nosyl-group. (b) Attempted cyano-amination using TMSCN as ligand exchange reagent. (c&d) *In situ* generation of *N*-Halo compounds towards halo-aminations.

Starting with the tosylate protecting group, we investigated whether different protecting groups are tolerated in this reaction (Scheme 25, a). The easier to remove nosylate protecting group was well tolerated by **[Cu]**, yielding product **34** in 93%, compared to the 94% yield achieved under standard conditions (Figure 2). Notably, the **[Ir]** catalyst did not tolerate the nosyl group as well, dropping from 74% (Figure 2) to 50% yield.

Nitrogen radicals in ATRA reactions: A holistic picture for three distinct ATRA mechanisms.

Recent literature demonstrated the possibility of TMSCN to partake in ATRA type reactions by transmetallating onto an inner-shell complex between a copper catalyst and an benzylic radical to achieve a formal substitution of the chlorine atom by a cyano-group.[93] However, test reactions of three styrene derivatives with rising electron deficiency only afforded the *N*-cyanated starting material next to styrene **15b**. The reaction between starting material **31** and TMSCN was determined to be too fast to enable any productive ATRA reactions with unsaturated compounds.

Lastly, the *in situ* formation of *N*-halo compounds and their subsequent ATRA reactions was investigated in order to increase the operational ease of our protocol. Initial test under standard conditions with **31** and 1.1 eq. **36** did not give rise to product **18b** under all conditions tested. However, when employing the conditions described in chapter 2.5.1 the chlorination of *N,4*-dimethylbenzenesulfonamide **31** by 1.1 eq. *N*-halo succinimide **36** and addition to **15b** yielded the corresponding product **18b/37** in 93% (X = Cl) or 96% (X = Br) yield. This demonstrated, that amides can be used directly as starting materials in this photoreaction without prior formation and isolation of the *N*-halogenated compounds.

2.5 Product distinction by Inner-Sphere Mechanism

Compelling evidence for the presence of three distinct ATRA mechanisms by elucidating their differing electronic substrate dependencies has been provided. However, we wanted to further establish the inner-shell mechanism as dominant pathway for **[Cu]** catalyzed ATRA reactions. To this end a mechanistic distinction by product selectivity was developed.
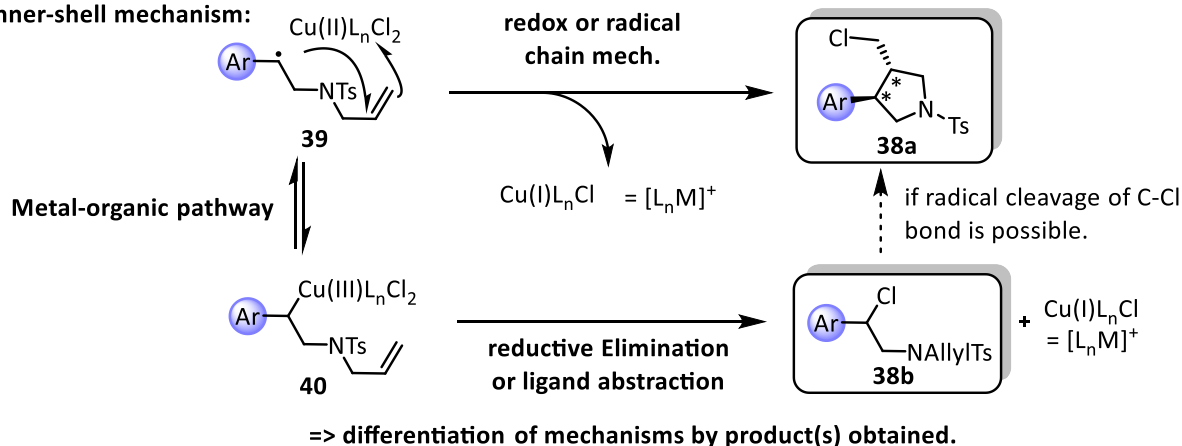
Scheme 26: Proposed influence of copper on radical cascade cyclizations.

S. V. Ley and co-workers demonstrated that activation of the *in situ* formed *N*-allyl-*N*-chloro-4-methylbenzenesulfonamide **17e** by [Ir(*d*F(CF$_3$)ppy)$_2$(dtbbpy)]PF$_6$ (**[Ir-F]**) will lead to a radical cascade reaction ultimately forming pyrrolidine **38a** in very good yield and a diastereomeric ratio of approx.. 0.7:0.3 in all cases (Scheme 26).[101] We envisioned, that the proposed interaction of the **[Cu]** catalyst with the initially created benzylic radical **39** blocks a subsequent 5-exo-trig cyclization. Copper(III) intermediate **40** then proceeds to yield an open-chained product **38b** by either a reductive elimination or a ligand abstraction mechanism. Thus, a simple distinction between different products will lead to information about which mechanism is dominant in any given ATRA reaction with styrenes.

2.5.1 Reaction Screening

In order to achieve comparable results, **[Ir-F]**, **[Ir]** and **[Cu]** had to be tested under the same conditions. Noteworthily, while Ley *et al.* used a similar solvent, the *N*-allyl compound was chosen as limiting reagent. In contrast, this protocol used the more expensive styrene derivatives as limiting reagent so far. Furthermore, literature conditions proceeded under elevated temperatures (35 °C) instead of room temperature.

Table 3: Reaction screening for N-allyl-N-chloro-4-methylbenzenesulfonamide **$$**.

Entry	λ [nm]	Catalyst (1 mol%)	Yield 3[b]	Yield 4
1	455	[Ir(dF(CF₃)ppy)₂(bpy)](PF₆) 0.5 mol%	67%	0%
2	455	[Ir(ppy)₂(dtbbpy)](PF₆)	40%	7%
3	455	[Cu(dap)₂]Cl	23%	51%
4	455	no	7%[c]	0%
5	367	no	66%	2%

(a) Reaction conditions: 0.3 mmol **15b**, 0.45 mmol **17e,** DCE abs. 6 mL (0.05 M). Reactions were irradiated using a 3 W blue LED for 6 h at room temperature. (b) **38a** was obtained in a approx. 0.7:0.3 d.r. in all reactions. (c) determined by ¹H-NMR analysis against tetrachloroethane as internal standard.

Applying the reaction conditions previously used with the **[Ir-F]** catalyst in 0.5 mol% catalyst loading lowered the yield from Leys' conditions (86%) to 67% for the cyclized product **$$** with no open-chained product observed. **[Ir]** achieved a combined yield of 47%, split between **38a** and the open-chained product **38b** in a 5.7:1 ratio. As expected, product selectivity inverted for **[Cu]** catalysis and a combined isolated yield of 74% with 1:2.2 product selectivity was obtained. Curiously, blue light irradiation alone was not enough to facilitate a radical-chain reaction, and only small amounts of cyclized product **38a** were detected. However, switching to 390 nm LED irradiation was sufficient to drive this radical-chain reaction and 66% product **38a** were obtained. To confirm that this switch in product selectivity is not an isolated case for styrene, two more substrates with differing electronic properties were tested (Figure 8).

38b
[Ir]: 40% **38a**, 7% **89a**.
[Cu] 23% **38a**, 51% **38a** .

39b
[Ir]: 77% **39a**, 10% **39b**.
[Cu] 12% **39a** 46% **39b** .

40b
[Ir]: 33% **40a**, 4% **40c**.
[Cu] 0% **40c** 43% **40c** .
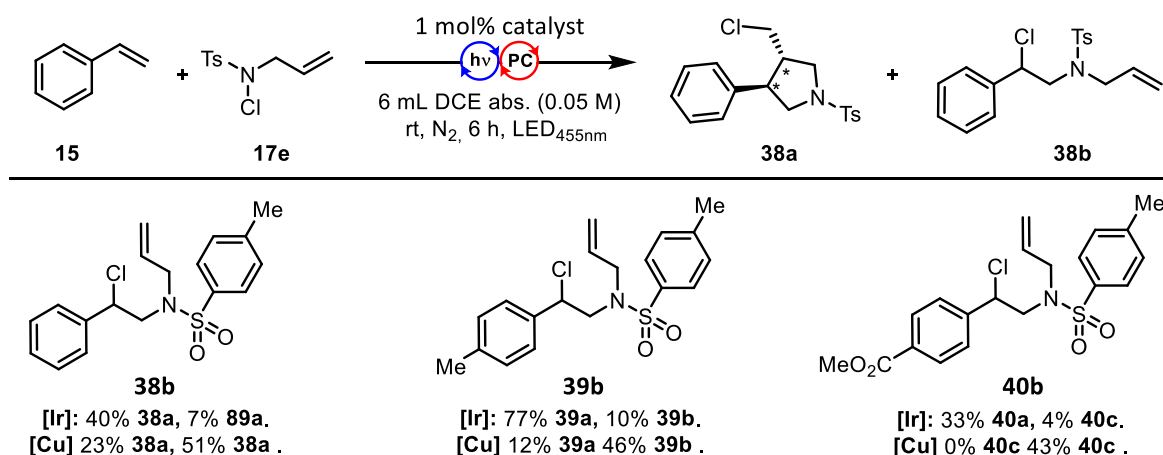
(a) Reaction conditions: 0.3 mmol **1**, 0.45 mmol **2**, DCE abs. 6 mL (0.05 M). Reactions were irradiated using a 3W blue LED$_{455nm}$ for 6 h at room temperature. Products **3** had an d.r. of approx.: 0.7:0.3 in all cases.

Figure 8: Screening of the electronic influence in three different styrene derivatives

As already demonstrated in the styrene substrate scope (Figure 3), yield for **[Ir]** catalysis decreased for styrenes. Methyl substituted styrene **15a** led to an good overall yield of 87% in a 7.7:1 product ratio, while for electron-poor derivative **15k** overall yield decreased to 37% in a 8.3:1 ratio towards the cyclized product **40a** for **[Ir]**. **[Cu]** catalysis led to selectivity towards the open-chained products **38b-40b**. Contrary to our expectations, overall yield decreased with more electron negative derivatives from 74% overall yield for **38a/38b** to 43% for **40c/40c**. However, product selectivity increased from 2.2:1 to a selective reaction, respectively. This was in line with our observation, that inner-shell mechanisms involving copper intermediates are more favored with increasing electron deficiency of the substrate. This led to the rationalization, that a radical-chain pathway – initiated by blue light irradiation – is operating in parallel to the inner-shell mechanism, ultimately leading to cyclized products **38a** and **39a**.

To confirm this hypothesis, we screened several different reaction parameters. While green light (530 nm) irradiation is still able to catalyze reaction with **[Cu]** (Table 4, entry 2), the yield for open-chained product **38a** decreased to 44% and no more cyclized product **38b** was observed. Thus, we set out to find reaction parameters more favorable towards inner-shell ATRA reactions by copper catalysis by increasing the yield of this reaction.

Nitrogen radicals in ATRA reactions: A holistic picture for three distinct ATRA mechanisms.

Table 4: Reaction optimization for NClAllylTs.
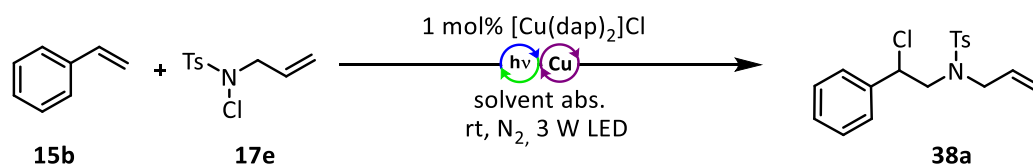
Entry	Solvent	Irradiation time	λ [nm]	Yield 38a[b]
1[c]	DCE (0.05 M)	6 h	455	51% **38a**, 23% **38b**
2[c]	DCE (0.05 M)	6 h	530	44%
3	DCE (0.05 M)	6 h	530	53%
4	DCE (0.25 M)	6 h	530	66%
5	DCM (0.25 M)	6 h	530	75%
6	$CF_3C_6H_5$ (0.25 M)	16 h	530	60%
7	DCM (0.5)	6 h	530	80% (57%)
8	**DCM (1 M)**	**16 h**	**530**	**88% (73%)**
9[d]	DCM (1 M)	16 h	530	100% (94%)

(a) Reaction conditions: 2 eq. **15b**, 1 eq. **17e**. Reactions were irradiated using a 3 W green LED$_{530nm}$ at room temperature. (b) ^{1}H-NMR yield *vs.* tetrachloroethane as internal standard. Isolated yield in parenthesis. (c) Stoichiometry: 1 eq. **15b**, 1.5 eq. **17e**. (d) Control reaction with NClMeTs **17a** instead of **17e**. Product **18b** isolated.

A direct comparison between blue (455 nm) and green (530 nm) light irradiation (entry 2) led to a decrease in overall yield to 44%, albeit in perfect product selectivity towards open-chained product **38a**. This established that green light is able to establish the copper catalyzed inner-shell mechanism as the dominant pathway in this reaction. However, the mediocre yield of 44% hinted towards efficiency problems within our initial protocol towards the productive coupling of nitrogen radicals to unsaturated bonds. Switching the reaction stoichiometry to conditions initially employed in the work of S. V. Ley and co-workers (2 eq. styrene, 1 eq. *N*-chloro compound) led to an increase in yield for open-chained product **38a**. Reaction time was increased to 16 hours to allow for full conversion under the more benign green light irradiation. A comparison of three different solvents at a 0.25 mol/L concentration demonstrated, dichloromethane as most optimal solvent with 75% yield by ^{1}H-NMR analysis. While structurally very similar to Dichloroethane (DCE), DCM is less toxic and easier to handle than DCE. Trifluorotoluol was chosen as potential solvent because it does not contain C-H bonds readily cleaved by the generated nitrogen radical through HAT abstraction mechanism.

Increasing the concentration to 1 M achieved the best result with an 73% isolated yield for **38a**. A control reaction with *N*-chloro-*N*,4-dimethylbenzenesulfonamide **17a** and the optimized conditions gave product **18b** in 94% yield

2.6 Substrate Scope – Improved conditions

Having established the optimal reaction conditions for inner-shell mechanism involving the **[Cu]** photocatalyst, we decided to reinvestigate substrates that only achieved mediocre yields for **[Cu]** catalysis. We expected to see an improvement for every example utilizing the optimized conditions to favor the inner shell mechanism. However, this means that the result obtained can no longer be directly compared with the previously established experiments on **[Ir]** catalysis. Nevertheless, the outcomes of these reactions can be directly compared to the yields obtained by the initial reaction protocol.

Figure 9: Selected substrates subjected to optimized conditions.
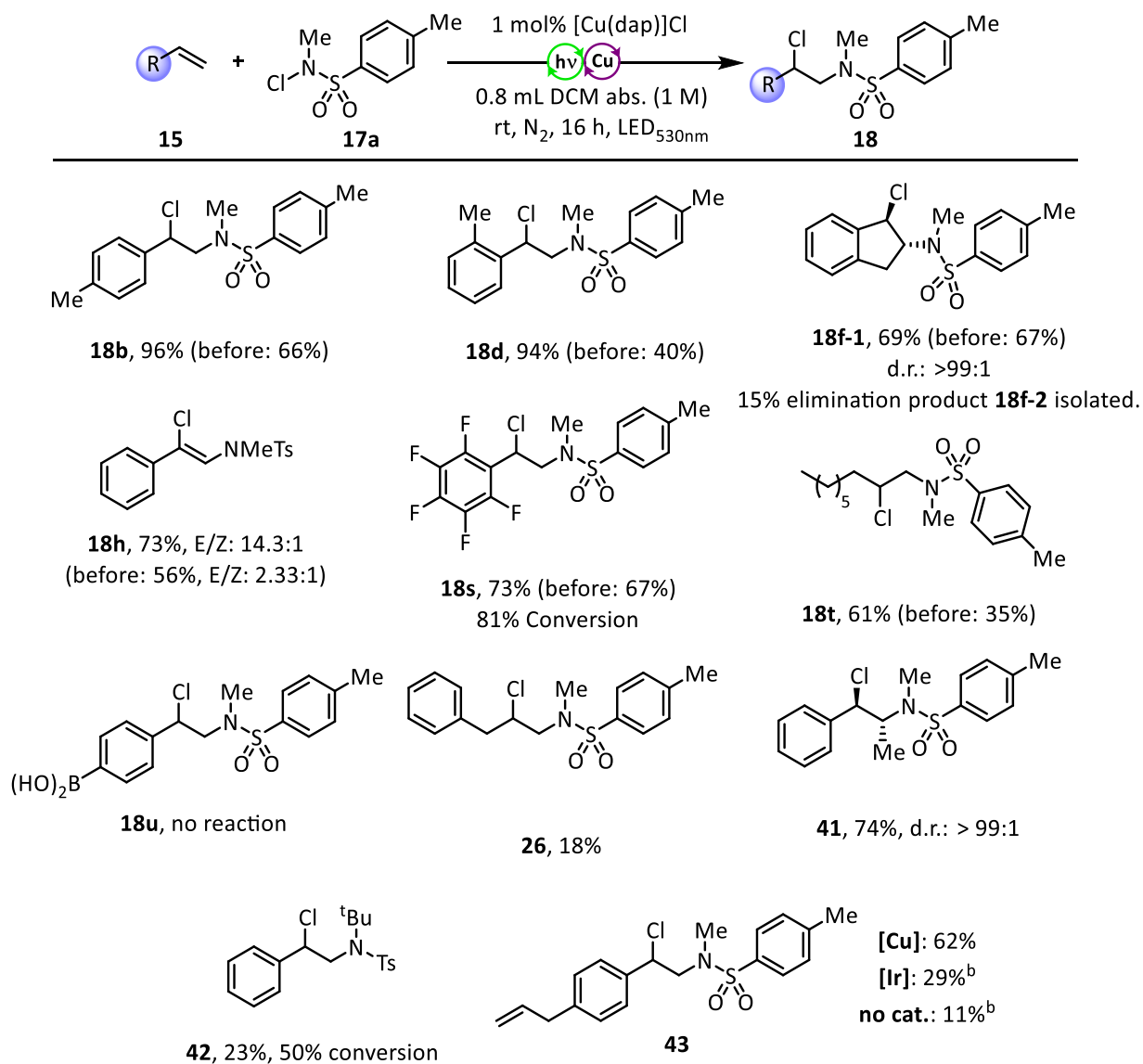
(a) Reaction conditions: Reaction conditions: 1.6 mmol **15**, 0.8 mmol **17b**, DCM abs. 0.8 mL (1 M). Reactions were irradiated using a 3 W green LED$_{530nm}$ for 16 h at room temperature. (b) 0.3 mmol alkene, 0.45 mmol **17b**, DCE abs. 6 mL (0.05 M). Reactions were irradiated using a 3W blue LED$_{455nm}$ for 6 h at room temperature

In agreement with our hypothesis, the new reaction protocol led to an improvement in yield for almost all substrates, while some new substrates were also accessible. 1-octene gave access to product **18t** in 61% yield. Both *ortho*- and *para*-methyl substituted styrenes **15b** & **15d** showed a dramatic increase in yield to almost quantitative levels. While the improvement in case of indene **15f** was miniscule (69%), the product **18f** was obtained in an enantioselective fashion and 15% of the unsaturated elimination product **44** could be isolated for the first time. Similarly, β-methyl styrene led to the enantioselective formation of **41** in 74%, demonstrating the *trans*-selectivity for this reaction. Curiously, **18h** was obtained in a 14.3:1 *E/Z* mixture in 73% yield, marking an improvement in diastereomeric selectivity from 2.3:1 *E/Z* ratio from the

previous reaction protocol for both the **[Cu]** reaction and the radical-chain mechanism (Figure 2). Pentafluoro derivative **18s** was obtained in 73% yield. However, only 81% conversion of the *N*-chloro reagent **17a** was observed, hinting towards a side reaction poisoning the catalyst. We were successful in demonstrating the chemo selectivity of this reaction with 4-vinyl styrene. **43** was obtained in 69% yield in case of **[Cu]**, whereas **[Ir]** and radical-chain reaction only afforded **43** in 29% and 11% yield respectively, using the initial reaction protocol with inverted stoichiometry (Table 2). When only allylbenzene **24** is added to the reaction mixture, ATRA product **26** was isolatable in 18% yield. This demonstrated, that this chemo selectivity is not purely achieved through reaction kinetics, but also through the unfavorable coupling to unactivated alkenes. Sterically hindered substituents on the nitrogen group, such as a *tert*-butyl group, inhibited the N-Cl bond cleavage and subsequently only gave 23% isolated yield with 50% conversion of the *N*-(*tert*-butyl)-*N*-chloro-4-methylbenzenesulfonamide reagent after 16 hours. Boronic acid derivative **15u** was still inaccessible by the improved protocol, leading to decomposition of *N*-Cl starting material **17a**. Evaluation of this substrate scope demonstrates that conditions tailored towards inner-shell copper intermediates improve reaction efficiency significantly. These promising results initiated further research into the previously unsuccessful chloroamination of unactivated alkenes.
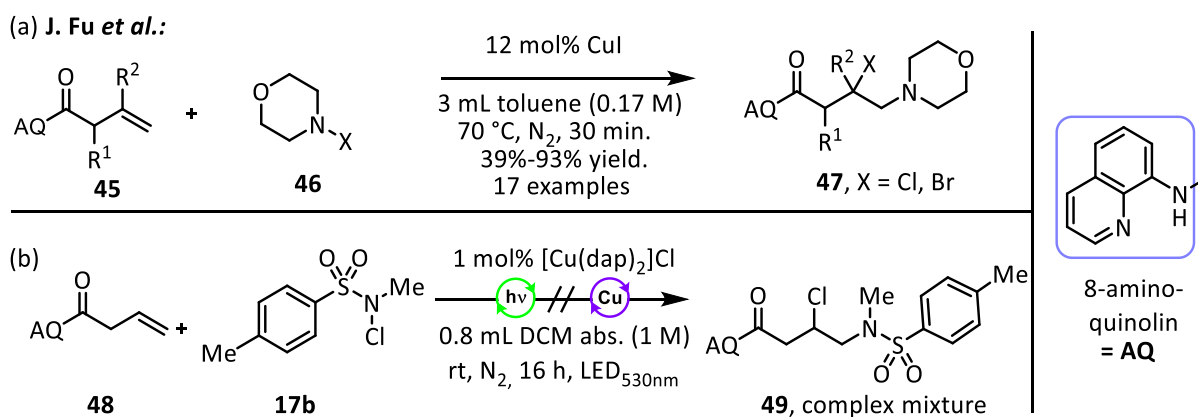
Scheme 27: Copper catalyzed functionalization of unactivated alkenes with an 8-aminoquinoline handle.

The group of Fu and co-workers demonstrated the use of an 8-aminochinoline handle to facilitate the coordination of a copper-ion in the vicinity of an unsaturated bond.[102] This coordination activated the double bond and enabled a halo-amination of β,γ-unsaturated amides **45** by *N*-halo morpholine **46** in good yields, which was not possible without the 8-aminoquinoline handle (Scheme 27, a). Following this strategy, the chloroamination of

unactivated alkene **48** by the previously optimized conditions was attempted. However, only a complex mixture of several products could be isolated, among them several derivatives of **48** with a chlorinated 8-aminochinoline auxiliary and an intact alkene group. This problem could be potentially solved by adding an additional copper salt to this reaction to saturate the auxiliary ligand with copper ions before initiating the ATRA reaction (Scheme 27, b). In order to determine the effect of intramolecular nucleophiles on the copper-based inner-shell transition state between benzylic radical **7** and a copper (II) complex, a chlorinated *N*-tosyl-*N*-chloro valinol **17f** was synthesized (Scheme 28).
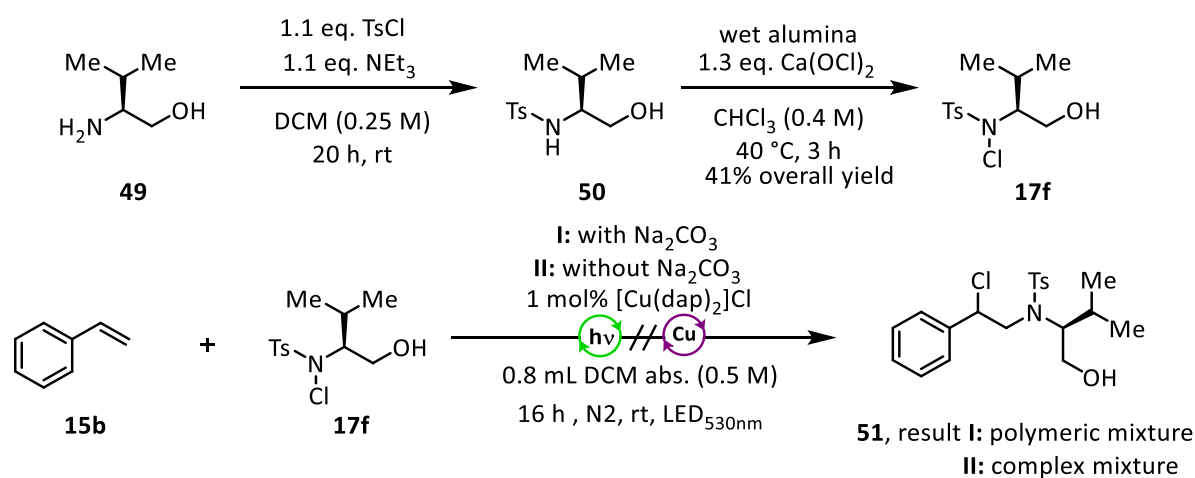
Scheme 28: **[Cu]**-catalyzed reaction between styrene **15b** and nitrogen radical precursor **17f**.

However, the nitrogen radical precursor (*S*)-*N*-chloro-*N*-(1-hydroxy-3-methylbutan-2-yl)-4-methylbenzenesulfonamide **17f** failed to achieve an efficient coupling between the generated *N*-centered radical and styrene **17b**. Neither product **51**, nor a morpholine derivative resulting from an attack of the alcohol on the benzylic position could be isolated from this reaction. In presence of a sodium carbonate base a polymeric mixture was obtained, while the absence of base led to a complex mixture of various different products.

Turning our attention to the effect of optimized conditions for inner-shell mechanisms on the *in situ* generation of *N*-halo compounds, NBS **36b** was investigated as halogenating agents (Scheme 29, a). The addition of 1.1 eq. *N*-halo succinimide **53** to *N*-allyl-4-methylbenzenesulfonamide **52** yielded the corresponding product **54b** in 82% yield. This demonstrated, that amides can be used directly as starting materials in this photoreaction without prior formation and isolation of the *N*-halogenated compounds.

Nitrogen radicals in ATRA reactions: A holistic picture for three distinct ATRA mechanisms.

Scheme 29: (a) *In situ generation of N-halo-N-allyl compounds. (b)Investigations into the chemoselectivity of bromo-aminations under varying conditions.*
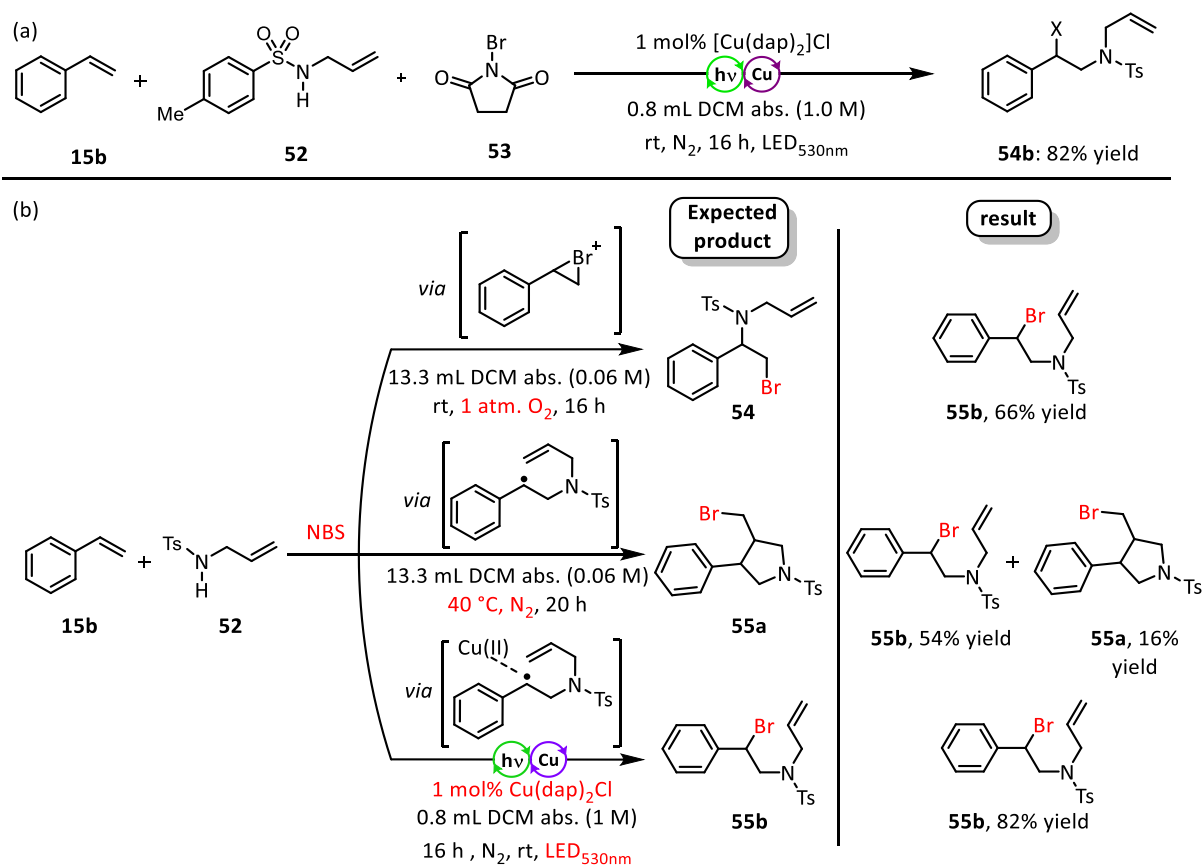
After the initial promising result of NBS **53** in the *in situ* bromo-amination of styrene (Scheme 25, d), the chemoselectivity of this reaction using *N*-radical precursor **52** was investigated. The group of Yu demonstrated the chemoselectivity control of bromo-aminations using tosylamide and NBS under two different metal-free conditions: The first protocol achieved selectivity for β-bromo products *via* a bromonium intermediate under an oxygen atmosphere at room temperature, while the second selectively yielded α-bromo products *via* an ATRA reaction at slightly elevated temperatures.[103] This rationale was expanded to *N*-allyl-4-methylbenzenesulfonamide **52** (Scheme 29). Judging from previous result and the work of Yu, we expected the β-bromo product **54** from the reaction, proceeding *via* a bromonium ion at room temperature under an oxygen atmosphere. Furthermore, the thermal reaction under elevated temperatures should yield the cyclized product **55a** in a radical-chain cascade, akin to the previous results (Table 3). In contrast to this, we hoped that copper photocatalysis might favor the open-chained product **55b** by an inner-shell mechanism. However, we found that the open-chained α-bromo product **55b** was favored in all three reaction conditions. The β-bromo product **54** could not be observed under an oxygen atmosphere, and elevated

temperature only led to 16% yield of the radical cascade product **55a**. These results were rationalized by a shift in kinetics towards shorter benzylic radical lifetimes, thus decreasing the chance for inner-shell mechanisms or 5-exo-trig cyclizations to occur. The high overall yields are due to more efficient radical-chain initiation caused by the more labile N-Br bond.

2.7 Experiments with chiral ligands

Encouraged by the performance of the copper catalyzed inner-shell mechanism in comparison to radical-chain or ionic mechanism for the halo-amination ATRA reactions, we envisioned the possibility to induct chirality at the benzylic position after reductive elimination or ligand abstraction, if a chiral ligand sphere at the metal-center is present. To achieve this enantioselective chloro-amination of styrenes, our investigations included five different chiral ligands. Three of which belong to the family of chiral bisoxazoline ligands, one chiral phosphine ligand and one chiral phosphoric acid (Figure 10). Concentration was lowered to 0.25 mol/L to allow for a homogeneous reaction solution. Additionally, 5 mol% copper salt and a slight excess of 6 mol% chiral ligand were added to ensure complete complexation of copper ions by at least one chiral ligand. To keep the choice of alkene consistent, styrene was chosen as substrate in favor of a more electron deficient styrene derivative to preserve comparability with previous screening experiments (Table 4, entry 9)

Reaction scheme:

15b + 17a, 5 mol% Cu(I/II) source, 6 mol% chiral ligand, hν, 1.6 mL DCM abs. (0.25 M), rt, N_2, 16 h, LED$_{530nm}$ → 18b, via 56

57 Ph-BOX

Cu(I)Cl: 95% yield
$[a]^{20\,°C} = 0.47°$

Cu(II)Cl$_2$: 66% yield
$[a]^{20\,°C} = 0.36°$

Cu(II)Cl$_2$ (450nm): 66% yield
$[a]^{20\,°C} = 0.95°$

58 ^{i}Pr-BOX

Cu(II)Cl$_2$: 55% yield
$[a]^{20\,°C} = 0.42°$[b]

59 Indanyl-Aza-BOX

Cu(I)Cl: 46% yield
$[a]^{20\,°C} = -1.11°$

Cu(II)Cl$_2$: 85% yield
$[a]^{20\,°C} = 2.41°$[b]

60 (S)-BINAP

Cu(I)Cl: 49% yield
$[a]^{20\,°C} = 0.92°$

Cu(II)Cl$_2$: 58% yield
$[a]^{20\,°C} = 0.25°$

61

Cu(I)Cl: 55% yield
$[a]^{20\,°C} = 0.92°$

Cu(II)Cl$_2$: 58% yield
$[a]^{20\,°C} = 0.25°$
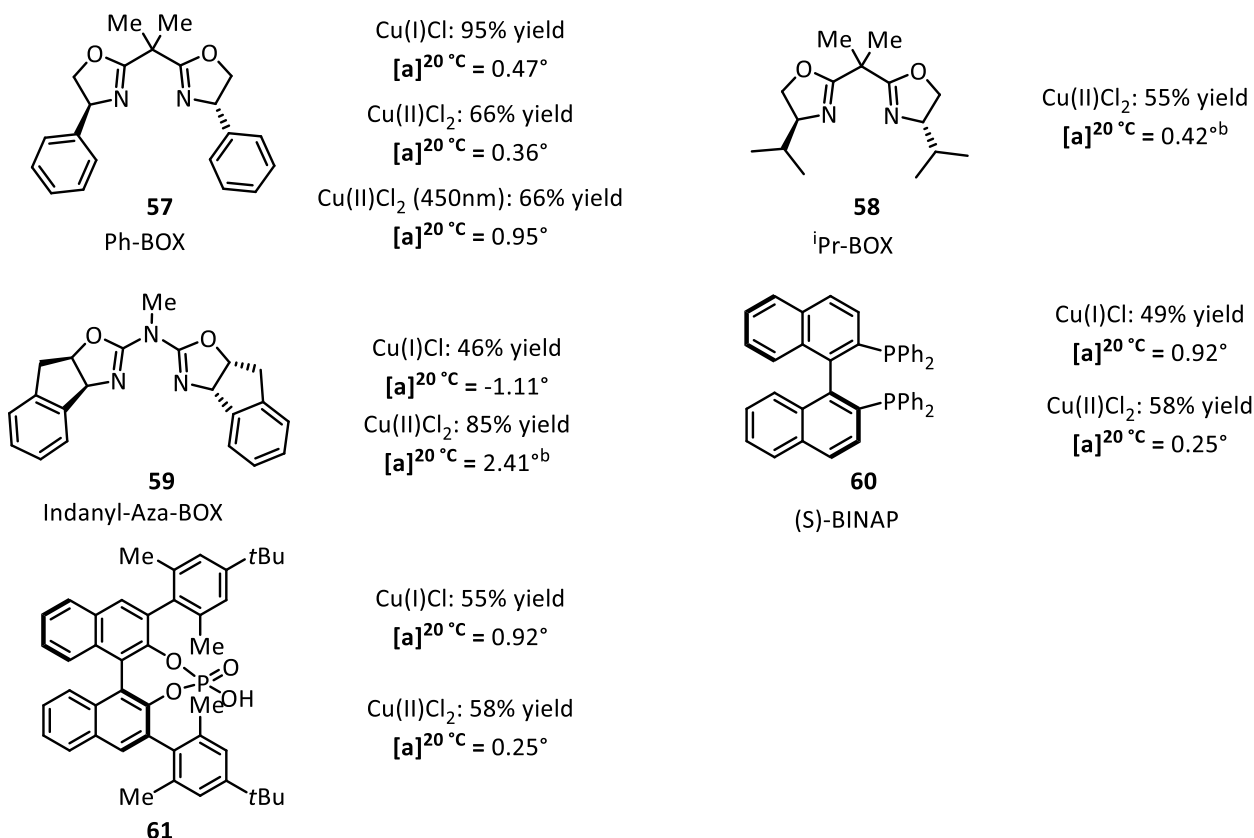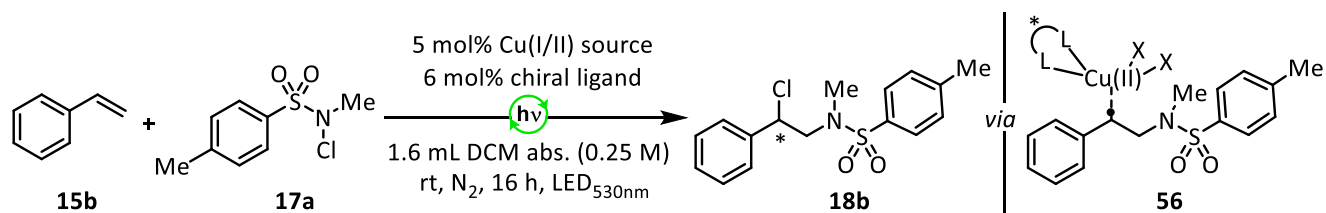
(a) Reaction conditions: 0.8 mmol **15b**, 0.4 mmol **17a**, DCM abs. 1.6 mL (0.25 M). Reactions were irradiated using a 3 W green LED$_{530nm}$ for 16 h at room temperature. (b) racemate confirmed by chiral HPLC.

Figure 10: Screening of various chiral ligands for asymmetric influence in the chloroamination of styrene.

The observation of moderate to good yields in all reactions suggest that any soluble copper (I/II) can catalyze this ATRA halo-amination reaction. This is notable, since this opens up the use of such Cu-salt/ligand mixture for investigations into other ATRA reactions. Bis (R)-phenyl oxazoline **57** (Ph-BOX) resulted in 95% yield when using Cu(I)Cl and 66% yield for both 455 and 530 nm irradiation when Cu(II)Cl$_2$ was used instead. However, measured optical rotation values were very low. A similar result was obtained with the structurally similar bis *iso*-propyl oxazoline ligand **58** (55%) and the reaction mixture was confirmed to be a racemate by chiral HPLC. Curiously, Indanyl-Aza-BOX ligand **59** was able to achieve 85% yield with Cu(II)Cl$_2$ and 54% yield with Cu(I)Cl, which marks an inversion in regard to the optimal Cu-ion source to the results obtained with Ph-BOX **57**. Despite the good yields, no reaction displayed potential for

chiral induction. Accordingly, both phosphorus based chiral ligands, (S)-BINAP **60** and chiral phosphoric acid **61**, gave access to product **18b** in mediocre yields (49%-58%) as a racemate regardless of copper source used. The implication of these results suggests, that an achiral ligand abstraction pathway is dominant in this reaction. This mechanism entails a direct attack from the benzylic radical **56** to a chloride ligand on the copper catalyst in favor of a copper(III) intermediate, subsequently followed by a reductive elimination. A possible way to remedy this issue is the use of electron-poor styrenes to favor the formation of a copper(III) intermediate over ligand abstraction processes. Alternatively, discouraging such abstraction processes by utilizing stronger Cu-F bonds,[104] formed by an initial cleavage of an *N*-F bond by photocatalytic means, is a viable option.

2.8 Mechanistic discussion

To investigate the mechanisms by which the three distinct ATRA pathways operate, we analyzed the radical-chain reaction. Mere irradiation by blue light led to high yields for electron-rich substrates without the addition of photocatalyst in a radical-chain reaction. Surprisingly, the UV-VIS absorption spectra of the substrates, products and reaction mixtures showed no significant absorbance in case of 4-methylstyrene (*cf.* chapter 7.2.3, Figure 27). Additionally, no change in absorption before/after degassing the reaction solution, or after irradiating for one or two hours with blue light could be observed. Thus, the formation of light absorbing donor-acceptor complexes under any conditions present during the reaction could not be detected. However, after two hours of irradiation 21% yield of product **18a** could be determined by ^{1}H-NMR spectroscopy. This has led to the conclusion, that 455 nm light can trigger the reaction. To investigate the cause of this behavior, the UV-VIS absorption spectra of *N*-Chlorosulfonamide **17a** at varying concentrations were analyzed (Figure 11).
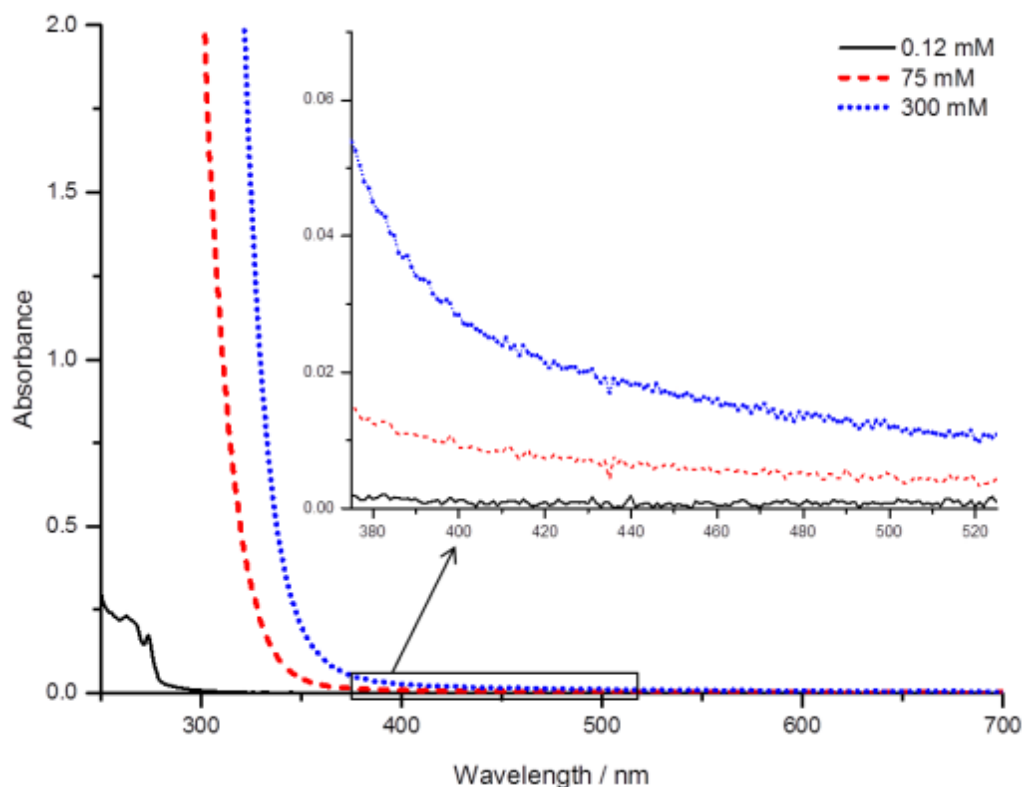
Figure 11: UV-Vis absorption spectra of *N*-Chlorosulfonamide **17a** at varying concentrations in DCE abs. Measurements performed by C. Lankes.

When increasing the concentration levels of the nitrogen radical precursor **17a** to levels similar to those present in the reaction mixture (75 mM) a small absorbance becomes apparent. Quadrupling the concentration of **17a** makes this absorbance band more evident. Considering the emission band of a LED_{455nm}, the overlap of light emission and **17a** absorption combined with the high light output power (3 W) achieved by internal irradiation seems to be sufficient to initiate a radical-chain reaction by homolytic cleavage of the labile N-Cl bond present in **17a**.

As part of an overarching goal to elucidate the varying reactivities of different styrenes depending on reaction conditions, the quantum yields of all three pathways were investigated (Table 5). We observed slower kinetics for the uncatalyzed reactions (entry 1, 4 & 6), so reaction time was increased to 6 hours in contrast to the catalyzed reactions, which were stopped after 1 hour to avoid saturation effects.

Table 5: Quantum yields for three selected substrates.
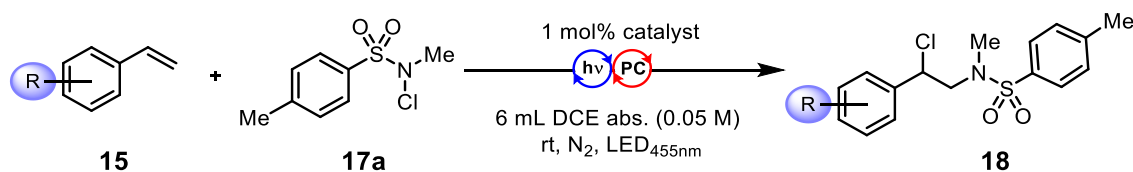
Entry	Product	catalyst	t [h]	^{1}H-NMR yield	Φ
1		no	6	30%	57%
2		[Ir]	1	39%	3%
3	18a	[Cu]	1	41%	3%
4		no	6	4%	2%
5		[Ir]	1	27%	2%
6	18l	[Cu]	1	34%	3%
7		no	6	---	---
8		[Ir]	1	9%	0.7%
9	18p	[Cu]	1	18%	1.4%

(a) Reaction conditions: 1 eq. **1**, 2 eq. **2**, DCE abs. (0.05 M). Reactions were irradiated using a blue LED$_{455nm}$ in a quantum yield apparatus at room temperature in a fluorescence cuvette. Reactions performed by C. Lankes.

It should be noted, that the quantum yield determination apparatus uses a different irradiation setup than the previously used internal irradiation setup, and that the light power within the quantum yield apparatus is significantly lower than in the standard reaction setup. This rationalizes the lower yield in entry 4 compared to standard conditions (44%). In general, quantum yield for catalyzed reactions were low (>> 1), pointing towards the absence of significant radical-chain processes. In consequence, catalytic pathways seem to be the dominant driving force in these reactions. In contrast, *para*-methyl styrene derivative **15a** displayed a comparatively high quantum yields of 0.57, a strong indication towards the presence of a dominant radical-chain pathway. Entry 7 failed to give any productive reaction, and no quantum yield could be calculated from this experiment. Nonetheless, the overall efficiency for catalyzed reactions is very poor and since only absorbed photons are considered for the calculation of the quantum yield, this points towards an unproductive deactivation pathway being present. The quantum yields for *para*-methyl and *para*-chloro derivatives **18a** and **18l** remained similar around 3%, while **[Ir]** declined to 2% quantum yield in case of **18l**.

Nitrogen radicals in ATRA reactions: A holistic picture for three distinct ATRA mechanisms.

This is in line with the lower yield for **18l** under **[Ir]** catalysis of 50% compared to 88% yield for **[Cu]**. *Para*-nitro styrene **15p** further highlights the advantage of **[Cu]** over **[Ir]** catalysis for electron-poor derivatives by achieving twice the quantum yield, albeit still being lower than for the other two derivatives.

Evaluation of preceding results led to the formulation of a comprehensive mechanistic picture of ATRA reactions for styrenes with varying electronic properties (Scheme 30). This reaction mechanism takes all three possible pathways into account and is thus compatible with previously established mechanisms.[58,105] The central intermediates in all three pathways are the *N*-centered radical of *N*-methyltosylamide **62** and the benzylic radical **63** resulting from condensation to a styrene derivative.
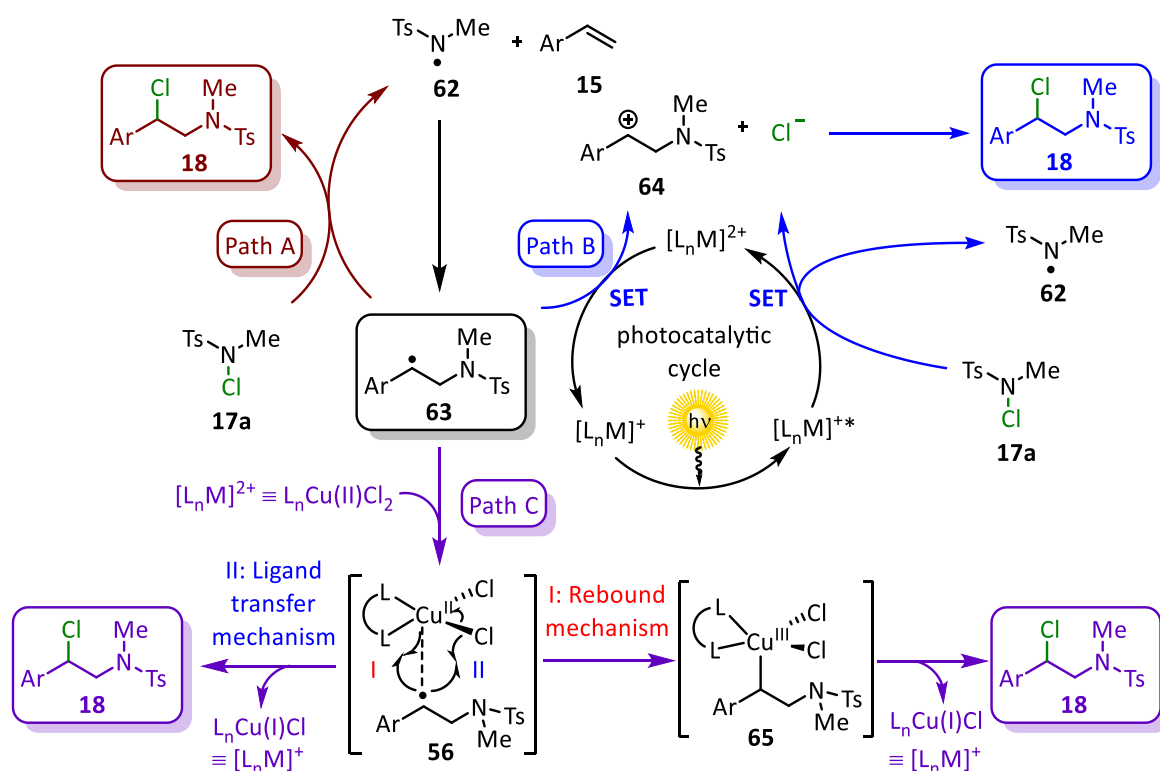
Scheme 30: Comprehensive mechanistic picture for the chloroaminations using *N*-chlorosulfonamide $$.

The initial *N*-centered radical **62** is generated either by homolytic cleavage, caused by absorption of near-UV photons, or by heterolytic cleavage after insertion of an electron into the σ*-orbital of the N-Cl bond of **17a** by an excited photocatalyst. After condensation to a styrene derivative **15**, benzylic radical **63** can react *via* three distinct mechanistic pathways (Scheme 30, path A, B & C): In the radical-chain pathway (Path A) radical **63** abstracts an chlorine atom from the *N*-chloro compound **17a**, leading to the desired product **18** and *N*-

centered radical **62**. This radical can proceed to react with the next unsaturated compound, continuing the chain reaction until all of precursor **17a** or styrene **15** are spent, or until all active radicals have terminated *via* chain termination mechanisms and no new radicals are formed by irradiation.

The introduction of a photoredox catalyst such as **[Ir]** favors a photoredox catalyzed pathway (Path B) as dominant reaction mechanism. This pathway is initiated by absorption of a photon in the VIS spectral region by the photocatalyst, accessing the excited $^3T_1$ triplet state. This triplet state reduces *N*-chloro-*N*-methylsulfonamide **17a** by inserting an electron into the σ^*-orbital of the N-Cl bond, oxidizing the catalyst in the process and subsequently causing heterolytic cleavage to the *N*-centered radical **62** and a chloride anion. After condensation to styrene derivative **15**, the long-lived benzylic radical **63** is oxidizable by $[L_nM]^{2+}$ upon collision and a second single electron transfer (SET) regenerates the catalyst in the ground state and results in benzylic cation **64**. Finally, **64** recombines with a chloride anion to give the desired product **18**.

Introducing metals with rapid ligand exchange capabilities such as copper into the reaction opens up the possibility of an inner-shell mechanism (Path C) involving the active participation of the metal atom in the radical mechanism. Initially, this path proceeds *via* the same mechanism as path B, however deviation occurs from the benzylic radical **63**. Instead of being oxidized by the photocatalyst to cation **64**, the open-shelled organic intermediate **63** interacts with another open-shell metal compound, *e.g.* a copper(II) complex, to form intermediate **56**, thus opening up two new mechanistic pathways: In a ligand transfer mechanism (II) the benzylic radical in **63** directly attacks a halide ligand, abstracting it and subsequently yielding the initial copper(I) complex as well as product **18**. This resulting copper(I) complex can then reenter the photocatalytic cycle to initiate the next catalytic cycle after photon absorption. The rebound mechanism (I) proceeds *via* the formation of copper(III) intermediate **65** by radical-radical coupling of both open-shelled structures, subsequently forming a metal-organic bond. This short-lived complex will react *via* a reductive elimination mechanism, giving access to product **18** and a copper(I) complex, thus closing the catalytic cycle.

Metal complexes such as **[Ir]** are characterized by very slow ligand exchange, making the metal atom inaccessible to inner-shell mechanisms. The difference in yields for electron-rich and electron-poor derivates in between **[Cu]** and **[Ir]** can be rationalized by the increasingly difficult oxidation of benzylic radical **63** to cation **64**, the more electron-poor the styrene derivative **15** is. Considering the *para*-cyanobenzene benzylic radical cannot be oxidized by **[Cu]** ($E_{1/2}(Cu^{2+}/Cu^{+})$ = + 0.62 V *vs.* 4- cyanobenzylradical: + 1.08 V)[106], yet is still converted to product **18** in very good yields, it is reasonable to assume that copper catalysis can proceed solely *via* path C for electron poor derivatives. While **[Ir]** is still able to oxidize electron-poor benzylic radicals ($E_{1/2}(Ir^{4+}/Ir^{3+})$ = + 1.21 V)[1], a drop in yield is observable for increasingly electronegative substituents (Figure 4). This suggests, that the oxidation to cation **64** becomes less feasible the more electron withdrawing the styrene substituents.

2.9 Conclusion

Investigations into the ATRA mechanism of halo-amination of various styrenes revealed three mechanisms at work (Scheme 31, a), depending on the reaction conditions: Radical-chain, photoredox and inner-shell mechanisms could be distinguished by adjusting the reaction conditions in suitable ways.
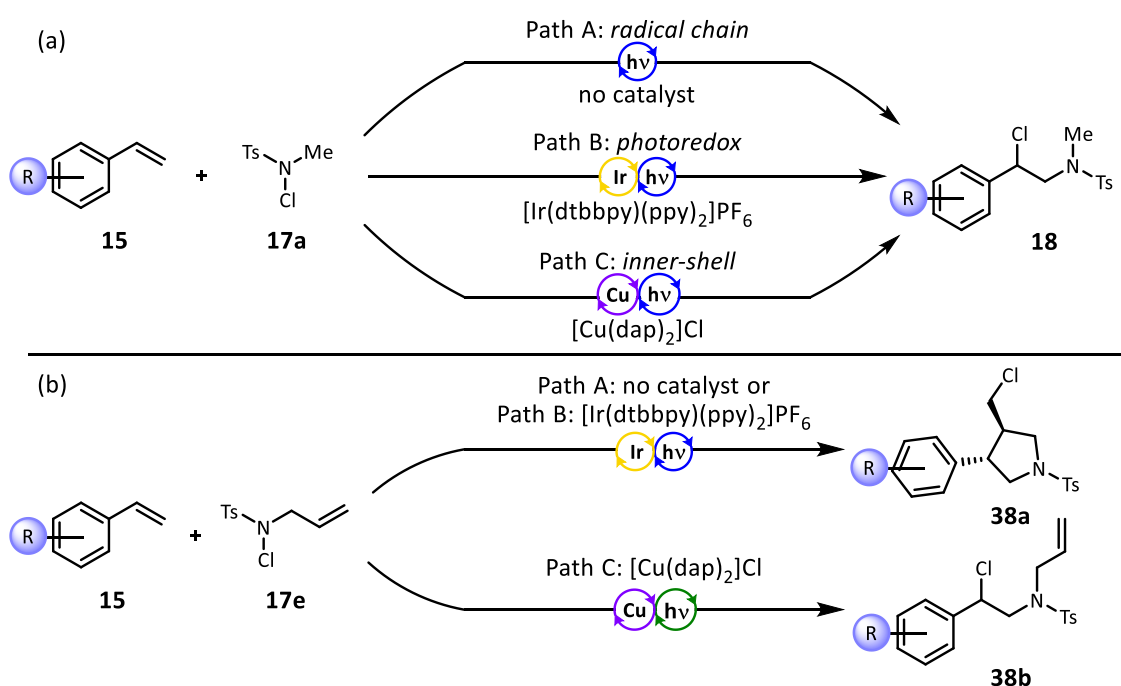
Scheme 31: (a) Three distinct ATRA mechanisms investigated in this work. (b) Varying product selectivity for different ATRA mechanisms.

Nitrogen radicals in ATRA reactions: A holistic picture for three distinct ATRA mechanisms.

The radical-chain mechanism could be established as dominant pathway in the absence of catalysts in the reaction solution, while irradiating with blue light. Another way to trigger this radical-chain reaction was to add 1 mol% of AIBN and stirring at 80 °C for 6 hours. While the radical-chain mechanism produced good results with electron-rich derivatives, yields dropped sharply when using electron-poor derivatives.

A photoredox mechanism is the dominant pathway when a photoredox catalyst with a stable ligand sphere, such as [Ir(dtbbpy)(ppy)$_2$]PF$_6$ is employed. Since ligand substitution reactions of 5d metals are slow, they do not allow for inner-shell mechanisms in the time-scales relevant to this reaction. Furthermore, the kinetics of this photo-catalyzed reaction were much faster compared to the radical-chain mechanism and yields for electron rich styrenes were high. However, similarly to the radical-chain mechanism, a drop in efficiency was observed when using electron-poor derivatives as substrates. However, this decrease in yield was less drastic compared to the radical-chain reaction.

In contrast to this, inner-shell mechanisms were enabled by using the copper-based photoredox catalyst [Cu(dap)$_2$]Cl. While yields for electron-rich substrates were comparable to those of the Iridium catalyst, yields increased with increasing substrate electronegativity. Contrary to this, the other two mechanisms displayed decreasing yields with increasing substrate electronegativity. This trend continued for substrate whose benzylic radical cannot be oxidized by [Cu(dap)$_2$]Cl, thus suggesting an inner-shell mechanism at work. A wide variety of styrene derivatives have been demonstrated for halo-amination reactions using copper photocatalysis, however unactivated alkenes were not convertible by this protocol in good yields with the exception of 1-octene **15t**.

Furthermore, the presence of an inner-shell mechanism has been demonstrated *via* the product selectivity between pure ATRA with allyl reagents leading to product **38b** and ATRA followed by a 5-exo-trig cyclization leading to product **38a**. The optimized conditions were shown to be very efficient and improved overall yields for ATRA by copper catalysis. *In situ* generation of *N*-chloro reagents as well as upscaling experiments were successful. However, exploiting inner-shell mechanism for chiral induction by a chiral ligand sphere failed, either through a poor choice of substrate or mechanistic incompatibility.

3 Synthesis of 2*H*-Pyrrols after remote C$_{sp}$^{3} functionalization by iminyl radicals.

3.1 Introduction

Nearly all pharmaceuticals or agrochemicals contain nitrogen atoms in their base motifs, and their efficient syntheses are of great interest in industrial applications.[10] The use of ionic or metal-organic pathways for synthesis of such compounds has been widespread, while the use of nitrogen centered radicals has not experienced the same success so far. Photocatalysis as a method to facilitate various radical reactions has witnessed tremendous developments in recent years.[1,3,107] However, despite their relevance the use of nitrogen radicals as intermediates in photoredox catalysis has only recently become a field of increased interest, even though their generation through conventional means is well explored.[13]

Depending on their electronic nature, nitrogen radicals can display vastly different reactivities. Ranging from the more nucleophilic nature of aminyl radicals, to the addition of ambiphilic iminyl-radicals to various π-systems, to C-H abstraction reactions and addition to aromatics by the electrophilic amidyl- and aminium-radicals (*cf.* chapter *1.2*).[36,49,108] Photoredox catalysis has proven to be a versatile and reliable method for the generation of those radicals, generally through three different approaches: A proton-coupled electron transfer (PCET), the use or *in situ* generation of precursor molecules or the direct oxidation of a nitrogen lone pair.[12,38,63,109] This work focuses on controlling the reactivity of iminyl radicals in a radical cascade reaction.

Radicals, such as **67** are generally accessible through precursor molecules like oximes **65** through cleavage of the labile N-O bond, or through unsaturated azides **66** after condensation with a radical followed by nitrogen extrusion. The use of vinyl azides **66** over oxime esters **65** as precursor species has the advantage of generating iminyl radicals after an intermolecular condensation reaction, instead of relying on purely intramolecular reactions of pre-functionalized substrates.
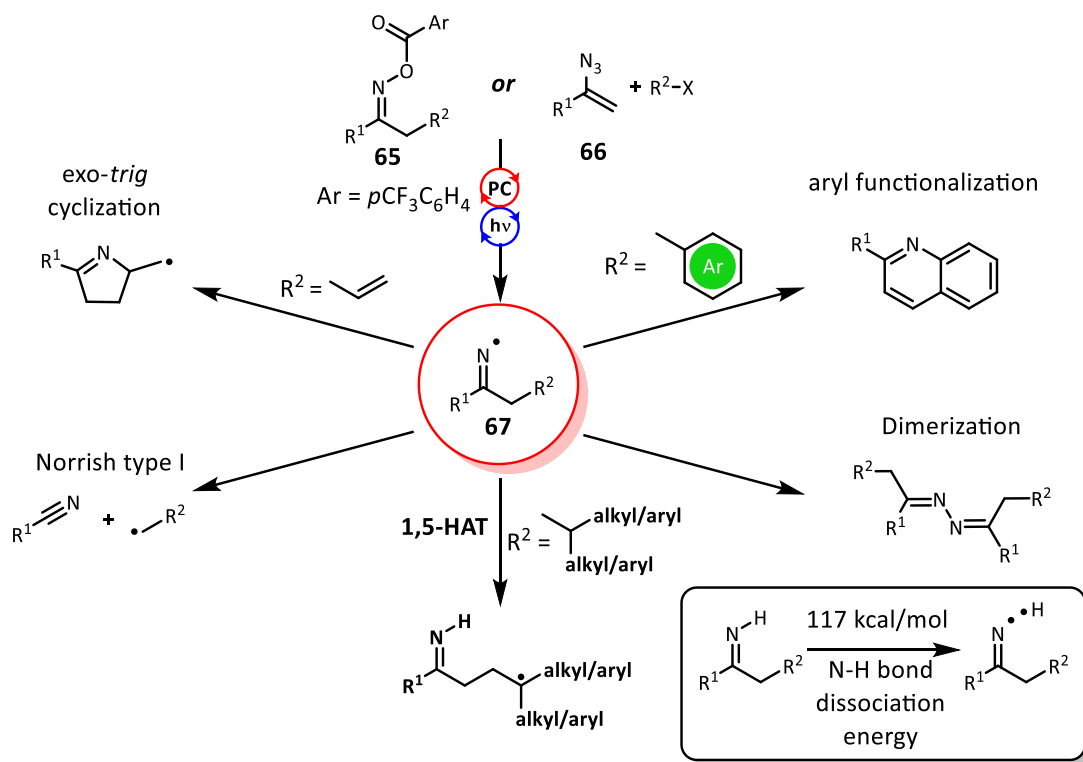
Scheme 32: Photocatalytic generation and modes of operation of Iminyl radicals.

In recent years, there has been an emergent rise in interest for the application of vinyl azides as pivotal three-atom synthon for the construction of complex *N*-heterocyclic scaffolds. Next to their function as radical acceptors, subsequently forming iminyl radicals upon radical addition, the unique features of the unsaturated azide group also allow it to react as nucleophile or electrophile. As such, the diverse reactivity has been used to highlight und investigate highly reactive intermediates with unusual mechanistic pathways.[110] When treated with heat or irradiation in the area of 350-450 nm, the unsaturated azide functions as a vinyl nitrene synthon, giving access to the highly strained 3-phenylazirine. Contact with various transition metal catalysts can trigger the extrusion of dinitrogen from the scaffold, resulting in transition metal nitrenes or comparable radical intermediates. Most relevant for this work, upon treatment with carbon-centered radicals and condensation to the unsaturated moiety, dinitrogen is extruded and highly reactive iminyl radicals (approx. 117

kcal/mol)[40]   are   obtained   (
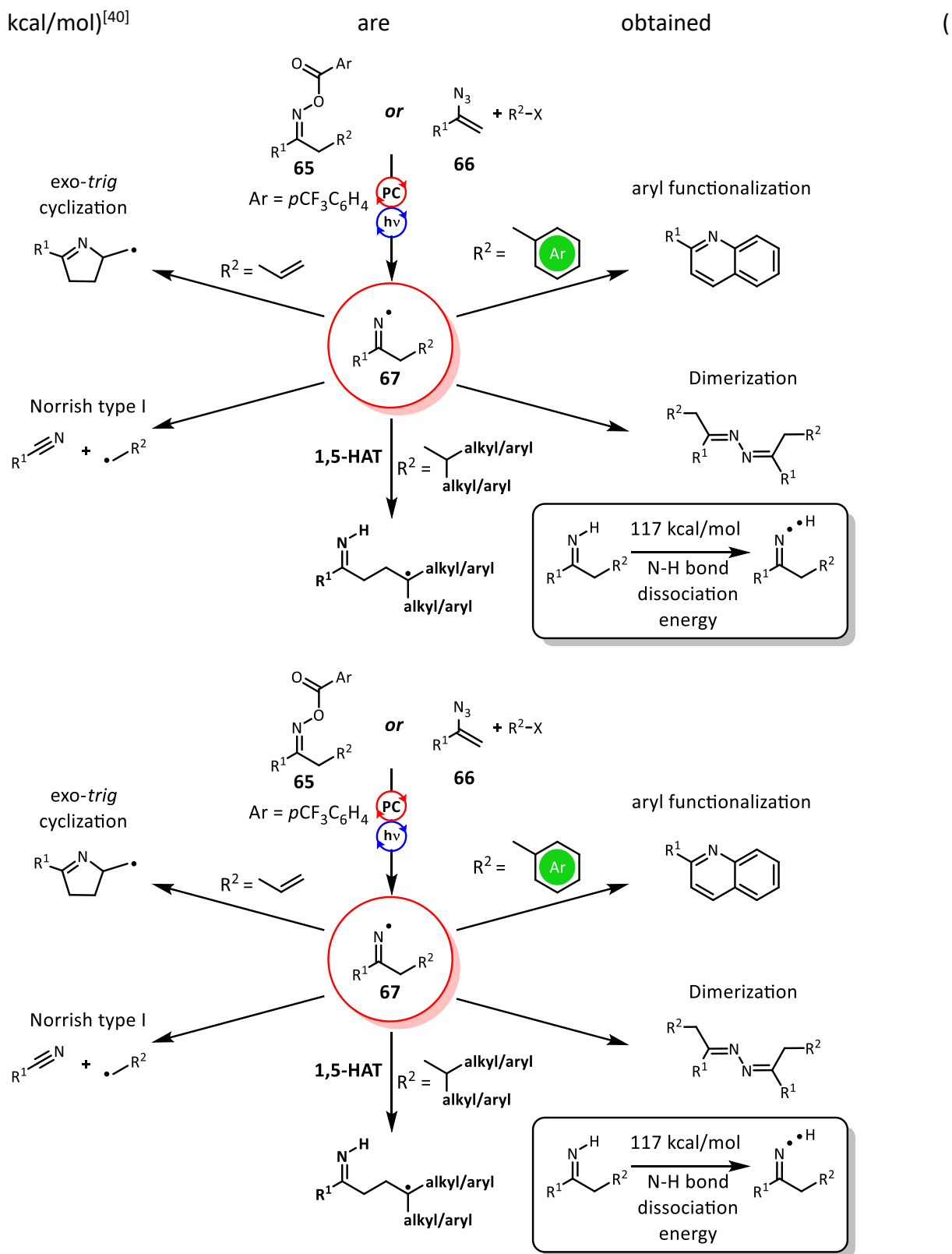
Scheme 32). While more reaction pathways *via* which unsaturated azides can react exist, only mechanisms relevant to this work are listed here (Scheme 33).[110]

Synthesis of 2H-Pyrrols after remote Csp3 functionalization by iminyl radicals.
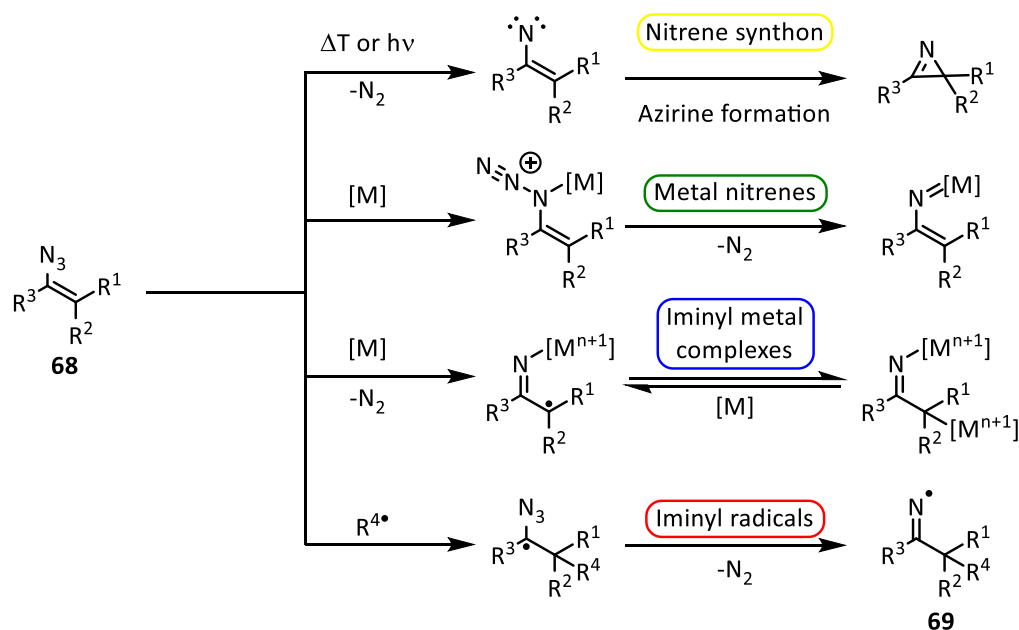
Scheme 33: Selected examples for the reactivity of unsaturated azides.

Since the ambiphilic iminyl σ-radical **69** can partake in cyclization-, Norrish type I-, dimerization-, aryl functionalization- and C-H abstraction reactions, reliably controlling the reactivity can be a challenging subject (Scheme 33).[66,74,75,111–114] Hereby, the C-H activation of remote C_{sp}^3 C-H bonds is of special interest, since its ubiquity in chemical structures make it an ideal albeit challenging target for functionalization.

However, the inert nature of this bond often makes harsh reaction conditions a necessity. In turn this limits functional group tolerance, decreases regioselectivity and narrows the substrate scope.[115] A radical based C-H activation mechanism as exemplified by the *Hoffman-Löffler-Freytag* reaction represents an viable alternative for site selective C-H functionalizations. The six-membered cyclic transition state of 1,5-hydrogen atom transfer (1,5-HAT) is a potentially valuable tool for the derivatization of remote C-H bonds, making laborious pre-functionalization or use of directing groups unnecessary. For this purpose, novel approaches utilizing *O-* and *N-*centered radical precursors have been successfully designed recently.[116] In the past, radical initiators such as $HSnBu_3$ or oxidants such as hypervalent iodine had to be used to drive these reactions.[72,117] Photoredox catalysis represents a powerful tool for the construction or activation of challenging bonds under mild conditions. Both site selective C(sp^2)- and C(sp^3)-H activations by nitrogen radicals have been previously reported.

Synthesis of 2H-Pyrrols after remote Csp3 functionalization by iminyl radicals.

C(sp²)-H functionalization:

Sanford, 2014:

10 eq.
70

71

5 mol% Ir(ppy)$_3$

MeCN, rt, 24 h, 26 W CFL
32%-89% yield

72

Leonori, 2019:

2 eq.
70

73

1.1 eq.
74

5 mol% [Ru(bpy)$_3$]Cl$_2$
MeCN, rt, 24 h

then HClO$_4$ (4.0 eq.),
rt, 1h, LED$_{455nm}$
21%-99% yield

75

Yu, 2015:

76

1 mol% Ir(ppy)$_3$

DMF, rt, 1 h
5 W white LED

Iminyl radical
intermediate

77

− N$_2$

58%-99%
yield

78

Yu, 2016:

79

1 mol% Ir(ppy)$_3$

DMF, rt, 24 h
5 W white LED

49%-90%
yield

78
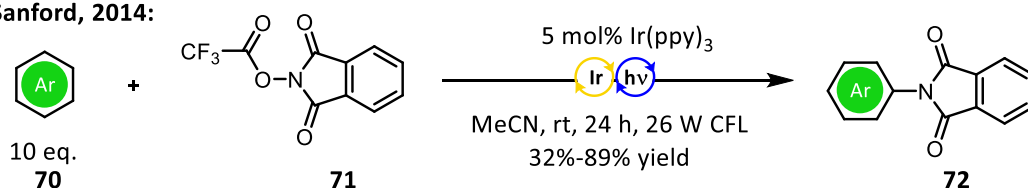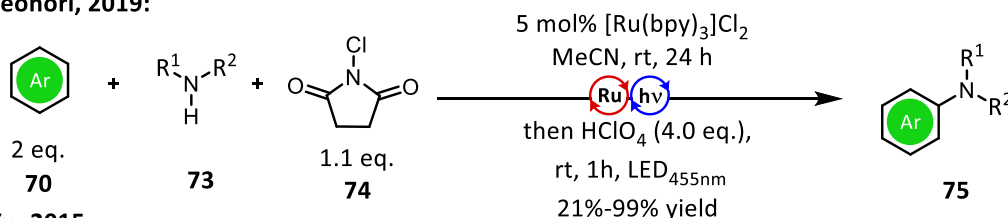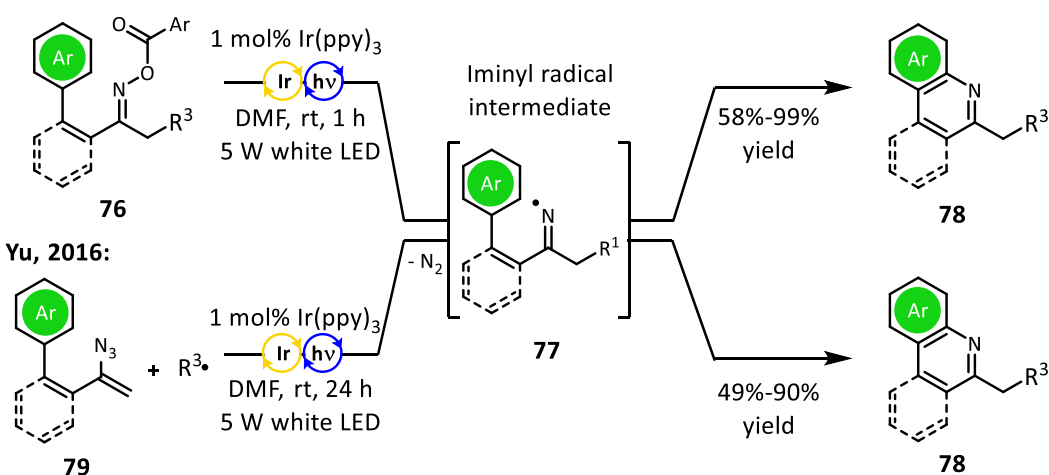
Scheme 34: Examples for photocatalyzed C(sp²)-H activation using nitrogen-centered radicals.

In 2014, the group of Sanford first reported the generation of amidyl radicals from *N*-acetylphatlimides **71**, an active ester previously employed in photocatalyzed decarboxylations.[118] Using a ten-fold excess of arene **70**, the direct functionalization of various inert arenes was achieved in good yields (Scheme 34).[38] Recently, a groundbreaking report on the activation of unactivated C(sp²)-H bonds by the Leonori group highlighted the *in situ* generation of *N*-chloro aminium ions by a reaction of amine **73** and NCS **74**. Such precursor molecules were capable of performing Buchwald-Hartwig type functionalizations after activation by a [Ru(bpy)$_3$]Cl$_3$ photocatalyst. A diverse scope of arenes **70** and amines **73** were compatible with this protocol in good yields, including complex alkaloid frameworks such as strychnine or a tropane derivative.[49] While the group of Yu reported on the C(sp²)-H activation through the photoredox-catalyzed generation of iminyl radicals **77** from vinyl azides **79** after condensation with a carbon-centered radical as well as oxime esters **76** in good yields,[35,67] to the best of our knowledge the photoredox-catalyzed C(sp³)-H activation has so

far only been reported using iminyl radicals.[119,120] Hereby, pre-functionalized oxime esters have been the precursor employed in C(sp^3)-H activation by nitrogen-centered radicals.
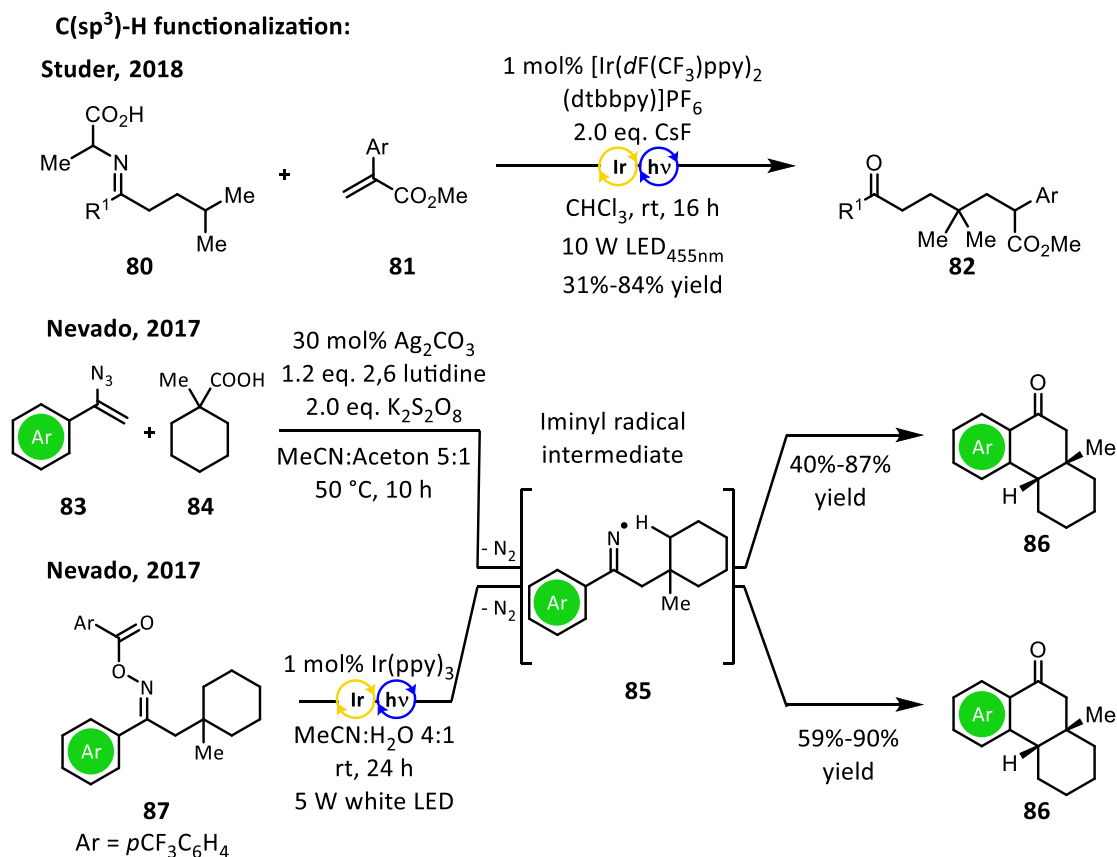
Scheme 35: Examples for C(sp^3)-H activation using iminyl radicals.

Studer and co-workers were able to realize the generation of iminyl radicals by oxidation of oxime precursor **80** by an Ir(dF(CF$_3$)ppy)$_2$(dtbbpy)]PF$_6$ (**[Ir-F]**) photocatalyst (Scheme 35). Following an 1,5-HAT event the tertiary carbon radical coupled with α,β-unsaturated ester **81** to give access to a scope of products **82** in good yields.[119] Nevado and co-workers reported two different pathways to access iminyl radical **85**: The intermolecular reaction between azido styrene **83** and an tertiary carbon-centered radical, generated by thermal decarboxylation of **84**, gave access to iminyl radical **85** which subsequently leads to ketone **86** after condensation to the aryl moiety and hydrolysis of the imine. Starting from oxime ester **87**, **85** is obtained after photocatalytic activation, ultimately yielding the same ketone product **86** in good yields. Hereby, the group of Nevado mentioned two substrates that cyclized to 2H-pyrroles instead of ketone **86** after an 1,5-HAT event followed by an oxidation and cyclization.[112,121]

This work: photocatalyic C$_{sp}^3$ C-H-functionalization from vinyl azides
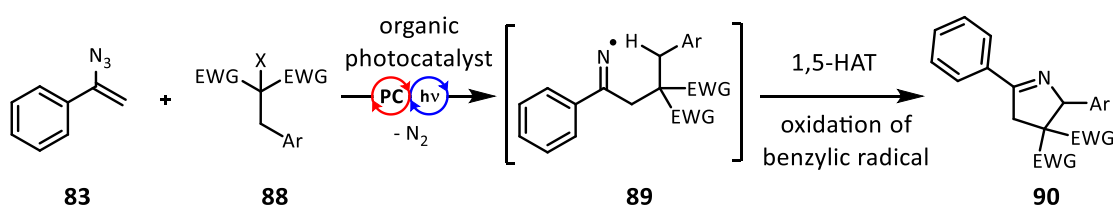
Scheme 36: Photocatalytic C(sp^3)-H activation by iminyl radicals and subsequent radical cascade.

Herein, we give the first report of 1,5-HAT reactions by iminyl radicals generated from vinyl azides though photocatalytic means. Selective activation of remote C(sp^3)-H bonds was achieved, subsequently yielding 2*H*-Pyrrols in favor of ketones in a radical cascade reaction, enabled by an organic photoredox catalysts.

3.2 Present work: Reaction Design towards 1,5-C(sp^3)-HAT by photocatalytically generated iminyl radicals.

The initial aim of the project was to develop a general protocol for the site selective activation of C-H bonds through nitrogen radicals generated by photocatalytic means. The radical reaction cascade envisioned involves three key steps: The generation of an iminyl radical, followed by a site selective hydrogen atom abstraction (HAT) and the utilization of the generated C$_{sp}^3$ radical to form a final product.

The aforementioned iminyl radicals can generally be accessed through two different means: Cleavage of a prefunctionalized oxime moiety by treating the N–O bond with triggers such as radical initiators, oxidants, thermal cleavage, or single electron reduction/oxidation by photocatalytic systems. A second way to generate iminyl radicals *in situ* is by reacting unsaturated azides with carbon-centered radicals, causing the extrusion of molecular nitrogen after condensation of the radical to the unsaturated bond, thus creating an iminyl radical.

Synthesis of 2H-Pyrrols after remote Csp3 functionalization by iminyl radicals.
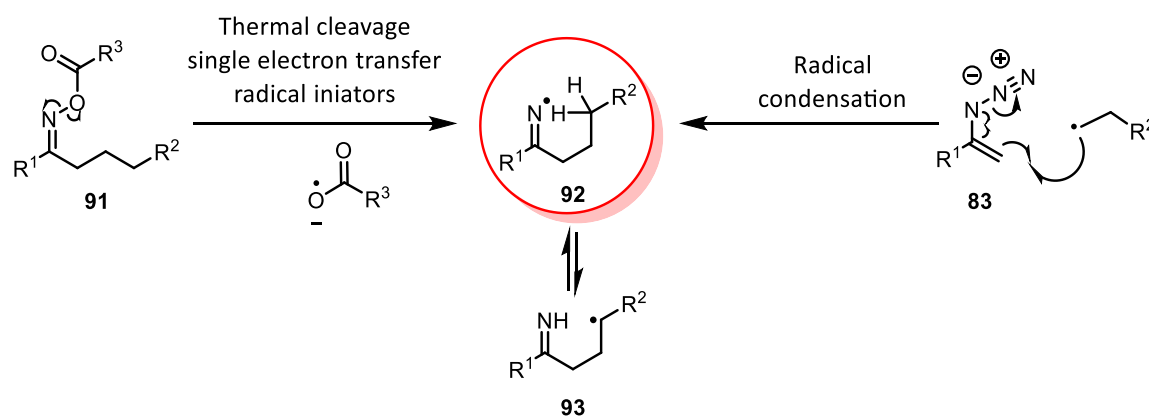
Scheme 37: Generation of iminyl radicals and the desired hydrogen atom transfer (HAT) reaction .

Accessing site selective 1,5 C-H functionalization *via* oxime precursors requires complex prefunctionalized starting materials, deemed to be too impractical for a general synthetic protocol.[75] Thus, unsaturated azides such as 1-azidostyrene **83a** and derivatives were chosen as most suitable iminyl radical precursor. However, this made a suitable carbon radical precursor towards **92** with a suitable radical-stabilizing R^2 a requirement (Scheme 37). The initial strategy was to use 2-Bromomalonate derivates as suitable precursor, since the cleavage of the electron deficient C–Br by photocatalytic means has been extensively studied and shown to work reliably.[84,86,122] Additionally, the steric bulk of the ester groups in intermediate **89** cause a Thorpe-Ingold-Effect, which favors 1,5-HAT and ring closure reactions through a contraction of the relevant dihedral angle (Scheme 36)**.** To add to this, the electron deficient quaternary carbon center stemming from the malonate motive can act as an effective handle for further functionalization or decarboxylation, opening a way to more potential product derivatizations. As such, the 2-bromomalonate motive **88** was chosen as initial radical precursor.

Having settled for a suitable radical precursor, further considerations were made towards the design of R^2 (Scheme 37). Even though the energy of the iminyl radical (approx. 117 kcal/mol)[40] is more than sufficient to homolytically cleave even a primary C_{sp}^3 C-H bond (approx. 100 kcal/mol), it was hypothesized that a radical stabilizing substituent, such as a phenyl group, would decrease the reactivity of the created transient carbon-centered radical and limit the number of possible side products. With these considerations in mind, 2-benzyl-2-bromomalonate **88a** was chosen as optimal second starting material to trigger the desired radical cascade (Scheme 38).
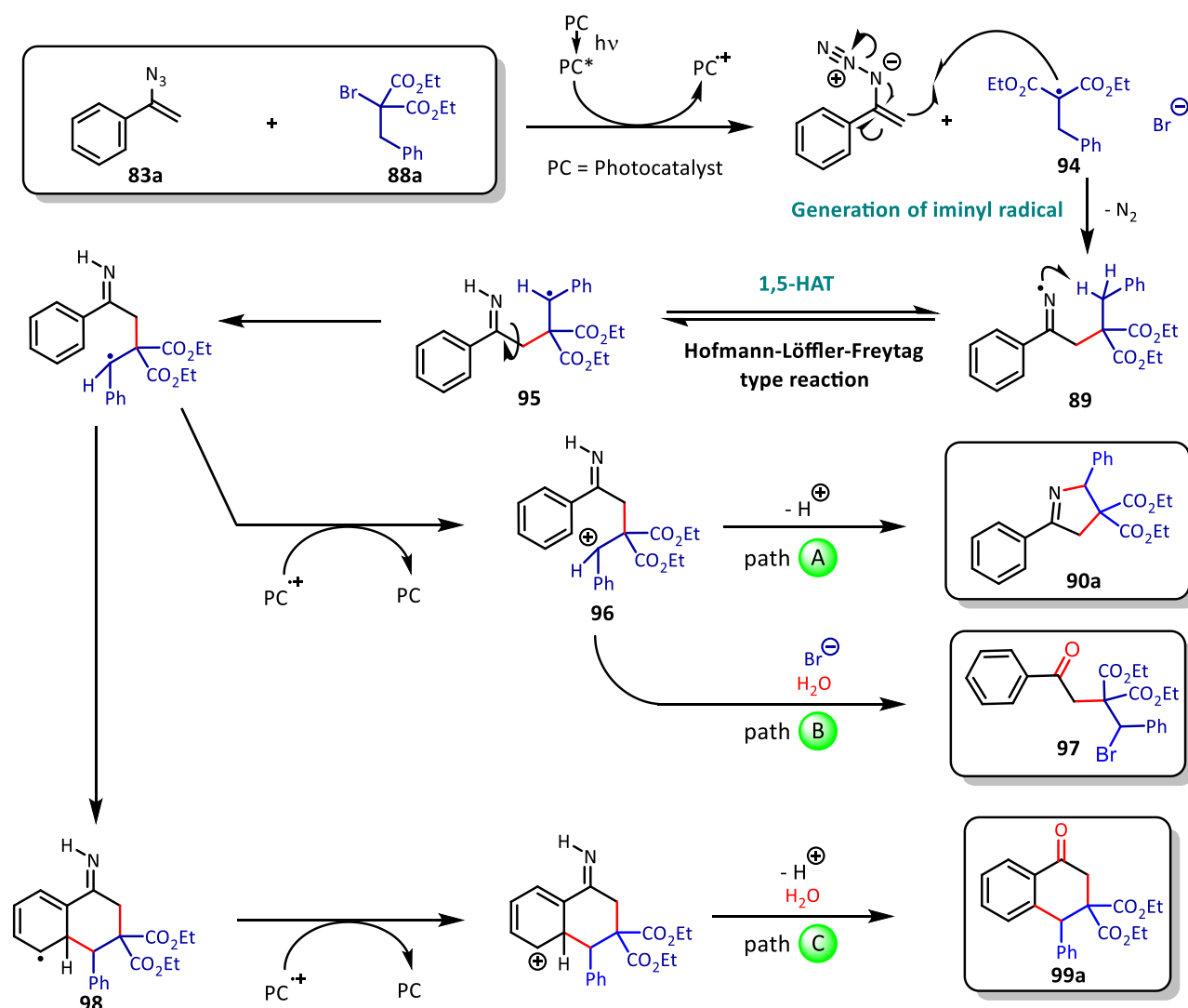
Scheme 38: Initial proposal for a 1,5-HAT radical cascade and possible products.

The focus then turned to the possible products formed by the benzylic radical **95**. Considering literature for comparable radical cascades[112,121] three possible products were considered (Scheme 38): Condensation to the aryl core originating from the 1-azidostyrene starting material, subsequent re-aromatization and hydrolysis of the imine moiety lead to cyclic ketone **99a** as major product (Scheme 38, path C). In contrast to this pathway, if the oxidation of the benzylic radical **95** outpaces the condensation two different products can be obtained. Attack of the imine moiety on the carbo-cation **96** leads to the 2*H*-pyrrole product **90a** in a reaction reminiscent of the classical *Hoffman-Löffler-Freytag* reaction (Scheme 38, path A), while the nucleophilic attack of a halide anion leads to a substituted product **97** in a cascade ATRA type reaction (Scheme 38, path B).
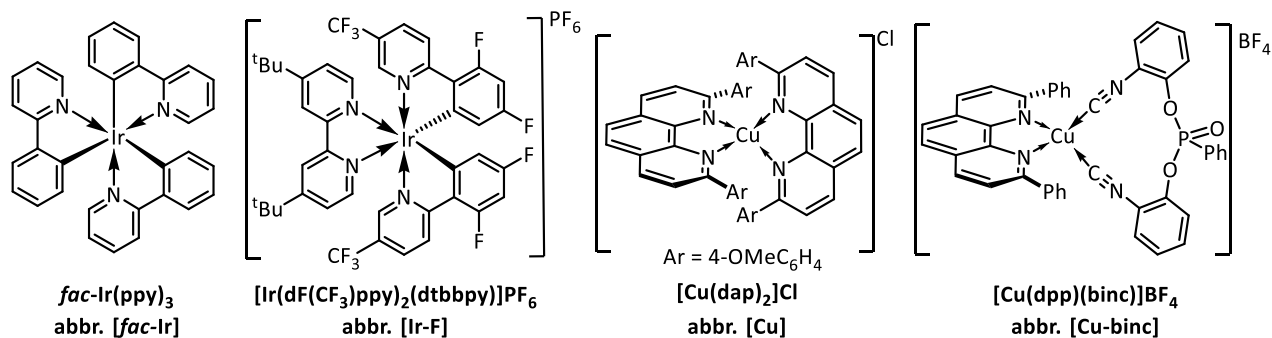
Figure 12: Photocatalysts for initial reaction screening.

Having established a general reaction design, screening for suitable reaction conditions and the optimal photocatalyst began. The initial strategy included four metal based photocatalysts, known for their ability to facilitate various photoredox reactions.[1,86,123] Two different iridium based-catalysts, *fac*-Ir(ppy)$_3$ and [Ir(dF(CF$_3$)ppy)$_2$(dtbbpy)]PF$_6$, were chosen for their varying redox potentials and tendencies to facilitate outer shell redox reaction. In contrast to these, copper catalysts show signs of directly interacting with radical intermediates in inner-shell mechanisms,[89,124] and were selected as potentially suitable catalysts.

3.1 Reaction optimization using metal-based catalysts.

To account for the various undesired side reactions of the very reactive azidostyrene starting material, a ratio of 1.5 eq. 1-azidostyrene **83a** to 1.0 eq. 2-benzyl-2-bromomalonate **88a** was employed (Table 6). Various solvents or solvent mixtures, whose suitability had been reported in comparable literature, were tested for their tolerance towards iminyl radical reactions.

Synthesis of 2H-Pyrrols after remote Csp3 functionalization by iminyl radicals.

Table 6: Initial reaction screening.
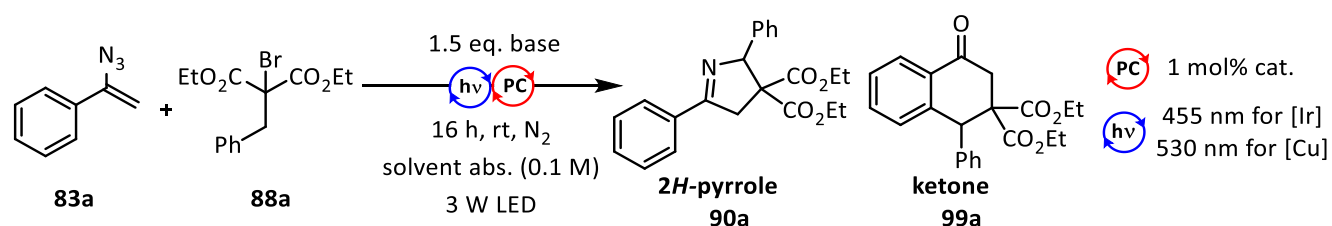
entry	base	catalyst	solvent	^{1}H-NMR yield
1	—	[Cu(dap)$_2$]Cl	MeCN	complex mixture
2	—	*fac*-Ir(ppy)$_3$	MeCN	2*H*-Azirine
3	—	[Ir(dF(CF$_3$)ppy)$_2$(dtbbpy)](PF$_6$)	MeCN	2*H*-Azirine
4	K$_2$HPO$_4$	[Cu(dap)$_2$]Cl	MeCN:EtOH 1:1	traces of 2*H*-pyrrole **90a**
5	K$_2$HPO$_4$	[Cu(dpp)(binc)](BF$_4$)	MeCN:EtOH 1:1	8% 2*H*-pyrrole **90a**
6	K$_2$HPO$_4$	*fac*-Ir(ppy)$_3$	MeCN:EtOH 1:1	17% 2*H*-pyrrole **90a**
7	K$_2$HPO$_4$	[Ir(dF(CF$_3$)ppy)$_2$(dtbbpy)](PF$_6$)	MeCN:EtOH 1:1	8% 2*H*-pyrrole **90a**
8	K$_2$HPO$_4$	[Cu(dap)$_2$]Cl	DMF	traces of 2*H*-pyrrole **90a**
9	K$_2$HPO$_4$	[Cu(dpp)(binc)](BF$_4$)	MeCN:H$_2$O 4:1	22% 2*H*-pyrrole **90a**[b]
10	**K$_2$HPO$_4$**	**[Cu(dap)$_2$]Cl (5 mol%)**	**MeCN:H$_2$O 4:1**	**27% 2*H*-pyrrole 90a**[b], 9% ketone **99a**[b]
11	AcOH	[Cu(dap)$_2$]Cl (5 mol%)	MeCN:EtOH 1:1	11% 2*H*-pyrrole **90a**
12	2,6-Lutidine	[Cu(dap)$_2$]Cl (5 mol%)	MeCN:H$_2$O 4:1	traces of 2*H*-pyrrole **90a**

(a) Reaction conditions: 0.6 mmol **83a**, 0.4 mmol **88a**. ^{1}H-NMR yield determined using tetrachloroethane as internal standard. (b): isolated yield

The initial variable investigated was the effect of various photocatalysts on this reaction (entry 1-3). Disappointingly, no product formation could be detected in absence of any additional additives. Notably, the 1-azidostyrene **83a** starting material quantitatively decomposed to the three membered unsaturated 1-phenyl-2*H*-azirine in case of iridium based photocatalysts (entry 2 & 3). To determine the effects of a base additive on the reaction, K$_2$HPO$_4$ was selected. In order to increase the solubility of the additive, a more polar acetonitrile/ethanol solvent mixture was necessary. Interestingly, iridium performed better than copper catalyst (entry 4 - 7), with a 17% yield of 2*H*-pyrrole **90a** detected (entry 6) next to completely decomposed starting material. While giving less product, the copper catalysts proved to be the more benign choice of reaction conditions (entries 4 & 5), since most of the starting material was left intact, in contrast to both iridium catalysts. While *N,N*-dimethylformamide (DMF) as solvent did not have any beneficial effect on the reaction (entry 8), the addition of water as co-solvent to acetonitrile increased the yield for [Cu(dpp)(binc)](BF$_4$) from 8% to 22% of 2*H*-Pyrrole **90a**

(entry 9). Investigating the effect of increased catalyst loading, the best result of a 3:1 product mixture of 2*H*-pyrrole **90a** and cyclic ketone **99a** in 36% combined isolated yield (entry 10) was obtained. Finally, exchanging K₂HPO₄ for acetic acid or 2,6-Lutidine had a negative influence on the reaction (entries 11 & 12). It is noteworthy, that only entry 10 displayed the formation of ketone **99a**. In no case the product of an ATRA type reaction **97** was observed. Since all attempts of optimization were dissatisfactory, it was concluded that the problem was either the choice of catalyst, or the choice of radical initiator. This has led to the synthesis of a scope of different starting material derivatives for this reaction in order to further investigate this reaction (Scheme 39).
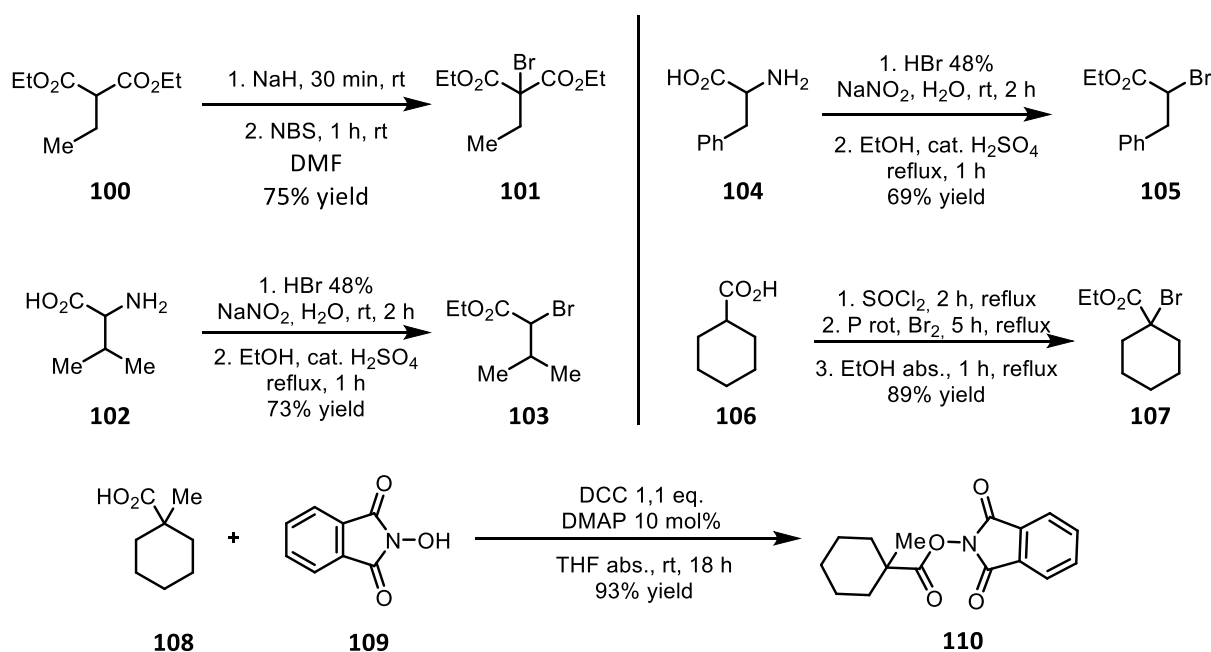
Scheme 39: Synthesis of variations of starting material 2-benzyl-2-bromomalonate **88**.

The scope included an α-bromomalonate derivative **101**, wherein the stabilizing substitution pattern was changed from a benzylic to a secondary C-H functionality. To rule out a negative effect of the sterically demanding malonate group three derivatives with only one ester group were synthesized. This included a benzylic (in **105**), a tertiary (in **103**), and a secondary carbon (in **107**) in 1,5-position of the generated iminyl radical in intermediate **89** (Scheme 38, C-H bond dissociation energies: Benzylic secondary carbon approx. 85 kcal/mol, secondary carbon approx. 98 kcal/mol, tertiary approx. 100 kcal/mol; N-H imine bond dissociation energy: approx. 117 kcal/mol).[40] To circumvent potential difficulties with radical initiation by cleavage of the electron deficient C-Br bond, the active ester 1,3-dioxoisoindolin-2-yl 1-

methylcyclohexane-1-carboxylate **110** (NPht = Phthalimide), cleavable by photocatalysis, with a secondary carbon in the relevant 1,5-position was synthesized.[125] With the derivatives at hand, suitable conditions for the efficient synthesis of 2H-pyrroles were searched (Table 7).

Table 7: Screening reactions with various starting material derivatives.

expected product:	screening result:
111	**[Cu] (5 mol%):** traces of **111** **[Cu-binc]^b:** no reaction **[fac-Ir]:** 80% 2H-azirine **116**
112	**[Cu]:** no reaction **[fac-Ir]:** 80% 2H-azirine **116** **[Ir-F]:** complex mixture
113	**[Cu] (5 mol%):** no reaction **[Cu-binc]:** complex mixture **[fac-Ir]:** 90% 2H-azirine **116** **[Ir-F]:** polymeric mixture
114	**[Cu]:** no reaction **[Cu-binc]:** complex mixture **[fac-Ir]:** quant. 2H-azirine **116** **[Ir-F]:** complex mixture
115	**[Cu]:** quant. 2H-azirine **116** **[Cu-binc]:** 40% 2H-azirine **116** **[fac-Ir]:** quant. 2H-azirine **116** **[Ir-F]:** quant. 2H-azirine **116**

(a) Reaction conditions: 0.6 mmol **83a**, 0.4 mmol carbon radical precursor. 2H-azirine yields were determined by ^{1}H-NMR analysis using tetrachloroethane as internal standard. (b) K_2HPO_4 was added instead of 2,6-lutidine.

In general, acetonitrile was used as solvent, since the use of solvent mixtures in the initial reaction screening was deemed to be to unreliable (Table 6). As part of an overarching question, whether a homo- or a heterogeneous base is preferable for this reaction, 2,6-lutidine was chosen as soluble pyridine base for two substrates (**111** and **114**). However, all

five substrates failed to give their corresponding product in any significant amount. Further studies showed that the main product of most reaction was the decomposition to the three-membered 2H**Reaction optimization using organic photoredox catalysts.**When compared to the reaction outcomes of the initial reaction screening (Table 6), it became apparent that the choice of starting materials was not the underlying issue of this reaction. Summing up the screening conducted with substrates **101** to **110** (Table 7), all five derivatives failed to deliver more than traces of a single expected product. Due to the inherent instability of 1-azdiostyrene **83a**, the reaction outcomes observed were either a quantitative decomposition to the azirine **116** (Scheme 40), or a complex reaction mixture most likely resulting from photoredox-reactions with 3-phenyl-2H-azirine **116** leading to a plethora of different products.
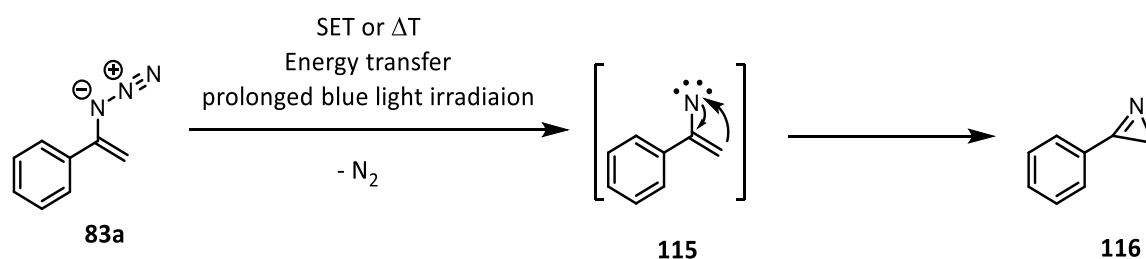
Scheme 40: Decomposition of 1-azidostyrene to 3-phenyl-2H-azirine **116**.

The aforementioned instability of 1-azidostyrene **83a** has been reported in literature, and while examples of 1-azidostyrene in photoredox reactions with iridium or ruthenium catalysts are known, those reactions can be rationalized by the possibility of the nitrene intermediate **115** to be the active species.[35,114,126] Other studies have highlighted the decomposition of **83a** to **116** by illustrating that 1-azidostyrene **83a** is merely a suitable precursor and demonstrating that 3-phenyl-2H-azirine **116** is the active starting material in their reactions.[127]

In light of these initial results with various starting materials, attention turned to the choice of catalyst. Having identified energy transfer as a problematic side reaction when working with 1-azidostyrene **83a**, the focus shifted from metal-based to organic photoredox catalysts, since they only very rarely participate in energy transfer reactions. However, most established organic photocatalyst are only active in the reductive quenching cycle, not in the oxidative quenching cycle necessary for the initial cleavage of the C-Br bond.

Synthesis of 2H-Pyrrols after remote Csp3 functionalization by iminyl radicals.
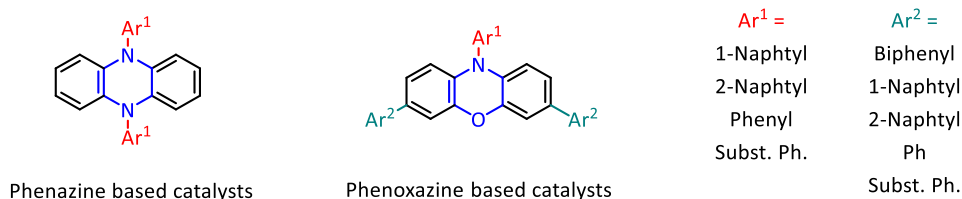
Figure 13: Organic photocatalysts developed by Miyake and co-workers and mechanism.

The Miyake group recently established a class of polyaromatic organic photocatalysts (Figure 13), and highlighted their ability to cleave carbon halogen bonds with several examples exemplifying the high reduction potentials calculated (between -1.6 to -2.1 V, depending on the choice of catalyst).[128,129] Interestingly, the exact mechanism differs slightly from the established photoredox mechanism for metal-based catalysts, that was initially proposed.[130] Orr-Ewing and co-workers observed to reactions of two dihydrophenazines with ultrafast time-resolved spectroscopy. Within this study, Orr-Ewing elucidated the dissociative bimolecular electron transfer between the phenazine catalyst and an α-bromo ester compound. He discovered that the biggest contributor to the initial dissociative electron transfer to be the S_1 state of the phenazine catalyst he investigated, as opposed to the longer lived T_1, which is the catalytically active state in most metal-based catalysts.
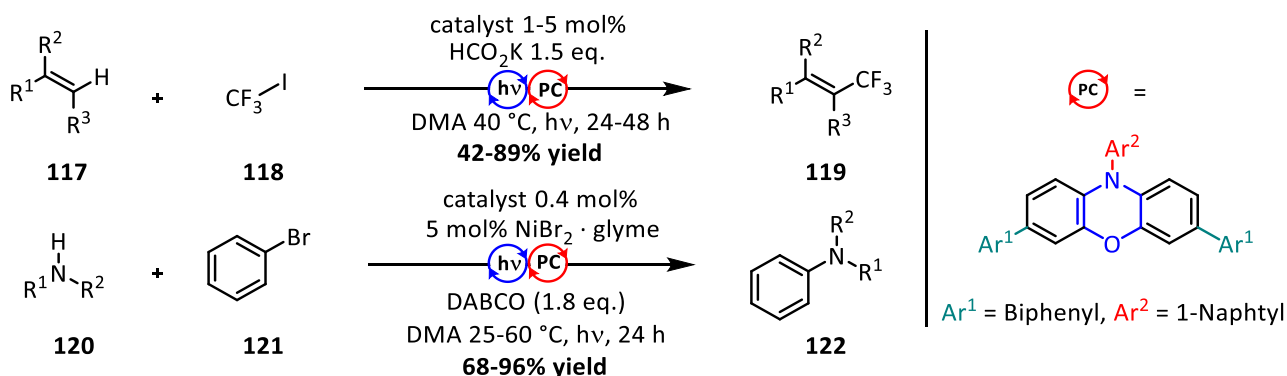
Scheme 41: Selected literature examples by Miyake and co-workers.

While the initial application for those catalysts resided in polymer chemistry,[131–133] Miyake *et al.* quickly managed to realize several photoredox reactions, *e.g.* an ATRA type reaction using •CF_3 radicals generated from CF_3I, or an *Hartwig-Buchwald* type reaction with a nickel co-catalyst (Scheme 41).[132,134] Encouraged by the success of this organic photocatalyst, a new set of screening reactions was devised, and the starting materials of the initial reaction screening **83a** and **88a** were used again. At the same time, the amount of additive, if present,

was kept constant. Reaction screening demonstrated that the presence of water was not detrimental to this reaction and judging from earlier experiments the presence of water even had a beneficial effect on the reaction. As a result of this, solvents and glassware were used without prior removal of trace amounts of water. Research by the group of Miyake demonstrated the suitability of *N,N*-dimethylacetamide (DMA) for reactions using 5,10-di(naphthalen-2-yl)-5,10-dihydrophenazine and related phenoxazine catalysts (Scheme 41) and related catalysts. As such, DMA has been chosen as base solvent for the reaction screening. Other reaction parameters were kept constant from previous screening attempts.

Synthesis of 2H-Pyrrols after remote Csp3 functionalization by iminyl radicals.

Table 8: Reaction screening with organic photocatalysts.
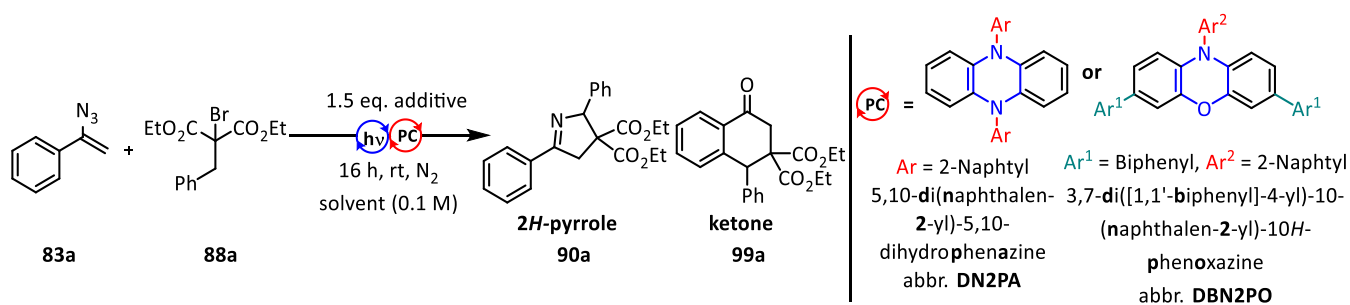
entry	additive	catalyst	solvent	^{1}H-NMR yield
1	—	DN2PA 5 mol%	DMA	10% 2H-pyrrole **90a**, 39% ketone **99a** [b]
2[c]	—	DN2PA 5 mol%	DMA	28% 2H-pyrrole **90a**, 43% ketone **99a** [b]
3	HCO$_2$Na	DN2PA 5 mol%	DMA	81% 2H-pyrrole**90a**
4	AcOH	DN2PA 5 mol%	DMA	38% 2H-pyrrole **90a**, 37% ketone **99a**
5	HCO$_2$Na	DN2PA 5 mol%	MeCN abs.	44% 2H-pyrrole **90a**
6	HCO$_2$Na	DN2PA 5 mol%	DMF abs.	78% 2H-pyrrole **90a**
7[c]	HCO$_2$Na	DBN2PO 5 mol%	DMA	80% 2H-pyrrole **90a**
8	**HCO$_2$Na**	**DN2PA 1 mol%**	**DMA**	**84% 2H-pyrrole 90a**
9	HCO$_2$Na	DN1PA 1 mol%	DMA	69% 2H-pyrrole **90a**, 15% ketone **99a**
10	HCO$_2$Na	DBN2PO 1 mol%	DMA	84% 2H-pyrrole **90a**
11	HCO$_2$Na	DN2PA 1 mol%	DMA	70% 2H-pyrrole **90a**

(a) Reaction conditions: 0.6 mmol **83a**, 0.4 mmol **88a**. ^{1}H-NMR yield determined using tetrachloroethane as internal standard (b): isolated yield. (c): Performed with 403 nm instead of 455 nm 3 W LED.

Pleasingly, even the first screening experiment (Table 8, entry 1) with 5 mol% DN2PA catalyst loading was more successful than any previous experiments, giving a combined yield of 49% compared to the best previous result of 36% (entry 10, Table 6). However, the reaction conditions employed favored the formation of ketone **99a** over 2H-pyrrole **90a** in a 4:1 ratio (entry 1). Although, the maximum absorption of the organic catalysts is around λ_{max} = 380 nm, with the absorption band only extending into the visible region, the light used to excite the catalyst (λ_{LED} = 455 nm) was sufficient to drive an efficient reaction. When using a near-UV LED (λ_{LED} = 403 nm) to better excite the catalyst, the yield increased to 71% combined yield with a decrease in selectivity to 1.5:1 in favor of ketone **99a** (entry 2). Gratifyingly, the addition of sodium formiate – based on a report by Miyake and co-workers for the trifluoromethylation of alkenes[132]– resulted in the selective formation of the 2H-pyrrole **90a** in a very good yield of 81% (entry 3). To test the effect of a weak acid on this reaction, acetic acid was added to the reaction mixture in absence of formiate salts.

While overall yield increased to 75% compared to 49% without any additive (entry 1), product selectivity dropped to a 1:1 ratio (entry 4). Encouraged by initial good results using sodium formiate, the solvent effects were investigated. Using Acetonitrile abs. or DMF abs. as solvent led to a decrease in yield to 44% and 78% respectively (entry 5 & 6). This was rationalized by the decrease in solubility for formiate salts in case of acetonitrile. Although the result of DMF and DMA were comparable, such a result was expected considering that the similarity of said solvents. With this information in hand, the phenoxazine catalyst 3,7-di([1,1'-biphenyl]-4-yl)-10-(naphthalen-2-yl)-10*H*-phenoxazine (DBN2PO, Table 8) was tested using a near-UV LED (λ_{LED} = 403 nm). However, no increase in 2*H*-pyrrole yield could be achieved, despite complete product selectivity (entry 7). 5,10-di(naphthalen-1-yl)-5,10-dihydrophenazine, a constitutional isomer of DN2PA differing in the attachment of both naphthalene groups to the phenazine moiety, achieved 84% overall yield in 1 mol% catalyst loading (entry 9), even though product selectivity decreased to 4.6:1 in favor of the 2*H*-pyrrole **90a** compared to ketone **99a**. The focus then turned to decreasing the catalyst loading below 5 mol%. Gratifyingly, both DN2PA and DBN2PO were able to outperform previous results with 84% yield of 2*H*-pyrrole **90a** (entry 8 & 10). In fact, even lowering the catalyst loading to 0.1 mol% in case of DN2PA resulted in a only slightly decreased yield to 70% (entry 11). While a low catalyst loading is desirable from an economic point of view, a catalyst loading of 1 mol% was chosen for further reaction screening, in order to ensure complete reaction with all future substrates. In no case the product of an ATRA type reaction **97** (Scheme 38, path B) was observed.

3.2 Determining the effect of base additives.

With optimized conditions in hand, the advantageous effect of sodium formiate in this reaction was investigated. To verify whether the reductive properties determine the reactivity, or its slightly basic properties are key to this reaction, a selection of various bases, some of which active in redox reactions, was made. Additionally, it was discovered that reaction time can be reduced to 10 hours from the screening experiments without any loss in yield (Table 9).

Synthesis of 2H-Pyrrols after remote Csp3 functionalization by iminyl radicals.

Table 9: Base screening.
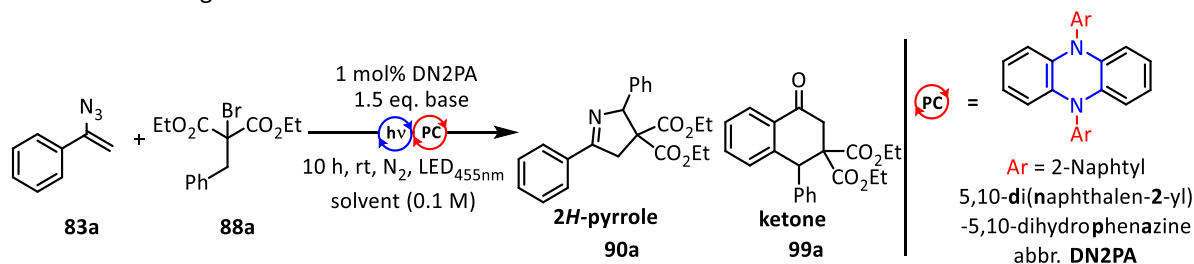
entry	base	comment	^{1}H-NMR yield
1	DIPEA	redox active organic base	26% 2H-pyrrole **90a**
2	2,6-Lutidine	non-oxidizable organic base	54% 2H-pyrrole **90a**, 21% ketone **99a**
3	K$_2$HPO$_4$	non-oxidizable inorganic base	52% 2H-pyrrole **90a**, 47% ketone **99a**
4	Na$_2$CO$_3$	non-oxidizable inorganic base	31% 2H-pyrrole **90a**, 54% ketone **99a**
5	**HCO$_2$K**	**redox active inorganic base**	**92% 2H-pyrrole 90a,4% ketone 99a** [b]

(a) Reaction conditions: 0.6 mmol **83a**, 0.4 mmol **88a**. ^{1}H-NMR yield determined using tetrachloroethane as internal standard. (b): isolated yields.

When comparing the reaction outcomes of the reaction screening with those of the base screening it becomes apparent, that the choice of base indeed has a crucial effect on product yield and selectivity (Table 9). Considering the mechanism, a similar reaction outcome to sodium formiate was expected for DIPEA (entry 1), since both of them could act as electron donor (D) in an oxidative quenching cycle. However, while product selectivity remained high, yield dropped dramatically to 26% for 2H-pyrrole **90**. Following this result, a organic base such a 2,6-lutidine, a pyridine base non oxidizable by most oxidants, was evaluated. While overall yield rose to 75%, product selectivity decreased (entry 2). From this it can be inferred that additives with reductive properties confer selectivity towards the 2H-pyrrole product **90a** (entry 2), even though DIPEA inhibited a productive reaction. Following this hypothesis Na$_2$CO$_3$ and K$_2$HPO$_4$ were tested as non-oxidizable inorganic bases and resulted in excellent combined yields with 85% and 99% respectively, albeit with close to no product selectivity (entry 4 & 5). By capitalizing on the increased solubility of HCO$_2$K in DMA compared to HCO$_2$Na, overall yield of the reaction could be increased to 96%, with 2H-pyrrole being isolated in 92% yield. With these optimized conditions at hand, the scope of this reaction was investigated.

3.3 Starting material synthesis

To start exploring the reaction scope, starting material synthesis had to be revisited. Both starting materials were synthesized from commonly available starting materials, and miscellaneous variations at different sites had to be contemplated. In case of unsaturated azides, product stability had to be considered, since the unsaturated azide functional groups tends to be unstable under various conditions.[110]

3.3.1 Synthesis of unsaturated azides.

A scope of 1-azidostyrene derivatives were considered as initial set of starting azides. 1-Azidostyrenes are more stable than various other unsaturated azides, and their synthesis, reactions and other relevant properties are comparatively well explored.[110] Within the scope of this work, three different synthesis pathways towards 1-azidostyrene derivatives were necessary to obtain the desired starting materials (Scheme 42). This was necessary due to inherent problems with regioselectivity or reactivity within certain derivatives, combined with the inability to separate regioisomers or byproducts reliably due to the instability of the obtained product mixtures during purification.
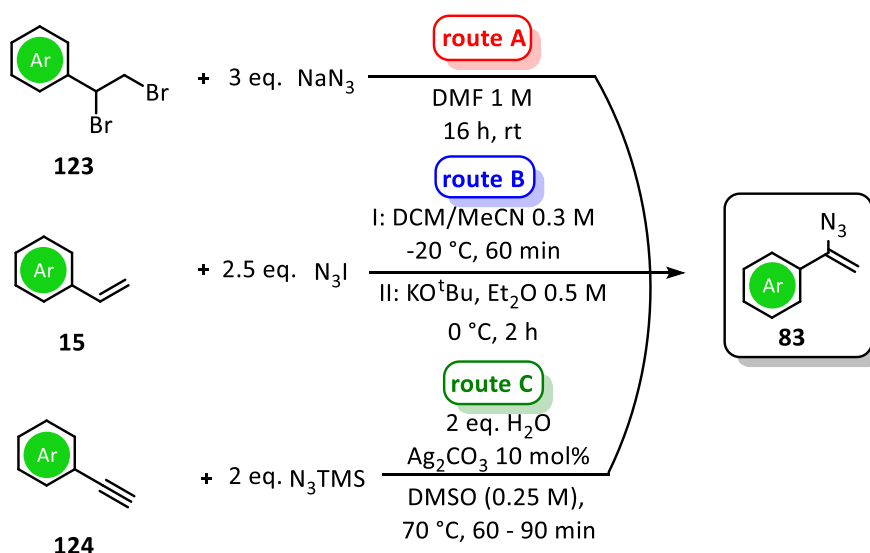
Scheme 42: The three pathways employed for the synthesis of vinyl azides.

Dibrominated styrenes **123** are easily available through common bromination procedures of corresponding styrenes **15**.[135] The products of these reactions were converted into the desired 1-azidostyrenes by treating them with a three-fold excess of sodium azide in DMF. A second pathways utilized the highly reactive iodoazide reagent N_3I, which can be prepared *in situ* from sodium azide and the interhalogen compound iodine monochloride (ICl). Carefully treating the crude iodoazide intermediate product from this reaction with a strong base in diethyl ether results in unsaturated azide products. Where monosubstituted alkynes of the desired derivatives are available, hydroazidation is a suitable pathway. Following a protocol established by professor X. Bi and co-workers, various alkynes can be efficiently converted into unsaturated azides by $TMSN_3$ in a silver-catalyzed reaction.[136] In an effort to enable a broad substrate scope a number of unsaturated azide derivates have been prepared (Figure 14).

83a
88% yield
route **A**

83b
95% yield
1.14:1 regioselectivity
route **A**

83c
96% yield
3.23:1 regioselectivity
route **A**

83d
86% yield
10:1 regioselectivity
route **A**

83e
92% yield
20:1 regioselectivity
route **A**

83f
75% yield
route **A**

83g
83% yield
route **B**

83h
69% yield
route **B**

83i
66% yield
route **B**

83j
no rxn.
route **B**

83k
83% yield
route **C**
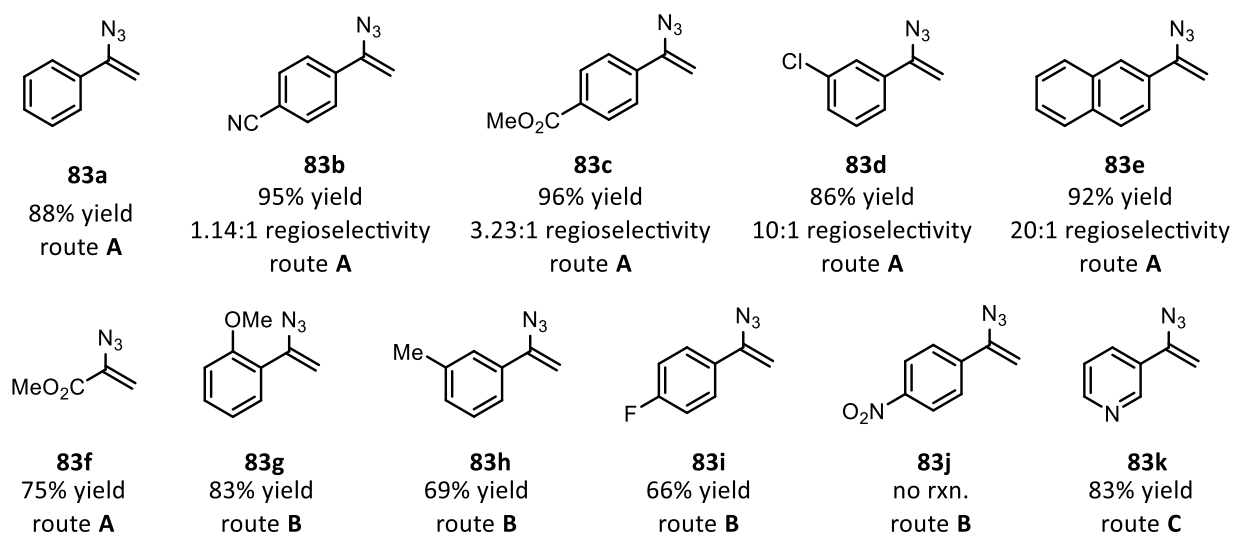
Figure 14: Unsaturated azides prepared as starting material.

Evaluating the results obtained from various synthesis routes, the various strengths and weaknesses of each route become apparent: While route A has the broadest applicability in terms of substrates and excellent yields, products **83b** and **83c** displayed severe problems with regioselectivity, resulting in product mixtures unsuitable for the planned reaction. Notably, methyl acrylate could be converted into methyl 2-azidoacrylate **83f** in 75% using this route. Contrary to route A, route B displayed no issues with regioselectivity, however it led to lower yields. Additionally, substrates with electron withdrawing substituents could not be successfully converted by this strategy, and **83j** could only be obtained as a mixture of starting

material and decomposition products of the desired product. The hydroazidation of alkynes (route C) was able to give access to product **83k** in good yields and full regioselectivity, establishing the silver catalyzed reaction pathway a suitable alternative wherever the corresponding alkynes **124** are available.

3.3.2 Syntheses of 2-benzyl-2-bromomalonate derivatives.

Starting from 2-benzylmalonates **127**, 2-benzyl-2-bromomalonate derivates **88** were synthesized by an acid catalyzed bromination in diethyl ether. In turn, 2-benzylmalonates could be obtained from 2 different synthetic procedures.
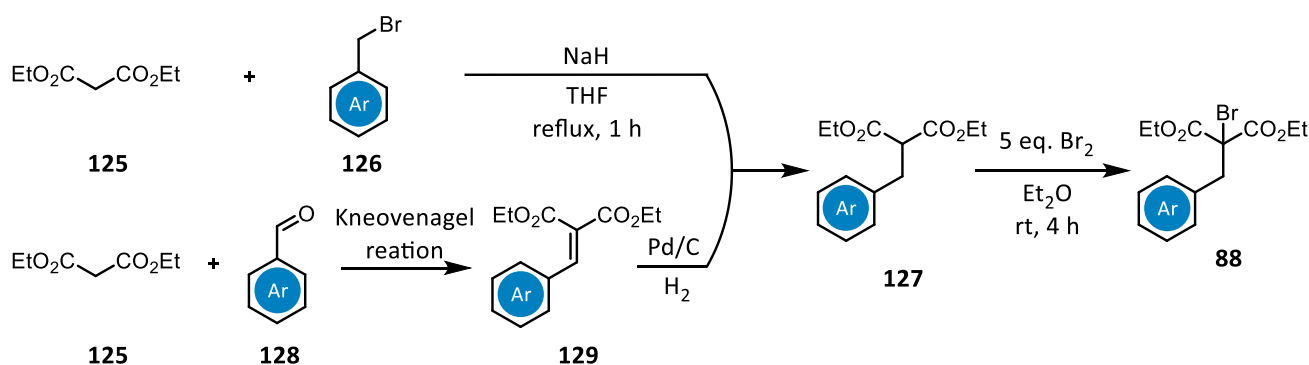
Scheme 43: General synthetic strategy to synthesize 2-benzyl-2-bromomalonates.

The initial strategy proceeded via a direct alkylation of malonate **125** via a S$_{N2}$ reaction after deprotonation by sodium hydride, followed by addition of various benzylic bromides **$$** to obtain 2-benzylated malonates **127** (Scheme 43, upper pathway). However, despite various alterations to reaction procedure, the dialkylation side product of malonate **125** was also obtained in low yields. While excess malonate **125** could be removed by vacuum distillation, a mixture of dialkylated malonate and monoalkylated product **127** proved to be exceedingly difficult to separate. This was problematic during the bromination step to obtain the final starting material **88**. It should be mentioned that using a two-step synthesis might in fact save time due to easier separation. The route utilizes a *Knoevenagel reaction* to obtain the unsaturated 2-benzylidenemalonate product **129**, followed by a direct hydrogenation of the crude material to afford diethyl 2-benzylmalonate **127** as only product of this reaction (Scheme 43, lower pathway). A radical bromination approach in order to brominate **127** was deemed unsuitable, since bromination of the benzylic position would have been the most likely reaction outcome. Instead, a modified literature procedure was developed to brominate

the α-malonate C-H functionality in presence of a benzylic position in what is presumed to be an acid catalyzed reaction. The initial formation of HBr during this reaction could be rationalized by the reaction of excess bromine with diethyl ether solvent molecules.

Figure 15: (a) Malonate derivatives synthesized (b) corresponding 2-bromo products.

As stated above, yields in the first step were lowered by a dialkylation side reaction, and subsequent difficulties during purification. In order to determine the effect of nitrile groups on the reaction 2-benzylmalononitrile **127g** was synthesized by the same protocol. The initial strategy to brominate an α-malonate C-H functionality in presence of a benzylic position proved to be an effective approach to this problem across the substrate scope, with two notable exceptions: The *para*-methyl derivative **88b** could only be isolated in very low yields, and the bromination reaction of 2-benzylmalononitrile **127g** only led to rapid decomposition of the starting material, with no isolatable product detected. **88h** and **88i** could also be isolated using the aforementioned procedure starting from available starting materials.

3.4 Substrate scope

Having identified ideal reaction conditions (Table 9, entry 5) and with a sufficient set of starting materials in hand, testing for the applicability of the optimized reaction conditions commenced. Reaction time was increased from 10 h to 16 h (Figure 16) to allow every substrate sufficient reaction time. No decomposition of product upon prolonged irradiation could be detected.

Figure 16: Substrate scope for 1,5-HAT by iminyl radicals.

Synthesis of 2H-Pyrrols after remote Csp3 functionalization by iminyl radicals.

Since 1-azidostyrenes **83b** and **83c** with strong electron withdrawing substituents were obtained as mixture of regioisomers they were deemed not suitable for the reaction (Figure 14). *Ortho*-methyl substitution on the malonate frame led to 73% yield of 2*H*-pyrrole **90b**. *Meta*-alkyl substituted azide **83h** gave a combined yield of 55%, with a low product selectivity of 1.3:1 towards **90c**. Interestingly, both possible meta-regioisomers for the ketone product **99c** were detected in a close to 1:1 ratio to each other, demonstrating that reaction of the benzylic radical in the proposed mechanism is slow enough to allow for rotation of the relevant phenyl group (Scheme 38).

The electron donating *ortho*-OMe substituent was tolerated in derivate **90d**, albeit yield dropped to 47% of the desired 2*H*-pyrrole. Notably 9% of the corresponding ketone **99d** were isolated, in a product selectivity of 5.2:1. Halogen substituents in *meta-* and *para-* position of the azide were well tolerated, achieving yields of 68% **90e** and 70% **90f**. Surprisingly, the para-fluoro-1-azidostyrene **83i** also yielded 9% of the corresponding ketone **99f** next to **90f** in 7.8:1 product selectivity with a combined yield of 78%. The product **90g**, with a *para*-bromo substituted malonate core, was obtained in 71% yield without detectable ketone formation. Gratifyingly, the 2*H*-pyrrole derivative of nicotine **90h** was isolated in 62% with no detectable traces of ketone. This product enables the possibility for a synthesis of various nicotine derivatives after stereoselective hydrogenation of the imine bond. For the naphthalene derivative **90i** a 1.5:1 inverse product selectivity in favor of the ketone **99i** was observed. This can be rationalized by the lower activation barrier for the radical attack on the aromatic core compared to phenyl derivatives. Substitution on the malonate frame only gave rise to the desired 2*H*-pyrrole products, and no product mixtures were obtained.

Overall, substitution on the malonate frame was well tolerated. However, when exchanging the benzylic position for the less stabilized tertiary position the yield dropped dramatically to 9% for product **90j**. Interestingly, an open-chained decarboxylated side product was obtained in 21% yield (*vide infra*, Table 10). Finally, malonate starting materials with nitro groups in their structure (**88f** and **88j**, Figure 15) only gave rise to their corresponding de-halogenated products. 1-azidomethylacrylate **83f** gave a mixture of two products with similar R_f and identical mass, which exact structure remains unknown at this point, but does not correspond to the expected product. It is worth pointing out that ^{1}H-NMR yields for the 2*H*-pyrrole products were consistently higher (5 – 15%) than those isolated, while ^{1}H-NMR yields for the

corresponding ketones remained consistent with isolated yields. This hints towards a loss of 2*H*-pyrrole during isolation by flash column chromatography.

In an effort to expand the substrate scope for the synthesis of 2*H*-pyrrols through iminyl radicals and remote $C_{sp}{}^3$ functionalization beyond 2-benzyl-2-bromomalonate derivates to other radical precursors, additional literature reports were investigated. In particular, the combination of two different kinds of iminyl radicals precursors -oxime esters and unsaturated azides – highlights the various reactivities of the iminyl radicals generated *in situ* in this radical cascade reaction.[137] The starting material synthesis for a cyclobutene oxime ester **$$** was realized in a four-step synthesis, starting from styrene **15a**.
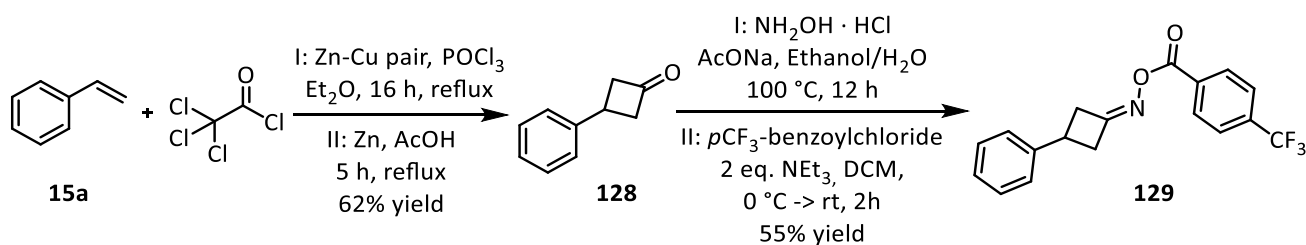
Scheme 44: Synthesis of a model cyclobutane oxime ester iminyl radical precursor.

The reaction sequence towards **129** proceeded *via* a [2+2] addition of **15a** to 2,2-dichloroethen-1-one, generated *in situ* from 2,2,2-trichloroacetyl chloride, followed by a reductive dehalogenation to product **128** in 62% yield. After imine condensation, followed by an esterification the desired starting material **129** was obtained in 34% overall yield starting from styrene. **129** was subjected to the previously optimized reaction conditions with four different unsaturated azides.

Synthesis of 2H-Pyrrols after remote Csp3 functionalization by iminyl radicals.
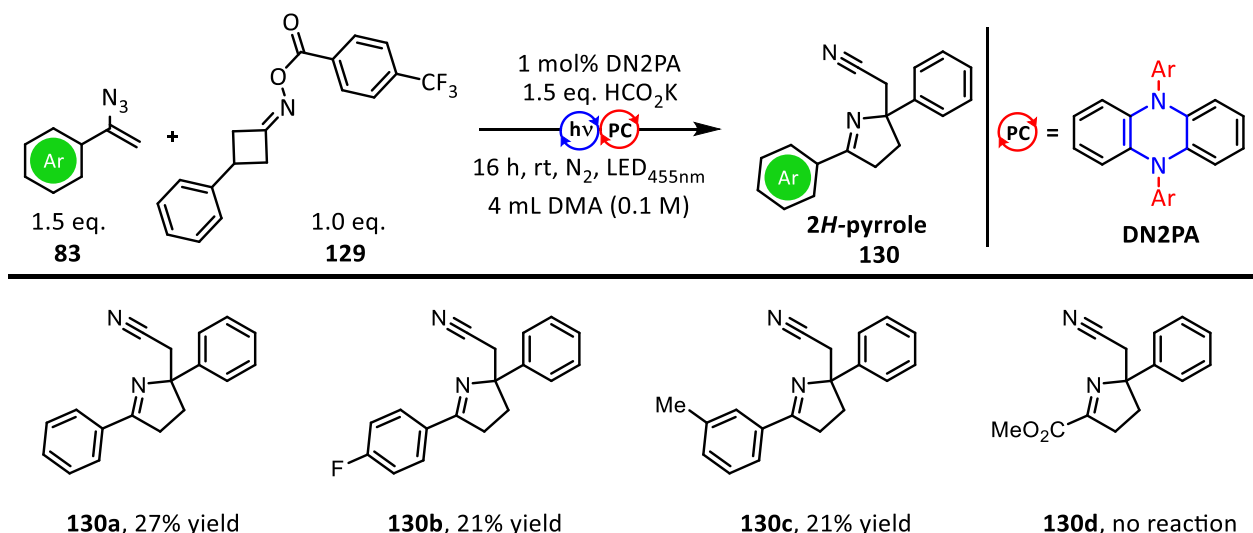
Figure 17: Substrate scope for the coupling of oxime esters to 1-azidostyrene

Isolated yields of 2*H*-pyrrole products **130** were low regardless of the substitution pattern of the unsaturated azide used. No ketone products could be isolated from any reaction. In case of the reaction with methyl 1-azidoacrylate no productive coupling between both reactants could be detected. The mechanism of this reaction proceeds as such: After an initial electron transfer from the catalyst to starting material **129**, the N-O bond homolytically cleaves to afford the first iminyl radical **131**. This radical reacts in a Norrish type reaction, releasing the ring strained stored in the cyclobutene ring and giving access to the primary radical **132**. This radical can then react with 1-azidostyrene **83a** to yield a second iminyl radical after dinitrogen extrusion (Scheme 45). After condensation of radical **132** with azidostyrene to the second iminyl radical **133** the mechanism proceeds as previously described (Scheme 38). Having illustrated this impressive radical cascade reaction involving two different modes of generation and reactivities for iminyl radicals, our attention turned to further diversify the scope of available substrates in hope of finding reactions with yields comparable to the optimized conditions.
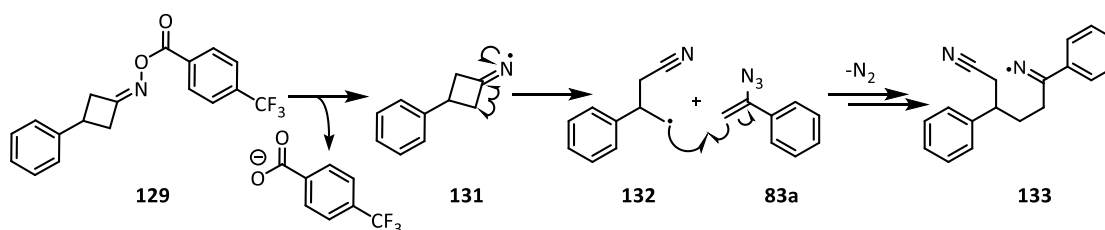
Scheme 45: Initial reaction steps towards product **133**.

3.5 Limits of the reaction

Having established two different ways of generating the desired iminyl radicals, the limits of the reaction's substrate scope were explored in depth. The scope of various already synthesized radical precursors (Scheme 39) was expanded by three additional derivatives: Two more phtalimide activated esters, both with benzylic C-H bonds in the relevant 1,5-HAT position (Scheme 46) were synthesized. Additionally, phenylmethanesulfonyl chloride **153** with α-benzylic C-H bonds was subjected to this protocol, to see if sulfur radicals are tolerated in this reaction.
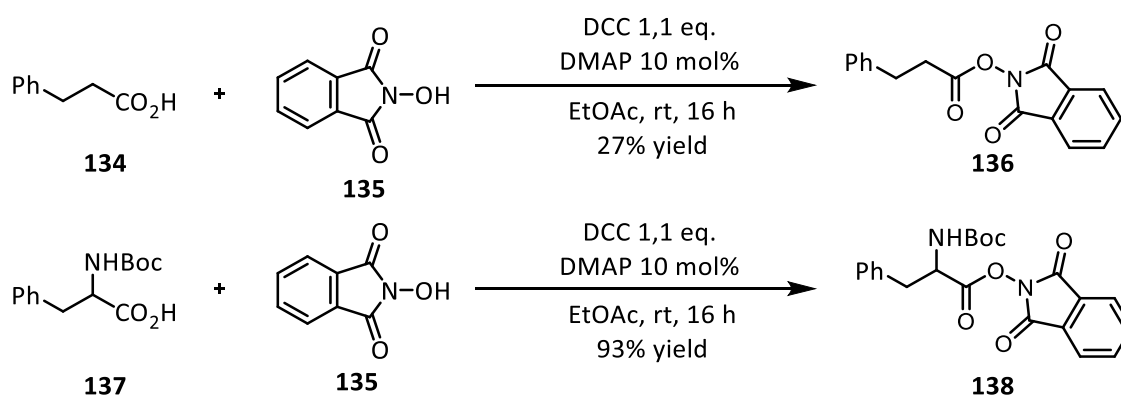
Scheme 46: Synthesis of additional carbon-centered radical precursors.

All available carbon radical precursors were tested using the previously optimized reaction conditions to investigate the available scope for this radical cascade reaction (Table 10).

Synthesis of 2H-Pyrrols after remote Csp3 functionalization by iminyl radicals.

Table 10: Unsuccessful radical precursors and isolated side products.
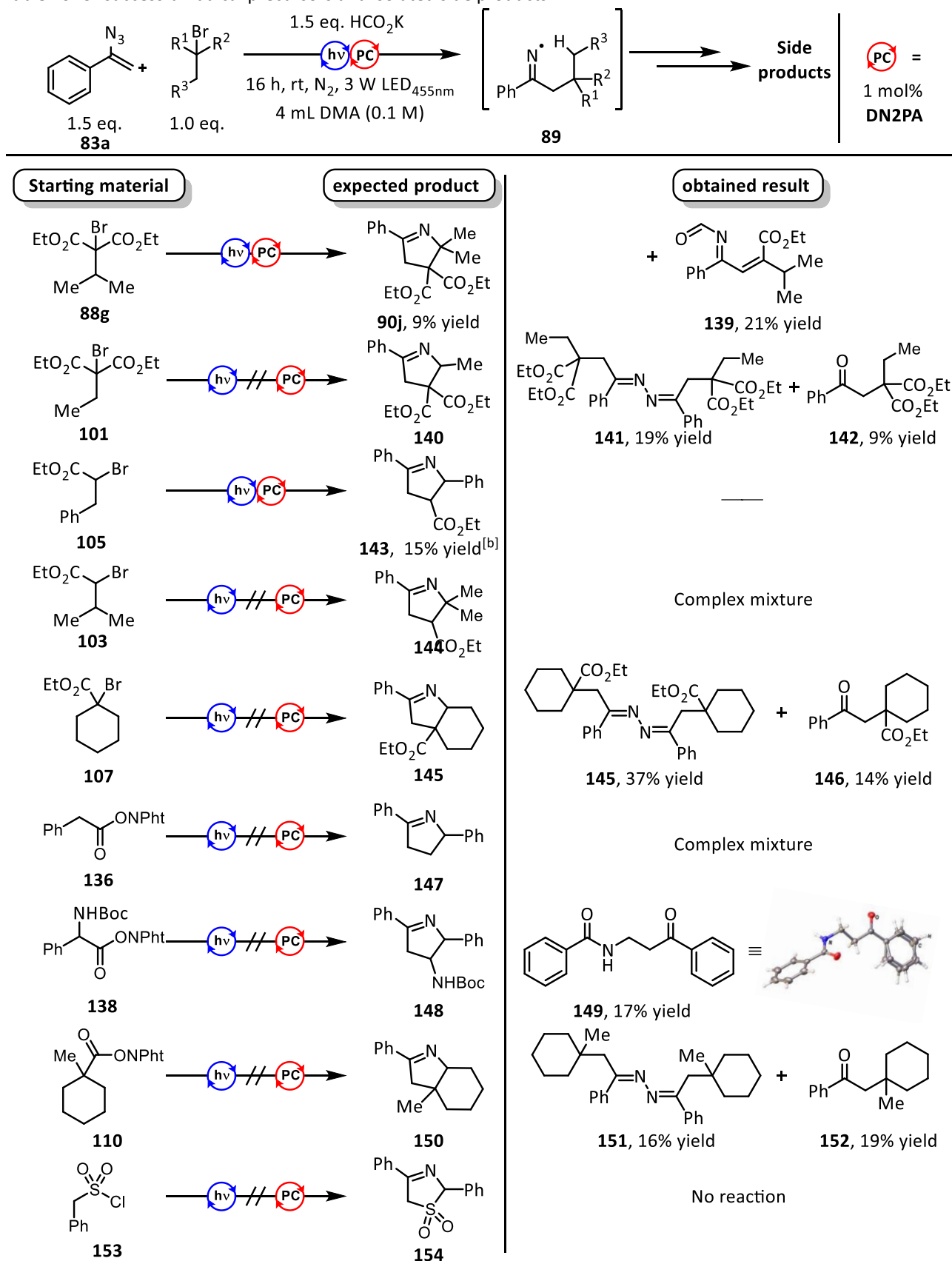
(a) Reaction conditions: 0.6 mmol **83a**, 0.4 mmol radical precursor. (b) Determined by ^{1}H-NMR analysis using 1,1,2,2-tetrachloroethane as internal standard.

Synthesis of 2H-Pyrrols after remote Csp3 functionalization by iminyl radicals.

The studies towards expanding the scope of radical precursors began by using various malonate derivates and varying the carbon center at which the 1,5-HAT takes place. Exchanging the benzylic position of the standard starting material **88a** with a tertiary carbon center dropped the yield dramatically to 9% isolated yield. However, the thus far unknown new side product ethyl (2Z,4Z)-4-(formylimino)-2-isopropyl-4-phenylbut-2-enoate **139** could be isolated from the reaction mixture in 21% yield. The mechanism, by which this unusual side product Is formed remains unknown to date. The structure of **139** was determined by NMR spectroscopy and mass spectrometry analysis.

Upon transition to a secondary carbon center (in **101**), dimerization of the iminyl radical intermediate was observed. After partial hydrolyzation during purification, ketone **142** is formed from the initial dimer product **141**. A combined yield of 28% was obtained for the radical dimerization products. Turning the focus to α-bromo ester derivatives, a benzylic carbon center was investigated first (compound **105**). The desired product ethyl 2,5-diphenyl-3,4-dihydro-2H-pyrrole-3-carboxylate **143** could be detected in the crude mixture in a low yield of 15% but was not isolated. A tertiary carbon center gave rise to a complex mixture of multiple products that could not be identified. A secondary carbon center (compound **107**) resulted in radical dimerization as observed before in compound **101**. Products of this reaction (**145**&**146**) had a combined yield of 47%, considerably higher than those of the malonate derivative. This indicates that not the generation of the initial carbon radical, but the coupling to 1-azidostyrene, or one of the subsequent reaction steps lead to a considerable loss in yield.

In order to study the impact of the electronic properties of the carbon-centered radical to the initial coupling to 1-azidostyrene, three different active esters (**110**, **136** and **138**) were investigated as precursors for electron rich carbon-centered radicals. While the active ester of Phenylacetic acid **136** gave rise to a complex reaction mixture, the active ester of *Boc*-protected phenylalanine **138** yielded the thus far unknown product **149** in 21% yield. The structure of product **149** has been confirmed by NMR spectroscopy, mass spectrometry and X-ray crystal structure analysis. The mechanism by which product **149** could have been formed was not investigated further. A secondary carbon in the 5-position of the iminyl radical led to the isolation of a combined yield of 35% of two products resulting from iminyl radical dimerization. Remarkably, the formation of these products confirms the presence of iminyl radical **89**, the same radical which was previously postulated by C. Nevado during the

formation of the corresponding ketones. However, the non-photocatalytic reaction conditions favored the formation of the corresponding ketone **99** in good yields and diastereoselectivites.[112] This highlights the enormous versatility of nitrogen radicals, and their ability to change reactivity depending on the reaction conditions utilized to generate it. The use of a sulfonyl chloride reagent **153** with an α-benzylic C-H functionality failed to give any productive coupling products with 1-azidostyrene **83a**.

3.6 Upscaling and product derivatization

To broaden the scope of applications, derivatizations of the isolated product were to be developed. To gain access to suitable amounts of product **90a** for derivatization reactions, the scalability of the developed reaction was demonstrated. Since the reaction mixture is a suspension of HCO₂K in DMA and a considerable amount of dinitrogen is extruded during the reaction a flow-setup for continuous synthesis was unsuitable for the purpose of upscaling. Instead a new batch photoreactor with an internal volume of 40 mL was designed within our group (Figure 18).
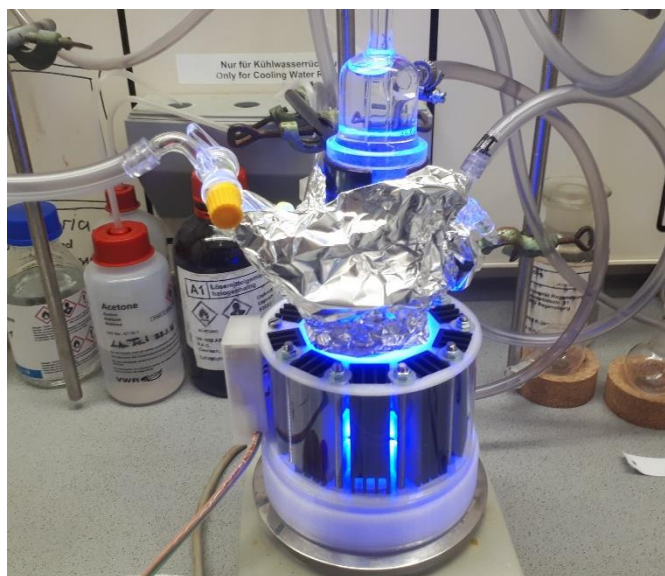
Figure 18: Batch reactor designed within the group of O. Reiser with an internal volume of 40 mL.

Irradiation was achieved by twenty 3 W LEDs, cooled by an air-flow setup. The reaction mixture was cooled by an internal cooling finger to keep reaction temperature constant at 23 °C. Building overpressure was vented through an attached bubbler, linked to the apparatus by a glass stopcock.
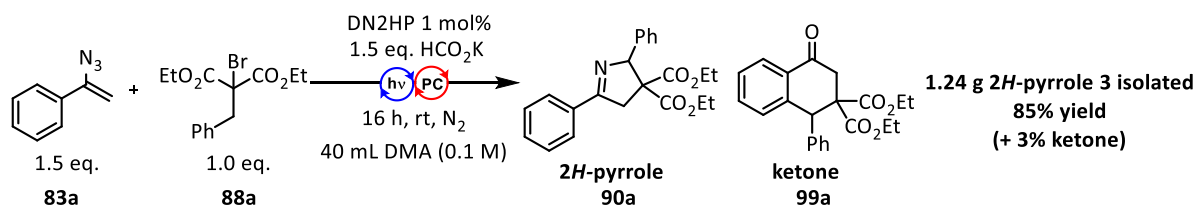
Scheme 47: Demonstration of the reaction scalability.

Gratifyingly, the standard reaction could be upscaled without encountering significant reaction problems. The yield of 85% of product **90a** compares well to the reaction screening result of 92% (Scheme 47). In both reactions a small amount of ketone side product **99a** was formed.

With a sufficient amount of isolated 2*H*-pyrrole in hand, various derivatizations were demonstrated. The synthesis of unnatural cyclic *β*-amino acids derivatives was of particular interest, since they can find many applications in medicinal and synthetic chemistry.[138]
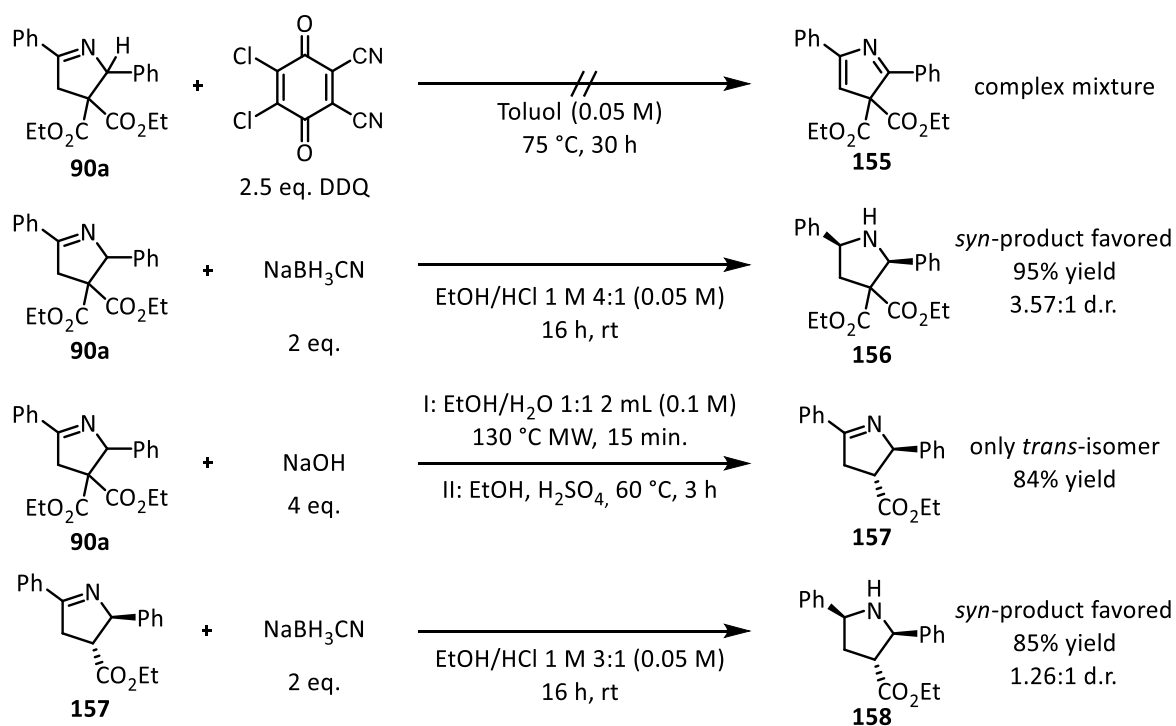
Scheme 48: Synthesis of various derivatives of standard product **90a**.

Synthesis of 2H-Pyrrols after remote Csp3 functionalization by iminyl radicals.

Following a literature report for the oxidation of similar 2*H*-pyrrols, an aromatization to a pyrrole derivative using 4,5-dichloro-3,6-dioxocyclohexa-1,4-diene-1,2-dicarbonitrile (DDQ) was attempted.[139] However, only a complex mixture could be observed. Direct reduction of **90a** to the pyrrolidine **156** proceeded in excellent yields with a diastereoselectivity of 3.57:1 towards the *syn*-diastereomer. Pleasingly, decarboxylation of **90a** yielded only one diastereomer, which was identified to be the *trans*-diastereomer in 84% yield. **157** could not be isolated as free carboxylic acid, and severe loss of product during isolation occurred that could not be avoided. As such, the free carboxylic acid was immediately esterified with ethanol to obtain **157**, which in turn could be easily isolated. Using the hydrogenation protocol established earlier for the hydrogenation of **90a**, the unnatural cyclic β-amino acids **158** was obtained in a 1.26:1 diastereomeric ratio favoring the diastereomer in which both phenyl groups are *syn* oriented. Configuration of products was determined by careful analysis and comparison of COSY- and NOESY-spectra.

3.7 Mechanistic discussion

The mechanistic discussion for this family of organic photoredox catalysts is still ongoing.[130,133,140] This class of catalysts has been of high interest for applications in organic atom transfer radical polymerization reaction (oATRP), but has also found applications in small molecule activation.[141] While the groups of Prof. G. Miyake and J. Orr-Ewing are mainly debating about whether the singlet catalyst (^{1}PC) or the triplet catalyst (^{3}PC) are the active species responsible for SET processes, the Königs group proposed a novel catalyst mechanism (Scheme 49, a and b).[140]
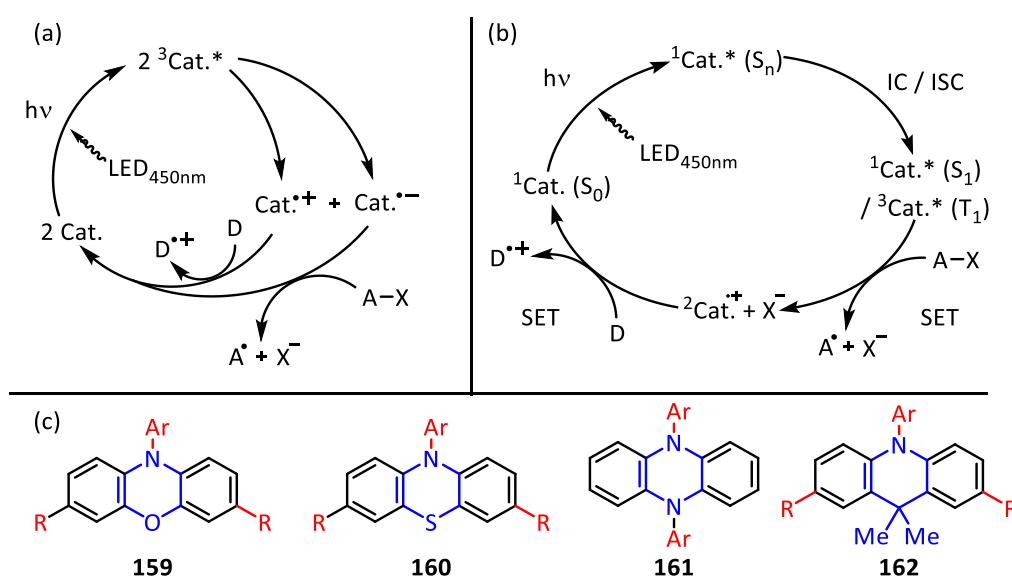
Scheme 49: (a) Mechanism as proposed for phenoxazine catalysts by König *et. al.* (b) Mechanism as proposed by Miyake/Orr-Ewing *et. al.* (c) Catalysts investigated in literature for oATRP reactions.

Based on results obtained from transient spectroscopy, König and co-workers discovered that the investigated phenoxazine catalyst 3,7-di([1,1'-biphenyl]-4-yl)-10-(naphthalen-2-yl)-10*H*-phenoxazine (DBN2PO) formed radical cations and anions in the absence of available quenchers. Ultimately, this led to the formulation of a dissociation mechanism, in which two excited photocatalyst molecules dissociate into a radical anion and radical cation upon collision. This could be rationalized by the exceptionally long lifetimes of the triplet state catalyst (^{3}Cat* (T$_1$), lifetime up to τ = 1 ms) allowing for the occurrence of ^{3}Cat* (T$_1$) collisions. The radical anion was found to catalyze the initiation step for the *in situ* formation of fluorophosgene the group was investigating.[140] Curiously, the addition of the reductive

quencher NEt_3 was necessary to intercept catalyst radical cations, regenerating them in the process (Scheme 49, a).[140]

In contrast to these results, the group of Orr-Ewing and co-workers analyzed two different dihydrophenazine catalysts using ultrafast time-resolved spectroscopic methods and reported an oxidative quenching cycle as mechanistic driving force. Notably, Orr-Ewing *et al.* discovered that the excited catalyst singlet state ($^1Cat^*$ (S_1)) and not the triplet state ($^3Cat^*$ (T_1)) was the main contributor to most single electron transfer (SET) events to alkyl halides.[130] In line with the theory, the S_1 state of catalyst was found to have an higher reductive potential than the corresponding T_1 state. Research by the group of Miyake an co-workers, highlighting this class as a whole (Scheme 49, c), has proposed the T_1 state to be the main contributor to SET reactions, due to the long lifetimes of the triplet state (Scheme 49, b).[128,129,131–133] Applying this knowledge to the reaction, the initiation step can proceed *via* multiple reactions pathways.
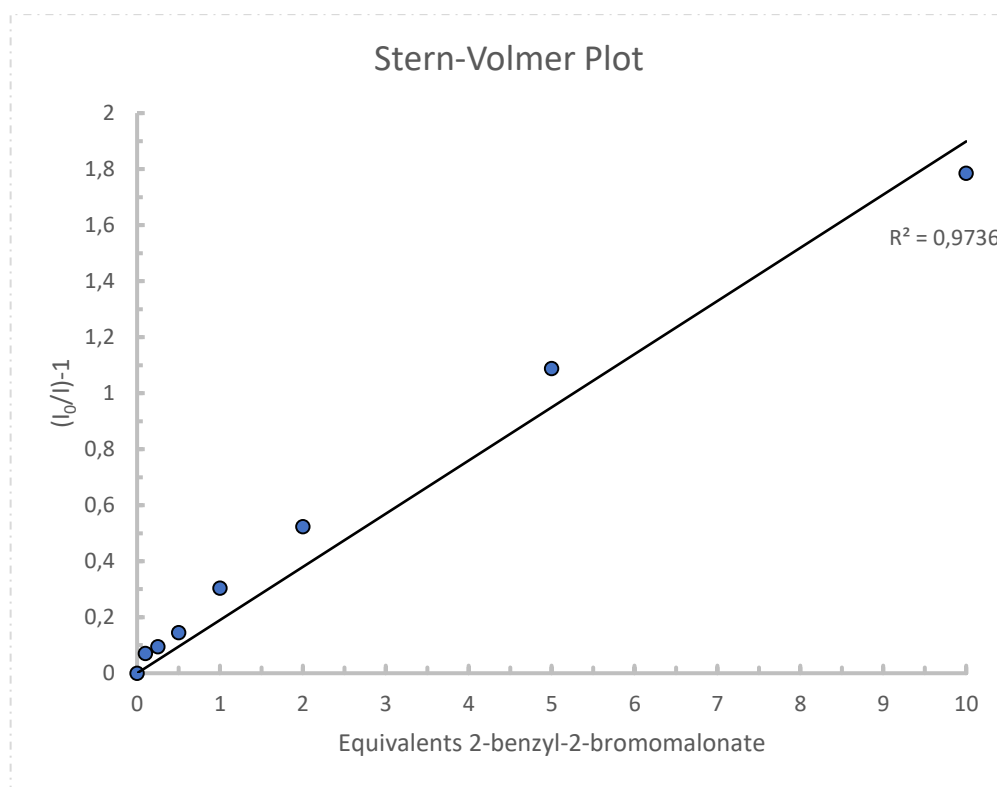
Figure 19: Stern-Volmer plot of DN2HP quenching with 2-benzyl-2-bromomalonate.

A Stern-Volmer plot displayed a diffusion-controlled quench of the phenazine catalyst emission by 2-bromo-2-benzyl-malonate **88a**. This allowed for the assumption, that due to a direct interaction between the excited catalyst and **88a**, an oxidative quenching cycle is operating in this reaction (Scheme 49, b). For a dissociative mechanism (Scheme 49, a), no effect of either reactant on catalyst emission combined with an increase in excited state lifetime with reduced catalyst concentrations would have been expected and in fact, such a behavior was reported by the Königs group.[140]

At the same time, 1-azidostyrene **83a** had no effect on DN2HP emission. Contrasting this to the metal-based catalysts employed at the start of the project, literature reports emission quenching of aforementioned catalysts by various unsaturated azides, subsequently forming nitrenes.[113,126,127,142] The absence of excited catalyst quenching by unsaturated azides might be rationalized by a reaction of the quencher 2-bromo-2-benzyl-malonate **88a** with the singlet state catalyst $^1Cat^*$ (S_1) without the catalyst entering the triplet state, or an inability of $^3Cat^*$ (T_1) to sensitize unsaturated azides. Thus, the initial reaction step was deemed to be the creation of radical **90** (Scheme 50) by SET with the excited catalyst.
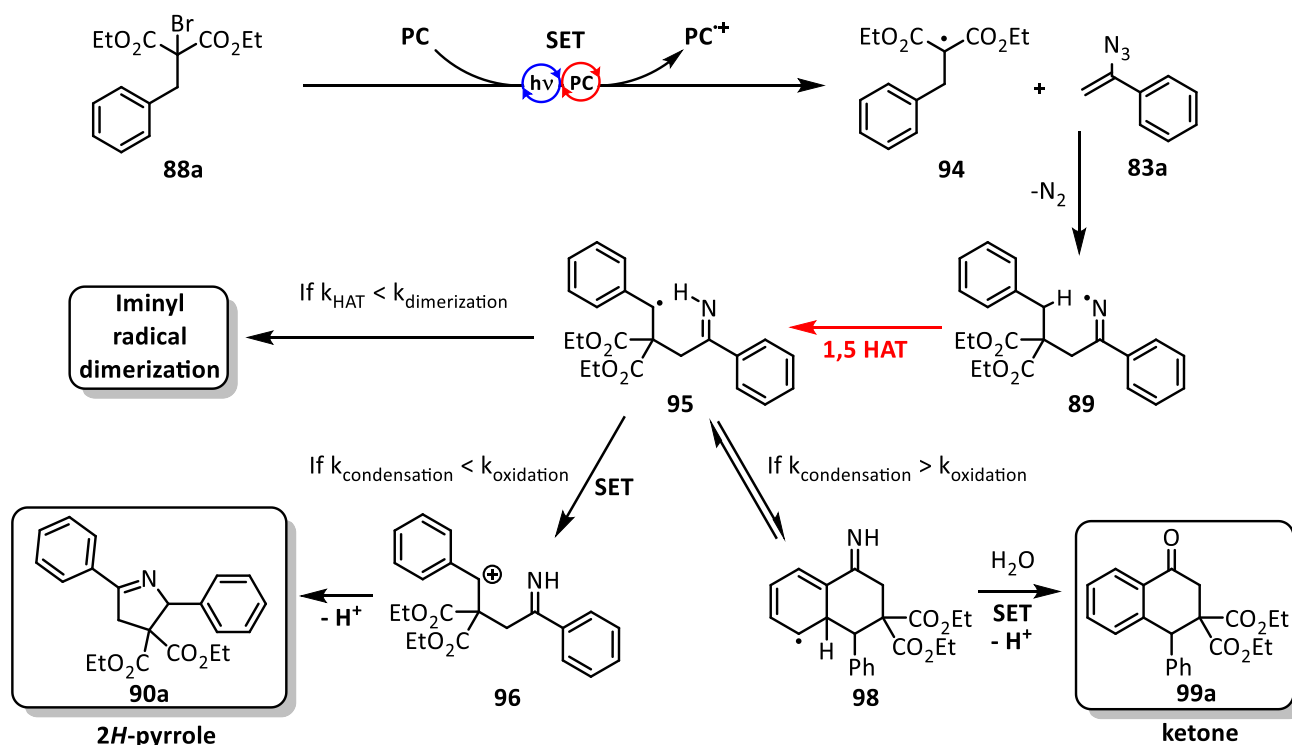
Scheme 50: Mechanistic proposal for the photocatalyzed reaction of 2-benzyl-2-bromomalonate **88a** with 1-azidostyrene.

Synthesis of 2H-Pyrrols after remote Csp3 functionalization by iminyl radicals.

After the cleavage of the electron deficient C-Br bond of **88a** by an excited DN2HP molecule through SET, the carbon-centered radical **94** is created. This radical can consequently react with 1-azidostyrene **83a** to form the iminyl radical **89** after nitrogen extrusion. The aforementioned iminyl radical is able to partake in a 1,5-HAT to a benzylic C-H functionality, initially part of 2-benzyl-2-bromomalonate **88a**, to yield the radical **95**. However, if radical dimerization of iminyl radical **95** is faster than the 1,5-HAT, radical dimers and their hydrolysis products are obtained. This has been demonstrated for non-benzylic C-H functionalities in 5-position to the iminyl radical (Table 10). The benzylic radical **95** allows for an attack of the phenyl ring in 6-position, giving rise to the reactive intermediate **98**. Intermediates such as **98** are considered to be strongly reducing and acidic, since the resulting product leads to re-aromatization and, after subsequent hydrolysis of the imine group, to the ketone **99a**. Alternatively, if oxidation of the benzylic radical **95** is favored kinetically, the benzylic cation **96** gives rise to 2*H*-pyrrole **90a** after cleavage of a proton from the iminyl group. Considering the results of the base screening for this reaction (Table 9), it is unknown at this point in time how the addition of the redox-active potassium formiate favors the formation of 2*H*-pyrrole **90a** over ketone **99a**, especially since the redox-active organic base diisopropylethylamine (DIPEA) failed to give **90a** in good yields (26%), while the inorganic base K_2HPO_4 yielded a mixture of **90a** and **99a** in a combined yield of 99%, albeit in a 1:1 product mixture.

3.8 Conclusion and Outlook

In summary, a protocol for the visible light mediate formation of 2*H*-pyrrole **90a** from 2-benzyl-2-bromomalonates and unsaturated azides in good yields has been developed. The mechanism involves a radical cascade including a site selective C-H functionalization of an *in situ* generated iminyl radical. Illustrating a unique advantage of organic photocatalysts over metal-based ones, the ability of organic catalysts to tolerate substrates prone to triplet sensitization has been demonstrated. A critical role of formiate salts for yield and selectivity in this reaction have been uncovered, however the exact function of the inorganic salt in this reaction is yet to be determined at this point. Regarding derivatizations, a necessity for a benzylic group in the 5-position of the created iminyl radical due to kinetic constraints has been discovered. However, derivatizations at the necessary benzyl core were well tolerated. Additionally, various unsaturated azides have been shown to be suitable coupling partners in this reaction. As part of an overarching goal to broaden the substrate scope additional non-styrene based unsaturated azides need to be explored. Furthermore, the up-scalability to multi-gram scale reactions and the applicability of the obtained products in diastereoselective decarboxylations and subsequent hydrogenations to obtain separable diastereomers of cyclic β-amino acids have been demonstrated in good yields.
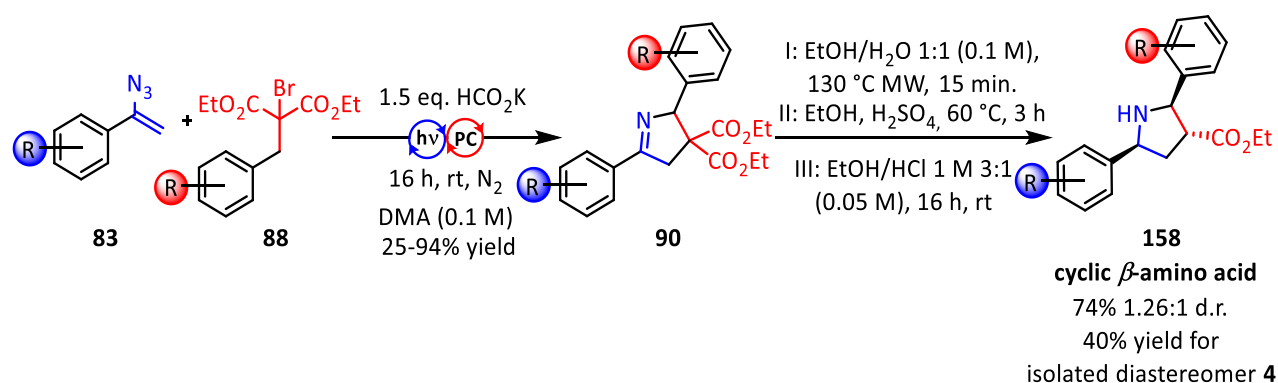
Scheme 51: Synthesis of 2*H*-pyrroles by a radical cascade reaction, and product application.

In future, more non-styrene based unsaturated azides should be explored to further broaden the substrate scope and demonstrate the versatility of this reaction cascade. Additionally, substituents on the benzylic position of 2-benzyl-2-bromomalonate **88** can be introduced to give access to more derivatives.

4 Photocatalyzed [2+2] additions of olefins

This chapter has been published:

S. K. Pagire, A. Hossain, L. Traub, S. Kerres, O. Reiser, Chem. Commun. **2017**; DOI: 10.1039/C7CC06710K. This work has been featured as a cover page of a journal.

The manuscript was prepared by S. K. Pagire and O. Reiser

4.1 Introduction

Cyclobutanes are strained four-membered cycloalkanes, found in various natural products, and formed most often by photocatalyzed [2+2] processes.[12] Naturally occurring cyclobutanes find diverse applications, displaying a variety of biological activities such as antitumor, antibacterial, antimicrobial, antifungal, and immunosuppressive properties.[143] Such compounds can mostly be found in fungi, insects and microbial species and have been of great interest in medical and pharmaceutical chemistry.[144] In regard to chemoselectivity of [2+2] cycloadditions of various alkenes either *head-to head*-isomers or *head-to-tail* regioisomers can be formed. In case for the dimerization of cinnamates the products are of interest for their biological activities.[145] Derived from truxinic or truxilic acid, compounds such as Endiandrin A, Magnosaline, Piperarborenine D, Incarvillateine and Dipiperamide B have been found to be bioactive compounds and hence found various applications (Figure 20).[146]
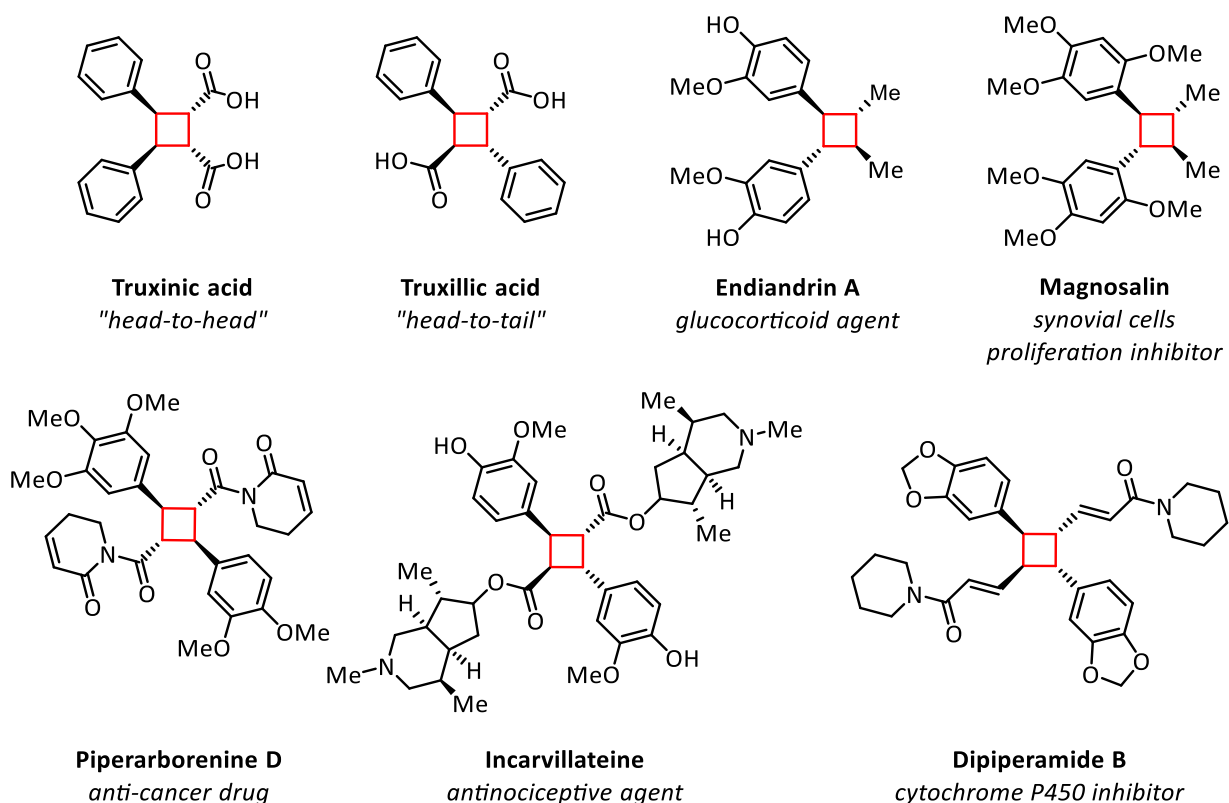
Figure 20: Selected examples of bioactive cinnamate and styrene dimer derivatives

While thermal [2+2] additions are rare but known, photochemical [2+2] cycloadditions have enjoyed a steadily growing interest within the synthetic community.[7,147] Photodimerizations and intramolecular [2+2] photocycloadditions require the use ultraviolet (UV) light to excite an unsaturated compound to an elevated electronic state and trigger the subsequent cycloaddition to another olefin. This leads to the formation of a variety of different isomers, since the orientation of two alkenes during cycloaddition is not predetermined. From a synthetic chemist's viewpoint, it is challenging to obtain cyclobutanes derived from two alkenes in a regio- and diastereoselective manner.[148,149] A severe disadvantage of [2+2] cycloadditions driven by UV light are side reactions (*e.g. Norrish Type I & II* reactions) enabled by excitation of olefins into higher electronic states by highly energetic UV light, which can severely harm the functional group tolerance and thus limit the available substrate scope.[150] In contrast, the use of visible light *via* photocatalytic systems has been established as a benign method to access alkene [2+2] products.[126] This method of activation can procced *via* two mechanistically distinct pathways: A single electron transfer from/to a suitable conjugated system initiates a radical condensation to cyclobutane ring structures, consequently followed by the regeneration of the catalyst to yield the desired product (Scheme 52, a).[1,9,83,151,152] Another way to catalyze cycloadditions not accessible by thermal reaction is by exploiting the

long lived triplet energy state of a metal based catalyst, attainable through the absorption of a photon in the visible spectrum of light and internal conversion processes to facilitate the direct transfer of energy to an olefin with an lower triplet energy state.[6,153,154] (Scheme 52, b). Due to the fast radiation-less decay of linear excited alkenes through *E/Z*-isomerization or related processes, the [2+2] cycloaddition of alkenes by triplet sensitization is most successful for intramolecular alkenes, or alkenes locked in carbocycles.[155]
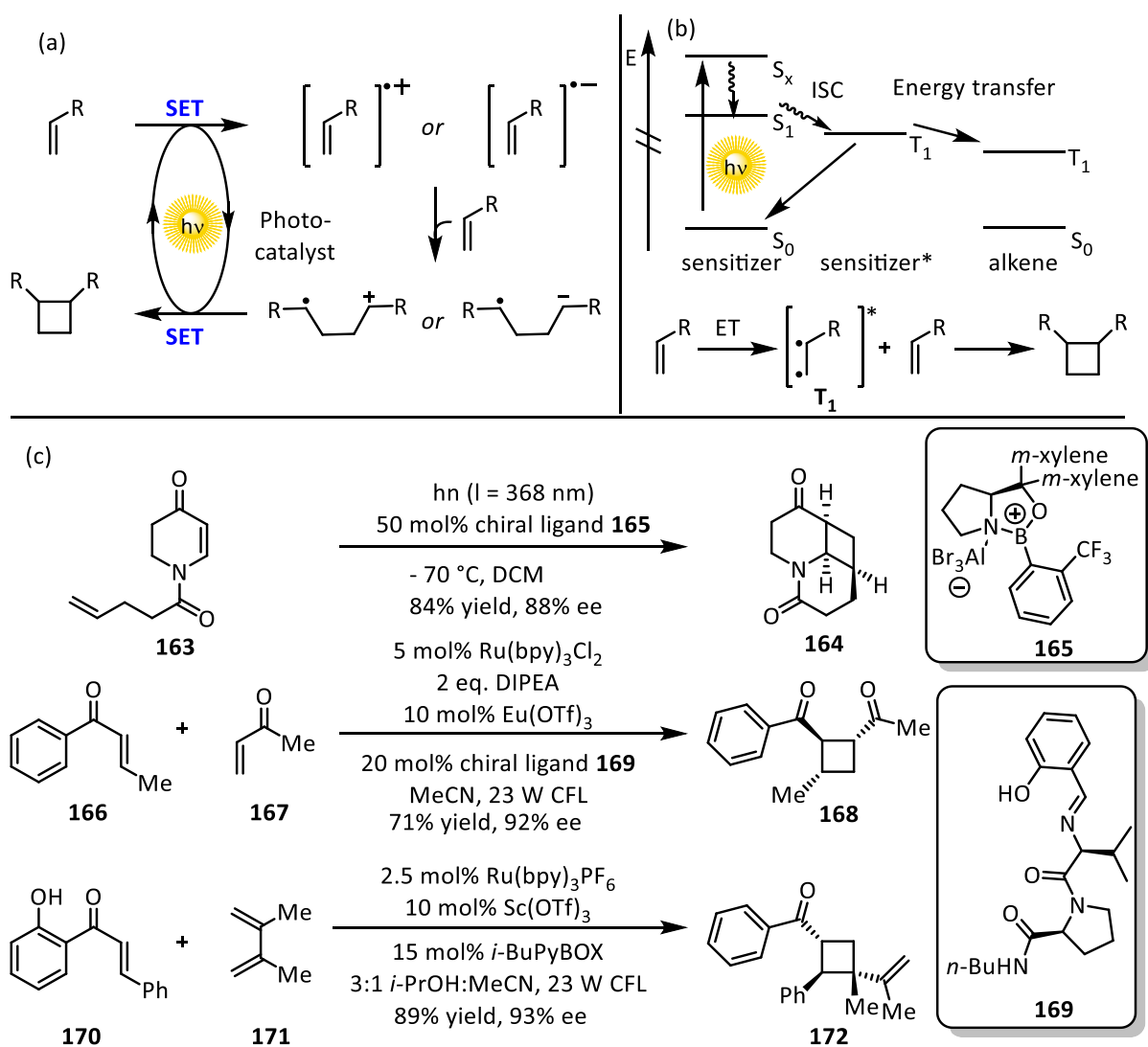
Scheme 52: (a) [2+2] cycloaddition facilitated by photoredox catalysis. (b) [2+2] cycloaddition facilitated by energy transfer. (c) selected examples for asymmetric [2+2] cycloadditions.

All three photochemical synthesis pathways for cyclobutanes (UV light, photoredox catalysis and energy transfer) have their own unique advantages and disadvantages, and their synthetic applicability has been demonstrated with challenging asymmetric reactions in good yields and stereoselectivities.[156] A wide range of cyclobutane derivates have been made accessible

starting from various alkenes by these method.[7,157] Curiously, despite the progress made towards cyclobutane derivates, dimerization of cinnamates and styrenes remain scarce.[7,158] This is partly due to the efficiency with which cinnamates and styrenes undergo *cis/trans*-isomerization in liquid phase, a characteristic emphasized by their use as UV-B absorbers in cosmetic sunscreens.[159] So far, in order to realize [2+2] cycloadditions of cinnamates and β-acrylic derivatives, the unsaturated reaction centers required tethering by covalent or non-covalent means to increase the likeliness of an [2+2] event by spatial proximity.[160] Highlighting the importance of experimental setup in UV light reactions, Beeler and co-workers have achieved the dimerization of cinnamates in a UV flow setup. Additionally, the addition of catalytic amounts of thiourea catalyst improved selectivity for the δ-truxinate isomer (d.r. 75/25).[161]

With the dimerization of cinnamates and styrenes several stereochemical considerations are necessary: The differentiation between *head-to-head* and *head-to-tail* orientation leads to two different constitutional isomers. *E/Z*-isomerization of monomers before undergoing dimerization leads to a variety of possible structural and stereochemical outcomes.[149] One way to solve this problem are the aforementioned tethering techniques to control the diastereoselectivity by controlling spatial orientation of the substrates.[162] Another way to control the diastereoselectivity and, more importantly, also the enantioselectivity of such reactions is the addition of chiral ligands in tandem with lewis acids such as Europium or Scandium triflate salts (Scheme 52, c). Lastly, Yoon *et al*. have recently achieved good diastereomeric ratios by using a Brønsted acid approach in tandem with cleavable auxiliary imidazole groups to lower the high triplet energy of the cinnamate coupling partner in an triplet sensitized reaction.[157]

4.2 Initial findings

The initial reaction was discovered by S. K. Pagire during his investigations into the chemistry of α-bromo cinnamates under photocatalytic conditions.[163] While investigating the generation of reactive vinyl radicals through an energy transfer processes in the presence of oxygen and their subsequent radical cascade reactions (Scheme 53, a),[164] a control experiment revealed a peculiar and unexpected result: The formation of [2+2] cycloadducts (Scheme 53, b).
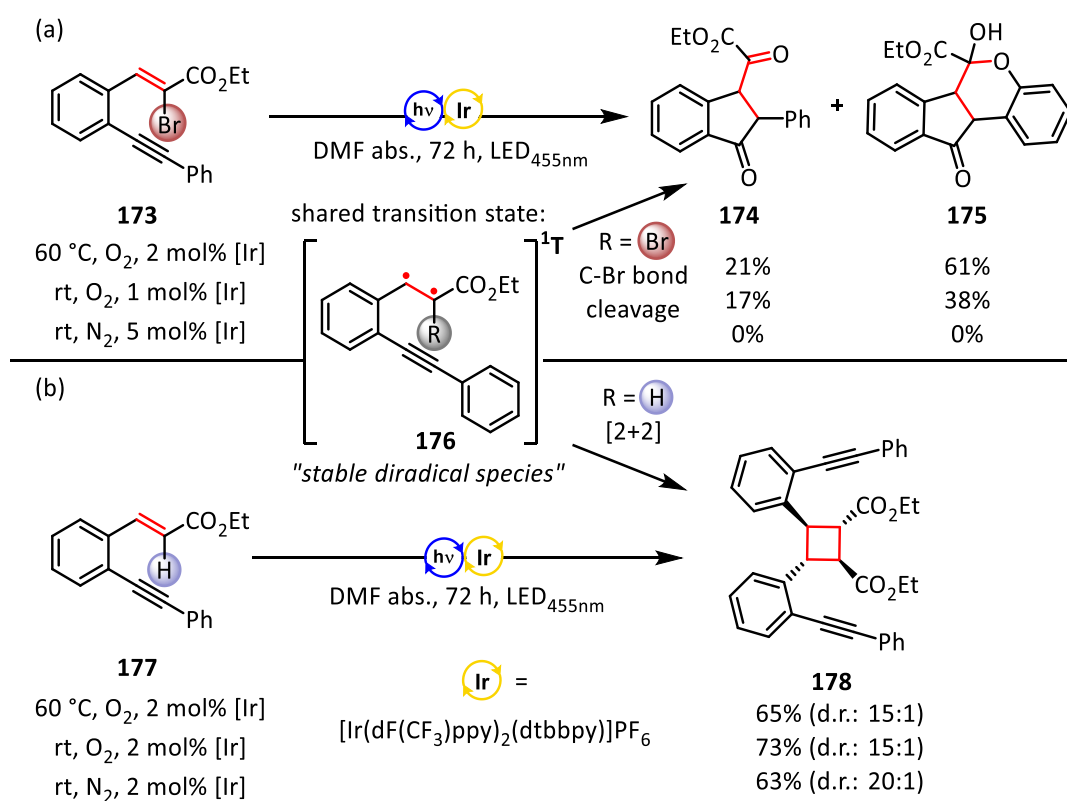
Scheme 53: (a) Vinyl radical generation through energy transfer. (b) [2+2] cycloaddition of cinnamates by energy transfer. Reactions were carried out by S. K. Pagire.

Energy transfer from the excited $[Ir(dF(CF_3)ppy)_2(dtbbpy)]PF_6$ ([*F*-Ir]*) catalyst to the cinnamate derivatives **173** or **177** gives rise to the triplet state **176**, an excited state that can be described as "stable diradical state". The presence of a halogen bond in intermediate **176** will lead to cleavage of the weak C-Br bond, while molecular oxygen O_2 is present in solution. The resulting vinyl radical can participate in a plethora of reactions,[165] although in this case a radical cascade mechanism involving molecular oxygen ultimately leads to products **174** or **175**, depending on the electronic properties of the substrate. Notably, due to the competitive

E/Z-isomerization relaxation mechanism of **176** to starting material(s) **173/177**, long reaction times were necessary and solely the isomerization of starting material **173** was observed under inert atmosphere with 5 mol% [*F*-Ir]. It was discovered, that the cyclobutane derivative **178** is obtained in a good yield and diastereomeric ratio when no C-X bond was present in intermediate **177**, regardless of atmosphere or temperature. Curiously, the presence of a vinyl bromide group in the α-cinnamate position inhibited the [2+2] reaction of **177** under inert atmosphere. Unexpectedly, no intramolecular side-reactions of diradical **176** with the triple bond were observed in any conditions probed and the aforementioned photocatalyzed [2+2] pathway turned out to be the dominant pathway next to the relaxation through *E/Z*-isomerization.

We were delighted to see, that no literature had described such visible light catalyzed dimerization reactions of cinnamates to date.[7] Following this general principle, we set out to establish this reaction as convenient route to various truxinate derivatives, while also enabling the visible light catalyzed [2+2] reaction of styrenes and chalcones, thus improving on existing literature protocols (Scheme 54).

Previous work:

Scharf *et al.*:

179
Only tethered
cinnamates

toluene, 60 h, 125 W UV-lamp
hν (>305 nm)
89% yield, 4.9:1 d.r.

180
Diastereocontrol
by tethering

Beeler *et al.*:

Ar = 3,5-C$_6$H$_3$(CF$_3$)$_2$

8 mol%

181
Only cinnamates

MeCN, 8 h, 500 W UV-lamp
hν (>305 nm)
40-80% yield, 1:1-4:1 d.r.

182
8 examples

This work:

[Ir(dF(CF$_3$)ppy)$_2$(dtbbpy)]PF$_6$

DMF abs., 72 h, 3 W LED$_{455nm}$
11-99% yield, 1:1 - 99:1 d.r.

183
cinnamates
styrenes
chalcones

184
30 examples
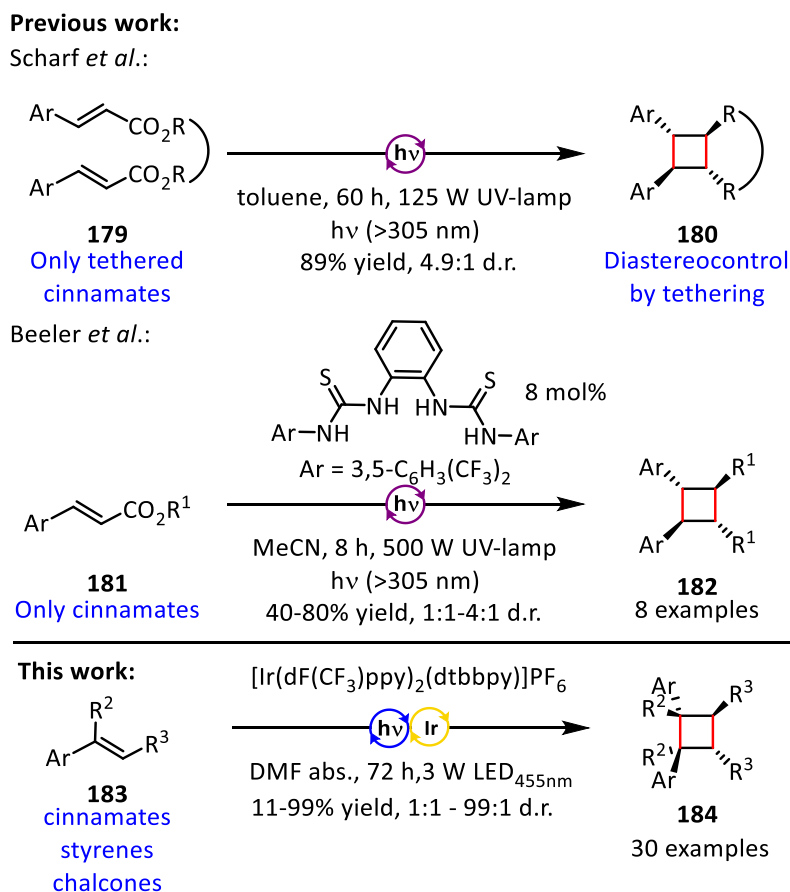
Scheme 54: Established methods for the photodimerization of cinnamates.

The aforementioned activation of cinnamates by energy transfer is especially interesting, since the activation of such substrates by single electron transfer (SET) is unfeasible. The redox potential of conjugated esters is out of range of most photocatalysts (approx. -1.79 V vs SCE) for one electron reductions.[2,166] As such, the use of photocatalysts with long triplet state lifetimes and high triplet state energies was paramount. Hereby, the triplet state energy of the catalyst defines the range of substrate available for activation by energy transfer, while the lifetime of the catalyst increases the likelihood of energy transfer events occurring in solution.[167]

4.3 Reaction screening

Following these underlying principles, the hypothesis was formed, that [Ir[dF(CF$_3$)ppy]$_2$(dtbbpy)](PF$_6$) with an excited state lifetime of τ = 2300 ns and a triplet state energy level of 61.8 kcal/mol should be the most suitable photocatalyst for a sensitization reaction.[168]

Table 11: Reaction screening for the synthesis of δ- and β-truxinates.
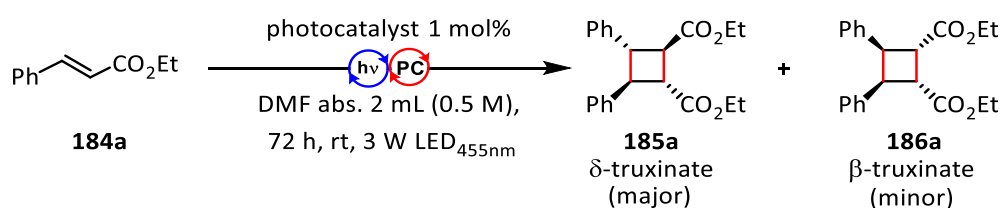
entry	catalyst [1 mol%]	atmosphere	Yield [%]	d.r. [δ/β][b]
1	[Ir[dF(CF$_3$)ppy]$_2$(dtbbpy)](PF$_6$)	O$_2$	63	9:1
2	fac-[Ir(ppy)$_3$]	O$_2$	44	9:1
3	[Ir(ppy)$_2$dtbbpy](PF$_6$)	O$_2$	18	9:1
4	[Cu(dap)$_2$]Cl	O$_2$	traces	–
5	[Ru(bpy)$_3$]Cl$_2$	O$_2$	traces	–
6	[Ir[dF(CF$_3$)ppy]$_2$(dtbbpy)](PF$_6$)	N$_2$	96	9:1
7[c]	[Ir[dF(CF$_3$)ppy]$_2$(dtbbpy)](PF$_6$)	N$_2$	78	–
8	Rose Bengal, 530 nm	N$_2$	0	–
9	No catalyst	N$_2$	0	–
10[d]	[Ir[dF(CF$_3$)ppy]$_2$(dtbbpy)](PF$_6$)	N$_2$	0	–

[a]: Ethyl cinnamate **184a** 1.0 mmol, catalyst 1 mol%, DMF abs. 2 mL (0.5 M), 3 W LED$_{455nm}$, 72 h, r.t. [b] determined by 1H-NMR analysis [c] 0.5 mol% catalyst, 84 h. [d] no light. – = not determined. Optimization was performed by S. K. Pagire and A. Hossain.

We started our investigations with ethyl cinnamate under an oxygen atmosphere (Table 11). Pleasingly, a good initial yield of 63% for **185a/186a** could be achieved. Additional evidence for the initial hypothesis of an energy transfer mechanism was obtained by the reactions of fac-Ir(ppy)$_3$ (τ = 1900 ns, E$_T$ = 58.1 kcal/mol)[168] and [Ir(ppy)$_2$dtbbpy](PF$_6$) (τ = 557 ns, E$_T$ = 49.2kcal/mol) resulting in lower yields, in line with our expectations for catalysts with worse physical properties for an energy transfer mechanism. [Cu(dap)$_2$]Cl (τ = 270 ns) and [Ru(bpy)$_3$]Cl$_2$ (τ = 1100ns, E$_T$ = 49.0 kcal/mol) failed to give the desired product under an

oxygen atmosphere. Having identified a promising catalyst for the sensitization of cinnamates, the influence of inert conditions was investigated. Standard conditions under inert conditions (entry 6) gave the best overall yield in 96% in a 9:1 d.r.. While the absence of oxygen had no effect on the diastereomeric ratio, an increase in yield was observed. This was probably due to the fact that oxygen competes with cinnamate for sensitization, while not being able to react further under the given conditions. Lowering the catalyst loading to 0.5 mol% while increasing the reaction time to 84 h lowered to yield to 78%. Control reactions with the triplet sensitizer Rose Bengal under green light (530 nm) irradiation, no catalyst under blue light irradiation and [Ir(ppy)$_2$dtbbpy](PF$_6$) without irradiation gave no desired product **185a/186a**, thus demonstrating the necessity of a Iridium based photocatalytic system as driving force for this reaction (Table 11).

4.4 Substrate Scope: Cinnamates and Chalcones

With the optimized conditions at hand, we started to examine the substrate scope-of styrene and chalcone [2+2] photocyclizations. With a triplet state energy level of about 54.7 kcal/mol for cinnamate esters,[167] dependent on the substitution pattern, all derivatives should be available for sensitization by [*F*-Ir]. The *trans*-configured starting materials were synthesized by *Horner-Wadsworth-Emmons* reactions starting from corresponding aldehydes.[169] Long reaction times (72 h) were necessary to overcome the efficient *cis/trans*-isomerization of alkenes as main relaxation pathway for linear alkenes in an excited triplet state.

Figure 21: Substrate scope for [2+2] cycloadditions of cinnamates and chalcones
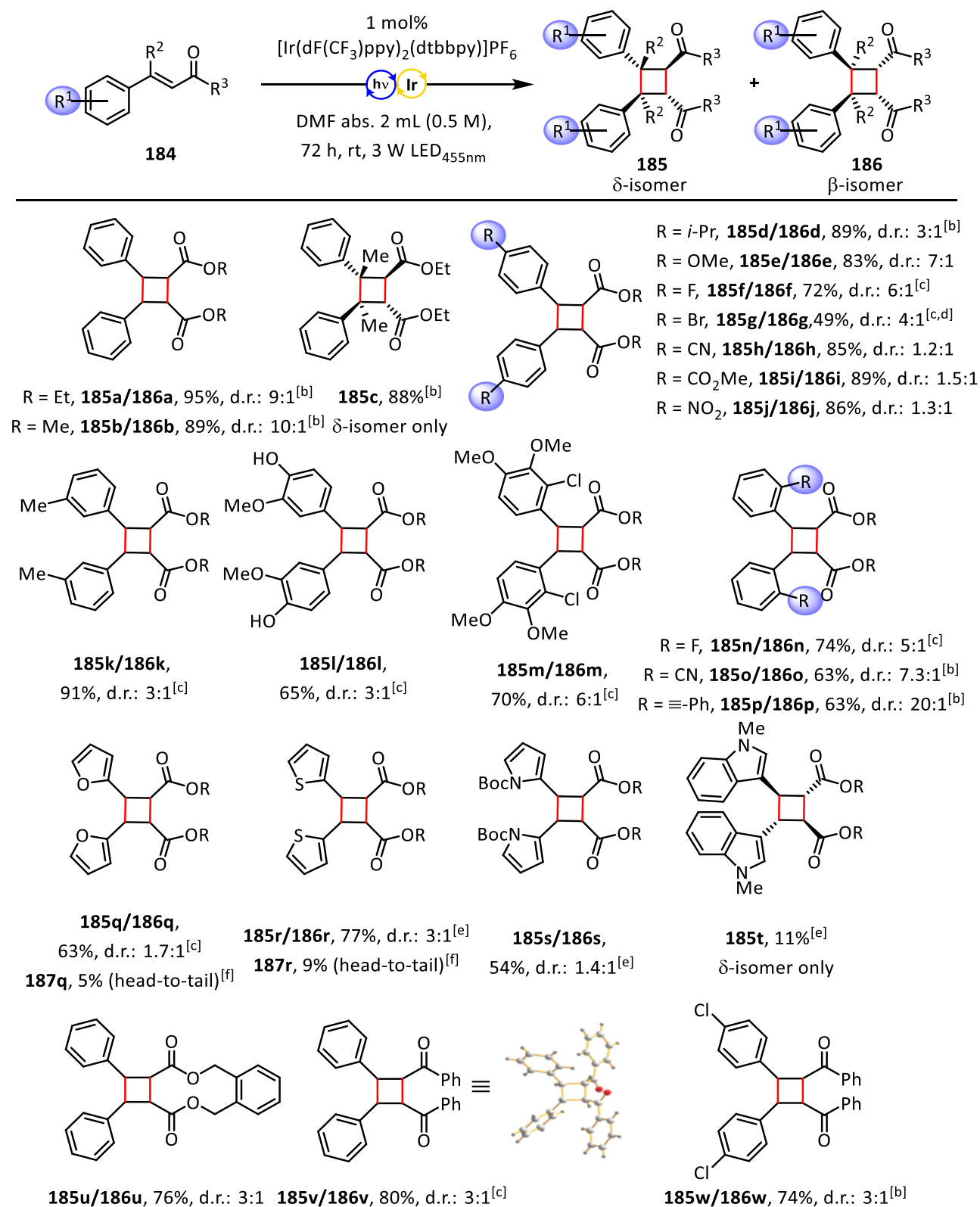
(a) Reaction conditions: substrate **184** (1.0 mmol), [Ir[dF(CF₃)ppy]₂(dtbbpy)](PF₆) 1 mol%, DMF abs. 2 mL (0.5 M), LED₄₅₅ₙₘ, rt, 72 h. (b) Prepared by S. K. Pagire. (c) Prepared by A. Hossain. (d) Reaction time 96 h (e) prepared by S. Kerres (f) Determined by ¹H-NMR analysis.

Photocatalyzed [2+2] additions of olefins

As an ideal approach to the substrate scope the effect of various ester groups was compared. Gratifyingly, methyl cinnamate afforded product **185b/186b** in 89% yield in good diastereoselectivity. As expected, this result was very similar to the result of the ethyl ester **184a** (96%, 9:1 diastereomeric ratio (d.r.)., Figure 21), and improved upon an example previously reported by Beeler *et al*. (60% yield, 4 :1 d.r., Scheme 54). The compatibility of methyl substitution in α-position of cinnamate **184c** was demonstrated by the synthesis of **185c/186c** as the only obtainable diastereomer in excellent yield. Strongly electron withdrawing substituents in *para*-position had a negative impact on the diastereoselectivity of this reaction (**184h**, **184i** and **184j**) , albeit while maintaining good yields. This was rationalized by a change in radical stability for the benzylic position in the relevant radical intermediate, influencing conformational equilibria (*c.f.* Chapter 4.7, Scheme 55)

Evaluating the impact of +M, +I and +M/-I effects from substituents in *para*-position, we were pleased to see that such substitution had no particularly negative influence on the diastereoselectivity of this [2+2] cycloaddition. While an isopropyl substituent led to the isolation of cycloadduct **185d/186d** in 89% yield in a 3:1 diastereomeric ratio. Similar results were obtained by methyl substitution in meta-position (**185k/186k**). An increase in +M effect led to better diastereoselectivites, regardless of the +/-I effect involved (**185e/186e** to **185g/186g**). Curiously, the disubstituted cinnamate **184l** only afforded **185l/186l** in a 3:1 diastereoselectivity, while three substituents gave rise to product **185m/186m** in a 6:1 d.r., both in good yields.

Considering the steric constraints imparted by substitutions in *ortho*-position, an increase in diastereoselectivity was observed from the comparatively small fluorine group (5:1 d.r.) to the sterically demanding *ortho*-tolane cinnamate derivative (**184n** to **184p**) that was initially investigated in this reaction (20:1 d.r.). A decrease in yield to 63-74% was observed and was explained by the steric effects of *ortho*-substitutions

Five membered heterocyclic cinnamate derivatives (**184q** to **184s**) gave good yields, although diastereoselectivites suffered when compared to other examples. It is noteworthy, that small amounts of head-to-tail products were observed in the ^{1}H-NMR spectra of crude product mixtures. An indole derivative led to the single isomer **185t** in 11% yield, demonstrating a limit of this method. An intermolecular example with a covalent tether led to 76% yield of **185u/186u**, however there was no observable positive effect on diastereoselectivity by tethering both unsaturated moieties together by an *ortho*-xylene group

Finally, chalcone derivatives were investigated (**184v** and **184w**). Chalcones are another class of α,β-unsaturated compounds that have rarely been successful in [2+2] reactions due to their fast *cis/trans*-isomerization processes and high triplet energy of approx. 54 kcal/mol.[153,170] Nevertheless, the protocol described herein was successful in the dimerization of two chalcones, giving access to the desired products **185v/186v** and **185w/186w** in good yields with a 3:1 d.r.. The δ-isomer **185v** could be crystallized and the supposed structure was confirmed by X-ray crystallography. The limits of this methodology could be demonstrated by the attempted dimerization of sulfone-, cyano- and nitro-substituted alkenes, which only afforded *E/Z*-isomerization of the starting materials. This indicated, that while triplet sensitization of the substrates by [Ir(ppy)$_2$dtbbpy](PF$_6$) was possible, relaxation by *E/Z*-isomerization was to efficient for any intermolecular [2+2] cycloadditions to take place.

4.5 Substrate Scope: Styrenes

Considering their uses as biologically active molecules, cyclobutanes derived from styrenes are of high interest in synthetic chemistry (*cf*. Figure 20). As such, we expanded our efforts in [2+2] photocyclizations by triplet sensitization to styrene derivatives. Previous reports on this reaction under visible light conditions either required intramolecular substrates or were limited to electron rich examples.[171] Considering the triplet excited state energy of styrenes (about 61.7 kcal/mol)[168] these substrates are at the very limit of what [Ir[dF(CF$_3$)ppy]$_2$(dtbbpy)](PF$_6$) (61.8 kcal/mol) is capable of activating by triplet sensitization mechanisms.
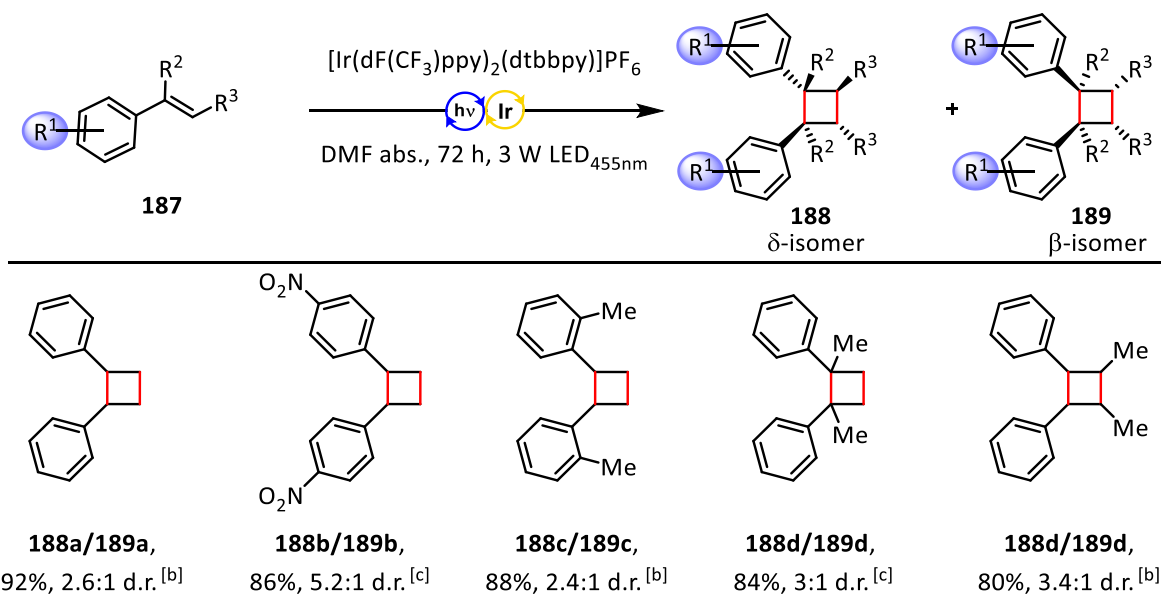
Figure 22: Scope of styrene [2+2] cycloadditions.

The feasibility of styrene sensitization by visible light catalysis was demonstrated by several edge cases. All cases gave good yields, regardless of substitution pattern. We were pleased to see that electron withdrawing group in *para*-position afforded product **$$b** in a good 5.2:1 d.r.. *Ortho*-, α- as well as β-methyl substitution produced comparable diastereomeric ratios of 2.4 to 3.4:1. In conclusion, we hereby demonstrated that our methodology is suitable for expanding the scope of [2+2] cycloadditions towards styrene derivatives.

4.6 2+2 Cross couplings

Research by various groups has highlighted the importance of unsymmetrical cyclobutanes.[172] The syntheses of such cyclobutanes is challenging, and a majority do not include [2+2] photocyclizations. Following this rationale, we set out to see if two electronically different cinnamates would allow for cross-coupling using our methodology in order to access unsymmetrical cyclobutane products.
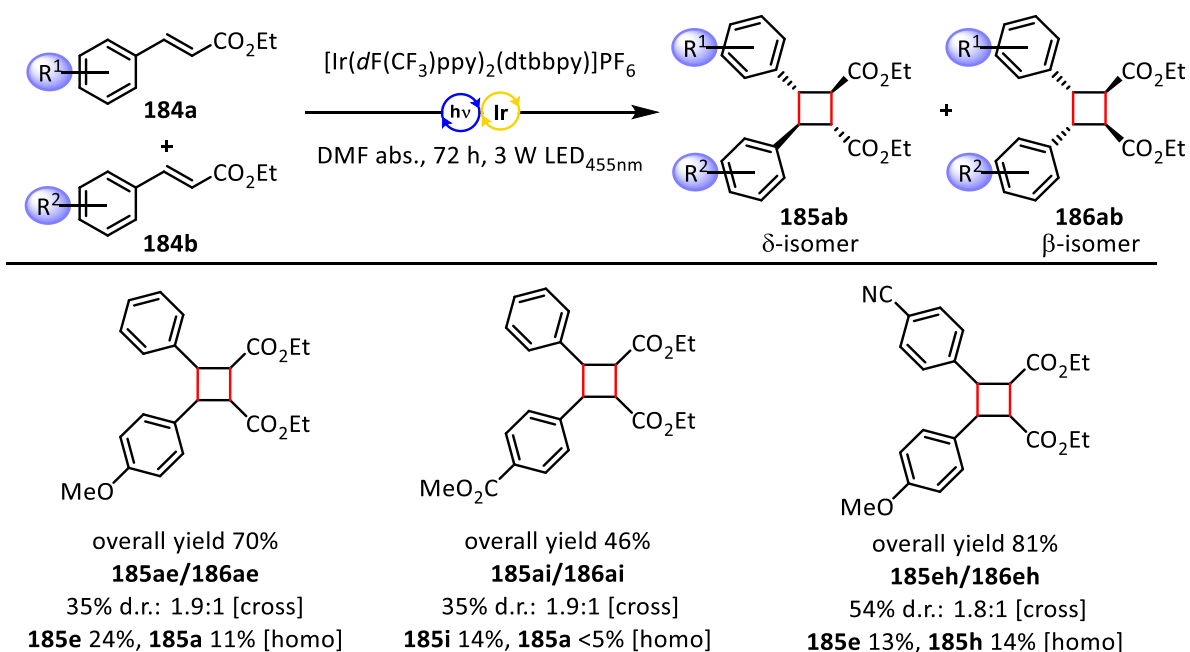
(a) Reaction conditions: substrate **184a** (0.5mmol), substrate **184b** (0.5 mmol) [Ir[dF(CF₃)ppy]₂(dtbbpy)](PF₆) 1 mol%, DMF abs. 2 mL (0.5 M), LED₄₅₅nm, rt, 72 h. d.r. were determined by ¹H-NMR or isolated products where applicable.

Figure 23: Cross coupling reaction for the [2+2] cycloaddition of different cinnamates.

Indeed, all cross-coupling products of two different cinnamates could be isolated from their corresponding reactions (Figure 23). However, only the cross-coupling reaction of an electronically rich with an electronically poor cinnamate displayed a slight bias towards cross-coupled over homo-coupled product. The d.r. of each cross-coupling product was similar to each other and in line with expectations.

4.7 Mechanistic discussion

In general, [2+2] cyclizations of conjugated alkenes have been realized with energy transfer as well as SET catalysis.[151,168] Considering the high redox potentials of cinnamate derivatives – being challenging to reduce or oxidize by most photocatalysts - we followed the rational proposed by Haag *et al.* for the dimerization of cinnamates by UV-light.[162] This includes the utilization of an activated cinnamate "diradical" triplet state (T_1), which is in turn accessed by an energy transfer mechanism.[173]

Photocatalyzed [2+2] additions of olefins
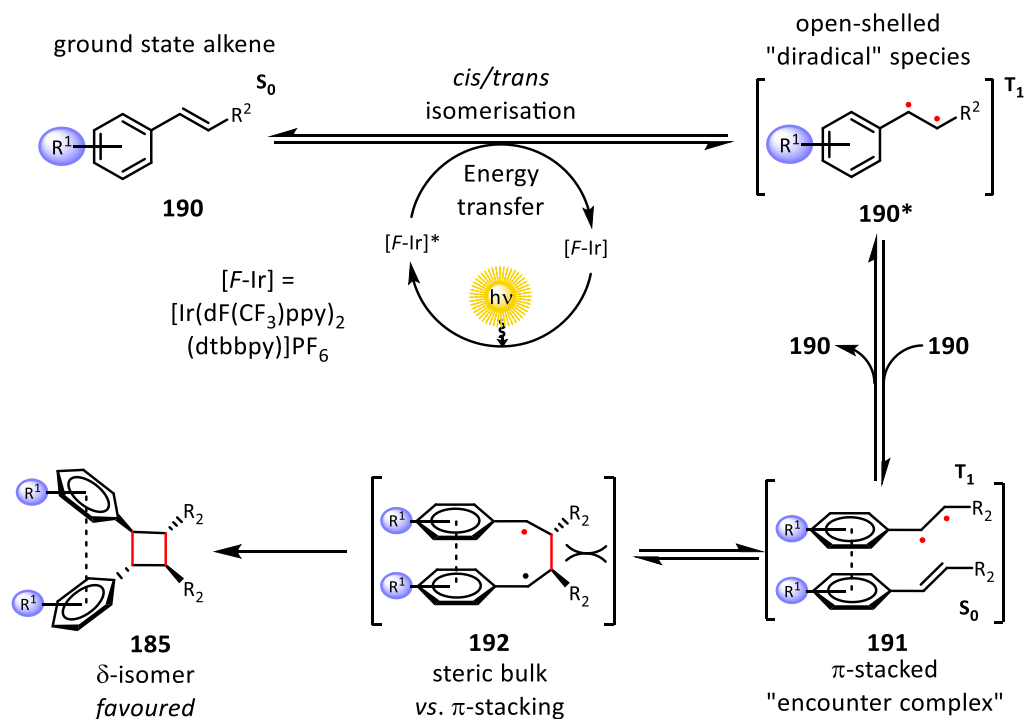
Scheme 55: Proposed reaction mechanism.

Absorption of a photon leads to excitation of the [Ir(dF(CF$_3$)ppy)$_2$(dtbbpy)](PF$_6$) (*F*-Ir) catalyst, followed by relaxation and ISC processes giving access to the T$_1$ state ([*F*-Ir]*) of the catalyst. Within its excited state lifetime (τ = 2200 ns) collision with substrate **190** can lead to an energy transfer event, giving T$_1$ **190*** and the ground state catalyst (*F*-Ir). **190*** can relax back to its ground state *via* a cis/trans mechanism (unproductive pathway) or form an "encounter complex" upon collision with a second **190** molecule. Since **190*** can be treated as diradical species, bond-formation in the α-position of cinnamate can occur, leading to the more stable benzylic diradical **191**. Within **191**'s lifetime bond rotations are possible, and a diastereomeric mixture between products **185/186** is formed (Scheme 55). As demonstrated in the substrate scope (Figure 21), electron-withdrawing substituents in *para*-position lead to a reduction in stereo control between the β- and δ-product. Since -M effects increase the C-H dissociation energy of benzylic C-H bonds, thus forming more reactive radicals,[40] it can be deducted that an decrease in lifetime through higher radical reactivity of intermediate **192** directly leads to lower diastereomeric ratios. This allows for the assumption, that the all-trans product selectivity (δ) is mainly determined by thermodynamic factors through minimization of steric strain. Following this rational, increasing the steric bulk in *ortho*-position leads to a higher lifetime of **192** and an increase in steric strain, thus increasing the selectivity towards the δ-isomer, which was in line with our experiments.

4.8 Conclusion

In conclusion, we were successful in expanding the existing scope and applicability for [2+2] photodimerizations under benign visible light conditions. For the first time, intermolecular dimerization of cinnamates, styrenes and chalcones was realized under such conditions, which gave access to a range of functionalized cyclobutanes in good yields and moderate diastereoselectivites. In addition, we have demonstrated the synthesis of valuable asymmetric cyclobutanes in moderate yields by combining two cinnamates of suitable electronic properties. Finally, isolated product **186l** has been shown to be a crucial intermediate for the formal synthesis of the lignan natural product (±)-Tanegool.[7,174]
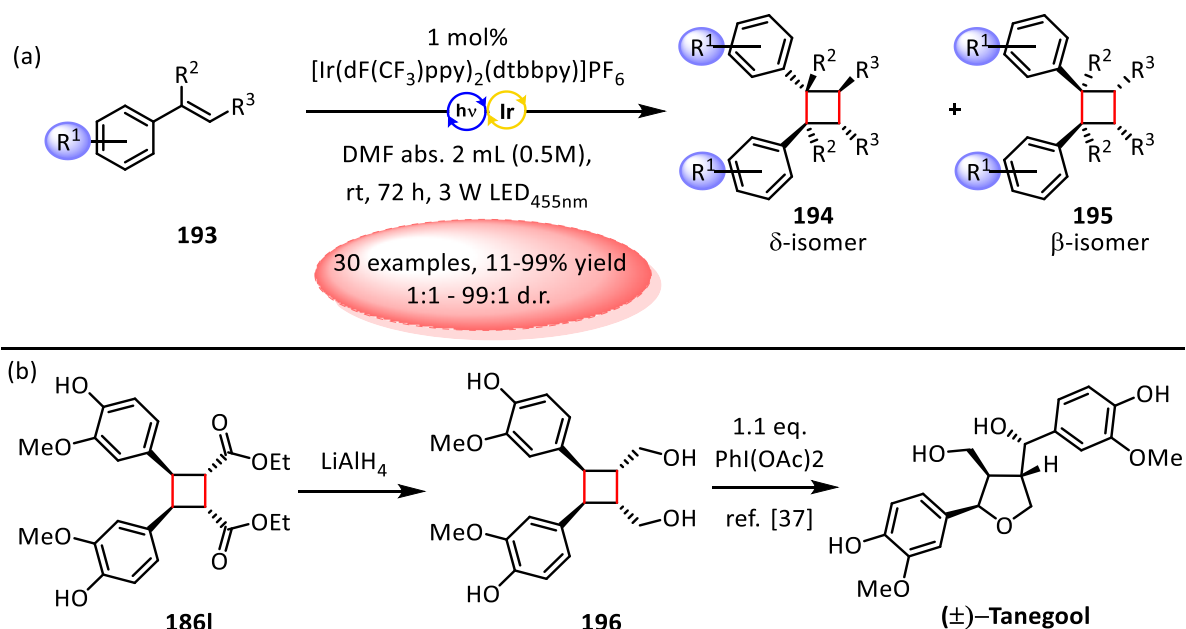
Scheme 56: (a) Summary for photocatalyzed [2+2] additions of olefins. (b) Formal synthesis of (±)-Tanegool.

5 Summary/Zusammenfassung

5.1 Summary

This thesis investigates the diverse reactivities of N-centered radicals, in particular ATRA-reactions with N-centered radicals in presence of copper photocatalysts and HAT reactions utilizing the highly reactive nature of nitrogen radicals.

In the **first chapter**, "nitrogen radicals in ATRA reactions: A holistic picture for three distinct ATRA mechanisms", the current mechanistic picture for ATRA reactions is expanded by a third possible mechanism. This third mechanistic pathway, called "inner-shell" mechanism, includes metal-organic intermediates enabled by the fast ligand exchange constant of the utilized copper photocatalyst. Contrasting this, the established radical-chain and photoredox mechanisms do not consider such intermediates for ATRA reactions. It was discovered, that the dominant pathway is strongly dependent on the catalyst, or lack of thereof, used and the electronic properties of the substrate. Hereby, styrene derivatives were the optimal substrate class due to their electronic tunability and comparatively stable benzylic radicals. After screening a selection of electron-rich and electron-poor styrene derivatives with all three possible mechanisms, the variations in electronic dependencies of each mechanism were visualized by plotting the obtained yields against the Hammett substituent constant of the substrate. The presence of this third mechanism was effectively demonstrated by enabling/disabling a 5-exo-trig radical cyclization cascade during halo-aminations with *N*-Allyl compounds. This reaction was optimized to give access to a powerful and selective protocol towards copper catalyzed halo-aminations of styrenes, eclipsing previous protocols for this reaction. Furthermore, upscaling and *in situ* formation of *N*-halo compounds further established the synthetic applicability of this reaction.

In the **second chapter**, "synthesis of 2*H*-Pyrrols after remote C_{sp}^3 functionalization by iminyl radicals", a radical cascade reaction, initiated by the generation of highly reactive iminyl radicals, followed by a site-selective C_{sp}^3-H functionalization was explored. It was discovered, that metal-based photoredox catalysts were incompatible with the unsaturated azide iminyl

radical precursor. However, an organic photoredox catalyst was shown to be effective, successfully coupling α-bromo malonate derivatives and unsaturated azides in a radical cascade reaction. Curiously, addition of potassium formiate induced product selectivity, favoring the formation of 2*H*-pyrrole over another possible ketone product in this radical cascade. A diverse scope of different iminyl radical precursors, as well as various carbon radical precursor were explored, demonstrating the possible scope of this reaction. After successfully upscaling this reaction to a multi-gram scale, the possibility of isolating a single diastereomer of the decarboxylated product and the cyclic β-amino acid derived from it was demonstrated through two steps. Insights into the mechanisms are given through quenching experiments and the formation of various side products during this radical cascade reaction is explained.

In the **third chapter**, "photocatalyzed [2+2] additions of olefins", the [2+2] additions of cinnamates, chalcones and styrenes by an energy transfer mechanism are explored. This transformation was challenging to achieve due to the high triplet energy state and fast relaxation pathways of these substrates. Despite this, the fluorinated iridium catalyst [Ir(*d*F(CF$_3$)ppy)$_2$(dtbbpy)]PF$_6$ was able to achieve this transformation in excellent yields and good diastereoselectivities for electron-rich derivatives within three days of irradiation time. Additionally, styrenes with substitutions in any position were tolerated. Moreover, cross-coupling reactions between substrates of opposing electronic properties were favored over the homo-coupling products, giving access to unsymmetrical cyclobutane derivatives. Lastly, the formal synthesis of (±)-Tanegool was demonstrated with a product obtained from this reaction protocol.

5.2 Zusammenfassung

Diese Arbeit beschäftigt sich mit den vielfältigen Reaktionsmechanismen, welche *N*-zentrierten Radikalen möglich sind. Im Besonderen werden hierbei ATRA-Reaktionen von Stickstoffradikalen mit kupferbasierten Photokatalysatoren und HAT-Reaktionen betrachtet, welche die hochreaktiven Eigenschaften der Stickstoffradikalen nutzen.

Im **ersten Kapitel**, „nitrogen-radicals in ATRA reactions: A holistic picture for three distinct ATRA-mechanisms", wurden die bekannten ATRA-Mechanismen um einen dritten Mechanismus erweitert. Dieser Reaktionspfad, welcher hier als „inner-shell"-Mechanismus bezeichnet wird, beinhaltet metallorganische Intermediate, welche durch einen schnellen Ligandenaustausch eines kupferbasierten Photokatalysators ermöglicht werden. Im Gegensatz dazu berücksichtigen die bisher etablierten Radikalketten- und Photoredox-Mechanismen keine Interaktionen dieser Art. Es wurde festegestellt, dass der dominante Reaktionsmechanismus stark vom verwendeten Katalysator und den elektronischen Eigenschaften des verwendeten Substrates abhängt. Hierbei waren Styrolderivate optimale Substrate, da sich ihre elektronischen Eigenschaften gut durch funktionelle Gruppen am aromatischen Kern verändern lassen und sie relativ stabile benzylische radikale als Intermediate bilden. Nach der Evaluation verschiedener elektronenreicher sowie -armer Styrole durch die drei möglichen Mechanismen konnten die verschiedenen elektronischen Abhängigkeiten der einzelnen Mechanismen dadurch verdeutlicht werden, dass die erhaltenen Ausbeuten gegen die Hammettkonstanten der funktionellen Gruppen aufgetragen wurden. Das Auftreten eines dritten „inner-shell"-Mechanismus' wurde nachgewiesen, indem eine radikalische 5-exo-trig Cyclisierung mit *N*-halo-*N*-allyl-Reagenzien durch die Anwesenheit eines Kupferkatalysators verhindert wurde, während andere Mechanismen nur das cyclisierte Produkt lieferten. Die Reaktionsbedingungen wurden optimiert, um ein selektives und effektives Protokoll für die Haloaminierung von Styrolen zu erhalten. Dieses Protokoll war dabei effektiver als vorheriger für die Haloaminierung von Styrolen. Darüber hinaus konnte durch Hochskalierung der Reaktion und der *in-situ* Bildung der *N*-halo-Verbindungen die synthetische Anwendbarkeit der Reaktion demonstriert werden.

Summary/Zusammenfassung

Im **zweiten Kapitel**, „synthesis of 2*H*-Pyrrols after remote C_{sp}^3 functionalization by iminyl radicals", wurde eine Radikalkaskadenreaktion untersucht, welche die Generierung eines hochreaktiven Iminylradikals beinhaltet, das wiederum eine regioselektive C_{sp}^3-H-Funktionalisierung auslöst. Hierbei wurde festgestellt, dass für diese Reaktion Photoredoxkatalysatoren auf Metallbasis nicht kompatibel mit den verwendeten ungesättigten Aziden waren. Es konnte jedoch gezeigt werden, dass ein organischer Photokatalysator erfolgreich die Kupplung zwischen α-Bromomalonat-Derivaten und ungesättigten Aziden in einer Radikalkaskade katalysieren kann. Die Zugabe von Kaliumformiat verursachte hierbei Produktselektivität. Dabei wurde die Bildung von 2*H*-Pyrrolen über ein anderes mögliches Ketonprodukt bevorzugt. Innerhalb dieser Arbeit wurden dabei diverse Iminylradikalvorläufer wie auch Kohlenstoffradikalvorläufer getestet, um die Grenzen dieser Reaktion aufzuzeigen. Nachdem diese neue Reaktion erfolgreich auf einen multi-gramm-Maßstab skaliert wurde, konnten verschiedene Derivatisierungen des Produktes demonstriert werden. Dabei konnte ein einzelnes Diastereomer des decarboxylierten Produktes sowie ein einzelnes Diastereomer eines cyclischen β-Aminoesters in zwei Stufen isoliert werden. Quenchingexperimente und die verschiedenen erhaltenen Nebenprodukte konnten hierbei Einsichten in den Mechanismus dieser Radikalkaskadenreaktion liefern.

Im **dritten Kapitel**, „photocatalyzed 2+2 additions of olefins", wurde die [2+2]-Addition von Zimtestern, Styrolen und Chalkonen durch einen Energietransfermechanismus untersucht. Diese Reaktion stellt hohe Ansprüche an die Reaktionsbedingungen, da sich diese Substrate durch eine hohe Triplettenergie und schnelle Relaxationsmechanismen auszeichnen. Nichtsdestotrotz konnte der fluorierte Iridiumkatalysator [Ir(*d*F(CF₃)ppy)₂(dtbbpy)]PF₆ diese Reaktion innerhalb von 72 Stunden in guten Ausbeuten und − im Falle der elektronenreichen Substrate − guten Diastereoselektivitäten realisieren. Dabei wurden auch Styrole mit Substitutionen in jeder Position toleriert. Zusätzlich konnte gezeigt werden, dass Substrate mit gegensätzlichen elektronischen Eigenschaften eine Kreuzkupplung gegenüber Homokupplungen bevorzugen. Dies ermöglichte den Zugang zu asymmetrischen Cyclobutanderivaten. Zuletzt konnte die formelle Synthese von (±)-Tanegool aus einem in dieser Arbeit erhaltenen Produkt aufgezeigt werden.

6 Literaturverzeichnis

[1] M. H. Shaw, J. Twilton, D. W. C. MacMillan, *J. Org. Chem.* **2016**, *81*, 6898.

[2] C. K. Prier, D. A. Rankic, D. W. C. MacMillan, *Chem. Rev.* **2013**, *113*, 5322.

[3] N. A. Romero, D. A. Nicewicz, *Chem. Rev.* **2016**, *116*, 10075.

[4] P. Renaud, M. P. Sibi, *Radicals in organic synthesis*, Wiley-VCH, Weinheim, **2001**.

[5] A. Studer, D. P. Curran, *Angew. Chem.* **2016**, *55*, 58.

[6] K. L. Skubi, T. R. Blum, T. P. Yoon, *Chem. Rev.* **2016**, *116*, 10035.

[7] S. Poplata, A. Tröster, Y.-Q. Zou, T. Bach, *Chem. Rev.* **2016**, *116*, 9748.

[8] B. M. Hockin, C. Li, N. Robertson, E. Zysman-Colman, *Catal. Sci. Technol.* **2019**, *9*, 889.

[9] M. D. Kärkäs, J. A. Porco, C. R. J. Stephenson, *Chem. Rev.* **2016**, *116*, 9683.

[10] S. A. Lawrence, *Cambridge University Press* **2004**, ISBN 0-521-78284-8.

[11] a) L. Jiang, S. L. Buchwald in *Metal-catalyzed cross-coupling reactions* (Eds.: A. de Meijere, F. Diederich), Wiley-VCH, Weinheim, **2004**, pp. 699–760; b) A. K. Yudin (Ed.) *Catalyzed carbon-heteroatom bond formation*, Wiley-VCH-Verl., Weinheim, **2011**.

[12] M. D. Kärkäs, *ACS Catal.* **2017**, *7*, 4999.

[13] S. Z. Zard, *Chem. Soc. Rev.* **2008**, *37*, 1603.

[14] J.-R. Chen, X.-Q. Hu, L.-Q. Lu, W.-J. Xiao, *Chem. Soc. Rev.* **2016**, *45*, 2044.

[15] K. Löffler, C. Freytag, *Ber. Dtsch. Chem. Ges.* **1909**, *42*, 3427.

[16] D. H. R. Barton, A. L. J. Beckwith, A. Goosen, *J. Chem. Soc.* **1965**, 181.

[17] a) A. W. Hofmann, *Ber. Dtsch. Chem. Ges.* **1885**, *18*, 109; b) M. E. Wolff, *Chem. Rev.* **1963**, *63*, 55.

[18] L. E. Kaim, C. Meyer, *J. Org. Chem.* **1996**, *61*, 1556.

[19] S. Kim, G. H. Joe, J. Y. Do, *J. Am. Chem. Soc.* **1993**, *115*, 3328.

[20] J. Guin, R. Fröhlich, A. Studer, *Angew. Chem.* **2008**, *47*, 779.

[21] H. Lu, C. Li, *Tetrahedron Lett.* **2005**, *46*, 5983.

[22] a) A.-C. Callier-Dublanchet, B. Quiclet-Sire, S. Z. Zard*, *Tetrahedron Lett.* **1997**, *38*, 2463;
b) A.-C. Callier-Dublanchet, B. Quiclet-Sire, S. Z. Zard, *Tetrahedron Lett.* **1995**, *36*, 8791.

[23] R. Alonso, P. J. Campos, B. García, M. A. Rodríguez, *Org. Lett.* **2006**, *8*, 3521.

[24] W.R. Bowman, D. N. Clark, R. J. Marmon, *Tetrahedron* **1994**, *50*, 1275.

[25] J. A. Blake, D. A. Pratt, S. Lin, J. C. Walton, P. Mulder, K. U. Ingold, *J. Org. Chem.* **2004**, *69*, 3112.

[26] A. R. Forrester, M. Gill, J. S. Sadd, R. H. Thomson, *J. Chem. Soc., Chem. Commun.* **1975**, 291.

[27] W.R. Bowman, D. N. Clark, R. J. Marmon, *Tetrahedron* **1994**, *50*, 1295.

[28] P. Gaudreault, C. Drouin, J. Lessard, *Can. J. Chem.* **2005**, *83*, 543.

[29] F. Gagosz, C. Moutrille, S. Z. Zard, *Org. Lett.* **2002**, *4*, 2707.

[30] D. C. Miller, K. T. Tarantino, R. R. Knowles, *Top. Curr. Chem.* **2016**, *374*, 30.

[31] H. Kim, T. Kim, D. G. Lee, S. W. Roh, C. Lee, *Chemical commun.* **2014**, *50*, 9273.

[32] K. Miyazawa, T. Koike, M. Akita, *Chemistry* **2015**, *21*, 11677.

[33] T. W. Greulich, C. G. Daniliuc, A. Studer, *Org. Lett.* **2015**, *17*, 254.

[34] Y. Chen, A. S. Kamlet, J. B. Steinman, D. R. Liu, *Nature chem.* **2011**, *3*, 146.

[35] X. Sun, S. Yu, *Chemical commun.* **2016**, *52*, 10898.

[36] J. Davies, S. P. Morcillo, J. J. Douglas, D. Leonori, *Chemistry* **2018**, *24*, 12154.

[37] G. Cecere, C. M. König, J. L. Alleva, D. W. C. MacMillan, *J. Am. Chem. Soc.* **2013**, *135*, 11521.

[38] L. J. Allen, P. J. Cabrera, M. Lee, M. S. Sanford, *J. Am. Chem. Soc.* **2014**, *136*, 5607.

[39] J. Xuan, B.-J. Li, Z.-J. Feng, G.-D. Sun, H.-H. Ma, Z.-W. Yuan, J.-R. Chen, L.-Q. Lu, W.-J. Xiao, *Chem.: Asian J.* **2013**, *8*, 1090.

[40] Y.-R. Luo, *Handbook of bond dissociation energies in organic compounds*, CRC Press, Boca Raton, Fla., **2003**.

[41] X.-Q. Hu, J.-R. Chen, Q. Wei, F.-L. Liu, Q.-H. Deng, A. M. Beauchemin, W.-J. Xiao, *Angew. Chem.* **2014**, *53*, 12163.

[42] D. C. Miller, G. J. Choi, H. S. Orbe, R. R. Knowles, *J. Am. Chem. Soc.* **2015**, *137*, 13492.

[43] J.-D. Wang, Y.-X. Liu, D. Xue, C. Wang, J. Xiao, *Synlett* **2014**, *25*, 2013.

[44] L. Benati, G. Bencivenni, R. Leardini, D. Nanni, M. Minozzi, P. Spagnolo, R. Scialpi, G. Zanardi, *Org. Lett.* **2006**, *8*, 2499.

[45] Z. Liu, J. Zhang, S. Chen, E. Shi, Y. Xu, X. Wan, *Angew. Chem.* **2012**, *51*, 3231.

[46] M. Tokuda, Y. Yamada, T. Takagi, H. Suginome, A. Furusaki, *Tetrahedron Lett.* **1985**, *26*, 6085.

[47] Y. L. Chow, W. C. Danen, S. F. Nelsen, D. H. Rosenblatt, *Chem. Rev.* **1978**, *78*, 243.

[48] T. D. Svejstrup, A. Ruffoni, F. Juliá, V. M. Aubert, D. Leonori, *Angew. Chem.* **2017**, *56*, 14948.

[49] A. Ruffoni, F. Juliá, T. D. Svejstrup, A. J. McMillan, J. J. Douglas, D. Leonori, *Nature chemistry* **2019**, *11*, 426.

[50] S. Maity, N. Zheng, *Angew. Chem.* **2012**, *51*, 9562.

[51] A. J. Musacchio, L. Q. Nguyen, G. H. Beard, R. R. Knowles, *J. Am. Chem. Soc.* **2014**, *136*, 12217.

[52] S. Maity, M. Zhu, R. S. Shinabery, N. Zheng, *Angew. Chem.* **2012**, *51*, 222.

[53] J. Davies, T. D. Svejstrup, D. Fernandez Reina, N. S. Sheikh, D. Leonori, *J. Am. Chem. Soc.* **2016**, *138*, 8092.

[54] J. Lessard, D. Griller, K. U. Ingold, *J. Am. Chem. Soc.* **1980**, *102*, 3262.

[55] a) R. Sutcliffe, D. Griller, J. Lessard, K. U. Ingold, *J. Am. Chem. Soc.* **1981**, *103*, 624; b) N. J. Gesmundo, J.-M. M. Grandjean, D. A. Nicewicz, *Org. Lett.* **2015**, *17*, 1316.

[56] J. H. Horner, O. M. Musa, A. Bouvier, M. Newcomb, *J. Am. Chem. Soc.* **1998**, *120*, 7738.

[57] Q. Qin, S. Yu, *Org. Lett.* **2014**, *16*, 3504.

[58] Q. Qin, D. Ren, S. Yu, *Org. Biomol. Chem.* **2015**, *13*, 10295.

[59] X. Ren, Q. Guo, J. Chen, H. Xie, Q. Xu, Z. Lu, *Chemistry* **2016**, *22*, 18695.

[60] G. J. Choi, R. R. Knowles, *J. Am. Chem. Soc.* **2015**, *137*, 9226.

[61] L. Zhu, P. Xiong, Z.-Y. Mao, Y.-H. Wang, X. Yan, X. Lu, H.-C. Xu, *Angew. Chem.* **2016**, *55*, 2226.

[62] Q. Qin, S. Yu, *Org. Lett.* **2015**, *17*, 1894.

[63] G. J. Choi, Q. Zhu, D. C. Miller, C. J. Gu, R. R. Knowles, *Nature* **2016**, *539*, 268.

[64] J. C. K. Chu, T. Rovis, *Nature* **2016**, *539*, 272.

[65] J. Fu, G. Zanoni, E. A. Anderson, X. Bi, *Chem. Soc. Rev.* **2017**, *46*, 7208.

[66] J. C. Walton, *Acc. Chem. Res.* **2014**, *47*, 1406.

[67] H. Jiang, X. An, K. Tong, T. Zheng, Y. Zhang, S. Yu, *Angew. Chem.* **2015**, *54*, 4055.

[68] H. Jiang, A. Studer, *Angew. Chem.* **2017**, *129*, 12441.

[69] J. Davies, N. S. Sheikh, D. Leonori, *Angew. Chem.* **2017**, *129*, 13546.

[70] D. F. Reina, E. M. Dauncey, S. P. Morcillo, T. D. Svejstrup, M. V. Popescu, J. J. Douglas, N. S. Sheikh, D. Leonori, *Eur. J. Org. Chem.* **2017**, *2017*, 2108.

[71] J. Davies, S. G. Booth, S. Essafi, R. A. W. Dryfe, D. Leonori, *Angew. Chem.* **2015**, *54*, 14017.

[72] Y.-F. Wang, G. H. Lonca, S. Chiba, *Angew. Chem.* **2014**, *53*, 1067.

[73] X.-Y. Yu, J.-R. Chen, P.-Z. Wang, M.-N. Yang, D. Liang, W.-J. Xiao, *Angew. Chem.* **2018**, *57*, 738.

[74] H.-T. Qin, S.-W. Wu, J.-L. Liu, F. Liu, *Chemical commun.* **2017**, *53*, 1696.

[75] E. M. Dauncey, S. P. Morcillo, J. J. Douglas, N. S. Sheikh, D. Leonori, *Angew. Chem.* **2018**, *57*, 744.

[76] L. Li, H. Chen, M. Mei, L. Zhou, *Chemical commun.* **2017**, *53*, 11544.

[77] X.-Y. Duan, N.-N. Zhou, R. Fang, X.-L. Yang, W. Yu, B. Han, *Angew. Chem.* **2014**, *53*, 3158.

[78] a) Q.-Q. Zhao, J. Chen, D.-M. Yan, J.-R. Chen, W.-J. Xiao, *Org. Lett.* **2017**, *19*, 3620; b) X.-Q. Hu, X. Qi, J.-R. Chen, Q.-Q. Zhao, Q. Wei, Y. Lan, W.-J. Xiao, *Nature commun.* **2016**, *7*, 11188.

[79] E. Brachet, L. Marzo, M. Selkti, B. König, P. Belmont, *Chem. Sci.* **2016**, *7*, 5002.

[80] Q.-Q. Zhao, X.-Q. Hu, M.-N. Yang, J.-R. Chen, W.-J. Xiao, *Chemical commun.* **2016**, *52*, 12749.

[81] X. Zhu, Y.-F. Wang, W. Ren, F.-L. Zhang, S. Chiba, *Organic letters* **2013**, *15*, 3214.

[82] a) F. Teplý, *Collect. Czech. Chem. Commun.* **2011**, *76*, 859; b) D. M. Schultz, T. P. Yoon, *Science* **2014**, *343*, 1239176; c) J. M. R. Narayanam, C. R. J. Stephenson, *Chem. Soc. Rev.* **2011**, *40*, 102.

[83] D. Ravelli, S. Protti, M. Fagnoni, *Chem. Rev.* **2016**, *116*, 9850.

[84] T. Courant, G. Masson, *J. Org. Chem.* **2016**, *81*, 6945.

[85] a) D. Menigaux, P. Belmont, E. Brachet, *Eur. J. Org. Chem.* **2017**, *2017*, 2008; b) X. Liu, K. Tong, A. H. Zhang, R. X. Tan, S. Yu, *Org. Chem. Front.* **2017**, *4*, 1354; c) L. Song, S. Luo, J.-P. Cheng, *Org. Chem. Front.* **2016**, *3*, 447; d) T. Tsuritani, H. Shinokubo, K. Oshima, *J. Org. Chem.* **2003**, *68*, 3246.

[86] M. Pirtsch, S. Paria, T. Matsuno, H. Isobe, O. Reiser, *Chemistry* **2012**, *18*, 7336.

[87] S. Paria, M. Pirtsch, V. Kais, O. Reiser, *Synthesis* **2013**, *45*, 2689.

[88] a) M. S. Kharasch, E. V. Jensen, W. H. Urry, *Science* **1945**, *102*, 128; b) M. S. Kharasch, P. S. Skell, P. Fisher, *J. Am. Chem. Soc.* **1948**, *70*, 1055; c) M. S. Kharasch, H. M. Priestley, *J. Am. Chem. Soc.* **1939**, *61*, 3425.

[89] A. Hossain, A. Bhattacharyya, O. Reiser, *Science* **2019**, *364*.

[90] D. B. Bagal, G. Kachkovskyi, M. Knorn, T. Rawner, B. M. Bhanage, O. Reiser, *Angew. Chem.* **2015**, *54*, 6999.

[91] a) T. Rawner, M. Knorn, E. Lutsker, A. Hossain, O. Reiser, *J. Org. Chem.* **2016**, *81*, 7139; b) S. K. Pagire, S. Paria, O. Reiser, *Org. Lett.* **2016**, *18*, 2106.

[92] B. Chen, C. Fang, P. Liu, J. M. Ready, *Angew. Chem.* **2017**, *56*, 8780.

[93] Z.-L. Li, G.-C. Fang, Q.-S. Gu, X.-Y. Liu, *Chem. Soc. Rev.* **2020**, *49*, 32.

[94] a) Y. Miyake, K. Nakajima, Y. Nishibayashi, *J. Am. Chem. Soc.* **2012**, *134*, 3338; b) M. S. Oderinde, M. Frenette, D. W. Robbins, B. Aquila, J. W. Johannes, *J. Am. Chem. Soc.* **2016**, *138*, 1760; c) S. H. Oh, Y. R. Malpani, N. Ha, Y.-S. Jung, S. B. Han, *Org. Lett.* **2014**, *16*, 1310; d) B. Sahoo, M. N. Hopkinson, F. Glorius, *J. Am. Chem. Soc.* **2013**, *135*, 5505; e) C.-

J. Wallentin, J. D. Nguyen, P. Finkbeiner, C. R. J. Stephenson, *J. Am. Chem. Soc.* **2012**, *134*, 8875.

[95] M. A. Cismesia, T. P. Yoon, *Chem. Sci.* **2015**, *6*, 5426.

[96] S. R. Chemler, M. T. Bovino, *ACS Catal.* **2013**, *3*, 1076.

[97] a) A. S. Kalgutkar, R. Jones, A. Sawant in *RSC drug discovery* (Ed.: D. A. Smith), Royal Society of Chemistry, Cambridge, **2010**, pp. 210–274; b) F. Carta, A. Scozzafava, C. T. Supuran, *Expert opinion on therapeutic patents* **2012**, *22*, 747; c) A. U. Meyer, A. L. Berger, B. König, *Chem. commun.* **2016**, *52*, 10918.

[98] a) T. Rawner, E. Lutsker, C. A. Kaiser, O. Reiser, *ACS Catal.* **2018**, *8*, 3950; b) A. Hossain, S. Engl, E. Lutsker, O. Reiser, *ACS Catal.* **2019**, *9*, 1103; c) A. Hossain, A. Vidyasagar, C. Eichinger, C. Lankes, J. Phan, J. Rehbein, O. Reiser, *Angew. Chem.* **2018**, *57*, 8288.

[99] X.-Y. Liu, P. Gao, Y.-W. Shen, Y.-M. Liang, *Adv. Synth. Catal.* **2011**, *353*, 3157.

[100] L. P. Hammett, *J. Am. Chem. Soc.* **1937**, *59*, 96.

[101] L. N. S. Crespin, A. Greb, D. C. Blakemore, S. V. Ley, *J. Org. Chem.* **2017**, *82*, 13093.

[102] Y. Li, Y. Liang, J. Dong, Y. Deng, C. Zhao, Z. Su, W. Guan, X. Bi, Q. Liu, J. Fu, *J. Am. Chem. Soc.* **2019**, *141*, 18475.

[103] W. Z. Yu, Y. A. Cheng, M. W. Wong, Y.-Y. Yeung, *Adv. Synth. Catal.* **2017**, *359*, 234.

[104] J. G. Speight, N. A. Lange, *Lange's handbook of chemistry*. Section 6, THERMODYNAMIC PROPERTIES, McGraw-Hill, New York, **2005**.

[105] W. T. Eckenhoff, T. Pintauer, *Catalysis Reviews* **2010**, *52*, 1.

[106] Y. Fu, L. Liu, H.-Z. Yu, Y.-M. Wang, Q.-X. Guo, *J. Am. Chem. Soc.* **2005**, *127*, 7227.

[107] a) D. M. Arias-Rotondo, J. K. McCusker, *Chem. Soc. Rev.* **2016**, *45*, 5803; b) B. König (Ed.) *Chemical Photocatalysis*, De Gruyter, Berlin, **2020**.

[108] J. Davies, S. G. Booth, S. Essafi, R. A. W. Dryfe, D. Leonori, *Angew. Chem.* **2015**, *127*, 14223.

[109] a) J.-Q. Liu, A. Shatskiy, B. S. Matsuura, M. D. Kärkäs, *Synthesis* **2019**, *51*, 2759; b) J. W. Beatty, C. R. J. Stephenson, *Acc. Chem. Res.* **2015**, *48*, 1474; c) B. N. Hemric, K. Shen, Q. Wang, *J. Am. Chem. Soc.* **2016**, *138*, 5813.

[110]   B. Hu, S. G. DiMagno, *Org. Biomol. Chem.* **2015**, *13*, 3844.

[111]   J. Davies, N. S. Sheikh, D. Leonori, *Angew. Chem.* **2017**, *56*, 13361.

[112]   W. Shu, A. Lorente, E. Gómez-Bengoa, C. Nevado, *Nature commun.* **2017**, *8*, 13832.

[113]   Q. Wang, J. Huang, L. Zhou, *Adv. Synth. Catal.* **2015**, *357*, 2479.

[114]   A. Hossain, S. Pagire, O. Reiser, *Synlett* **2017**, *28*, 1707.

[115]   J. Wencel-Delord, T. Dröge, F. Liu, F. Glorius, *Chem. Soc. Rev.* **2011**, *40*, 4740.

[116]   a) S. Chiba, H. Chen, *Org. Biomol. Chem.* **2014**, *12*, 4051; b) H. Chen, S. Chiba, *Org. Biomol. Chem.* **2014**, *12*, 42.

[117]   a) H. Chen, S. Sanjaya, Y.-F. Wang, S. Chiba, *Org. Lett.* **2013**, *15*, 212; b) V. Snieckus, J. C. Cuevas, C. P. Sloan, H. Liu, D. P. Curran, *J. Am. Chem. Soc.* **1990**, *112*, 896; c) Y.-F. Wang, K. K. Toh, S. Chiba, K. Narasaka, *Organic letters* **2008**, *10*, 5019; d) E. A. Wappes, S. C. Fosu, T. C. Chopko, D. A. Nagib, *Angew. Chem.* **2016**, *55*, 9974.

[118]   K. Okada, K. Okamoto, N. Morita, K. Okubo, M. Oda, *J. Am. Chem. Soc.* **1991**, *113*, 9401.

[119]   H. Jiang, A. Studer, *Angew. Chem.* **2018**, *130*, 1708.

[120]   a) Y. Li, R. Mao, J. Wu, *Org. Lett.* **2017**, *19*, 4472; b) J. Li, P. Zhang, M. Jiang, H. Yang, Y. Zhao, H. Fu, *Org. Lett.* **2017**, *19*, 1994; c) X. Shen, J.-J. Zhao, S. Yu, *Org. Lett.* **2018**, *20*, 5523; d) H. Chen, L. Guo, S. Yu, *Org. Lett.* **2018**, *20*, 6255; e) L. M. Stateman, K. M. Nakafuku, D. A. Nagib, *Synthesis* **2018**, *50*, 1569.

[121]   W. Shu, C. Nevado, *Angew. Chem.* **2017**, *56*, 1881.

[122]   P. Riente, M. A. Pericàs, *ChemSusChem* **2015**, *8*, 1841.

[123]   B. König (Ed.) *Chemical Photocatalysis*. ISBN: 978-3-11-057676-4, De Gruyter, Berlin, **2020**.

[124]   S. Engl, O. Reiser, *Eur. J. Org. Chem.* **2019**, *116*, 9683.

[125]   S. Murarka, *Adv. Synth. Catal.* **2018**, *360*, 1735.

[126]   E. P. Farney, T. P. Yoon, *Angew. Chem.* **2014**, *53*, 793.

[127]   W.-L. Lei, T. Wang, K.-W. Feng, L.-Z. Wu, Q. Liu, *ACS Catal.* **2017**, *7*, 7941.

[128]   B. G. McCarthy, R. M. Pearson, C.-H. Lim, S. M. Sartor, N. H. Damrauer, G. M. Miyake, *J. Am. Chem. Soc.* **2018**, *140*, 5088.

[129]   S. M. Sartor, B. G. McCarthy, R. M. Pearson, G. M. Miyake, N. H. Damrauer, *J. Am. Chem. Soc.* **2018**, *140*, 4778.

[130]   D. Koyama, H. J. A. Dale, A. J. Orr-Ewing, *J. Am. Chem. Soc.* **2018**, *140*, 1285.

[131]   J. C. Theriot, C.-H. Lim, H. Yang, M. D. Ryan, C. B. Musgrave, G. M. Miyake, *Science* **2016**, *352*, 1082.

[132]   R. M. Pearson, C.-H. Lim, B. G. McCarthy, C. B. Musgrave, G. M. Miyake, *J. Am. Chem. Soc.* **2016**, *138*, 11399.

[133]   B. L. Buss, C.-H. Lim, G. M. Miyake, *Angew. Chem.* **2020**, *59*, 3209.

[134]   Y. Du, R. M. Pearson, C.-H. Lim, S. M. Sartor, M. D. Ryan, H. Yang, N. H. Damrauer, G. M. Miyake, *Chemistry* **2017**, *23*, 10962.

[135]   D. B. Ramachary, G. S. Reddy, S. Peraka, J. Gujral, *ChemCatChem* **2017**, *9*, 263.

[136]   Z. Liu, P. Liao, X. Bi, *Org. Lett.* **2014**, *16*, 3668.

[137]   Y.-Q. Tang, J.-C. Yang, Le Wang, M. Fan, L.-N. Guo, *Org. Lett.* **2019**, *21*, 5178.

[138]   a) X. Liu, Y. Wang, Y. Xing, J. Yu, H. Ji, M. Kai, Z. Wang, D. Wang, Y. Zhang, D. Zhao et al., *J. Med. Chem.* **2013**, *56*, 3102; b) A. D. Hobson, C. M. Harris, E. L. van der Kam, S. C. Turner, A. Abibi, A. L. Aguirre, P. Bousquet, T. Kebede, D. B. Konopacki, G. Gintant et al., *J. Med. Chem.* **2015**, *58*, 9154; c) F. Fülöp, T. A. Martinek, G. K. Tóth, *Chem. Soc. Rev.* **2006**, *35*, 323.

[139]   B. Liu, Z.-M. Zhang, B. Xu, S. Xu, H.-H. Wu, Y. Liu, J. Zhang, *Org. Chem. Front.* **2017**, *4*, 1772.

[140]   D. Petzold, P. Nitschke, F. Brandl, V. Scheidler, B. Dick, R. M. Gschwind, B. König, *Chemistry* **2019**, *25*, 361.

[141]   T. G. Ribelli, F. Lorandi, M. Fantin, K. Matyjaszewski, *Macromol. Rapid Comm.* **2019**, *40*, e1800616.

[142]   S. Cludius-Brandt, L. Kupracz, A. Kirschning, *Beilstein J. Org. Chem.* **2013**, *9*, 1745.

[143]   V. M. Dembitsky, *Phytomedicine* **2014**, *21*, 1559.

[144]   J. C. Namyslo, D. E. Kaufmann, *Chem. Rev.* **2003**, *103*, 1485.

[145]   A. Sergeiko, V. V. Poroikov, L. O. Hanus, V. M. Dembitsky, *Open J. Med. Chem* **2008**, *2*, 26.

[146]   a) S. Tsukamoto, K. Tomise, K. Miyakawa, B.-C. Cha, T. Abe, T. Hamada, H. Hirota, T. Ohta, *Bioorgan. Med. Chem* **2002**, *10*, 2981; b) I.-L. Tsai, F.-P. Lee, C.-C. Wu, C.-Y. Duh, T. Ishikawa, J.-J. Chen, Y.-C. Chen, H. Seki, I.-S. Chen, *Planta Med.* **2005**, *71*, 535; c) M. Nakamura, Y.-M. Chi, W.-M. Yan, Y. Nakasugi, T. Yoshizawa, N. Irino, F. Hashimoto, J. Kinjo, T. Nohara, S. Sakurada, *J. Nat. Prod.* **1999**, *62*, 1293; d) R. N. Mahindru, S. C. Taneja, K. L. Dhar, R. T. Brown, *Phytochemistry* **1993**, *32*, 1073; e) R. A. Davis, A. R. Carroll, S. Duffy, V. M. Avery, G. P. Guymer, P. I. Forster, R. J. Quinn, *J. Nat. Prod.* **2007**, *70*, 1118.

[147]   M. W. Smith, P. S. Baran, *Science* **2015**, *349*, 925.

[148]   F. D. Lewis, S. L. Quillen, P. D. Hale, J. D. Oxman, *J. Am. Chem. Soc.* **1988**, *110*, 1261.

[149]   W. R. Gutekunst, P. S. Baran, *J. Am. Chem. Soc.* **2011**, *133*, 19076.

[150]   a) S. E. Paulson, D.-L. Liu, G. E. Orzechowska, L. M. Campos, K. N. Houk, *J. Org. Chem.* **2006**, *71*, 6403; b) R. G. W. NORRISH, C. H. BAMFORD, *Nature* **1937**, *140*, 195.

[151]   J. Du, T. P. Yoon, *J. Am. Chem. Soc.* **2009**, *131*, 14604.

[152]   a) M. A. Ischay, M. E. Anzovino, J. Du, T. P. Yoon, *J. Am. Chem. Soc.* **2008**, *130*, 12886; b) T. P. Yoon, *Accounts Chem. Res.* **2016**, *49*, 2307; c) S. Lin, S. D. Lies, C. S. Gravatt, T. P. Yoon, *Org. Lett.* **2017**, *19*, 368.

[153]   T. R. Blum, Z. D. Miller, D. M. Bates, I. A. Guzei, T. P. Yoon, *Science* **2016**, *354*, 1391.

[154]   J. Du, K. L. Skubi, D. M. Schultz, T. P. Yoon, *Science* **2014**, *344*, 392.

[155]   T. Ni, R. A. Caldwell, L. A. Melton, *J. Am. Chem. Soc.* **1989**, *111*, 457.

[156]   Y. Xu, M. L. Conner, M. K. Brown, *Angew. Chem.* **2015**, *54*, 11918.

[157]   E. M. Sherbrook, H. Jung, D. Cho, M.-H. Baik, T. P. Yoon, *Chem. Sci.* **2020**, *11*, 856.

[158]   a) S. Karthikeyan, V. Ramamurthy, *J. Org. Chem.* **2007**, *72*, 452; b) N. Nguyen, A. R. Clements, M. Pattabiraman, *New J. Chem.* **2016**, *40*, 2433.

[159]   V. G. Stavros, *Nature chem.* **2014**, *6*, 955.

[160] D. M. Bassani, V. Darcos, S. Mahony, J.-P. Desvergne, *J. Am. Chem. Soc.* **2000**, *122*, 8795.

[161] R. Telmesani, S. H. Park, T. Lynch-Colameta, A. B. Beeler, *Angew. Chem.* **2015**, *54*, 11521.

[162] D. Haag, H.-D. Scharf, *J. Org. Chem.* **1996**, *61*, 6127.

[163] a) S. K. Pagire, O. Reiser, *Green Chem.* **2017**, *19*, 1721; b) S. Paria, V. Kais, O. Reiser, *Adv. Synth. Catal.* **2014**, *356*, 2853; c) S. Paria, O. Reiser, *Adv. Synth. Catal.* **2014**, *356*, 557.

[164] S. K. Pagire, P. Kreitmeier, O. Reiser, *Angew. Chem.* **2017**, *56*, 10928.

[165] S. K. Pagire, T. Föll, O. Reiser, *Acc. Chem. Res.* **2020**.

[166] a) I. Fussing, M. Güllü, O. Hammerich, A. Hussain, M. F. Nielsen, J. H. P. Utley, *J. Chem. Soc., Perkin Trans. 2* **1996**, *38*, 649; b) H. Roth, N. Romero, D. Nicewicz, *Synlett* **2016**, *27*, 714.

[167] M. Montalti, *Handbook of Photochemistry*, CRC Press, Hoboken, **2006**.

[168] F. Strieth-Kalthoff, M. J. James, M. Teders, L. Pitzer, F. Glorius, *Chem. Soc. Rev.* **2018**, *47*, 7190.

[169] W. S. Wadsworth in *Organic reactions*, Wiley Online Library, [Hoboken, N.J.], **2003-**, pp. 73–253.

[170] F. Toda, K. Tanaka, M. Kato, *J. Chem. Soc., Perkin Trans. 1* **1998**, 1315.

[171] a) Z. Lu, T. P. Yoon, *Angew. Chem.* **2012**, *51*, 10329; b) R. Li, B. C. Ma, W. Huang, L. Wang, Di Wang, H. Lu, K. Landfester, K. A. I. Zhang, *ACS Catal.* **2017**, *7*, 3097.

[172] a) A. Throup, L. H. Patterson, H. M. Sheldrake, *Org. Biomol. Chem.* **2016**, *14*, 9554; b) R. A. Panish, S. R. Chintala, J. M. Fox, *Angew. Chem.* **2016**, *55*, 4983; c) W. R. Gutekunst, P. S. Baran, *J. Org. Chem.* **2014**, *79*, 2430.

[173] J. B. Metternich, D. G. Artiukhin, M. C. Holland, M. von Bremen-Kühne, J. Neugebauer, R. Gilmour, *J. Org. Chem.* **2017**, *82*, 9955.

[174] A. K. F. Albertson, J.-P. Lumb, *Angew. Chem.* **2015**, *54*, 2204.

[175]   W. L. F. Armarego, C. L. L. Chai, *Purification of laboratory chemicals*, Elsevier/BH, Oxford, **2009**.

[176]   a) K. A. Teegardin, J. D. Weaver, *Org. Synth.* **2018**, *95*, 29; b) M. Knorn, T. Rawner, R. Czerwieniec, O. Reiser, *ACS Catal.* **2015**, *5*, 5186; c) M. S. Oderinde, J. W. Johannes in *Organic Syntheses Based on Name Reactions* (Eds.: A. Hassner, C. Stumer), Elsevier, Burlington, **2002**, pp. 77–92.

[177]   D. Rackl, V. Kais, P. Kreitmeier, O. Reiser, *Beilstein journal of organic chemistry* **2014**, *10*, 2157.

[178]   G. Heuger, R. Göttlich, *Beilstein J. Org. Chem.* **2015**, *11*, 1226.

[179]   T. J. Barker, E. R. Jarvo, *Journal of the American Chemical Society* **2009**, *131*, 15598.

[180]   Q. Qin, D. Ren, S. Yu, *Org. Biomol. Chem.* **2015**, *13*, 10295.

[181]   U. Megerle, R. Lechner, B. König, E. Riedle, *Photochem. Photobiol. Sci.* **2010**, *9*, 1400.

[182]   H. Zhang, K. Muñiz, *ACS Catal.* **2017**, *7*, 4122.

[183]   B. C. Ranu, S. Samanta, *Tetrahedron* **2003**, *59*, 7901.

[184]   X. Zhang, J. E. de Los Angeles, M. Y. He, J. T. Dalton, G. Shams, L. Lei, P. N. Patil, D. R. Feller, D. D. Miller, F. L. Hsu, *J. Med. Chem.* **1997**, *40*, 3014.

[185]   M. Turský, D. Nečas, P. Drabina, M. Sedlák, M. Kotora, *Organometallics* **2006**, *25*, 901.

[186]   M. Adamczyk, D. S. Watt, D. A. Netzel, *J. Org. Chem.* **1984**, *49*, 4226.

[187]   E. Dulière, J. Marchand-Brynaert, *Synthesis* **2002**, *2002*.

[188]   G. Cahiez, M. Alami, *Tetrahedron* **1989**, *45*, 4163.

[189]   S. J. Garden, C. R. W. Guimarães, M. B. Corréa, C. A. F. de Oliveira, A. d. C. Pinto, R. Bicca de Alencastro, *J. Org. Chem.* **2003**, *68*, 8815.

[190]   H. Shimakoshi, M. Abiru, S.-i. Izumi, Y. Hisaeda, *Chem. commun.* **2009**, 6427.

[191]   Y. Sasson, O. W. Webster, *Chem. commun.* **1992**, 1200.

[192]   G. Suez, V. Bloch, G. Nisnevich, M. Gandelman, *Eur. J. Org. Chem.* **2012**, *2012*, 2118.

[193]   I. Sasaki, H. Doi, T. Hashimoto, T. Kikuchi, H. Ito, T. Ishiyama, *Chem. commun.* **2013**, *49*, 7546.

[194]   X.-Y. Yu, P.-Z. Wang, D.-M. Yan, B. Lu, J.-R. Chen, W.-J. Xiao, *Adv. Synth. Catal.* **2018**, *360*, 3601.

[195]   L. Xiang, Y. Niu, X. Pang, X. Yang, R. Yan, *Chem. commun.* **2015**, *51*, 6598.

[196]   P. Gu, Y. Su, X.-P. Wu, J. Sun, W. Liu, P. Xue, R. Li, *Org. Lett.* **2012**, *14*, 2246.

[197]   Y.-F. Wang, K. K. Toh, S. Chiba, K. Narasaka, *Organic letters* **2008**, *10*, 5019.

[198]   B. K. Dinda, A. K. Jana, D. Mal, *Chemical commun.* **2012**, *48*, 3999.

[199]   Y. Wang, Z. Li, H. Zhao, Z. Zhang, *Synthesis* **2019**, *51*, 3250.

[200]   S. K. Pagire, A. Hossain, L. Traub, S. Kerres, O. Reiser, *Chem. commun.* **2017**, *53*, 12072.

7 Experimental Part

7.1 General Remarks

All commercially available reagents were used as supplied without further purification unless stated otherwise. Anhydrous solvents were prepared according to established laboratory procedures.[175] Moisture sensitive reactions were carried out in flame-dried glassware. Oxygen sensitive reactions were performed by degassing the reaction mixture with three freeze-pump-thaw cycles. The various catalysts used in the scope of this work were synthesized by literature procedures.[86,176]

All photochemical were performed under dry and oxygen-free conditions using Schlenk techniques. The reaction mixture was irradiated using an internal irradiation setup, which was developed by O. Reiser et. al. (Figure 24).[177] The setup consists of a Schlenk pressure tube (A) and a LED-setup (LED (B) on top of a quartz glass rod (C)), which channels light directly into the reaction mixture (D). A screw cap with a Teflon adaptor (E) allows for air-tight closure of the reaction vessel and a stable fixation of the glass rod (C). For irradiation, a light emitting diode (LED) (700 mA, λmax = 455 nm, Osram Oslon 80) for blue light reactions or a LED (700 mA, λ_{max} = 530 nm, Cree XP-E) for green light reactions was used.
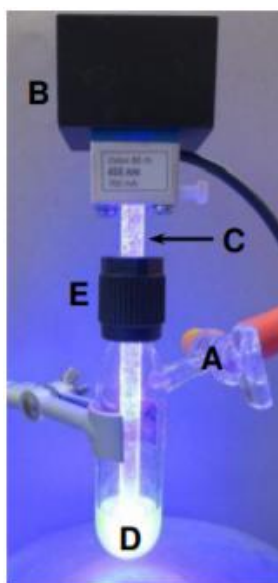
Figure 24: Internal Irradiation setup using a LED and a Quarz rod.

The photochemical upscaling reaction was performed in a 200 mL Schlenk reaction vessel, custom designed at the university of Regensburg by O. Reiser et. al. (Figure 25). The setup consists of a 200 mL Schlenk vessel (A) containing the reaction solution (C), while being cooled by an outer cooling mantle. Irradiation was achieved by an LED array (B) consisting of 30 LEDs (Osram Oslon SSL 80 deep blue ca. 1W/LED @ 700 mA, λ_{max} = 455 nm). The LED array (B) was water cooled by a second water cooling circuit. The LED array (B) was separated by the reaction solution (C) by a glass finger. The reaction was stirred by a flat Teflon stirring bar (D), providing additional circulation from bottom to top through a hollow glass handle (not visible).
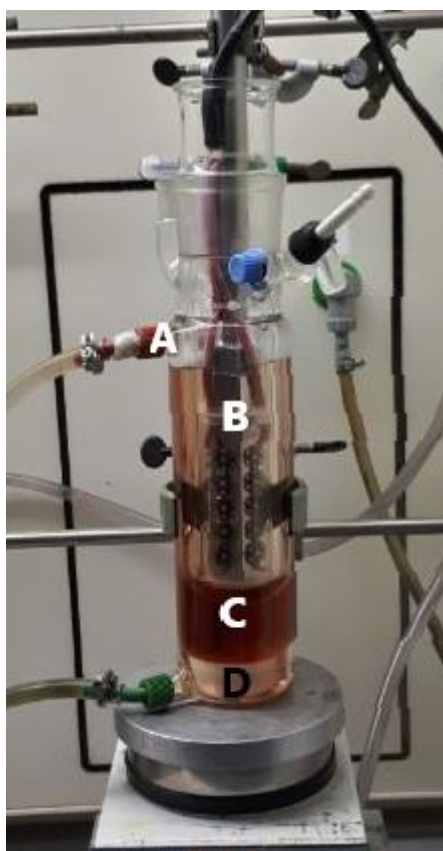
Figure 25: 200 mL reaction vessel for photochemical reactions.

The smaller photochemical upscaling reaction was performed in a 40 mL Schlenk reaction vessel, custom designed at the university of Regensburg by O. Reiser et. al. (Figure 26). The setup consists of an inner cooling mantle (A), cooling the reaction mixture during the reaction, giving an internal reactor volume of 40 mL with a short irradiation path after solvent displacement by the cooling mantle. Building overpressure was released *via* a glass stopcock (B), connected to an overpressure valve (not visible).

Irradiation was achieved by twenty Osram Oslon SSL 80 deep blue ca. 3W/LED @ 700 mA, λ_{max} = 455 nm LEDs, arranged around the outside wall of the reaction vessel in an LED array (C). The LEDs were air-cooled by a fan driven by the magnetic stirplate. This LED array (C) contained the glass reaction vessel itself (D) sitting directly on top of the magnet stirrer.
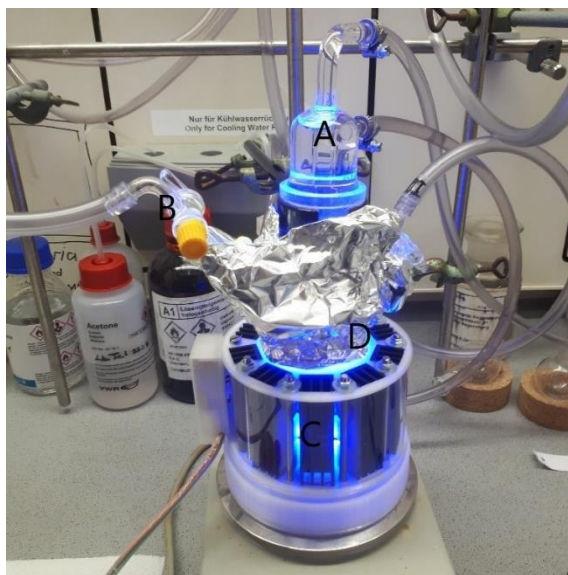
Figure 26: 40 mL reaction vessel for photochemical reactions.

Preparative column chromatography was performed with silica gel 60 from *Merck* (0.040-0.063 μm, 240-400 mesh). Conditioning of the column was performed by the "wet-packing" technique. Yields refer to chromatographically pure compounds unless otherwise stated. Flash column chromatography was performed using the *Reveleris X2* chromatography system by *BÜCHI Labortechnik AG*.

All reactions were monitored using precoated *TLC sheets ALUGRAM Xtra SIL G/UV254* from *Macherey-Nagel GmbH & Co. KG,* Düren. TLC sheets were coated with 0.2 mm silica gel 60 with fluorescent indicator UV254. UV active spots were detected at 254 nm and 366 nm. Petroleum ether and ethyl acetate mixtures (= PE:EA, reported as volume-% solutions of Ethyl acetate in Petroleum ether) were used as mobile phase, unless stated otherwise. For visualization, a 254 nm/366 nm UV-lamp or commonly used vanillin and permanganate stains followed by heating were employed.

^{1}H-NMR, ^{13}C-NMR and ^{19}F-NMR measurements were recorded either on a Bruker Avance 300 (300 MHz for ^{1}H, 75 MHz for ^{13}C, 282 MHz for ^{19}F), a Bruker Avance 400 (400 MHz for ^{1}H, 101 MHz for ^{13}C) or on a Bruker Avance III 600 MHz (600 MHz for ^{1}H, 151 MHz for ^{13}C) spectrometer at room temperature. Chemical shifts [δ] are reported in parts per million [ppm] relative to the residual solvent peak of deuterated chloroform (CDCl$_3$, 7.26 ppm for ^{1}H, 77.16 ppm for ^{13}C). The spectra were analyzed first order, and the coupling constants [J] are reported in Hertz (Hz). The multiplicity of the signals is reported as follows: s = singlet, d = doublet, t = triplet, q = quartet, m = multiplet, dd = doublet of doublets, etc. The integrals represent the relative number of hydrogen atoms related to the corresponding signals. Data is reported as follows: chemical shift, multiplicity, coupling constant J.

Infrared spectra were recorded on a *Cary 630 FTIR* spectrometer and the wavenumbers are reported in (cm^{-1}).

Mass spectrometry was performed by the Central Analytic Department of the University of Regensburg on a *Jeol AccuTOF GCX*, a *Finnigan MAT SSQ 710 A*, a *ThermoQuest Finnigan TSQ 7000* or an *Agilent Q-TOF 6540 UHD*.

UV-VIS absorption measurements were performed on a *Varian Cary 50 Bio* UV/VIS spectrophotometer. Decay time measurements were performed on a *Fluorolog 3-22* spectrometer, a *Picobrite PB-375L* pulsed diode laser with an excitation wavelength of 378 nm and a pulse width of < 100 ps was used as the excitation source.

Melting points (mps) were recorded on an automated system: Stanford Research Systems *OptiMelt MPA 100*.

7.2 Nitrogen radicals in ATRA reactions: A holistic picture for three distinct ATRA mechanisms.

7.2.1 Synthesis of *N*-Chlorosulfonamides

General procedure for the synthesis of *N*-Chlorosulfonamides[178]

To a mixture of calcium hypochlorite (65% wt, 1.3 eq.) in chloroform (0.4 M) was added 250 mg aluminum oxide per mmol of calcium hypochloride. After stirring at 40 °C for 15 min the corresponding sulfonamide (1 eq.) was added to the suspension. After 1.5-3 h at 40 °C (conversion tracked by TLC analysis), the suspension was filtered over a frit and concentrated *in vacuo.* The crude mixture was purified by column chromatography using PE:EA mixtures to afford the desired product. *N*-chlorosaccharin **17b** was supplied by commercial sources and *N*-chloroamine **17c** was synthesized according to literature procedure.[179]

N-chloro-*N*,4-dimethylbenzenesulfonamide (17a)
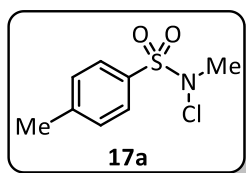
According to the general procedure, (**17a**) was prepared from calcium hypochlorite (2.86 g, 13.0 mmol, 1.3 eq.) and *N*,4-dimethylbenzenesulfonamide (3.70 g, 20.0 mmol, 1.0 eq.). After 2 h, the suspension was filtered and concentrated *in vacuo* and purified by column chromatography using PE:EA 20% (R_f = 0.6 in PE:EA 20%) to afford the desired product as white solid (3.78 g, 86%). The data was in accordance with literature.[178]

^{1}H-NMR (400 MHz, CDCl$_3$): δ = 7.81 (d, *J* = 8.4 Hz, 2H), 7.39 (d, *J* = 8.0 Hz, 2H), 3.08 (s, 3H), 2.47 (s, 3H). **^{13}C-NMR** (101 MHz, CDCl$_3$): δ = 145.7, 130.0, 129.8, 128.7, 45.5, 21.9. **IR** (neat, cm^{-1}): 3071, 2986, 2933, 1595, 1494, 1454, 1429, 1403, 1353, 1308, 1297, 1101, 1088, 1029, 802, 779, 663. **M.p.**: 77 °C. **HRMS** (ESI): m/z calculated for C$_8$H$_{11}$ClNO$_2$S [MH$^+$]: 220.0194, found: 220.0196.

N-chloro-*N*-methyl-4-nitrobenzenesulfonamide (17d)
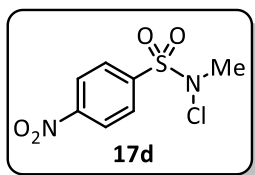
To an ice-cooled mixture of *N*-methyl-4-nitrobenzenesulfonamide (1.51 g, 7.0 mmol, 1.0 eq.) in dichloromethane (70 mL, 0.1 M) was added 1,3,5-trichloro-1,3,5-triazinane-2,4,6-trione (TCCA, 1.79 g, 7.7 mmol, 1.1 eq.). After 4 h, the reaction was complete (as judged by TLC) and the mixture was diluted with 70 mL of water. After layer separation the aqueous phase was extracted with dichloromethane (3 x 40 mL), dried over Na_2SO_4 as well as filtered and concentrated *in vacuo*. The crude mixture was purified by column chromatography using PE:EA 33% (R_f = 0.55 in PE:EA 33%) to afford the desired product as white solid (1.70 g, 97%).

1H-NMR (300 MHz, $CDCl_3$): δ = 8.53 – 8.42 (m, 2H), 8.21 – 8.09 (m, 2H), 3.17 (s, 3H). **13C-NMR** (75 MHz, $CDCl_3$): δ = 151.3, 137.5, 131.2, 124.4, 45.4. **IR** (neat, cm^{-1}): 3108, 2937, 2870, 1733, 1607, 1528, 1453, 1405, 1349, 1311, 1182, 1085, 1036, 857, 798, 738, 682. **M.p.**: 156 - 158 °C. **HRMS** (ESI): m/z calculated for $C_7H_8ClN_2O_4S$ [MH$^+$]: 250.9888, found: 250.9869.

N-allyl-*N*-chloro-4-methylbenzenesulfonamide (17e)
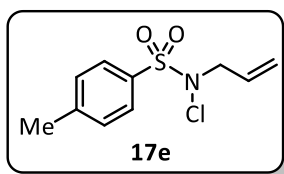
To a solution of 7.7 mL Triethylamine (5.62 g, 55 mmol, 1.1 eq.) in dichloromethane (250 mL, 0.25 M) was added Allylamine (3.20 g, 55 mmol, 1.1 eq.). 9.73 g of Tosyl chloride (98% wt, 50 mmol, 1.0 eq.) was added over 10 minutes at 0 °C. The reaction mixture was left stirring for 3 h until the reaction was complete as judged by TLC. The crude mixture was added to 250 mL NaHCO$_3$ sat. in a separatory funnel. The phases were separated, and the aqueous phase was extracted 3x with 50 mL of dichloromethane. The combined organic phases were dried over Na_2SO_4 and concentrated *in vacuo*. The crude mixture was treated according to the general procedure with calcium hypochloride (14.3 g, 65.0 mmol, 1.3 eq.). After 1.5 h the crude mixture was filtered and concentrated *in vacuo* and purified by column chromatography using PE:EA 30% (Rf = 0.65 in PE:EA 30%) to afford the desired product *N*-allyl-*N*-chloro-4-methylbenzenesulfonamide (**3**) as white solid (10.52 g, 42.8 mmol, 86% overall yield).

¹H NMR (400 MHz CDCl₃): δ = 7.83 (d, *J* = 8.3 Hz, 2H), 7.40 (d, *J* = 8.1 Hz, 2H), 5.82 (ddt, *J* = 16.8, 10.3, 6.4 Hz, 1H), 5.34 − 5.26 (m, 2H), 3.86 (d, *J* = 6.4 Hz, 2H), 2.48 (s, 3H) **¹³C-NMR** (101 MHz, CDCl₃): δ =145.5, 130.7, 130.0, 129.8, 129.6, 121.2, 59.3, 21.8. **IR** (neat, cm⁻¹): 3071, 2922, 2363, 1595, 1361, 1167, 1088, 988, 932, 809. **M.p.**: 77 °C. **HRMS** (ESI): m/z calculated for $C_{10}H_{13}ClNO_2S$ [MH⁺]: 246.0350, found: 246.0353.

N-(tert-butyl)-*N*-chloro-4-methylbenzenesulfonamide (17f)
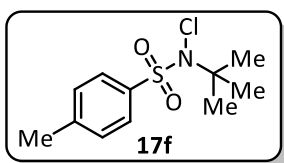
According to the general procedure, **17f** was prepared from calcium hypochloride (2.86 g, 13.0 mmol, 1.3 eq.) and *N*-(tert-butyl)-4-methylbenzenesulfonamide (3.70 g, 20.0 mmol, 1.0 eq.) in chloroform (50 mL). After 2 h, the suspension was filtered and concentrated *in vacuo* and purified by column chromatography using PE:EA 20% (R_f = 0.48 in PE:EA 20%) to afford the desired product as white solid (3.78 g, 86%).

¹H NMR (400 MHz CDCl₃): δ = 7.85 (d, *J* = 8.3, 2H), 7.32 (d, *J* = 8.0, 2H), 2.44 (s, 3H), 1.48 (s, 9H). **¹³C-NMR** (101 MHz, CDCl₃): δ = 144.8, 135.6, 129.6, 129.0, 68.1, 29.3, 21.8. **IR** (neat, cm⁻¹): 2986, 2937, 1599, 1461, 1357, 11163, 1088, 880, 913, 705, 664. **M.p.**: 147 - 148 °C. **HRMS** (ESI): m/z calculated for $C_{11}H_{17}ClNO_2S$ [MH⁺]: 262.0663, found: 262.0659.

(S)-*N*-chloro-*N*-(1-hydroxy-3-methylbutan-2-yl)-4-methylbenzenesulfonamide (17g)
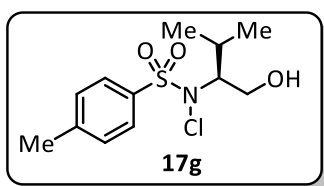
According to the general procedure, (**17g**) was prepared from calcium hypochlorite (1.67 g, 7.60 mmol, 1.3 eq.) and (S)-*N*-(1-hydroxy-3-methylbutan-2-yl)-4-methylbenzenesulfonamide (1.68 g, 5.85 mmol, 1.0 eq.). After 3 h, the suspension was filtered and concentrated *in vacuo* and purified by column chromatography using PE:EA 50% (R_f = 0.52 in PE:EA 50%) to afford the desired product as colorless oil (700.1 mg, 41%).

¹H-NMR (400 MHz, CDCl₃): δ = 7.82 (d, *J* = 8.4, 2H), 7.32 (d, *J* = 8.1, 2H), 4.04 (ddd, *J* = 8.8, 7.0, 4.9, 1H), 3.77 − 3.70 (m, 2H), 2.42 (s, 3H), 2.11 (s, 1H), 1.89 − 1.76 (m, 1H), 0.98 (dd, *J* = 9.0, 6.7, 6H). **¹³C-NMR** (101 MHz, CDCl₃): δ = 145.0, 133.7, 129.7, 129.0, 70.2, 60.7, 28.2, 21.7, 20.1, 19.8. **IR** (neat, cm⁻¹): 3548, 2967, 2878, 1595, 1468, 2334, 1163, 1092, 1021, 910, 813, 727, 667. **HRMS** (ESI): m/z calculated for $C_{12}H_{19}ClNO_3S$ [MH⁺]: 292.0769, found: 292.0772.

7.2.2 General Procedures for Chloroamination of Olefins

General procedure A

An oven dried pressure tube (25 mL size) equipped with a magnetic stir bar was charged with the corresponding *N*-chloro-4-methylbenzenesulfonamide **17a** (98.9 mg, 0.45 mmol, 1.5 eq.), [Cu(dap)$_2$]Cl (2.7 mg, 0.003 mmol, 1.0 mol%) and anhydrous 1,2-dichloroethane (DCE, 6.00 mL). The mixture was degassed using three freeze-pump-thaw cycles. Olefin (0.30 mmol, 1.0 eq.) was added under a slight nitrogen overpressure and the tube was equipped with a LED setup and sealed. The reaction mixture was irradiated at room temperature with a blue LED (λ_{max} = 455 nm) while being stirred and the reaction progress was monitored by TLC. After 6 h the reaction was stopped by switching off the light source. For determining the yield by NMR, either *1,1,2,2*-tetrachloroethane (25.2 mg, 0.15 mmol, 15.8 μL) was added to the crude mixture or a sample of 1.00 mL was taken, and 2-nitropropane was added as an internal standard. The remaining crude reaction mixture were concentrated and purified by column chromatography on silica gel by using PE:EA mixtures to afford the desired product.

General procedure B

A flame-dried pressure tube (5 mL) was equipped with a magnetic stir bar and charged with the corresponding *N*-chloro-4-methylbenzenesulfonamide **17a** (176.8 mg, 0.8 mmol, 1.0 eq.), [Cu(dap)$_2$]Cl (7.1mg, 0.008 mmol, 1.0 mol%) and anhydrous dichloromethane (DCM, 0.8 mL, 1M) . The mixture was degassed using three freeze-pump-thaw cycles. Olefin (1.60 mmol, 2.0 eq.) was added under a slight nitrogen overpressure and the tube was equipped with a LED setup and sealed. The reaction mixture was irradiated at room temperature with a green LED (λ_{max} = 530 nm) while being stirred. After 16 hours the reaction was stopped by switching off the light source. The crude mixture was transferred with DCM and concentrated *in* vacuo. For determining the crude yield by NMR 42 μL *1,1,2,2*-tetrachloroethane (67.4 mg, 0.4 mmol) were added to the crude mixture. The crude mixture was purified by column chromatography on silica gel by using PE:EA mixtures to afford the desired product.

N-(2-chloro-2-(*p*-tolyl)ethyl)-*N*,4-dimethylbenzenesulfonamide (18a)
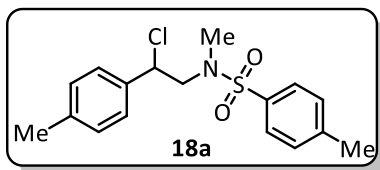
According to general procedure **B**, **18a** was prepared from 4-methylstyrene (**15a**) (213 µL, 1.6 mmol, 2.0 eq.) using [Cu(dap)₂]Cl (7.1 mg, 0.008 mmol, 1.0 mol%) as a catalyst. The crude product was purified by column chromatography on silica gel using PE:EA 3%-10% (R_f = 0.21 in PE:EA 7.5%) to afford **18a** as a white solid (249.5 mg, 96% yield).

¹H-NMR (300 MHz, CDCl₃): δ = 7.64 (d, *J* = 8.3 Hz, 2H), 7.30 (dd, *J* = 8.1, 1.9 Hz, 4H), 7.17 (d, *J* = 7.7 Hz, 2H), 5.08 (t, *J* = 7.3 Hz, 1H), 3.57 (dd, *J* = 14.5, 7.4 Hz, 1H), 3.39 (dd, *J* = 14.4, 7.3 Hz, 1H), 2.64 (s, 3H), 2.42 (s, 3H), 2.35 (s, 3H). **¹³C-NMR** (75 MHz, CDCl₃): δ = 143.7, 138.8, 135.8, 134.8, 129.8, 129.5, 127.5, 127.4, 61.3, 58.0, 37.0, 21.6, 21.3. **IR** (neat, cm⁻¹): 3034, 2922, 2865, 1595, 1513, 1460, 1342, 1156, 1088, 984, 924, 857, 820, 734. **M.p.**: 91 - 94 °C. **HRMS** (ESI): m/z calculated for $C_{17}H_{21}ClNO_2S$ [MH⁺]: 338.0976, found: 338.0985. The data is in accordance with the data reported in literature.[58]

N-(2-chloro-2-phenylethyl)-*N*,4-dimethylbenzenesulfonamide (18b)
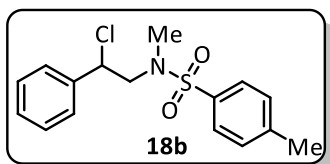
According to general procedure **A**, **18b** was prepared in a 200 ml photoreactor setup (Figure 25) from distilled styrene (**15b**) (1.09 mL, 9.5 mmol, 1.0 eq.) and *N*-chloro-*N*,4-dimethylbenzenesulfonamide (**17a**) (3.19 g, 14.25 mmol, 1.5 eq.) using [Cu(dap)₂]Cl (84 mg, 0.0095 mmol, 1.0 mol%) as a catalyst. The crude product was purified by column chromatography on silica gel using PE:EA 20% (Rf = 0.14 in PE:EA 20%) to afford **18b** as a light yellow oil (2.96 g, 96% yield).

¹H-NMR (400 MHz, CDCl₃): δ = 7.64 (d, *J* = 8.3 Hz, 2H), 7.48 – 7.25 (m, 7H), 5.11 (t, *J* = 7.3 Hz, 1H), 3.59 (dd, *J* = 14.5, 7.4 Hz, 1H), 3.40 (dd, *J* = 14.5, 7.3 Hz, 1H), 2.63 (s, 3H), 2.42 (s, 3H). **¹³C-NMR** (101 MHz, CDCl₃) δ = 143.6, 138.6, 134.5, 129.7, 128.8, 128.7, 127.4, 127.2, 61.2, 57.8, 36.8, 21.4. **IR** (neat, cm-1): 3063, 3034, 2926, 1599, 1495, 1454, 1338, 1156, 1088, 988, 932, 813, 738, 697. **HRMS** (ESI): m/z calculated for $C_{15}H_{16}ClN_2O_4S$ [MH⁺]: 355.0514, found: 355.0517. The data is in accordance with the data reported in literature.[58]

N-(2-hydroxy-2-(4-methoxyphenyl)ethyl)-*N*,4-dimethylbenzenesulfonamide (18c)
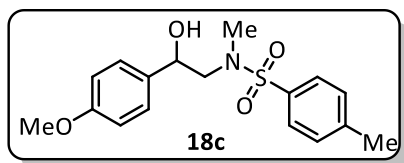
According to general procedure **A**, **18c** was prepared from 4-methoxystyrene (**15c**) (40 µL, 0.30 mmol, 1.0 eq.) using no catalyst. The crude product was purified by column chromatography on silica gel using PE:Et$_2$O 50% (R$_f$ = 0.16 in PE:Et$_2$O 50%) to afford **18c** as a colorless oil (18.9 mg, 18% yield) with slight impurities of *N*,4-dimethylbenzenesulfonamide.

^{1}H-NMR (400 MHz, CDCl$_3$): δ = 7.66 (d, *J* = 8.2 Hz, 2H), 7.30 (d, *J* = 8.7 Hz, 4H), 6.88 (d, *J* = 8.7 Hz, 2H), 4.87 (dd, *J* = 8.9, 3.4 Hz, 1H), 3.80 (s, 3H), 3.27 (dd, *J* = 14.1, 8.9 Hz, 1H), 2.98 (dd, *J* = 14.1, 3.5 Hz, 1H), 2.79 (s, 3H), 2.41 (s, 3H). **^{1}H-NMR** (400 MHz, DMSO-d$_6$): δ = 7.61 (d, *J* = 8.2 Hz, 2H), 7.42 – 7.39 (m, 2H), 7.24 (d, *J* = 8.6 Hz, 2H), 6.89 (d, *J* = 8.6 Hz, 2H), 5.44 (d, *J* = 4.5 Hz, 1H), 4.67 (dt, *J* = 7.8, 4.8 Hz, 1H), 3.74 (s, 3H), 3.01 (qd, *J* = 13.5, 6.4 Hz, 2H), 2.66 (s, 3H), 2.39 – 2.38 (m, 3H). **^{13}C NMR** (101 MHz, CDCl$_3$): δ = 159.6, 143.8, 134.4, 133.3, 129.9, 127.6, 127.4, 114.1, 71.9, 58.5, 55.4, 36.9, 21.7. **IR** (neat, cm^{-1}): 3507, 3295, 3076, 2922, 2839, 1610, 1513, 1457, 1327, 1245, 1156, 1088, 1033, 947, 813, 719. **HRMS** (APCI): m/z calculated for C$_{17}$H$_{22}$NO$_4$S [MH$^+$]: 336.1264, found: 336.1262.

This compound had already been reported as chloro- substituted (N-(2-chloro-2-(4-methoxyphenyl)ethyl)-N,4-dimethylbenzenesulfonamide): The NMR-data of the product we isolated is in full accordance with the data reported in the literature.[58] According to our data we concluded, that the compound is in fact hydroxy-, and not chloro-substituted. The IR spectrum shows a typical broad O-H stretching vibration in the region of 3500 cm^{-1}. Concerning the NMR-data, the predicted ^{13}C-carbon shift the C-OH carbon is in the range of 71 ppm for the hydroxy-substituted compound, which fits well with the experimental value of 71.9 ppm. In contrast to that, for a Cl-substituted compound this carbon shift is predicted to appear in the range of 59 ppm, which is in accordance with the measured values of the chloro-substituted compounds synthesized herein. Moreover, measuring the ^{1}H-NMR in DMSO-d$_6$ disclosed an additional doublet at 5.44 ppm which could be assigned to the proton of the hydroxy group. HRMS data also confirmed the hydroxy-substitution, while no chloro-substituted product could be detected.

N-(2-chloro-2-(*o*-tolyl)ethyl)-*N*,4-dimethylbenzenesulfonamide (18d)
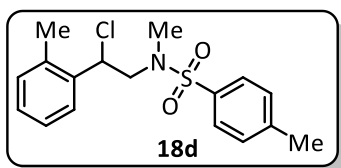
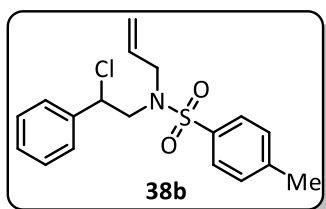According to general procedure **B**, **18d** was prepared from 2-methylstyrene (**15d**) (211 µL, 1.6 mmol, 2.0 eq.) using [Cu(dap)₂]Cl (7.1 mg, 0.008 mmol, 1.0 mol%) as a catalyst. The crude product was purified by column chromatography on silica gel using PE:EA 5%-15% (R_f = 0.16 in PE:EA 5%) to afford **18d** as a colorless oil (253,4 mg, 94% yield).

¹H-NMR (400 MHz, CDCl₃): δ = 7.66 (d, *J* = 8.2, 2H), 7.50 – 7.46 (m, 1H), 7.35 – 7.29 (m, 2H), 7.27 – 7.16 (m, 3H), 5.49 (dd, *J* = 7.8, 6.6, 1H), 3.51 (qd, *J* = 14.6, 7.2, 2H), 2.73 (s, 3H), 2.47 (s, 3H), 2.42 (s, 3H). **¹³C-NMR** (101 MHz, CDCl₃): δ = 143.7, 137.0, 136.0, 134.6, 130.7, 129.9, 128.6, 127.3, 127.1, 126.6, 58.0, 57.5, 37.3, 21.5, 19.4. **IR** (neat, cm⁻¹): 3067, 2922, 2868, 1599, 1490, 1461, 1342, 1156, 1088, 984, 924, 816, 753, 723. **HRMS** (ESI): m/z calculated for C₁₇H₂₁ClNO₂S [MH⁺]: 338.0976, found: 338.0986.

N-(2-chloro-2-(2-methoxyphenyl)ethyl)-*N*,4-dimethylbenzenesulfonamide (18e)
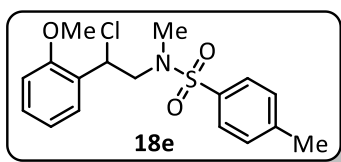
According to general procedure **A**, **18e** was prepared from 2-methoxystyrene (**15e**) (40 µL, 0.30 mmol, 1.0 eq.) using [Cu(dap)₂]Cl (2.7 mg, 0.003 mmol, 1.0 mol%) as a catalyst. The crude product was purified by column chromatography on silica gel using PE:Et₂O 50% (R_f = 0.45 in PE:Et₂O 50%) to afford **18e** as a light yellow oil (47.3 mg, 56% yield).

¹H-NMR (400 MHz, CDCl₃): δ = 7.67 – 7.60 (m, 2H), 7.48 (dd, *J* = 7.6, 1.7 Hz, 1H), 7.35 – 7.27 (m, 3H), 6.99 (td, *J* = 7.5, 1.1 Hz, 1H), 6.88 (dd, *J* = 8.3, 1.0 Hz, 1H), 5.56 (dd, *J* = 7.7, 6.5 Hz, 1H), 3.85 (s, 3H), 3.62 – 3.51 (m, 2H), 2.76 (s, 3H), 2.42 (s, 3H). **¹³C-NMR** (101 MHz, CDCl₃): δ = 156.7, 143.5, 135.1, 130.1, 129.8, 128.8, 127.5, 126.8, 121.1, 111.0, 56.5, 55.8, 55.2, 36.3, 21.6. **IR** (neat, cm⁻¹): 3070, 2922, 2840, 1599, 1491, 1461, 1342, 1249, 1159, 1088, 1025, 929, 818, 752, 730. **HRMS** (ESI): m/z calculated for C₁₇H₂₁ClNO₃S [MH⁺]: 354.0925, found: 354.0935.

N-(1-chloro-2,3-dihydro-1*H*-inden-2-yl)-*N*,4-dimethylbenzenesulfonamide (18f)

18f-1
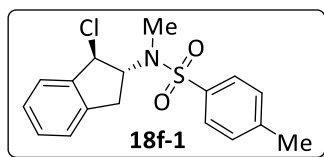
According to general procedure **B**, **18f** was prepared from 1*H*-indene (**15f**) (185.9 mg, 0.30 mmol, 2.0 eq.) using [Cu(dap)$_2$]Cl (7.1 mg, 0.008 mmol, 1.0 mol%) as a catalyst. The crude product was purified by column chromatography on silica gel using PE:EA 5%-15% (R$_f$ = 0.31 in PE:EA 20%) to afford the diastereomer **18f-1** as a light yellow oil (185.9 mg, 69% yield) next t **18f-2**.

¹H-NMR (400 MHz, CDCl$_3$, *E*-isomer) δ = 7.70 (d, *J* = 8.2 Hz, 2H), 7.27 (d, *J* = 7.8 Hz, 3H), 7.18 (t, *J* = 3.6 Hz, 2H), 7.09 (dd, *J* = 6.6, 2.2 Hz, 1H), 5.04 (d, *J* = 5.7 Hz, 1H), 4.87 (dt, *J* = 8.2, 6.6 Hz, 1H), 3.05 (dd, *J* = 16.4, 8.2 Hz, 1H), 2.73 (dd, *J* = 16.4, 6.5 Hz, 1H), 2.60 (s, 3H), 2.38 (s, 3H). **¹³C-NMR** (101 MHz, CDCl$_3$, *E*-isomer) δ = 143.6, 140.0, 139.4, 136.2, 129.8, 129.3, 127.7, 127.4, 125.0, 124.6, 66.9, 62.7, 33.1, 29.7, 21.6. **IR** (neat, cm⁻¹): 3030, 2955, 2922, 2857, 1599, 1492, 1461, 1338, 1156, 1088, 965, 816, 746, 701. **HRMS** (ESI): m/z calculated for C$_{17}$H$_{19}$ClNO$_2$S [MH⁺]: 336.0822, found: 336.0820. The data is in accordance with the data reported in literature.[58]

N-(1H-inden-2-yl)-*N*,4-dimethylbenzenesulfonamide (4f-2, LT617 F1)

18f-1
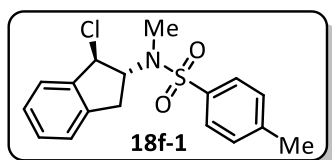
According to general procedure **B**, **18f-2** was prepared from 1*H*-indene (**15f**) (185.9 mg, 0.30 mmol, 2.0 eq.) using [Cu(dap)$_2$]Cl (7.1 mg, 0.008 mmol, 1.0 mol%) as a catalyst. The crude product was purified by column chromatography on silica gel using PE:EA 5%-15% (R$_f$ = 0.31 in PE:EA 20%) to afford **18f-2** as a light colorless oil (35.1 mg, 15% yield) next to **18f-1**.

¹H-NMR (400 MHz, CDCl$_3$) δ = 7.68 (d, *J* = 8.3, 2 H), 7.41 (d, *J* = 7.3, 1H), 7.36 – 7.29 (m, 2 H), 7.30 – 7.23 (m, 2 H), 7.22 – 7.15 (m, 1 H), 6.16 (s, 1 H), 3.89 (s, 2 H), 3.28 (s, 3 H), 2.45 (s, 3 H). **¹³C-NMR** (101 MHz, CDCl$_3$) δ = 147.2, 144.1, 143.2, 139.7, 134.6, 129.9, 127.2, 126.7, 124.1, 123.4, 120.1, 115.1, 40.7, 37.2, 21.7. **IR** (neat, cm⁻¹): 3291, 3064, 2922, 1718, 1599, 1461, 1402, 1327, 1159, 1092, 816, 753, 664. **HRMS** (ESI): m/z calculated for C$_{17}$H$_{18}$NO$_2$S [MH⁺]: 300.1053, found: 300.1057.

N-(2-chloro-2-(naphthalen-2-yl)ethyl)-*N*,4-dimethylbenzenesulfonamide (18g)
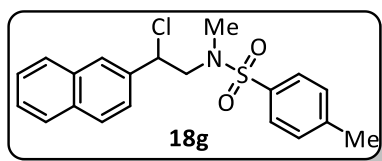
According to general procedure **A**, **18g** was prepared from 2-vinylnaphthalene (**15g**) (46.3 mg, 0.30 mmol, 1.0 eq.) using [Cu(dap)$_2$]Cl (2.7 mg, 0.003 mmol, 1.0 mol%) as a catalyst. The crude product was purified by column chromatography on silica gel using PE:EA 7.5% (R$_f$ = 0.09 in PE:EA 7.5%) to afford **18g** as a colorless oil (62.4 mg, 70% yield).

^{1}H-NMR (300 MHz, CDCl$_3$): δ = 7.92 – 7.78 (m, 4H), 7.63 (d, *J* = 8.3 Hz, 2H), 7.59 – 7.46 (m, 3H), 7.31 – 7.27 (m, 1H), 7.26 – 7.22 (m, 1H), 5.28 (t, *J* = 7.4 Hz, 1H), 3.69 (dd, *J* = 14.5, 7.2 Hz, 1H), 3.52 (dd, *J* = 14.5, 7.5 Hz, 1H), 2.63 (s, 3H), 2.41 (s, 3H). **^{13}C-NMR** (75 MHz, CDCl$_3$): δ = 143.8, 136.0, 134.9, 133.5, 133.1, 129.9, 129.0, 128.3, 127.9, 127.4, 127.3, 126.9, 126.8, 124.6, 61.7, 58.0, 37.2, 21.7. **IR** (neat, cm^{-1}): 3056, 2922, 2851, 1599, 1495, 1443, 1342, 1156, 1088, 988, 932, 820, 779, 723. **HRMS** (ESI): m/z calculated for C$_{20}$H$_{21}$ClNO$_2$S [MH$^+$]: 374.0983, found 374.0976.

N-(1-chloro-1-phenylprop-1-en-2-yl)-*N*,4-dimethylbenzenesulfonamide (18h)
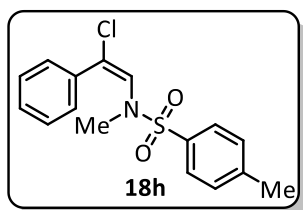
According to general procedure **B**, **18h** was prepared from phenylacetylene (**15h**) (176 μL, 1.6 mmol, 2.0 eq.) using [Cu(dap)$_2$]Cl (7.1 mg, 0.008 mmol, 1.0 mol%) as a catalyst. The crude product was purified by column chromatography on silica gel using PE:EA 5%-15% (R$_f$ = 0.10 in PE:EA 7.5%) to afford **18h** as a colorless oil (186.8 mg, 73% yield of a mixture of non-separable diastereomers: *E*:*Z* = 16.7:1).

^{1}H-NMR (300 MHz, CDCl$_3$, *E*-isomer): δ = 8.08 (d, *J* = 8.3 Hz, 2H), 7.80 – 7.72 (m, 2H), 7.68 – 7.54 (m, 5H), 7.04 (s, 1H), 2.95 (s, 3H), 2.83 (s, 3H). **^{13}C-NMR** (101 MHz, CDCl$_3$, *E*-isomer): δ = 144.3, 135.4, 134.0, 130.0, 129.3, 128.9, 128.3, 127.5, 127.1, 126.0, 36.7, 21.7. ^{13}C-NMR (101 MHz, CDCl$_3$, *Z*-isomer): δ = 144.2, 136.5, 135.2, 130.0, 129.4, 129.2, 128.6, 127.4, 126.8, 126.7, 125.1, 36.5, 21.8. **HRMS** (ESI, *E*-isomer): m/z calculated for C$_{16}$H$_{17}$ClNO$_2$S [MH$^+$]: 322.0663, found: 322.0668. The data of the *E*-isomer is in accordance with the data reported in literature.[99]

N-(2-chloro-2-(4-cyanophenyl)ethyl)-*N*,4-dimethylbenzenesulfonamide (18i)
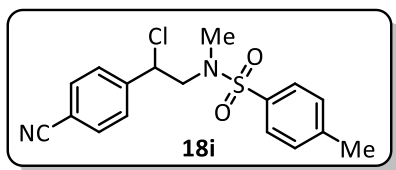
According to general procedure **A**, **18i** was prepared from 4-cyanostyrene (**15i**) (39 μL, 0.30 mmol, 1.0 eq.) using [Cu(dap)$_2$]Cl (2.7 mg, 0.003 mmol, 1.0 mol%) as a catalyst. The crude product was purified by column chromatography on silica gel using PE:EA 10%-25% (R$_f$ = 0.29 in PE:EA 25%) to afford **18i** as a colorless oil (80.0 mg, 96% yield).

^{1}H-NMR (400 MHz, CDCl$_3$): δ = 7.68 (d, *J* = 8.4 Hz, 2H), 7.63 (d, *J* = 8.3 Hz, 2H), 7.56 (d, *J* = 8.3 Hz, 2H), 7.32 (d, *J* = 8.0 Hz, 2H), 5.15 (t, *J* = 7.4 Hz, 1H), 3.52 (dd, *J* = 14.5, 7.0 Hz, 1H), 3.41 (dd, *J* = 14.5, 7.8 Hz, 1H), 2.63 (s, 3H), 2.43 (s, 3H). **^{13}C-NMR** (101 MHz, CDCl$_3$): δ = 144.1, 143.8, 134.4, 132.7, 130.0, 128.6, 127.4, 118.4, 112.9, 60.1, 58.1, 37.4, 21.7. **IR** (neat, cm^{-1}): 3065, 3027, 2926, 2823, 2229, 1599, 1495, 1457, 1338, 1156, 1088, 988, 932, 816, 760, 720. **HRMS** (ESI): m/z calculated for C$_{17}$H$_{18}$ClN$_2$O$_2$S [MH$^+$]: 349.0772, found: 349.0773.

N-(2-chloro-2-(4-nitrophenyl)ethyl)-*N*,4-dimethylbenzenesulfonamide (18j)
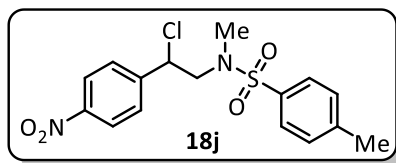
According to general procedure **A**, **18j** was prepared from 4-nitrostyrene (**15j**) (45 mg, 0.30 mmol, 1.0 eq.) using [Cu(dap)$_2$]Cl (2.7 mg, 0.003 mmol, 1.0 mol%) as a catalyst. The crude product was purified by column chromatography on silica gel using PE:Et$_2$O 50% (R$_f$ = 0.30 in PE: Et$_2$O 50%) to afford **18j** as a yellow oil (90.0 mg, 98% yield).

^{1}H NMR (400 MHz, CDCl$_3$): δ = 8.24 (d, *J* = 8.7 Hz, 2H), 7.69 – 7.56 (m, 4H), 7.32 (d, *J* = 8.0 Hz, 2H), 5.21 (t, *J* = 7.4 Hz, 1H), 3.54 (dd, *J* = 14.5, 6.9 Hz, 1H), 3.44 (dd, *J* = 14.5, 7.8 Hz, 1H), 2.65 (s, 3H), 2.43 (s, 3H). **^{13}C-NMR** (101 MHz, CDCl$_3$): δ = 148.2, 145.7, 144.1, 134.4, 130.1, 128.8, 127.5, 124.1, 59.7, 58.1, 37.4, 21.7. **IR** (neat, cm^{-1}): 3112, 3083, 2926, 2866, 1599, 1521, 1457, 1342, 1156, 1092, 932, 857, 813, 742. **HRMS** (ESI): m/z calculated for C$_{16}$H$_{18}$ClN$_2$O$_4$S [MH$^+$]: 369.0670; found: 369.0674.

Methyl 4-(1-chloro-2-((*N*,4-dimethylphenyl)sulfonamido)ethyl)benzoate (18k)
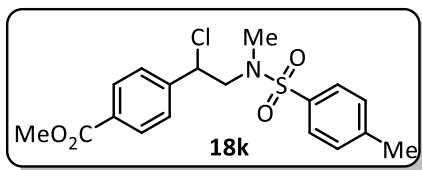
According to general procedure **A**, **18k** was prepared from methyl 4-vinylbenzoate (**15k**) (49 mg, 0.30 mmol, 1.0 eq.) using [Cu(dap)$_2$]Cl (2.7 mg, 0.003 mmol, 1.0 mol%) as a catalyst. The crude product was purified by flash column chromatography on silica gel using PE:EA 5-20% (R$_f$ = 0.23, PE:EA 20%) to afford **18k** as a yellow oil (87.0 mg, 95% yield).

^{1}H NMR (300 MHz, CDCl$_3$): δ = 8.03 (d, *J* = 8.2, 2H), 7.62 (d, *J* = 8.2, 2H), 7.49 (d, *J* = 8.3, 2H), 7.29 (d, *J* = 8.0, 2H), 5.14 (t, *J* = 7.3, 1H), 3.91 (s, 3H), 3.57 (dd, *J* = 14.5, 7.2, 1H), 3.38 (dd, *J* = 14.5, 7.6, 1H), 2.60 (s, 3H), 2.41 (s, 3H). **^{13}C-NMR** (75 MHz, CDCl$_3$): δ = 166.5, 143.8, 143.5, 134.5, 130.6, 130.1, 129.9, 127.7, 127.3, 60.5, 58.0, 52.3, 37.1, 21.6. **IR** (neat, cm^{-1}): 3064, 2926, 2855, 2356, 1595, 1439, 1342, 1163, 1088, 936, 816, 746. **HRMS** (ESI): m/z calculated for C$_{18}$H$_{21}$ClNO$_4$S [MH$^+$]: 382.0874; found: 382.0878.

Methyl 4-(1-chloro-2-((*N*,4-dimethylphenyl)sulfonamido)ethyl)benzoate (18l)
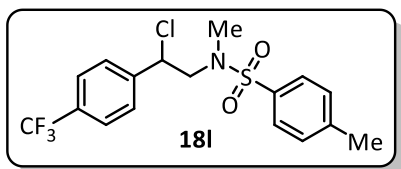
According to general procedure **A**, **18l** was prepared from 1-(trifluoromethyl)-4-vinylbenzene (**15l**) (49.0 mg, 0.30 mmol, 1.0 eq.) using [Cu(dap)$_2$]Cl (2.7 mg, 0.003 mmol, 1.0 mol%) as a catalyst. The crude product was purified by flash column chromatography on silica gel (PE:EA 5-20%, R$_f$ = 0.12 in PE:EA 10%) to afford **18l** as a colorless oil (100.2 mg, 85% yield).

^{1}H-NMR (400 MHz, CDCl$_3$): δ = 7.68 – 7.60 (m, 4H), 7.56 (d, *J* = 8.4, 2H), 7.31 (dt, *J* = 7.9, 0.8, 2H), 5.17 (t, *J* = 7.3, 1H), 3.54 (dd, *J* = 14.5, 7.2, 1H), 3.43 (dd, *J* = 14.5, 7.5, 1H), 2.64 (s, 3H), 2.43 (s, 3H). **^{13}C-NMR** (101 MHz, CDCl$_3$) δ = 144.0, 142.7, 134.6, 131.1 (q, *J* = 32.6), 130.0, 128.2, 127.5, 125.9 (d, *J* = 3.6), 123.9 (d, *J* = 272.2), 60.3, 58.1, 37.3, 21.7. **^{19}F-NMR** (377 MHz, CDCl$_3$) δ = -63.2. **IR** (neat, cm^{-1}): 2930, 2359, 1621, 1420, 1323, 1159, 1122, 932, 813, 734. **HRMS** (ESI): m/z calculated for C$_{17}$H$_{18}$ClF$_3$NO$_2$S [MH$^+$]: 392.0693; found: 392.0701.

N-(2-chloro-2-(4-fluorophenyl)ethyl)-*N*,4-dimethylbenzenesulfonamide (18m)
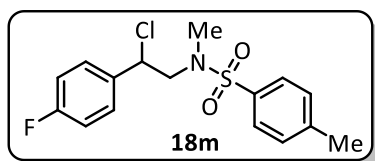
According to general procedure **A**, **18m** was prepared from 4-fluorostyrene (**15m**) (36 µL, 0.30 mmol, 1.0 eq.) using [Cu(dap)$_2$]Cl (2.7 mg, 0.003 mmol, 1.0 mol%) as a catalyst. The crude product was purified by column chromatography on silica gel using PE:EA 7.5% (R$_f$ = 0.18 in PE:EA 7.5%) to afford **18m** as a colorless oil (65.3 mg, 80% yield).

^{1}H-NMR (400 MHz, CDCl$_3$): δ = 7.69 − 7.60 (m, 2H), 7.43 − 7.37 (m, 2H), 7.34 − 7.28 (m, 2H), 7.12 − 7.01 (m, 2H), 5.10 (t, *J* = 7.4 Hz, 1H), 3.55 (dd, *J* = 14.5, 7.1 Hz, 1H), 3.39 (dd, *J* = 14.5, 7.6 Hz, 1H), 2.63 (s, 3H), 2.43 (s, 3H). **^{13}C-NMR** (101 MHz, CDCl$_3$): δ = 163.0 (d, *J*$_{C-F}$ = 248.0 Hz), 143.9, 134.8, 134.7 (d, *J*$_{C-F}$ = 3.3 Hz), 130.0, 129.5 (d, *J*$_{C-F}$ = 8.3 Hz), 127.5, 115.9 (d, *J*$_{C-F}$ = 21.9 Hz), 60.6, 58.2, 37.2, 21.7. **^{19}F-NMR** (282 MHz, CDCl$_3$): δ = -113.0. **IR** (neat, cm^{-1}): 3049, 2926, 2827, 1603, 1513, 1457, 1338, 1226, 1159, 1088, 988, 932, 839, 734. **HRMS** (ESI): m/z calculated for C$_{16}$H$_{18}$ClFNO$_2$S [MH$^+$]: 342.0725, found: 342.0739. The data is in accordance with the data reported in the literature.[58]

N-(2-chloro-2-(4-chlorophenyl)ethyl)-*N*,4-dimethylbenzenesulfonamide (18n)
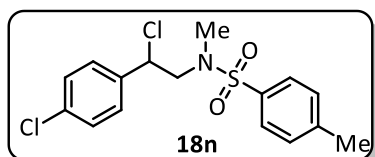
According to general procedure **A**, **18n** was prepared from 4-chlorostyrene (**15n**) (36 µL, 0.30 mmol, 1.0 eq.) using [Cu(dap)$_2$]Cl (2.7 mg, 0.003 mmol, 1.0 mol%) as a catalyst. The crude product was purified by column chromatography on silica gel using PE:EA 7.5% (R$_f$ = 0.11 in PE:EA 7.5%) to afford **18n** as a colorless oil (78.0 mg, 88% yield).

^{1}H-NMR (300 MHz, CDCl$_3$): δ = 7.63 (d, *J* = 8.3 Hz, 2H), 7.35 (s, 4H), 7.36 − 7.26 (m, 2H), 5.08 (t, *J* = 7.4 Hz, 1H), 3.54 (dd, *J* = 14.5, 7.1 Hz, 1H), 3.37 (dd, *J* = 14.4, 7.7 Hz, 1H), 2.63 (s, 3H), 2.43 (s, 3H). **^{13}C-NMR** (75 MHz, CDCl$_3$): δ = 143.9, 137.3, 134.9, 134.6, 130.0, 129.1, 129.1, 127.4, 60.5, 58.1, 37.2, 21.7. **IR** (neat, cm^{-1}): 3034, 2968, 2922, 1596, 1491, 1457, 1342, 1156, 1088, 988, 928, 813, 749, 686. **HRMS** (ESI): m/z calculated for C$_{16}$H$_{18}$Cl$_2$NO$_2$S [MH$^+$]: 358.0430, found: 358.0436. The data is in accordance with the data reported in literature.[58]

N-(2-(4-bromophenyl)-2-chloroethyl)-*N*,4-dimethylbenzenesulfonamide (18o)
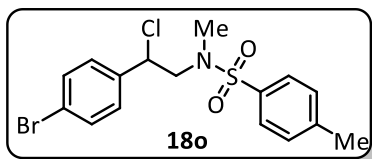
According to general procedure **A**, **18o** was prepared from 4-bromostyrene (**15o**) (39 µL, 0.30 mmol, 1.0 eq.) using [Cu(dap)$_2$]Cl (2.7 mg, 0.003 mmol, 1.0 mol%) as a catalyst. The crude product was purified by column chromatography on silica gel using PE:EA 7.5% (R_f = 0.10 in PE:EA 7.5%) to afford **18o** as a colorless oil (78.3 mg, 81% yield).

^{1}H-NMR (300 MHz, CDCl$_3$): δ = 7.63 (d, *J* = 8.3 Hz, 2H), 7.56 – 7.45 (m, 2H), 7.36 – 7.28 (m, 4H), 5.07 (t, *J* = 7.4 Hz, 1H), 3.53 (dd, *J* = 14.5, 7.1 Hz, 1H), 3.37 (dd, *J* = 14.4, 7.7 Hz, 1H), 2.63 (s, 3H), 2.43 (s, 3H). **^{13}C-NMR** (75 MHz, CDCl$_3$): δ = 143.9, 137.9, 134.7, 132.1, 130.0, 129.4, 127.5, 123.0, 60.5, 58.1, 37.2, 21.7. **IR** (neat, cm^{-1}): 3053, 2952, 2922, 2848, 1596, 1491, 1462, 1445, 1405, 1346, 1156, 1088, 988, 924, 824, 746, 667. **HRMS** (ESI): m/z calculated for C$_{16}$H$_{18}$BrClNO$_2$S [MH$^+$]: 401.9925, found: 401.9929.

N-(2-chloro-2-(3-chlorophenyl)ethyl)-*N*,4-dimethylbenzenesulfonamide (18p)
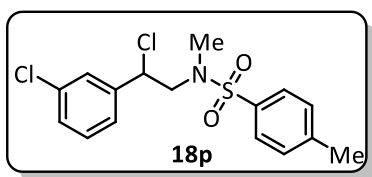
According to general procedure **A**, **18p** was prepared from 3-chlorostyrene (**15p**) (38 µL, 0.30 mmol, 1.0 eq.) using [Cu(dap)$_2$]Cl (2.7 mg, 0.003 mmol, 1.0 mol%) as a catalyst. The crude product was purified by column chromatography on silica gel using PE:EA 7.5% (R_f = 0.13 in PE:EA 7.5%) to afford **18p** as a colorless oil (74.0 mg, 86% yield).

^{1}H-NMR (400 MHz, CDCl$_3$): δ = 7.64 (d, *J* = 8.3 Hz, 2H), 7.41 – 7.36 (m, 1H), 7.36 – 7.27 (m, 5H), 5.07 (t, *J* = 7.3 Hz, 1H), 3.54 (dd, *J* = 14.6, 7.3 Hz, 1H), 3.40 (dd, *J* = 14.5, 7.3 Hz, 1H), 2.66 (s, 3H), 2.43 (s, 3H). **^{13}C-NMR** (101 MHz, CDCl$_3$): δ = 143.9, 140.8, 134.8, 134.8, 130.2, 130.0, 129.2, 127.8, 127.5, 125.9, 60.5, 58.1, 37.3, 21.7. **IR** (neat, cm^{-1}): 3064, 2922, 2818, 1595, 1576, 1476, 1431, 1338, 1156, 1088, 992, 932, 816, 753, 727, 690. **HRMS** (ESI): m/z calculated for C$_{16}$H$_{18}$Cl$_2$NO$_2$S [MH$^+$]: 358.0430, found: 358.0438.

N-(2-chloro-2-(3-methoxyphenyl)ethyl)-*N*,4-dimethylbenzenesulfonamide (18q)
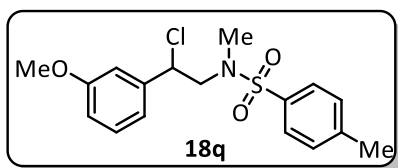
According to general procedure **A**, **18q** was prepared from 3-methoxystyrene (**15q**) (42 μL, 0.30 mmol, 1.0 eq.) using [Cu(dap)$_2$]Cl (2.7 mg, 0.003 mmol, 1.0 mol%) as a catalyst. The crude product was purified by column chromatography on silica gel using PE:Et$_2$O 50% (R$_f$ = 0.38 in PE:Et$_2$O 50%) to afford **18q** as a light yellow oil (81.9 mg, 96% yield).

^{1}H-NMR (400 MHz, CDCl$_3$): δ = 7.69 − 7.60 (m, 2H), 7.34 − 7.27 (m, 3H), 7.03 − 6.95 (m, 1H), 6.95 (t, *J* = 2.1 Hz, 1H), 6.87 (ddd, *J* = 8.3, 2.6, 0.9 Hz, 1H), 5.07 (t, *J* = 7.3 Hz, 1H), 3.82 (s, 3H), 3.57 (dd, *J* = 14.5, 7.4 Hz, 1H), 3.41 (dd, *J* = 14.5, 7.2 Hz, 1H), 2.65 (s, 3H), 2.42 (s, 3H). **^{13}C-NMR** (101 MHz, CDCl$_3$): δ = 159.9, 143.8, 140.3, 134.9, 130.0, 129.9, 127.4, 119.9, 114.6, 113.1, 61.4, 58.1, 55.5, 37.1, 21.6. **IR** (neat, cm^{-1}): 3067, 2930, 2840, 1599, 1491, 1457, 1342, 1260, 1156, 1088, 1040, 936, 768, 731, 697. **HRMS** (ESI): m/z calculated for C$_{17}$H$_{21}$ClNO$_3$S [MH$^+$]: 354.0925, found: 354.0930.

N-(2-chloro-2-(pyridin-2-yl)ethyl)-*N*,4-dimethylbenzenesulfonamide (18r)
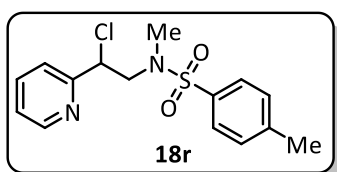
According to general procedure **A**, **18r** was prepared from 2-vinylpyridine (**15r**) (32 mg, 0.30 mmol, 1.0 eq.) using [Cu(dap)$_2$]Cl (2.7 mg, 0.003 mmol, 1.0 mol%) as a catalyst. The crude product was purified by flash column chromatography on silica gel using PE:EA 5%-20% (R$_f$ = 0.35 in PE:EA 33%) to afford **18r** as a yellow oil (81.0 mg, 83% yield).

^{1}H NMR (400 MHz, CDCl$_3$): δ = 8.64 − 8.52 (m, 1H), 7.71 (dd, *J* = 7.7, 1.8, 1H), 7.65 (d, *J* = 8.3, 2H), 7.44 (dt, *J* =7 .8, 1.1, 1H), 7.35 − 7.08 (m, 3H), 5.21 (t, *J* = 7.3, 1H), 3.84 − 3.54 (m, 2H), 2.68 (s, 3H), 2.40 (s, 3H). **^{13}C-NMR** (101 MHz, CDCl$_3$): δ = 157.1, 149.6, 143.8, 137.3, 134.4, 129.9, 127.5, 123.7, 123.6, 60.6, 55.8, 37.2, 21.6. **IR** (neat, cm^{-1}): 3064, 2926, 2855, 2356, 1595, 1439, 1342, 1163, 1088, 936, 816, 746. **HRMS** (ESI): m/z calculated for C$_{15}$H$_{18}$ClN$_2$O$_2$S [MH$^+$]: 325.0772; found: 325.0778.

N-(2-chloro-2-(perfluorophenyl)ethyl)-*N*,4-dimethylbenzenesulfonamide (18s)
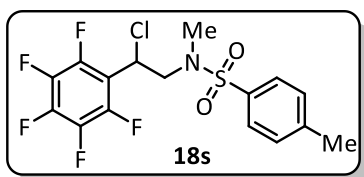
According to general procedure **B**, **18s** was prepared from distilled 2,3,4,5,6-pentafluorostyrene (**15s**) (230 μL, 1.6 mmol, 2.0 eq.) using [Cu(dap)$_2$]Cl (7.1 mg, 0.008 mmol, 1.0 mol%) as a catalyst. The crude product was purified by column chromatography on silica gel using PE:EA 15-25% (R$_f$ = 0.57 in PE:EA 25%) to afford **18s** as a colorless oil (242,9 mg, 73% yield, 81% Conversion of **17f** after 16 h).

¹H-NMR (300 MHz, CDCl$_3$): δ = 7.64 (d, *J* = 8.3 Hz, 2H), 7.36 − 7.30 (m, 2H), 5.48 − 5.35 (m, 1H), 3.93 (dd, *J* = 14.4, 9.1 Hz, 1H), 3.40 (dd, *J* = 14.4, 6.3 Hz, 1H), 2.82 (s, 3H), 2.44 (s, 3H). **¹³C-NMR** (151 MHz, CDCl$_3$): δ = 145.5 (d, *J*$_{C-F}$ = 252.7 Hz), 144.2, 141.9 (d, *J*$_{C-F}$ = 256.8 Hz), 137.8 (d, *J*$_{C-F}$ = 252.9 Hz), 134.2, 130.0, 127.5, 112.5 (td, *J*$_{C-F}$ = 14.5, 3.8 Hz), 55.0, 48.1, 37.0, 21.6. **¹⁹F-NMR** (282 MHz, CDCl$_3$): δ = -140.8 (d, *J* = 20.9 Hz), -152.4 (tt, *J* = 21.1, 2.8 Hz), -161.3 (td, *J* = 21.9, 8.1 Hz). **IR** (neat, cm⁻¹): 3032, 2929, 2847, 1655, 1599, 1523, 1506, 1457, 1349, 1162, 1133, 1021, 980, 949, 816, 734. **HRMS** (ESI): m/z calculated for C$_{16}$H$_{14}$ClF$_5$NO$_2$S [MH⁺]: 414.0348, found 414.0351.

N-(2-chlorooctyl)-*N*,4-dimethylbenzenesulfonamide (18t)
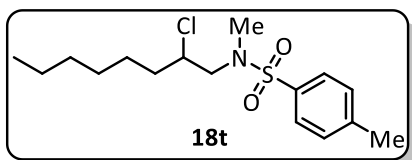
According to general procedure **A**, **18t** was prepared from distilled 1-octene (**15t**) (47 μL, 0.30 mmol, 1.0 eq.) using [Cu(dap)$_2$]Cl (2.7 mg, 0.003 mmol, 1.0 mol%) as a catalyst. The crude product was purified by column chromatography on silica gel PE:EA 5% (R$_f$ = 0.32 in PE:EA 5%) to afford **18t** as a colorless oil (28.3 mg, 35% yield).

¹H-NMR (400 MHz, CDCl$_3$): δ = 7.68 (d, *J* = 8.3 Hz, 2H), 7.33 (d, *J* = 7.9 Hz, 2H), 4.11 − 4.00 (m, 1H), 3.37 (dd, *J* = 14.2, 6.7 Hz, 1H), 3.08 (dd, *J* = 14.2, 6.8 Hz, 1H), 2.83 (s, 3H), 2.43 (s, 3H), 1.96 − 1.86 (m, 1H), 1.69 − 1.53 (m, 2H), 1.46 − 1.26 (m, 7H), 0.92 − 0.87 (m, 3H). **¹³C-NMR** (101 MHz, CDCl$_3$): δ = 143.8, 134.6, 129.9, 127.6, 61.0, 57.0, 37.1, 35.5, 31.8, 28.9, 26.2, 22.7, 21.7, 14.2. **IR** (neat, cm⁻¹): 2957, 2930, 2859, 1599, 1494, 1457, 1341, 1159, 1088, 973, 932, 816, 738. **HRMS** (ESI): m/z calculated for C$_{16}$H$_{26}$ClNO$_2$S [MH⁺] 332.1446, found: 296.1682 [MH⁺, -HCl]. The data are in accordance with the data reported in the literature.[180]

N-(2-chloro-3-phenylpropyl)-*N*,4-dimethylbenzenesulfonamide (26)
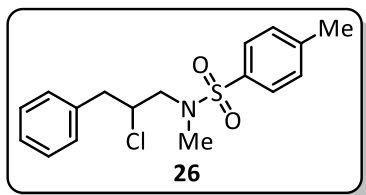
According to general procedure **B**, **26** was prepared from allylbenzene (**24**) (212 µL, 1.6 mmol, 2.0 eq.) using [Cu(dap)$_2$]Cl (2.7 mg, 0.003 mmol, 1.0 mol%) as a catalyst and adding 84.8 mg (0.8 mmol, 1.0 eq.) Na$_2$CO$_3$. The crude product was purified by column chromatography on silica gel using PE:EA 5% (R$_f$ = 0.08 in PE:EA 5%) to afford **26** as a colorless oil (47.8 mg, 18% yield).

^{1}H-NMR (400 MHz, CDCl$_3$): δ = 7.62 (d, *J* = 8.2 Hz, 2H), 7.38 − 7.25 (m, 5H), 7.26 − 7.23 (m, 2H), 4.30 (dtd, *J* = 9.0, 6.6, 4.8 Hz, 1H), 3.46 (dd, *J* = 14.4, 6.4 Hz, 1H), 3.28 (dd, *J* = 14.4, 4.8 Hz, 1H), 3.09 (dd, *J* = 14.3, 7.0 Hz, 1H), 2.94 (dd, *J* = 14.4, 9.0 Hz, 1H), 2.85 (s, 3H), 2.43 (s, 3H). **^{13}C-NMR** (101 MHz, CDCl$_3$) δ= 143.8, 137.3, 134.4, 129.9, 129.5, 128.6, 127.6, 127.1, 61.1, 56.8, 42.1, 37.3, 21.7. **IR** (neat, cm^{-1}): 3064, 3030, 2922, 2855, 1599, 1495, 1454, 1342, 1159, 1088, 943, 816, 738, 701. **HRMS** (ESI): m/z calculated for C$_{17}$H$_{21}$ClNO$_2$S [MH$^+$]: 338.0976, found: 338.0981.

2-(2-chloro-3-phenylpropyl)benzo[*d*]isothiazol-3(2H)-one 1,1-dioxide (28)
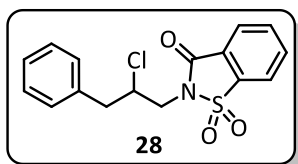
According to general procedure **B**, **28** was prepared from allylbenzene (**24**) (106 µL, 0.8 mmol, 2.0 eq.) using [Cu(dap)$_2$]Cl (3.5 mg, 0.008 mmol, 1.0 mol%) as a catalyst. The crude product was purified by column chromatography on silica gel using PE:EA 5% (R$_f$ = 0.07 in PE:EA 5%) to afford **28** as a colorless oil (28.7 mg, 21% yield)

^{1}H-NMR (400 MHz, CDCl$_3$): δ = 8.04 (d, *J* = 6.5, 1H), 7.93 − 7.77 (m, 3H), 7.34 − 7.20 (m, 5H), 4.73 − 4.60 (m, 1H), 4.22 (dd, *J* = 11.6, 8.9, 1H), 3.83 (dd, *J* = 11.6, 5.7, 1H), 3.49 − 3.32 (m, 2H). **^{13}C-NMR** (101 MHz, CDCl$_3$) δ = 159.1, 137.5, 136.5, 135.0, 134.5, 129.3, 128.9, 127.4, 125.4, 121.0, 57.8, 43.1, 37.0, 31.1. **IR** (neat, cm^{-1}): 3064, 3030, 2922, 2855, 1599, 1495, 1454, 1342, 1159, 1088, 943, 816, 738, 701. **HRMS** (ESI): m/z calculated for C$_{16}$H$_{15}$ClNO$_3$S [MH$^+$]: 336.0462, found 336.0456.

N-(2-chloro-2-phenylethyl)-*N*-methyl-4-nitrobenzenesulfonamide (34)
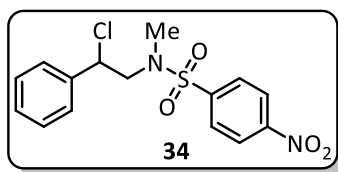
According to general procedure **A**, **34** was prepared from distilled styrene (**15b**) (34 µL, 0.30 mmol, 1.0 eq.) and *N*-chloro-*N*-methyl-4-nitrobenzenesulfonamide (**17d**) (112.8 mg, 0.45 mmol, 1.5 eq.) using [Cu(dap)$_2$]Cl (2.7 mg, 0.003 mmol, 1.0 mol%) as a catalyst. The crude product was purified by column chromatography on silica gel using PE:EA 7.5% (R_f = 0.09 in PE:EA 7.5%) to afford **34** as a light yellow oil (79.2 mg, 93% yield).

^{1}H-NMR (400 MHz, CDCl$_3$): δ = 8.34 (d, *J* = 8.7 Hz, 2H), 7.93 (d, *J* = 8.7 Hz, 2H), 7.48 – 7.32 (m, 5H), 5.10 (t, *J* = 7.3 Hz, 1H), 3.66 (dd, *J* = 14.6, 7.6 Hz, 1H), 3.51 (dd, *J* = 14.5, 7.1 Hz, 1H), 2.73 (s, 3H). **^{13}C-NMR** (101 MHz, CDCl$_3$): δ = 150.3, 144.0, 138.3, 129.3, 129.1, 128.6, 127.6, 124.6, 61.0, 58.1, 36.9. **IR** (neat, cm^{-1}): 3105, 3034, 2930, 2868, 1606, 1528 (vs), 1454, 1349, 1311, 1163, 1088, 932, 857, 758, 742, 697. **HRMS** (ESI): m/z calculated for C$_{15}$H$_{16}$ClN$_2$O$_4$S [MH$^+$]: 355.0514, found: 355.0517. The data are in accordance with the data reported in the literature.[180]

N-(2-bromo-2-phenylethyl)-N,4-dimethylbenzenesulfonamide (37)
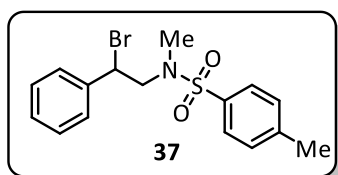
According to general procedure **B**, **37** was prepared from styrene (**15b**) (183 µL, 1.6 mmol, 2.0 eq.), *N*,4-dimethylbenzenesulfonamide (151.2 mg, 0.8 mmol, 1.0 eq.) and 1-bromopyrrolidine-2,5-dione (NBS, 159.8 mg, 0.88 mmol, 1.1 eq.) using [Cu(dap)$_2$]Cl (7.1 mg, 0.008 mmol, 1.0 mol%) as a catalyst. The crude product was purified by flash column chromatography on silica gel using PE:EA 5-15% (R_f = 0.14 in PE:EA 20%) to afford **37** as a colorless oil (290.1 mg, 98% yield).

^{1}H-NMR (400 MHz, CDCl$_3$): δ = 7.63 (d, *J* = 8.3, 2H), 7.42 (dd, *J* = 8.0, 1.7, 2H), 7.40 – 7.27 (m, 5H), 5.15 (dd, *J* = 8.4, 6.9, 1H), 3.73 (dd, *J* = 14.5, 6.9, 1H), 3.54 (dd, *J* = 14.5, 8.4, 1H), 2.59 (s, 3H), 2.42 (s, 3H). **^{13}C-NMR** (101 MHz, CDCl$_3$): δ = 143.8, 139.1, 134.8, 129.9, 129.0, 129.0, 128.1, 127.5, 57.8, 52.0, 36.9, 21.6. **IR** (neat, cm^{-1}): 3062, 3033, 29276, 1599, 1496, 1458, 1338, 1154, 1088, 987, 932, 813, 737, 697. **HRMS** (ESI): m/z calculated for C$_{15}$H$_{16}$ClN$_2$O$_4$S [MH$^+$]: 368.0314, found: 368.0318.

3-(chloromethyl)-4-phenyl-1-tosylpyrrolidine (38a)

anti-38a
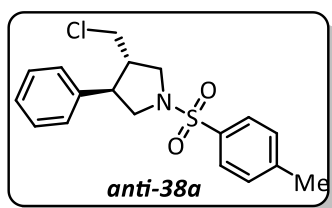
According to general procedure **A**, **38a** was prepared from styrene (**15b**) (34 µL, 0.3 mmol, 1.0 eq.) using [Ir[dF(CF$_3$)ppy]$_2$(dtbpy)]PF$_6$ (1.7 mg, 0.0015 mmol, 0.5 mol%) as a catalyst and *N*-allyl-*N*-chloro-4-methylbenzenesulfonamide (**17e**) (111.7 mg, 0.45 mmol, 1.5 eq.). The crude product was purified by column chromatography on silica gel using PE:EA 15% (R$_f$ = 0.21 in PE:EA 15%) to afford **38a** as an inseparable 0.71:0.29 mixture of diastereomers as colorless oil (70.5 mg, 67% yield)

^{1}H-NMR (400 MHz, CDCl3, major diastereomer (*anti*)): δ = 7.76 (d, *J* = 8.2 Hz, 2H), 7.38 (d, *J* = 8.0 Hz, 2H), 7.34 – 7.22 (m, 3H), 7.14 – 7.06 (m, 2H), 3.72 (td, *J* = 10.1, 7.9 Hz, 2H), 3.45 (dd, *J* = 11.3, 4.0 Hz, 1H), 3.39 – 3.23 (m, 3H), 3.08 – 2.96 (m, 1H), 2.60 – 2.46 (m, 1H), 2.47 (s, 3H). **^{1}H-NMR** (400 MHz, CDCl3, minor diastereomer (*syn*)): δ = 7.80 (d, *J* = 8.2 Hz, 2H), 7.40 – 7.36 (m, 2H), 7.32 – 7.23 (m, 3H), 7.05 (dd, *J* = 7.3, 2.3 Hz, 2H), 3.67 – 3.59 (m, 3H), 3.50 (dd, *J* = 7.0, 4.8 Hz, 1H), 3.37 – 3.31 (m, 1H), 3.07 – 2.98 (m, 1H), 2.81 (dd, *J* = 11.0, 9.2 Hz, 1H), 2.62 (ddd, *J* = 10.3, 7.9, 6.7 Hz, 1H), 2.47 (s, 3H). **^{13}C-NMR** (101 MHz, CDCl$_3$, major diastereomer): δ = 143.8, 138.4, 133.5, 129.8, 129.0, 127.6, 127.4, 127.3, 54.6, 51.3, 48.0, 47.3, 44.2, 21.6. **^{13}C-NMR** (101 MHz, CDCl$_3$, minor diastereomer): δ = 143.8, 137.5, 133.8, 129.9, 128.8, 127.8, 127.5, 127.3, 52.5, 50.3, 45.8, 45.6, 43.1, 21.6 **IR** (neat, cm^{-1}): 3291, 3090, 2952, 2885, 1599, 1495, 1342, 1159, 1092, 1033, 816, 701. **HRMS** (ESI): m/z calculated for C$_{18}$H$_{21}$ClNO$_2$S [MH$^+$]: 350.0976, found: 350.0981. The spectral data was in accordance with literature.[101]

N-allyl-*N*-(2-chloro-2-phenylethyl)-4-methylbenzenesulfonamide (38b)

38b

According to general procedure **B**, Fehler! Verweisquelle konnte nicht gefunden werden. was prepared from styrene (Fehler! Verweisquelle konnte nicht gefunden werden.) (183 µL, 1.6 mmol, 2.0 eq.) and *N*-allyl-*N*-chloro-4-methylbenzenesulfonamide (**3**) (196.6 mg, 0.8 mmol, 1.0 eq.) using [Cu(dap)$_2$]Cl (7.1 mg, 0.008 mmol, 1.0 mol%) as a catalyst. The crude product was purified by flash column chromatography on silica gel using PE:EA 5-15% (R$_f$ = 0.30, PE:EA 15%) to afford **5e** as a colorless oil (203.0 mg, 73% yield).

¹H-NMR (400 MHz, CDCl₃): δ = 7.68 (d, *J* = 8.3, 2H), 7.42 – 7.33 (m, 5H), 7.32 – 7.26 (m, 2H), 5.31 (ddt, *J* = 16.8, 10.1, 6.5, 1H), 5.18 (t, *J* = 7.4, 1H), 5.09 – 4.95 (m, 2H), 3.82 (dd, *J* = 15.8, 6.4, 1H), 3.68 (dd, *J* = 14.9, 7.2, 1H), 3.49 (dd, *J* = 14.9, 7.6, 1H), 3.38 (dd, *J* = 15.7, 6.8, 1H), 2.43 (s, 3H). **¹³C-NMR** (101 MHz, CDCl3): δ = 143.7, 138.9, 136.8, 132.4, 129.9, 128.9, 128.8, 127.8, 127.4, 119.8, 61.2, 54.1, 52.0, 21.6. <u>**IR**</u> (neat, cm⁻¹): 3030, 2952, 2885, 1599, 1454, 1341, 1088, 1159, 1014, 813, 757. **HRMS** (ESI): m/z calculated for C₁₈H₂₁ClNO₂S [MH⁺]: 350.0976, found: 350.0985.

3-(chloromethyl)-4-(p-tolyl)-1-tosylpyrrolidine (39a)

anti-39a
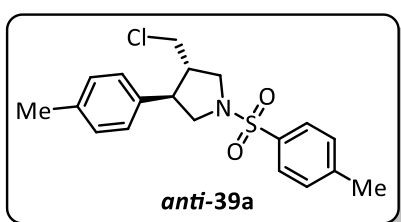
According to general procedure **A**, **39a** was prepared from 1-methyl-4-vinylbenzene (**15a**) (34 μL, 0.3 mmol, 1.0 eq.) using [Ir[dF(CF₃)ppy]₂(dtbpy)]PF₆ (1.7 mg, 0.003 mmol, 1 mol%)[as a catalyst and *N*-allyl-*N*-chloro-4-methylbenzenesulfonamide (**17d**) (111.7 mg, 0.45 mmol, 1.5 eq.). The crude product was purified by column chromatography on silica gel using PE:EA 1-15% (R_f = 0.21 in PE:EA 15%) to afford **39a** as an inseparable 0.7:0.3 mixture of diastereomers as colorless oil (83.6 mg, 77% yield)

¹H-NMR (400 MHz, CDCl3, major diastereomer (*anti*)): δ = 7.76 (d, *J* = 8.2 Hz, 2H), 7.37 (d, *J* = 8.0 Hz, 2H), 7.10 (d, *J* = 7.9 Hz, 2H), 6.98 (d, *J* = 8.1 Hz, 2H), 3.71 (ddd, *J* = 10.3, 7.9, 6.9 Hz, 2H), 3.45 (dd, *J* = 11.3, 3.9 Hz, 1H), 3.34 – 3.24 (m, 3H), 3.07 – 2.92 (m, 1H), 2.80 (dd, *J* = 11.0, 9.2 Hz, 1H), 2.47 (s, 3H), 2.31 (s, 3H). **¹H-NMR** (400 MHz, CDCl3, minor diastereomer (*syn*)): δ = 7.79 (d, *J* = 8.2 Hz, 2H), 7.40 – 7.36 (m, 2H), 7.06 (d, *J* = 7.8 Hz, 2H), 6.93 (d, *J* = 8.1 Hz, 2H), 3.67 – 3.55 (m, 3H), 3.46 (d, *J* = 3.9 Hz, 1H), 3.36 – 3.29 (m, 1H), 3.05 – 3.00 (m, 1H), 2.80 (dd, *J* = 11.0, 9.2 Hz, 1H), 2.67 – 2.53 (m, 1H), 2.47 (s, 3H), 2.31 (d, *J* = 2.4 Hz, 3H). **¹³C-NMR** (101 MHz, CDCl₃, both diastereomers): δ = 143.9, 137.5, 137.3, 135.4, 134.5, 133.7, 130.0, 130.0, 129.8, 129.6, 127.8, 127.8, 127.7, 127.4, 54.8, 52.7, 51.5, 50.4, 48.1, 47.2, 45.7, 45.6, 44.4, 43.3, 21.7, 21.2, 21.1. **IR** (neat, cm⁻¹2952, 2922, 2870, 1595, 1517, 1443, 1342, 1159, 1088, 1014, 813. **HRMS** (ESI): m/z calculated for C₁₉H₂₃ClNO₂S [MH⁺]: 364.1133, found: 364.1143.

N-allyl-*N*-(2-chloro-2-(p-tolyl)ethyl)-4-methylbenzenesulfonamide (39b)
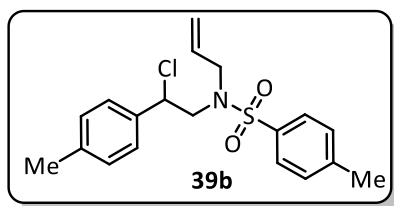
According to general procedure **A**, **$$** was prepared from 1-methyl-4-vinylbenzene (**$$**) (34 µL, 0.3 mmol, 1.0 eq.) using [Cu(dap)₂]Cl (2.7 mg, 0.003 mmol, 1 mol%) as a catalyst and *N*-allyl-*N*-chloro-4-methylbenzenesulfonamide (**3**) (111.7 mg, 0.45 mmol, 1.5 eq.). The crude product was purified by column chromatography on silica gel using PE:EA 15% (R$_f$ = 0.32 in PE:EA 15%) to afford **$$** as colorless oil (50.3 mg, 46% yield)

¹H-NMR (400 MHz, CDCl₃): δ = 7.66 (d, J=8.3, 2H), 7.32 − 7.21 (m, 4H), 7.14 (d, *J* = 7.9, 2H), 5.40 − 5.25 (m, 1H), 5.12 (t, *J* = 7.3, 1H), 5.10 − 4.95 (m, 2H), 3.83 (ddt, *J* = 15.8, 6.3, 1.5, 1H), 3.66 (dd, *J* = 14.8, 7.2, 1H), 3.48 (dd, *J* = 14.8, 7.5, 1H), 3.38 (ddt, *J* = 15.8, 6.8, 1.3, 1H), 2.41 (s, 3H), 2.34 (s, 3H). **¹³C-NMR** (101 MHz, CDCl3): δ = 143.6, 138.7, 136.8, 135.8, 132.4, 129.8, 129.4, 127.6, 127.3, 119.7, 61.1, 53.9, 51.8, 21.5, 21.2. **IR** (neat, cm⁻¹): 3030, 2952, 2885, 1599, 1454, 1341, 1088, 1159, 1014, 813, 757. **HRMS** (ESI): m/z calculated for C₁₉H₂₃ClNO₂S [MH⁺]: 364.1133, found: 364.1136.

Methyl 4-(4-(chloromethyl)-1-tosylpyrrolidin-3-yl)benzoate (40a)

According to general procedure **A**, **40a** was prepared from methyl 4-vinylbenzoate (**15k**) (48.7 mg, 0.3 mmol, 1.0 eq.) using [Ir[dF(CF₃)ppy]₂(dtbpy)]PF₆ (1.7 mg, 0.003 mmol, 1 mol%)[as a catalyst and *N*-allyl-*N*-chloro-4-methylbenzenesulfonamide (**17d**) (111.7 mg, 0.45 mmol, 1.5 eq.). The crude product was purified by column chromatography on silica gel using PE:EA 1-15% (R$_f$ = 0.21 in PE:EA 15%) to afford **40a** as an inseparable 0.7:0.3 mixture of diastereomers as colorless oil (40.5 mg, 33% yield)

¹H-NMR (400 MHz, CDCl3, major diastereomer (*anti*)): δ = 8.02 (d, *J* = 8.3 Hz, 2H), 7.82 (d, *J* = 8.2 Hz, 2H), 7.44 (d, *J* = 8.0 Hz, 2H), 7.25 (d, *J* = 8.3 Hz, 2H), 3.96 (s, 3H), 3.79 (dt, *J* = 10.3, 8.1 Hz, 2H), 3.73 – 3.66 (m, 1H), 3.51 (dd, *J* = 11.4, 4.2 Hz, 1H), 3.44 – 3.31 (m, 2H), 3.19 (q, *J* = 8.8 Hz, 1H), 2.67 – 2.57 (m, 1H), 2.54 (d, *J* = 2.3 Hz, 3H). **¹H-NMR** (400 MHz, CDCl3, minor diastereomer (*syn*)): δ = 8.02 (d, *J* = 8.3 Hz, 2H), 7.82 (d, *J* = 8.2 Hz, 2H), 7.44 (d, *J* = 8.0 Hz, 2H), 7.25 (d, *J* = 8.3 Hz, 2H), 3.96 (s, 3H), 3.79 (dt, *J* = 10.3, 8.1 Hz, 2H), 3.73 – 3.66 (m, 1H), 3.51 (dd, *J* = 11.4, 4.2 Hz, 1H), 3.44 – 3.31 (m, 2H), 3.19 (q, *J* = 8.8 Hz, 1H), 2.67 – 2.57 (m, 1H), 2.54 (d, *J* = 2.3 Hz, 3H). **¹³C-NMR** (101 MHz, CDCl$_3$, both diastereomers): 166.6, 144.1, 144.0, 144.0, 143.0, 133.7, 133.4, 130.3, 130.0, 130.0, 130.0, 129.6, 129.4, 128.0, 127.7, 127.5, 127.5, 77.5, 77.2, 76.8, 54.3, 52.6, 52.2, 51.2, 50.2, 48.0, 47.2, 45.7, 45.6, 44.1, 42.8, 23.9, 21.7, 21.6. **IR** (neat, cm^{-1}): 2997, 2952, 1714, 1614, 1439, 1341, 1286, 1159, 1115, 1021, 809, 768, 664. **HRMS** (ESI): m/z calculated for C$_{22}$H$_{23}$ClNO$_4$S [MH$^+$]: 408.1031, found: 408.1034.

Methyl 4-(2-((*N*-allyl-4-methylphenyl)sulfonamido)-1-chloroethyl)benzoate (40b)

According to general procedure **A**, **40b** was prepared from methyl 4-vinylbenzoate (**15k**) (48.7 mg, 0.3 mmol, 1.0 eq.) using Cu(dap)$_2$]Cl (2.7 mg, 0.003 mmol, 1 mol%) as a catalyst and *N*-allyl-*N*-chloro-4-methylbenzenesulfonamide (**17d**) (111.7 mg, 0.45 mmol, 1.5 eq.). The crude product was purified by column chromatography on silica gel using PE:EA 1-20% (R$_f$ = 0.38 in 20% EA/PE) to afford **40b** as colorless oil (52.4 mg, 43% yield).

¹H-NMR (400 MHz, CDCl$_3$): δ = 8.02 (d, *J* = 8.3 Hz, 2H), 7.67 (d, *J* = 8.3 Hz, 2H), 7.47 (d, *J* = 8.3 Hz, 2H), 7.38 – 7.22 (m, 2H), 5.36 – 5.18 (m, 2H), 5.13 – 4.94 (m, 2H), 3.92 (s, 3H), 3.71 (ddd, *J* = 46.0, 15.2, 6.6 Hz, 2H), 3.42 (ddd, *J* = 36.3, 15.3, 7.3 Hz, 2H), 2.42 (s, 3H). **¹³C-NMR** (101 MHz, CDCl3): δ = 166.6, 143.9, 143.7, 136.4, 132.2, 130.6, 130.0, 130.0, 127.9, 127.4, 120.1, 60.4, 54.1, 52.4, 52.3, 21.7. **IR** (neat, cm^{-1}): 3030, 2952, 2885, 1715, 1454, 1341, 1088, 1159, 1014, 813, 757. **HRMS** (ESI): m/z calculated for C$_{22}$H$_{23}$ClNO$_4$S [MH$^+$]: 408.1031, found: 408.1038.

N-((1R,2R)-1-chloro-1-phenylpropan-2-yl)-*N*,4-dimethylbenzenesulfonamide (41)

According to general procedure **B**, **41** was prepared from *trans*-β-methylstyrene (210 µL, 1.6 mmol, 2.0 eq.) using [Cu(dap)$_2$]Cl (7.1 mg, 0.008 mmol, 1.0 mol%) as a catalyst. The crude product was purified by column chromatography on silica gel using 5%-15% PE:EA (R$_f$ = 0.18 in PE:EA 10%) to afford the diastereomer **41** as a colorless oil (201,1 mg, 74% yield).

^{1}H-NMR (400 MHz, CDCl$_3$) δ = 7.46 (d, *J* = 8.3, 2H), 7.42 (dd, *J* = 7.9, 1.6, 2H), 7.40 – 7.30 (m, 3H), 7.21 (d, *J* = 8.1, 2H), 5.03 (d, *J* = 6.5, 1H), 4.49 (p, *J* = 6.7, 1H), 2.73 (s, 3H), 2.39 (s, 3H), 1.16 (d, *J* = 6.8, 3H). **^{13}C-NMR** (101 MHz, CDCl$_3$) δ = 143.4, 139.1, 129.7, 128.6, 128.5, 127.6, 127.2, 67.6, 58.2, 29.7, 21.6, 13.0. **IR** (neat, cm^{-1}): 3060, 2986, 1599, 1495, 1454, 1338, 1267, 1152, 939, 887, 816, 734, 697. **HRMS** (ESI): m/z calculated for C$_{17}$H$_{21}$ClNO$_2$S [MH$^+$]: 338.0976, found: 338.0978.

N-(tert-butyl)-*N*-(2-chloro-2-phenylethyl)-4-methylbenzenesulfonamide (42)

According to general procedure **B**, **42** was prepared from styrene (**15b**) (166.6 mg, 1.6 mmol, 2 eq.) using [Cu(dap)$_2$]Cl (7.1 mg, 0.008 mmol, 1.0 mol%) as a catalyst and **17f** (209.4 mg, 0.8 mmol, 1 eq.). The crude product was purified by flash column chromatography on silica gel using PE:EA 5-15% (R$_f$ = 0.51 in PE:EA 20%) to afford 171.3 mg of a colorless oil as a 0.61:0.39 mixture of starting material **17f** to product **42** (66.8 mg, 23% yield, 50% Conversion of **17f**), which could not be further separated by flash column chromatography.

^{1}H-NMR (400 MHz, CDCl$_3$): δ = 7.81 (d, *J* = 8.3, 2H), 7.54 – 7.47 (m, 2H), 7.43 – 7.32 (m, 3H), 7.32 – 7.24 (m, 2H), 5.56 (dd, *J* = 8.8, 4.6, 1H), 3.89 (dd, *J* = 15.5, 4.6, 1H), 3.69 (dd, *J* = 15.5, 8.8, 1H), 2.42 (s, 3H), 1.24 (s, 9H). **^{13}C-NMR** (101 MHz, CDCl$_3$): δ = 143.1, 141.2, 139.5, 129.7, 128.8, 128.7, 127.7, 127.4, 63.0, 59.8, 53.4, 29.7, 21.6. **IR** (neat, cm^{-1}): 2982, 2941, 2363, 1599, 1454, 1338, 1163, 1088, 895, 813, 700, 664. **HRMS** (ESI): m/z calculated for C$_{19}$H$_{24}$ClNNaO$_2$S [MNa$^+$]: 388.1108, found 388.1107.

N-(2-(4-allylphenyl)-2-chloroethyl)-*N*,4-dimethylbenzenesulfonamide (43)

According to general procedure **B**, **43** was prepared from 1-allyl-4-vinylbenzene (83.5 mg, 0.58 mmol, 1.5 eq.) and *N*-chloro-*N*,4-dimethylbenzenesulfonamide (**17a**) (85.7 mg, 0.386 mmol, 1.0 eq.) using [Cu(dap)$_2$]Cl (3.4 mg, 0.0039 mmol, 1.0 mol%) as a catalyst. The crude product was purified by flash column chromatography on silica gel (PE:EA 5-15%, R$_f$ = 0.42 in PE:EA 20%) to afford **43** as a colorless oil (87.5 mg, 62% yield).

^{1}H-NMR (400 MHz, CDCl$_3$): δ = 7.64 (d, *J* = 8.3, 2H), 7.38 – 7.27 (m, 4H), 7.20 (d, *J* = 8.1, 2H), 6.03 – 5.88 (m, 1H), 5.14 – 5.04 (m, 3H), 3.57 (dd, *J* = 14.5, 7.4, 1H), 3.46 – 3.36 (m, 3H), 2.64 (s, 3H), 2.42 (s, 3H). **^{13}C-NMR** (101 MHz, CDCl$_3$) δ = 143.7, 141.0, 137.0, 136.6, 134.9, 129.9, 129.1, 127.7, 127.4, 116.3, 61.3, 58.1, 40.0, 37.1, 21.6. . **IR** (neat, cm^{-1}): 3030, 2978, 2907, 2359, 1598, 1454, 1342, 1211, 1163, 1088, 992, 932, 816, 746. **HRMS** (ESI): m/z calculated for C$_{19}$H$_{23}$ClNO$_2$S [MH$^+$]: 364.1133; found: 364.1137.

3-(bromomethyl)-4-phenyl-1-tosylpyrrolidine (55a)

According to general procedure **B**, **55a** was prepared from styrene (**15b**) (137 μL, 1.2 mmol, 1.5 eq.), *N*-allyl-4-methylbenzenesulfonamide (169.0 mg, 0.8 mmol, 1.0 eq.) and 1-bromopyrrolidine-2,5-dione (NBS, 156.8 mg, 0.88 mmol, 1.1 eq.). Instead of adding a catalyst, the reaction mixture was stirred at 40 °C for 20 hours under an inert atmosphere without irradiation. The crude product was purified by flash column chromatography on silica gel using PE:EA 5-15% (R$_f$ = 0.28 in PE:EA 20%) to afford **55a** as an inseparable 0.7:0.3 mixture of diastereomers as colorless oil (40.5 mg, 33% yield).

¹H-NMR (400 MHz, CDCl3, major diastereomer (*anti*)): δ = 7.67 − 7.60 (m, 2H), 7.25 (dd, J = 8.1, 3.4 Hz, 2H), 7.19 − 7.12 (m, 3H), 7.04 − 6.95 (m, 2H), 3.67 − 3.58 (m, 2H), 3.56 − 3.48 (m, 1H), 3.27 − 3.09 (m, 2H), 3.01 (dd, J = 10.5, 7.8 Hz, 1H), 2.86 (td, J = 9.6, 8.1 Hz, 1H), 2.57 − 2.50 (m, 1H), 2.35 (s, 3H). **¹H-NMR** (400 MHz, CDCl3, minor diastereomer (*syn*)): δ = 7.67 (d, J = 8.2 Hz, 2H), 7.25 (dd, J = 8.1, 3.4 Hz, 2H), 7.19 − 7.12 (m, 3H), 6.96 − 6.91 (m, 2H), 3.56 − 3.49 (m, 1H), 3.35 (td, J = 6.7, 4.7 Hz, 1H), 3.27 − 3.09 (m, 3H), 2.74 (q, J = 4.8 Hz, 1H), 2.61 − 2.52 (m, 1H), 2.44 − 2.36 (m, 1H), 2.35 (s, 3H). **¹³C-NMR** (101 MHz, CDCl₃, both diastereomers): 143.9, 138.3, 137.6, 133.9, 133.7, 130.0, 130.0, 129.1, 128.9, 127.9, 127.8, 127.7, 127.6, 127.6, 127.5, 54.8, 52.7, 52.5, 51.3, 48.6, 47.9, 46.5, 45.8, 32.8, 31.3, 21.7. **IR** (neat, cm⁻¹): 3064, 3030, 2922, 2885, 1599, 1495, 1342, 1156, 1088, 1014, 757, 701. **HRMS** (ESI): m/z calculated for $C_{18}H_{21}BrNO_2S$ [MH⁺]: 394.0471, found: 394.0475.

N-allyl-*N*-(2-bromo-2-phenylethyl)-4-methylbenzenesulfonamide (55b)

According to general procedure **B**, **55b** was prepared from styrene (**15b**) (137 μL, 1.2 mmol, 1.5 eq.) and *N*-chloro-*N*,4-dimethylbenzenesulfonamide (**17e**) (170.7 mg, 0.8 mmol, 1.0 eq.) using [Cu(dap)₂]Cl (7.1mg, 0.008 mmol, 1.0 mol%) as a catalyst. The crude product was purified by flash column chromatography on silica gel (PE:EA 5-15%, Rf = 0.38 in PE:EA 20%) to afford **55b** as a colorless oil (259.5 mg, 82% yield).

¹H-NMR (400 MHz, CDCl3): δ = 7.60 (d, J = 8.3 Hz, 2H), 7.35 (dd, J = 7.8, 1.8 Hz, 2H), 7.31 − 7.19 (m, 5H), 5.32 − 5.18 (m, 1H), 5.17 (dd, J = 8.8, 6.6 Hz, 1H), 5.06 − 4.90 (m, 2H), 3.76 (td, J = 14.2, 13.6, 6.3 Hz, 2H), 3.59 (dd, J = 14.9, 8.8 Hz, 1H), 3.25 (dd, J = 15.8, 7.0 Hz, 1H), 2.36 (s, 3H). **¹³C-NMR** (101 MHz, CDCl3): δ = 143.7, 139.0, 136.5, 132.2, 129.8, 128.8, 128.7, 128.2, 127.2, 119.7, 53.8, 52.0, 51.7, 21.5. **IR** (neat, cm⁻¹): 3030, 2952, 2885, 1599, 1454, 1341, 1088, 1159, 1014, 813, 757. **HRMS** (ESI): m/z calculated for $C_{18}H_{21}BrNO_2S$ [MH⁺]: 394.0471, found 394.0474.

7.2.3 Absorption spectra

All compounds were measured in concentrations used for the standard reaction conditions.

Product **18a** was measured in a lower concentration of 12.5 mmol/L.

Figure 27: UV-VIS absorption spectra of N-chlorosulfonamide **17a** (TsNMeCl, black line), 4-methylstyrene (**15a**, blue triangles), degassed reaction mixture of compound **18a** before irradiation with blue LED (455 nm) (red dots) and product **18a** (black squares) in DCE.

Mixture of TsNMeCl (**17a**) (75 mM) and 4-methylstyrene (**15a**) (50 mM) in DCE. Conditions: mixture exposed to air, no light irradiation (green squares); degassed mixture before light irradiation (red dots); degassed mixture after irradiation with blue LED (455 nm) for 1 h (blue triangles); degassed mixture after irradiation with blue LED for 2 h (black triangles).

Figure 28: UV-Vis absorption spectra of the reaction mixture under different conditions.

7.2.4 Quantum Yield Determination

The quantum yield Φ of the visible light driven chloro-amination of various substituted styrenes with *N*-chloro-*N*,4-dimethylbenzenesulfonamide (**17a**) was determined using a method developed by E. Riedle *et al.*.[181] For irradiation, a blue LED (950 mA operating current, λ_{max} = 455 nm, OSRAM LD-CQ7P-1U3U) was used. The radiant power was measured with a commercial power meter (PowerMax USB - PS19Q Power Sensor from Coherent) using computer-aided read out with PowerMax software.

An oven-dried pressure tube was charged with *N*-chloro-*N*,4-dimethylbenzenesulfonamide (**17a**) (66.0 mg, 0.30 mmol, 1.5 eq.) and [Cu(dap)$_2$]Cl (1.8 mg, 2.0 μmol, 1.0 mol%) under nitrogen atmosphere. Anhydrous 1,2-dichloroethane (DCE, 4.00 mL) was added and the reaction mixture was degassed by three pump-freeze-thaw cycles. Styrene derivative **15** (0.20 mmol, 1.0 eq.) was added under a slight nitrogen overpressure. An oven dried fluorescence cuvette equipped with a magnetic stir bar and a septum was flushed with nitrogen. Immediately prior to the quantum yield measurement, 2.00 mL of the reaction solution (corresponding to 0.10 mmol of styrene derivative) was transferred to the measuring cuvette under a nitrogen atmosphere. In order to minimize ambient light, the measurement was accomplished in a dark room. The radiant power of light transmitted by the cuvette with a blank solution (Pref) was measured. The cuvette with the blank solution was exchanged by the cuvette containing the reaction mixture and the transmitted radiant power (Psample) was determined. The transmitted radiant power was monitored during the whole irradiation and remained constant. The sample was irradiated for the indicated time while being stirred (cf.

Table 12) and the yield was determined by 1H-NMR analysis using 2-nitropropane as internal standard. The light power at the sample was significantly lower compared to the photocatalytic setup using the internal irradiation.

The quantum yield Φ was calculated as follows:

$$\Phi = \frac{N_{prod}}{N_{ph,abs}} = \frac{n_{prod} * N_A * h * c}{P_{abs} * \Delta t * \lambda} = \frac{n_{prod} * N_A * h * c}{\left(P_{ref} - P_{sample}\right) * f * \Delta t * \lambda}$$

Here, Φ is quantum yield, N_{prod} is the number of molecules created, $N_{ph,\,abs}$ is the number of photons absorbed, N_A is Avogadro´s constant in mol^{-1}, n_{prod} is the molar amount of product molecules created in mol, P_{abs} is the radiant power absorbed in Watt, Δt is the irradiation time in seconds, h is Planck´s constant in Js, c is the speed of light in ms^{-1}, λ is the wavelength of the irradiation source in meters, P_{ref} is the radiant power transmitted by a blank cuvette in Watt, P_{sample} is the radiant power transmitted by the cuvette with the reaction mixture in Watt and f is a correction factor. The correction factor f depends on the reflection coefficient R of the air-glass-interface. Neglecting second order effects, f can be calculated from:

$$f = \frac{1 + R * \dfrac{P_{sample}}{P_{ref}}}{1 - R}$$

For a fused silica cuvette and a wavelength of λ = 443 nm, R is 0.0357.

$$P_{abs} = \left(P_{ref} - P_{sample}\right) * f$$

Example using the data of entry 1 (

Experimental Part

Table **12**)

$$f = \frac{1 + R * \dfrac{P_{sample}}{P_{ref}}}{1 - R} = \frac{1 + 0.0357 * \dfrac{99.9mW}{100.5mW}}{1 - 0.0357} = 1.0738$$

$$\Phi = \frac{n_{prod} * N_A * h * c}{\left(P_{ref} - P_{sample}\right) * f * \Delta t * \lambda} =$$

$$= \frac{0.030 * 10^{-3}mol * 6.022 * 10^{23}mol^{-1} * 6.626 * 10^{-34}Js * 2.998 * 10^{8}ms^{-1}}{(100.5 - 99.9) * 10^{-3}Js^{-1} * 1.0738 * 21600s * 455 * 10^{-9}m} = 0.567$$

$$\Phi \cong 57\%$$

Table **12**: Results of quantum yield measurements.
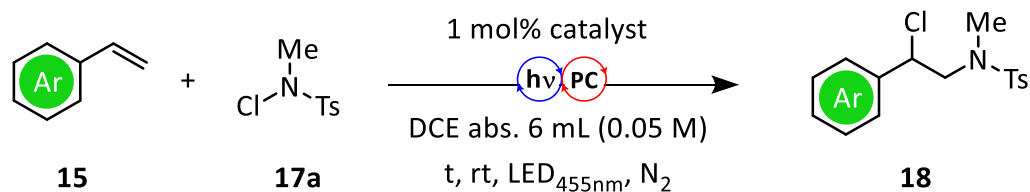
Entry	Product	Catalyst	Δt / h	P_{ref} [mW]	P_{sample} [mW]	P_{abs} [mW]	^{1}H-NMR Yield	Φ
1		no	6	100.5	99.9	0.64	30%	57%
2		[Ir]	1	97.6	7.6	93.6	39%	3%
3		[Cu]	1	96.6	6.2	94.0	41%	3%
4		no	6	102.0	99.8	2.36	4%	2%
5		[Ir]	1	99.7	6.4	97.0	27%	2%
6		[Cu]	1	99.6	6.1	97.2	34%	3%
7		[Ir]	1	99.7	6.1	97.3	9%	0.7%
8		[Cu]	1	99.4	7.6	95.5	18%	1.4%

Reaction conditions: *N*-chloro-*N*,4-dimethylbenzenesulfonamide (**17a**) (1.5 eq., 0.15 mmol), catalyst (1.0 mol%), anhydrous DCE (2.00 mL), degassed solution, alkene (0.10 mmol, 1.0 eq.), rt, irradiation with blue LED (455 nm), stirred reaction mixture. The NMR yields were determined by ^{1}H-NMR using 2-nitropropane as internal standard. Used catalysts: [Cu(dap)$_2$]Cl (**[Cu]**), [Ir(ppy)$_2$(dtbbpy)]PF$_6$ (**[Ir]**) or no catalyst (no).

7.3 Synthesis of 2*H*-Pyrrols after remote C$_{sp}$^{3} functionalization by iminyl radicals.

7.3.1 Starting materials

7.3.1.1 Synthesis of 2-Bromo-2-alkylmalonates
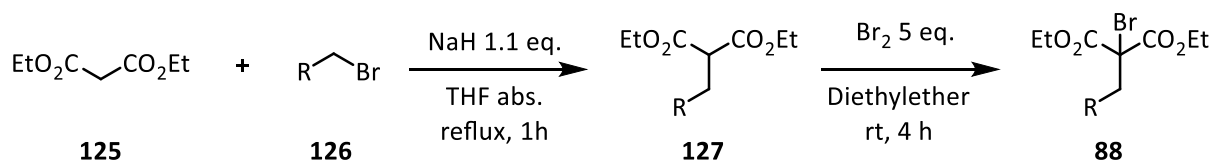
Scheme 57: Two step Synthesis of brominated malonate derivatives.

General procedure for the synthesis of alkylated malonates

Benzylated malonates were prepared according to a literature procedure.[182] Diethyl malonate (1.05 eq.) was added to a suspension of NaH (60%, 1.1 eq.) in THF abs. drop-wise over the course of 15 minutes at 0 °C. After gas evolution had ceased, benzyl bromide (1.0 eq.) was added and the mixture was refluxed for 1 h. Excess base was quenched by the addition of 100 mL water. The organic phase was concentrated *in vacuo*, dissolved in diethyl ether and washed with water (3x). The organic phase was dried over MgSO$_4$, concentrated *in vacuo* and the crude product was purified by column chromatography.

Diethyl 2-benzylmalonate (127a)
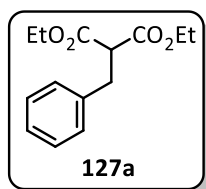
Was synthesized according the general procedure using 8.58 g diethyl malonate (52.50 mmol, 1.05 eq.), 2.20 g NaH (55.00 mmol, 1.1 eq.) and 8.64 g benzyl bromide (50.00 mmol, 1.1 eq.). **127a** was obtained after column chromatography (PE:EA 10%, R$_f$ = 0.23 in PE:EA 10%,) as colorless oil (7.63 g, 61%).

^{1}H-NMR (300 MHz, CDCl$_3$): δ = 7.33 − 7.15 (m, 5H), 4.15 (qd, J = 7.1, 1.4, 4H), 3.64 (t, J = 7.9, 1H), 3.22 (d, J = 7.8, 2H), 1.20 (t, J = 7.1, 6H). **^{13}C-NMR** (75 MHz, CDCl$_3$): δ = 169.0, 138.0, 128.9, 128.6, 126.8, 61.6, 54.0, 34.8, 14.1. The data was in accordance with literature.[183]

Diethyl 2-(2-methylbenzyl)malonate (127b)
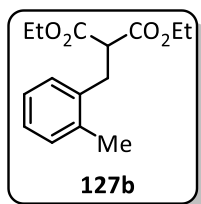
Was synthesized according the general procedure using 858.1 mg diethyl malonate (5.25 mmol, 1.05 eq.), 210.0 mg NaH (5.25 mmol, 1.05 eq.) and 934.7 mg 1-(bromomethyl)-2-methylbenzene (5.00 mmol, 1.0 eq.). **127b** was obtained after column chromatography (PE:EA 10%, R$_f$ = 0.5 in PE:EA 20%))) as colorless oil (933.0 mg, 70%).

^{1}H-NMR (300 MHz, CDCl$_3$): δ = 7.16 − 7.07 (m, 4H), 4.16 (qd, J = 7.1, 1.1, 4H), 3.65 (t, J = 7.8, 1H), 3.23 (d, J = 7.8, 2H), 2.34 (s, 3H), 1.21 (t, J = 7.1, 6H). The data was in accordance with literature.[184]

Diethyl 2-(4-methylbenzyl)malonate (127c)
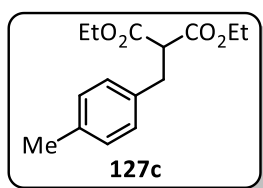
Was synthesized according the general procedure using 858.1 mg diethyl malonate (5.25 mmol, 1.05 eq.), 210.0 mg NaH (5.25 mmol, 1.05 eq.) and 944.2 mg 1-(bromomethyl)-4-methylbenzene (0.88 mmol, 1.0 eq.). **127c** was obtained after column chromatography (PE:EA 10%, R$_f$ = 0.5 in PE:EA 20%) as colorless oil (789.0 mg, 60%).

^{1}H-NMR (300 MHz, CDCl$_3$): δ = 7.10 − 7.05 (m, 4H), 4.16 (qd, J = 7.1, 2.2 Hz, 4H), 3.62 (t, J = 7.8 Hz, 1H), 3.17 (d, J = 7.8 Hz, 2H), 2.30 (s, 3H), 1.21 (t, J = 7.1 Hz, 6H). The data was in accordance with literature.[185]

Diethyl 2-(4-bromobenzyl)malonate (127d)
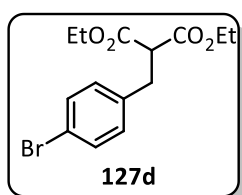
Was synthesized according the general procedure using 150.7 mg diethyl malonate (0.92 mmol, 1.05 eq.), 36.9 mg NaH (0.92 mmol, 1.05 eq.) and 224.0 mg 1-bromo-4-(bromomethyl)benzene (0.88 mmol, 1.0 eq.). **127d** was obtained after column chromatography (PE:EA 10%, R$_f$ = 0.45 in PE:EA 20%) as colorless oil (203.1 mg, 70%).

^{1}**H-NMR** (300 MHz, CDCl$_3$): δ = 7.40 (d, J = 8.4, 2H), 7.09 (d, J = 8.6, 2H), 4.16 (qd, J = 7.1, 2.4, 4H), 3.59 (t, J = 7.8, 1H), 3.16 (d, J = 7.8, 2H), 1.22 (t, J = 7.1, 6H). The data was in accordance with literature.[186]

Diethyl 2-(4-nitrobenzyl)malonate (127e)
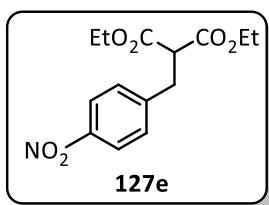
Was synthesized according the general procedure using 858.1 mg diethyl malonate (5.25 mmol, 1.05 eq.), 210.0 mg NaH (5.25 mmol, 1.05 eq)and 1.09 g 1-(bromomethyl)-4-nitrobenzene (0.88 mmol, 1.0 eq.). **127e** was obtained after column chromatography (PE:EA 10%, R$_f$ = 0.35 in PE:EA 20%) as colorless oil (636.0 mg, 43%).

^{1}**H-NMR** (300 MHz, CDCl$_3$): δ = 8.15 (d, J = 8.8, 2H), 7.39 (d, J = 8.9, 2H), 4.17 (qq, J = 7.2, 3.7, 4H), 3.66 (dd, J = 8.1, 7.5, 1H), 3.31 (d, J = 7.8, 2H), 1.22 (t, J = 7.1, 6H). The data was in accordance with literature.[187]

Diethyl 2-isopropylmalonate (127f)
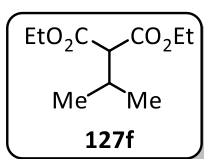
Was synthesized according the general procedure using 4.09 g diethyl malonate (25.00 mmol, 1.0 eq.), 210.0 mg NaH (27.50 mmol, 1.1 eq.) and 3.45 g 2-bromopropane (27.50 mmol, 1.1 eq.). **127f** was obtained after column chromatography (PE:EA 10%, R$_f$ = 0.4 in PE:EA 20%) as colorless oil (4.96 g, 98%).

^{1}**H-NMR** (400 MHz, CDCl$_3$): δ = 4.19 (q, J = 7.1, 4H), 3.10 (d, J = 8.7, 1H), 2.39 (ddt, J = 13.5, 8.7, 6.7, 1H), 1.26 (t, J = 7.1, 6H), 1.00 (d, J = 6.8, 6H).The data was in accordance with literature.[188]

2-isocyano-3-phenylpropanenitrile (127g)
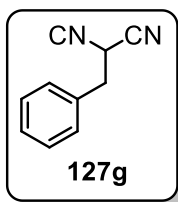
Was synthesized according the general procedure using 1.69 g 2-isocyanoacetonitrile (25.00 mmol, 1.0 eq.), 1.1 g NaH (27.50 mmol, 1.1 eq.) and 4.8 g (bromomethyl)benzene (27.50 mmol, 1.1 eq.). **127g** was obtained after sublimation (80 °C, 1 mbar) as colorless crystalline solid (1.61 g, 41%).

^{1}**H-NMR** (300 MHz, CDCl$_3$): δ = 7.57 − 7.28 (m, 5H), 3.91 (t, J = 7.0, 1H), 3.30 (d, J = 7.0, 2H). The data was in accordance with literature.[189]

General procedure for brominated malonate derivatives

Brominated malonates were prepared according to a modified literature procedure.[190] Diethyl malonate derivative (1.0 eq.) was dissolved in diethyl ether (0.2 M). Bromine (5 eq.) was added to the solution and left stirring for 4 h as judged by TLC control. After the starting material was consumed, the reaction was quenched by adding 10% $Na_2S_2O_3$ solution and stirring for 30 minutes. After all excess bromine was consumed phases were separated. The organic phase was diluted with some diethyl ether and washed with $Na_2S_2O_3$ solution, water (2x) and brine. The organic phase was dried over $MgSO_4$, filtered and concentrated *in vacuo* and the crude product was purified by column chromatography.

Diethyl 2-benzyl-2-bromomalonate (88a)
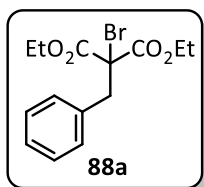
Was synthesized according the general procedure using 2.58 g diethyl 2-benzylmalonate **127a** (10.20 mmol, 1.0 eq.), and 8.16 g bromine (51.06 mmol, 2.6 mL, 5.0 eq.). **88a** was obtained after column chromatography (PE:EA 10%, R_f = 0.55 in PE:EA 20%) as colorless oil (2.91 g, 87%).

¹H-NMR (400 MHz, CDCl₃): δ = 7.31 − 7.23 (m, 5H), 4.26 (qd, *J* = 7.1, 2.4, 4H), 3.64 (s, 2H), 1.27 (t, *J* = 7.1, 6H). **¹³C-NMR** (101 MHz, CDCl₃): δ = 166.8, 134.5, 130.5, 128.3, 127.8, 63.4, 63.2, 43.7, 13.9. The data was in accordance with literature.[190]

Diethyl 2-bromo-2-(2-methylbenzyl)malonate (88b)
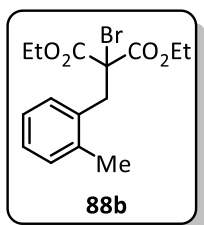
Was synthesized according the general procedure using 297 mg diethyl 2-(2-methylbenzyl)malonate **127b** (1.10 mmol, 1.0 eq.), and 879 mg bromine (5.51 mmol, 282 µL, 5.0 eq.). **88b** was obtained after column chromatography (PE:EA 10%, R_f = 0.66 in PE:EA 15%) as colorless oil (176 mg, 47%).

¹H-NMR (300 MHz, CDCl₃): δ = 7.19 − 7.08 (m, 4H), 4.28 (qd, *J* = 7.1, 3.8, 4H), 3.73 (s, 2H), 2.38 (s, 3H), 1.27 (t, *J* = 7.1, 6H).

Diethyl 2-bromo-2-(4-methylbenzyl)malonate (88c)
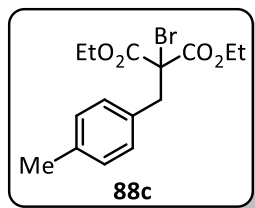
Was synthesized according the general procedure using 798.0 mg diethyl 2-(4-methylbenzyl)malonate **127c** (2.96 mmol, 1.0 eq.), and 2.36 g bromine (14.79 mmol, 758 µL, 5.0 eq.). **88c** was obtained after column chromatography (PE:EA 10%, R_f = 0.68 in PE:EA 20%) as colorless oil (176 mg, 47%).

¹H-NMR (400 MHz, CDCl₃): δ = 7.21 − 7.04 (m, 4H), 4.27 (qd, *J* = 7.2, 1.1 Hz, 4H), 3.60 (s, 2H), 2.31 (s, 3H), 1.28 (t, *J* = 7.1 Hz, 6H).

Diethyl 2-bromo-2-(4-bromobenzyl)malonate (88d)
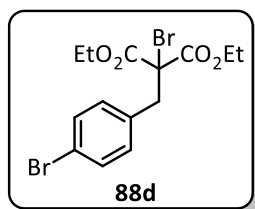
Was synthesized according the general procedure using 203 mg diethyl 2-(4-bromobenzyl)malonate **127d** (0.62 mmol, 1.0 eq.), and 493 mg bromine (3.08 mmol, 158 µL, 5.0 eq.). **88d** was obtained after column chromatography (PE:EA 5%, R_f = 0.58 (PE:EA 10%)) as colorless oil (221 mg, 88%).

¹H-NMR (300 MHz, CDCl₃): δ = 7.45 − 7.38 (m, 2H), 7.17 − 7.09 (m, 2H), 4.26 (qd, *J* = 7.1, 1.2, 4H), 3.59 (s, 2H), 1.27 (t, *J* = 7.1, 6H).). **¹³C-NMR** (101 MHz, CDCl₃): δ = 166.6, 133.5, 132.3, 131.5, 122.0, 63.4, 62.8, 43.0, 14.0.

Diethyl 2-bromo-2-(4-nitrobenzyl)malonate (88e)
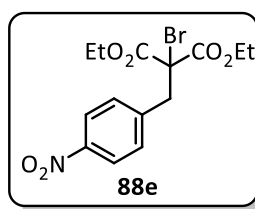
Was synthesized according the general procedure using 492 mg diethyl 2-(4-nitrobenzyl)malonate **127e** (1.63 mmol, 1.0 eq.), and 1.30 g bromine (8.16 mmol, 418 µL, 5.0 eq.). **88e** was obtained after column chromatography (PE:EA 10%, R_f = 0.5 (PE:EA 15%)) as light yellow oil (558.3 mg, 91%).

¹H-NMR (400 MHz, CDCl₃): δ = 8.20 − 8.11 (m, 2H), 7.48 − 7.40 (m, 2H), 4.28 (qd, *J* = 7.1, 1.2, 4H), 3.73 (s, 2H), 1.28 (t, *J* = 7.1, 6H). **¹³C-NMR** (101 MHz, CDCl₃): δ = 166.3, 147.7, 142.1, 131.6, 123.4, 63.6, 62.0, 43.2, 14.0.

Diethyl 2-bromo-2-isopropylmalonate (88f)
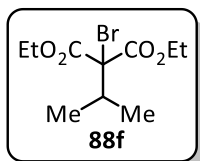
Was synthesized according the general procedure using 1.01 g diethyl 2-isopropylmalonate **127f** (5.00 mmol, 1.0 eq.), and 4.0 g bromine (25.00 mmol, 1.28 mL, 5.0 eq.). **88f** was obtained after column chromatography (PE:Et$_2$O 20%, R$_f$ = 0.35 in PE:Et$_2$O 20%,) as colorless oil (1.01 g, 72%).

^{1}H-NMR (300 MHz, CDCl$_3$): δ = 4.26 (q, J = 7.1, 4H), 2.55 (hept, J = 6.6, 1H), 1.29 (t, J = 7.1, 6H), 1.09 (d, J = 6.6, 6H).

Diethyl 2-bromo-2-ethylmalonate (88h)
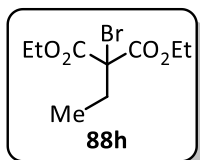
Was synthesized according the general procedure using 941 mg diethyl 2-ethylmalonate (5.00 mmol, 1.0 eq.), and 4.0 g bromine (25.00 mmol, 1.28 mL, 5.0 eq.). **88h** was obtained after distillation (b.p.: 76 °C, 1.2 mbar) as colorless oil (990.3 mg, 74%).

^{1}H-NMR (300 MHz, CDCl$_3$): δ = 4.26 (q, J = 7.1, 4H), 2.29 (q, J = 7.3, 2H), 1.27 (t, J = 7.1, 6H), 1.01 (t, J = 7.3, 3H). The data was in accordance with literature.[191]

Diethyl 2-bromo-2-(2-nitro-1-phenylethyl)malonate (88i)
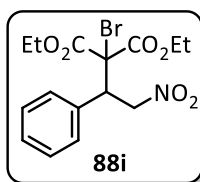
Was synthesized according the general procedure using 577 mg diethyl 2-(2-nitro-1-phenylethyl)malonate (1.87 mmol, 1.0 eq.), and 1.49 g bromine (9.33 mmol, 478 µL, 5.0 eq.). **88i** was obtained after column chromatography (PE:EA 10%, R$_f$ = 0.28) as white solid (345.5 mg, 56%).

^{1}H-NMR (400 MHz, CDCl$_3$): δ = 7.39 (dd, J = 6.8, 3.0, 2H), 7.34 – 7.29 (m, 3H), 5.28 (dd, J = 13.5, 3.2, 1H), 5.03 (dd, J = 13.5, 10.4, 1H), 4.54 (dd, J = 10.4, 3.2, 1H), 4.29 (qd, J = 7.1, 1.8, 2H), 4.13 – 4.00 (m, 2H), 1.28 (t, J = 7.1, 3H), 1.14 (t, J = 7.1, 3H). The data was in accordance with literature.[192]

7.3.1.2 Synthesis of brominated non-malonate compounds

Ethyl 2-bromo-3-methylbutanoate (103)
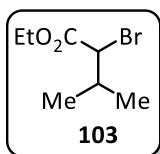
Was synthesized by dissolving 3.98 g (30.00 mmol, 1.0 eq.) Valine in 27 mL H_2O and 30 mL 48% HBr solution. 3.3 g (48.00 mmol, 1.6 eq.) sodium nitrite dissolved in 7.5 mL water was added dropwise at 0 °C and the reaction mixture was stirred for 2.5 h. The reaction mixture was extracted four times with 20 mL Et_2O. The combined organic phases were washed with 10 mL brine, dried over Na_2SO_4, filtered and concentrated *in vacuo*. The colorless oil was dissolved in 25 mL EtOH, acidified with 0.7 mL H_2SO_4 and refluxed for 4 h. 20 mL Et_2O was added and the mixture was neutralized with 5% $NaHCO_3$. The organic phase was washed with brine, dried over Na_2SO_4, filtered and concentrated *in vacuo*. **103** was obtained after column chromatography (PE:EA 5-10%, R_f = 0.4 in PE:EA 10%) as colorless oil (3.89 g, 73%)

¹H-NMR (400 MHz, CDCl₃): δ = 4.21 (q, *J* = 7.1, 2H), 4.01 (d, *J* = 7.9, 1H), 2.21 (dp, *J* = 8.0, 6.7, 1H), 1.27 (t, *J* = 7.1, 3H), 1.07 (d, *J* = 6.6, 3H), 1.00 (d, *J* = 6.7, 3H). **¹³C-NMR** (101 MHz, CDCl₃): δ = 169.6, 61.9, 54.8, 32.4, 20.1, 20.0, 14.1.

ethyl 2-bromo-3-phenylpropanoate (105)
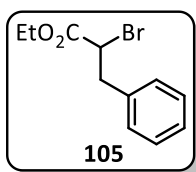
Was synthesized by dissolving 1.65 g *L*-phenylalanine (10.00 mmol, 1.0 eq.) in 9 mL H_2O and 10 mL 48% HBr solution. 1.1 g (16 mmol, 1.6 eq.) sodium nitrite dissolved in 2.5 mL water was added dropwise at 0 °C and the reaction mixture was stirred for 2.5 h. The reaction mixture was extracted four times with 5 mL Et_2O. The combined organic phases were washed with 10 mL brine, dried over Na_2SO_4, filtered and concentrated *in vacuo*. The colorless oil was dissolved in 20 mL EtOH, acidified with 0.3 mL H_2SO_4 and refluxed for 1 h. 20 mL Et_2O was added and the mixture was neutralized with 5% $NaHCO_3$. The organic phase was washed with brine, dried over Na_2SO_4, filtered and concentrated *in vacuo*. **105** was obtained after column chromatography (PE:EA 5%, R_f = 0.3 in PE:EA 5%) as colorless oil (1.77 g, 69%)

¹H-NMR (300 MHz, CDCl₃): δ = 7.38 – 7.15 (m, 5H), 4.39 (dd, *J* = 8.5, 7.1, 1H), 4.18 (qd, *J* = 7.1, 2.2, 2H), 3.46 (dd, *J* = 14.0, 8.5, 1H), 3.25 (dd, J=14.1, 7.1, 1H), 1.22 (t, *J* = 7.1, 3H).**¹³C-NMR** (75 MHz, CDCl₃): δ = 169.5, 136.9, 129.3, 128.8, 127.4, 62.1, 45.6, 41.3, 14.0.

Ethyl 1-bromocyclohexane-1-carboxylate (107)
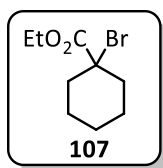
9.1 mL thionylchloride (14.87 g, 125.00 mmol, 1.25 eq.) was added dropwise to 12.7 mL (13.08 g, 100.00 mmol, 1.0 eq.) cyclohexanecarboxylic acid. The reaction mixture was stirred at 90 °C for 2 h. After cooling, 160 mg of red phosphorus (5 mol%) followed by a dropwise addition of 6.5 mL (125.00 mmol, 20.2 g, 1.25 eq.) bromine. The reaction mixture was stirred at 100 °C for 5 h, after which the reaction mixture was cooled to 0 °C and 33 mL EtOH was added dropwise. The reaction mixture was refluxed for another hour. The reaction was ended by adding 50 g of ice, and 10 mL 50% $Na_2S_2O_3$ solution. The mixture was extracted three times with Et_2O. The combined organic phases were washed with 10% $Na_2S_2O_3$, two times with $NaHCO_3$ and with brine. The organic Phase was dried over Na_2SO_4, filtered and concentrated *in vacuo*. **107** was obtained after vacuum distillation (b.p.: 51 °C at 0.6 mbar) as colorless oil (21.0 g, 89%).

¹H-NMR (400 MHz, CDCl₃): δ = 4.25 (q, *J* = 7.1, 2H), 2.23 – 2.09 (m, 4H), 1.78 – 1.69 (m, 2H), 1.54 – 1.38 (m, 4H), 1.31 (t, *J* = 7.1, 3H). The data was in accordance with literature.[193]

7.3.1.3 General procedure for the synthesis of activated esters

Activated esters were synthesized by dissolving 1.0 eq. carboxylic acid in EtOAc (0.1 M). 1.2 eq. dicyclohexylmethanediimine (DCC) and 1 mol% N,N-dimethylpyridin-4-amine (DMAP) were added to this solution. After 15 minutes 1.2 eq. 2-hydroxyisoindoline-1,3-dione was added and the mixture was stirred for 16 h. After 16 h, the suspension was cooled in a freezer for 1 h and filtered while cold. The residue was washed with cold EtOAc, and the filtrate was concentrated *in vacuo*.

1,3-dioxoisoindolin-2-yl 1-methylcyclohexane-1-carboxylate (110)
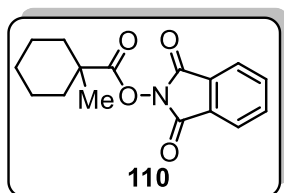
Was synthesized according to the general procedure. 3.55 g (25.00 mmol, 1.0 eq.) 1-methylcyclohexane-1-carboxylic acid, 5.67 g (27.50 mmol, 1.1 eq.) DCC, 4.62 g (27.50 mmol, 1.1 eq.) 2-hydroxyisoindoline-1,3-dione and 304.4 mg (10 mol%) DMAP were dissolved in 125 mL THF (0.2 M). **110** was obtained after column chromatography (PE:EA 5-10%, R_f = 0.40 in PE:EA 10%) as slightly yellow oil (6.66 g, 93%)

¹H-NMR (300 MHz, CDCl₃): δ = 7.90 − 7.85 (m, 2H), 7.82 − 7.75 (m, 2H), 2.29 − 2.18 (m, 2H), 1.71 − 1.49 (m, 6H), 1.43 (s, 3H), 1.40 − 1.18 (m, 3H). **¹³C-NMR** (75 MHz, CDCl₃): δ = 173.8, 162.4, 134.8, 129.2, 124.0, 77.6, 77.2, 76.7, 43.3, 35.8, 26.9, 25.6, 23.2.

1,3-dioxoisoindolin-2-yl 3-phenylpropanoate (136)
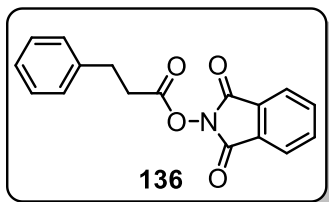
Was synthesized according to the general procedure. 1.50 g (10.00 mmol, 1.0 eq. phenylacetic acid, 2.48 g (12.00 mmol, 1.2 eq.) DCC, 1.96 g (12.00 mmol, 1.2 eq.) 2-hydroxyisoindoline-1,3-dione and 12.2 mg (1 mol%) DMAP were used. **136** was obtained after recrystallization from ethanol as colorless crystals (0.67 g, 27%)

¹H-NMR (400 MHz, CDCl₃): δ = 7.92 (dd, *J* = 5.5, 3.1 Hz, 2H), 7.82 (dd, *J* = 5.5, 3.1 Hz, 2H), 7.40 − 7.34 (m, 2H), 7.29 (dd, *J* = 5.3, 3.4 Hz, 3H), 3.22 − 3.11 (m, 2H), 3.02 (ddd, *J* = 8.4, 7.0, 1.1 Hz, 2H). **¹³C-NMR** (101 MHz, CDCl₃): δ = 169.0, 162.0, 139.3, 134.9, 129.1, 128.9, 128.5, 126.9, 124.1, 32.9, 30.7. **IR** (neat, cm⁻¹): 1815, 1737, 1495, 1454, 1372, 1185, 1066, 969, 880, 783, 697. **HRMS** (EI): m/z calculated for $C_{17}H_{14}NO_4$ [MH⁺]: 296.0917 found 296.0919.

1,3-dioxoisoindolin-2-yl (tert-butoxycarbonyl)phenylalaninate (138)
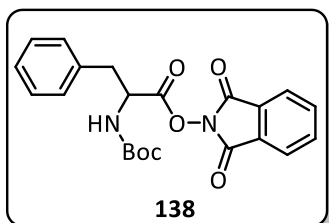
Was synthesized according to the general procedure. 1.00 g (3.77 mmol, 1.0 eq.) (tert-butoxycarbonyl)phenylalanine, 933.3 mg (4.52 mmol, 1.2 eq.) DCC, 4.62 g (4.52 mmol, 1.2 eq.) 2-hydroxyisoindoline-1,3-dione and 4.6 mg (1 mol%) DMAP were used. **138** was obtained after recrystallization from ethanol as colorless crystals (6.66 g, 93%)

¹H-NMR (300 MHz, CDCl₃): δ = 7.90 (dd, *J* = 5.5, 3.1 Hz, 2H), 7.80 (dd, *J* = 5.5, 3.1 Hz, 2H), 7.39 − 7.24 (m, 5H), 5.09 − 4.91 (m, 1H), 4.73 (s, 1H), 3.41 − 3.12 (m, 2H), 1.42 (s, 9H). **¹³C-NMR** (75 MHz, CDCl₃): δ = 168.8, 161.6, 154.8, 135.0, 134.8, 129.8, 128.9, 128.8, 127.5, 124.2, 80.7, 52.8, 38.3, 28.4.

7.3.1.1 Synthesis of 3-phenylcyclobutan-1-one O-(4-(trifluoromethyl)-benzoyl) oxime (129)
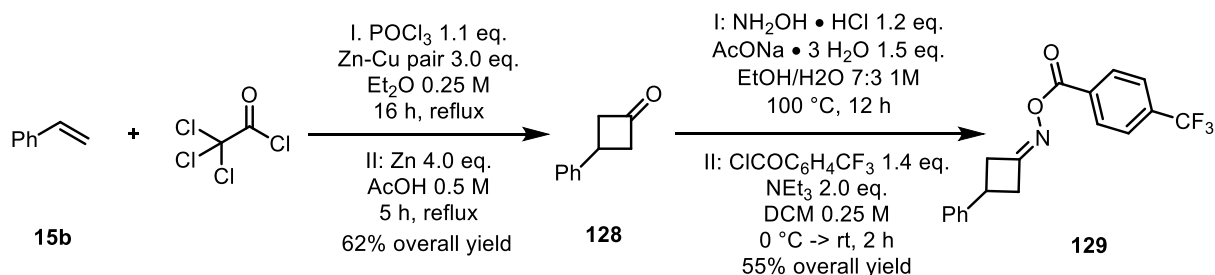
Scheme 58: Synthetic route to 3-phenylcyclobutan-1-one O-(4-(trifluoromethyl)benzoyl) oxime **129**.

3-phenylcyclobutan-1-one (128)
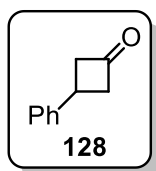
Was synthesized according to a modified literature procedure.[194] The Zn-Cu pair was prepared by suspending 350 mg Cu(OAc)$_2$•H$_2$O (6 wt%) in 10 mL AcOH and adding 6.00 g of Zn dust. After 30 seconds dust was allowed to settle, and the solution was decanted. The dust was washed once with 10 mL AcOH and three times with Et$_2$O and dried by a stream of dried N$_2$. 3.12 g styrene **15b** (30.00 mmol, 1.0 eq.) was dissolved in 60 mL of Et$_2$O and the Zn-Cu pair was added. 10.91 g trichloroacetyl chloride (60.00 mmol, 2.0 eq.) and 5.06 g POCl$_3$ (33.00 mmol, 1.1 eq.) were dissolved in 60 mL Et$_2$O, and this solution was added *via* a dropping funnel. Afterwards, the mixture was refluxed for 16 h. The zinc was removed from the crude mixture by filtering through a celite pad and washing with 30 mL Et$_2$O. The crude mixture was extracted once with each of 100 mL of H$_2$O, NaHCO$_3$ and brine. The organic phase was dried over MgSO$_4$, filtered and concentrated *in vacuo*. **128** was obtained after column chromatography (PE:EA 5-15%, R$_f$ = 0.46 in PE:EA 20%) as colorless oil (2.70 g, 62%)

^{1}H-NMR (400 MHz, CDCl$_3$): δ = 7.38 (t, *J* = 7.5, 2H), 7.35 − 7.25 (m, 3H), 3.66 (p, J = 7.6, 1H), 3.54 − 3.42 (m, 2H), 3.23 (dd, *J* = 20.0, 7.4, 2H). **^{13}C-NMR** (101 MHz, CDCl$_3$): δ = 206.2, 143.5, 128.5, 126.4, 126.3, 54.4, 28.2. **IR** (neat, cm^{-1}): 3064, 3030, 2974, 2922, 1782, 1603, 1495, 1454, 1379, 1163, 1103, 984, 869, 757, 701. **HRMS** (EI): m/z calculated for C$_{10}$H$_{11'0}$O [M$^•$]: 146.0726, found: 146.0722.

3-phenylcyclobutan-1-one oxime
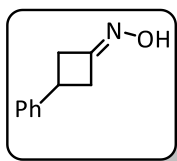
Was synthesized according to a modified literature procedure.[194] 417.0 mg (6.0 mmol, 1.2 eq.) hydroxylamine hydrochloride and 1.02 g (7.50 mmol, 1.5 eq.) sodium acetate trihydrate were dissolved in 5 mL EtOH/H_2O 7:3. 731.0 mg (5.0 mmol, 1.0 eq.). 3-phenylcyclobutan-1-one **XX** was added and stirred at 100 °C in a closed vessel for 12 h. The reaction mixture was diluted with water and extracted three times with 45 mL Et_2O. The combined organic phases were dried over $MgSO_4$, filtered and concentrated *in vacuo*. 3-phenylcyclobutan-1-one oxime was obtained after column chromatography (PE:EA 15-25%, R_f = 0.17 in PE:EA 20%) as colorless oil (595.2 mg, 74%)

^{1}H-NMR (400 MHz, $CDCl_3$): δ = 9.76 (s, 1H), 7.40 (t, *J* = 7.6, 2H), 7.31 (dd, *J* = 16.2, 7.7, 3H), 3.74 – 3.60 (m, 1H), 3.54 (ddt, *J* = 17.0, 9.2, 3.1, 1H), 3.50 – 3.37 (m, 1H), 3.12 (ddt, *J* = 16.4, 6.9, 3.4, 2H).**^{13}C-NMR** (101 MHz, $CDCl_3$): δ = 156.5, 144.0, 128.6, 126.5, 126.4, 39.2, 38.3, 32.8. **IR** (neat, cm^{-1}): 3243, 3146, 3027, 2922, 2369, 1703, 1603, 1495, 1454, 1402, 1174, 969, 910, 746, 697. **HRMS** (EI): m/z calculated for $C_{10}H_{11}{'}_0O$ [M$^\bullet$]: 161.0835; found: 161.0833

3-phenylcyclobutan-1-one O-(4-(trifluoromethyl)benzoyl) oxime (129)
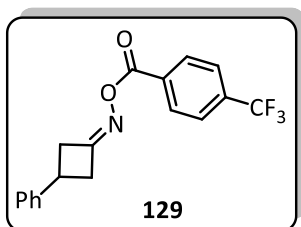
Was synthesized according to a modified literature procedure.[194] 570.7 mg (3.54 mmol, 1.0 eq.) 3-phenylcyclobutan-1-one oxime was dissolved in 14 mL DCM. 0.99 mL NEt_3 (7.08 mmol, 2.0 eq.) and 0.74 mL (4.96 mmol, 1.4 eq.) 4-(trifluoromethyl)benzoyl chloride were added at 0 °C. The mixture was allowed to warm to room temperature and stirred for 2 h. The reaction mixture was diluted with 20 mL H_2O and 40 mL Et_2O. The phases were separated, and the organic phase was washed with 20 mL H_2O. The organic phases were dried over $MgSO_4$, filtered and concentrated *in vacuo*. **129** was obtained after column chromatography (PE:EA 5-10%, R_f = 0.32 in PE:EA 20%) as colorless solid (595.2 mg, 74%)

¹H-NMR (400 MHz, CDCl₃): δ = 8.17 (d, *J* = 8.1, 2H), 7.73 (d, *J* = 8.2, 2H), 7.37 (dd, *J* = 8.0, 6.9, 2H), 7.33 – 7.23 (m, 3H), 3.80 – 3.53 (m, 3H), 3.34 – 3.19 (m, 2H).**¹³C-NMR** (101 MHz, CDCl₃): δ = 166.9 , 162.9 , 142.9 , 134.8 (q, *J* = 32.8), 132.4 , 130.1 , 128.9 , 127.1 , 126.4 , 125.7 (q, *J* = 3.8), 123.6 (d, *J* = 272.8), 39.6 , 32.6 .**¹⁹F NMR** (377 MHz, CDCl₃) δ = -63.7 (s). **IR** (neat, cm⁻¹): 3474, 3071, 1744, 1677, 1409, 1323, 1256, 1163, 1121, 1066, 1010, 846, 768, 693. **m.p.**: 112 - 114 °C. **HRMS** (ESI) m/z: calculated for $C_{18}H_{15}F_3NO_2$ [M-H⁺]: 334.1049; found: 334.1052.

7.3.1.5 Synthesis of vinyl azides

Handling vinyl azides – caution advised: While no incidents occurred during my work with vinyl azides, they should be treated with utmost care due to their inherent toxicity, instability and explosive properties. Isolated vinyl azides can be stored in the dark in a freezer (-16 °C) for up to several months without significant degradation. For optimal results purification after prolonged storage (>1-2 weeks) by flash column chromatography (1% EA/PE) is recommended.[110]

General procedure A (dibromination)
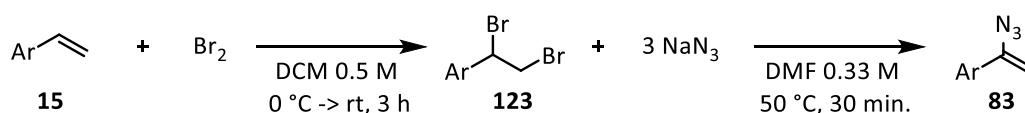
Scheme 59: Overview scheme for the synthesis of vinyl azides **83** through dibrominated alkenes **123**.

Was synthesized according to a modified literature procedure.[195] Styrene (1.0 eq.) was dissolved in DCM 0.5 M). The solution was cooled to 0° C and 1.1 eq. bromine was added dropwise. The reaction was allowed to warm to room temperature and left stirring for 3 hours. The reaction mixture was diluted with 10% Na₂S₂O₃ and 20% NaHCO₃ solution as well as Et₂O and left stirring for 15 minutes. Phases were separated and the organic phase was washed with 10% Na₂S₂O₃, sat. NaHCO₃ and brine. The crude **123** could be used in without further purification

The dibromo species **123** (1.0 eq.) was dissolved in DMF (0.33 M) and NaN₃ (3.1 eq.) was added to the solution. The suspension was stirred at 50 °C for 30 minutes. The reaction mixture was cooled to room temperature and conversion was checked by TLC. If conversion was not complete, several drops of DBU were added to the solution, left stirring at room temperature

and conversion was checked every 15 minutes. The suspension was diluted with Et_2O and H_2O, phases were separated, and the aqueous phase was washed three times with Et_2O. The combined organic phases were dried over Na_2SO_4, filtered and concentrated *in vacuo* (max. 40 °C). Vinyl azides were purified by flash column chromatography using 1% EA/PE.

General procedure B (ICl)
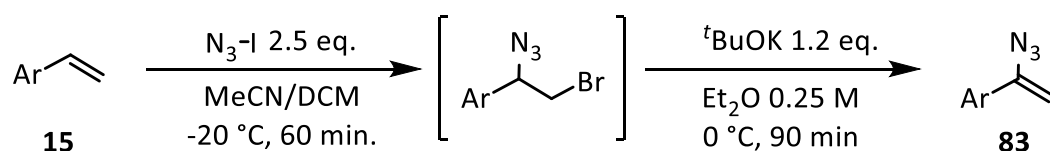
Scheme 60: Overview scheme for the synthesis of vinyl azides **83** through iodoazide.

83 was synthesized according to a modified literature procedure.[74] ICl (1.5 eq.) was dissolved in DCM (1.0 M) and added to a suspension of NaN_3 (2.5 eq.) in MeCN (3 M) at -20 °C and stirred for 60 minutes. A solution of the corresponding styrene derivative **15** (1.0 eq.) in DCM (1 M) was added to the suspension. After 90 minutes (as judged by TLC control) the reaction was quenched by addition of a 10% $Na_2S_2O_3$ solution and left stirring for 10 minutes. The phases were separated, and the aqueous phase was washed two times with Et_2O. The combined organic phases were washed with sat. $NaHCO_3$ solution and brine. The organic phase was dried over Na_2SO_4, filtered and concentrated *in vacuo* (max. 40 °C). The crude mixture was immediately dissolved in Et_2O (0.25 M) and cooled to 0 °C. *t*BuOK (1.2 eq.) was added slowly over 15 minutes, and the reaction was monitored by TLC for up to 90 minutes. After the reaction was complete, solids were removed by filtering through a celite pad and washing with Et_2O. The filtrate was concentrated *in vacuo* and purified by flash column chromatography (PE:EA 1%, R_f = 0-7 – 0-95 in PE:EA 1%, for all azidostyrenes, bright orange stain with vanillin staining solution) to give the corresponding vinyl azides.

4-(1,2-dibromoethyl)benzonitrile (123b)
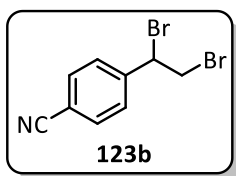
Was synthesized according to general procedure **A** using 189.0 mg (1.39 mmol, 95%, 1.0 eq.) methyl 4-vinylbenzonitrile, 2.8 mL DCM and 78 µL bromine (1.53 mmol, 1.1 eq.). **123b** was obtained as white oil after column chromatography (PE:EA 10%, R_f = 0.45 in PE:EA 10%) in 335.0 mg (83%) yield.

^{1}H-NMR (400 MHz, CDCl$_3$): δ = 7.72 – 7.65 (m, 2H), 7.55 – 7.48 (m, 2H), 5.12 (dd, J = 11.2, 4.9, 1H), 4.07 (dd, J = 10.4, 4.9, 1H), 3.96 (dd, J = 11.2, 10.4, 1H). **^{13}C-NMR** (101 MHz, CDCl$_3$): δ = 143.7, 132.8, 128.7, 118.3, 113.1, 48.5, 34.0.

Methyl 4-(1,2-dibromoethyl)benzoate (123c)
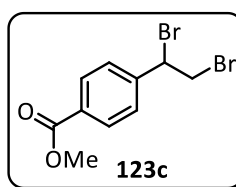
Was synthesized according to general procedure **A** using 496.5 mg (3.00 mmol, 98%, 1.0 eq.) methyl 4-vinylbenzoate, 6 mL DCM and 169 µL bromine (3.30 mmol, 1.1 eq.). **123c** was obtained as colorless crystals in 958.2 mg (99%) yield.

^{1}H-NMR (400 MHz, CDCl$_3$): δ = 8.06 (d, J = 8.5, 2H), 7.48 (d, J = 8.2, 2H), 5.15 (dd, J = 10.9, 5.2, 1H), 4.11 – 3.97 (m, 2H), 3.93 (s, 3H). **^{13}C-NMR** (101 MHz, CDCl$_3$): δ = 166.5, 143.5, 130.9, 130.3, 127.9, 52.4, 49.5, 34.5.

1-chloro-3-(1,2-dibromoethyl)benzene (123d)
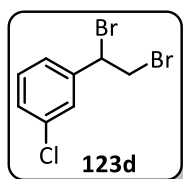
Was synthesized according to general procedure **A** using 424.3mg (3.00 mmol, 98%, 1.0 eq.) 1-chloro-3-vinylbenzene, 6 mL DCM and 169 µL bromine (3.30 mmol, 1.1 eq.). **123d** was obtained as colorless oil after filtration through a short silica pad (PE) in 782.0 mg (87%) yield.

^{1}H-NMR (400 MHz, CDCl$_3$): δ = 7.34 (d, J = 1.4, 1H), 7.30 – 7.18 (m, 3H), 5.01 (dd, J = 10.9, 5.2, 1H), 4.00 (dd, J = 10.4, 5.1, 1H), 3.91 (t, J = 10.6, 1H). **^{13}C-NMR** (101 MHz, CDCl$_3$): δ = 140.7, 134.8, 130.2, 129.5, 128.0, 126.0, 49.4, 34.7.

2-(1,2-dibromoethyl)naphthalene (123e)
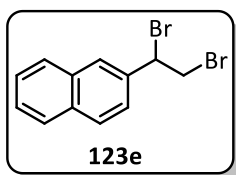
Was synthesized according to general procedure **A** using 477.0 mg (3.00 mmol, 97%, 1.0 eq.) 2-vinylnaphthalene, 6 mL DCM and 169 µL bromine (3.30 mmol, 1.1 eq.). **123e** was obtained as colorless crystals after filtration through a short silica pad (PE) in 721.4 mg (77%) yield.

^{1}H-NMR (400 MHz, CDCl$_3$): δ = 7.93 − 7.78 (m, 4H), 7.57 − 7.48 (m, 3H), 5.34 (dd, J = 9.4, 6.7, 1H), 4.19 − 4.14 (m, 2H). **^{13}C-NMR** (101 MHz, CDCl$_3$): δ = 135.8, 133.6, 133.0, 129.2, 128.3, 127.9, 127.6, 127.1, 126.8, 124.5, 51.5, 34.9.

Methyl 2,3-dibromopropanoate (123f)
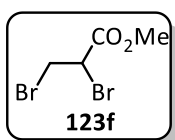
Was synthesized according to general procedure **A** using 5.0 g (58.2 mmol, 1.0 eq.) methylacrylate, 100 mL DCM and 3.3 mL bromine (64.00 mmol, 1.1 eq.). **123f** was obtained as colorless oil in 11.8 g (82%) yield.

^{1}H-NMR (400 MHz, CDCl$_3$): δ = 4.44 (dd, J = 11.3, 4.4, 1H), 3.95 − 3.86 (m, 1H), 3.83 (s, 3H), 3.67 (dd, J = z9.9, 4.4, 1H). **^{13}C-NMR** (101 MHz, CDCl$_3$): δ = 168.2, 53.5, 40.8, 29.7.

(1-azidovinyl)benzene (83a)
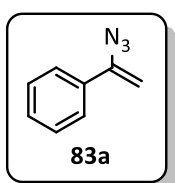
Was synthesized according to general procedure **A** using 15.35 g (58.14 mmol 1.0 eq.) (1,2-dibromoethyl)benzene, 150 mL DMF and 11.34 g sodium azide (174.42 mmol, 99%, 3.0 eq.). **83a** was obtained as slightly yellow oil after flash column chromatography in 7.39 g (88%) yield.

^{1}H-NMR (400 MHz, CDCl$_3$): δ = 7.61 − 7.55 (m, 2H), 7.37 (dd, J = 5.1, 2.0, 3H), 5.45 (d, J = 2.4, 1H), 4.98 (d, J = 2.4, 1H). **^{13}C-NMR** (101 MHz, CDCl$_3$): δ = 145.1, 134.3, 129.1, 128.5, 125.6, 98.0. The data was in accordance with literature.[136]

4-(1-azidovinyl)benzonitrile (83b)
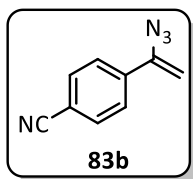
Was synthesized according to general procedure **A** using 258.0 mg (0.89 mmol 1.0 eq.) 4-(1,2-dibromoethyl)benzonitrile **123b**, 2.7 mL DMF and 182 mg sodium azide (2.77 mmol, 99%, 3.1 eq.). **83b** was obtained as orange oil after flash column chromatography in 144.4 mg (95%) yield as a non-separable 1.14:1 mixture of both azide regioisomers.

^{1}H-NMR (300 MHz, CDCl$_3$) (1-azidovinyl regioisomer): δ = 7.81 − 7.45 (m, 4H), 5.59 (d, J = 3.0, 1H), 5.11 (d, J = 2.9, 1H). **^{1}H-NMR** (300 MHz, CDCl$_3$) (2-azidovinyl regioisomer): δ = 7.81 − 7.45 (m, 4H), 6.24 (d, J=2.4, 1H), 5.94 (d, J=2.4, 1H). The data was in accordance with literature.[196]

methyl 4-(1-azidovinyl)benzoate (83c)
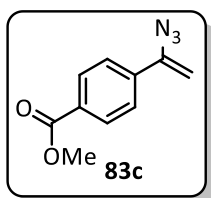
Was synthesized according to general procedure **A** using 429.0 mg (1.33 mmol 1.0 eq.) methyl 4-(1,2-dibromoethyl)benzoate **123c**, 4.0 mL DMF and 271 mg sodium azide (2.77 mmol, 99%, 3.1 eq.). **83c** was obtained as orange oil after flash column chromatography in 259.2 mg (96%) yield as a non-separable 3.23:1 mixture of both azide regioisomers.

^{1}H-NMR (300 MHz, CDCl$_3$) (1-azidovinyl regioisomer): δ = 8.03 − 7.97 (m, 2H), 7.63 (d, J = 0.6, 2H), 5.56 (d, J = 2.7, 1H), 5.06 (d, J = 2.7, 1H), 3.92 (s, 3H). **^{1}H-NMR** (300 MHz, CDCl$_3$) (2-azidovinyl regioisomer): δ = 8.03 − 7.97 (m, 2H), 7.68 − 7.62 (m, 2H), 6.22 (d, J = 2.2, 1H), 5.88 (d, J = 2.2, 1H), 3.92 (s, 3H). The data was in accordance with literature.[197]

1-(1-azidovinyl)-3-chlorobenzene (83d)
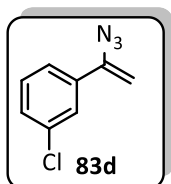
Was synthesized according to general procedure **A** using 301.1 mg (1.00 mmol 1.0 eq.) 1-chloro-3-(1,2-dibromoethyl)benzene **123d**, 3.0 mL DMF and 203.6 mg sodium azide (3.10 mmol, 99%, 3.1 eq.). **83d** was obtained as yellow oil in 154.6 mg (86%) yield as 10:1 mixture of both azide regioisomers. The crude product was used as starting material without further purification.

¹H-NMR (300 MHz, CDCl₃, 1-azidovinyl regioisomer): δ = 7.55 (td, *J* = 1.8, 0.7, 1H), 7.45 (dt, *J* = 6.8, 1.9, 1H), 7.33 – 7.21 (m, 2H), 5.47 (d, *J* = 2.6, 1H), 5.00 (d, *J* = 2.7, 1H). **¹H-NMR** (300 MHz, CDCl₃, 2-azidovinyl regioisomer): δ = 7.55 (td, *J* = 1.8, 0.7 Hz, 1H), 7.45 (dt, *J* = 6.8, 1.9 Hz, 1H), 7.36 – 7.23 (m, 2H), 6.14 (d, *J* = 2.2 Hz, 1H), 5.82 (d, *J* = 2.2 Hz, 1H). The data was in accordance with literature.[195]

2-(1-azidovinyl)naphthalene (83e)
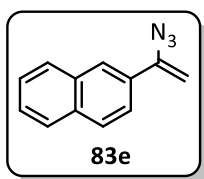
Was synthesized according to general procedure **A** using 349.0 mg (1.09 mmol 1.0 eq.) 2-(1,2-dibromoethyl)naphthalene **123e**, 10.0 mL DMF (0.1 M) and 221.7 mg sodium azide (3.10 mmol, 99%, 3.1 eq.). **83e** was obtained as yellow oil after flash column chromatography in 194.7 mg (92%) yield as 20:1 mixture of both azide regioisomers.

¹H-NMR (300 MHz, CDCl₃) (1-azidovinyl regioisomer): δ = 8.10 – 8.03 (m, 1H), 7.84 (dddd, *J* = 9.4, 7.4, 3.9, 0.8, 3H), 7.74 – 7.61 (m, 1H), 7.53 – 7.41 (m, 2H), 5.59 (d, *J* = 2.5, 1H), 5.06 (d, *J* = 2.5, 1H). The data was in accordance with literature.[197]

Methyl 2-azidoacrylate (83f)
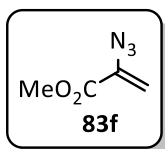
Was synthesized according to general procedure **A** using 1.42 g (5.72 mmol 1.0 eq.) methyl 2,3-dibromopropanoate **123f**, 5.7 mL DMF (1 M) and 1.15 g sodium azide (17.72 mmol, 99%, 3.1 eq.). **83f** was obtained as yellow oil after flash column chromatography in 547.0 mg (75%) yield.

¹H-NMR (300 MHz, CDCl₃): δ = 5.86 (d, *J* = 1.5, 1H), 5.36 (d, *J* = 1.5, 1H), 3.84 (s, 3H). **¹³C-NMR** (101 MHz, CDCl₃): δ = 162.6, 136.2, 111.2, 53.0. The data was in accordance with literature.[198]

1-(1-azidovinyl)-2-methoxybenzene (83g)
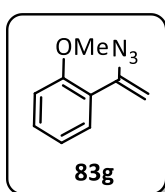
Was synthesized according to general procedure **B** using 507.0 mg (3.70 mmol, 98%, 1.0 eq.) 1-methoxy-2-vinylbenzene, 607.9 mg (9.26 mmol, 99%, 2.5 eq.) sodium azide, 901.8 mg (5.55 mmol, 1.5 eq.) iodine chloride and 498.6 mg potassium 2-methylpropan-2-olate (6.00 mmol, 1.20 eq.). **83g** was obtained as slightly yellow oil after flash column chromatography in 536.4 mg (83%) yield.

¹H-NMR (400 MHz, CDCl₃): δ = 7.39 – 7.32 (m, 2H), 6.96 (td, J = 7.7, 1.0, 2H), 5.04 (d, *J* = 0.7, 1H), 4.93 (d, *J* = 0.7, 1H), 3.89 (s, 3H). The data was in accordance with literature.[197]

1-(1-azidovinyl)-3-methylbenzene (83h)

83h
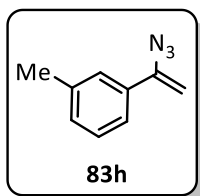
Was synthesized according to general procedure **B** using 634.0 mg (5.26 mmol, 98%, 1.0 eq.) 1-methyl-3-vinylbenzene, 854.5 mg (13.14 mmol, 99%, 2.5 eq.) sodium azide, 1.28 g (7.89 mmol, 1.5 eq.) iodine chloride and 708.0 mg potassium 2-methylpropan-2-olate (6.31 mmol, 1.20 eq.). **83h** was obtained as yellow oil after flash column chromatography in 580.0 mg (69%) yield.

¹H-NMR (300 MHz, CDCl₃): δ = 7.42 – 7.32 (m, 2H), 7.31 – 7.19 (m, 1H), 7.21 – 7.14 (m, 1H), 5.41 (d, *J* = 2.3, 1H), 4.94 (d, *J* = 2.3, 1H), 2.37 (s, 3H). The data was in accordance with literature.[199]

1-(1-azidovinyl)-4-fluorobenzene (83i)

83i
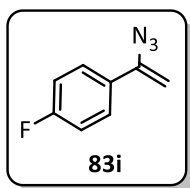
Was synthesized according to general procedure **B** using 736.0 mg (5.97 mmol, 96%, 1.0 eq.) 1-fluoro-4-vinylbenzene, 979.4 mg (14.91 mmol, 99%, 2.5 eq.) sodium azide, 1.45 g (8.95 mmol, 1.5 eq.) iodine chloride and 803.3 mg potassium 2-methylpropan-2-olate (7.16 mmol, 1.20 eq.). **83i** was obtained as orange oil after flash column chromatography in 642.1 mg (66%) yield.

¹H-NMR (400 MHz, CDCl₃): δ = 7.76 (dd, J = 8.9, 5.3, 2H), 7.26 (dd, J = 8.9, 8.5, 2H), 5.59 (d, J = 2.5, 1H), 5.16 (dd, J = 2.6, 0.5, 1H). The data was in accordance with literature.[196]

3-(1-azidovinyl)pyridine (83j)

83j
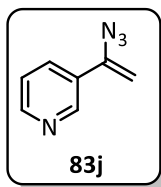
Was synthesized according to literature.[136] 3-Ethynylpyridine (221.7 mg, 2.15 mmol, 1.0 eq.) and azidotrimethylsilane (495.4 mg, 4.30 mmol, 2.0 eq.) were solved in 8 mL of dry DMSO. 55 mg of Ag₂CO₃ (10 mol%) and 72 µL H₂O (4 mmol, 2 eq.) added. The suspension was heated to 70 °C for 90 minutes. Afterwards, the suspension was diluted with 20 mL diethyl ether and washed with brine three times. The organic phase was dried over MgSO₄ and concentrated *in vacuo*. The crude product mixture was purified by column chromatography on silica gel using PE:EA 1% (Rf = 0.6, PE:EA 1%) to afford **83j** as light yellow oil (262.0 mg, 83% yield).

¹H-NMR (400 MHz, CDCl₃): δ = 8.82 (dd, J = 2.3, 0.9, 1H), 8.57 (dd, J = 4.8, 1.6, 1H), 7.83 (ddd, J = 8.1, 2.4, 1.7, 1H), 7.29 (ddd, J = 8.1, 4.8, 0.9, 1H), 5.51 (d, J = 2.8, 1H), 5.05 (d, J = 2.8, 1H). The data was in accordance with literature.[136]

7.3.2 General procedure for the preparation of 2*H*-Pyrrols

A Schlenk tube (5 mL) equipped with a magnetic stir bar was charged with 5,10-di(naphthalen-2-yl)-5,10-dihydrophenazine (D2NDHP, 1.7 mg, 0.004 mmol, 1 mol%), Potassium formiate (50.4 mg, 0.6 mmol, 1.5 eq.), 4 mL *N,N*-dimethylacetamide (DMA, 0.1 M) and diethyl 2-benzyl-2-bromomalonate **88a** (131.7 mg, 0.4 mmol, 1 eq.). The resulting suspension was degassed by three pump-freeze-thaw cycles. azidostyrene **83a** (91.7 mg, 0.6 mmol, 1.5 eq) was added under a slight nitrogen overpressure and the tube was equipped with a LED setup and sealed. The reaction mixture was irradiated at room temperature with a blue LED (λ_{max} = 455 nm) while being stirred for 10 h. Afterwards, the reaction was stopped by switching off the light source. The crude mixture was diluted with 15 mL Diethylether (Et₂O) and washed 15 mL of 50% NaHCO₃, 15 mL of water and 15 mL Brine. The combined aqueous phases were reextracted with 10 mL of Et₂O. The combined organic phases were dried over MgSO₄, filtered and concentrated *in vacuo*. For determining the yield by NMR the crude product was dissolved in CDCl₃ and *1,1,2,2*-tetrachloroethane (33.5 mg, 0.2 mmol, 21.0 µL) was added. The crude mixture was purified by column chromatography on silica gel by using PE:EA (reported as volume% of EA in PE) mixtures to afford the desired product.

Diethyl 2,5-diphenyl-2,4-dihydro-2*H*-pyrrole-3,3-dicarboxylate (90a)
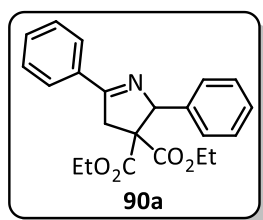
Was synthesized according to the general procedure. The crude product mixture was purified by column chromatography on silica gel using PE:EA 5%-15% (R_f = 0.35 in PE:EA 10%) to afford **90a** as light brown oil (164.0 mg, 92% yield).

¹H-NMR (400 MHz, CDCl₃): δ = 7.98 – 7.91 (m, 2H), 7.51 – 7.40 (m, 3H), 7.30 – 7.19 (m, 5H), 6.30 (s, 1H), 4.39 – 4.17 (m, 2H), 4.13 (dd, *J* = 17.8, 2.1, 1H), 3.69 (dq, *J* = 10.7, 7.1, 1H), 3.50 – 3.35 (m, 2H), 1.29 (t, *J* = 7.1, 3H), 0.82 (t, *J* = 7.1, 3H). **¹³C-NMR** (101 MHz, CDCl₃): δ = 171.0, 170.7, 169.0, 138.1, 133.5, 131.2, 128.7, 128.3, 128.1, 128.1, 127.9, 80.8, 65.1, 62.2, 61.7, 44.3, 14.2, 13.5. **IR** (neat, cm⁻¹): 3034, 29386, 2933, 2904, 1756, 1722, 1629, 1580, 1454, 1342, 1312, 1245, 1163, 1111, 1047, 1017, 760, 693. **m.p.**: 61 °C. **HRMS** (ESI): m/z calculated for C₂₂H₂₄NO₄ [M-H⁺]: 366.1700, found 366.1704.

Diethyl 5-phenyl-2-(o-tolyl)-2,4-dihydro-2*H*-pyrrole-3,3-dicarboxylate (90b)
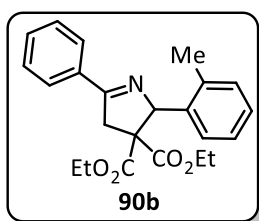
Was synthesized according to the general procedure using diethyl 2-bromo-2-(4-bromobenzyl)malonate **88b** (95%, 171.8 mg, 0.4 mmol, 1.0 eq.) instead of diethyl 2-benzyl-2-bromomalonate **88a**. The crude product mixture was purified by column chromatography on silica gel using PE: Et₂O 10%-20% (R_f = 0.25 in PE:Et₂O 20%) to afford **90b** as light yellow oil (103.3 mg, 73% yield).

¹H-NMR (400 MHz, CDCl₃): δ = 7.96 (d, *J* = 7.3 Hz, 2H), 7.47 (ddd, *J* = 12.6, 7.8, 6.0 Hz, 3H), 7.16 – 7.09 (m, 2H), 7.05 (td, *J* = 7.3, 2.1 Hz, 1H), 6.78 (dd, *J* = 7.6, 1.3 Hz, 1H), 6.71 (d, *J* = 2.4 Hz, 1H), 4.40 – 4.17 (m, 3H), 3.70 (dd, *J* = 10.7, 7.2 Hz, 1H), 3.50 (d, *J* = 18.2 Hz, 1H), 3.44 – 3.28 (m, 1H), 2.54 (s, 3H), 1.29 (t, *J* = 7.1 Hz, 3H), 0.85 (t, *J* = 7.2 Hz, 3H). **¹³C-NMR** (101 MHz, CDCl₃): δ = 171.0, 169.0, 138.5, 138.1, 132.1, 128.6, 128.6, 128.3, 128.1, 128.0, 125.4, 80.7, 65.1, 62.2, 61.7, 44.3, 21.5, 14.2, 13.6. **IR** (neat, cm⁻¹): 3034, 2982, 2933, 1726, 1625, 1454, 1252, 1178, 1051, 910, 731, 697. **HRMS** (ESI): m/z calculated for C₂₃H₂₆NO₄ [M-H⁺]: 380.1856, found 380.1856.

Diethyl 2-phenyl-5-(m-tolyl)-2,4-dihydro-3*H*-pyrrole-3,3-dicarboxylate (90a) & Diethyl 6-methyl-4-oxo-1-phenyl-3,4-dihydronaphthalene-2,2(1*H*)-dicarboxylate (99c)
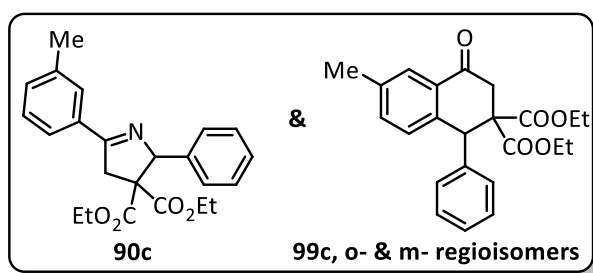
Was synthesized according to the general procedure using 1-(1-azidovinyl)-3-methylbenzene **83c**, 90%, 106.1 mg, 0.6 mmol, 1.5 eq.) in place of azidostyrene **83a**. The crude product mixture was purified by column chromatography on silica gel using PE:EA 5%-15% (Rf = 0.39 (2*H*-pyrrol), 0.35 (ketone) in PE:EA 10%) to afford 22.1 mg of **90c** as colorless oil and 61.8 mg colorless oil as a 1:1.46 mixture of **99c** ortho- and meta-regioisomers, which were not separated further by column chromatography (**90c**: 25.1 mg, 31% yield; **99c**: 36.7 mg, 24% yield).

2*H*-pyrrole 90c: ^{1}H-NMR (400 MHz, CDCl$_3$): δ = 7.82 (s, 1H), 7.70 (d, *J* = 7.4, 1H), 7.34 (t, *J* = 7.4, 1H), 7.32 − 7.18 (m, 6H), 6.29 (s, 1H), 4.39 − 4.17 (m, 2H), 4.13 (dd, *J* = 17.9, 2.2, 1H), 3.76 − 3.63 (m, 1H), 3.49 − 3.35 (m, 2H), 2.40 (s, 3H), 1.30 (t, *J* = 7.1, 3H), 0.83 (t, *J* = 7.1, 3H). ^{13}**C-NMR** (101 MHz, CDCl$_3$): δ = 171.1, 170.9, 169.0, 138.5, 138.2, 133.4, 132.0, 128.6, 128.6, 128.3, 128.1, 127.9, 125.3, 80.8, 65.1, 62.2, 61.7, 44.3, 21.5, 14.2, 13.6. **IR** (neat, cm^{-1}): 3034, 2982, 2933, 1726, 1625, 1454, 1252, 1178, 1051, 910, 731, 697. **HRMS** (ESI): m/z calculated for C$_{23}$H$_{26}$NO$_4$ [M-H$^+$]: 380.1856, found: 380.1856.

Ketone 99c, ortho- and meta-methyl mixture: ^{1}H-NMR (400 MHz, CDCl$_3$): δ = 8.01 − 7.87 (m, 1H), 7.26 (s, 5H), 7.06 − 6.97 (m, 3H), 4.18 − 3.99 (m, 4H), 3.34 − 3.19 (m, 2H), 2.39 − 2.17 (m, 3H), 1.22 − 1.03 (m, 6H). **IR** (neat, cm^{-1}):): 3034, 2982, 2933, 1726, 1625, 1454, 1252, 1178, 1051, 910, 731, 697. **HRMS** (ESI): m/z calculated for C$_{23}$H$_{25}$O$_5$ [MH$^+$]: 381.1697, found: 385.1704.

Diethyl 5-(2-methoxyphenyl)-2-phenyl-2,4-dihydro-2*H*-pyrrole-3,3-dicarboxylate (90d)
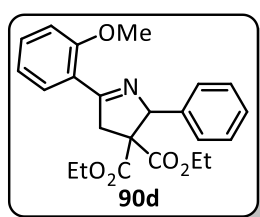
Was synthesized according to the general procedure using 1-(1-azidovinyl)-2-methoxybenzene **83d** (95%, 110.7 mg, 0.6 mmol, 1.5 eq.) in place of azidostyrene **83a.** The crude product mixture was purified by column chromatography on silica gel using PE:EA 5%-15% (Rf = 0.4 in PE:EA 20%) to afford **90d** as colorless crystals (75.0 mg, 47% yield).

¹H-NMR (400 MHz, CDCl₃): δ = 8.04 (dd, J = 7.7, 1.8 Hz, 1H), 7.48 – 7.41 (m, 1H), 7.34 – 7.23 (m, 5H), 7.08 – 6.93 (m, 2H), 6.27 – 6.17 (m, 1H), 4.40 – 4.15 (m, 3H), 3.78 – 3.67 (m, 1H), 3.57 (dd, J = 18.6, 1.1 Hz, 1H), 3.46 (dd, J = 10.7, 7.2 Hz, 1H), 1.31 (t, J = 7.1 Hz, 3H), 0.86 (t, J = 7.1 Hz, 3H) **¹³C-NMR** (101 MHz, CDCl₃): δ = 171.3, 171.1, 169.1, 158.6, 138.2, 132.1, 130.7, 128.3, 127.9, 127.7, 123.1, 120.8, 111.4, 79.1, 65.4, 61.9, 61.4, 55.6, 47.3, 14.1, 13.5. **IR** (neat, cm⁻¹): 3064, 2974, 2933, 1718, 1599, 1454, 1245, 1021, 753. **m.p.**: 67 °C. **HRMS** (ESI): m/z calculated for $C_{22}H_{24}NO_4$ [M-H⁺]: 396.1805, found: 396.1811.

Diethyl 5-(3-chlorophenyl)-2-phenyl-2,4-dihydro-2*H*-pyrrole-3,3-dicarboxylate (90e)
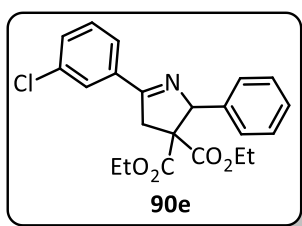
Was synthesized according to the general procedure using 1-(1-azidovinyl)-3-chlorobenzene **83e** (90%, 119.7 mg, 0.6 mmol, 1.5 eq.) in place of azidostyrene **83a**. The crude product mixture was purified by column chromatography on silica gel using PE:EA 10%-20% (R$_f$ = 0.24 in PE:EA 10%) to afford **90e** as yellow oil (109.3 mg, 68% yield).

¹H-NMR (400 MHz, CDCl₃): δ = 7.96 (t, J = 1.9 Hz, 1H), 7.80 (d, J = 7.7 Hz, 1H), 7.50 – 7.42 (m, 1H), 7.38 (t, J = 7.8 Hz, 1H), 7.32 – 7.22 (m, 5H), 6.29 (s, 1H), 4.29 (ddd, J = 37.6, 10.8, 7.1 Hz, 2H), 4.10 (dd, J = 17.9, 2.2 Hz, 1H), 3.76 – 3.63 (m, 1H), 3.46 – 3.36 (m, 2H), 1.30 (t, J = 7.1 Hz, 3H), 0.82 (t, J = 7.1 Hz, 3H). **¹³C-NMR** (101 MHz, CDCl₃): δ = 170.8, 169.6, 168.9, 137.9, 135.1, 134.9, 131.2, 130.0, 128.2, 128.1, 128.1, 128.0, 126.2, 80.8, 77.5, 77.2, 76.8, 65.1, 62.2, 61.8, 44.2, 14.2, 13.5. **IR** (neat, cm⁻¹): 2982, 2937, 2359, 1726, 1628, 1569, 1428, 1256, 1215, 1182, 1051, 861, 768, 701. **HRMS** (ESI): m/z calculated for C21H22ClNO4 [M-H⁺]: 400.1310, found 400.1312.

Diethyl 5-(4-fluorophenyl)-2-phenyl-2,4-dihydro-2*H*-pyrrole-3,3-dicarboxylate (90f) & diethyl 7-fluoro-4-oxo-1-phenyl-3,4-dihydronaphthalene-2,2(1*H*)-dicarboxylate (99f)
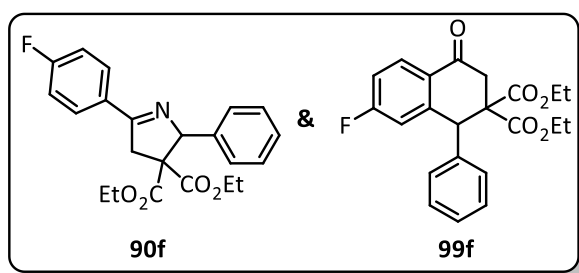
Was synthesized according to the general procedure using 1-(1-azidovinyl)-4-fluorobenzene **83f** (95%, 103.1 mg, 0.6 mmol, 1.5 eq.) in place of azidostyrene **83a**. The crude product mixture was purified by column chromatography on silica gel using PE:EA 5%-15% (R_f = 0.58 (3*H*-pyrrol), 0.54 (ketone) in PE:EA 20%) to afford 120.0 mg light yellow crystals as a 5.67:1 mixture of (**90f**) and (**99f**), which was not separated further by column chromatography (**90f**: 102.0 mg, 67% yield; **99f**: 18.0 mg, 12% yield).

2*H*-Pyrrole 90f: **^{1}H-NMR** (400 MHz, CDCl$_3$): δ = 7.94 (dd, *J* = 8.7, 5.5, 2H), 7.32 − 7.19 (m, 5H), 7.12 (t, *J* = 8.6, 2H), 6.28 (s, 1H), 4.39 − 4.17 (m, 2H), 4.11 (dd, *J* = 17.8, 2.2, 1H), 3.69 (dq, *J* = 10.7, 7.1, 1H), 3.47 − 3.34 (m, 2H), 1.29 (t, *J* = 7.1, 3H), 0.81 (t, *J* = 7.2, 3H). **^{13}C-NMR** (101 MHz, CDCl$_3$): δ = 170.8, 169.5, 168.9, 164.6 (d, J=251.8), 138.0, 130.2, 130.1, 128.2, 128.0, 127.9, 115.7 (d, J=21.7), 80.7, 65.1, 62.1, 61.7, 44.2, 14.1, 13.4. **^{19}F NMR** (377 MHz, CDCl$_3$) δ = -109.2. **IR** (neat, cm^{-1}): 3064, 2986, 2933, 1722, 1603, 1510, 1215, 947, 842. **m.p.**: 74 °C. **HRMS** (ESI): m/z calculated for C$_{22}$H$_{24}$FNO$_4$ [M-H$^+$]: 384.1606, found 384.1611.

Diethyl 2-(4-bromophenyl)-5-phenyl-2,4-dihydro-2*H*-pyrrole-3,3-dicarboxylate (90g)
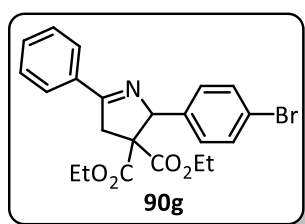
Was synthesized according to the general procedure using diethyl 2-bromo-2-(4-bromobenzyl)malonate **83g** (95%, 171.8 mg, 0.4 mmol, 1.0 eq.) instead of diethyl 2-benzyl-2-bromomalonate **83a**. The crude product mixture was purified by column chromatography on silica gel using PE:EA 5%-15% (R_f = 0.49 in PE:EA 20%) to afford **90g** as light yellow oil (127.0 mg, 74% yield).

¹H-NMR (400 MHz, CDCl₃): δ = 7.92 (d, *J* = 6.6, 2H), 7.51 − 7.37 (m, 5H), 7.18 (d, J=8.5, 2H), 6.23 (t, *J* = 1.6, 1H), 4.39 − 4.17 (m, 2H), 4.10 (dd, *J* = 17.8, 2.1, 1H), 3.80 − 3.67 (m, 1H), 3.55 − 3.38 (m, 2H), 1.29 (t, *J* = 7.1, 3H), 0.86 (t, *J* = 7.1, 3H). **¹³C-NMR** (101 MHz, CDCl₃): δ = 171.2, 170.7, 168.8, 137.4, 133.2, 131.3, 131.1, 130.0, 128.7, 128.0, 121.8, 80.0, 64.9, 62.2, 61.8, 44.4, 14.1, 13.5. **IR** (neat, cm⁻¹): 3060, 2982, 1722, 1487, 1252, 1178, 1044, 1010, 757, 693. **HRMS** (ESI): m/z calculated for $C_{22}H_{23}BrNO_4$ [M-H⁺]: 444.0805, found: X.

Diethyl 2-phenyl-5-(pyridin-3-yl)-2,4-dihydro-2*H*-pyrrole-3,3-dicarboxylate (90f)
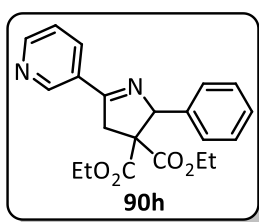
Was synthesized according to the general procedure using 3-(1-azidovinyl)pyridine **83f** (95%, 92.3 mg, 0.6 mmol, 1.5 eq.) in place of azidostyrene **83a**. The crude product mixture was purified by column chromatography on silica gel using PE:EA 5%-15% (R_f = 0.17, PE:EA 10%) to afford **90h** as light yellow crystalline solid (91.0 mg, 62% yield).

¹H-NMR (400 MHz, CDCl₃): δ = 8.71 (d, *J* = 3.2, 1H), 8.30 (d, *J* = 8.0, 1H), 7.44 − 7.36 (m, 1H), 7.33 − 7.20 (m, 5H), 6.30 (s, 1H), 4.41 − 4.19 (m, 2H), 4.14 (dd, *J* = 17.9, 2.2, 1H), 3.69 (dq, *J* = 10.7, 7.1, 1H), 3.49 − 3.33 (m, 2H), 1.30 (t, *J* = 7.1, 3H), 0.81 (t, *J* = 7.1, 3H). **¹³C-NMR** (101 MHz, CDCl₃): δ = 170.7, 168.8, 168.5, 151.9, 149.2, 137.7, 135.2, 129.2, 128.2, 128.1, 128.1, 123.7, 80.8, 65.0, 62.2, 61.8, 44.1, 14.1, 13.5. **IR** (neat, cm⁻¹): 3437, 3373, 2982, 1722, 1416, 1252, 1185, 1055, 752, 700. **m.p.**: 76 °C. **HRMS** (ESI): m/z calculated for $C_{21}H_{22}N_2O_4$ [M-H⁺]: 367.1652, found 367.1656.

Diethyl 5-(naphthalen-2-yl)-2-phenyl-2,4-dihydro-2*H*-pyrrole-3,3-dicarboxylate (90i) & diethyl 4-oxo-1-phenyl-3,4-dihydroanthracene-2,2(1*H*)-dicarboxylate (99i)
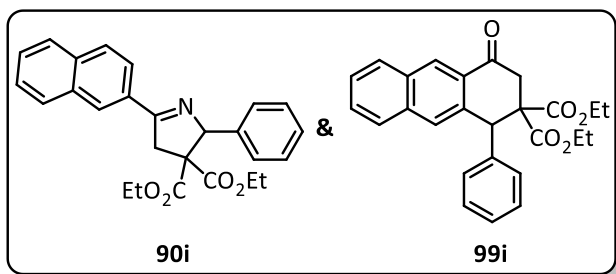
Was synthesized according to the general procedure using 2-(1-azidovinyl)naphthalene **83i** (95%, 123.3 mg, 0.6 mmol, 1.5 eq.) in place of azidostyrene **83a**. The crude product mixture was purified by column chromatography on silica gel using PE:EA 5%-20% (R_f = 0.33 **90i**, 0.27 **99i** in PE:EA 20%) to afford **90i** as yellow solid (40.8 mg, 25% yield) and **99i** as yellow solid (60.9 mg, 37% yield).

2*H*-pyrrole 90i: **¹H-NMR** (400 MHz, CDCl₃): δ = 8.29 (s, 1H), 8.18 (dd, *J* = 8.6, 1.7, 1H), 7.90 (q, *J* = 8.7, 7.4, 3H), 7.60 − 7.49 (m, 2H), 7.33 − 7.22 (m, 5H), 6.36 (s, 1H), 4.42 − 4.20 (m, 3H), 3.71 (dq, *J* = 10.7, 7.1, 1H), 3.59 (dd, *J* = 17.8, 1.1, 1H), 3.44 (dq, *J* = 10.7, 7.2, 1H), 1.32 (t, *J* = 7.1, 3H), 0.84 (t, *J* = 7.2, 3H). **¹³C-NMR** (101 MHz, CDCl₃): δ = 171.1, 170.7, 169.1, 138.2, 134.8, 133.0, 131.0, 128.9, 128.9, 128.5, 128.4, 128.1, 128.0, 128.0, 127.6, 126.7, 124.7, 81.0, 65.2, 62.2, 61.7, 44.3, 14.2, 13.6. **IR** (neat, cm⁻¹): 3060, 2982, 2933, 2363, 1726, 1621, 1454, 1368, 1252, 1051, 861, 749, 701. **HRMS** (ESI): m/z calculated for $C_{26}H_{26}NO_4$ [MH⁺]: 416.1856, found: 416.1863.

Ketone 99i: **¹H-NMR** (400 MHz, CDCl₃): δ = 8.16 (d, *J* = 8.7, 1H), 8.09 (d, *J* = 9.0, 1H), 7.82 (d, *J* = 8.4, 2H), 7.54 (ddd, *J* = 8.1, 6.9, 1.2, 1H), 7.46 (ddd, *J* = 8.3, 6.9, 1.4, 1H), 7.27 − 7.18 (m, 3H), 7.18 − 7.11 (m, 2H), 5.95 (s, 1H), 4.14 (qd, *J* = 7.2, 5.6, 2H), 4.11 − 3.93 (m, 2H), 3.36 (s, 2H), 1.22 (t, *J* = 7.1, 3H), 0.98 (t, *J* = 7.1, 3H). **¹³C-NMR** (101 MHz, CDCl₃): δ = 195.3, 169.5, 168.1, 141.8, 136.8, 136.7, 130.6, 129.3, 129.3, 128.8, 128.8, 128.6, 128.4, 127.9, 127.3, 125.6, 122.0, 77.3, 77.2, 77.0, 76.7, 62.3, 62.1, 60.3, 46.2, 38.3, 13.9, 13.7. **IR** (neat, cm⁻¹): 3064, 2982, 2933, 2363, 1733, 1677, 1621, 1461, 1368, 1245, 1174, 1044, 824, 738, 701. **HRMS** (ESI): m/z calculated for $C_{26}H_{25}O_5$ [M-H⁺]: 417.1697, found: 417.1702.

Diethyl 2,2-dimethyl-5-phenyl-2,4-dihydro-2*H*-pyrrole-3,3-dicarboxylate (90j) & Ethyl (2Z,4Z)-4-(formylimino)-2-isopropyl-4-phenylbut-2-enoate (139)
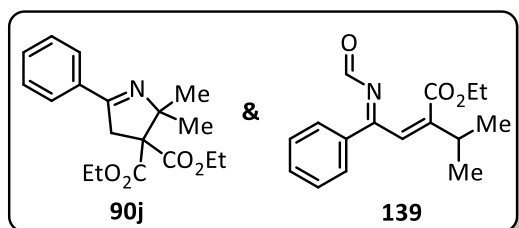
Was synthesized according to the general procedure using diethyl diethyl 2-bromo-2-isopropylmalonate **88f** (95%, 118.4 mg, 0.4 mmol, 1.0 eq.) instead of diethyl 2-benzyl-2-bromomalonate **88a**. The crude product mixture was purified by column chromatography on silica gel using PE:Et₂O 5%-15% (R_f = 0.24 in PE: Et₂O 20%) to afford **90f** as yellow oil (11 mg, 9% yield), and **139** as brown oil (with PE:EA 50%, R_f = 0.05 in PE:EA 20%) (27.0 mg, 21% yield)

90j: **¹H-NMR** (400 MHz, CDCl₃): δ = 7.83 (dd, *J* = 7.8, 1.9, 2H), 7.49 − 7.38 (m, 3H), 4.22 (q, *J* = 7.1, 4H), 3.56 (s, 2H), 1.46 (s, 6H), 1.27 (t, *J* = 7.1, 6H). **¹³C-NMR** (101 MHz, CDCl₃): δ = 170.1, 130.9, 128.6, 127.9, 127.7, 127.6, 76.6, 66.7, 61.6, 42.7, 25.1, 14.1. **IR** (neat, cm⁻¹): 3060, 2978, 1722, 1625, 1446, 1252, 1185, 1100, 1055, 1018, 865, 760, 693. **HRMS** (ESI): m/z calculated for $C_{18}H_{24}NO_4$ [M-H⁺]: 318.1700, found: 318.1704.

136: ¹H-NMR (400 MHz, CDCl₃): δ = 8.84 (s, 1H), 7.55 (dd, J = 8.2, 1.5, 2H), 7.46 – 7.37 (m, 3H), 5.64 (d, J=2.2, 1H), 4.20 (q, J = 7.1, 2H), 2.66 (hept, J = 6.8, 1H), 1.25 (t, J = 7.1, 3H), 1.03 (d, J = 6.8, 3H), 0.98 (d, J = 6.9, 3H). **¹³C-NMR** (101 MHz, CDCl₃): δ = 177.6, 169.0, 162.9, 142.4, 129.5, 129.0, 125.0, 103.0, 66.8, 61.8, 34.1, 18.5, 17.2, 14.2. **IR** (neat, cm⁻¹): 3213, 3064, 2967, 2353, 1744, 1707, 1454, 1416, 1290, 1215, 1040, 746, 693. **HRMS** (ESI): m/z calculated for $C_{16}H_{20}NO_3$ [M-H⁺]: 274.1438, found: 274.1443.

2-(2,5-Diphenyl-3,4-dihydro-2*H*-pyrrol-2-yl)acetonitrile (130a)
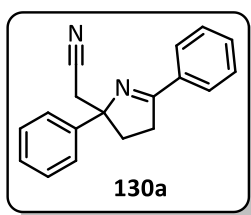
Was synthesized according to the general procedure using diethyl 3-phenylcyclobutan-1-one O-(4-(trifluoromethyl)benzoyl) oxime **129** (133.3 mg, 0.4 mmol, 1.0 eq.) instead of diethyl 2-benzyl-2-bromomalonate **88a**. The crude product mixture was purified by column chromatography on silica gel using PE:EA 5%-15% (R_f = 0.35 in PE:EA 20%) to afford **130a** as yellow oil (28.1 mg, 27% yield).

¹H-NMR (400 MHz, CDCl₃): δ = 7.98 (d, J = 6.4, 2H), 7.57 – 7.52 (m, 2H), 7.51 – 7.43 (m, 3H), 7.37 (t, J = 7.6, 2H), 7.31 – 7.25 (m, 1H), 3.30 (ddd, J = 17.3, 9.6, 6.1, 1H), 3.07 (ddd, J = 17.4, 9.8, 5.9, 1H), 2.98 (s, 2H), 2.59 (ddd, J = 13.3, 9.6, 5.9, 1H), 2.48 (ddd, J = 13.3, 9.8, 6.1, 1H). **¹³C-NMR** (101 MHz, CDCl₃): δ = 174.1, 145.3, 133.7, 131.4, 128.8, 128.7, 128.4, 127.7, 125.7, 117.7, 79.0, 35.9, 35.2, 32.6. **IR** (neat, cm⁻¹): 3060, 3030, 2926, 2341, 2251, 1744 1618, 1577, 1495, 1446, 1342, 1260, 1170, 1129, 1066, 1014, 760, 697. **HRMS** (EI): m/z calculated for $C_{18}H_{16}N_2$ [M-H⁺]: 259.1235, found: 259.1230.

2-(2-(4-fluorophenyl)-5-phenyl-3,4-dihydro-2*H*-pyrrol-2-yl)acetonitrile (130b)
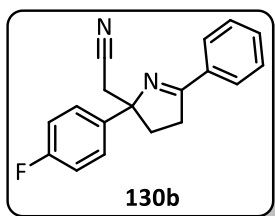
Was synthesized according to the general procedure using 1-(1-azidovinyl)-4-fluorobenzene **83f** (95%, 103.1 mg, 0.6 mmol, 1.5 eq.) instead of azidostyrene **83a** and diethyl 3-phenylcyclobutan-1-one O-(4-(trifluoromethyl)benzoyl) oxime **129** (133.3 mg, 0.4 mmol, 1.0 eq.) instead of diethyl 2-benzyl-2-bromomalonate **88a**. The crude product mixture was purified by column chromatography on silica gel using PE:EA 5%-15% (R_f = 0.30 in PE:EA 20%) to afford **130b** as yellow oil (23.3mg, 21% yield).

¹H-NMR (400 MHz, CDCl₃): δ = 7.99 (dd, *J* = 8.6, 5.6, 2H), 7.57 − 7.48 (m, 2H), 7.37 (t, *J* = 7.5, 2H), 7.31 − 7.25 (m, 1H), 7.14 (t, *J* = 8.7, 2H), 3.28 (ddd, *J* = 17.3, 9.6, 6.1, 1H), 3.05 (ddd, *J* = 17.3, 9.8, 5.8, 1H), 2.97 (d, *J* = 3.6, 2H), 2.59 (ddd, *J* = 13.3, 9.6, 5.8, 1H), 2.48 (ddd, *J* = 13.3, 9.8, 6.1, 1H).**¹³C-NMR** (101 MHz, CDCl₃): δ = 172.9, 164.8 (d, J=252.0), 145.2, 130.5 (d, J=8.7), 128.8, 127.7, 125.7, 117.7, 115.9, 115.7, 79.1, 36.0, 35.3, 32.7. **IR** (neat, cm⁻¹): 3064, 2930, 2251, 1778, 1685, 1603, 1510, 1413, 1338, 1230, 1156, 1096, 1062, 1014, 842, 764, 701. **HRMS** (EI): m/z calculated for $C_{18}H_{14}FN_2$ [M-H⁺]: 277.1141, found: 277.1135.

2-(5-phenyl-2-(m-tolyl)-3,4-dihydro-2*H*-pyrrol-2-yl)acetonitrile (130c)
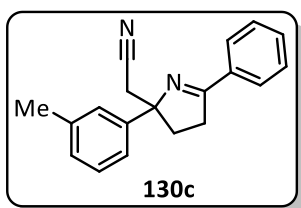
Was synthesized according to the general procedure using 1-(1-azidovinyl)-3-methylbenzene **83c** (95%, 100.5 mg, 0.6 mmol, 1.5 eq.) instead of azidostyrene **83a** and diethyl 3-phenylcyclobutan-1-one O-(4-(trifluoromethyl)benzoyl) oxime **129** (133.3 mg, 0.4 mmol, 1.0 eq.) instead of diethyl 2-benzyl-2-bromomalonate **88a**. The crude product mixture was purified by column chromatography on silica gel using PE:EA 10%-20% (R_f = 0.37 in PE:EA 20%) to afford **130a** as yellow oil (23.0 mg, 21% yield).

¹H-NMR (400 MHz, CDCl₃): δ = 7.84 (s, 1H), 7.72 (d, *J* = 7.2, 1H), 7.57 − 7.50 (m, 2H), 7.40 − 7.27 (m, 5H), 3.29 (ddd, *J* = 15.8, 9.6, 6.1, 1H), 3.06 (ddd, *J* = 17.2, 10.5, 5.9, 1H), 2.98 (s, 2H), 2.57 (ddd, *J* = 13.3, 9.6, 5.9, 1H), 2.52 − 2.36 (m, 1H), 2.43 (s, 3H). **¹³C-NMR** (101 MHz, CDCl₃): δ = 174.3, 145.4, 138.4, 132.2, 128.8, 128.8, 128.6, 127.6, 125.7, 125.6, 117.8, 78.9, 36.0, 35.2, 32.6, 21.5. **IR** (neat, cm⁻¹): 3056, 3027, 2952, 2922, 2251, 1685, 1618, 1491, 1446, 1334, 1178, 1062, 1018, 790, 764, 701.**HRMS** (EI): m/z calculated for $C_{19}H_{17}N_2$ [M-H⁺]: 273.1392, found: 277.1381.

Diethyl 2,5-diphenylpyrrolidine-3,3-dicarboxylate (156)
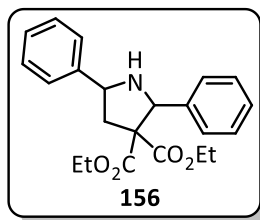
Was synthesized by dissolving 229.0 mg (0.63 mmol, 1.0 eq.) diethyl 2,5-diphenyl-2,4-dihydro-3H-pyrrole-3,3-dicarboxylate **90a** in 12.5 mL EtOH/1M HCl 3:1 (0.05 M) and adding 165.8 mg (2.51 mmol, 95%, 4.0 eq.) sodium cyanoborohydride and stirring the solution for 16 hours at room temperature. The reaction mixture was diluted with 10 mL sat. NaHCO$_3$ and 10 mL DCM and phases were separated. The aqueous phase was washed two times with 5 mL of DCM. The combined organic phases were dried over MgSO$_4$, filtered and concentrated *in vacuo*. The crude product mixture was purified by column chromatography on silica gel using PE:EA 5%-15% (R$_f$ = 0.38 in PE:EA 20%) to afford **157** as a mixture of both diastereomers as colorless oil (217.8 mg, 95% yield) in a 3.57:1 d.r.

¹H-NMR (400 MHz, CDCl$_3$, major diastereomer): δ = 7.63 – 7.52 (m, 2H), 7.50 – 7.40 (m, 1H), 7.38 (t, *J* = 7.5, 2H), 7.36 – 7.20 (m, 5H), 5.24 (s, 1H), 4.39 – 4.17 (m, 3H), 3.79 – 3.66 (m, 1H), 3.40 (dq, *J* = 10.7, 7.2, 1H), 2.88 (dd, *J* = 13.5, 10.7, 1H), 2.56 (dd, *J* = 13.4, 6.5, 1H), 1.28 (t, *J* = 7.1, 3H), 0.78 (t, *J* = 7.2, 3H). **¹H-NMR** (400 MHz, CDCl$_3$, minor diastereomer): δ = 7.63 – 7.52 (m, 2H), 7.50 – 7.40 (m, 1H), 7.38 (t, *J* = 7.5, 2H), 7.36 – 7.20 (m, 5H), 5.37 (s, 1H), 4.98 (t, *J* = 7.4, 1H), 4.38 – 4.19 (m, 1H), 4.14 (ddd, *J* = 14.2, 7.0, 3.7, 1H), 3.81 (dq, *J* = 10.7, 7.1, 1H), 3.53 (dq, *J* = 10.7, 7.1, 1H), 3.22 (dd, *J* = 13.5, 7.4, 1H), 2.30 (dd, *J* = 13.5, 7.4, 1H), 1.19 (t, *J* = 7.0, 3H), 0.81 (t, *J* = 7.2, 3H). **¹³C-NMR** (101 MHz, CDCl$_3$, mixture of diastereomers): δ = 171.9, 169.7, 142.3, 140.1, 128.7, 128.6, 128.2, 128.2, 127.9, 127.8, 127.7, 127.6, 127.2, 126.4, 66.8, 65.6, 61.7, 61.3, 60.8, 60.5, 43.0, 21.2, 14.3, 14.2, 14.1, 13.5. **IR** (neat, cm⁻¹): 3332, 3064, 3030 2982, 2904, 1722, 1603, 1454, 1390, 1256, 1178, 1051, 865, 746, 701. **HRMS** (EI): m/z calculated for C$_{22}$H$_{26}$NO$_4^+$ [M-H⁺]: 368.1856, found: 368.1860.

Experimental Part

Ethyl 2,5-diphenyl-3,4-dihydro-2H-pyrrole-3-carboxylate (157)
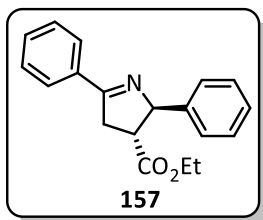
Was synthesized by dissolving 100.5 mg (0.28 mmol, 1.0 eq.) diethyl 2,5-diphenyl-2,4-dihydro-3H-pyrrole-3,3-dicarboxylate **90a** in 2.8 mL EtOH/H_2O 2:1 (0.1 M) and adding 45.1 mg (1.13 mmol, 4.1eq.) sodium hydroxide and heating the solution to 130 °C for 20 minutes in a microwave apparatus. The reaction mixture was diluted with 10 EtOH, acidified with several drops of H_2SO_4 and stirred at 60 °C for 2 hours. The solution was diluted with EtOAc and phases were separated. The organic phase was washed three times with H_2O. The organic phase was dried over $MgSO_4$, filtered and concentrated *in vacuo*. The crude product mixture was purified by column chromatography on silica gel using PE:EA 5%-15% (R_f = 0.48 in PE:EA 20%) to afford **157** as a single diastereomers as colorless oil (67.9 mg, 84% yield).

¹H-NMR (400 MHz, CDCl₃): δ = 7.96 (dd, *J* = 7.9, 1.7 Hz, 2H), 7.54 − 7.41 (m, 3H), 7.41 − 7.21 (m, 5H), 5.58 (d, *J* = 6.5 Hz, 1H), 4.25 (qq, *J* = 10.8, 7.1 Hz, 2H), 3.57 − 3.33 (m, 2H), 3.19 (ddd, *J* = 9.4, 7.7, 6.5 Hz, 1H), 1.31 (t, *J* = 7.1 Hz, 3H). **¹³C-NMR** (101 MHz, CDCl₃): δ = 174.1, 171.8, 143.2, 133.8, 131.0, 128.7, 128.6, 128.0, 127.4, 126.6, 79.7, 61.2, 51.3, 39.5, 14.4. **IR** (neat, cm⁻¹): 3060, 3030, 2982, 2930, 1726, 1621, 1577, 1495, 1446, 1338, 1230, 1174, 1025, 869, 760, 693. **HRMS** (EI): m/z calculated for $C_{19}H_{20}NO_2$ [M-H⁺]: 294.1489, found: 294.1495.

Ethyl 2,5-diphenylpyrrolidine-3-carboxylate (158)
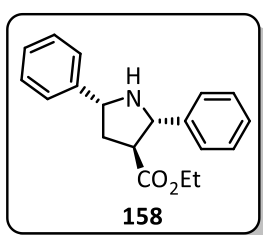
Was synthesized by dissolving 66.3 mg (0.23 mmol, 1.0 eq.) ethyl 2,5-diphenyl-3,4-dihydro-2H-pyrrole-3-carboxylate **157** in 4.8 mL EtOH/1M HCl 3:1 (0.05 M) and adding 59.8 mg (0.90 mmol, 95%, 4.0 eq.) sodium cyanoborohydride and stirring the solution for 16 hours at room temperature. The reaction mixture was diluted with 10 mL sat. $NaHCO_3$ and 10 mL DCM and phases were separated. The aqueous phase was washed two times with 5 mL of DCM. The combined organic phases were dried over $MgSO_4$, filtered and concentrated *in vacuo*. The crude product mixture was purified by column chromatography on silica gel using PE:EA 5%-15% (R_f = 0.41 (*syn*-**158**), R_f = 0.32 (*anti*-**158**) in PE:EA 20%) to afford (*syn*-**158**) as a colorless oil (31.7 mg, 47% yield) and (*anti*-**158**) as a colorless oil (25.2 mg, 38% yield).

¹H-NMR (400 MHz, CDCl₃, *syn*-diastereomer): δ = 7.54 (ddd, *J* = 12.5, 8.2, 1.2 Hz, 4H), 7.36 (ddd, *J* = 7.5, 6.6, 1.4 Hz, 4H), 7.32 – 7.25 (m, 2H), 4.57 (d, *J* = 7.6 Hz, 1H), 4.47 (t, *J* = 8.1 Hz, 1H), 4.17 (qd, *J* = 7.2, 4.3 Hz, 2H), 2.97 (ddd, *J* = 10.4, 7.6, 5.3 Hz, 1H), 2.53 (ddd, *J* = 12.8, 7.5, 5.2 Hz, 1H), 2.22 (s, 1H), 2.10 (ddd, *J* = 12.8, 10.4, 8.7 Hz, 1H), 1.24 (t, *J* = 7.1 Hz, 3H). **¹H-NMR** (400 MHz, CDCl₃, *anti*-diastereomer): δ = 7.50 – 7.42 (m, 4H), 7.35 (td, *J* = 7.4, 2.2 Hz, 4H), 7.31 – 7.22 (m, 2H), 4.79 (s, 1H), 4.57 (dd, *J* = 9.4, 6.4 Hz, 1H), 4.15 (qd, *J* = 7.1, 1.0 Hz, 2H), 3.15 (dt, *J* = 10.3, 7.7 Hz, 1H), 2.66 (ddd, *J* = 12.5, 7.7, 6.4 Hz, 1H), 2.24 (ddd, *J* = 12.6, 10.3, 9.5 Hz, 1H), 2.05 (s, 1H), 1.22 (t, *J* = 7.2 Hz, 3H). **¹³C-NMR** (101 MHz, CDCl₃, *syn*-diastereomer): 174.8, 144.1, 143.3, 128.5, 128.5, 127.6, 127.3, 127.1, 126.8, 65.8, 61.5, 60.8, 52.0, 39.0, 14.4. δ = **¹³C-NMR** (101 MHz, CDCl₃, *anti*-diastereomer): δ = 174.1, 144.1, 143.9, 128.7, 128.7, 127.4, 127.4, 126.7, 126.6, 65.4, 62.5, 60.9, 53.8, 40.1, 14.3. **IR** (neat, cm⁻¹): 3332, 3064, 3030, 2982, 2855, 1726, 1602, 1491, 1454, 1372, 1271, 1163, 1029, 865, 757, 701. **HRMS** (EI): m/z calculated for $C_{19}H_{22}NO_2$ [M-H⁺]: 296.1645, found 296.1650.

7.4 Photocatalyzed [2+2] additions of olefins

7.4.1 General procedure for the photocatalyzed [2+2] addition of cinnamates and styrenes.

A Schlenk tube (5 mL), equipped with a magnetic stir bar, was charged with olefin (1.00 mmol, 1.0 eq.), [Ir(dF(CF₃)ppy}₂(dtb-bpy)]PF₆ (11.2 mg, 0.01 mmol, 1 mol%) and 2 mL dry *N,N*-dimethylformamide (DMA abs., 0.5 M). The resulting solution was degassed by three pump-freeze-thaw cycles. The tube was equipped with a LED setup and sealed. The reaction mixture was irradiated at room temperature with a blue LED (λ_max = 455 nm) while being stirred for 72 h. Afterwards, the reaction was stopped by switching off the light source. The crude mixture was diluted with 15 mL Ethyl acetate (EtOAc) and brine (15 mL), phases were separated, and the aqueous phase was washed two times with ethyl acetate washed (20 mL). The combined organic phases were dried over Na₂SO₄, filtered and concentrated *in vacuo*. The crude mixture was purified by column chromatography on silica gel by using PE:EA (reported as volume% of EA in PE) mixtures to afford the desired product(s).

Product data for molecules synthesized and isolated by Santosh Pagire, Asik Hossain or Sabine Kerres is available in the corresponding publication.[200]

Diethyl 3,4-bis(4-methoxyphenyl)cyclobutane-1,2-dicarboxylate (185e/186e)

185e/186e
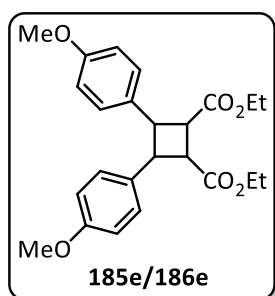
Was synthesized according to the general procedure. 206.2 mg Ethyl (*E*)-3-(4-methoxyphenyl)acrylate (1.00 mmol, 1.0 eq.) **184e** were used. The crude mixture was purified by column chromatography (20% PE:EA, R_f = 0.4) to afford the *trans*-diastereomer **185e** as 122 mg of a colorless oil (59% yield), and a 1:0.84 mixture of both diastereomers **185e/186e** as 49 mg yellow oil (27% yield)

^{1}H-NMR (400 MHz, CDCl$_3$, *trans* diastereomer): δ = 7.21 (d, *J* = 8.7, 4H), 6.85 (d, *J* = 8.7, 4H), 4.19 (q, *J* = 7.1, 4H), 3.79 (s, 6H), 3.66 – 3.58 (m, 2H), 3.44 – 3.33 (m, 2H), 1.26 (t, *J* = 7.1, 6H).
^{1}H-NMR (300 MHz, CDCl$_3$, mixture of diastereomers): δ = 7.21 – 7.13 (m, 2H), 6.85 – 6.74 (m, 2H), 6.85 – 6.76 (m, 2H), 4.14 (q, *J* = 7.1, 2H), 3.77 – 3.70 (m, 6H), 3.61 – 3.54 (m, 1H), 3.36 – 3.28 (m, 1H), 1.21 (t, *J* = 7.1 Hz, 6H). **^{13}C-NMR** (75 MHz, CDCl$_3$, *trans* diastereomer): δ = 172.8, 158.8, 133.5, 128.1, 114.1, 77.5, 77.2, 76.8, 61.0, 55.4, 47.0, 45.1, 14.4. **IR** (neat, cm^{-1}): 2982, 2836, 1722, 1610, 1513, 1461, 1245, 1033, 826, 731. **HRMS** (ESI): m/z calculated for C$_{24}$H$_{29}$O$_6$ [M-H$^+$]: 413.1959, found 413.1959.

Diethyl 3,4-bis(4-cyanophenyl)cyclobutane-1,2-dicarboxylate (185h/186h)

185h/186h
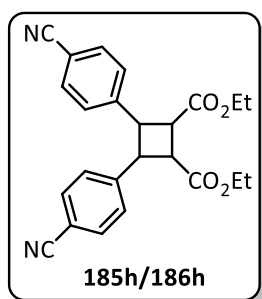
Was synthesized according to the general procedure. 201.2 mg Ethyl (*E*)-3-(4-cyanophenyl)acrylate (1.00 mmol, 1.0 eq.) **184h** were used. The crude mixture was purified by column chromatography (20% PE:EA, R_f = 0.2) to afford a 1.15:1 mixture of both diastereomers of **185h/186h** as 171 mg of a white solid (85% yield).

¹H-NMR (400 MHz, CDCl₃, *trans* diastereomer): δ = 7.66 − 7.59 (m, 4H), 7.38 (d, *J* = 8.3, 4H), 4.22 (qd, *J* = 7.1, 1.6, 4H), 3.90 − 3.68 (m, 2H), 3.52 − 3.35 (m, 2H), 1.27 (t, *J* = 7.1, 6H). **¹H-NMR** (300 MHz, CDCl₃, mixture of diastereomers): δ = 7.67 − 7.61 (m, 2H), 7.47 − 7.33 (m, 4H), 7.02 (d, *J* = 8.4, 2H), 4.49 (d, *J* = 6.1, 1H), 4.27 − 4.17 (m, 4H), 3.84 − 3.74 (m, 2H), 3.45 (d, *J* = 9.5, 1H), 1.28 (td, *J* = 7.1, 4.2, 6H). **¹³C-NMR** (75 MHz, CDCl₃, *trans* diastereomer): δ = 171.8, 145.7, 132.8, 127.7, 118.7, 111.6, 77.6, 77.2, 76.7, 61.7, 46.5, 44.6, 14.3. **IR** (neat, cm⁻¹): 3064, 2989, 2229, 1715, 1607, 1506, 1372, 1312, 1200, 1163, 1014, 828. **m.p.:** 121-122 °C. **HRMS** (ESI): m/z calculated for $C_{24}H_{23}N_2O_6$ [M-H⁺]: 403.1652, found 403.1652.

Diethyl 3,4-bis(4-(methoxycarbonyl)phenyl)cyclobutane-1,2-dicarboxylate (185i/186i)
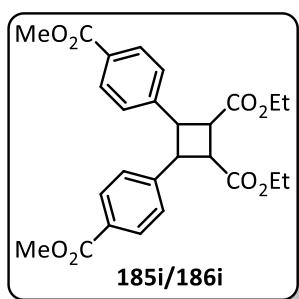
Was synthesized according to the general procedure. 234.3 mg Methyl (*E*)-4-(3-ethoxy-3-oxoprop-1- en-1-yl)benzoate (1.00 mmol, 1.0 eq.) **184i** were used. The crude mixture was purified by column chromatography (20% PE:EA, Rf = 0.25) to afford the *trans*-diastereomer **185h** as 130 mg of a colorless oil (56% yield), and the *cis* diastereomer **186h** as 79 mg colorless oil (34% yield).

¹H-NMR (400 MHz, CDCl₃, *trans* diastereomer): δ = 8.00 (d, 4H), 7.35 (d, *J* = 8.4, 4H), 4.21 (q, *J* = 7.1, 4H), 3.90 (s, 6H), 3.83 − 3.76 (m, 2H), 3.53 − 3.42 (m, 2H), 1.27 (t, *J* = 7.1, 6H). **¹H-NMR** (400 MHz, CDCl₃, *cis* diastereomers): δ = 7.71 (d, 4H), 6.94 (d, *J* = 8.4, 4H), 4.42 (dd, *J* = 3.9, 2.2, 2H), 4.16 (q, *J* = 7.1, 4H), 3.84 (d, *J* = 1.6, 2H), 3.78 (s, 6H), 1.23 (t, *J* = 7.1, 6H). **¹³C-NMR** (75 MHz, CDCl₃, *trans* diastereomer): δ = 172.8, 158.8, 133.5, 128.1, 114.1, 77.5, 77.2, 76.8, 61.0, 55.4, 47.0, 45.1, 14.4. **IR** (neat, cm⁻¹): 2952, 1718, 1610,1435, 1159, 1275, 1193, 1103, 1018, 965, 857, 768, 701. **HRMS** (ESI): m/z calculated for $C_{26}H_{29}O_6$ [M-H⁺]: 469.1857, found 469.1862.

Diethyl 3,4-bis(4-nitrophenyl)cyclobutane-1,2-dicarboxylate (185j/186j)
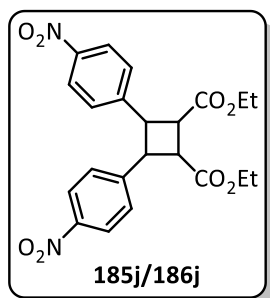
Was synthesized according to the general procedure. 221.2 mg (*E*)-3-(4-nitrophenyl)acrylate (1.00 mmol, 1.0 eq.) **184j** were used. The crude mixture was purified by column chromatography (10% PE:EA, R_f = 2 (trans), 0.15 (cis)) to afford the *trans*-diastereomer of **185j** as 115 mg orange oil (9% yield), and the *cis* diastereomer o**186j** as 87 mg orange oil (37% yield).

¹H-NMR (400 MHz, CDCl₃, *trans* diastereomer): δ = 8.24 − 8.16 (m, 4H), 7.45 (d, *J* = 8.7, 4H), 4.24 (qd, *J* = 7.1, 1.4, 4H), 3.90 − 3.81 (m, 2H), 3.53 − 3.43 (m, 2H), 1.33 − 1.23 (m, 6H). **¹H-NMR** (400 MHz, CDCl₃, *cis* diastereomers): δ = 8.01 (d, *J* = 8.8, 4H), 7.11 (d, *J* =8.7, 4H), 4.57 (d, *J* = 6.2, 2H), 4.24 (q, *J* = 7.1, 4H), 3.86 (dd, *J* = 3.7, 2.4, 2H), 1.30 (t, *J* = 7.1, 6H).**¹³C-NMR** (101 MHz, CDCl₃, *trans* diastereomer): δ = 171.7, 147.6, 147.4, 127.8, 124.3, 61.7, 46.5, 44.7, 14.3. **IR** (neat, cm⁻¹): 2982, 2937, 1722, 1603, 1517, 1342, 1200, 1159, 1111. 1014, 854, 746. **HRMS** (ESI): m/z calculated for $C_{22}H_{23}N_2O_8$ [M-H⁺]: 443.1449, found 443.1455.

Diethyl 3,4-di(furan-2-yl)cyclobutane-1,2-dicarboxylate (185q/186q)
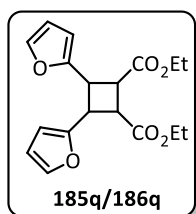
Was synthesized according to the general procedure. 166.2 mg Ethyl (*E*)-3-(furan-2-yl)acrylate (1.00 mmol, 1.0 eq.) **184q** were used. The crude mixture was purified by column chromatography (20% PE:EA, R_f = 0.4-0.2) to afford the head-to-tail conformer **187q** as 27 mg orange oil (16% yield), and a mixture of both head-to-head diastereomers **185q/186q** as 88 mg orange oil (53%).

¹H-NMR (300 MHz, CDCl₃, *trans* diastereomer): δ = 7.36 (dd, *J* = 1.8, 0.8 Hz, 2H), 6.30 (dd, *J* = 3.2, 1.9 Hz, 2H), 6.16 (dd, *J* = 3.2, 0.7 Hz, 2H), 4.18 (qd, *J* =7.1, 0.6 Hz, 4H), 3.82 − 3.72 (m, 2H), 3.53 − 3.44 (m, 2H), 1.25 (t, *J* = 7.1, 6H). **¹H-NMR** (300 MHz, CDCl₃, *cis* diastereomers): δ = 7.22 (dd, *J* = 1.8, 0.8 Hz, 2H), 6.20 (dd, *J* = 3.2, 1.8 Hz, 2H), 5.94 (d, *J* = 2.8 Hz, 2H), 4.25 (dd, *J* = 3.8, 2.2, 2H), 4.18 (qd, *J* = 7.1, 1.5 Hz, 4H), 3.85 (dd, *J* = 3.7, 2.2, 2H), 1.26 (td, *J* =7.1, 3.6 Hz, 6H). **¹H-NMR** (300 MHz, CDCl₃, head-to-tail conformer): δ = 7.35 − 7.30 (m, 1H), 7.20 (dd, *J* = 3.4, 1.5, 1H), 6.28 (td, *J* = 4.1, 3.7, 1.8, 1H), 6.23 − 6.14 (m, 2H), 5.97 (dd, *J* = 5.7, 3.3, 1H), 4.50 − 4.20 (m, 1H), 4.21 − 4.12 (m, 3H), 4.06 − 3.94 (m, 2H), 3.85 − 3.76 (m, 1H), 3.74 − 3.40 (m, 1H), 1.27 − 1.20 (m, 2H), 1.03 (t, *J* = 7.1, 3H). **¹³C-NMR** (101 MHz, CDCl₃, *trans* diastereomer): δ =

171.9, 153.4, 142.2, 110.4, 106.6, 61.1, 43.4, 39.4, 14.2. **IR** (neat, cm^{-1}): 2982, 2941, 1800, 1726, 1372, 1200, 1096, 1014, 924, 738. **HRMS** (ESI): m/z calculated for $C_{18}H_{21}O_6$ [M-H$^+$]: 333.1338, found 333.1335.

1,2-diphenyl-1,2,2a,5,10,12a-hexahydrobenzo[c]cyclobuta[h][1,6]dioxecine-3,12-dione (185u/186u)
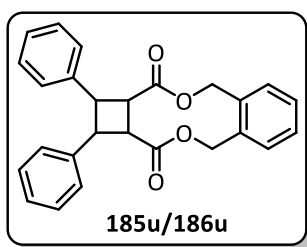
Was synthesized according to the general procedure. 398.5 mg 1,2-phenylenebis(methylene) (2E,2'E)-bis(3-phenylacrylate) (1.00 mmol, 1.0 eq.) **184u** was used. The crude mixture was purified by column chromatography (20% PE:EA, R$_f$ = 0.3) to afford the major-diastereomer **185u** as 168 mg white solid (42% yield), and a 1:1.36 mixture of both diastereomers **185h/186h** as 142 mg colorless oil (35%).

^{1}H-NMR (400 MHz, CDCl$_3$, major diastereomer): δ = 7.48 − 7.38 (m, 4H), 7.14 − 7.01 (m, 6H), 6.91 (dd, J = 5.2, 3.2 Hz, 4H), 5.27 (dd, J = 109.2, 12.2 Hz, 4H), 4.46 (dd, J = 3.8, 2.3 Hz, 2H), 3.81 (dd, J = 3.8, 2.3 Hz, 2H). **^{13}C-NMR** (101 MHz, CDCl$_3$, major*s* diastereomer): δ = 171.6, 138.4, 135.3, 131.7, 129.4, 128.2, 127.9, 126.6, 67.8, 44.4, 43.8. IR (neat, cm^{-1}): 3027, 2060, 2963, 1730, 1498, 1446, 1256, 1185, 1163, 1048, 1018, 839, 749, 697. **m.p.:** 153-154 °C (decomposition) **HRMS** (ESI): m/z calculated for $C_{26}H_{23}O_4$ [M-H$^+$]: 399.1591, found 399.1590.

Diethyl 3-(4-methoxyphenyl)-4-phenylcyclobutane-1,2-dicarboxylate (185ae/186ae)
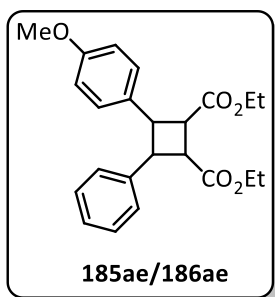
Was synthesized according to the general procedure. 88.1 mg Ethyl cinnamate **184a** (0.50 mmol, 1.0 eq.) and 103.1 mg ethyl-3-(4-methoxyphenyl)acrylate **184e** (0.50 mmol, 1.0 eq.) were used. The crude mixture was purified by column chromatography (20% PE:EA, R$_f$ = 0.3) to afford **185ae** as 67 mg colorless oil (35% yield), as well the homocoupling products **185e** as yellow oil (46 mg, 24% yield) and **185a** as colorless oil (21 mg, 11% yield).

^{1}H-NMR (400 MHz, CDCl$_3$): $\delta = 7.36 - 7.20$ (m, 7H), $6.90 - 6.84$ (m, 2H), 4.20 (qd, J = 7.0, 4.4, 4H), 3.79 (s, 3H), $3.75 - 3.63$ (m, 2H), $3.46 - 3.35$ (m, 2H), 1.27 (td, J = 7.1, 3.3, 6H). **^{13}C-NMR** (101 MHz, CDCl$_3$): $\delta = $ 172.8, 172.7, 158.8, 141.4, 133.4, 128.7, 128.1, 127.1, 126.9, 114.1, 61.1, 61.1, 55.4, 47.4, 46.8, 45.4, 44.7, 14.4. **IR** (neat, cm^{-1}): 2982, 1722, 1610, 1513, 1457, 1249, 1178, 1033, 828, 701. **HRMS** (ESI): m/z calculated for C$_{23}$H$_{27}$O$_5$ [M-H$^+$]: 383.1859, found 383.1586.

Diethyl 3-(4-(methoxycarbonyl)phenyl)-4-phenylcyclobutane-1,2-dicarboxylate (185ai/186ai)
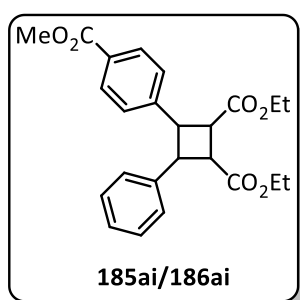
Was synthesized according to the general procedure. 88.1 mg Ethyl cinnamate **184a** (0.50 mmol, 1.0 eq.) and 117.1 mg Methyl-4-(3-ethoxy-3-oxoprop-1-en-1- yl)benzoate **184i** (0.50 mmol, 1.0 eq.) were used. The crude mixture was purified by column chromatography (20% PE:EA, R$_f$ = 0.4-0.1) to afford **185ai/186ai** as 76 mg colorless oil (32% yield, 1.9:1 d.r.), as well the homocoupling product **185i** as colorless oil (25 mg, 14% yield).

^{1}H-NMR (400 MHz, CDCl$_3$): $\delta = 7.99$ (d, J=8.3, 2H), 7.32 (ddd, J = 19.6, 15.8, 7.8, 7H), $4.26 - 4.16$ (m, 4H), 3.90 (s, 3H), $3.84 - 3.71$ (m, 2H), $3.51 - 3.41$ (m, 2H), $1.33 - 1.22$ (m, 6H). **^{13}C-NMR** (101 MHz, CDCl$_3$): 172.2, 166.9, 145.9, 130.2, 129.6, 129.3, 127.8, 127.0, 61.4, 61.4, 52.3, 52.1, 46.9, 45.0, 44.7, 43.4, 14.3, 14.3. **IR** (neat, cm^{-1}): 2952, 1718, 1610, 1435, 1275, 1185, 1103, 1017, 965, 857, 767, 705. **HRMS** (ESI): m/z calculated for C$_{24}$H$_{27}$O$_6$ [M-H$^+$]: 411.1808, found 411.1807.

Diethyl 3-(4-cyanophenyl)-4-(4-(methoxycarbonyl)phenyl)cyclobutane-1,2-dicarboxylate (185eh/186eh)

185eh/186eh
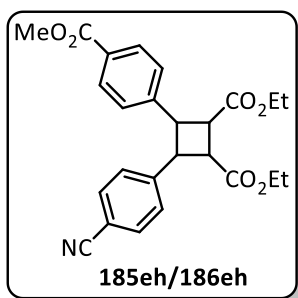
Was synthesized according to the general procedure. 103.1 mg Ethyl-3-(4-methoxyphenyl)acrylate **184e** (0.50 mmol, 1.0 eq.) and 100.6 mg Ethyl-3-(4-cyanophenyl)acrylate **184h** (0.50 mmol, 1.0 eq.) were used. The crude mixture was purified by column chromatography (20% PE:EA, R_f = 0.4-0.1) to afford **185h/186h** as 111.3 mg white solid (54% yield, 1.75:1 d.r.), as well the homocoupling products **185e** as white solid (26 mg, 13% yield) and **185h** as colorless oil (17 mg, 14% yield).

^{1}H-NMR (300 MHz, CDCl$_3$): δ = 7.65 – 7.53 (m, 2H), 7.38 (d, J = 8.1, 2H), 7.23 – 7.19 (m, 2H), 6.91 – 6.85 (m, 2H), 4.20 (p, J = 7.2, 4H), 3.77 – 3.58 (m, 2H), 3.47 – 3.34 (m, 2H), 1.27 (q, J = 7.1, 6H). **^{13}C-NMR** (101 MHz, CDCl$_3$): δ = 172.4, 172.2, 159.1, 146.7, 132.6, 132.5, 128.1, 127.7, 118.9, 114.3, 111.0, 61.4, 61.3, 55.4, 47.0, 46.7, 45.5, 44.1, 14.3. **IR** (neat, cm^{-1}): 2981, 2937, 2840, 229, 1718, 1610, 1513, 1245, 1178, 114, 1036, 828. **m.p.:** 54-56 °C (decomposed). **HRMS** (ESI): m/z calculated for C$_{24}$H$_{26}$NO$_5$ [M-H$^+$]: 408.1811, found 408.1805.

8 Appendix

8.1 NMR-Spectra

N-chloro-*N*,4-dimethylbenzenesulfonamide (17a)

¹H-NMR (400 MHz, CDCl₃):
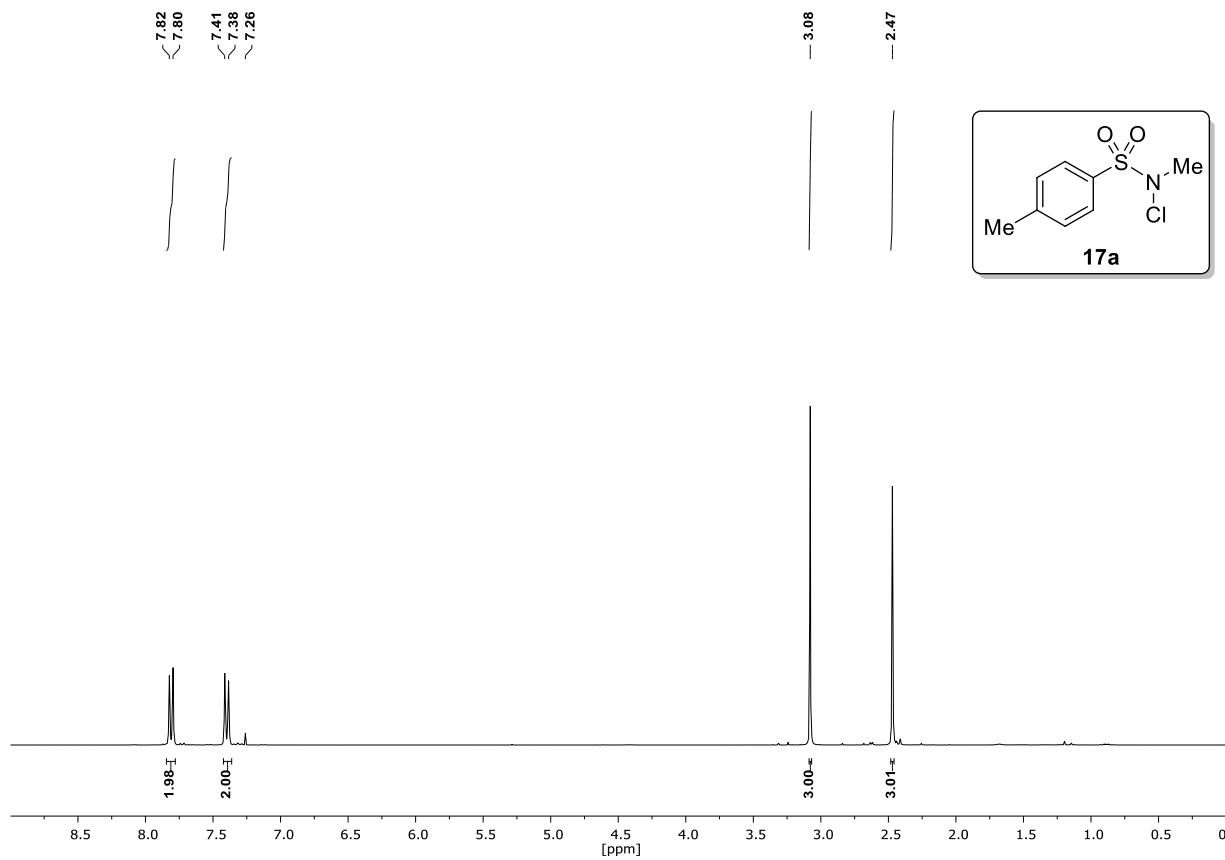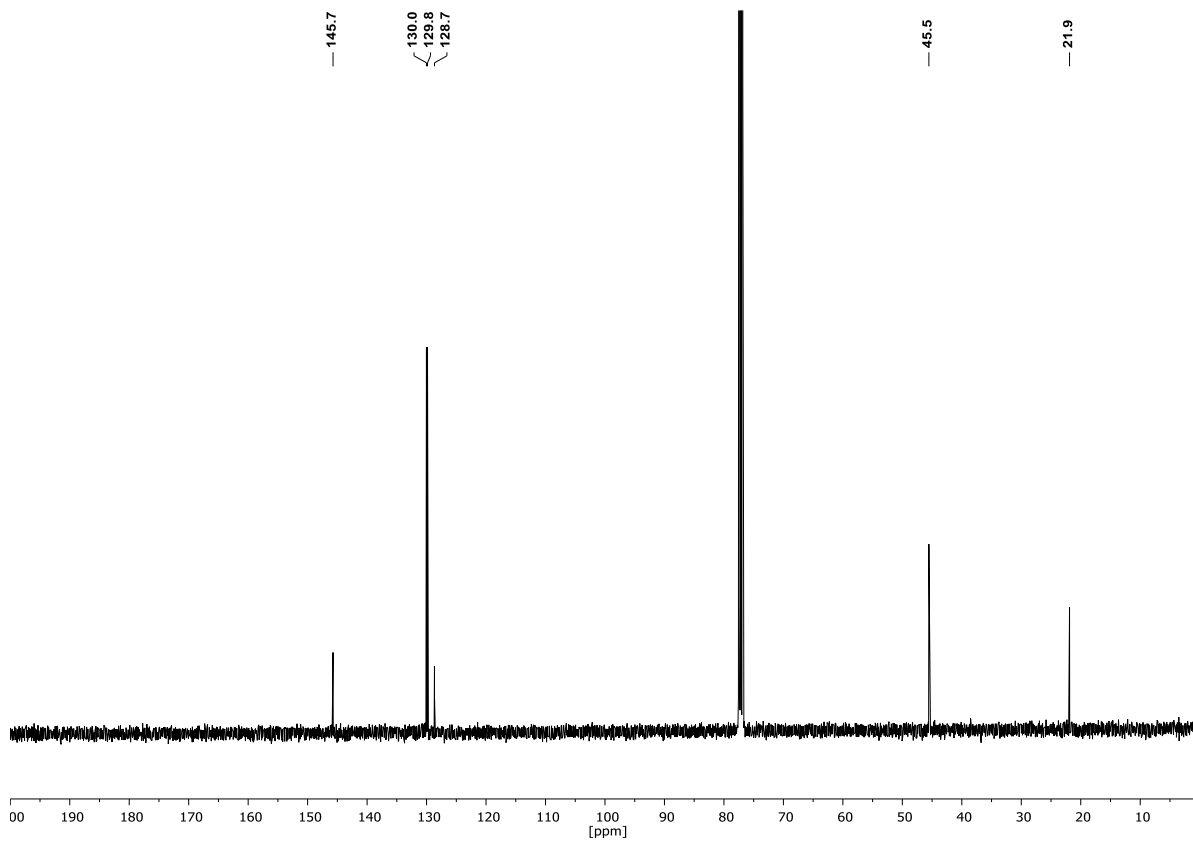
¹³C-NMR (101 MHz, CDCl₃):

N-chloro-*N*-methyl-4-nitrobenzenesulfonamide (17d)

^{1}H-NMR (300 MHz, CDCl$_3$):
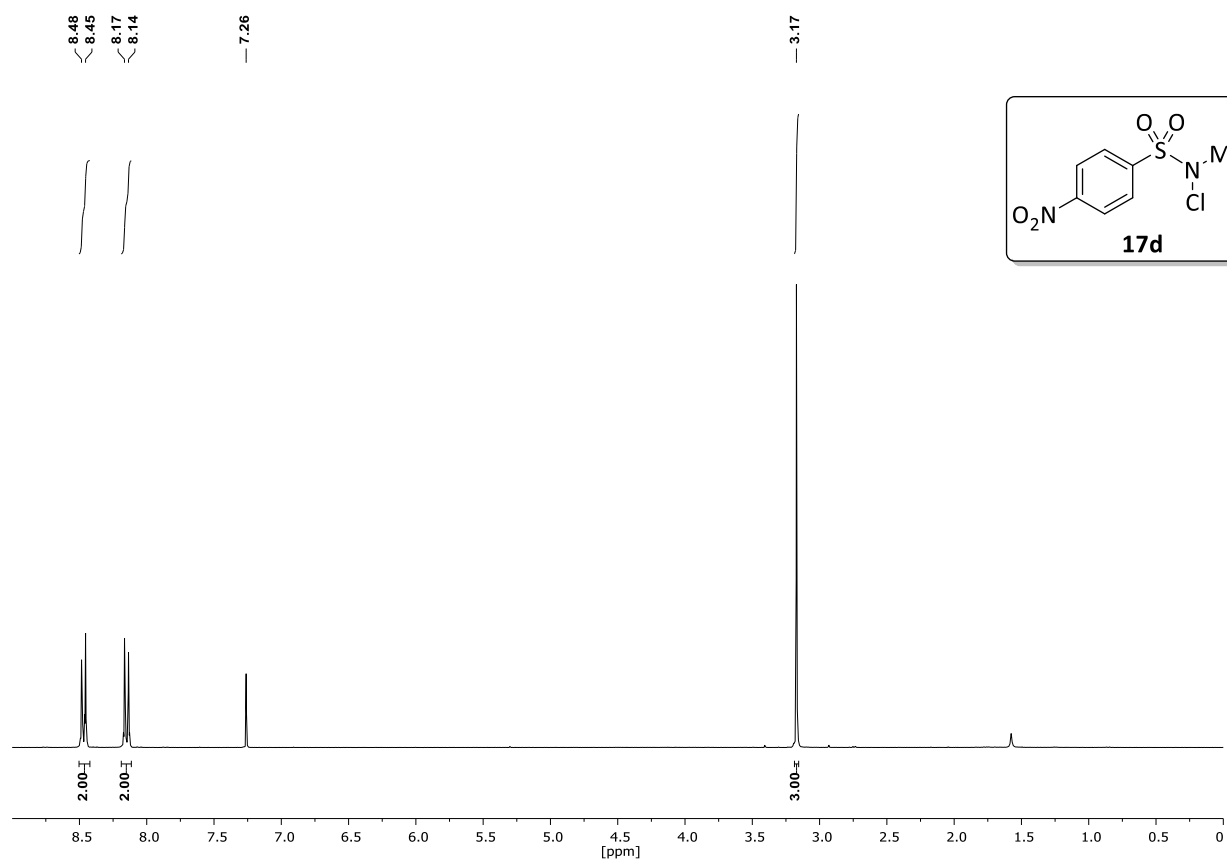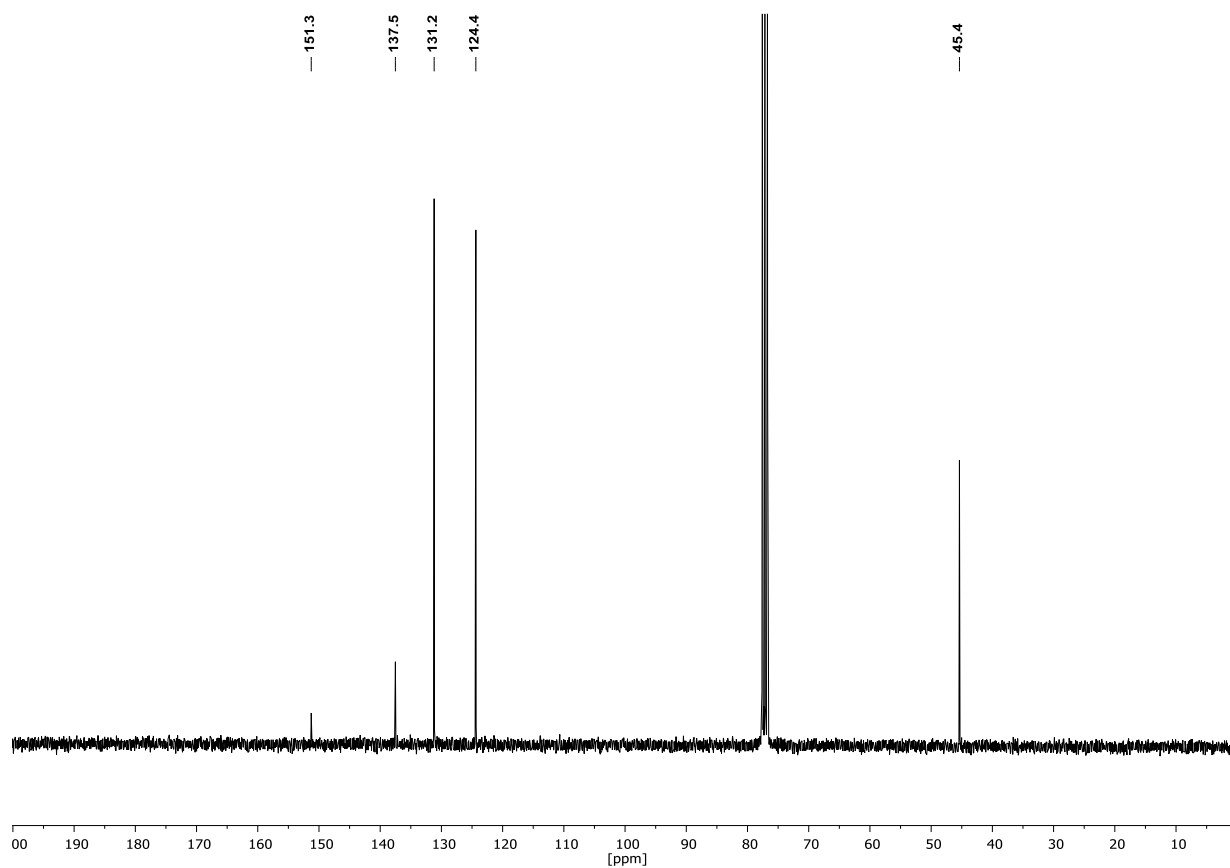
^{13}C-NMR (75 MHz, CDCl$_3$):

N-allyl-*N*-chloro-4-methylbenzenesulfonamide (17e)

^{1}H-NMR (400 MHz, CDCl$_3$):
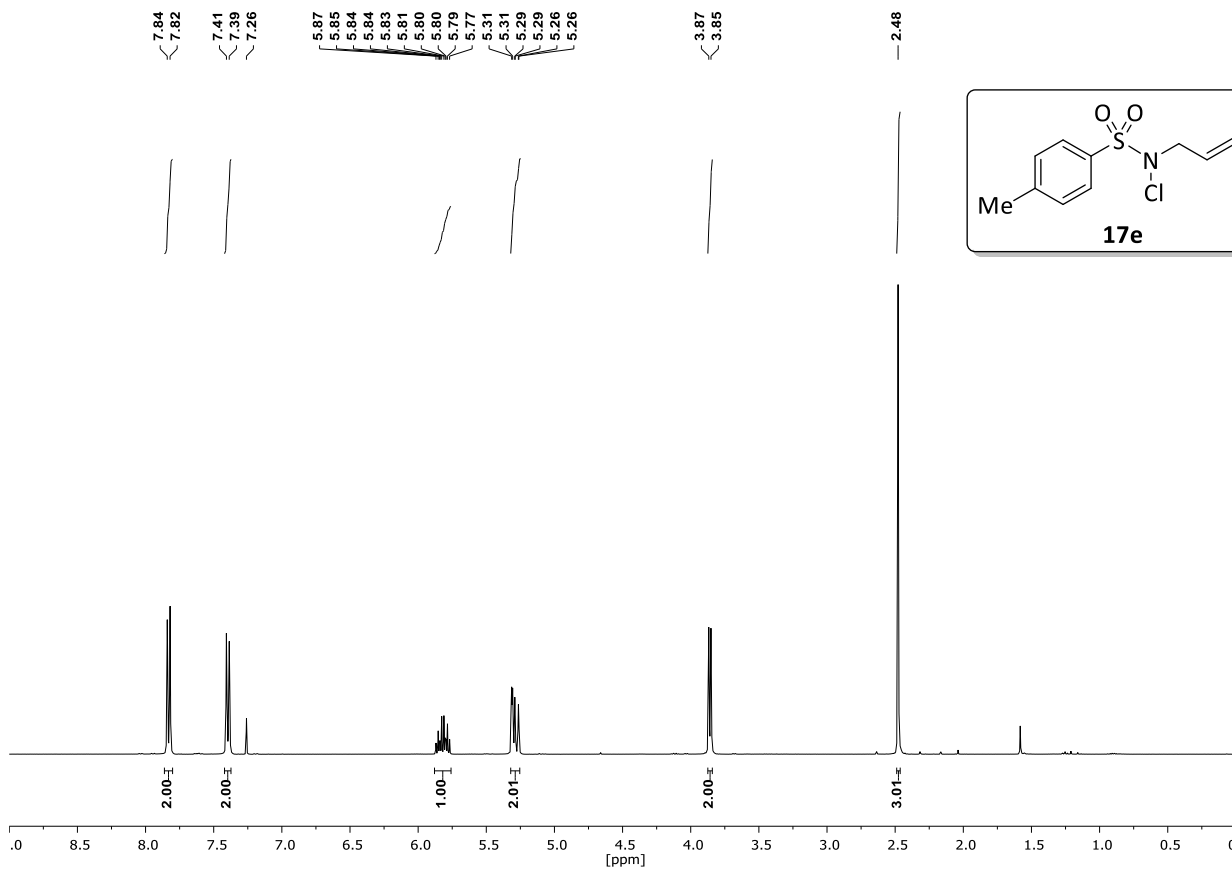
^{13}C-NMR (101 MHz, CDCl$_3$) & **DEPT135** (101 MHz, CDCl$_3$):
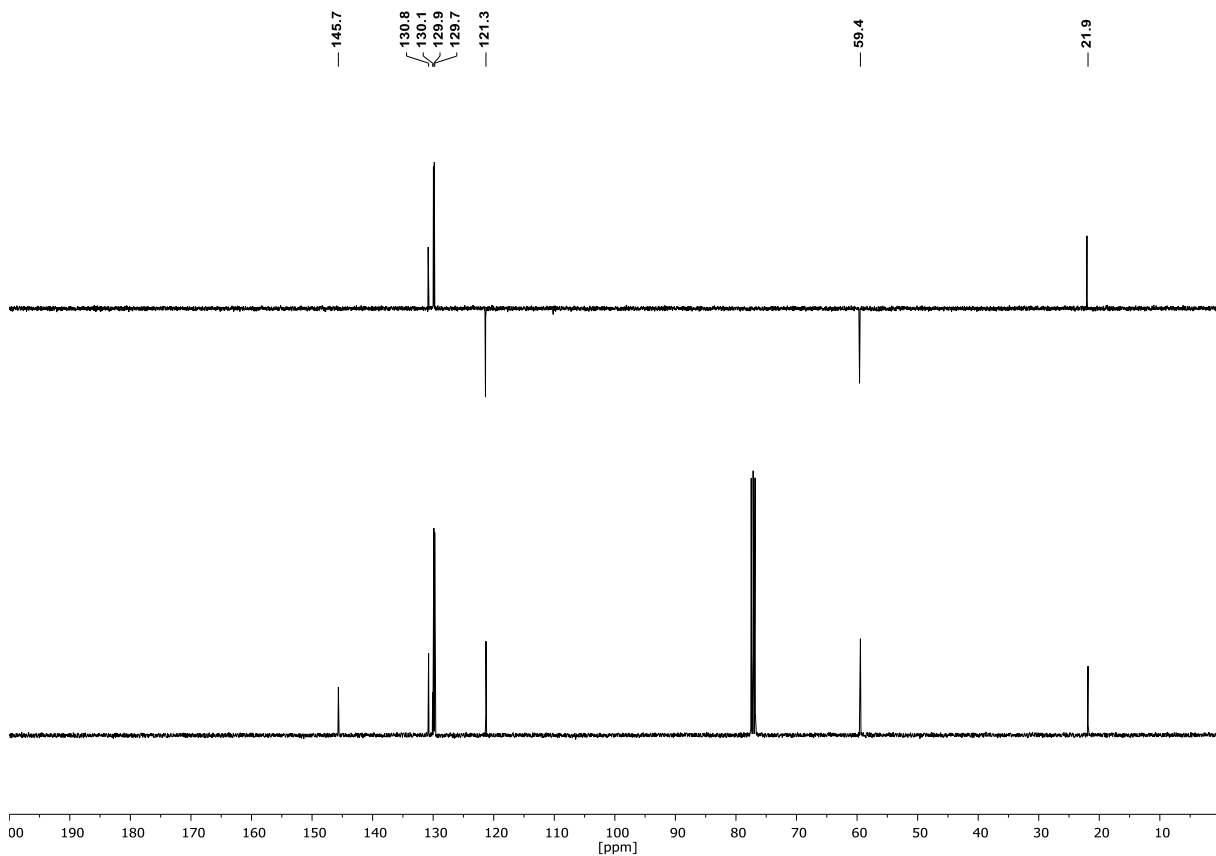
N-(tert-butyl)-N-chloro-4-methylbenzenesulfonamide (17f)

¹H-NMR (400 MHz, CDCl₃):
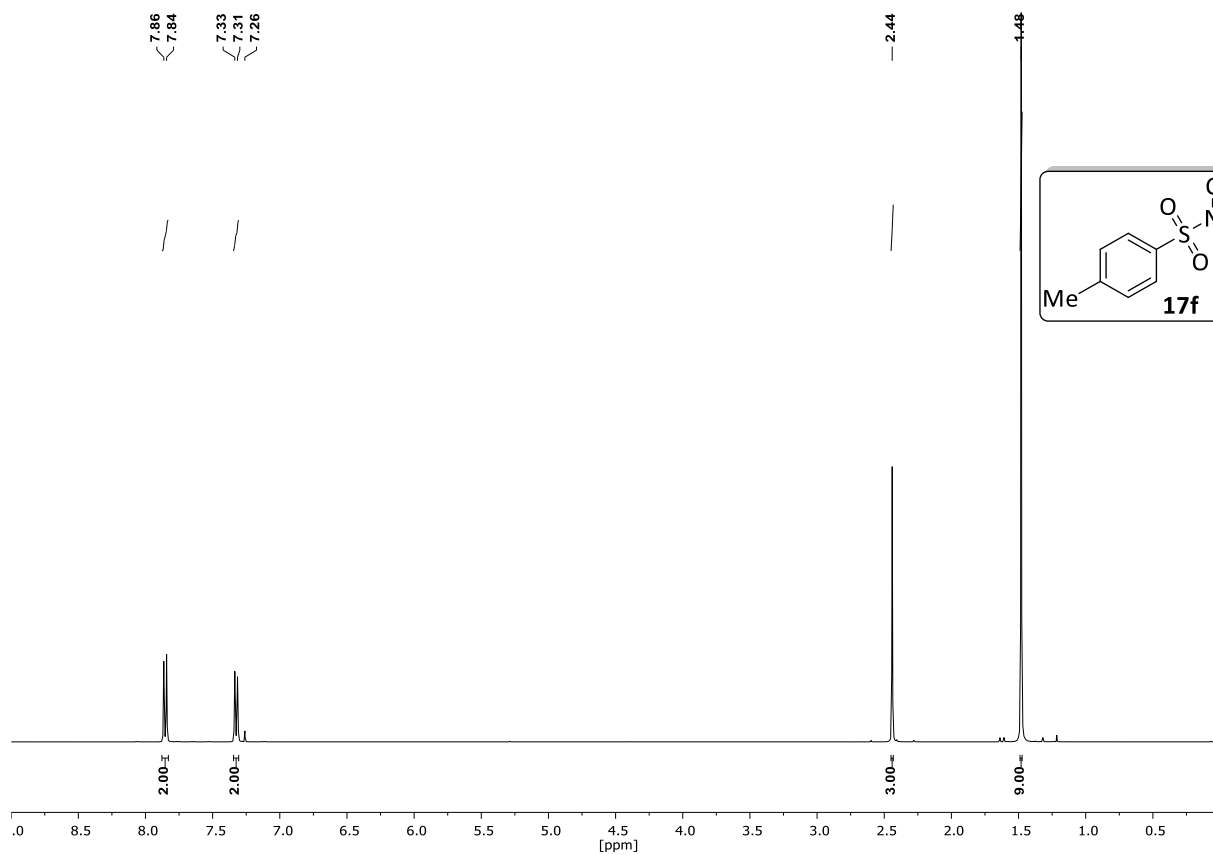
¹³C-NMR (101 MHz, CDCl₃) & **DEPT135** (101 MHz, CDCl₃):
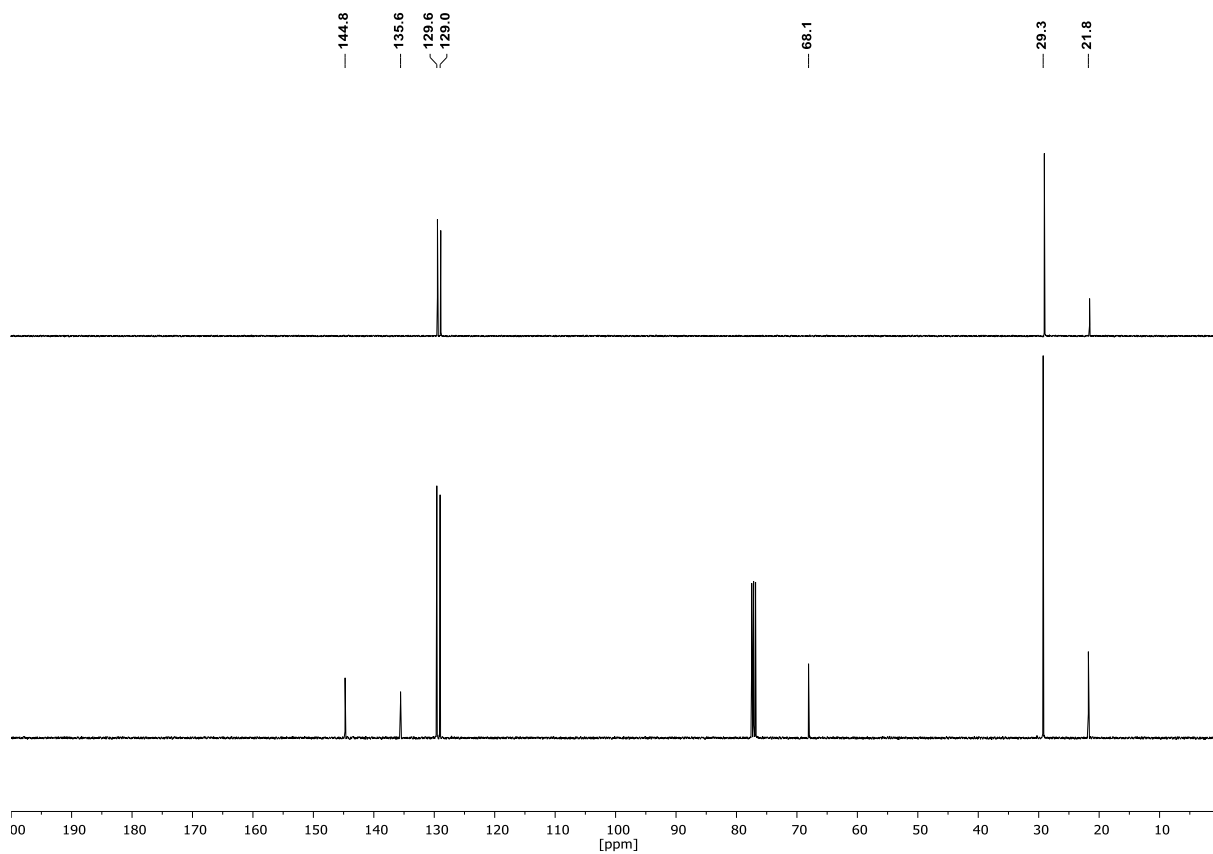
(S)-*N*-chloro-*N*-(1-hydroxy-3-methylbutan-2-yl)-4-methylbenzenesulfonamide (17g)

¹H-NMR (400 MHz, CDCl₃):
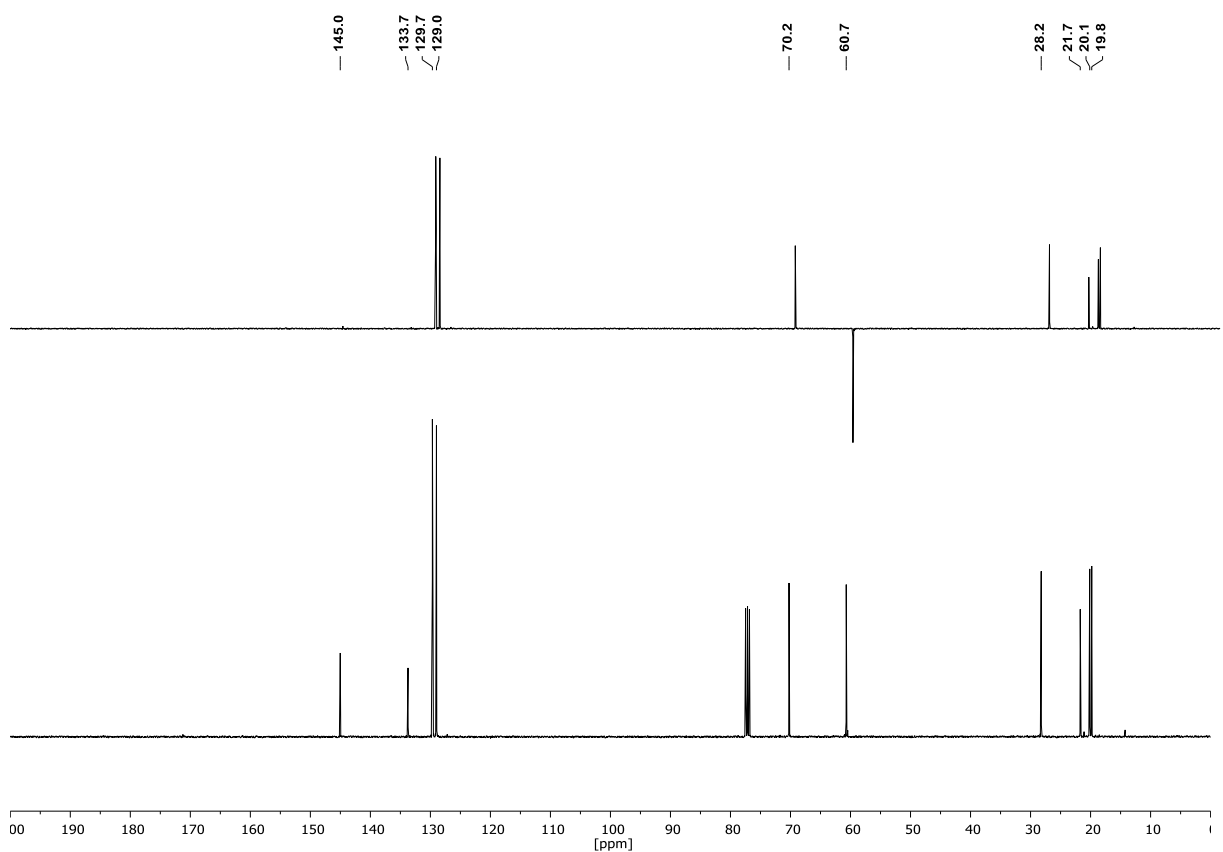
¹³C-NMR (101 MHz, CDCl₃):

N-(2-chloro-2-(*p*-tolyl)ethyl)-*N*,4-dimethylbenzenesulfonamide (18a)

^{1}H-NMR (400 MHz, CDCl$_3$):
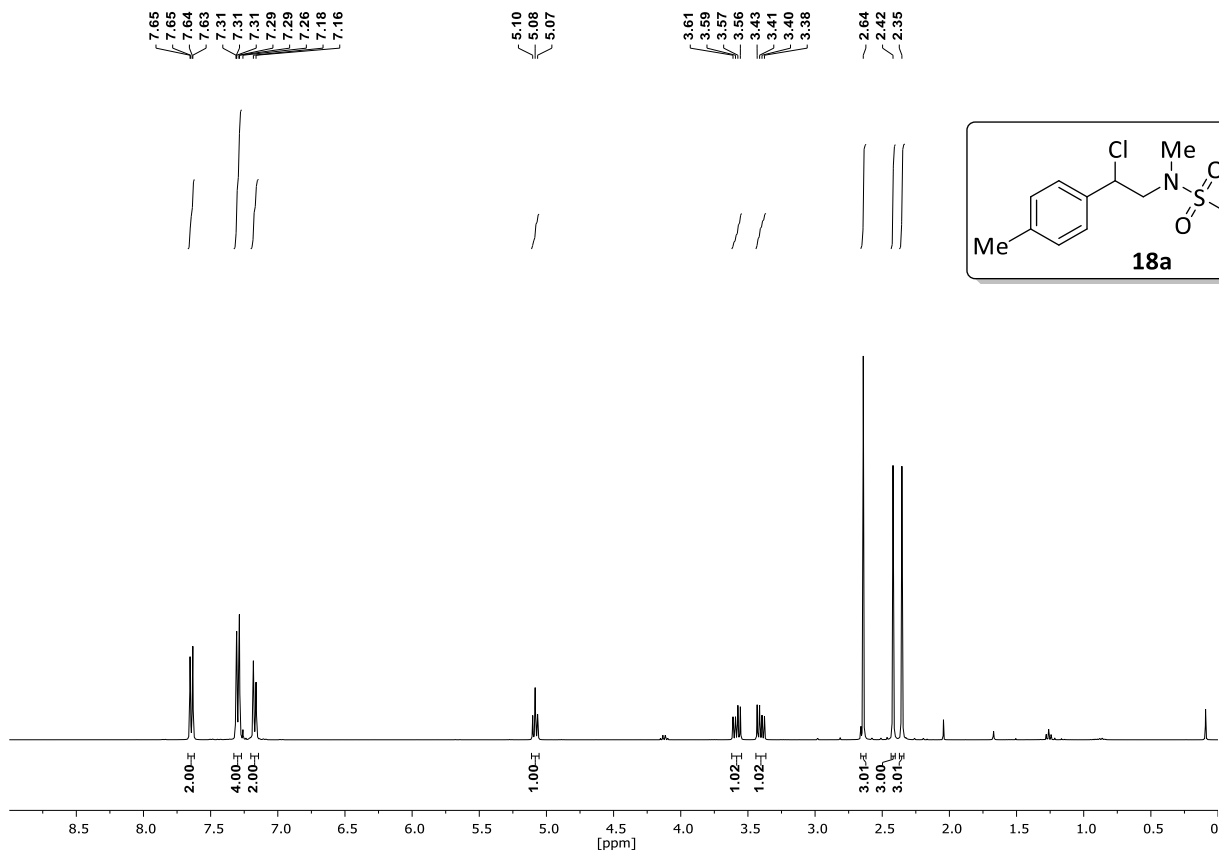
^{13}C-NMR (101 MHz, CDCl$_3$) & **DEPT135** (101 MHz, CDCl$_3$):
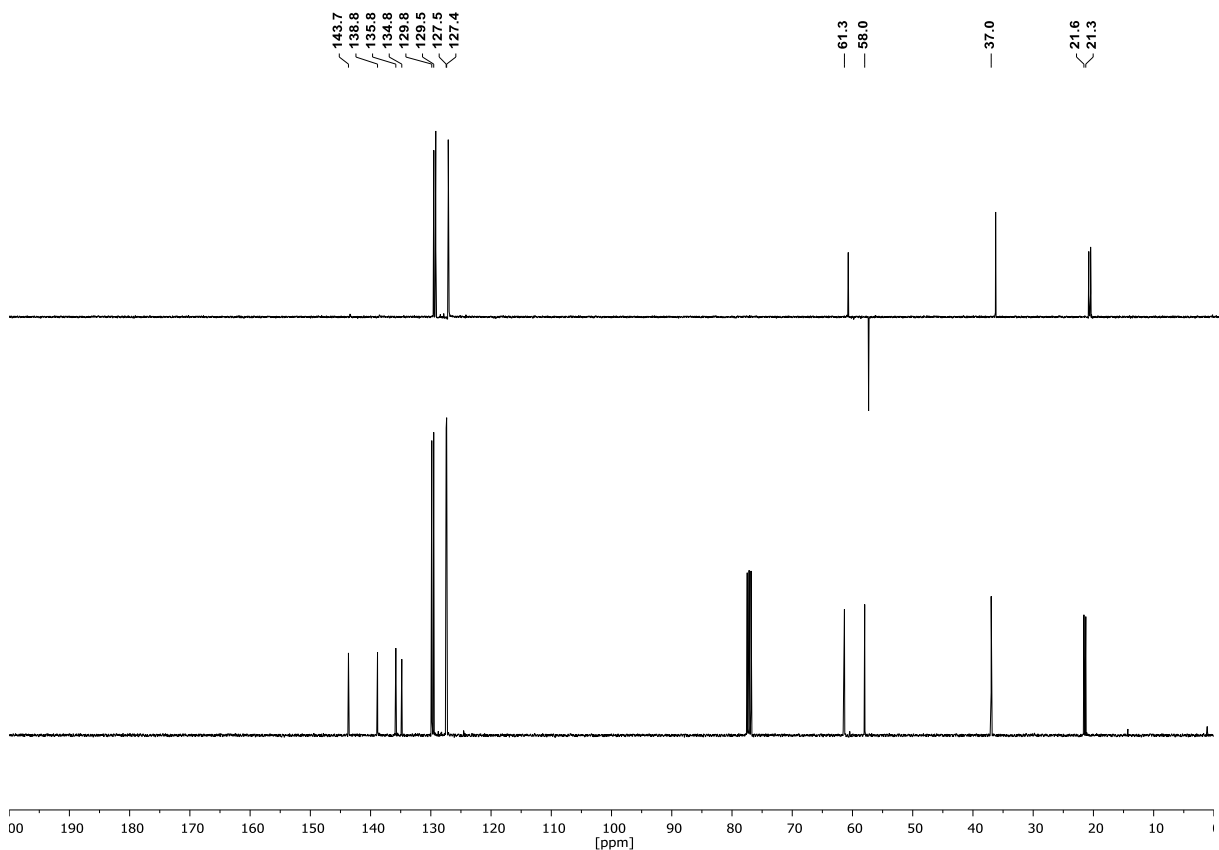
N-(2-chloro-2-phenylethyl)-*N*,4-dimethylbenzenesulfonamide (18b)

¹H-NMR (400 MHz, CDCl₃):
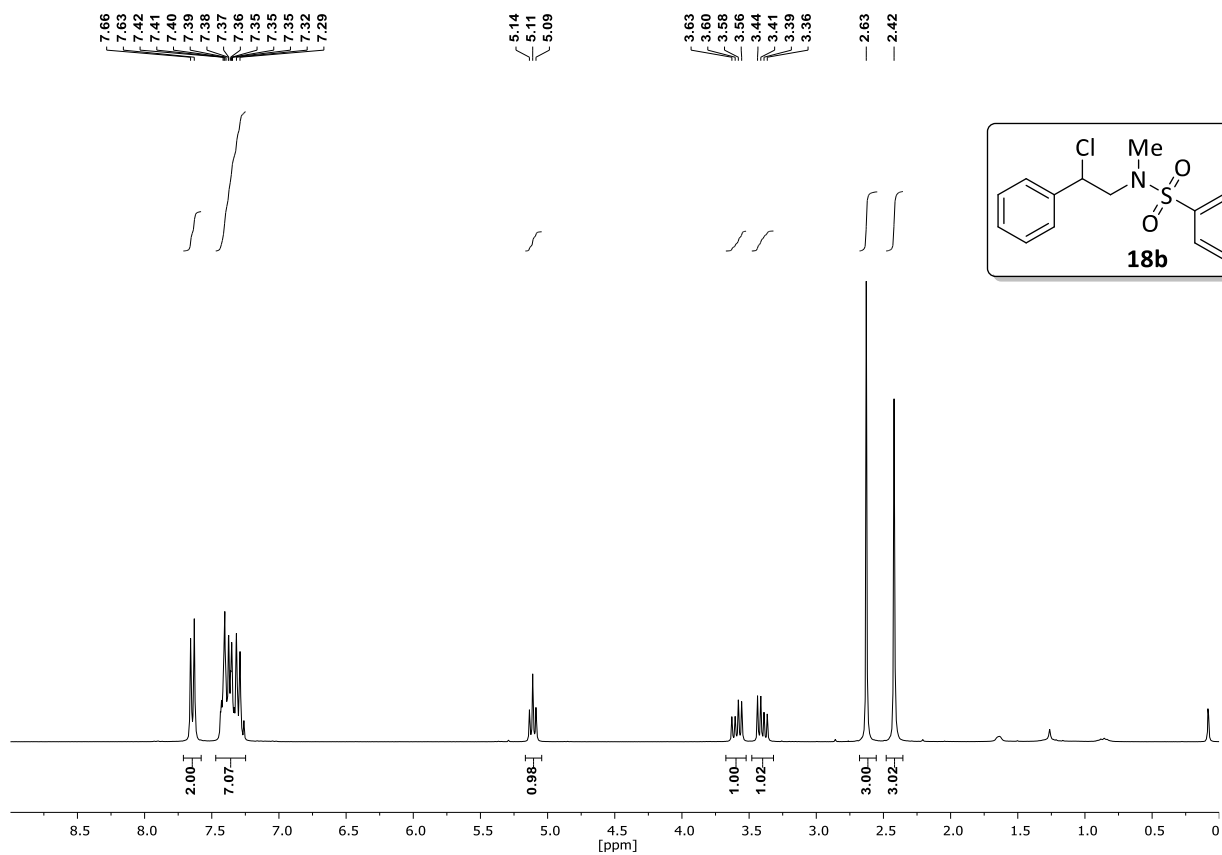
¹³C-NMR (101 MHz, CDCl₃) & **DEPT135** (101 MHz, CDCl₃):
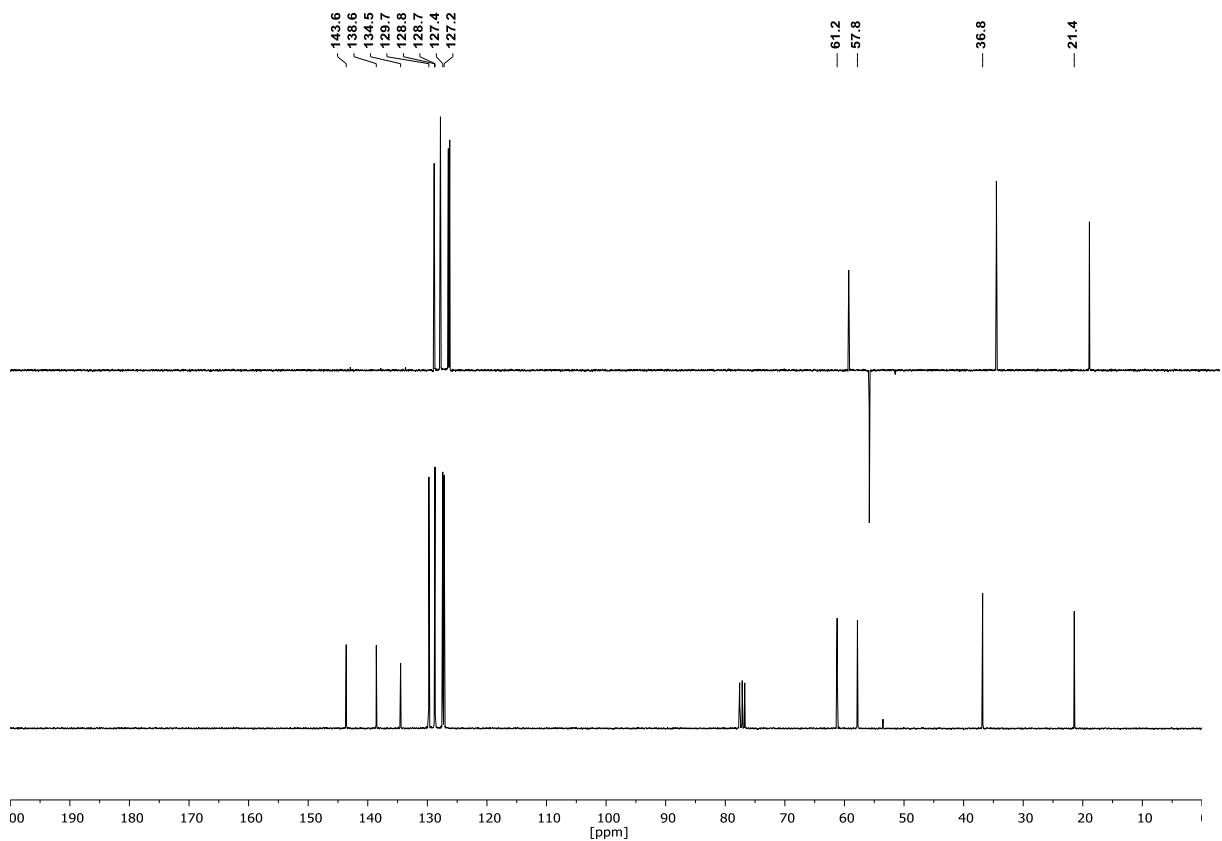
N-(2-hydroxy-2-(4-methoxyphenyl)ethyl)-N,4-dimethylbenzenesulfonamide (18c)

¹H-NMR (400 MHz, CDCl₃):
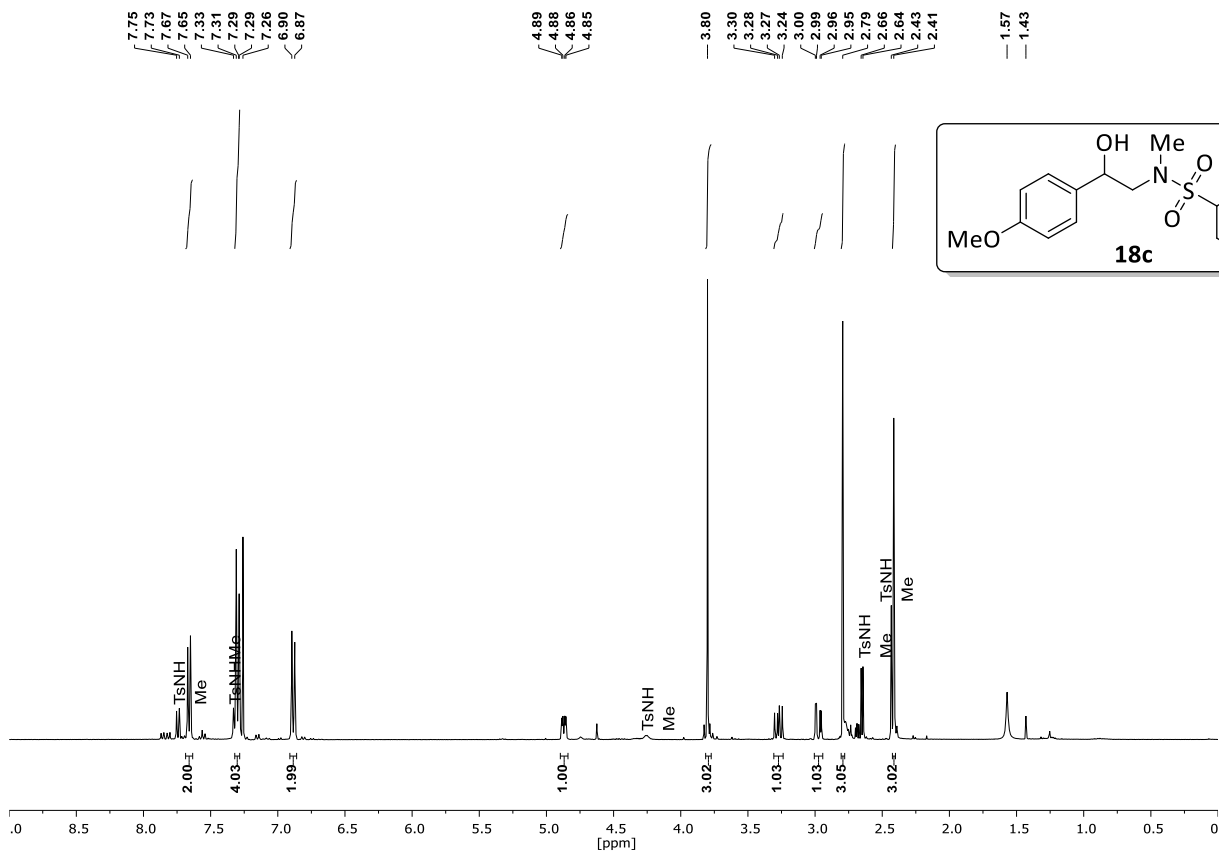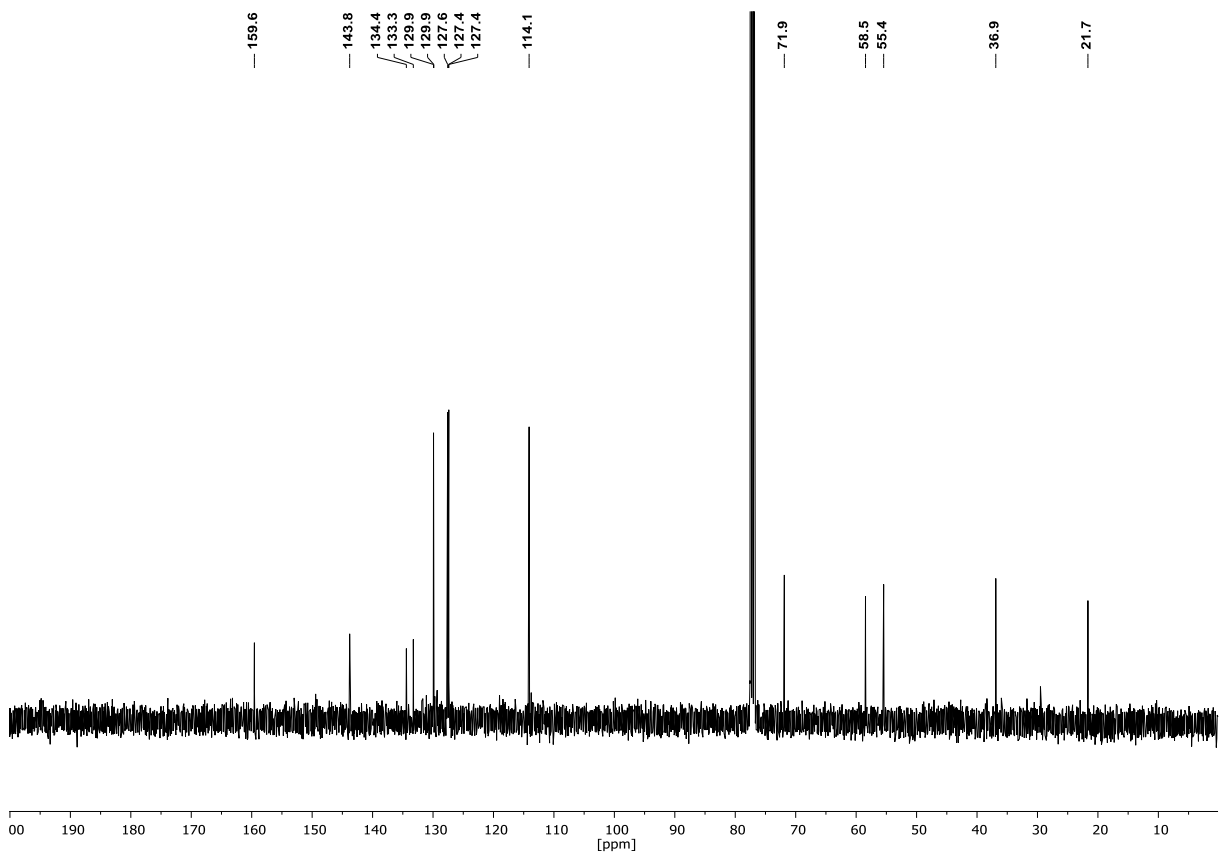
¹³C-NMR (101 MHz, CDCl₃):

¹H-NMR (400 MHz, DMSO-d₆):

8.31
7.67
7.65
7.61
7.59
7.41
7.39
7.39
7.25
7.23
6.90
6.87

5.44
5.43

4.69
4.67
4.67
4.66
4.66
4.64

3.74

3.32
3.07
3.05
3.03
3.01
2.99
2.98
2.96
2.95
2.66
2.50
2.49
2.38

CHCl3

TsNHMe

TsNHMe + product

OH

water

TsNHMe + product

2.02
2.65
2.00
2.00

0.90

1.01

3.01

2.05

3.01

4.75

.0   8.5   8.0   7.5   7.0   6.5   6.0   5.5   5.0   4.5   4.0   3.5   3.0   2.5   2.0   1.5   1.0   0.5   0

[ppm]

COSY (400 MHz, DMSO-d₆):

9.0   8.5   8.0   7.5   7.0   6.5   6.0   5.5   5.0   4.5   4.0   3.5   3.0   2.5   2.0   1.5   1.0   0.5

[ppm]

f1 (ppm)

1   2   3   4   5   6   7   8   9
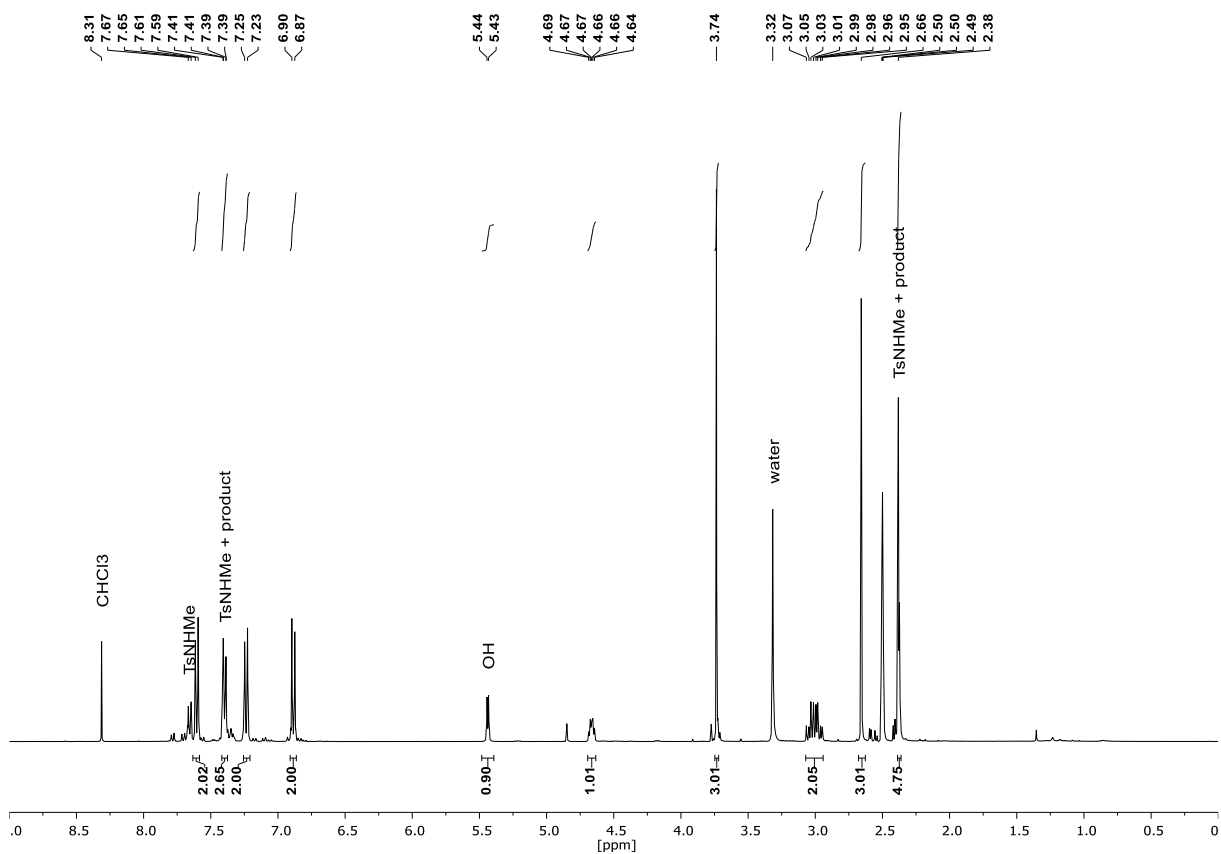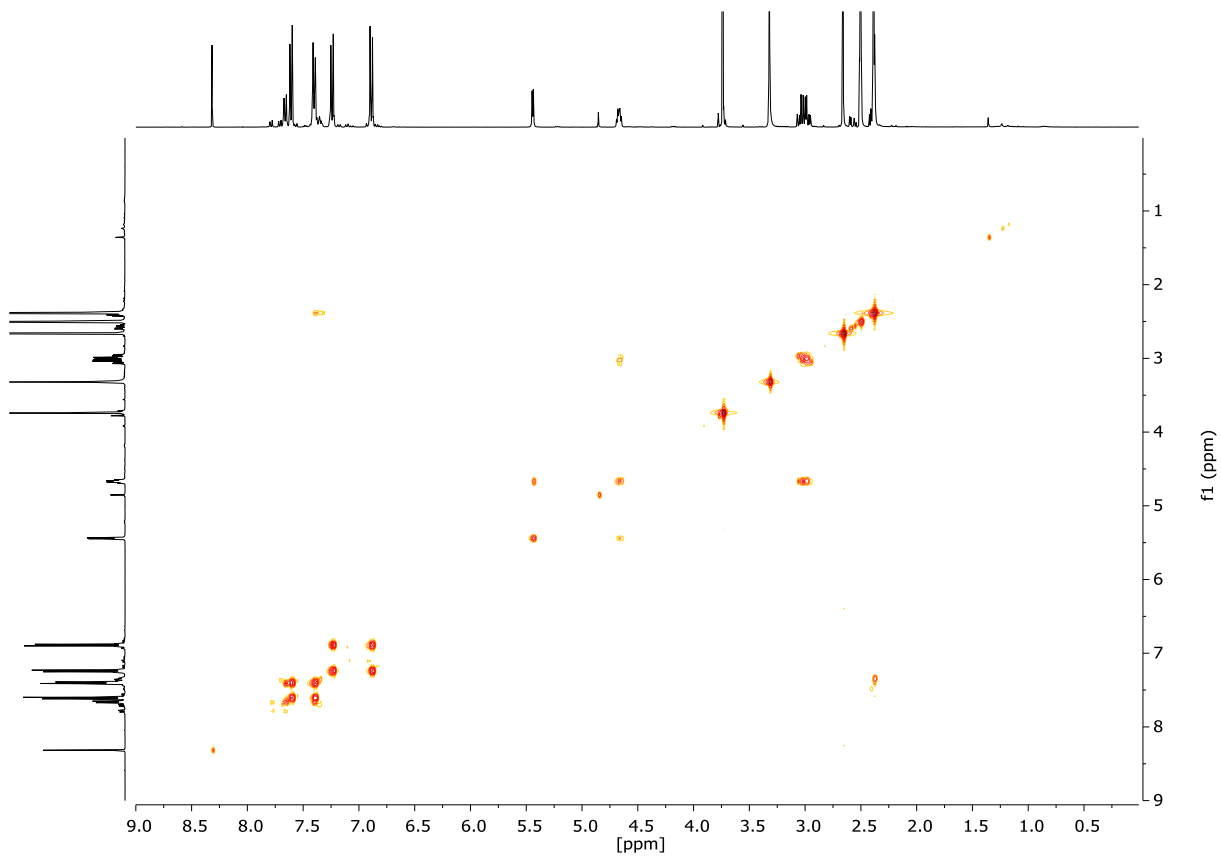
N-(2-chloro-2-(*o*-tolyl)ethyl)-*N*,4-dimethylbenzenesulfonamide (18d)

¹H-NMR (400 MHz, CDCl₃):
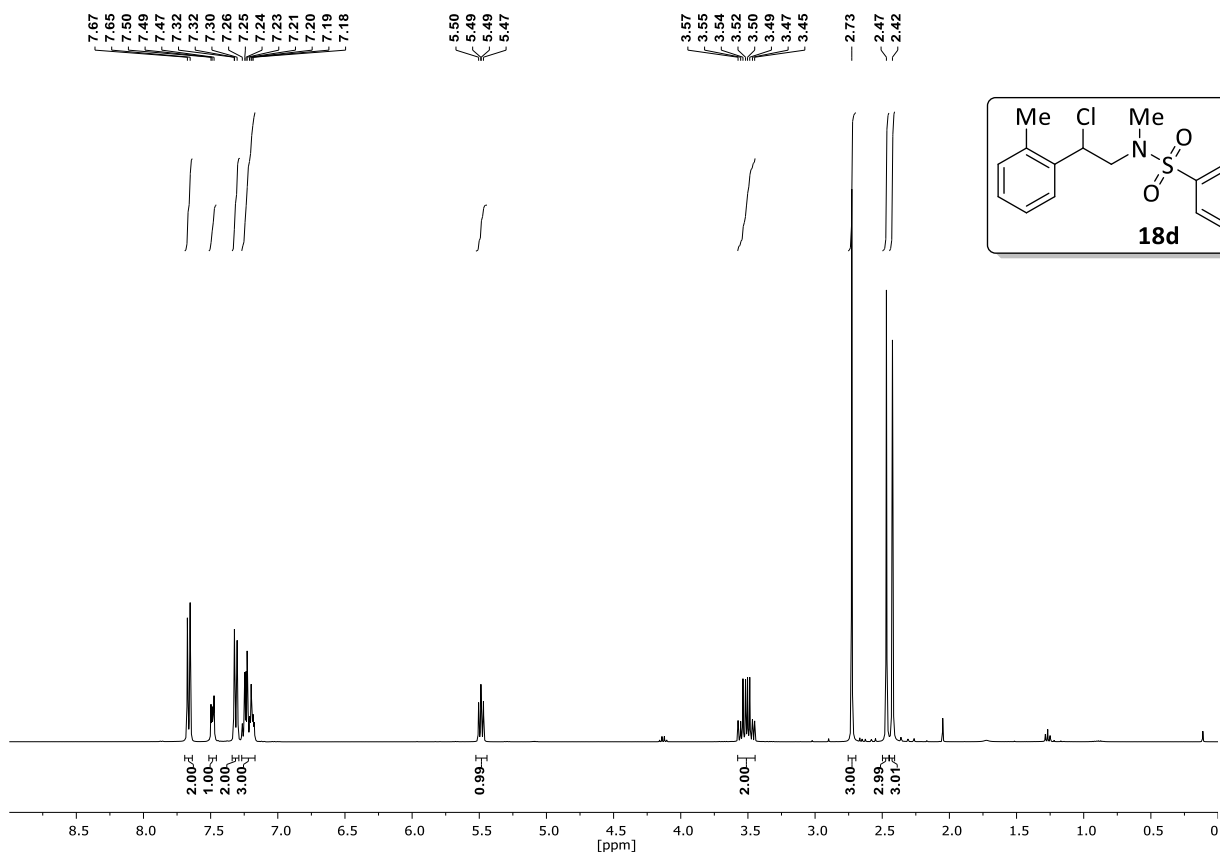
¹³C-NMR (101 MHz, CDCl₃) & **DEPT135** (101 MHz, CDCl₃):
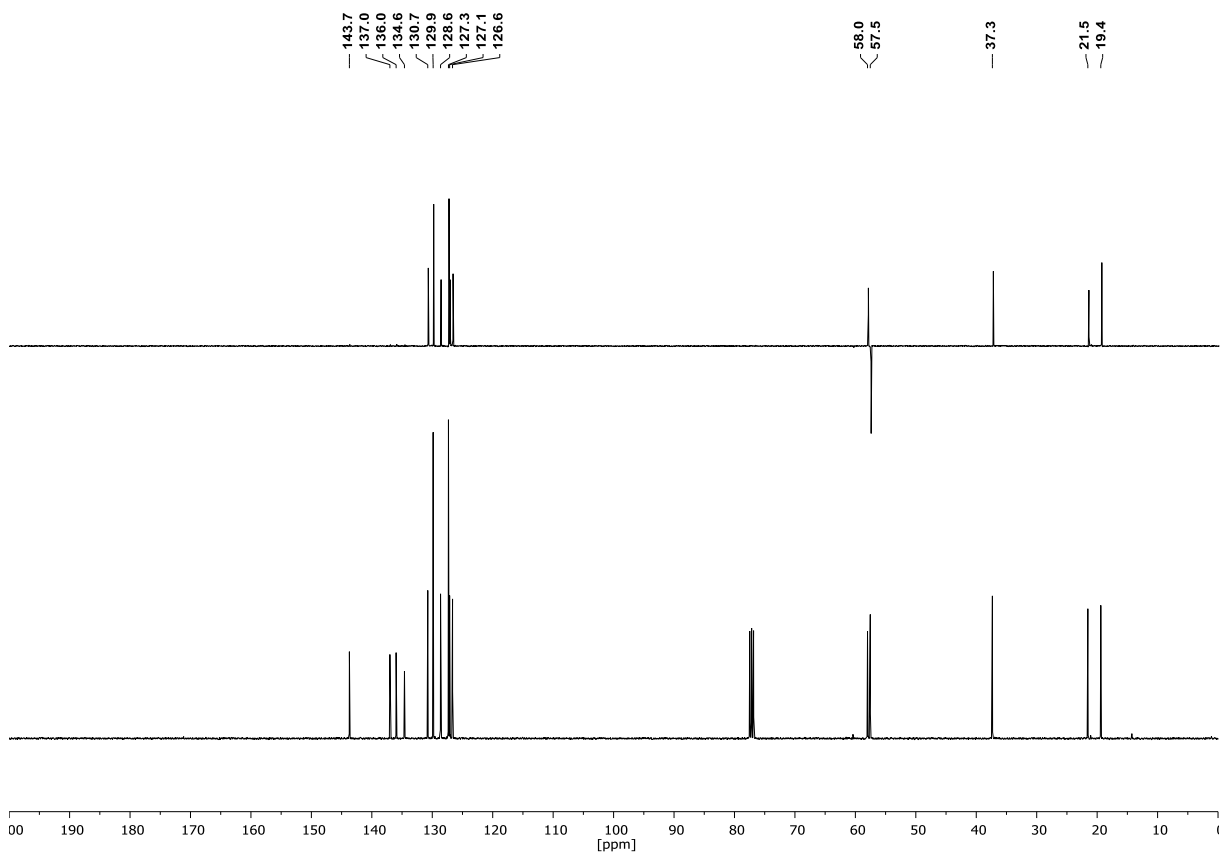
N-(2-chloro-2-(2-methoxyphenyl)ethyl)-*N*,4-dimethylbenzenesulfonamide (18e)

¹H-NMR (400 MHz, CDCl₃):
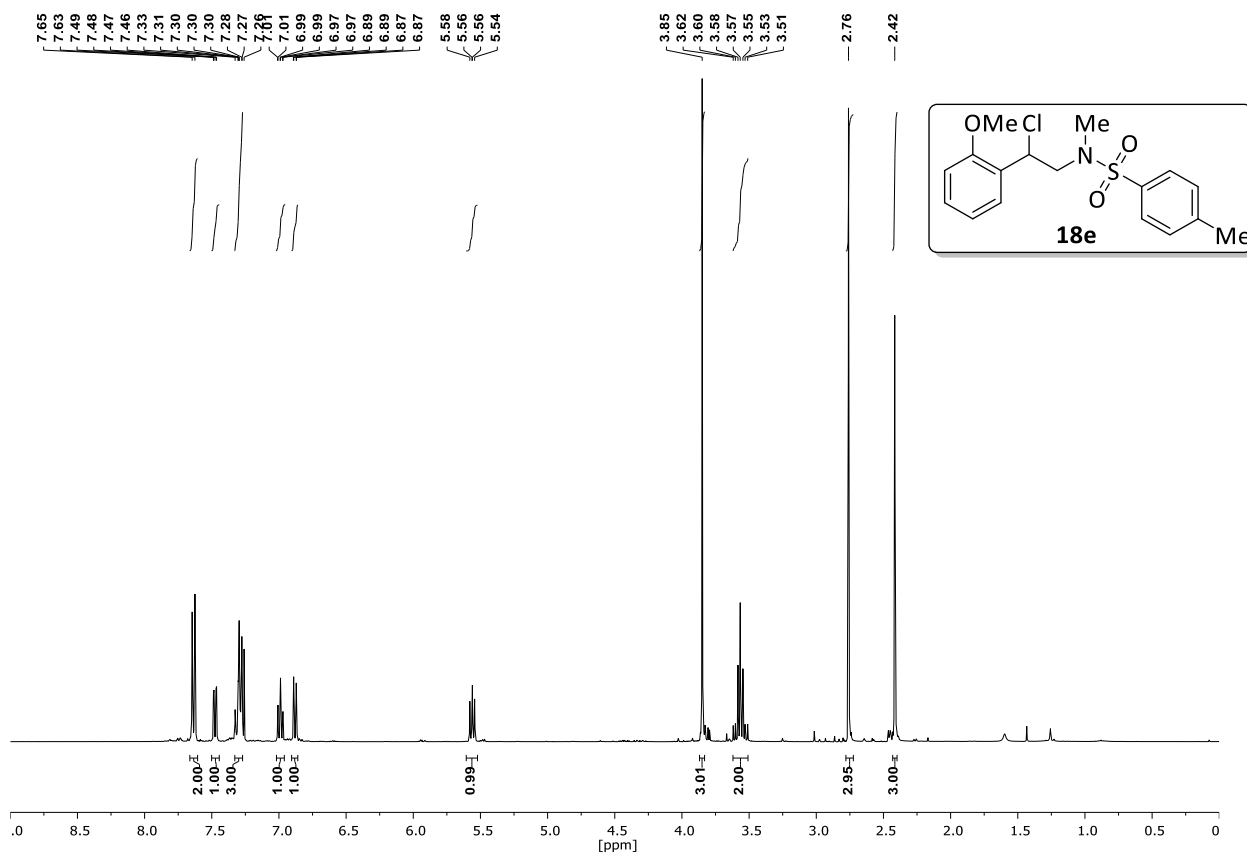
¹³C-NMR (101 MHz, CDCl₃) & **DEPT135** (101 MHz, CDCl₃):
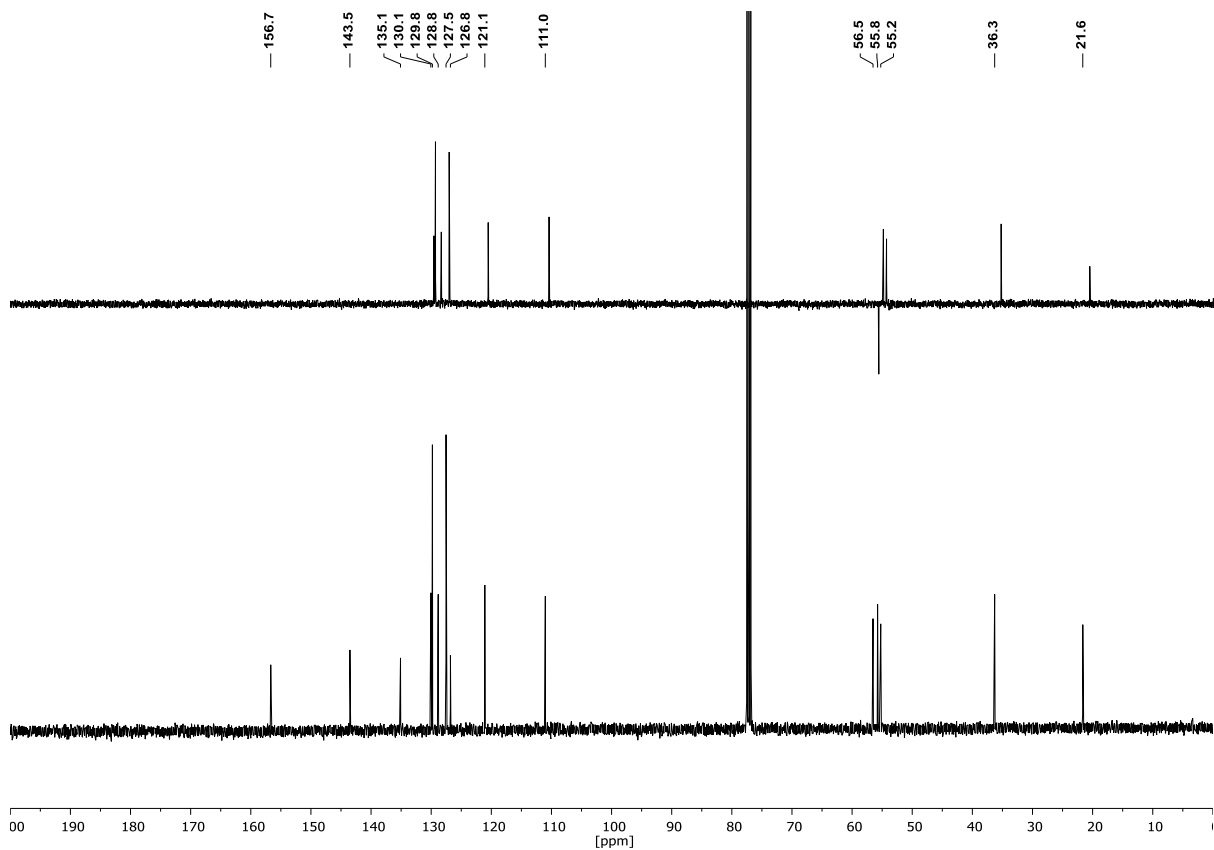
N-(1-chloro-2,3-dihydro-1H-inden-2-yl)-N,4-dimethylbenzenesulfonamide (Fehler! v erweisquelle konnte nicht gefunden werden – **1LT617F2**)

1H-NMR (400 MHz, CDCl3):
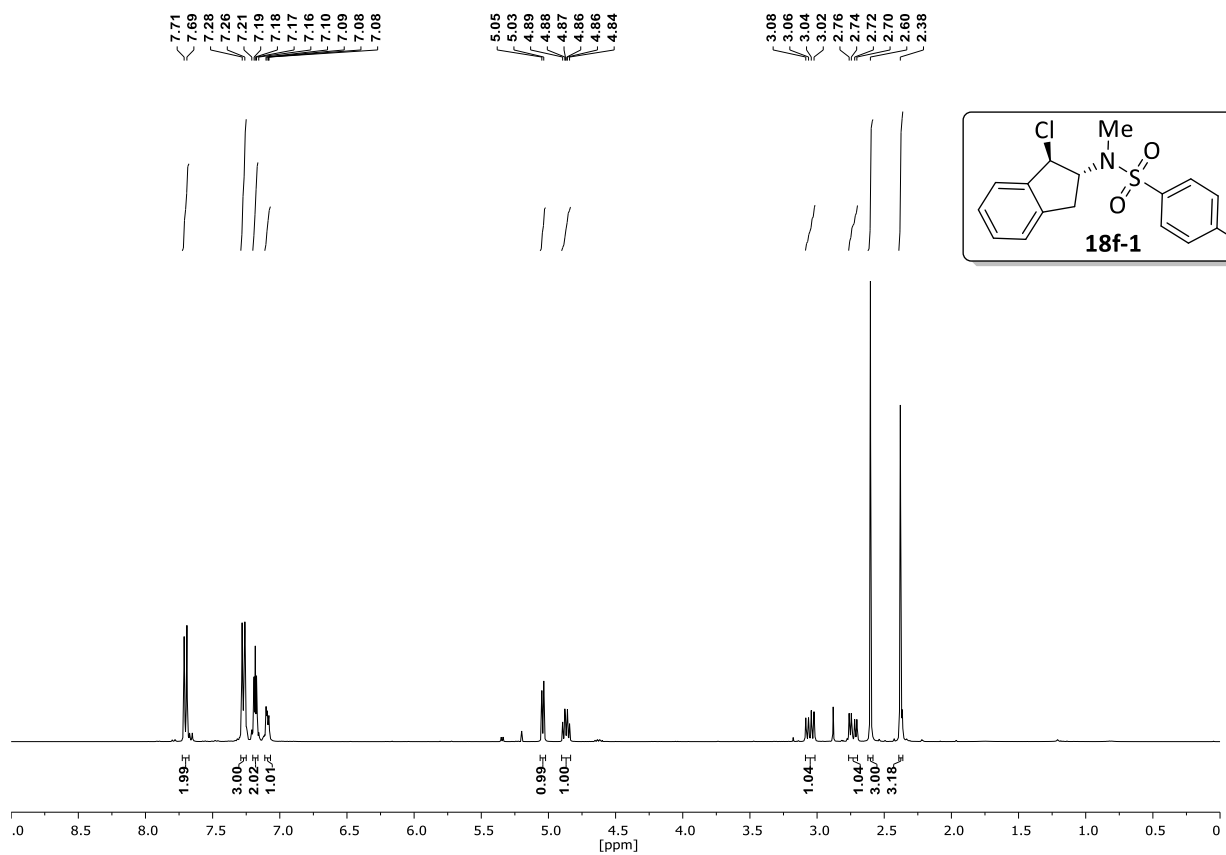
13C-NMR (101 MHz, CDCl3) & **DEPT135** (101 MHz, CDCl3):
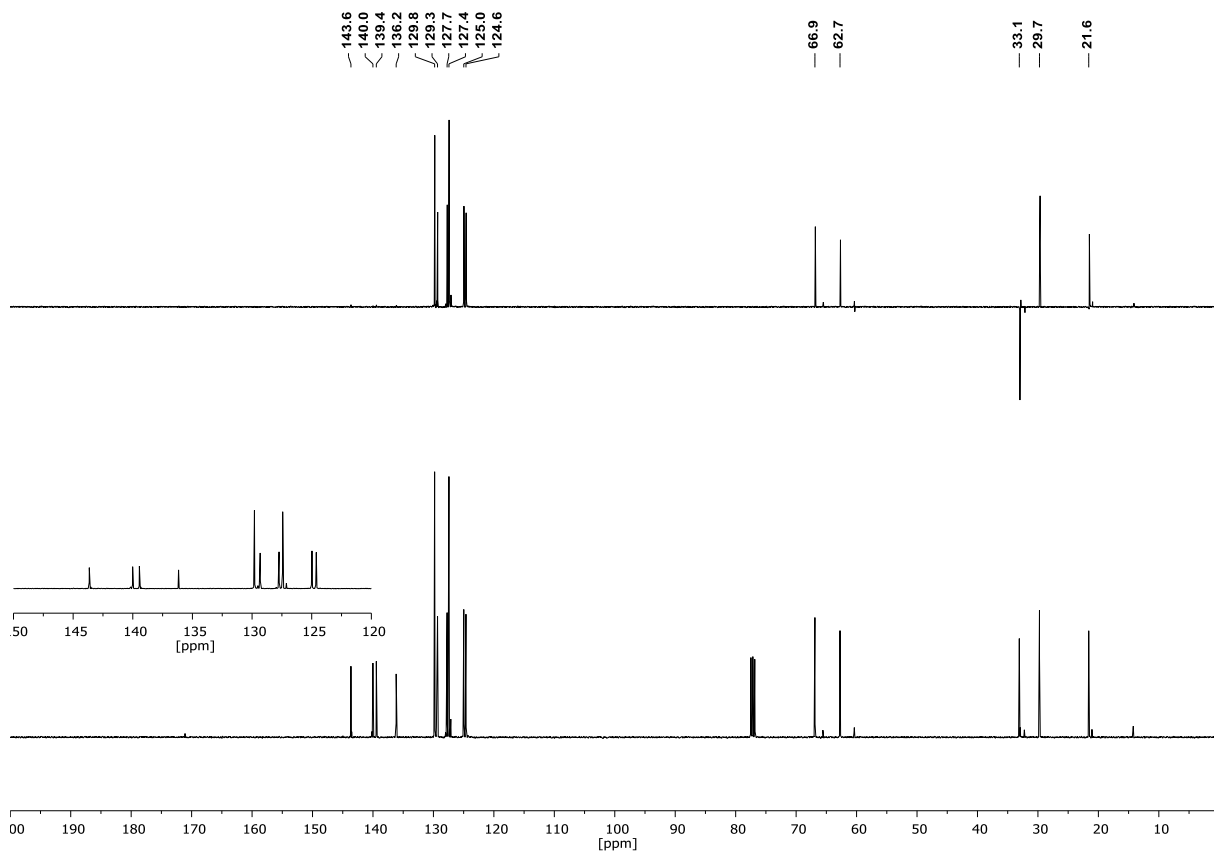
N-(1H-inden-2-yl)-*N*,4-dimethylbenzenesulfonamide (18f-2)

¹H-NMR (400 MHz, CDCl₃):
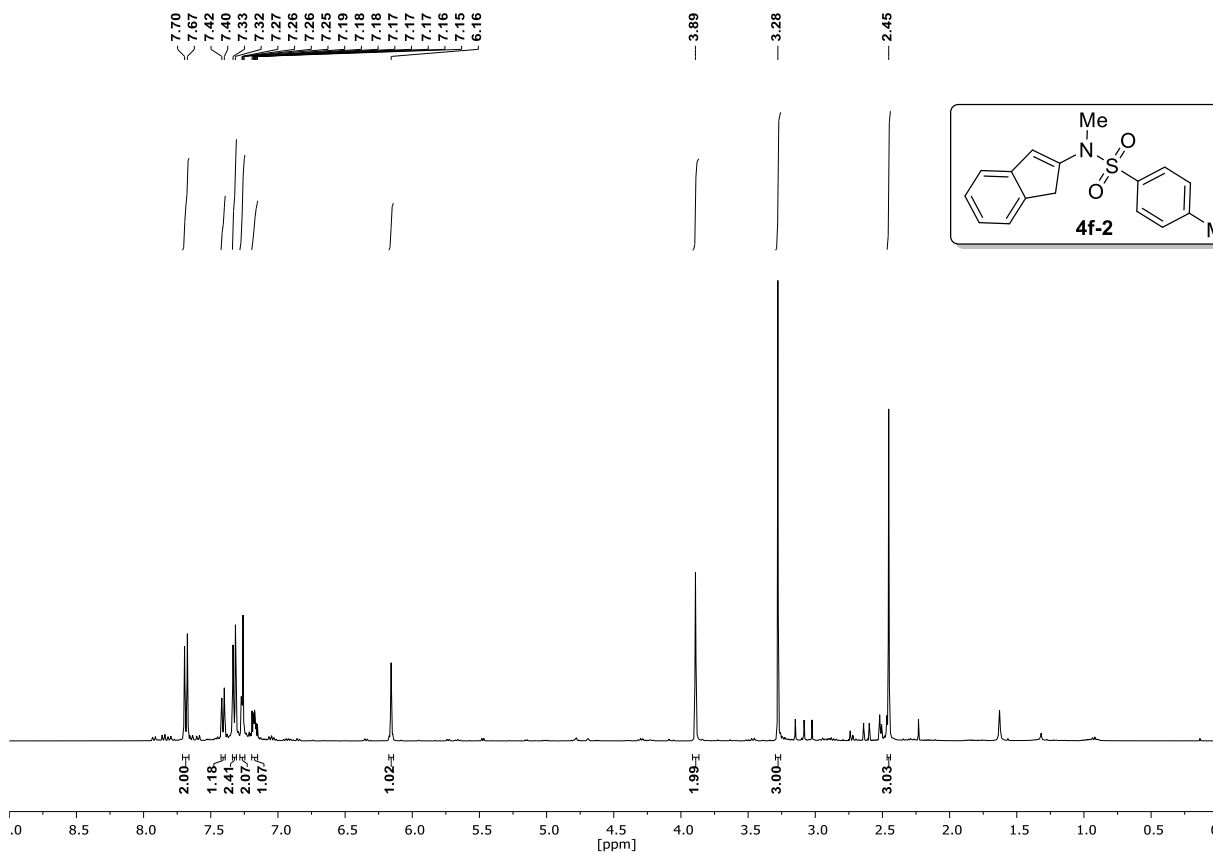
¹³C-NMR (101 MHz, CDCl₃) & **DEPT135** (101 MHz, CDCl₃):

147.2 144.1 143.2 139.7 134.6 129.9 127.2 126.7 124.1 123.4 120.1 115.1

40.7 37.2

21.7
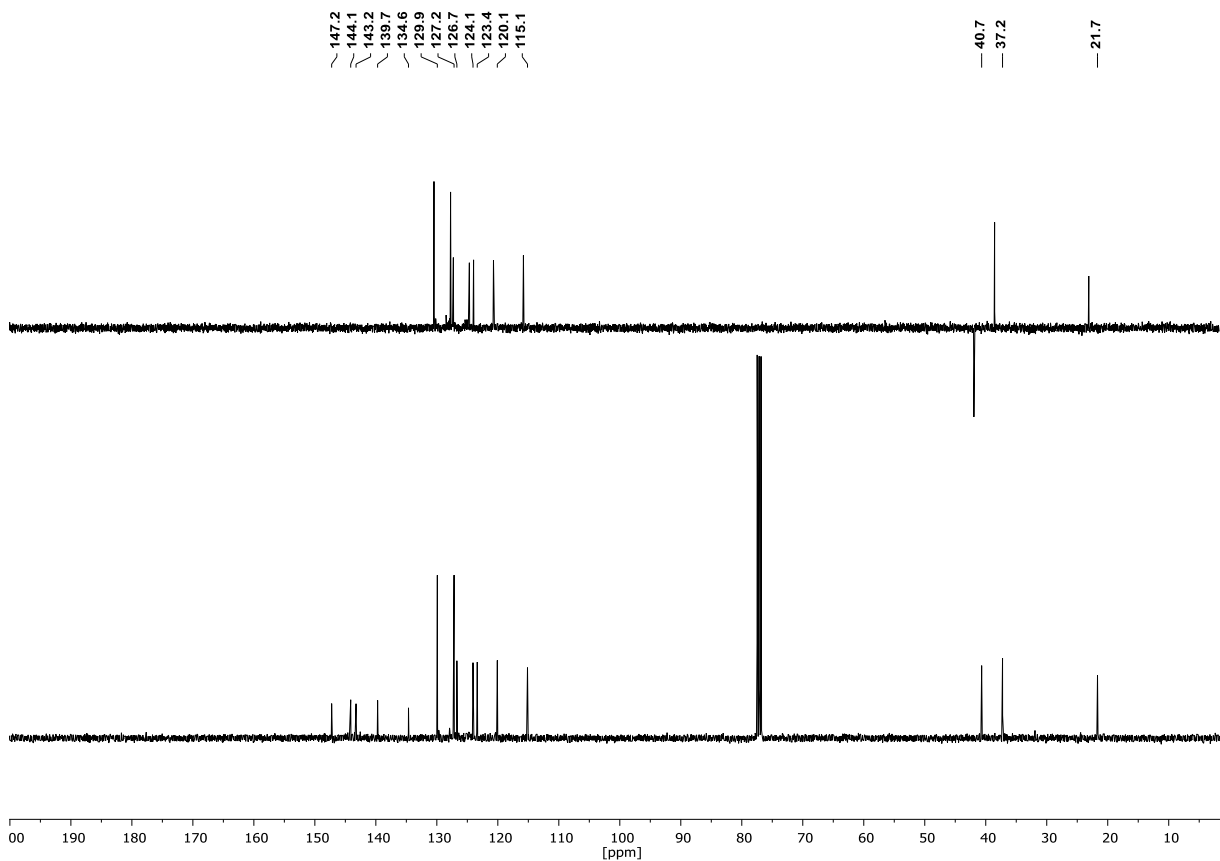
N-(2-chloro-2-(naphthalen-2-yl)ethyl)-N,4-dimethylbenzenesulfonamide (18g)

¹H-NMR (300 MHz, CDCl₃):

7.88 7.85 7.83 7.64 7.61 7.56 7.55 7.53 7.53 7.52 7.51 7.50 7.28 7.26 7.25

5.30 5.28 5.25

3.73 3.70 3.68 3.65 3.55 3.53 3.50 3.48

2.63 2.41

4.00 2.01 3.00 2.87 1.00 1.01 1.00 2.99 3.00

¹³C-NMR (75 MHz, CDCl₃) & **DEPT135** (75 MHz, CDCl₃):

144.142.140.138.136.134.132.130.128.126 [ppm]
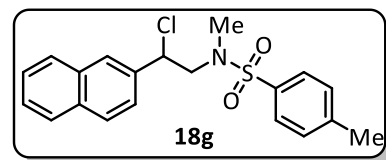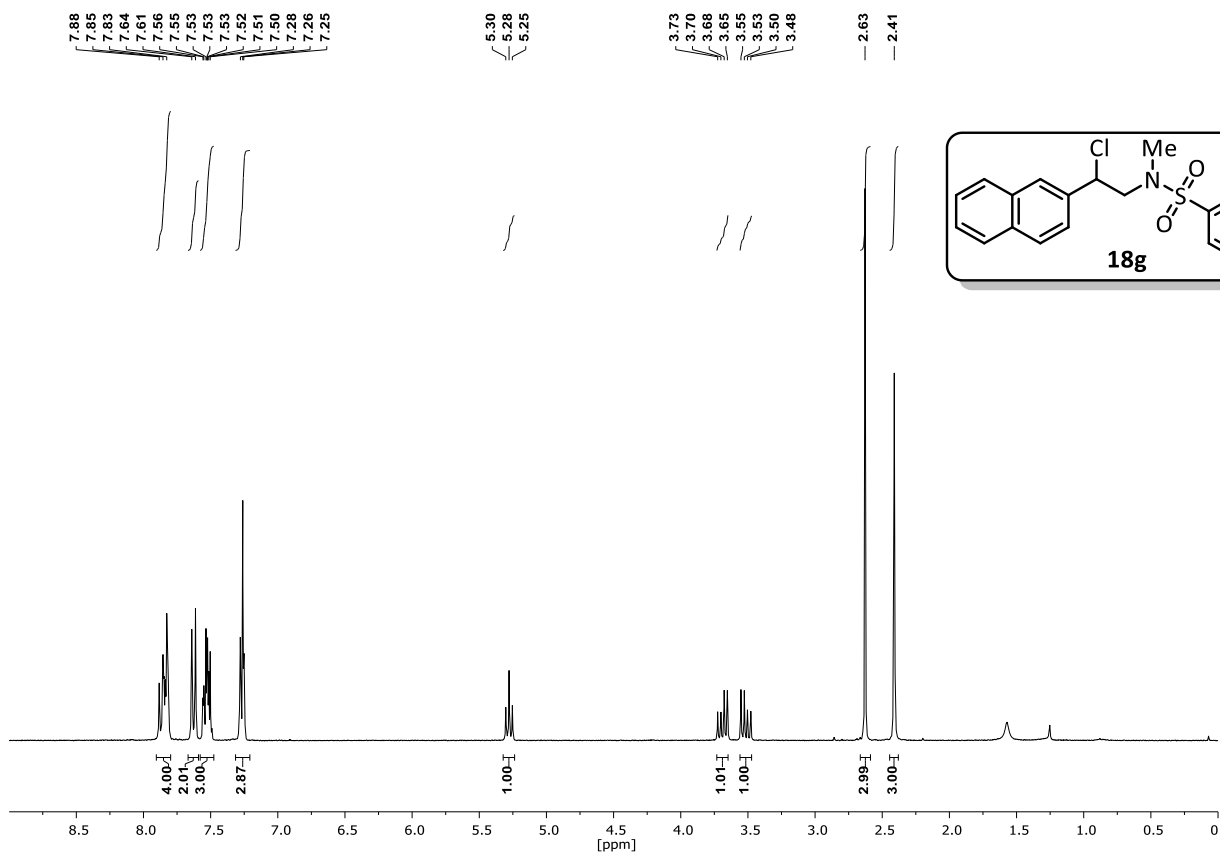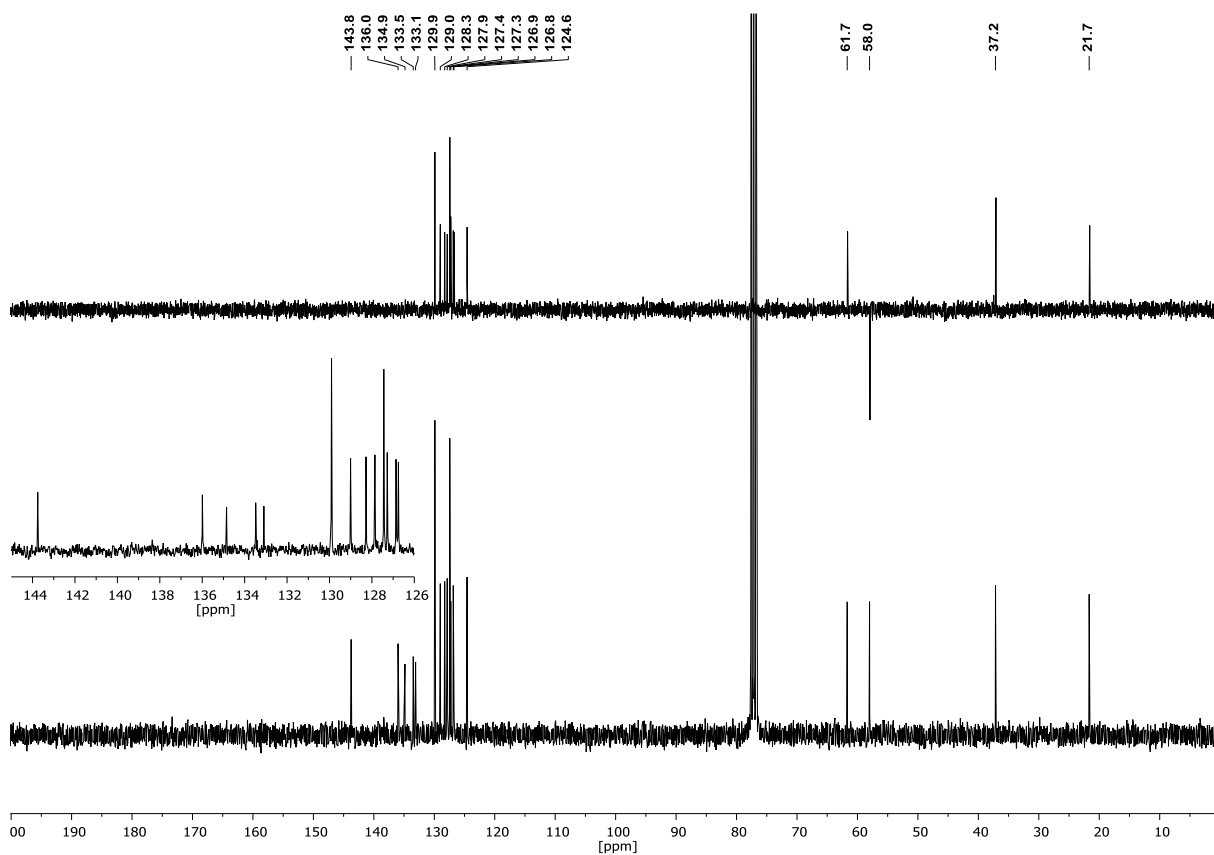
(E)-N-(2-chloro-2-phenylvinyl)*-N,4*-dimethylbenzenesulfonamide (Z)-N-(2-chloro-2-phenylvinyl)-N,4-dimethylbenzenesulfonamide) (18h)

¹H-NMR (300 MHz, CDCl₃):
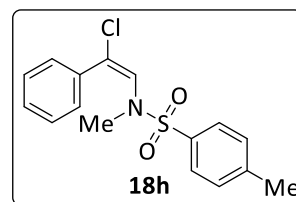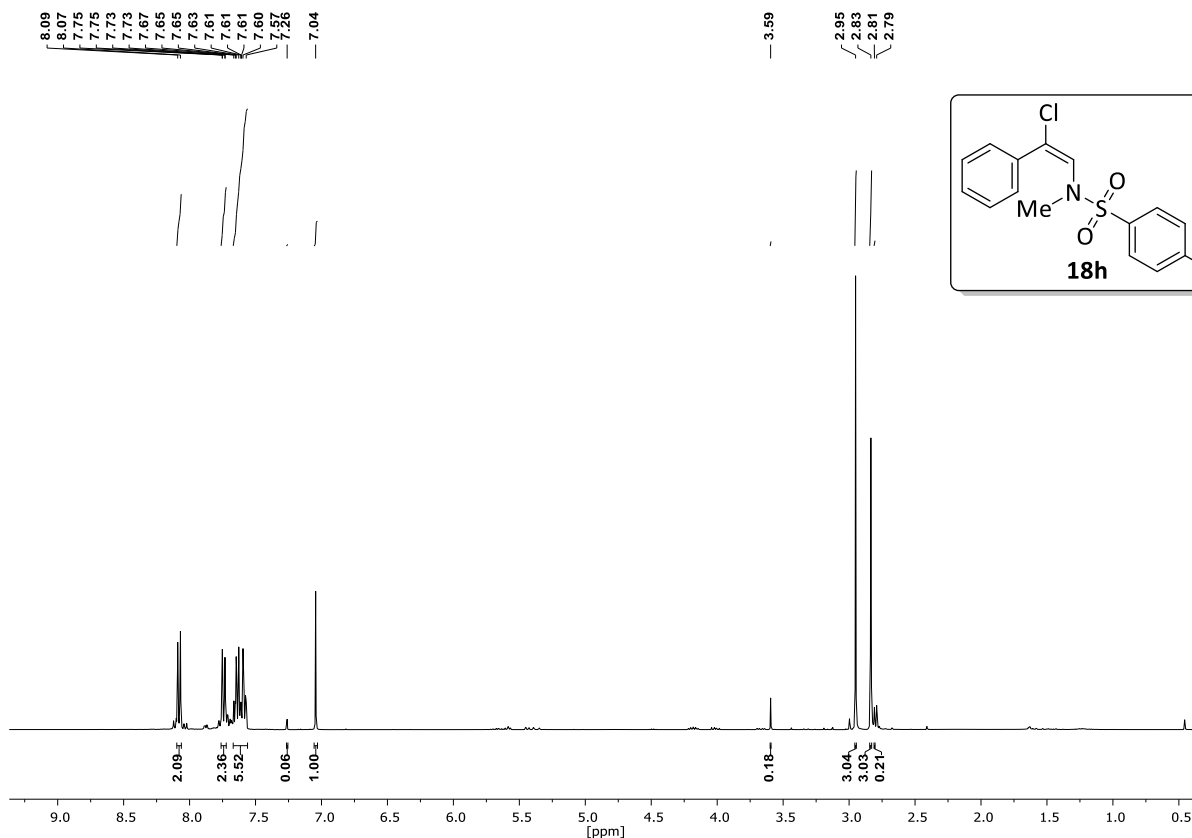
¹³C-NMR (75 MHz, CDCl₃) & **DEPT135** (75 MHz, CDCl₃):
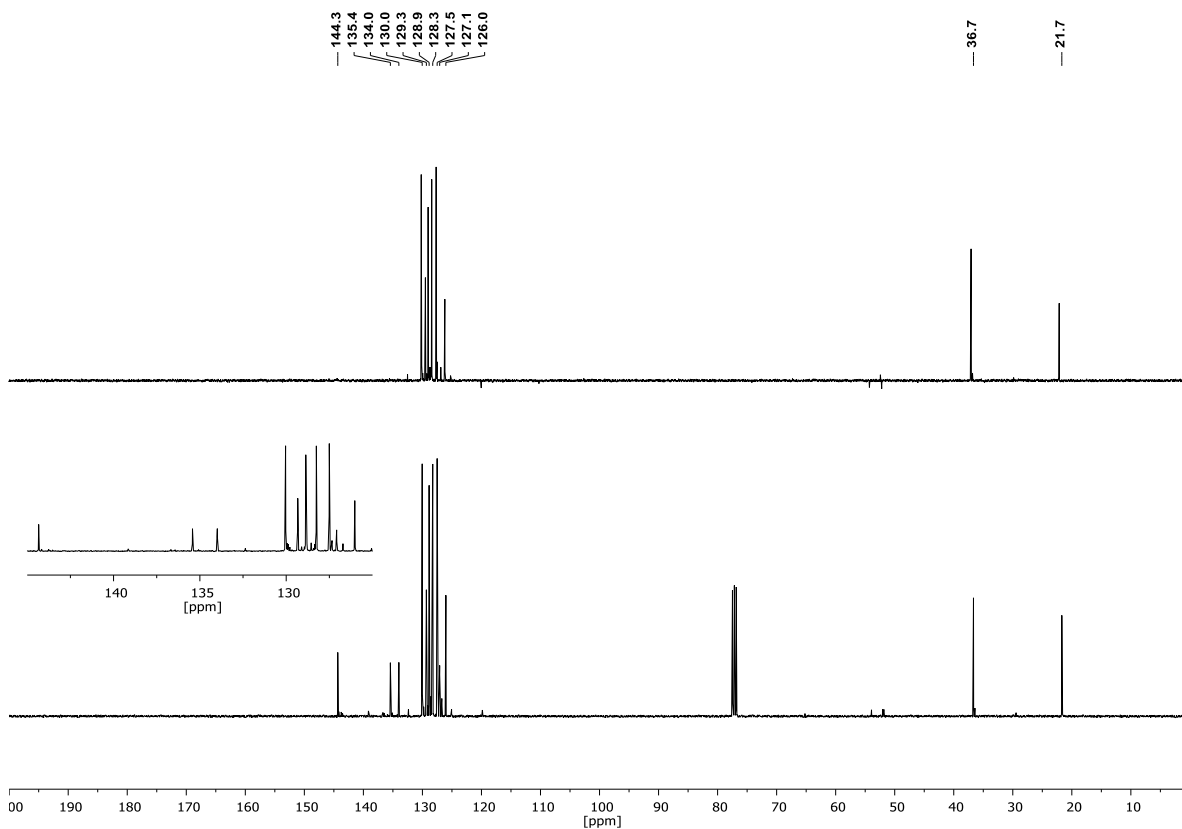
N-(2-chloro-2-(4-cyanophenyl)ethyl)-N,4-dimethylbenzenesulfonamide (18i)

^{1}H-NMR (400 MHz, CDCl$_3$):
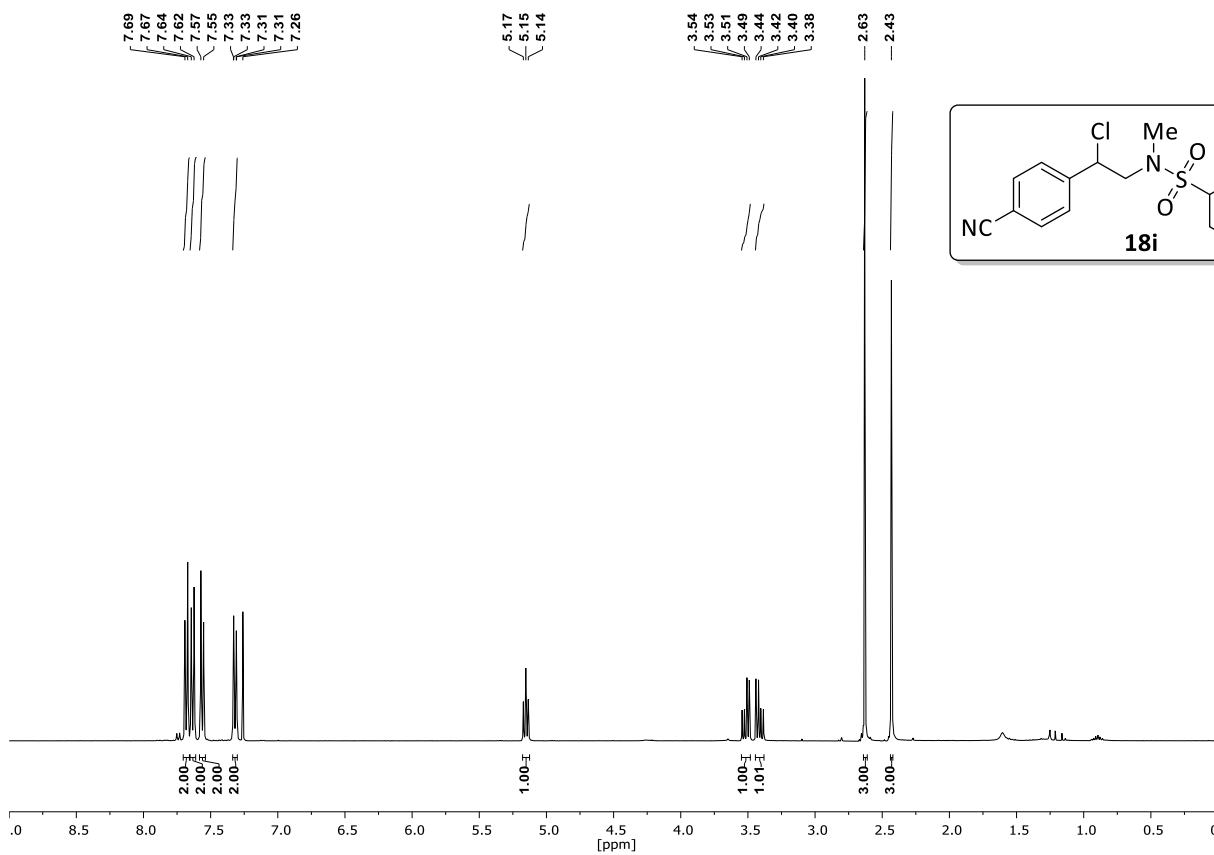
^{13}C-NMR (101 MHz, CDCl$_3$) & **DEPT135** (101 MHz, CDCl$_3$):
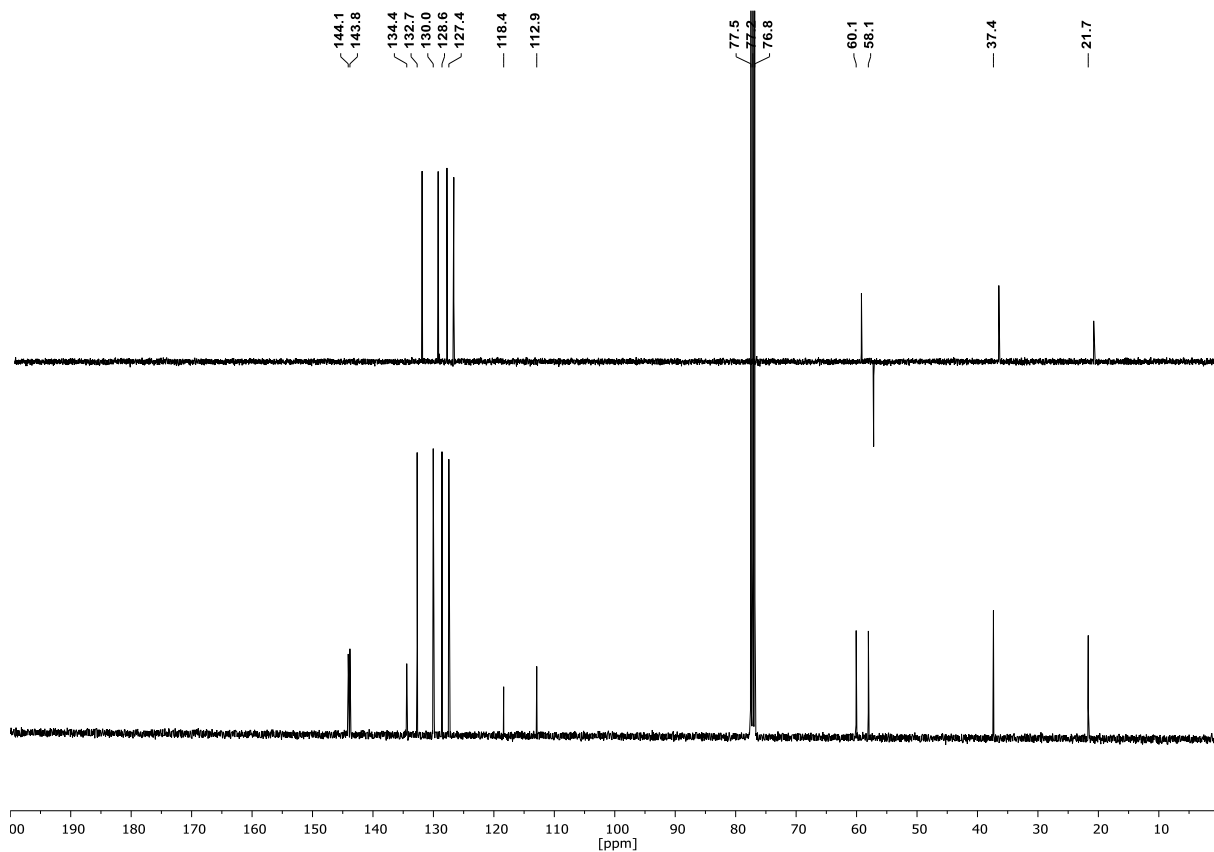
N-(2-chloro-2-(4-nitrophenyl)ethyl)-N,4-dimethylbenzenesulfonamide (18j)

¹H-NMR (400 MHz, CDCl₃):
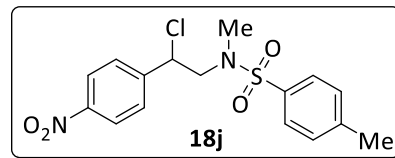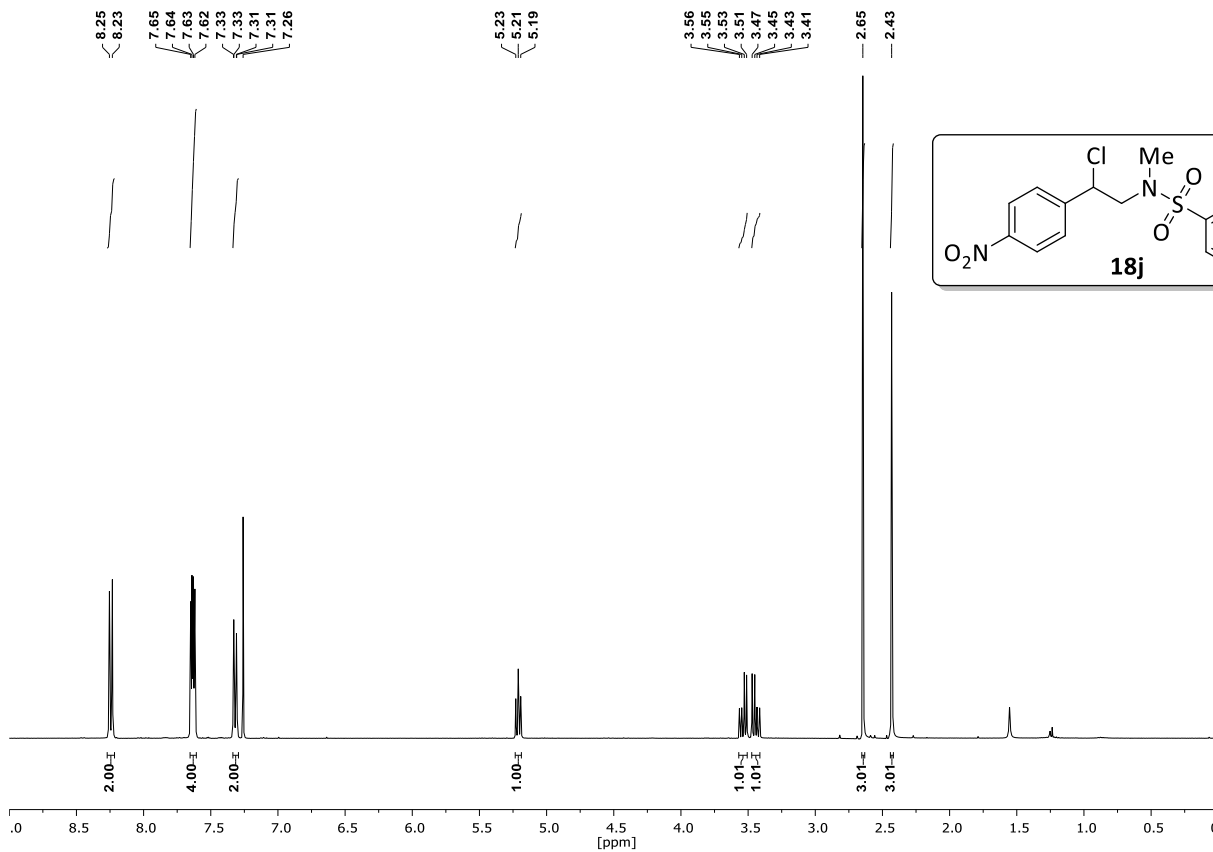
¹³C-NMR (101 MHz, CDCl₃) & **DEPT135** (101 MHz, CDCl₃):

13C-NMR peaks: 148.2, 145.7, 144.1, 134.4, 130.1, 128.8, 127.5, 124.1, 59.7, 58.1, 37.4, 21.7
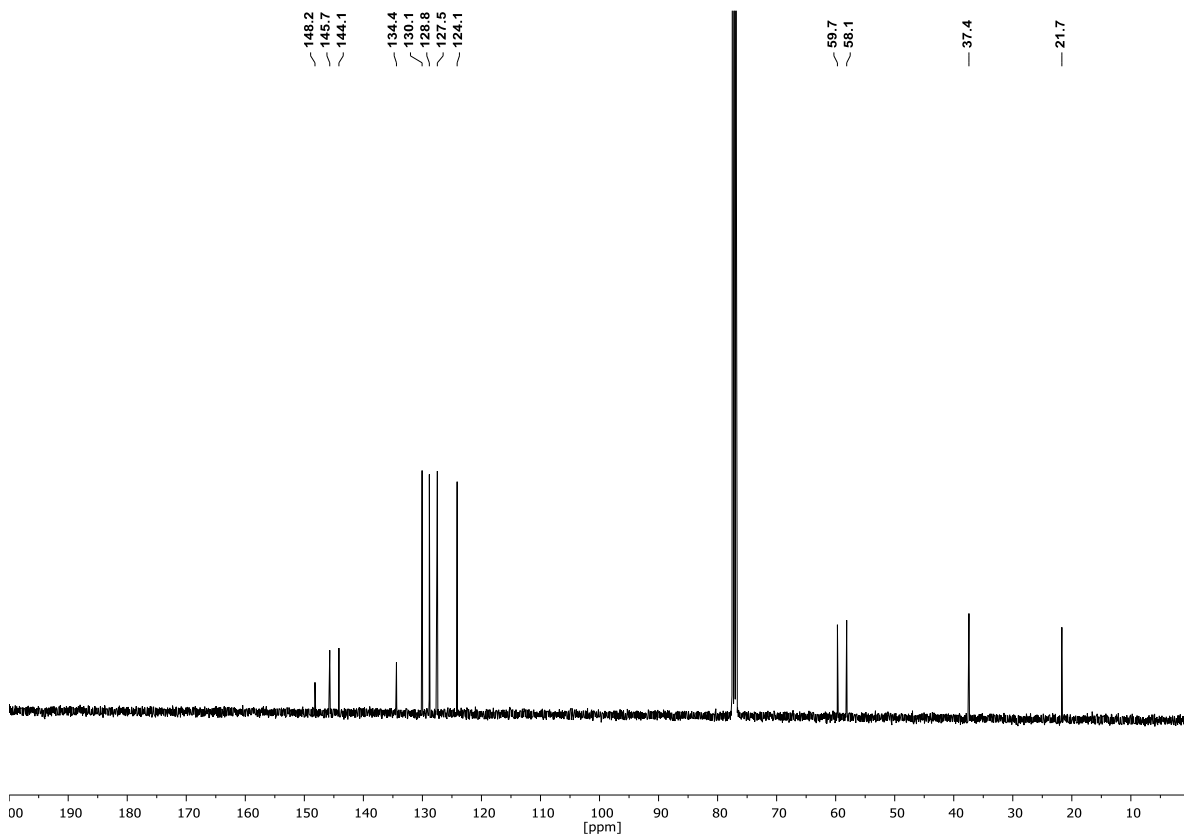
Methyl 4-(1-chloro-2-((*N*,4-dimethylphenyl)sulfonamido)ethyl)benzoate (18k)

¹H-NMR (300 MHz, CDCl₃):
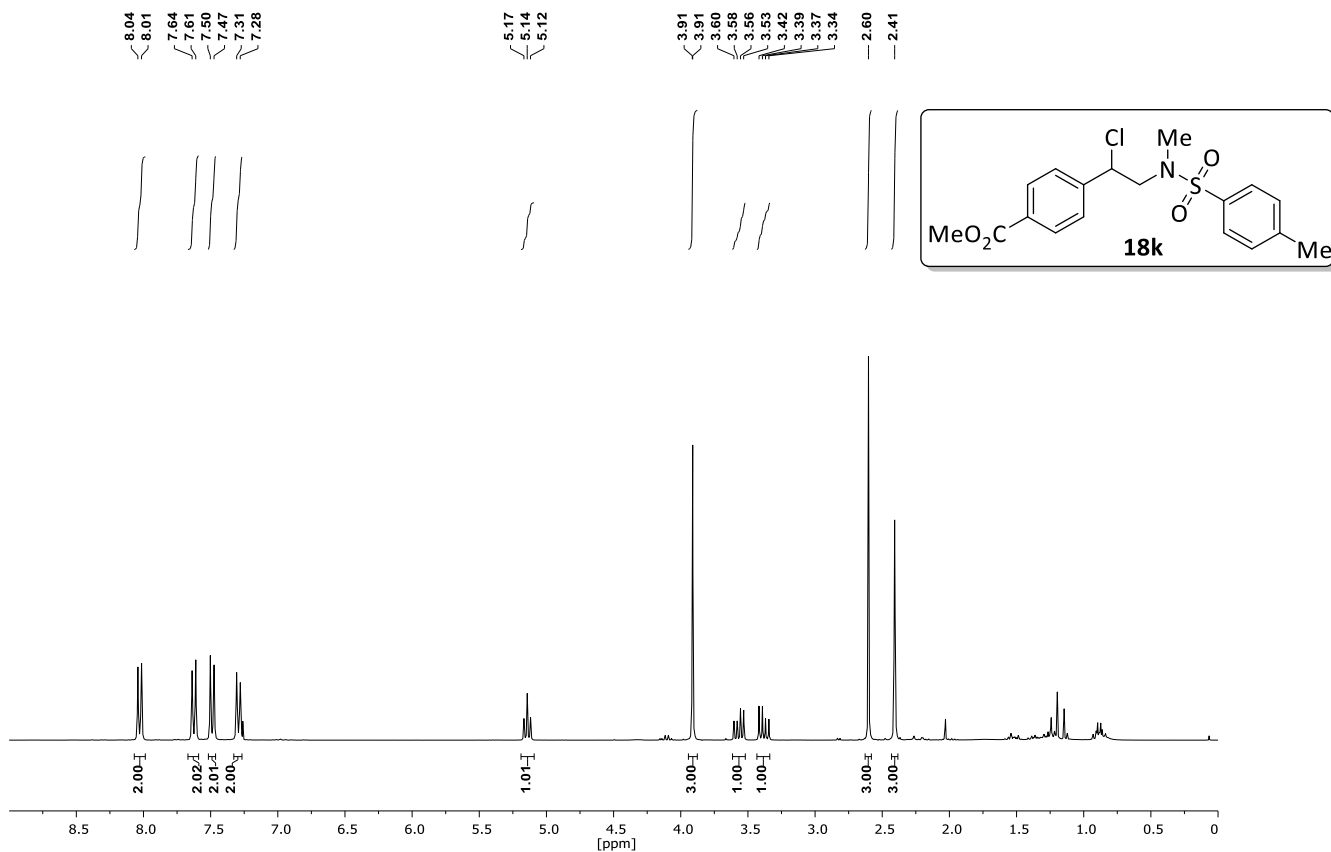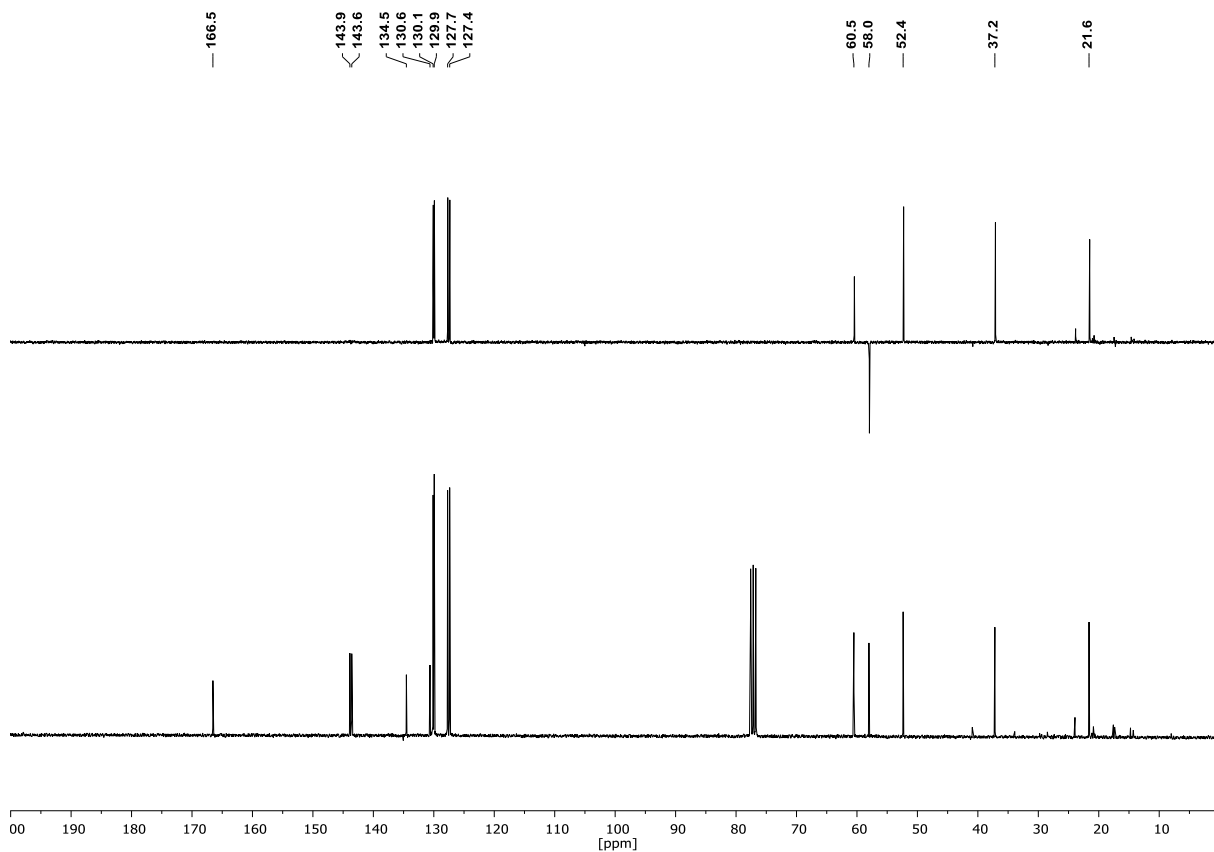
¹H-NMR peaks: 8.04, 8.01, 7.64, 7.61, 7.50, 7.47, 7.31, 7.28, 5.17, 5.14, 5.12, 3.91, 3.91, 3.60, 3.58, 3.56, 3.53, 3.42, 3.39, 3.37, 3.34, 2.60, 2.41

Integrations: 2.00, 2.02, 2.01, 2.00, 1.01, 3.00, 1.00, 1.00, 3.00, 3.00

¹³C-NMR (75 MHz, CDCl₃) & **DEPT135** (75 MHz, CDCl₃):

13C peaks: —166.5 143.9 143.6 134.5 130.6 130.1 129.9 127.7 127.4 60.5 58.0 52.4 37.2 21.6

[ppm scale: 00 190 180 170 160 150 140 130 120 110 100 90 80 70 60 50 40 30 20 10]

Methyl 4-(1-chloro-2-((*N*,4-dimethylphenyl)sulfonamido)ethyl)benzoate (18l)

1H-NMR (400 MHz, CDCl$_3$):

1H peaks: 7.65 7.65 7.64 7.64 7.63 7.63 7.62 7.57 7.55 7.32 7.32 7.32 7.30 7.30 7.30 7.26 5.19 5.17 5.15 3.57 3.55 3.54 3.52 3.46 3.44 3.42 3.40 2.64 2.43

Structure label: **18l**, CF$_3$, Cl, Me, N, S, O, O, Me

Integrations: 3.94 / 2.00 / 1.99 ; 1.00 ; 1.01 / 1.01 ; 2.98 / 3.00

[ppm scale: .0 8.5 8.0 7.5 7.0 6.5 6.0 5.5 5.0 4.5 4.0 3.5 3.0 2.5 2.0 1.5 1.0 0.5 0]
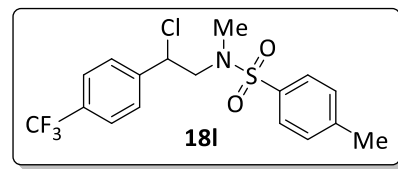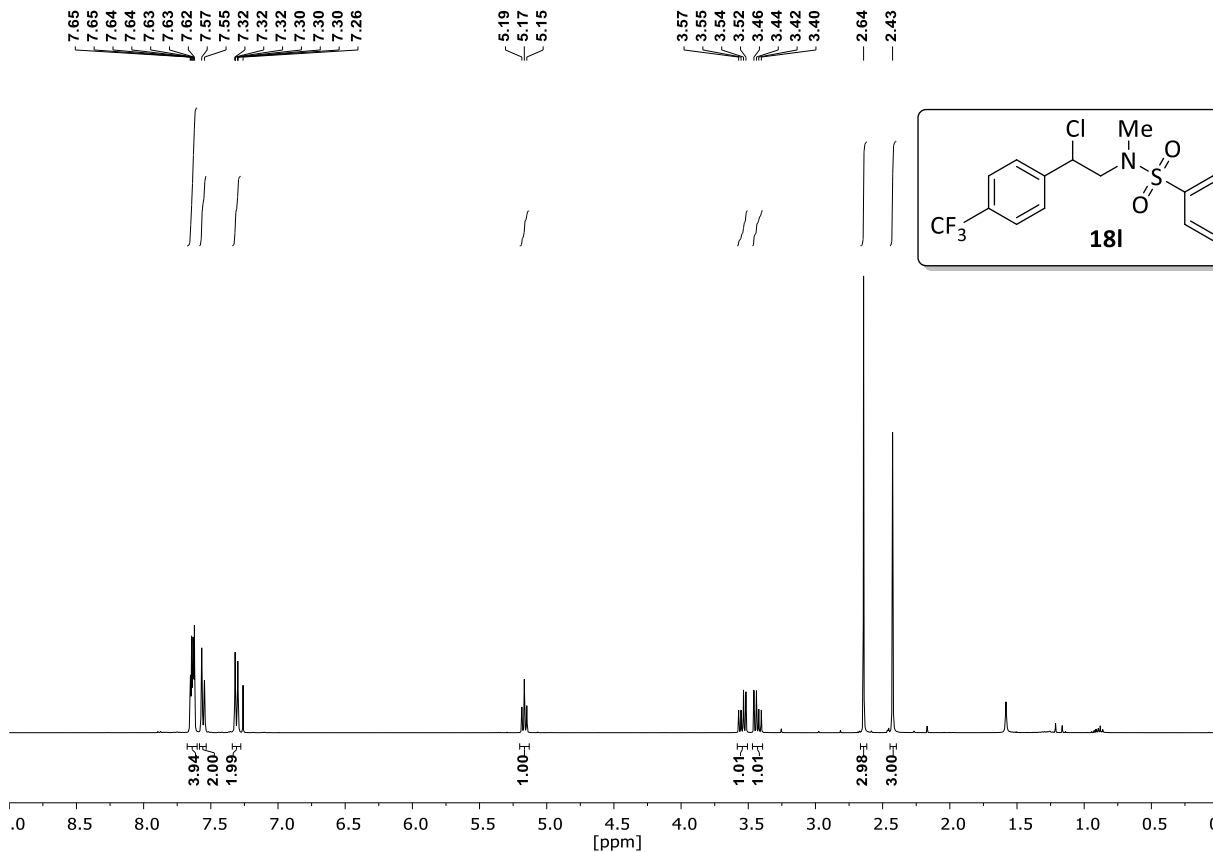
13C-NMR (101 MHz, CDCl$_3$) & **DEPT135** (101 MHz, CDCl$_3$):
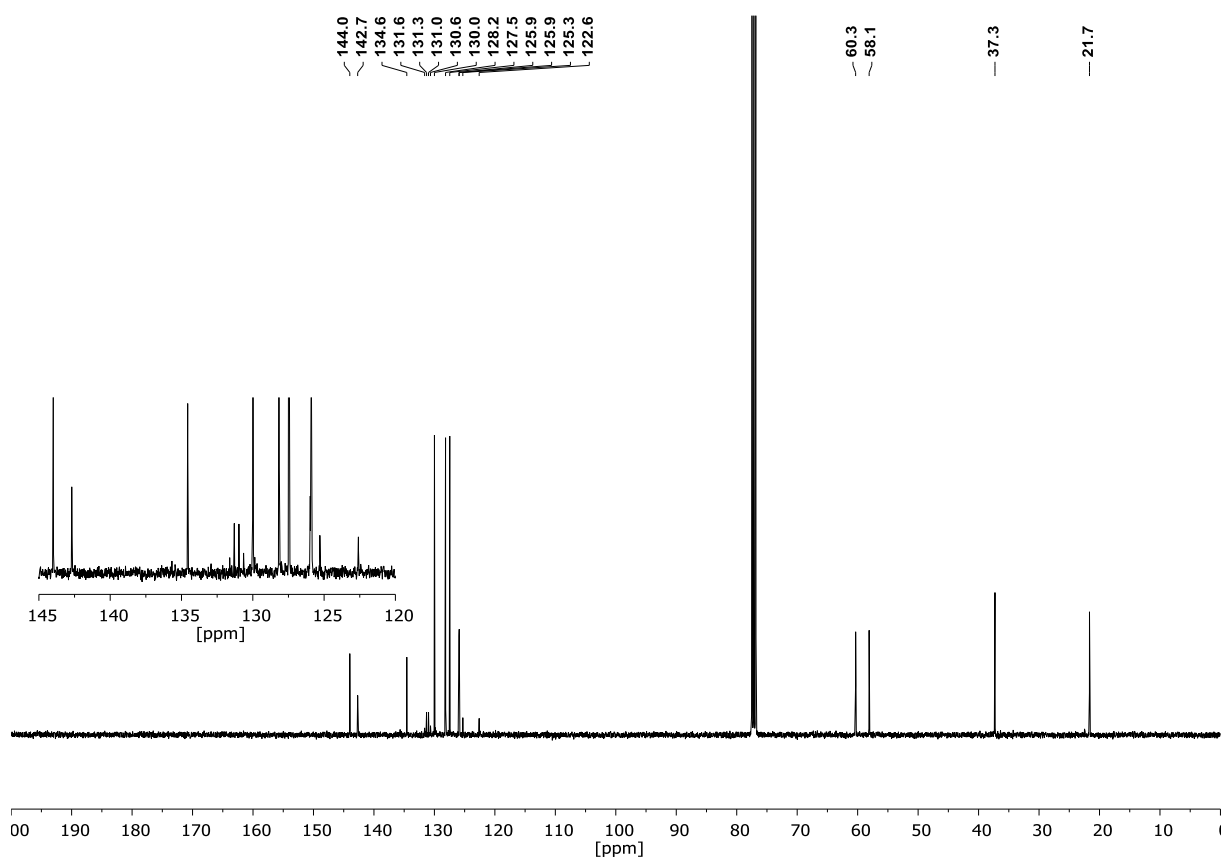
¹⁹F-NMR (377 MHz, CDCl₃):
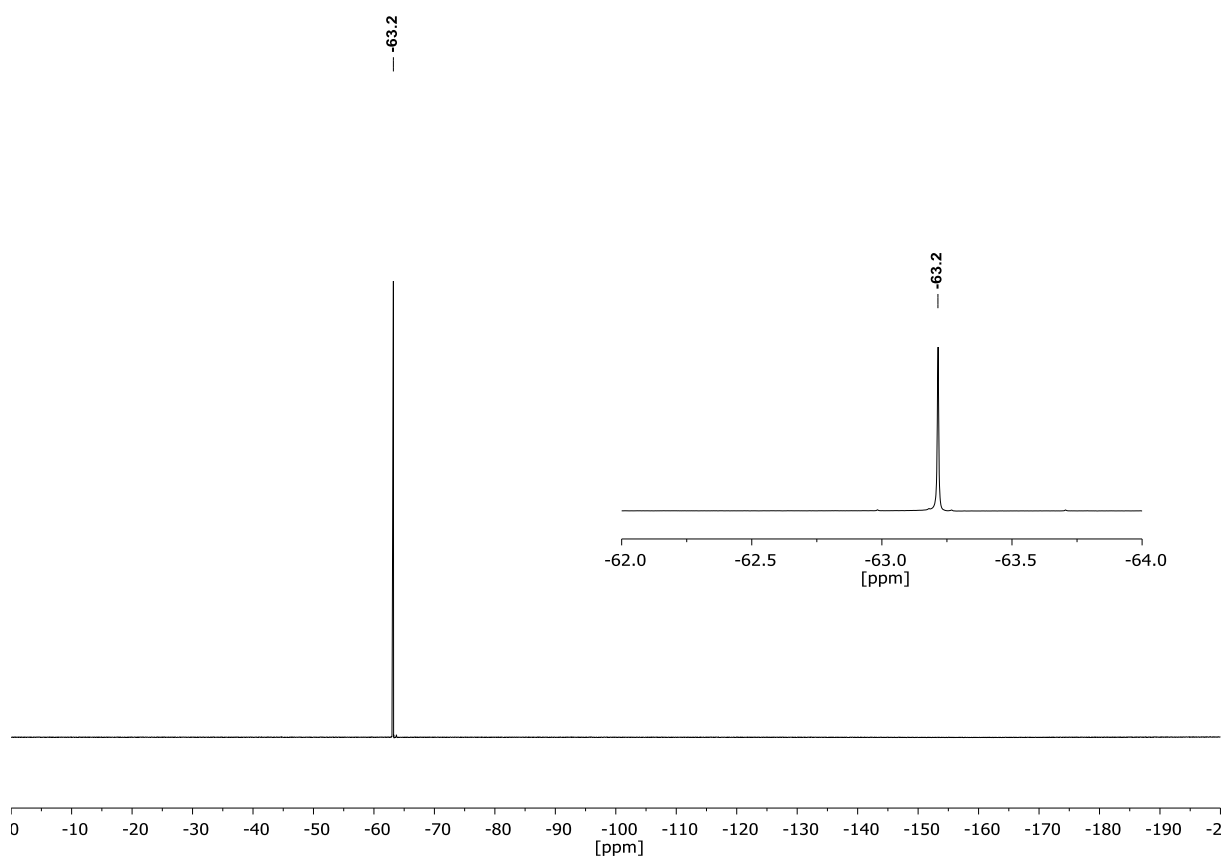
N-(2-chloro-2-(4-fluorophenyl)ethyl)-*N*,4-dimethylbenzenesulfonamide (18m)

¹H-NMR (400 MHz, CDCl₃):
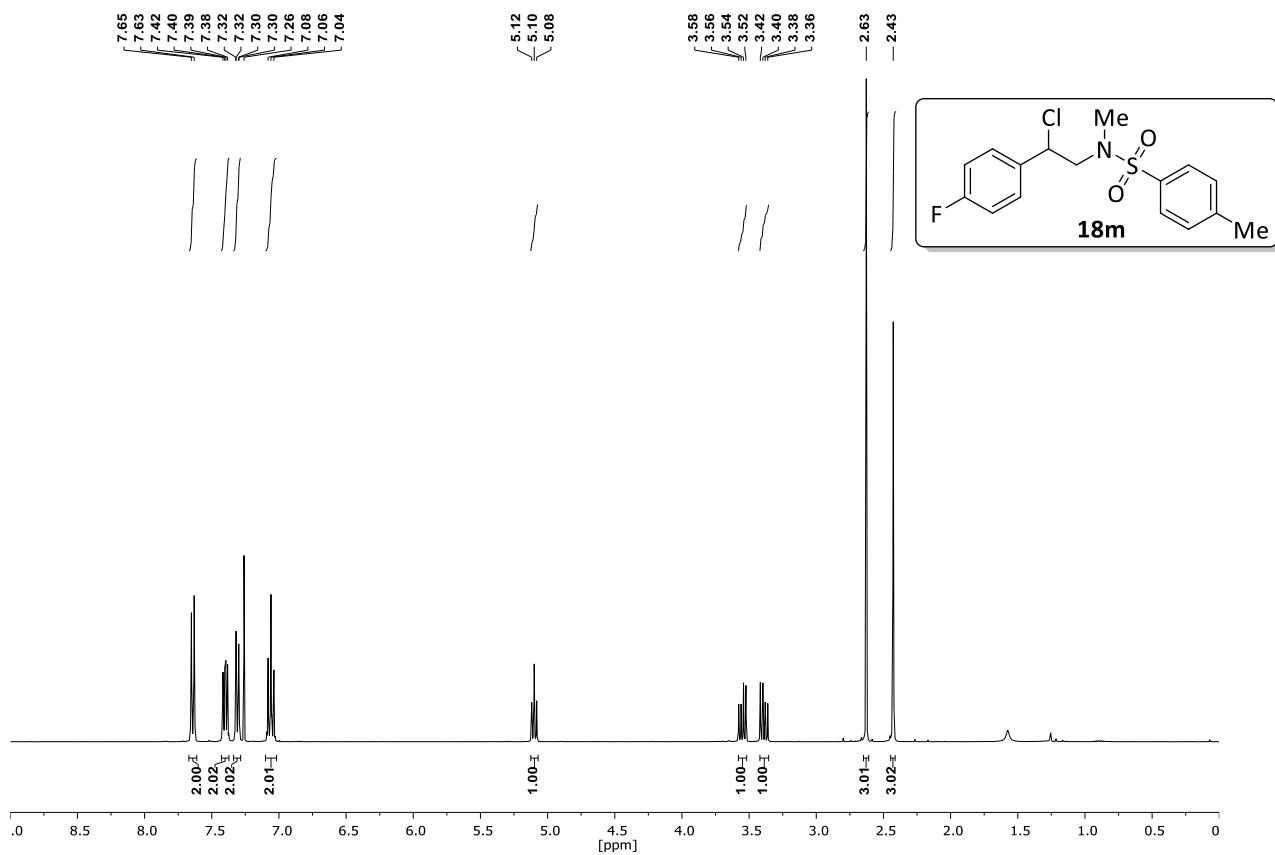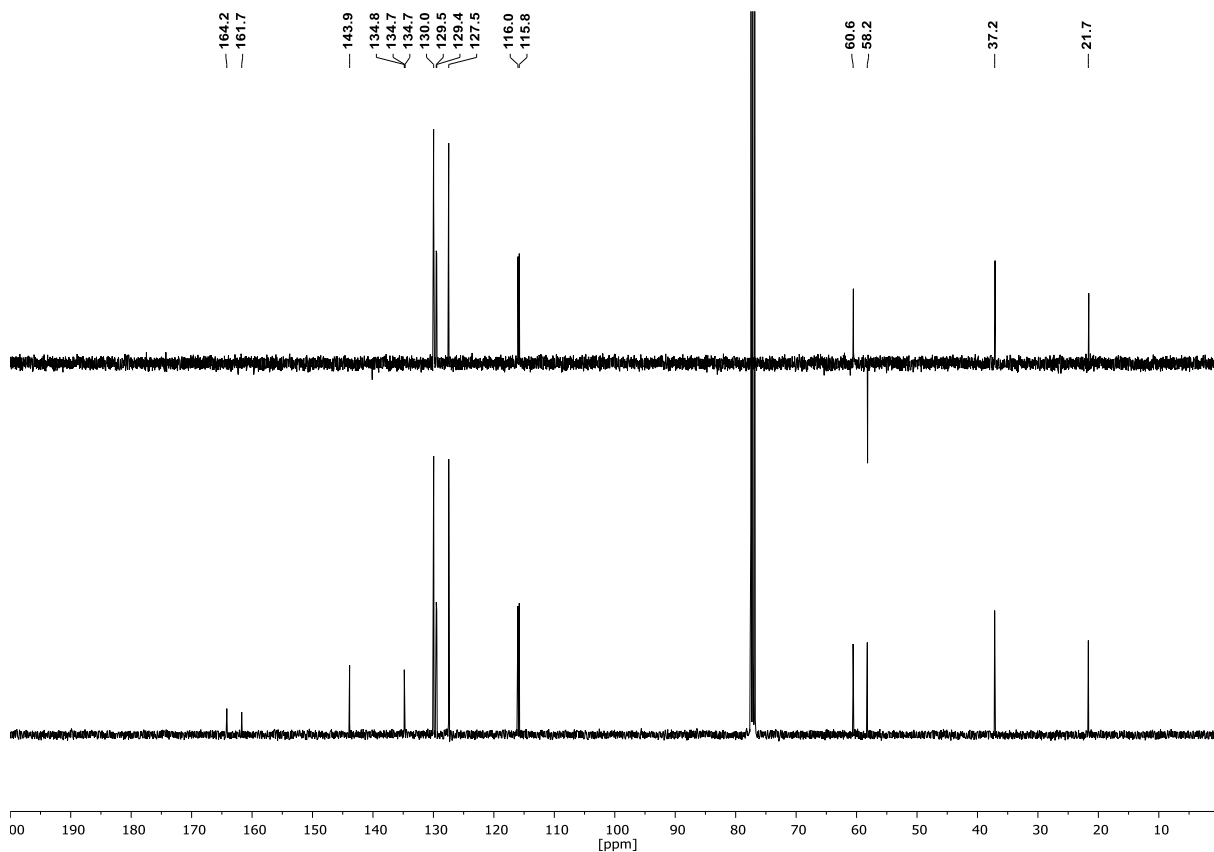
¹³C-NMR (101 MHz, CDCl₃) & **DEPT135** (101 MHz, CDCl₃):

¹⁹F-NMR (282 MHz, CDCl₃):

—-113.0

0   -10   -20   -30   -40   -50   -60   -70   -80   -90   -100   -110   -120   -130   -140   -150   -160   -170   -180   -190   -2
[ppm]
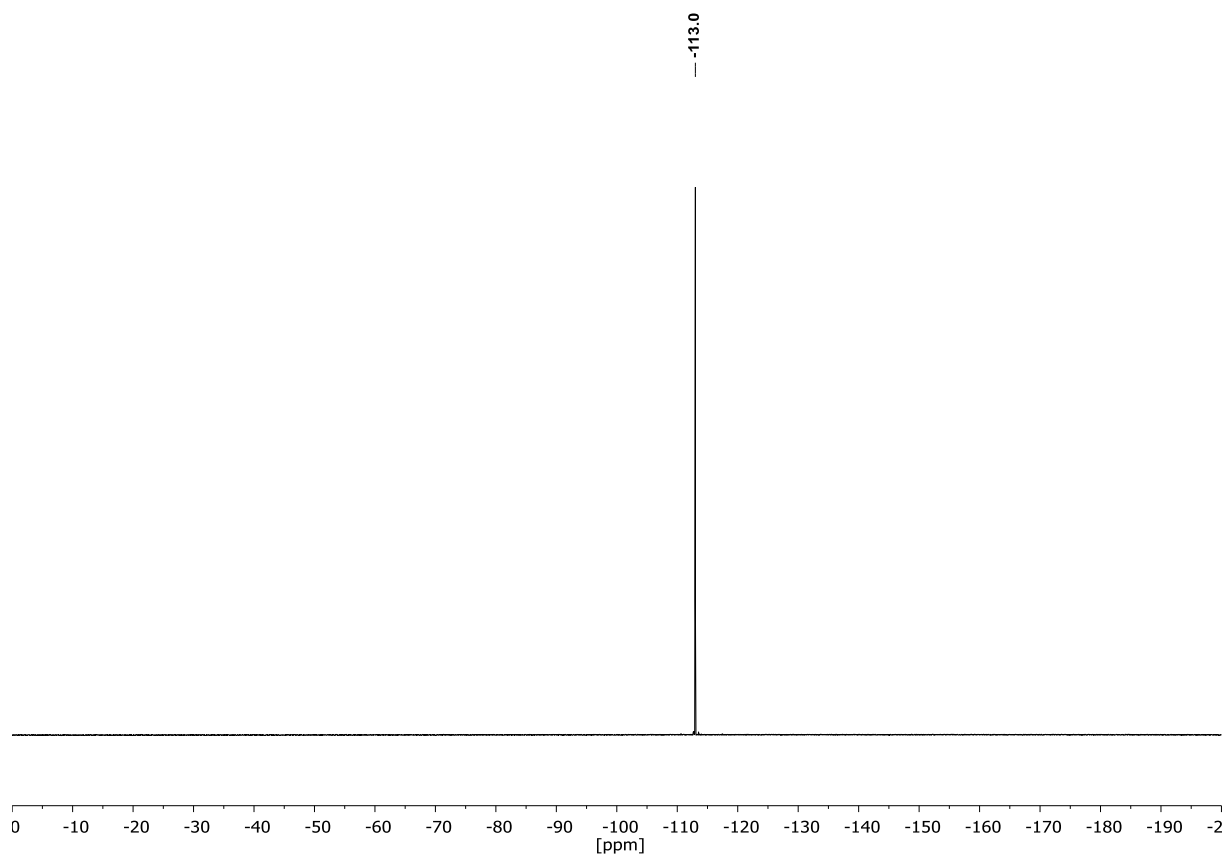
N-(2-chloro-2-(4-chlorophenyl)ethyl)-*N*,4-dimethylbenzenesulfonamide (18n)

¹H-NMR (300 MHz, CDCl₃):
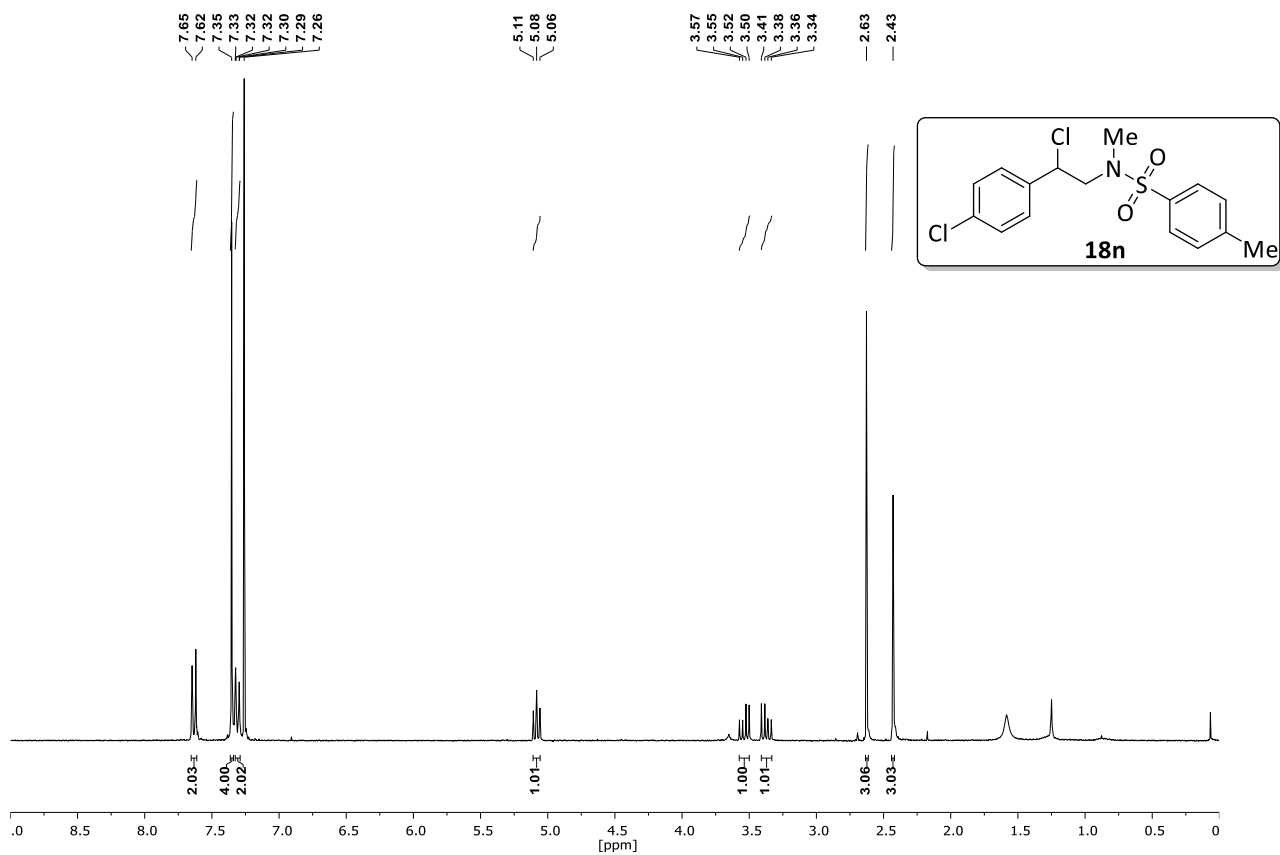
¹³C-NMR (75 MHz, CDCl₃) & **DEPT135** (75 MHz, CDCl₃):
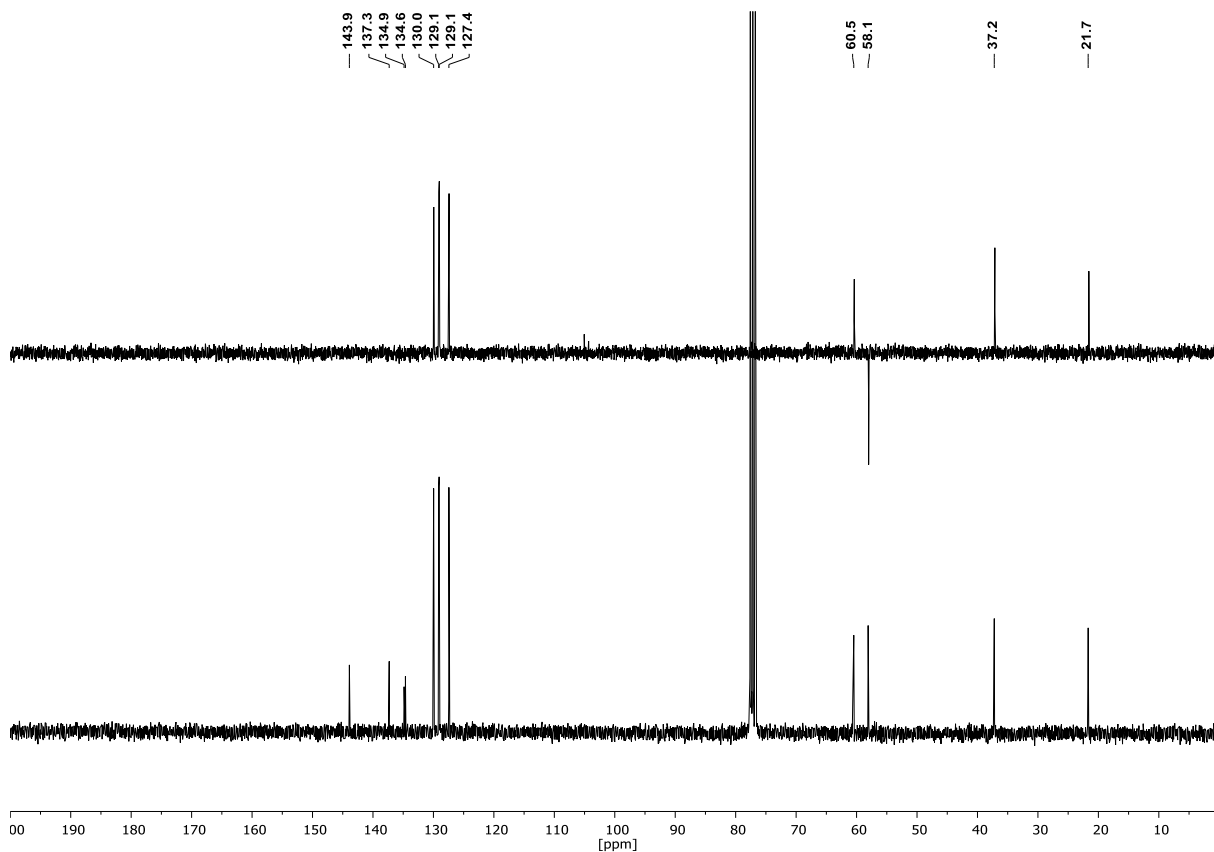
N-(2-(4-bromophenyl)-2-chloroethyl)-*N*,4-dimethylbenzenesulfonamide (18o)

^{1}H-NMR (300 MHz, CDCl$_3$):
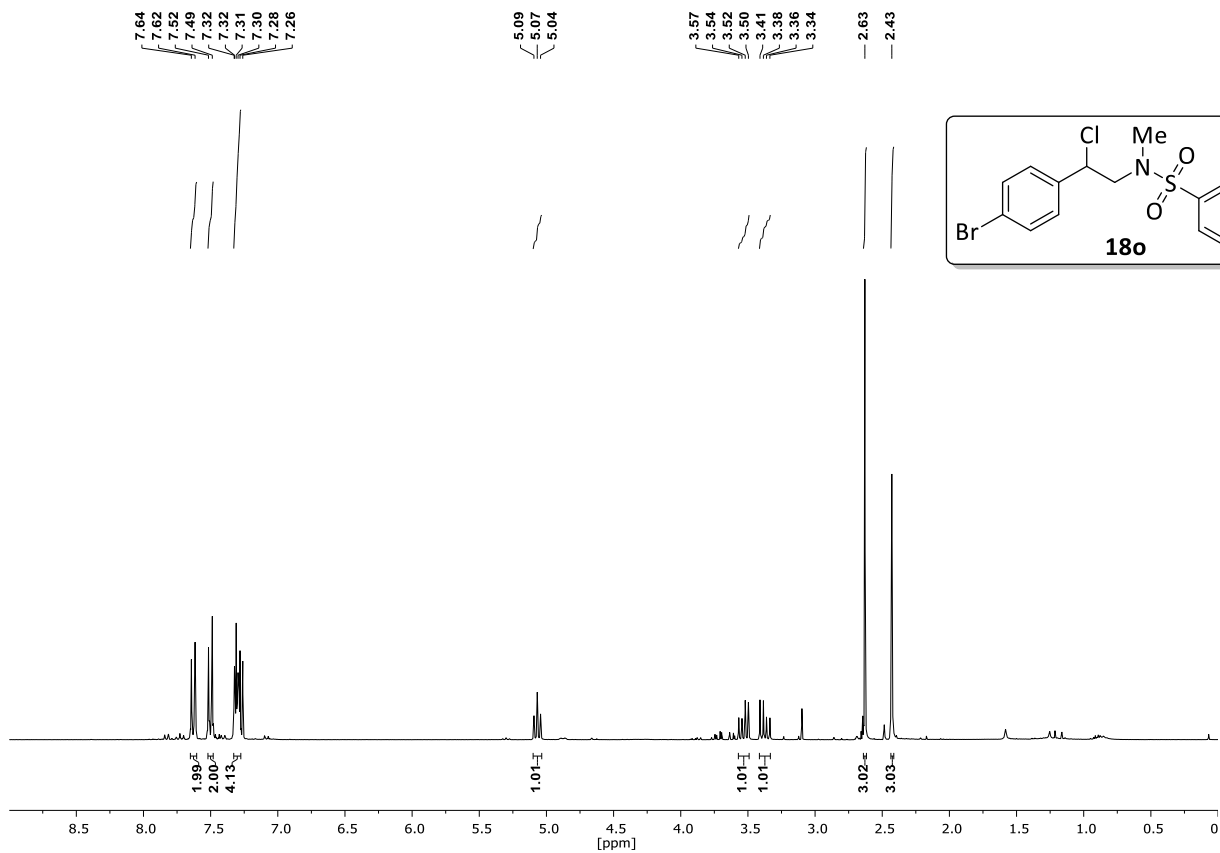
^{13}C-NMR (75 MHz, CDCl$_3$) & **DEPT135** (75 MHz, CDCl$_3$):
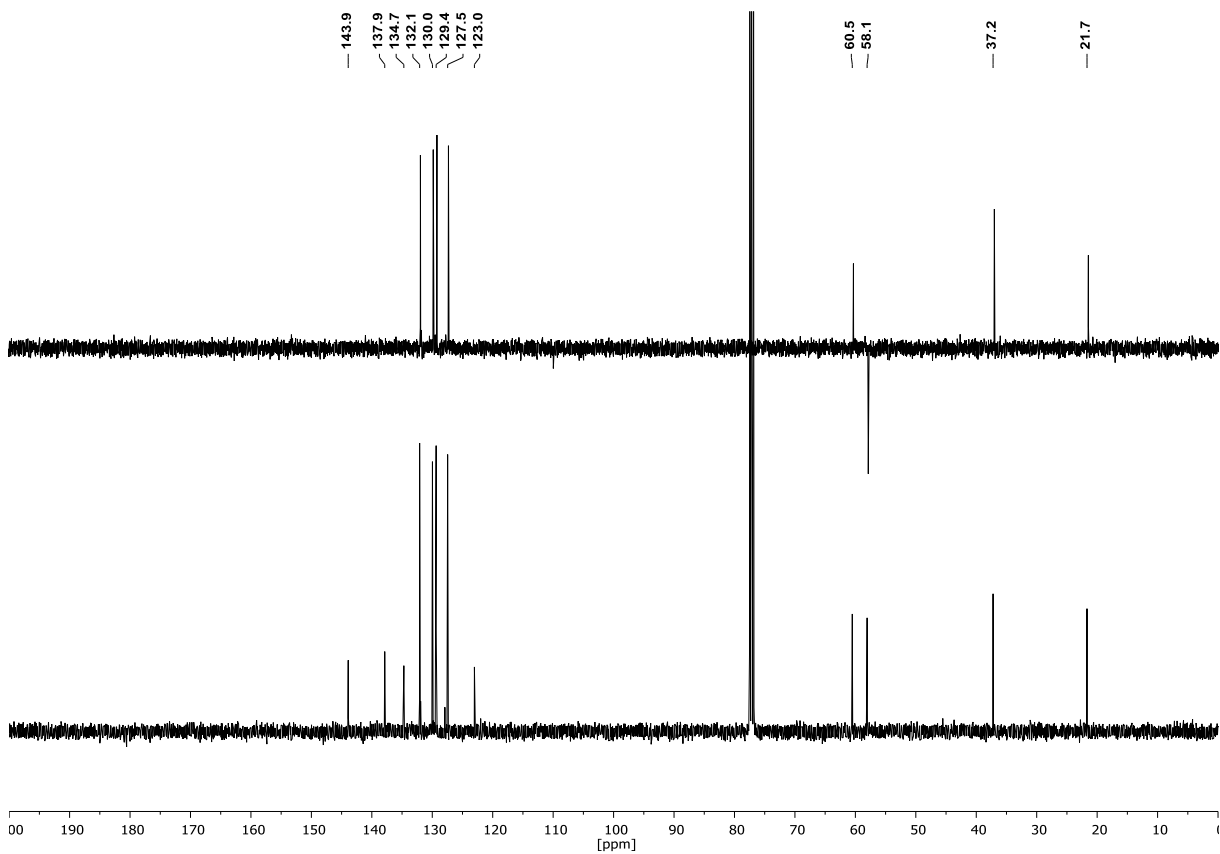
N-(2-chloro-2-(3-chlorophenyl)ethyl)-*N*,4-dimethylbenzenesulfonamide (18p)

¹H-NMR (400 MHz, CDCl₃):
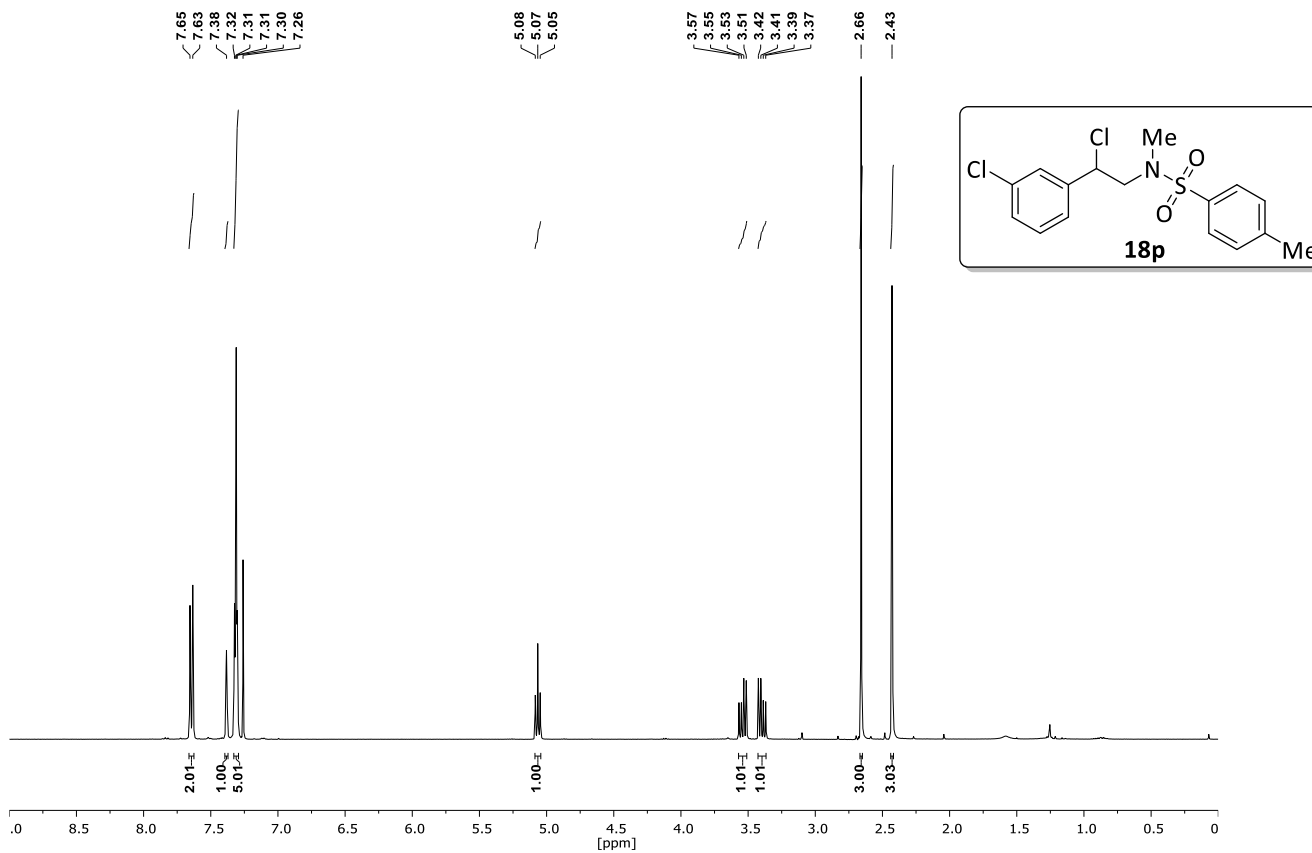
¹³C-NMR (101 MHz, CDCl₃) & **DEPT135** (101 MHz, CDCl₃):
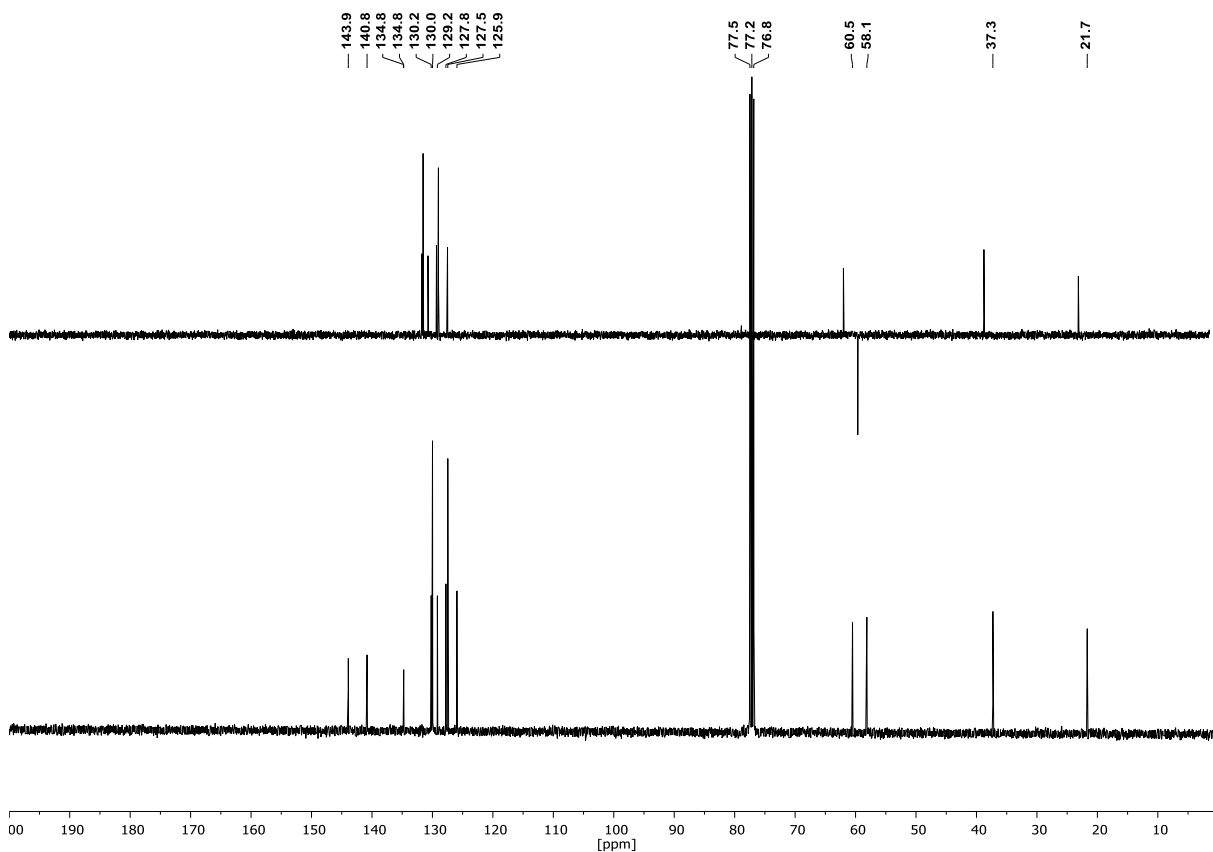
N-(2-chloro-2-(3-methoxyphenyl)ethyl)-*N*,4-dimethylbenzenesulfonamide (18q)

¹H-NMR (400 MHz, CDCl₃):
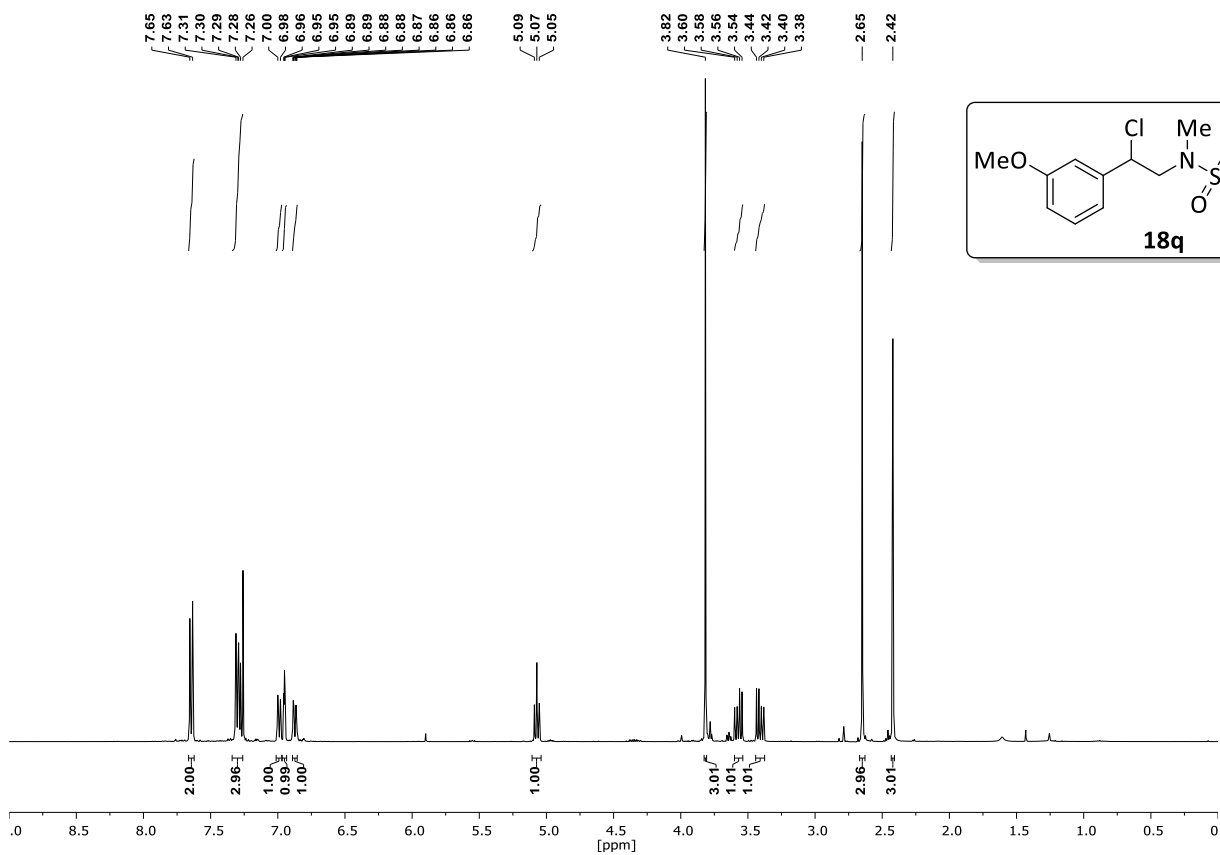
¹³C-NMR (101 MHz, CDCl₃) & **DEPT135** (101 MHz, CDCl₃):
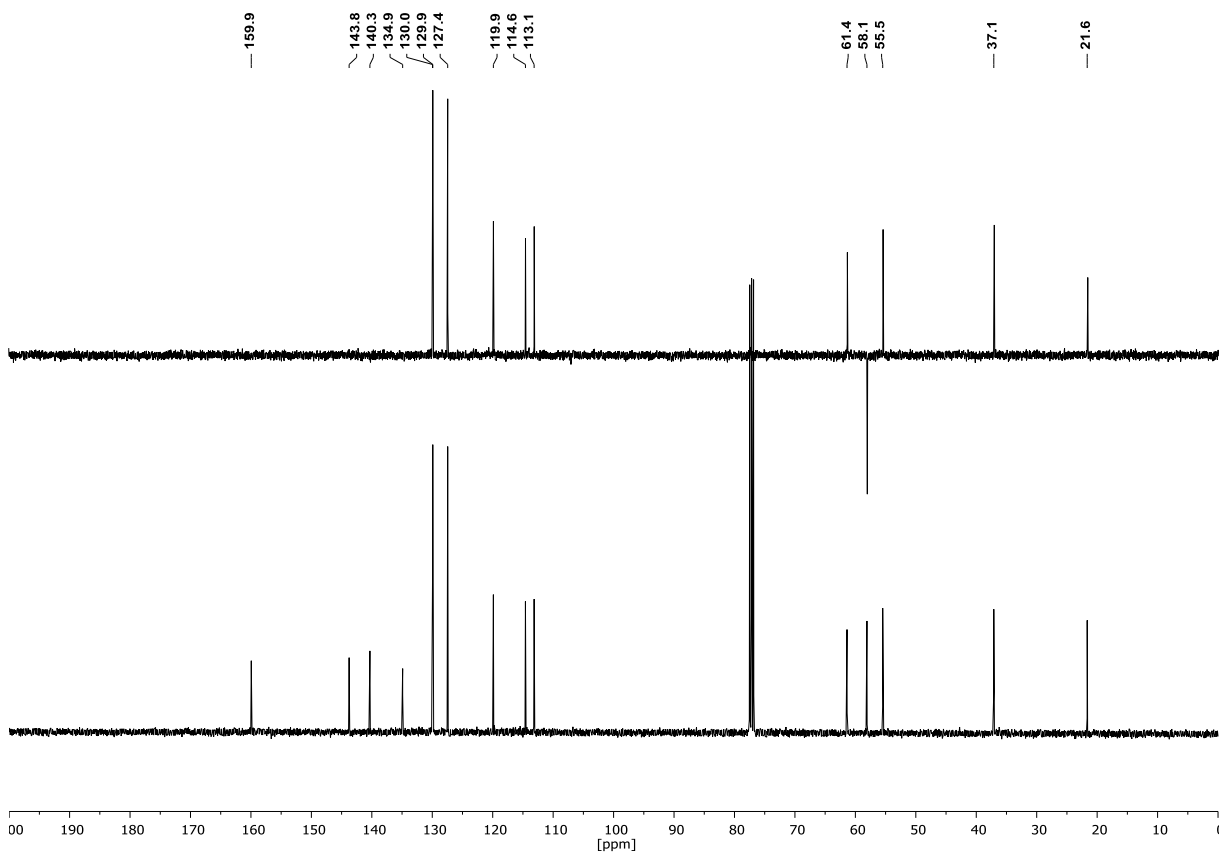
N-(2-chloro-2-(pyridin-2-yl)ethyl)-*N*,4-dimethylbenzenesulfonamide (18r)

¹H-NMR (400 MHz, CDCl₃):
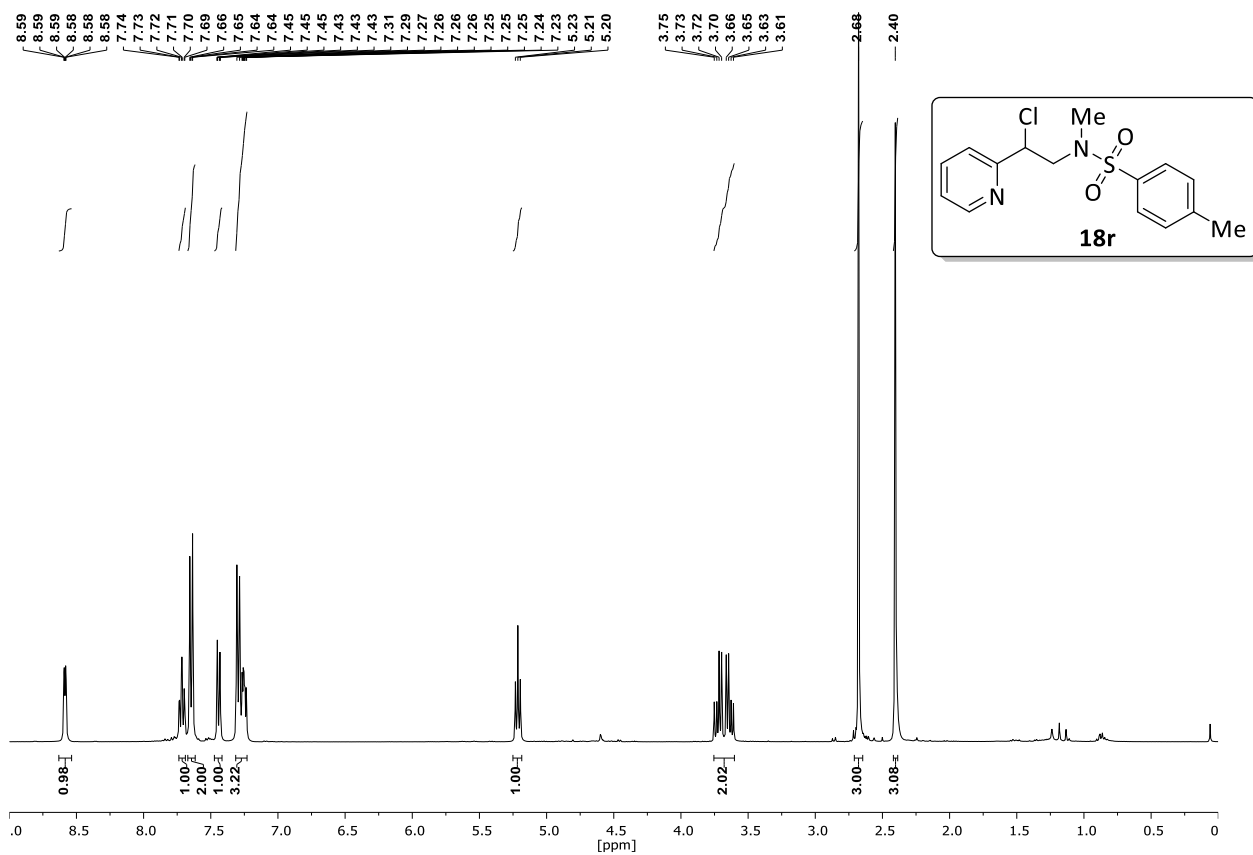
¹³C-NMR (101 MHz, CDCl₃) & **DEPT135** (101 MHz, CDCl₃):
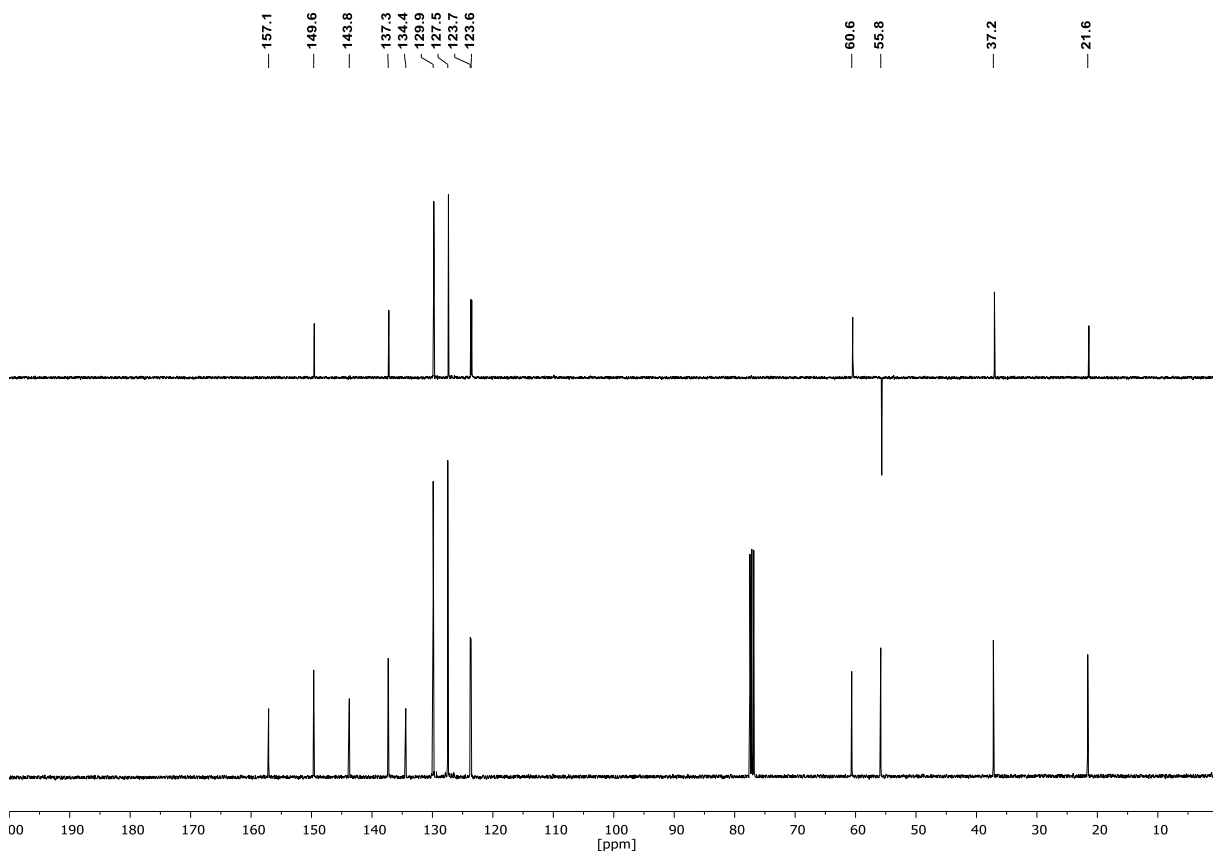
N-(2-chloro-2-(perfluorophenyl)ethyl)-N,4-dimethylbenzenesulfonamide (18s)

¹H-NMR (400 MHz, CDCl₃):
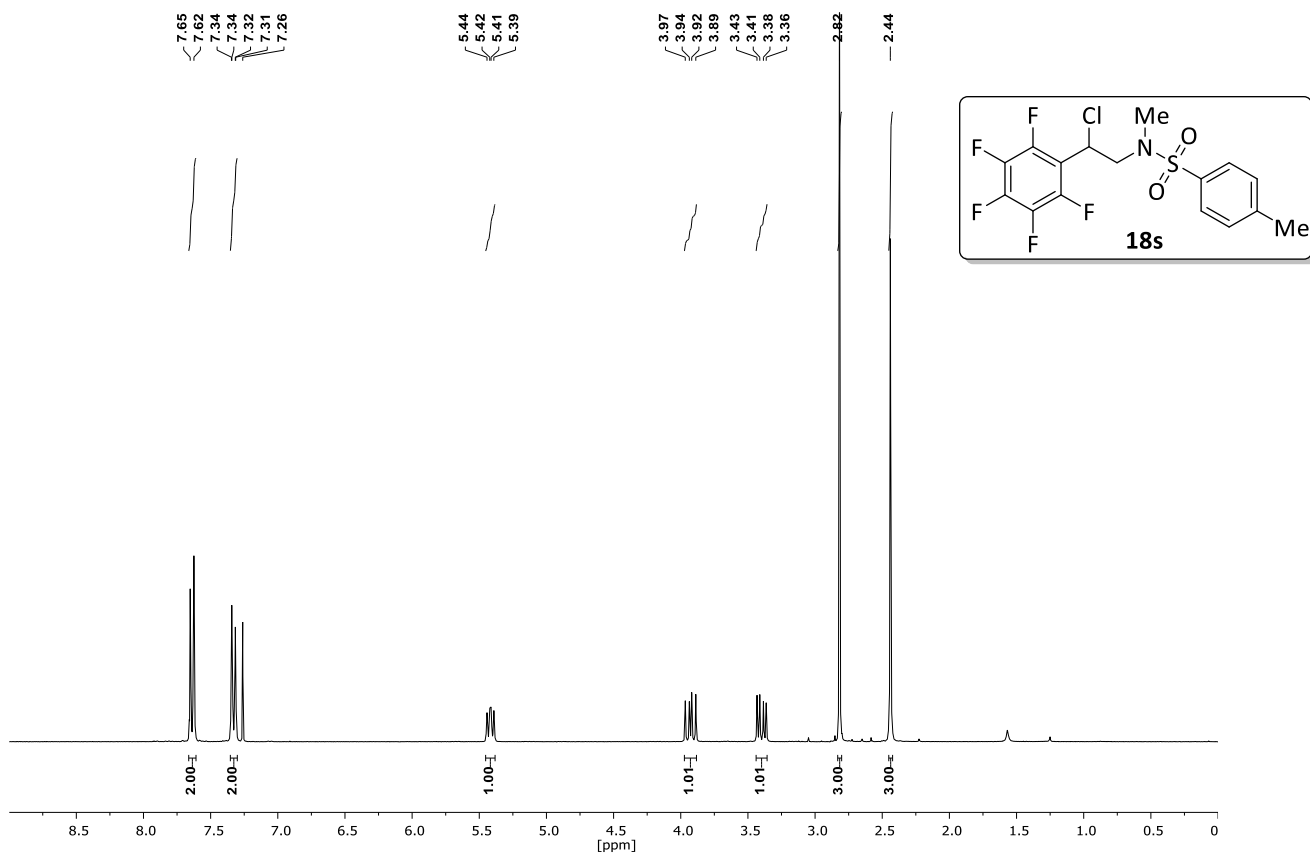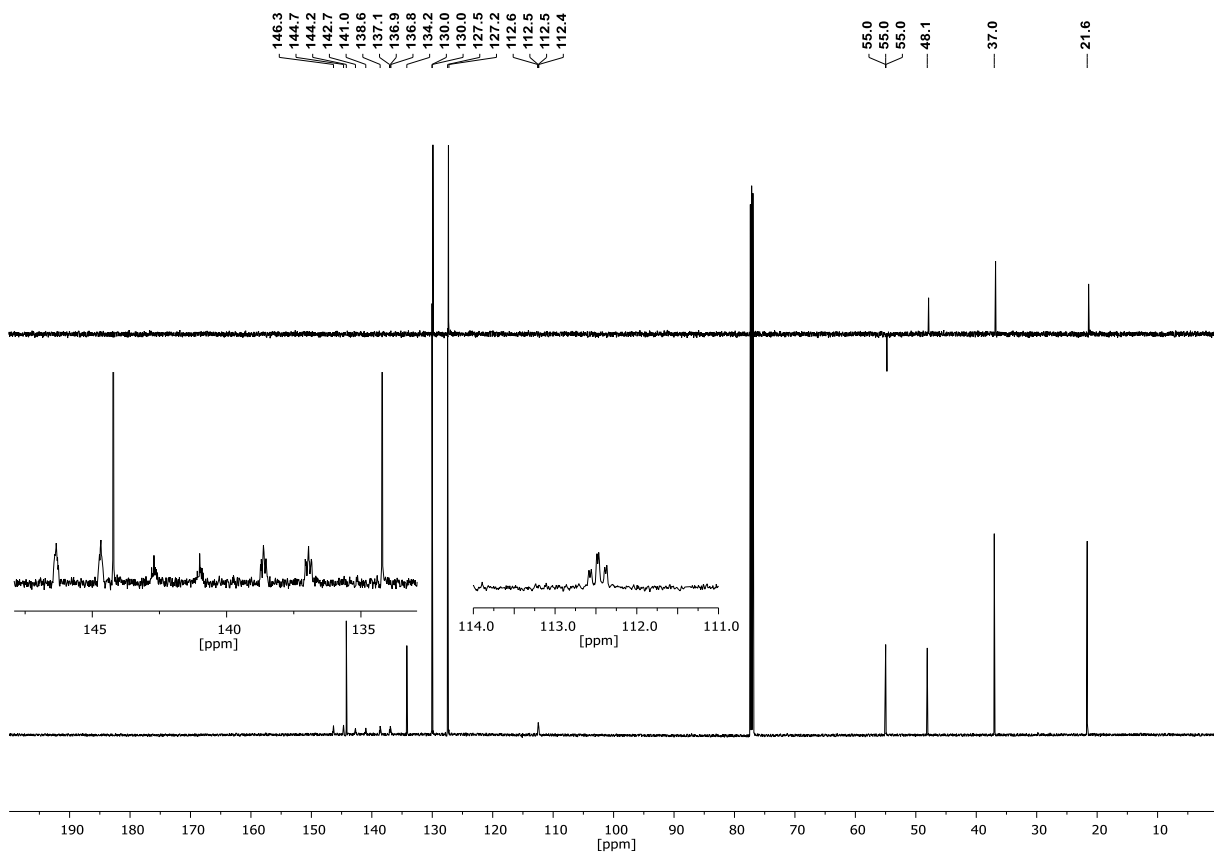
¹³C-NMR (101 MHz, CDCl₃) & **DEPT135** (101 MHz, CDCl₃):

¹⁹F-NMR (377 MHz, CDCl₃):
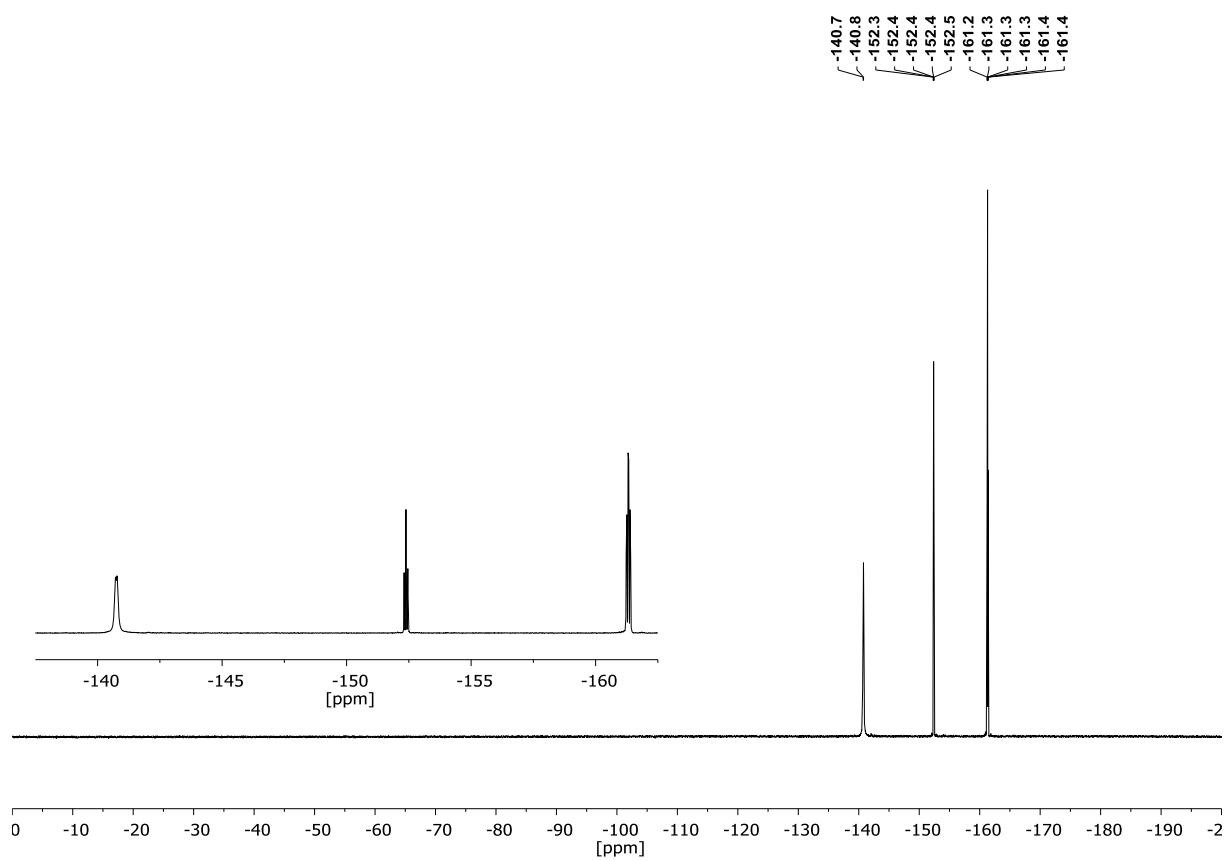
N-(2-chlorooctyl)-*N*,4-dimethylbenzenesulfonamide (18t)

¹H-NMR (300 MHz, CDCl₃):
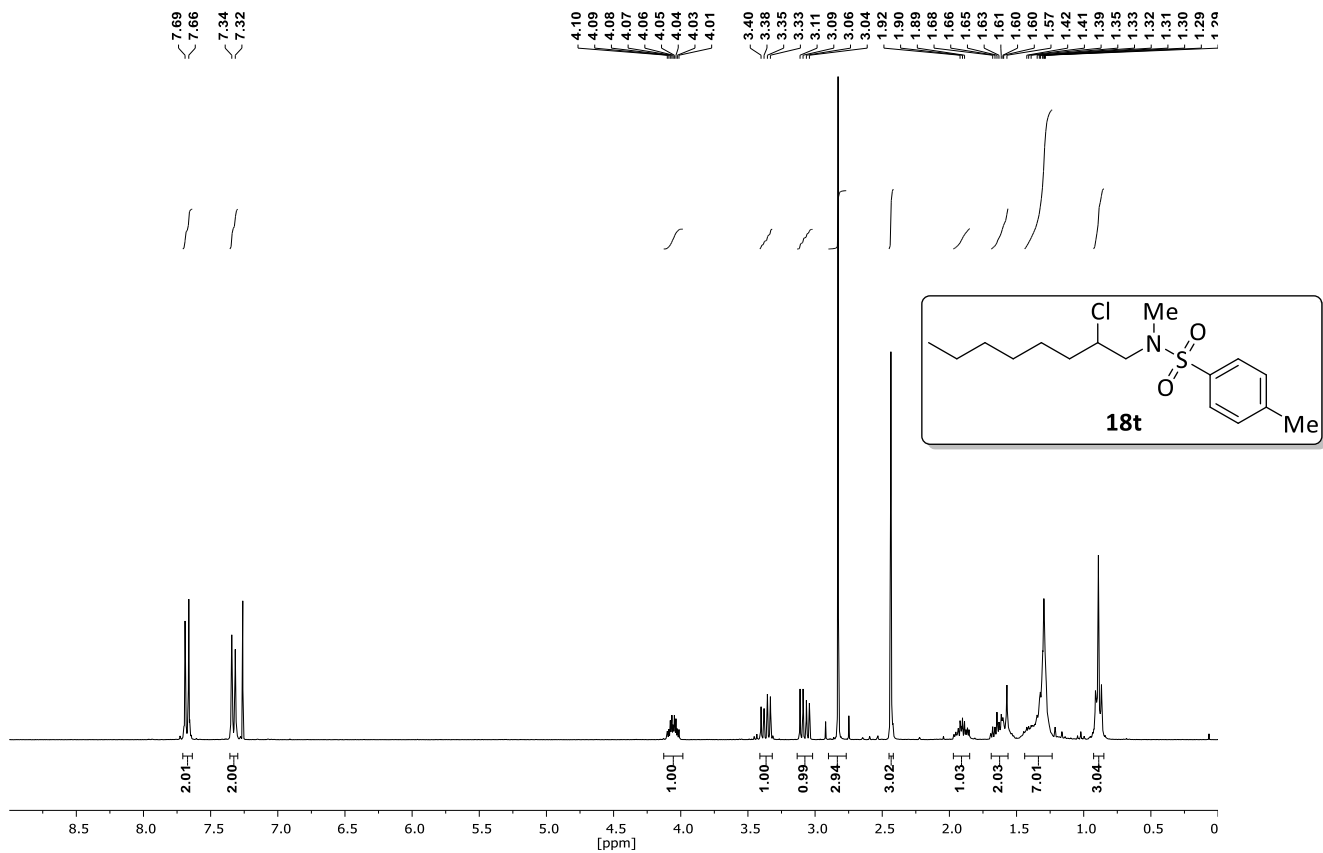
¹³C-NMR (75 MHz, CDCl₃) & **DEPT135** (75 MHz, CDCl₃):
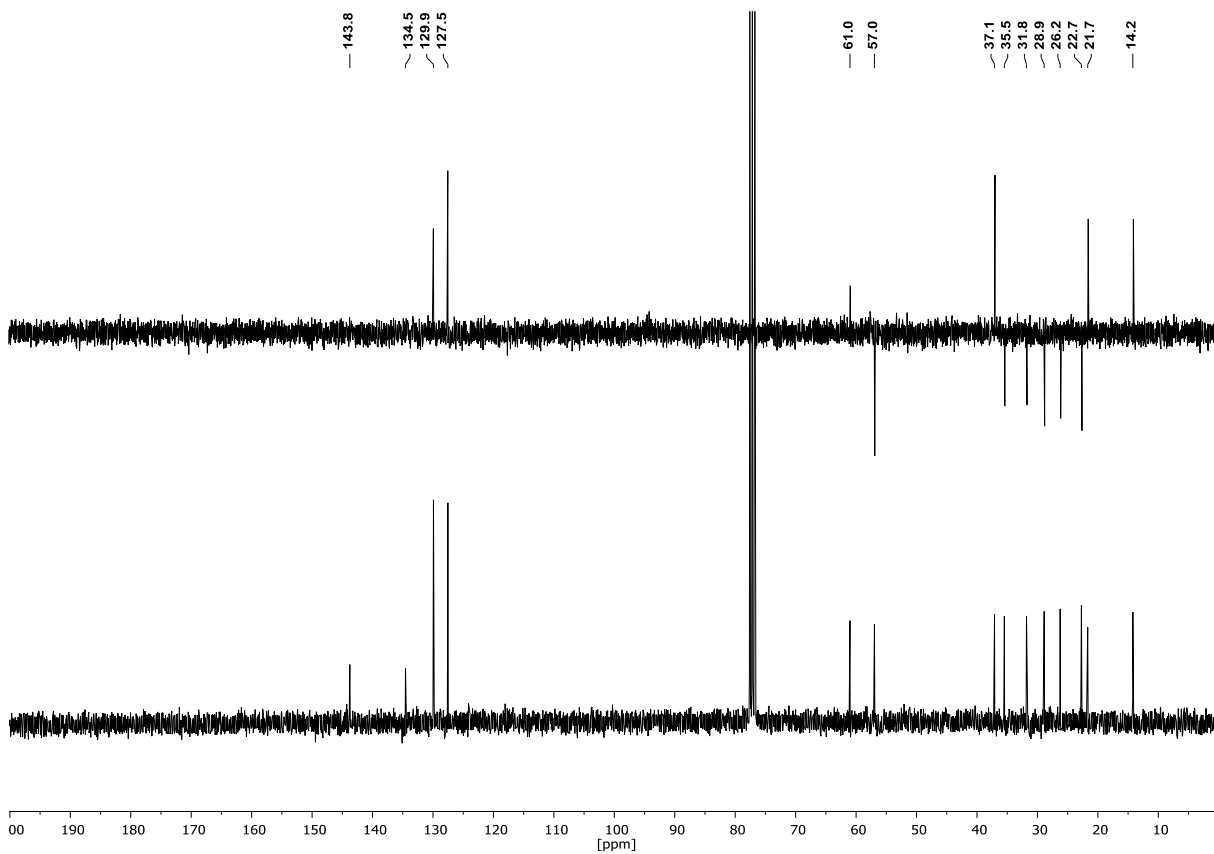
N-(2-chloro-3-phenylpropyl)-*N*,4-dimethylbenzenesulfonamide (26)

¹H-NMR (400 MHz, CDCl₃):
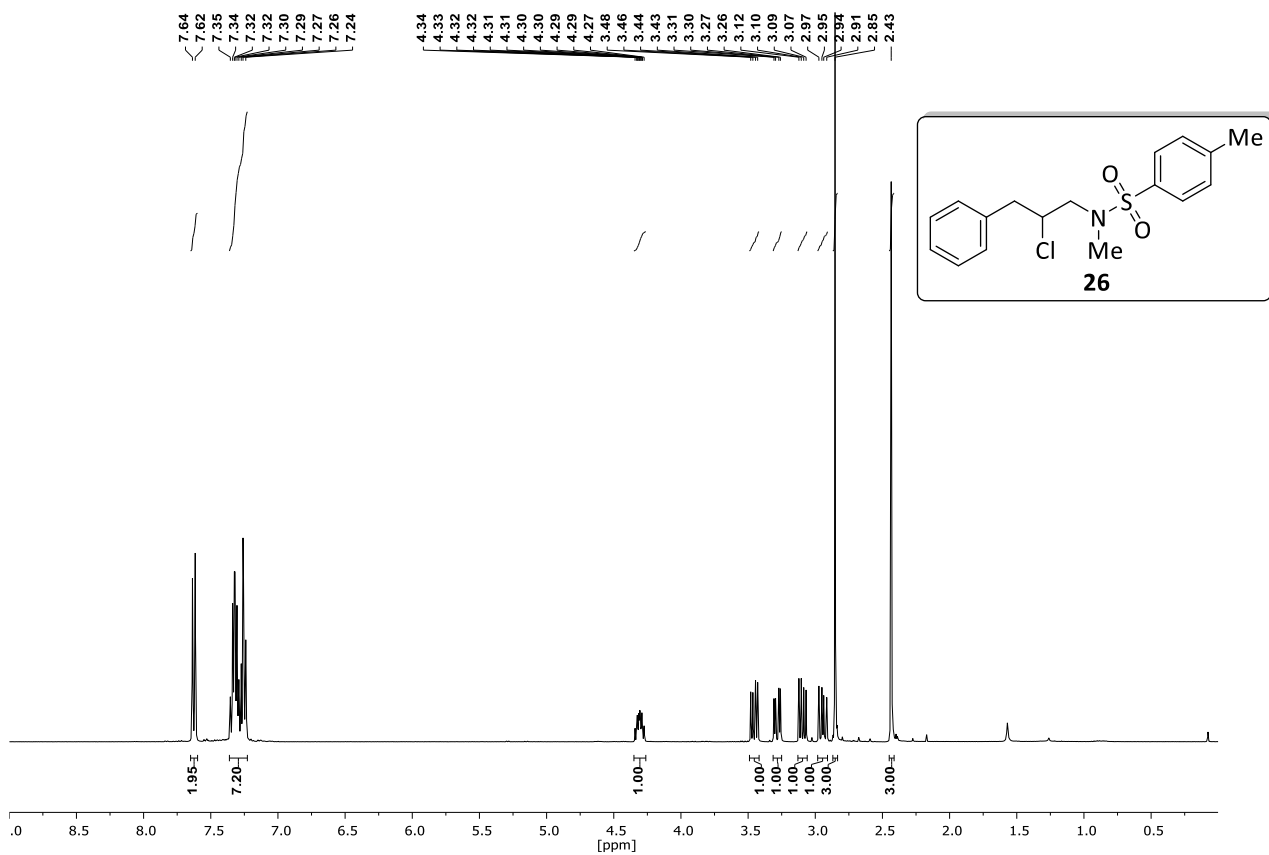
¹³C-NMR (101 MHz, CDCl₃) & **DEPT135** (101 MHz, CDCl₃):
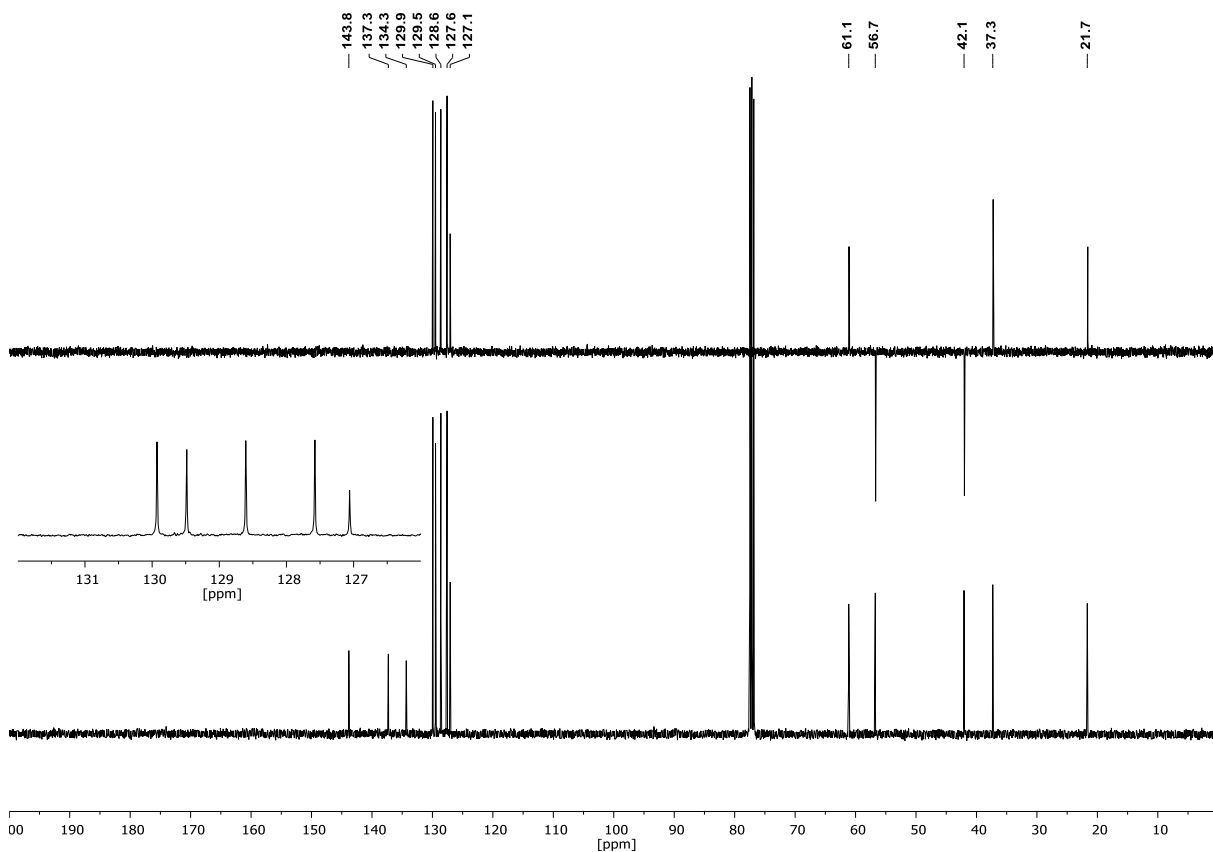
2-(2-chloro-3-phenylpropyl)benzo[*d*]isothiazol-3(2H)-one 1,1-dioxide (28)

¹H-NMR (400 MHz, CDCl₃):
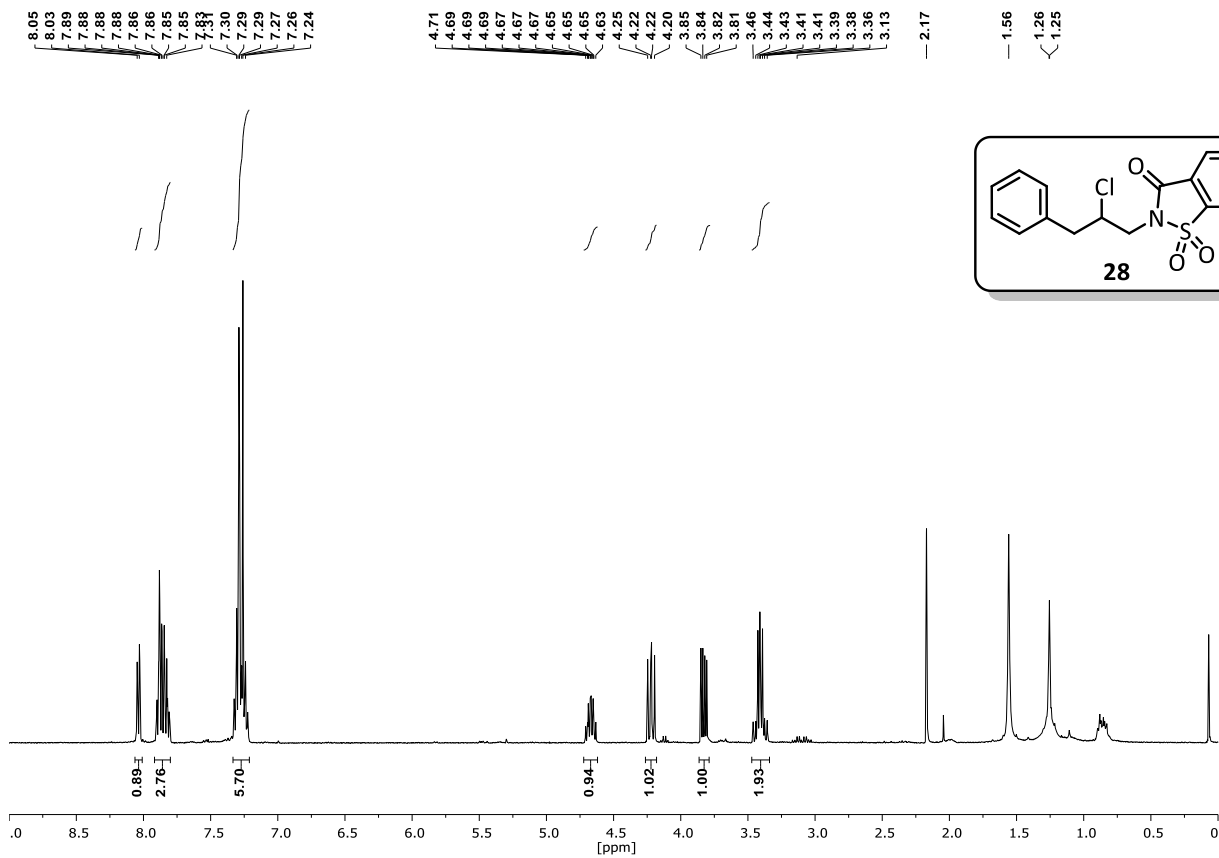
¹³C-NMR (101 MHz, CDCl₃) & **DEPT135** (101 MHz, CDCl₃):
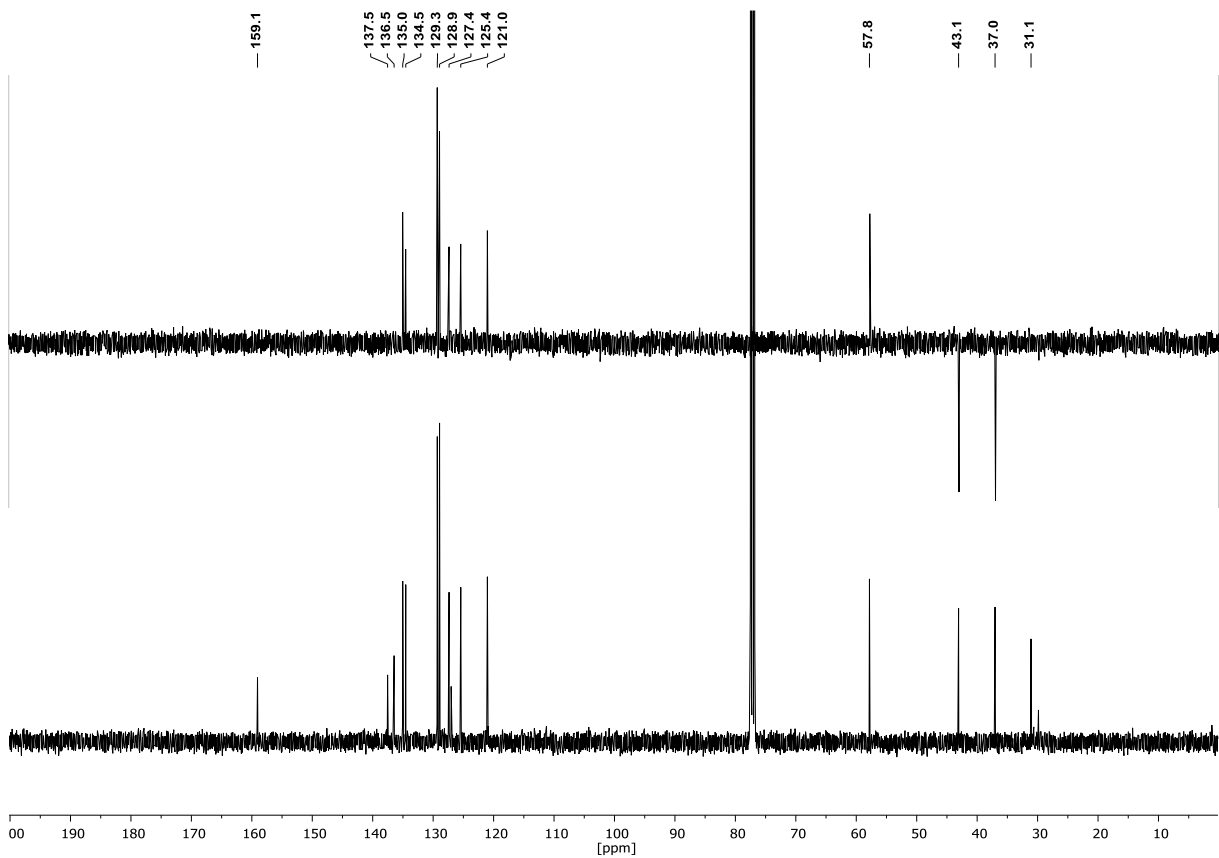
N-(2-chloro-2-phenylethyl)-*N*-methyl-4-nitrobenzenesulfonamide (34)

1H-NMR (400 MHz, CDCl$_3$):
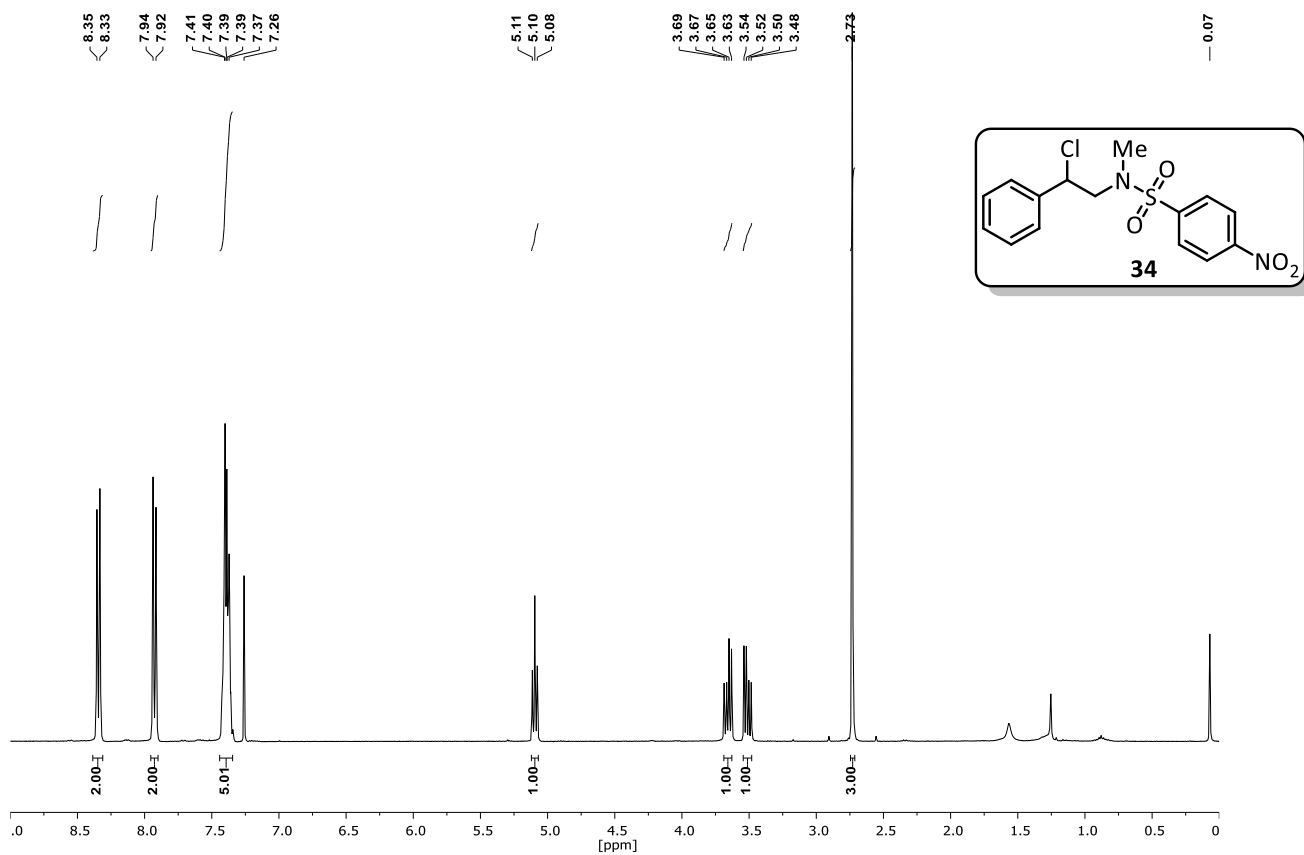
13C-NMR (101 MHz, CDCl$_3$) & **DEPT135** (101 MHz, CDCl$_3$):
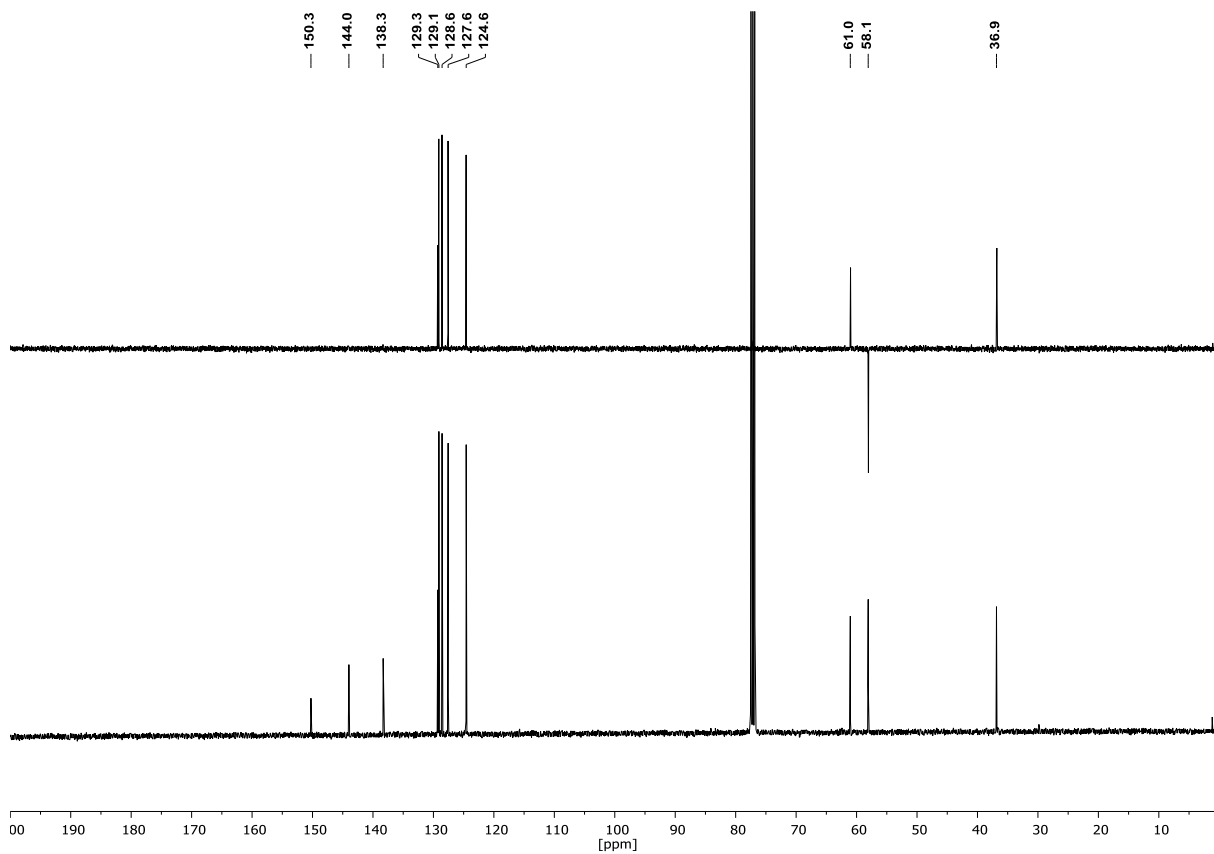
N-(2-bromo-2-phenylethyl)-N,4-dimethylbenzenesulfonamide (37)

^{1}H-NMR (400 MHz, CDCl$_3$):
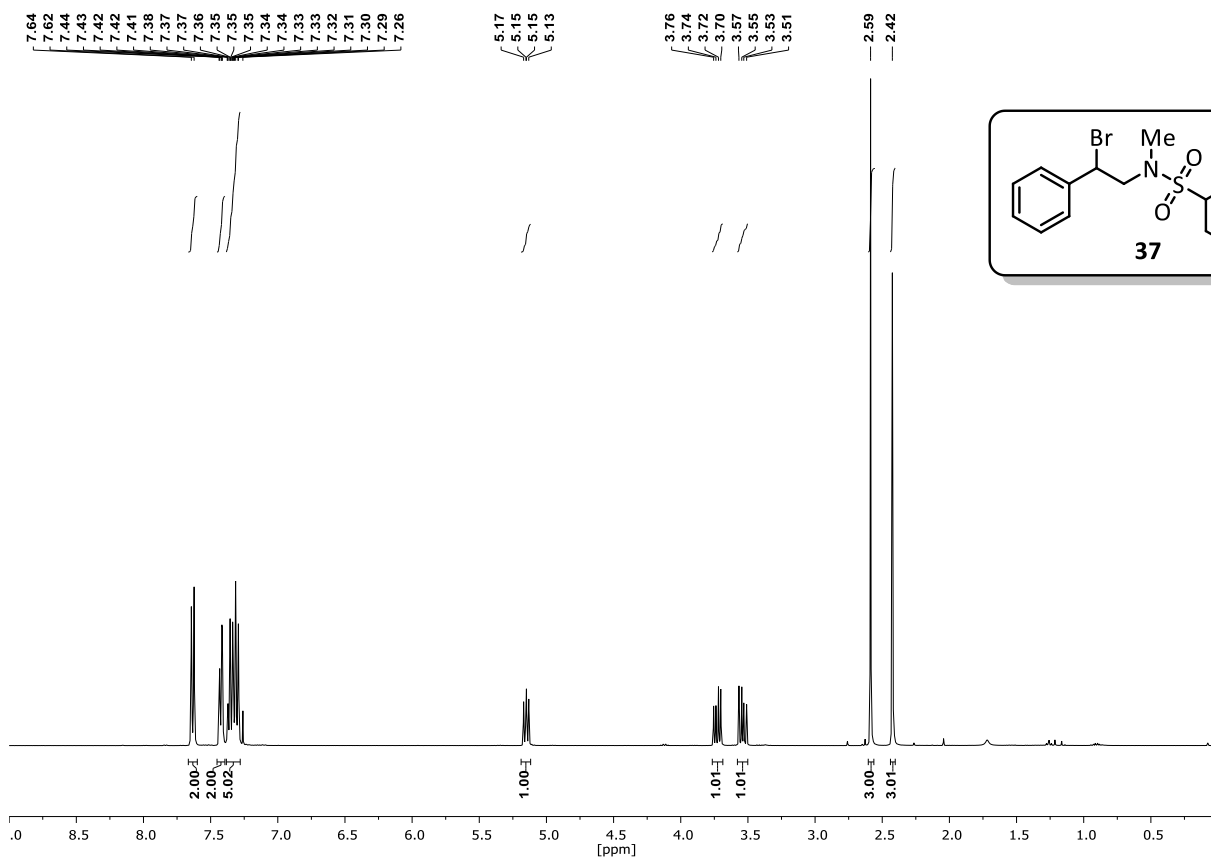
^{13}C-NMR (101 MHz, CDCl$_3$) & **DEPT135** (101 MHz, CDCl$_3$):
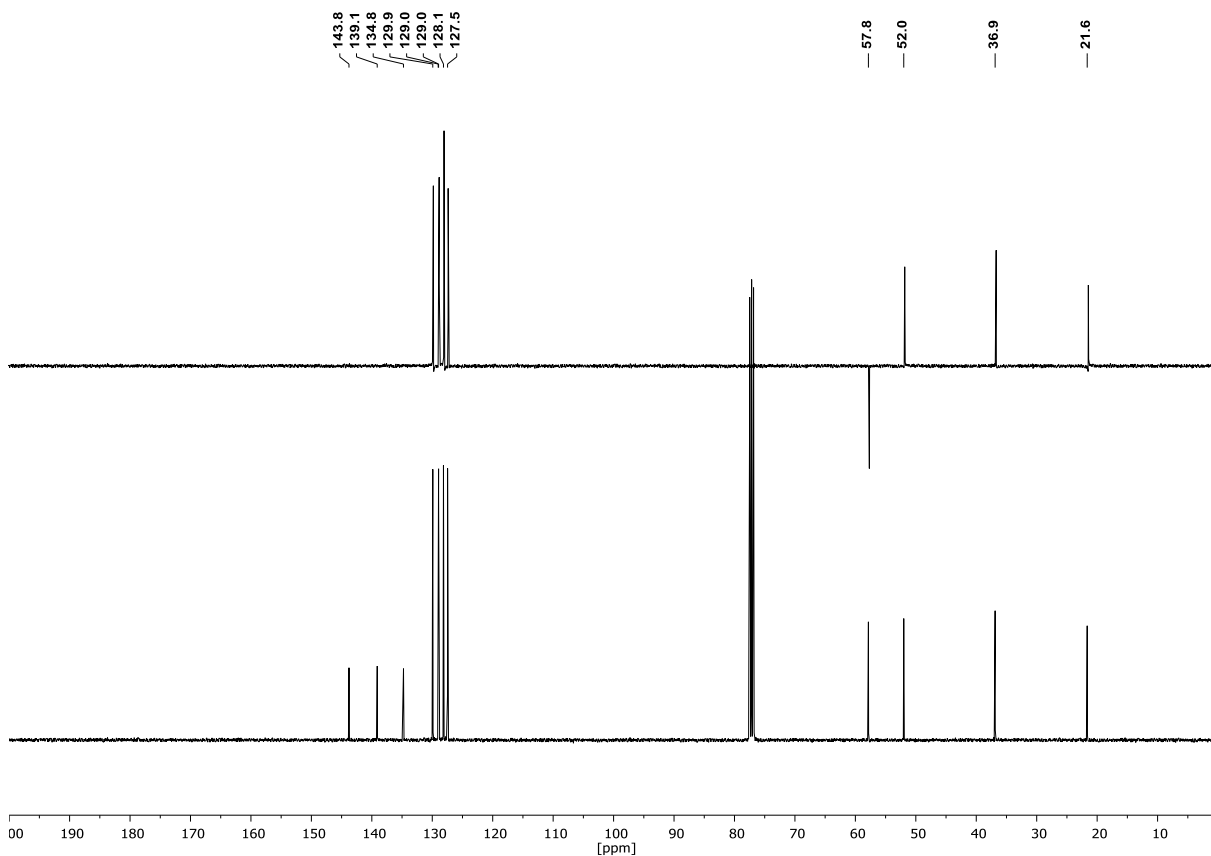
3-(chloromethyl)-4-phenyl-1-tosylpyrrolidine (38a) (d.r.: 0.71:0.29)

¹H-NMR (400 MHz, CDCl₃):
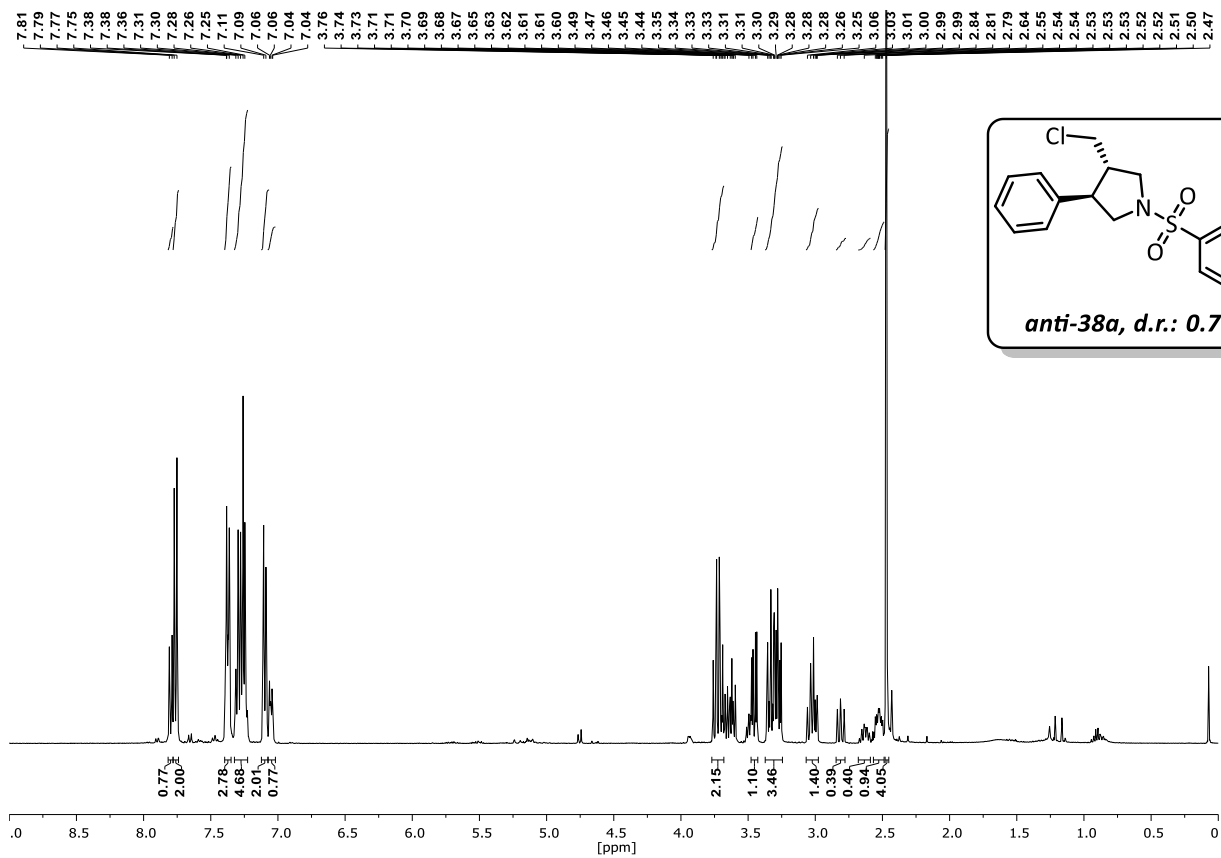
anti-38a, d.r.: 0.71:0.29

¹³C-NMR (101 MHz, CDCl₃) & **DEPT135** (101 MHz, CDCl₃):
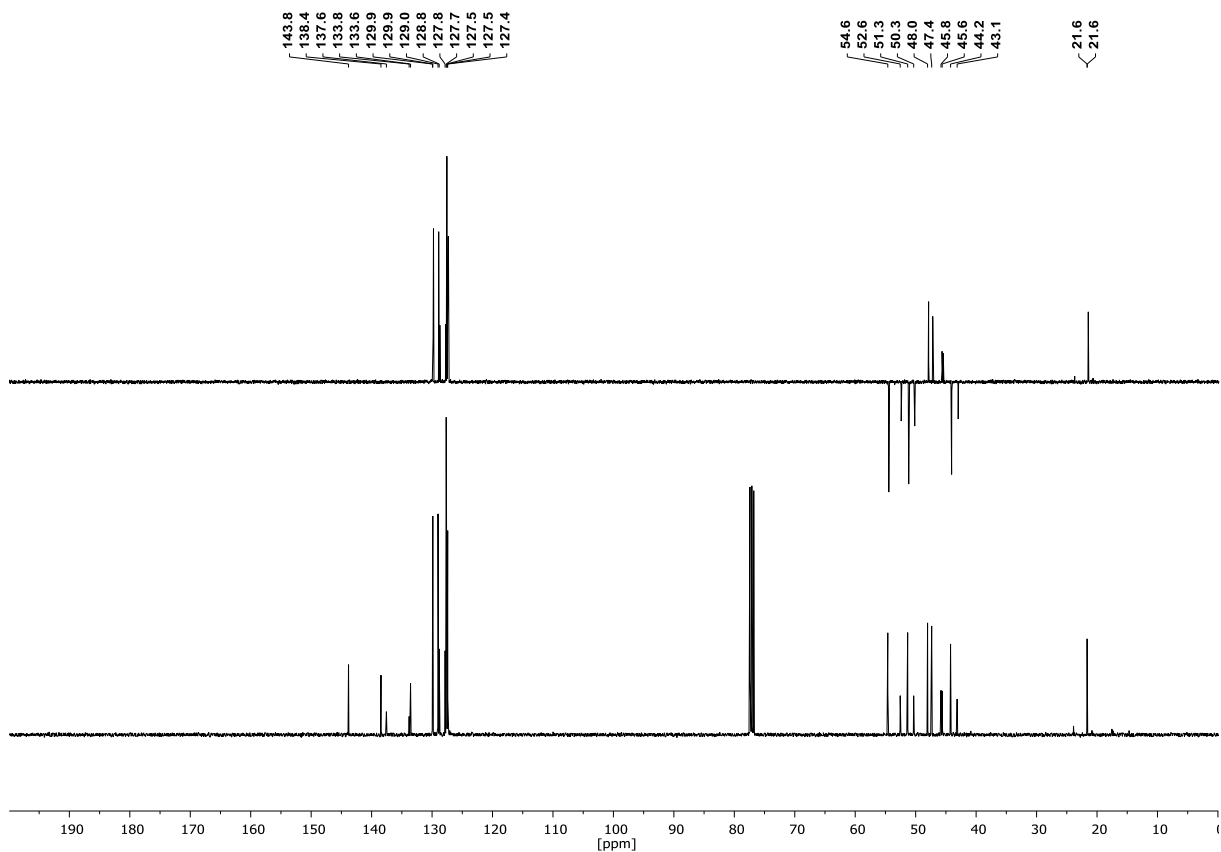
N-allyl-*N*-(2-chloro-2-phenylethyl)-4-methylbenzenesulfonamide (38b)

¹H-NMR (400 MHz, CDCl₃):
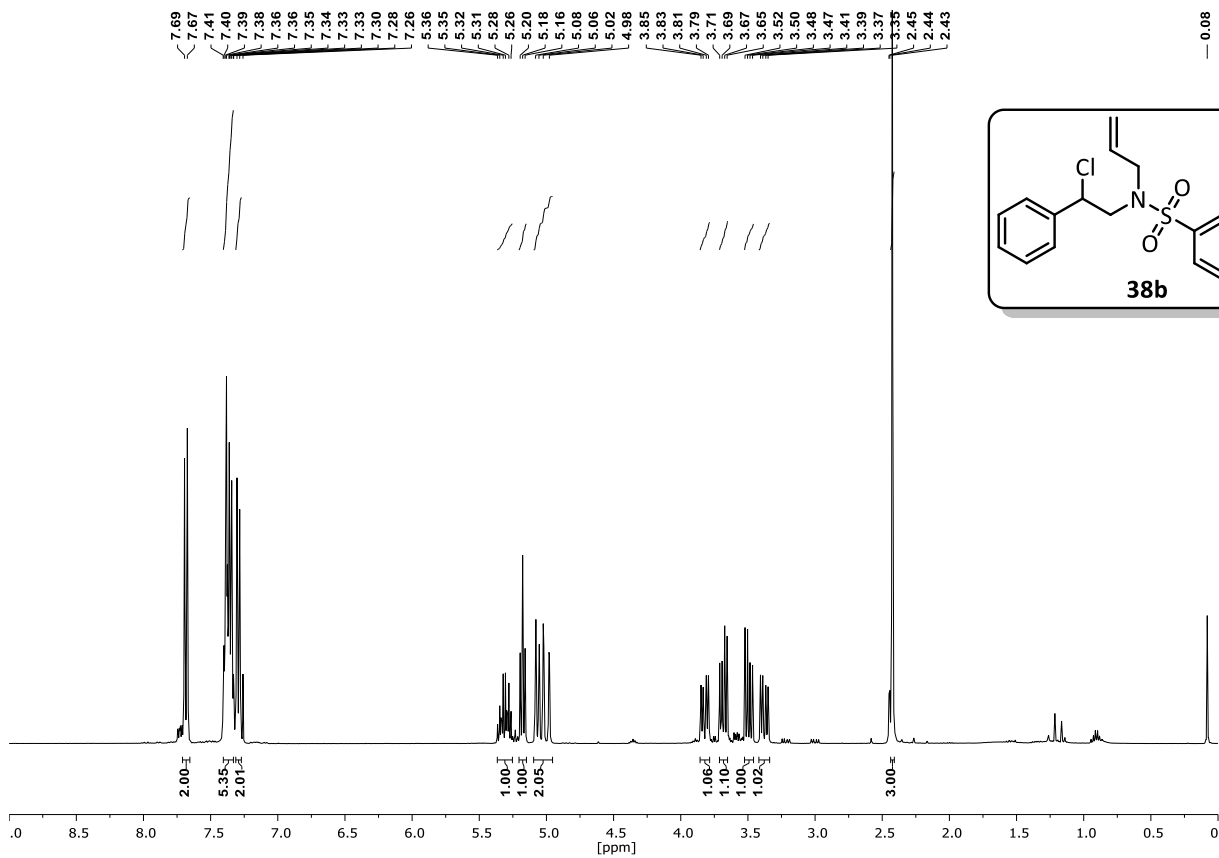
¹³C-NMR (101 MHz, CDCl₃) & **DEPT135** (101 MHz, CDCl₃):
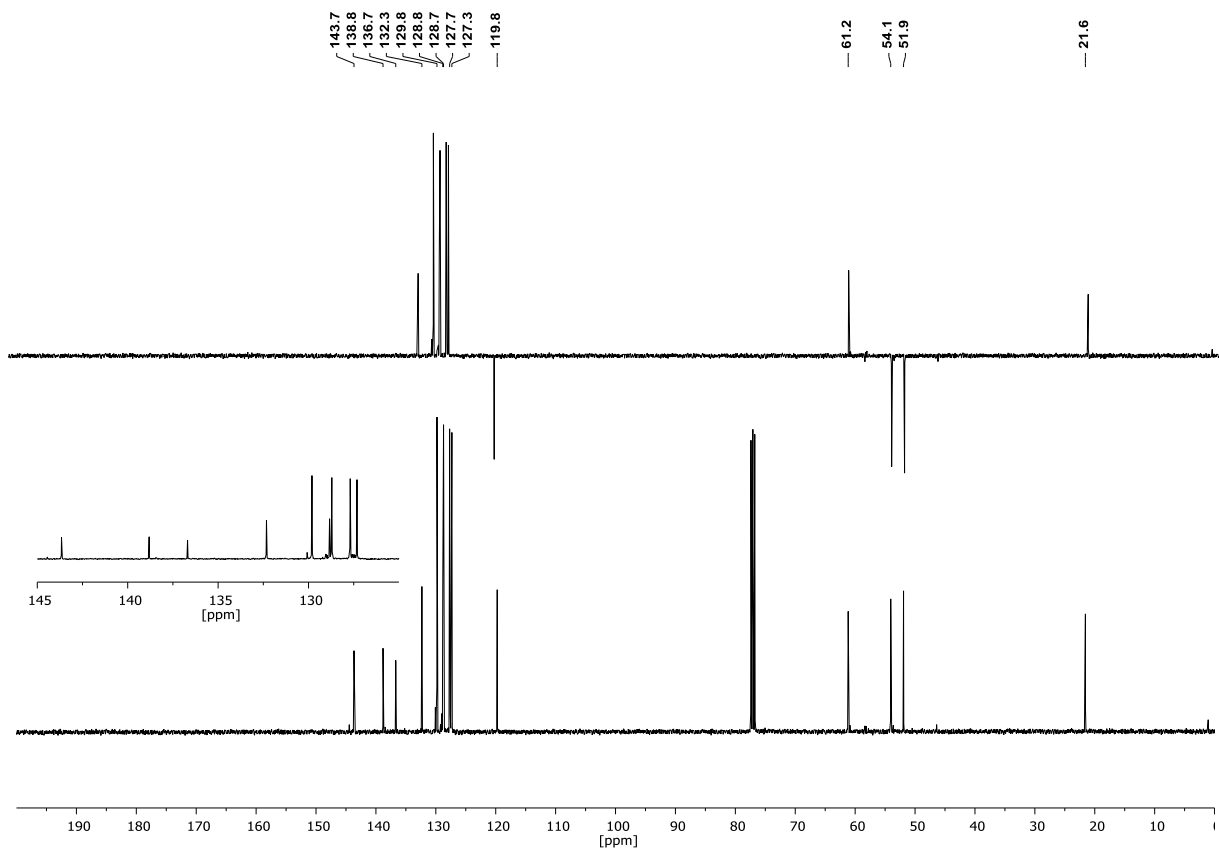
3-(chloromethyl)-4-(p-tolyl)-1-tosylpyrrolidine (39a)

^{1}H-NMR (400 MHz, CDCl$_3$):
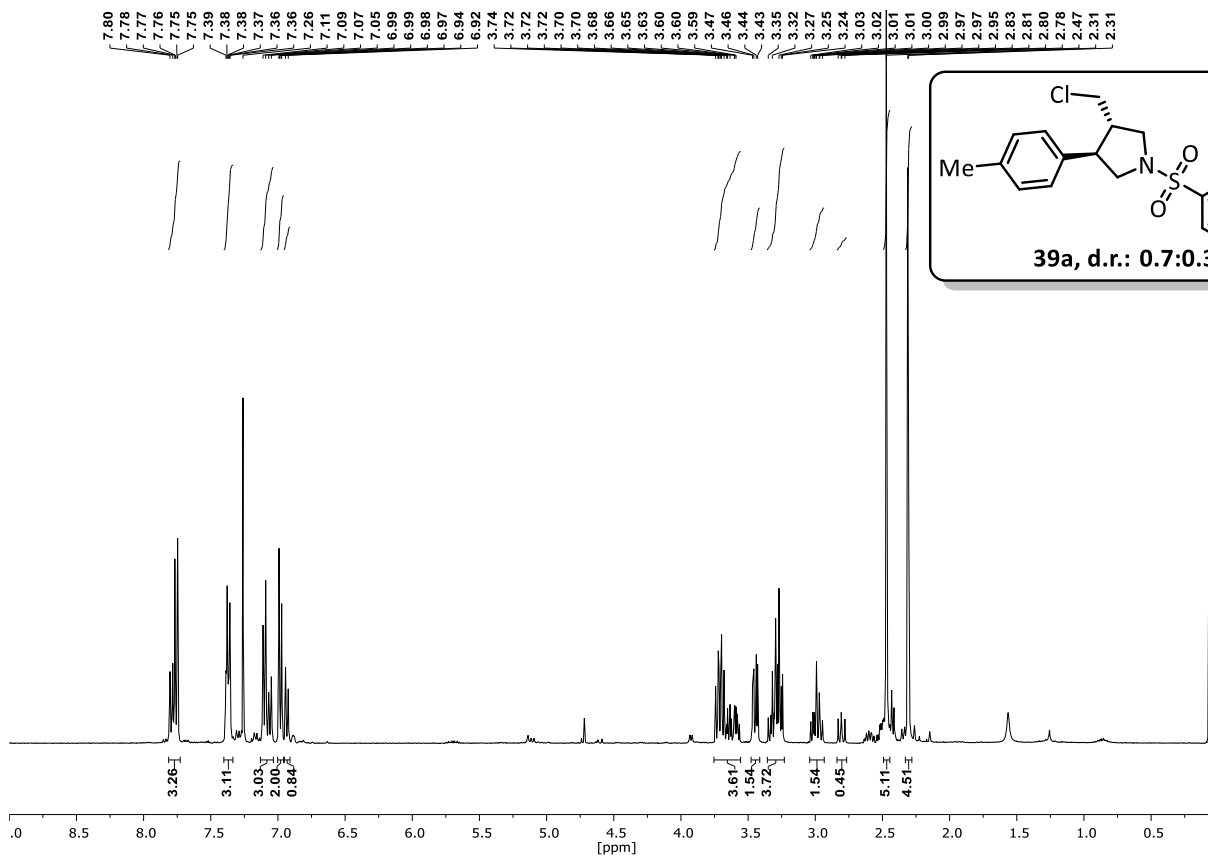
^{13}C-NMR (101 MHz, CDCl$_3$) & **DEPT135** (101 MHz, CDCl$_3$):
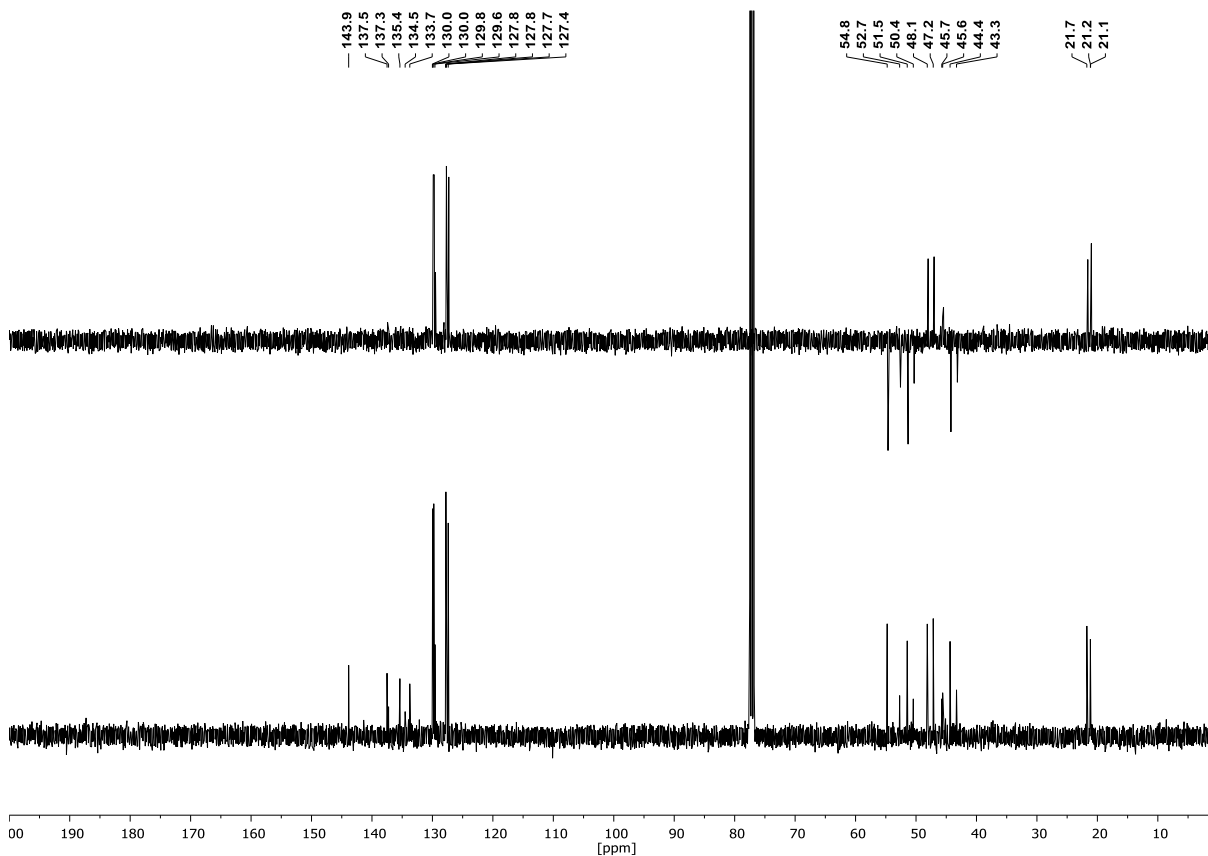
N-allyl-*N*-(2-chloro-2-(p-tolyl)ethyl)-4-methylbenzenesulfonamide (39b)

¹H-NMR (400 MHz, CDCl₃):
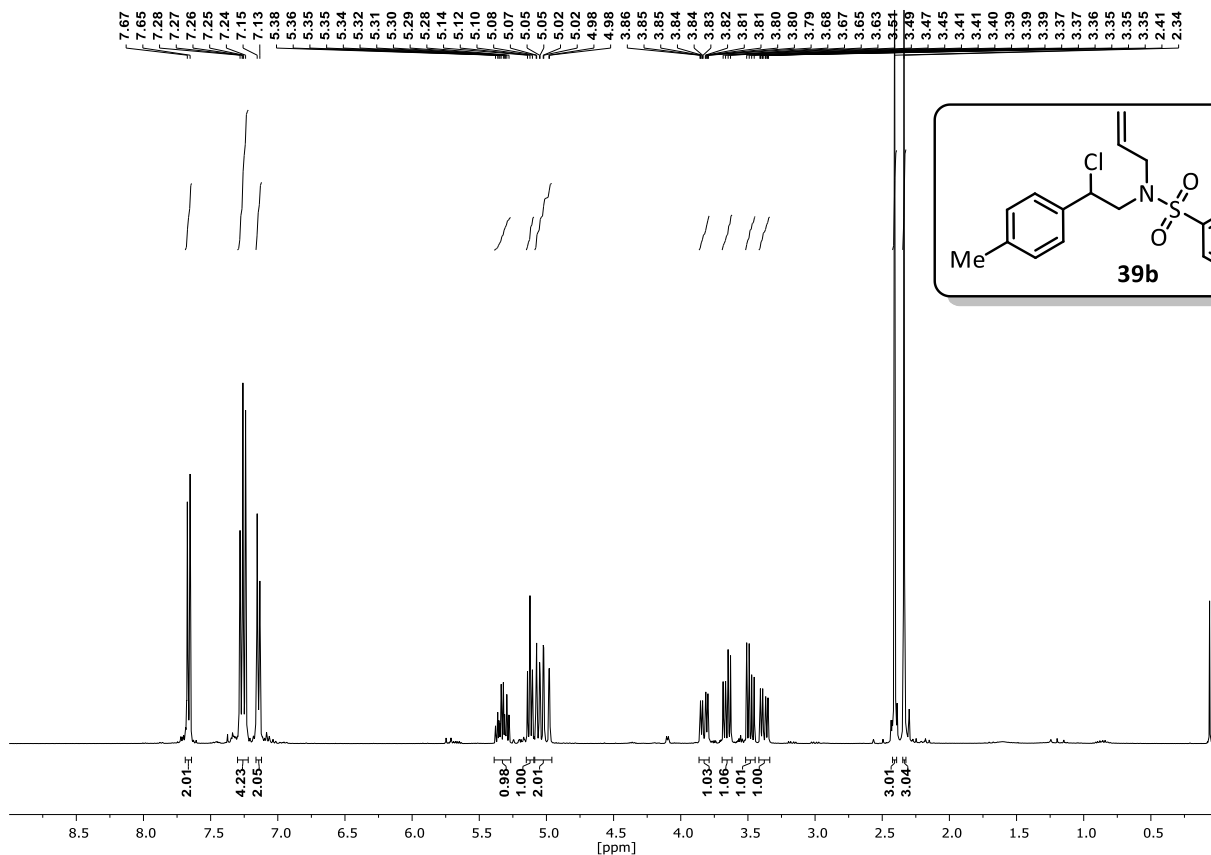
¹³C-NMR (101 MHz, CDCl₃) & **DEPT135** (101 MHz, CDCl₃):
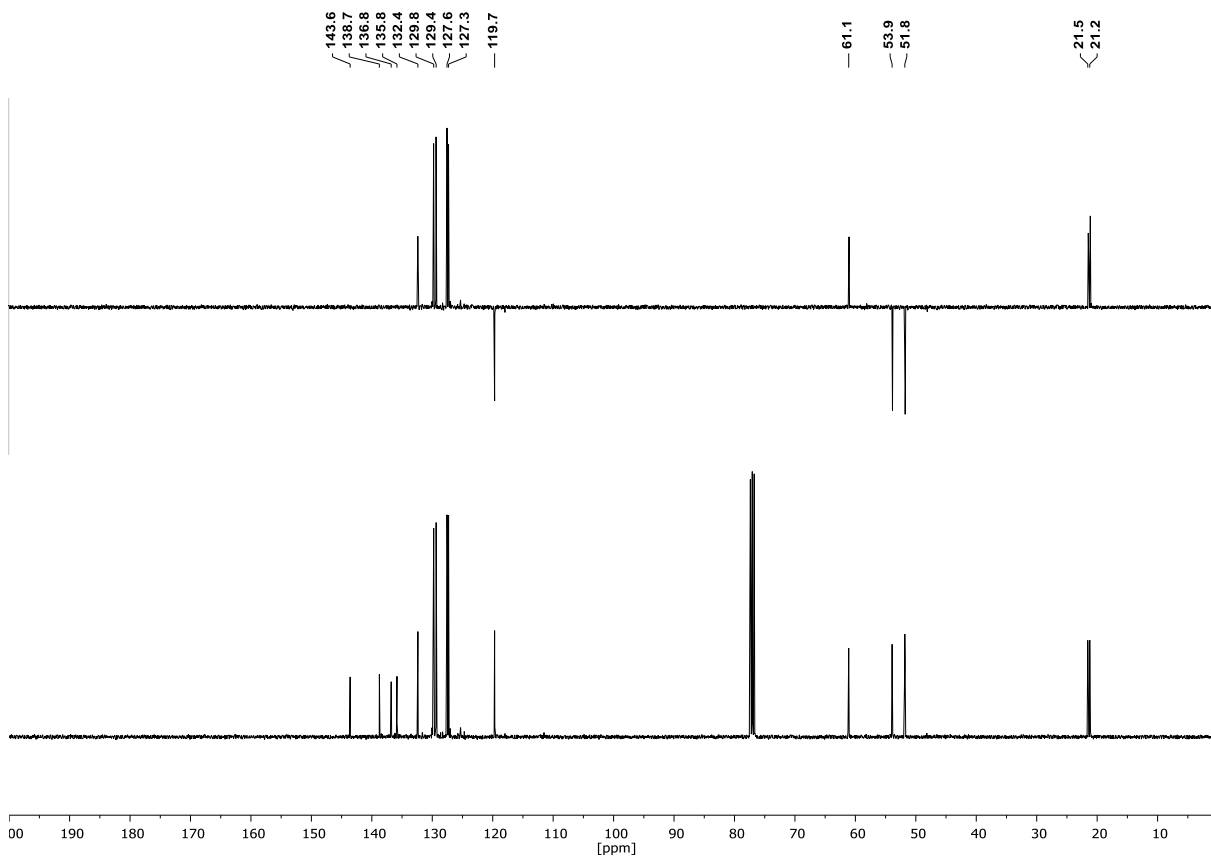
Methyl 4-(4-(chloromethyl)-1-tosylpyrrolidin-3-yl)benzoate (40a)

^{1}H-NMR (400 MHz, CDCl$_3$):
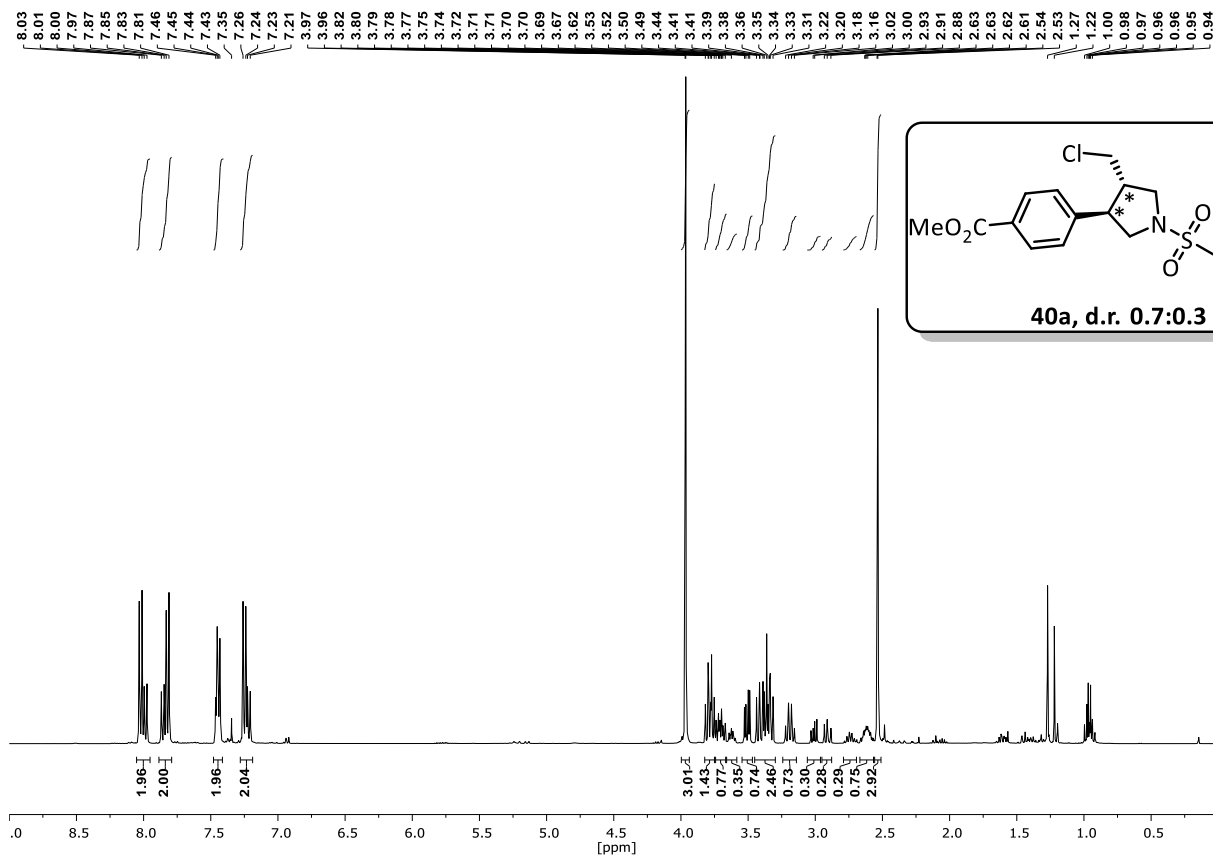
^{13}C-NMR (101 MHz, CDCl$_3$) & **DEPT135** (101 MHz, CDCl$_3$):
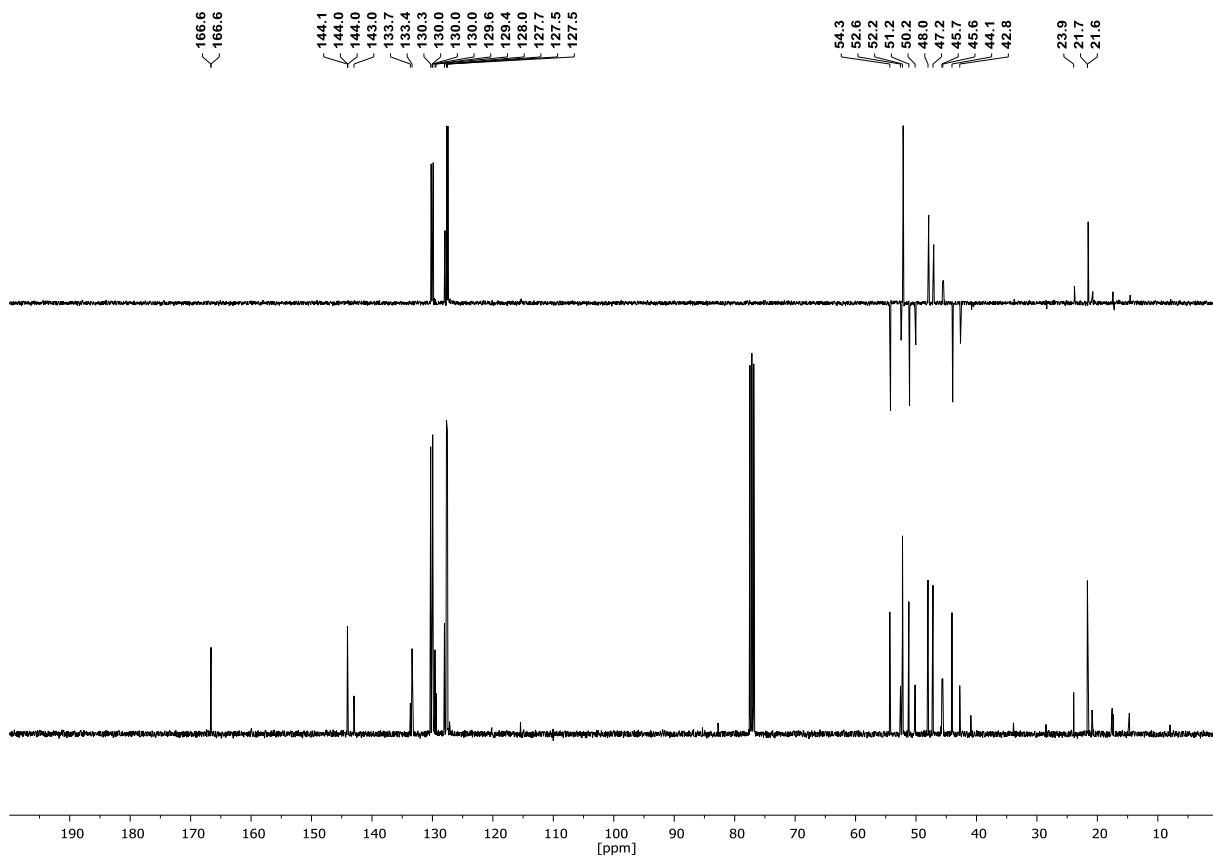
Methyl 4-(2-((*N*-allyl-4-methylphenyl)sulfonamido)-1-chloroethyl)benzoate (40b)

¹H-NMR (400 MHz, CDCl₃):
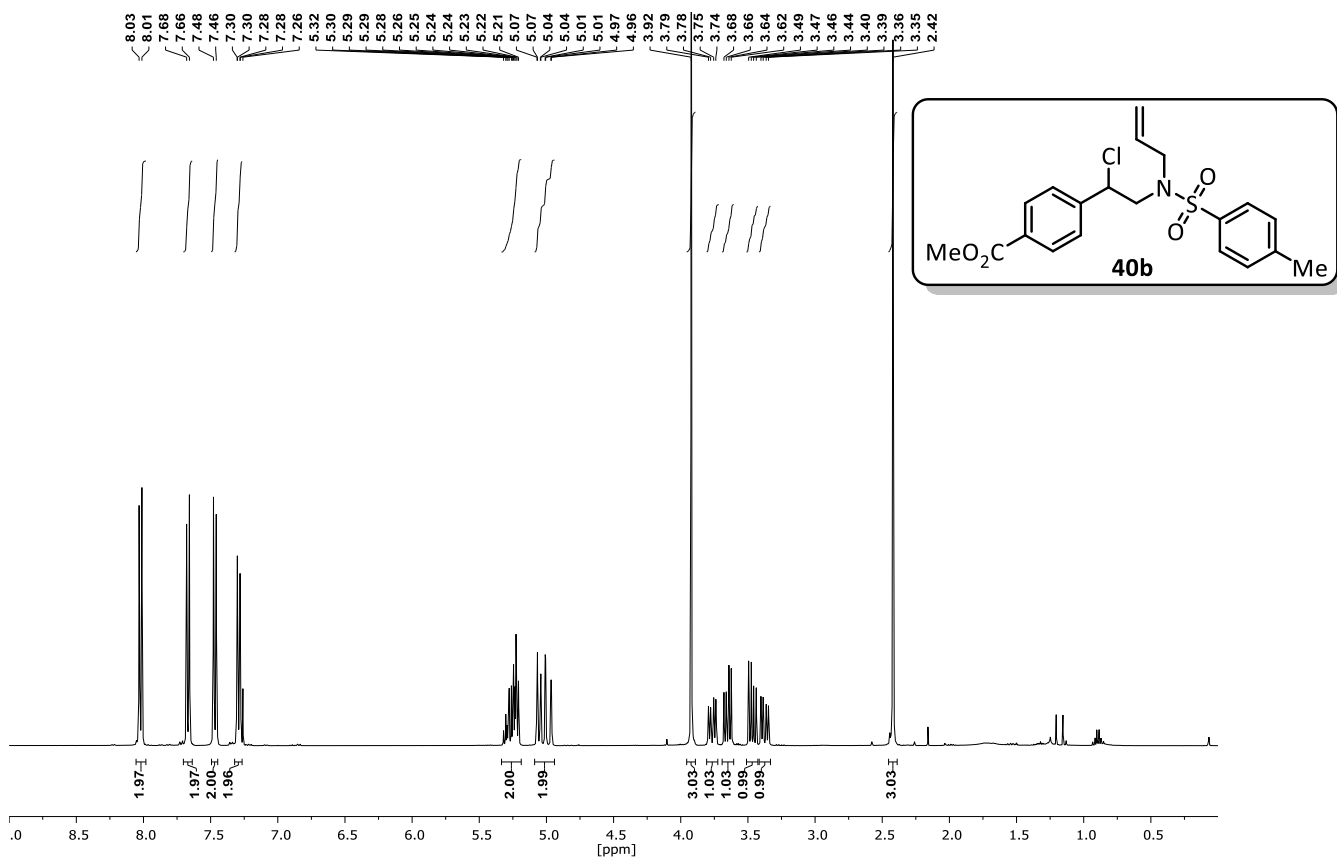
¹³C-NMR (101 MHz, CDCl₃) & **DEPT135** (101 MHz, CDCl₃):
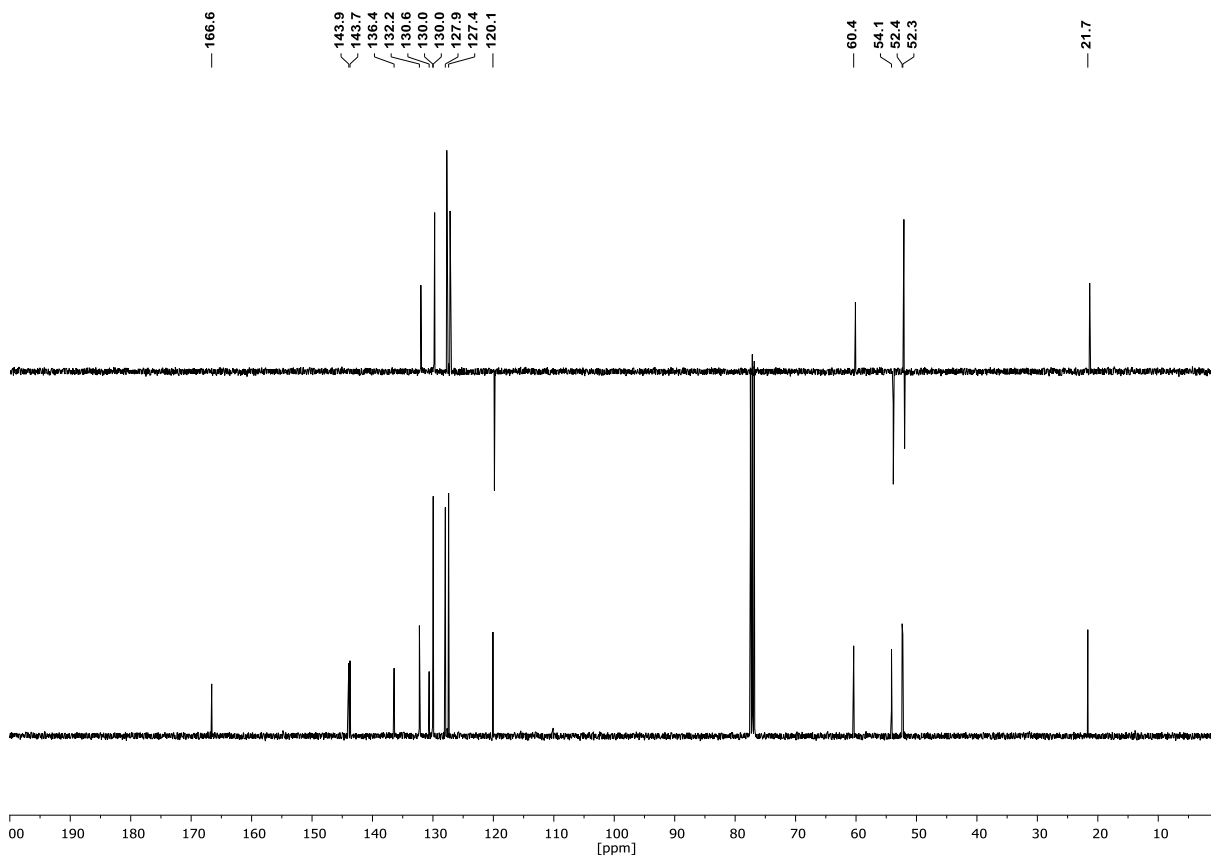
***N*-((1R,2R)-1-chloro-1-phenylpropan-2-yl)-*N*,4-dimethylbenzenesulfonamide (41)**

¹H-NMR (400 MHz, CDCl₃):
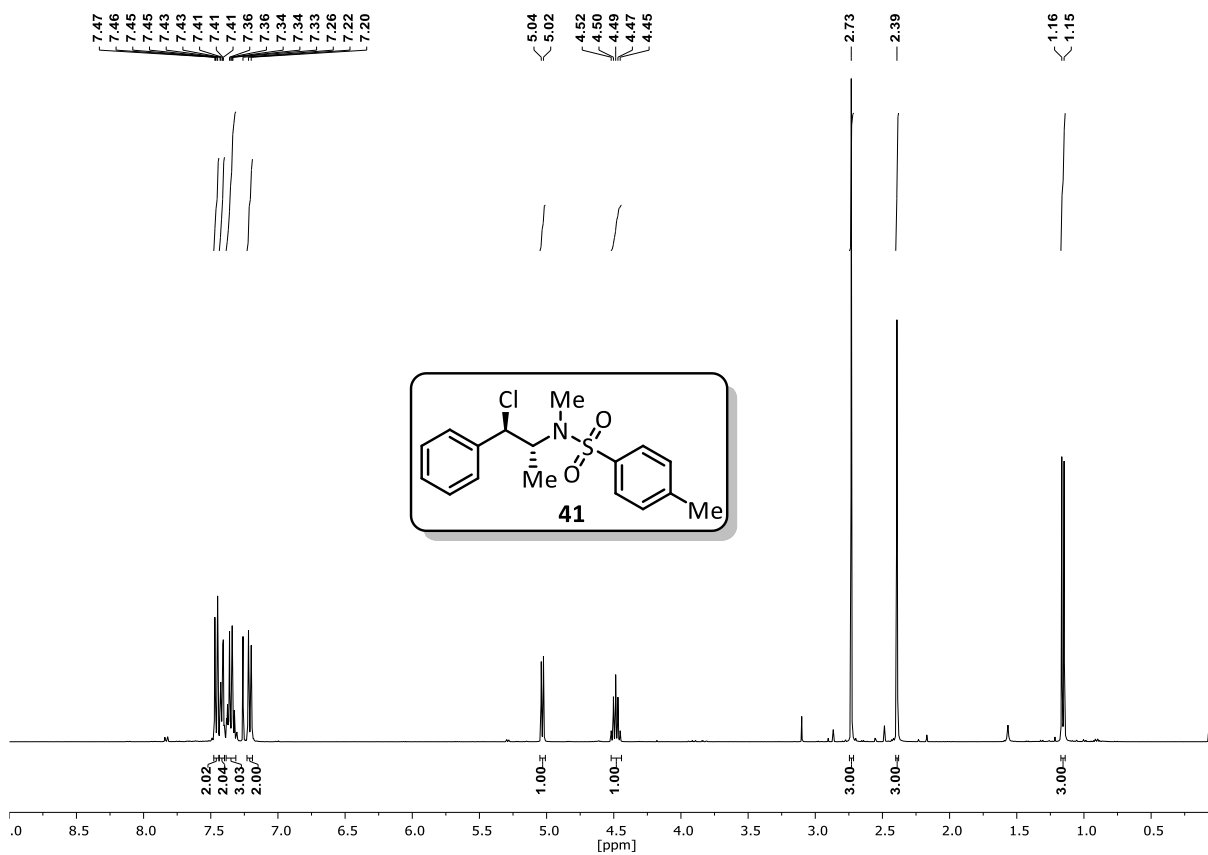
¹³C-NMR (101 MHz, CDCl₃) & **DEPT135** (101 MHz, CDCl₃):
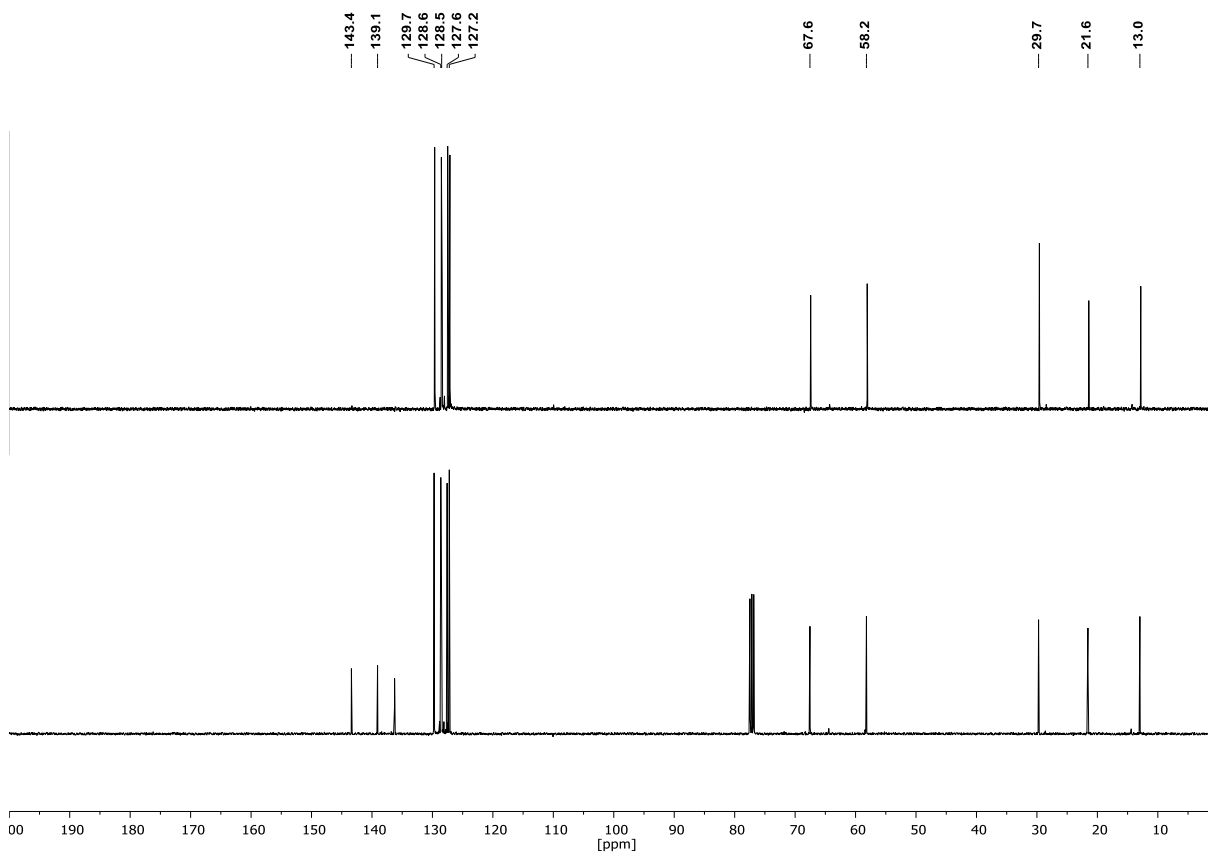
N-(tert-butyl)-*N*-(2-chloro-2-phenylethyl)-4-methylbenzenesulfonamide (42)

¹H-NMR (400 MHz, CDCl₃):
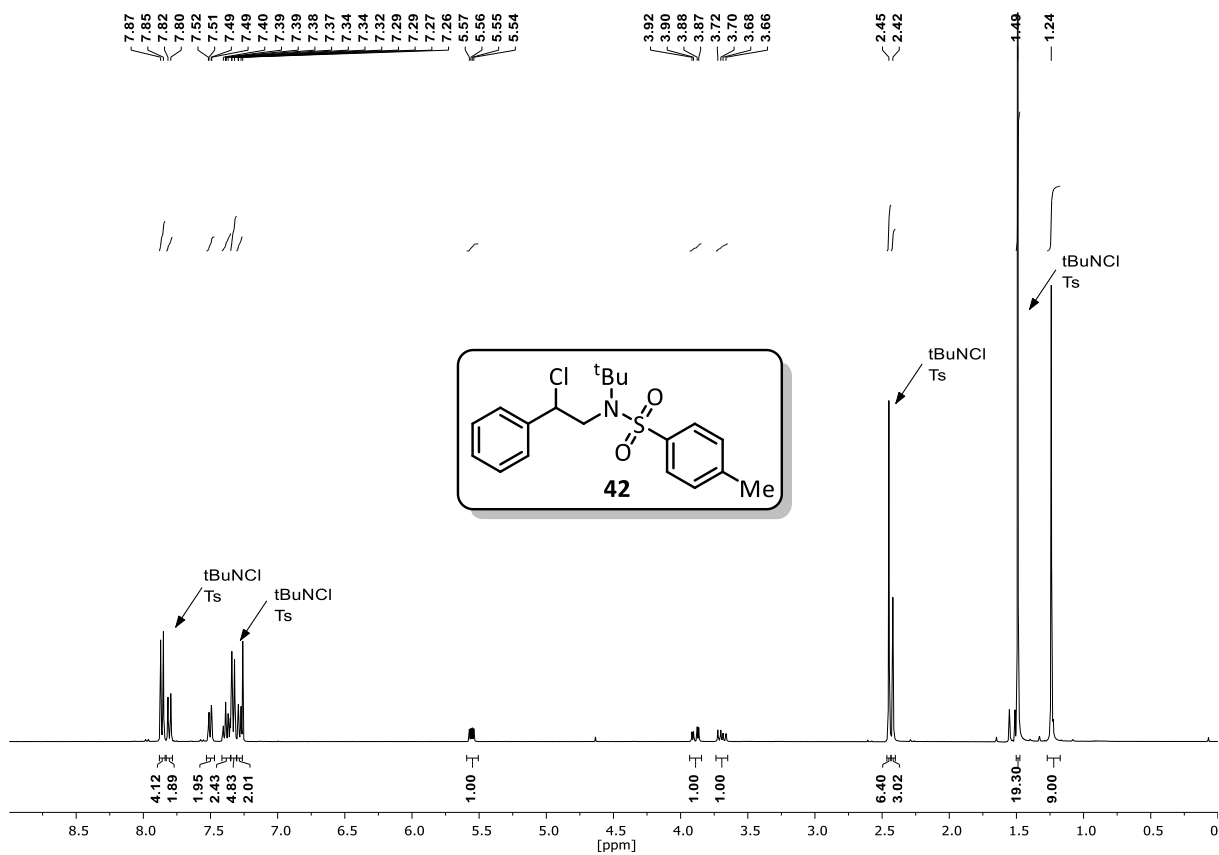
¹³C-NMR (101 MHz, CDCl₃) & **DEPT135** (101 MHz, CDCl₃):
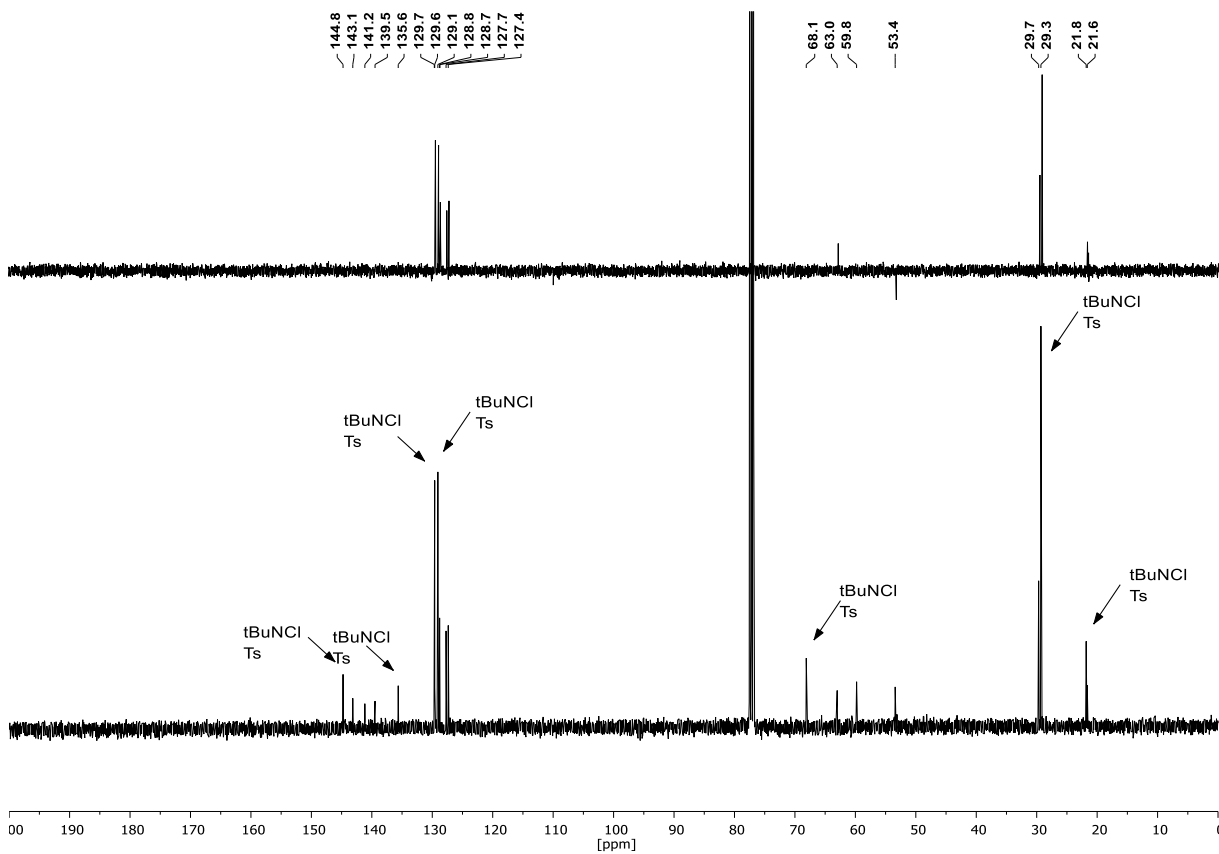
N-(2-(4-allylphenyl)-2-chloroethyl)-*N*,4-dimethylbenzenesulfonamide (43)

¹H-NMR (400 MHz, CDCl₃):
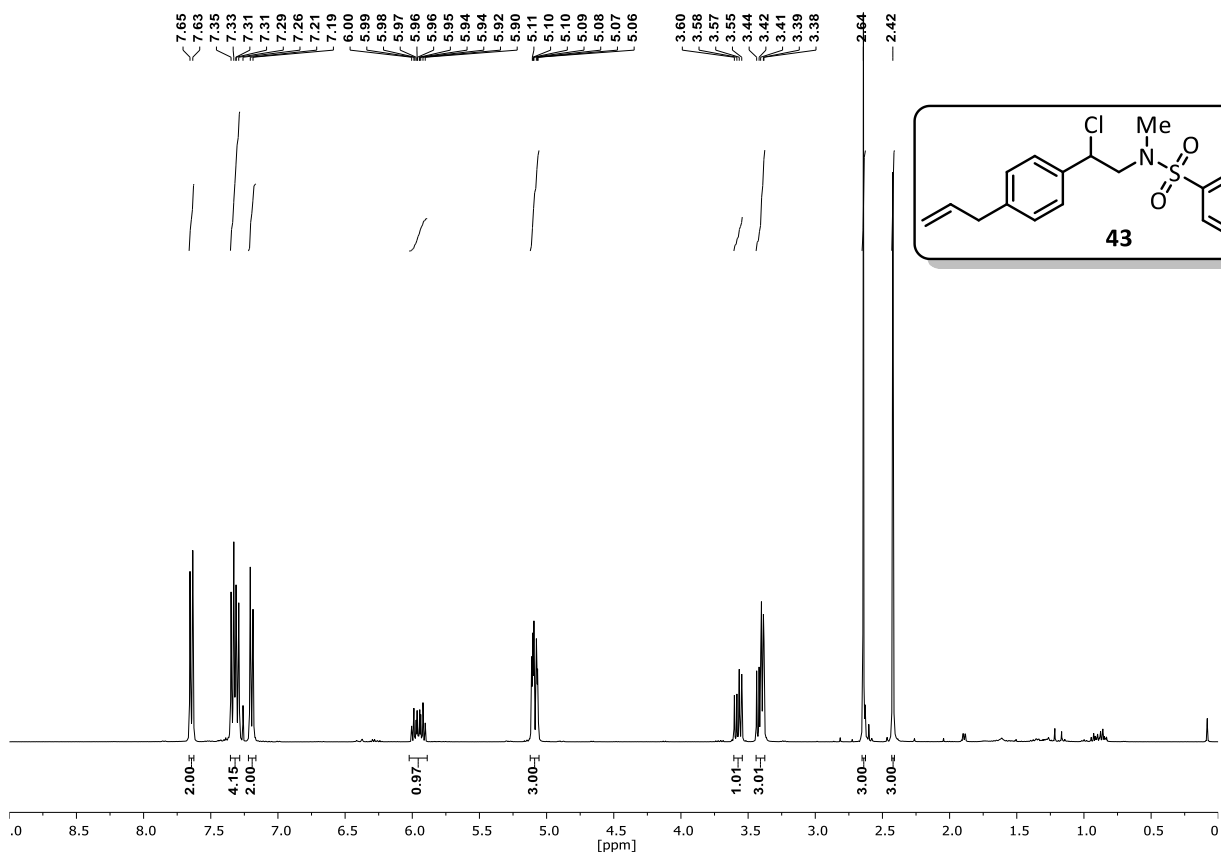
¹³C-NMR (101 MHz, CDCl₃) & **DEPT135** (101 MHz, CDCl₃):
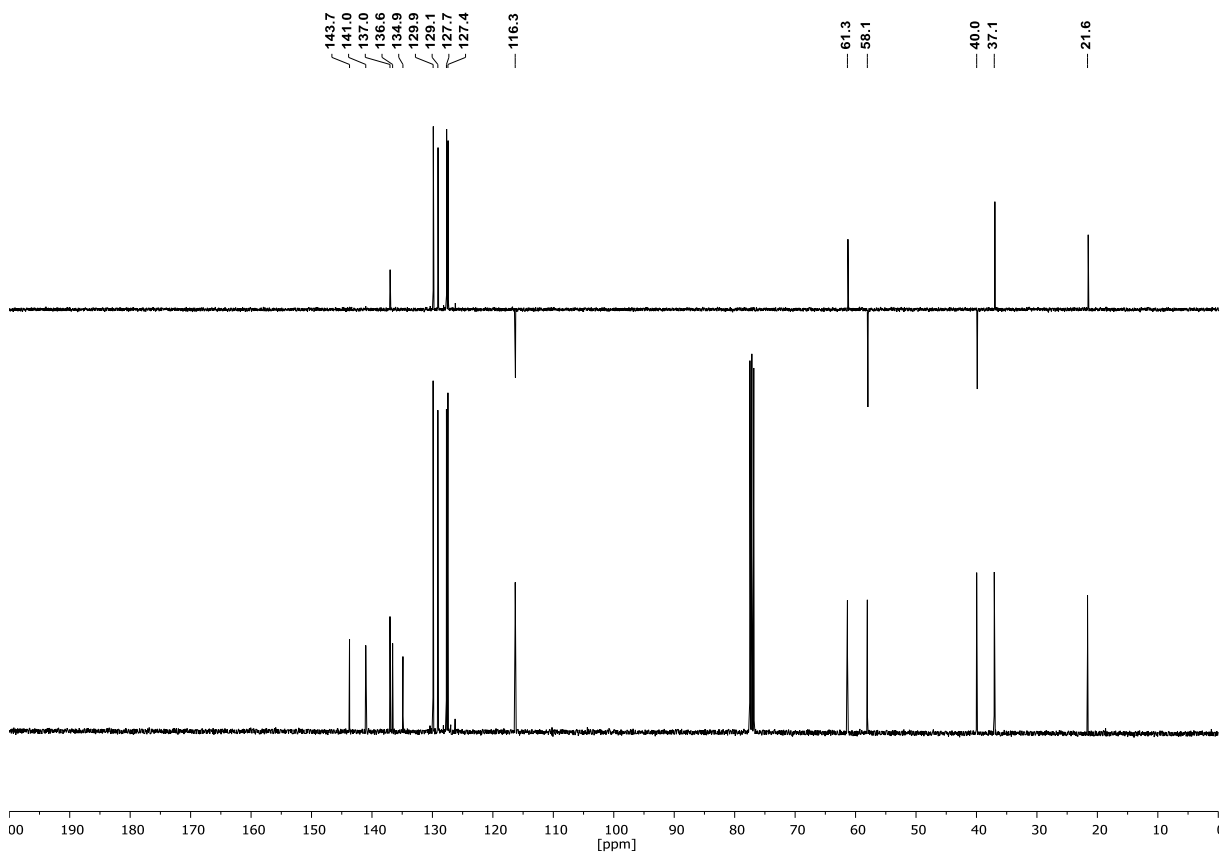
3-(bromomethyl)-4-phenyl-1-tosylpyrrolidine (55a)

¹H-NMR (400 MHz, CDCl₃):
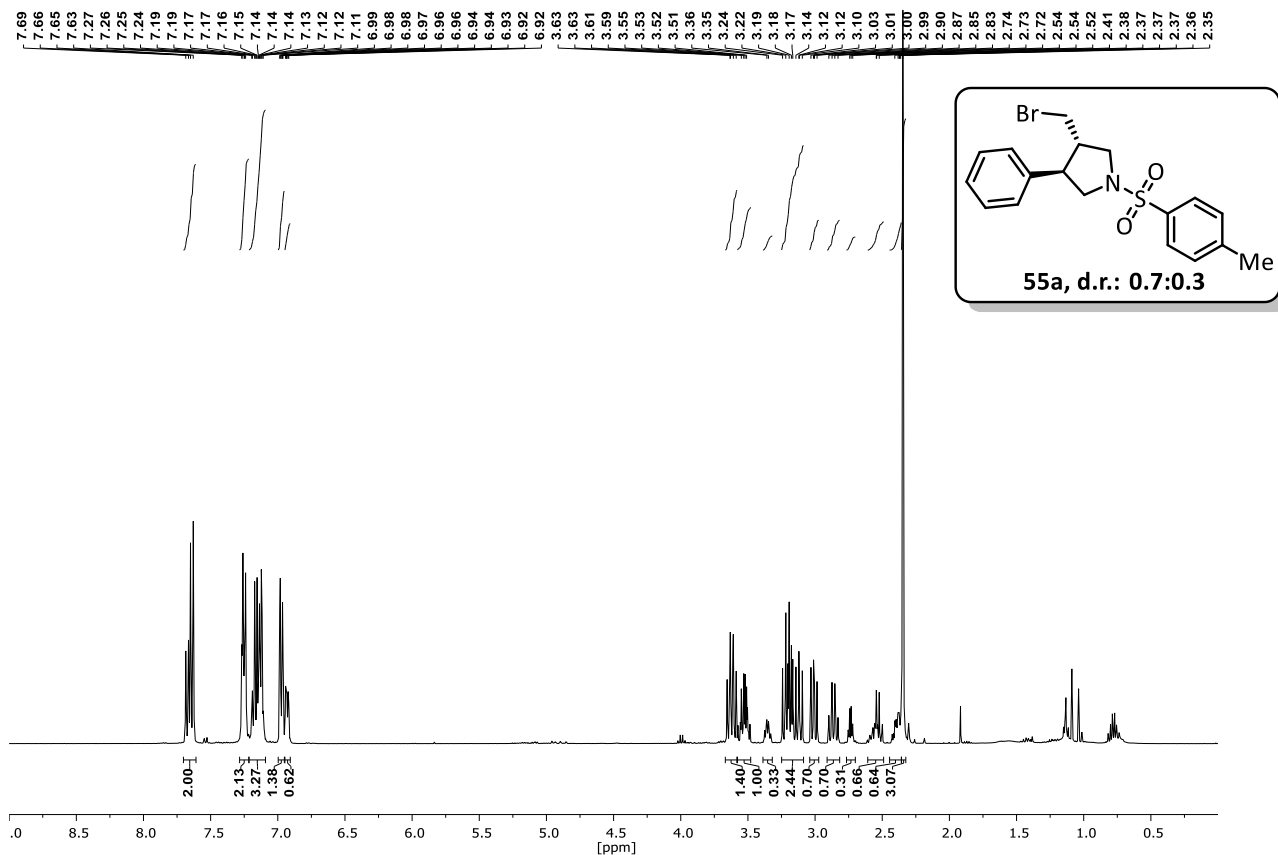
¹³C-NMR (101 MHz, CDCl₃) & **DEPT135** (101 MHz, CDCl₃):
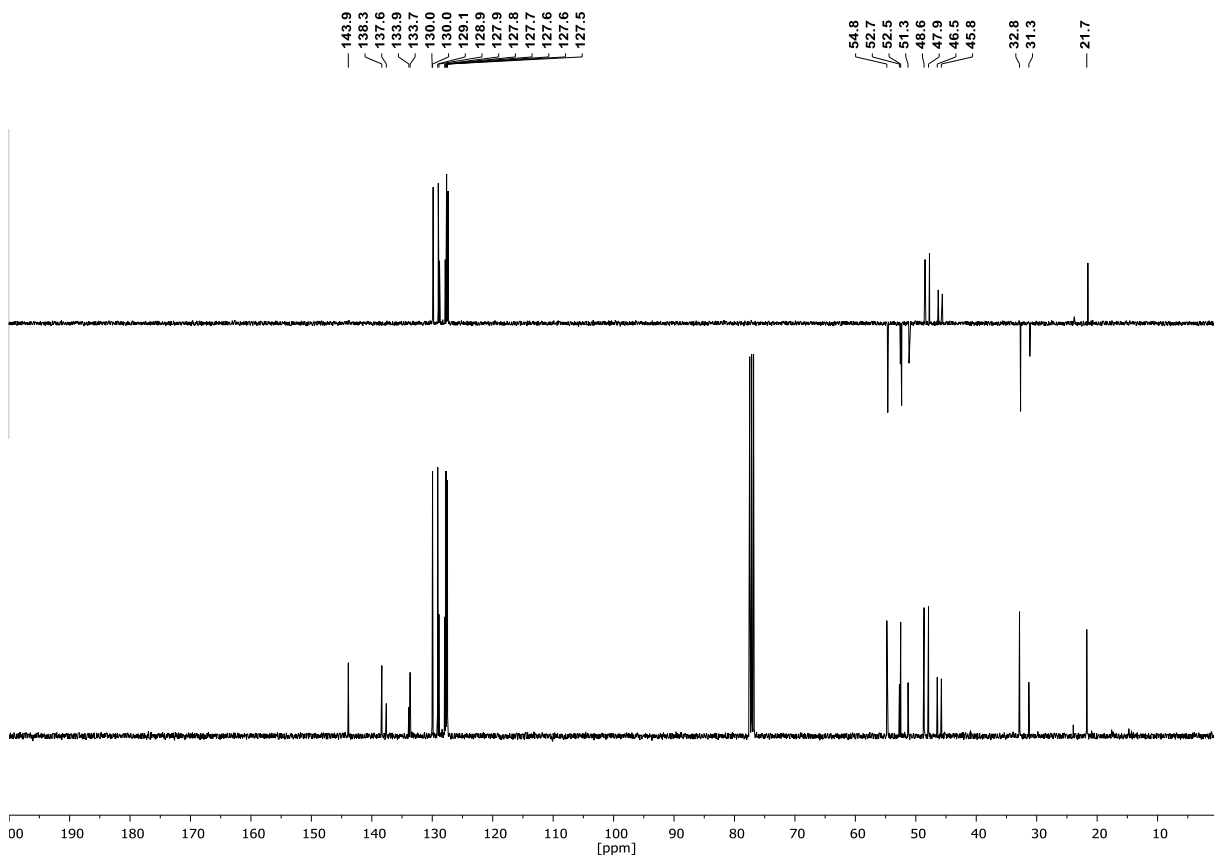
N-allyl-*N*-(2-bromo-2-phenylethyl)-4-methylbenzenesulfonamide (55b)

¹H-NMR (400 MHz, CDCl₃):
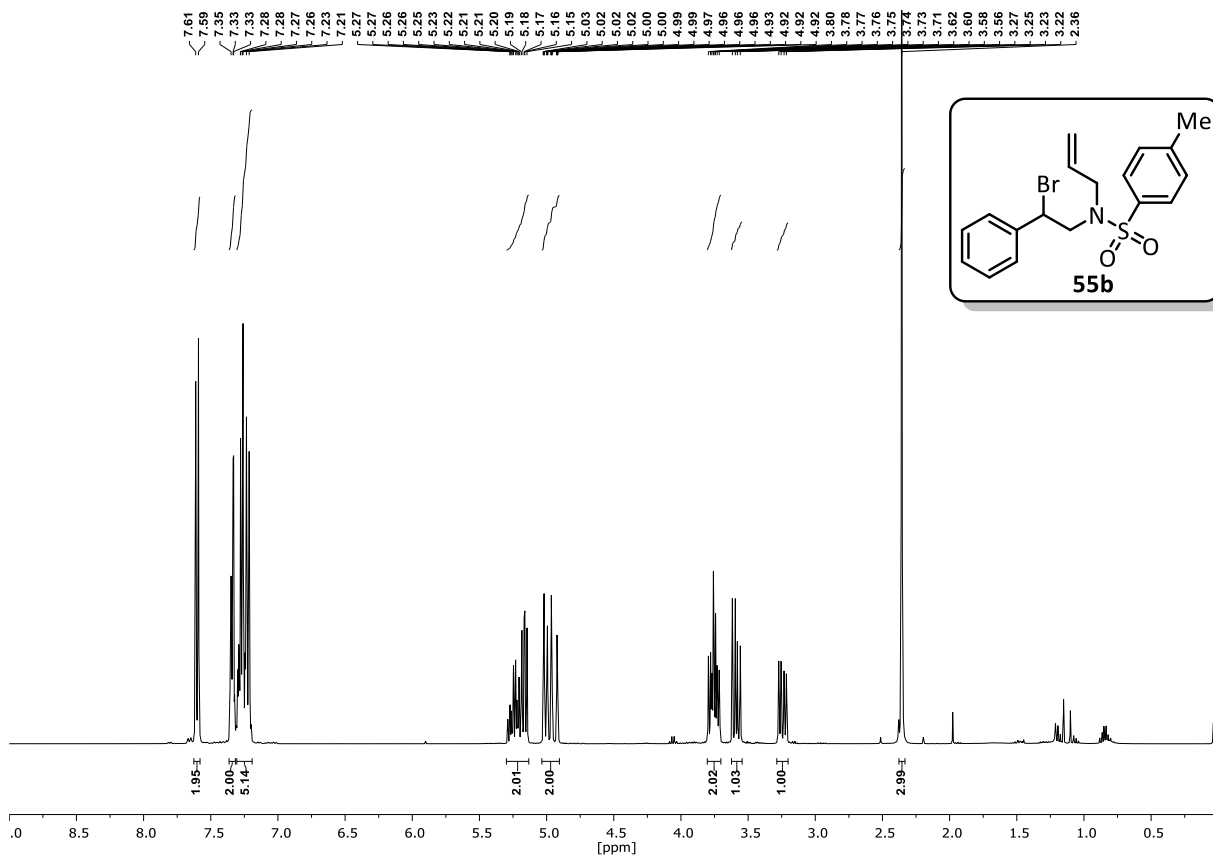
¹³C-NMR (101 MHz, CDCl₃) & **DEPT135** (101 MHz, CDCl₃):
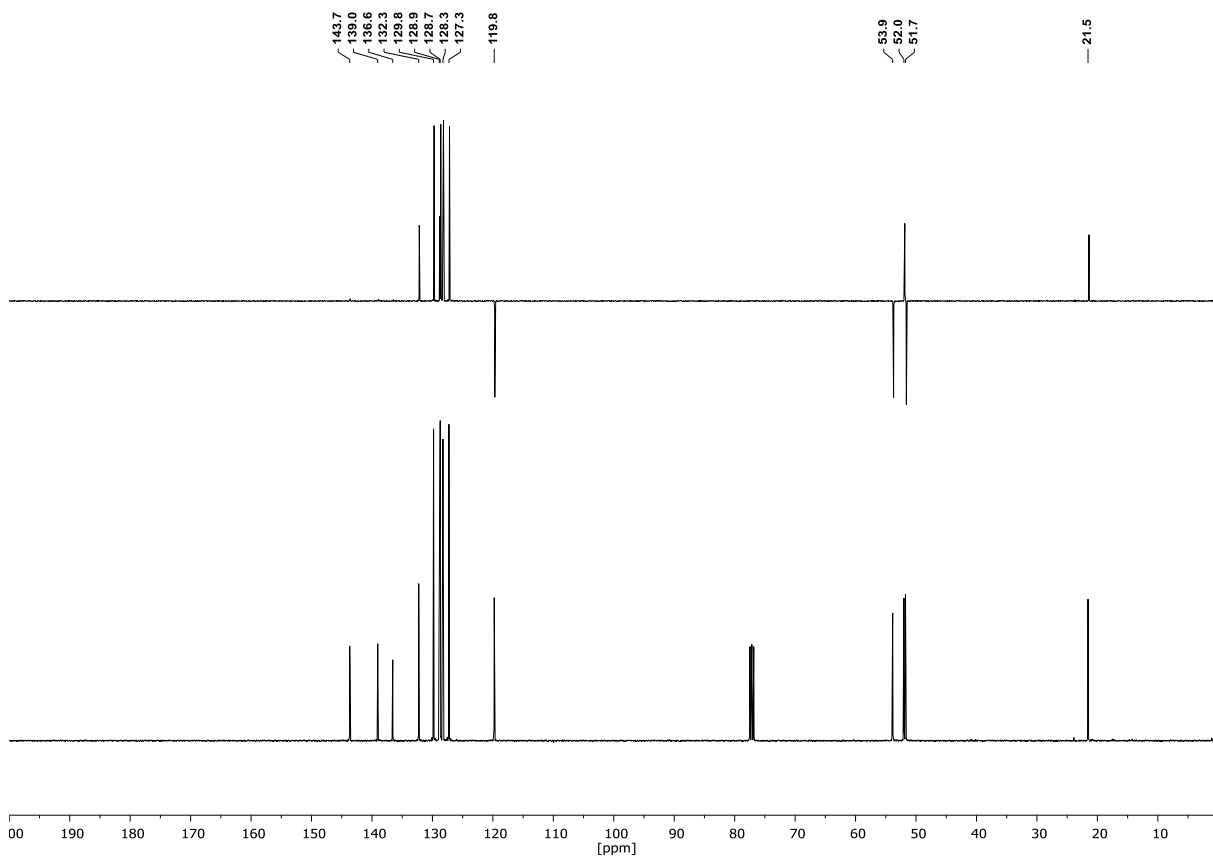
Diethyl 2-benzylmalonate (127a)

^{1}H-NMR (300 MHz, CDCl$_3$):
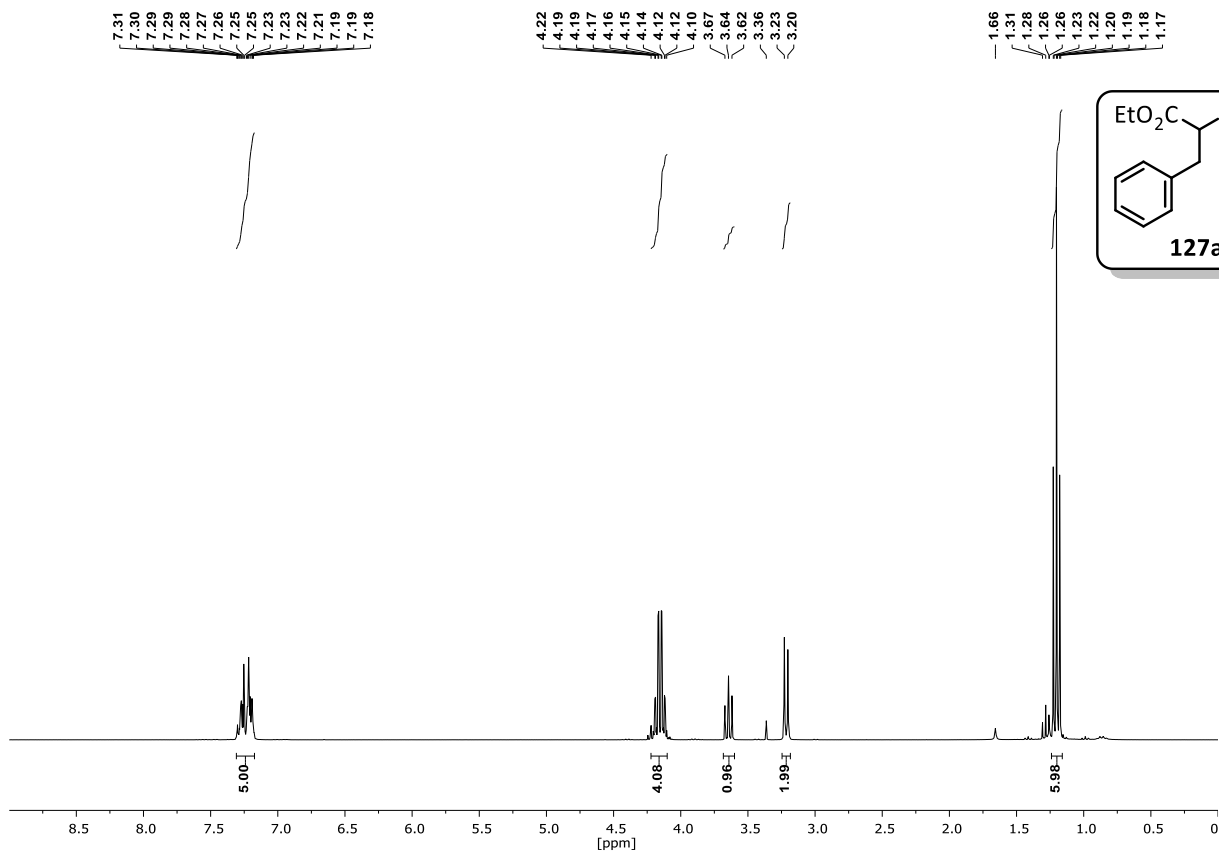
^{13}C-NMR (75 MHz, CDCl$_3$):
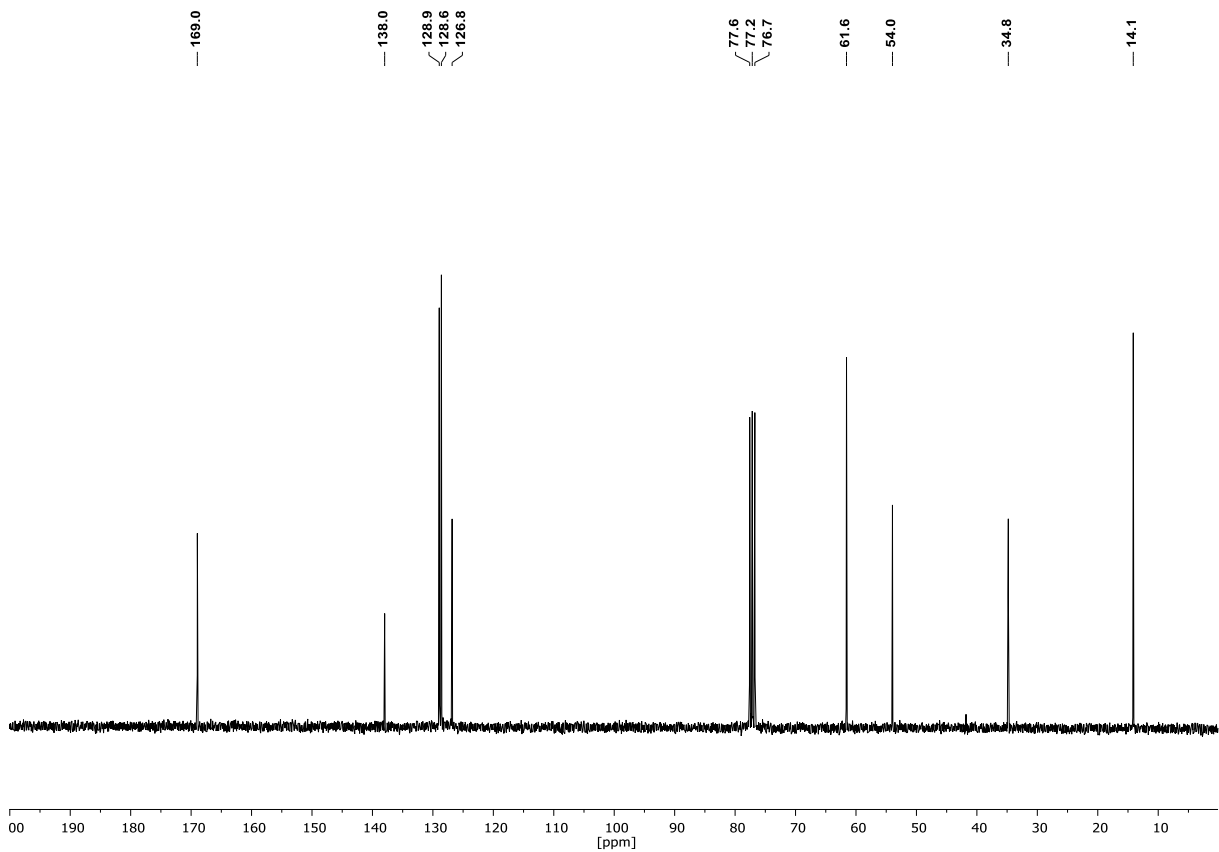
Diethyl 2-(2-methylbenzyl)malonate (127b)

¹H-NMR (300 MHz, CDCl₃):
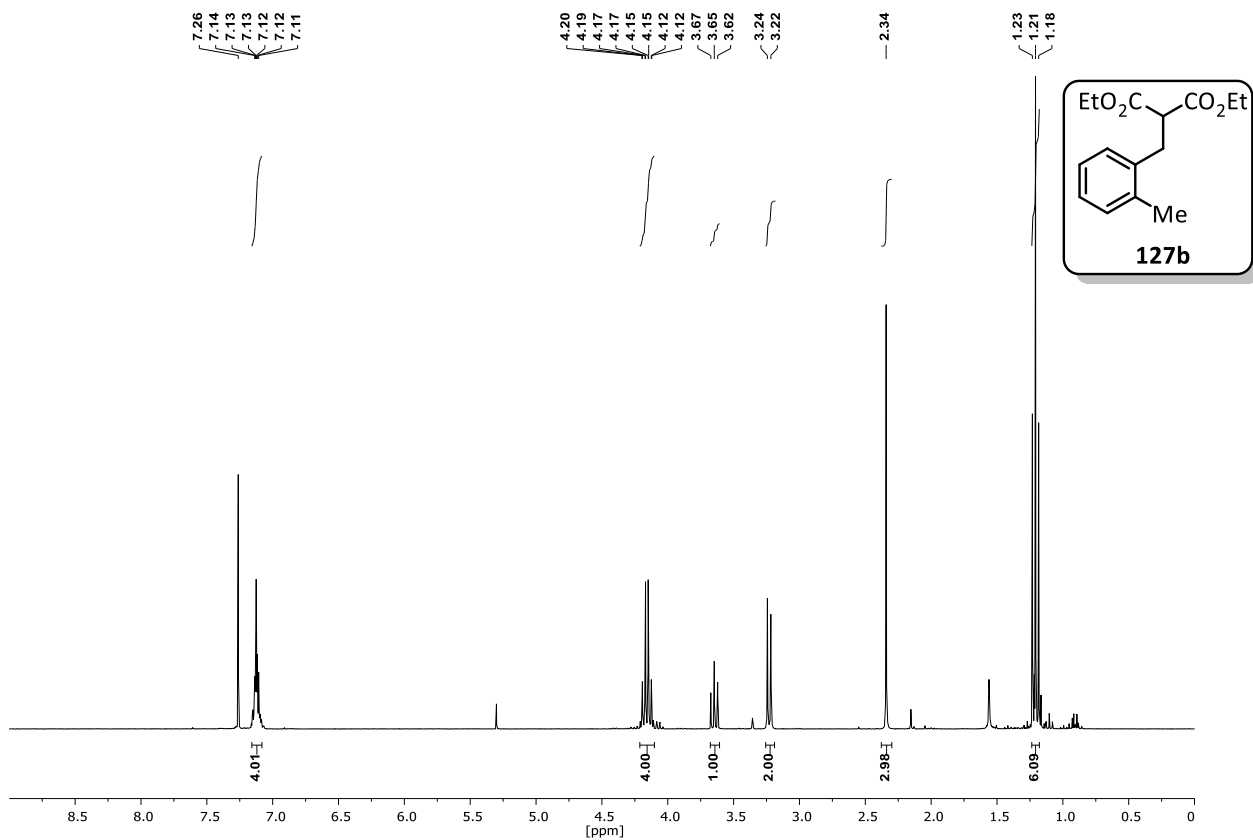
Diethyl 2-(4-methylbenzyl)malonate (127c)

¹H-NMR (300 MHz, CDCl₃):
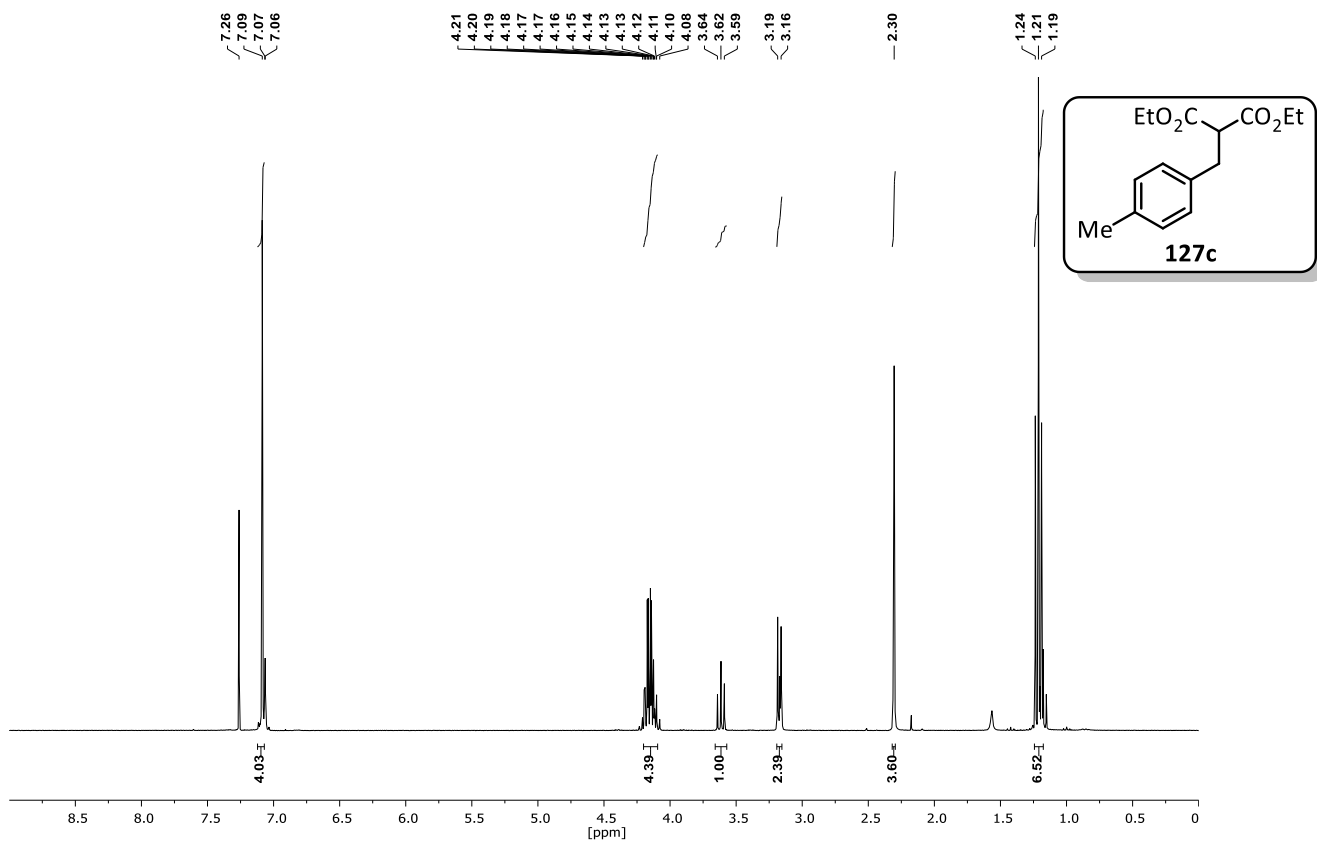
Diethyl 2-(4-bromobenzyl)malonate (127d)

¹H-NMR (300 MHz, CDCl₃):
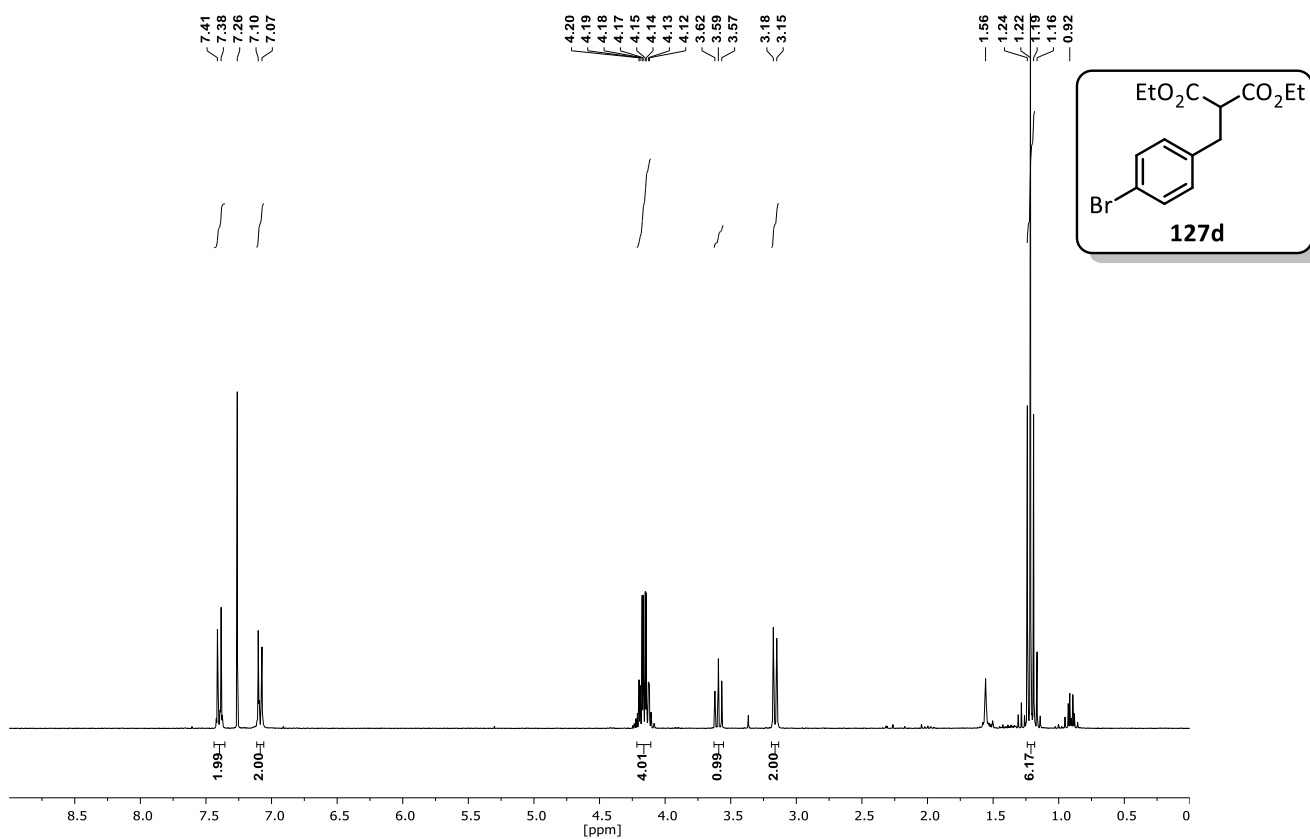
Diethyl 2-(4-nitrobenzyl)malonate (127e)

¹H-NMR (300 MHz, CDCl₃):
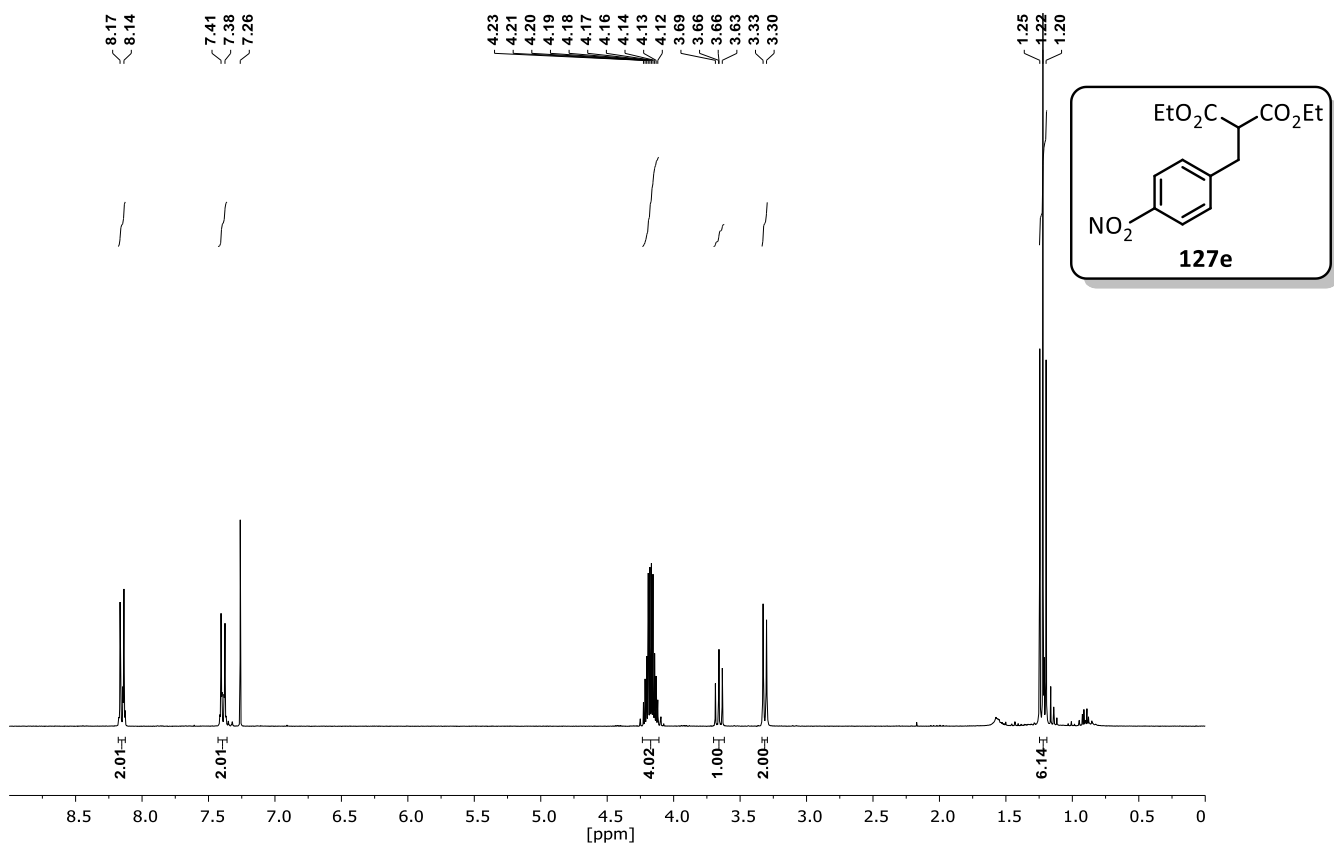
Diethyl 2-isopropylmalonate (127f)

¹H-NMR (400 MHz, CDCl₃):
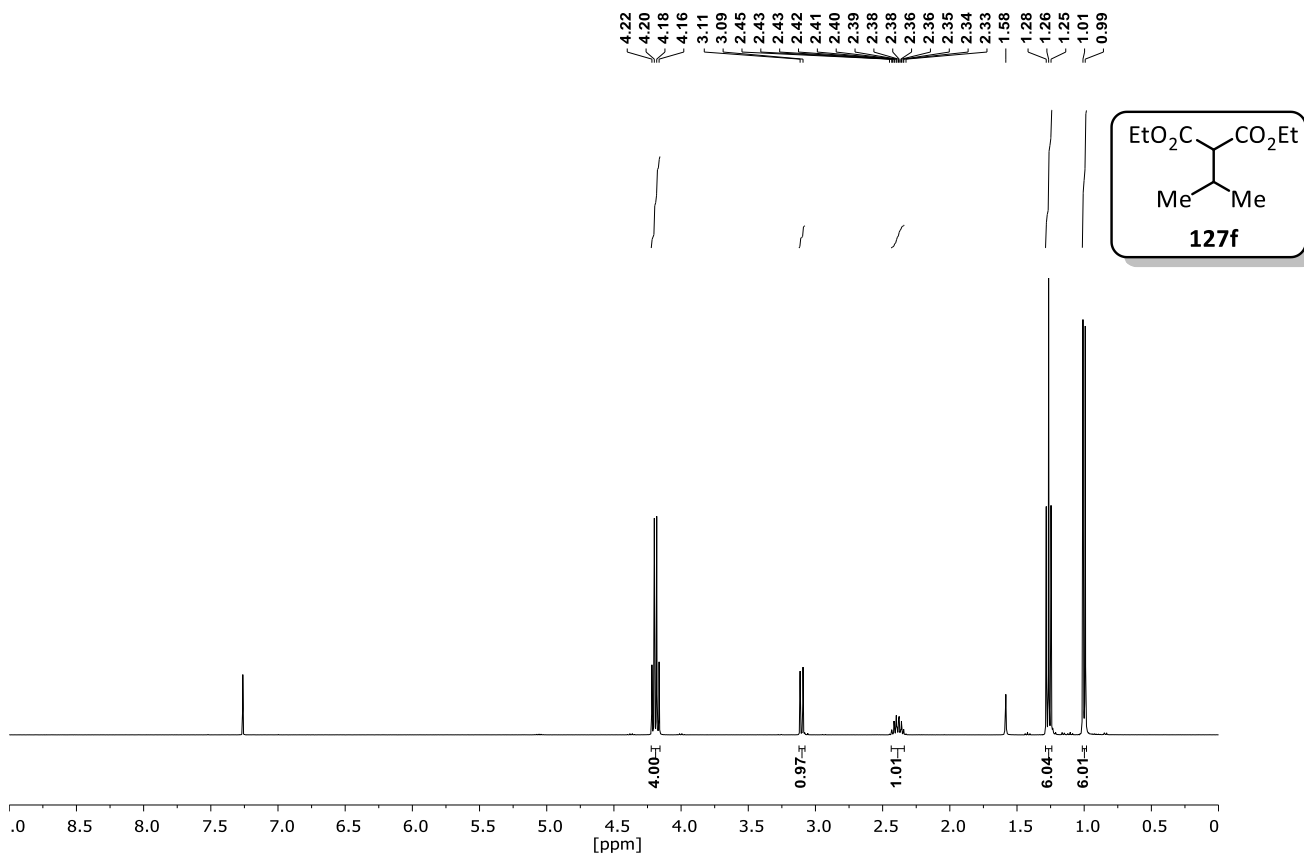
2-isocyano-3-phenylpropanenitrile (127g)

¹H-NMR (300 MHz, CDCl₃):
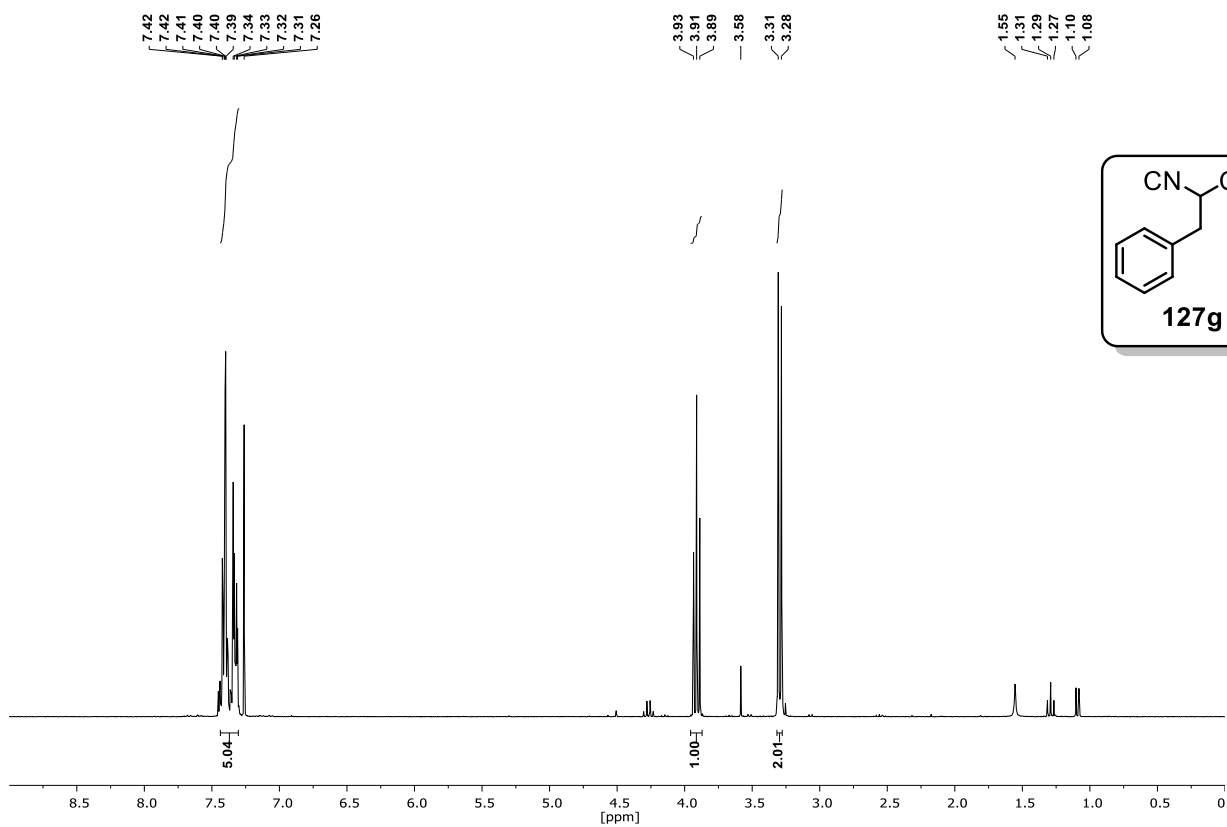
Diethyl 2-benzyl-2-bromomalonate (88a)

^{1}H-NMR (400 MHz, CDCl$_3$):
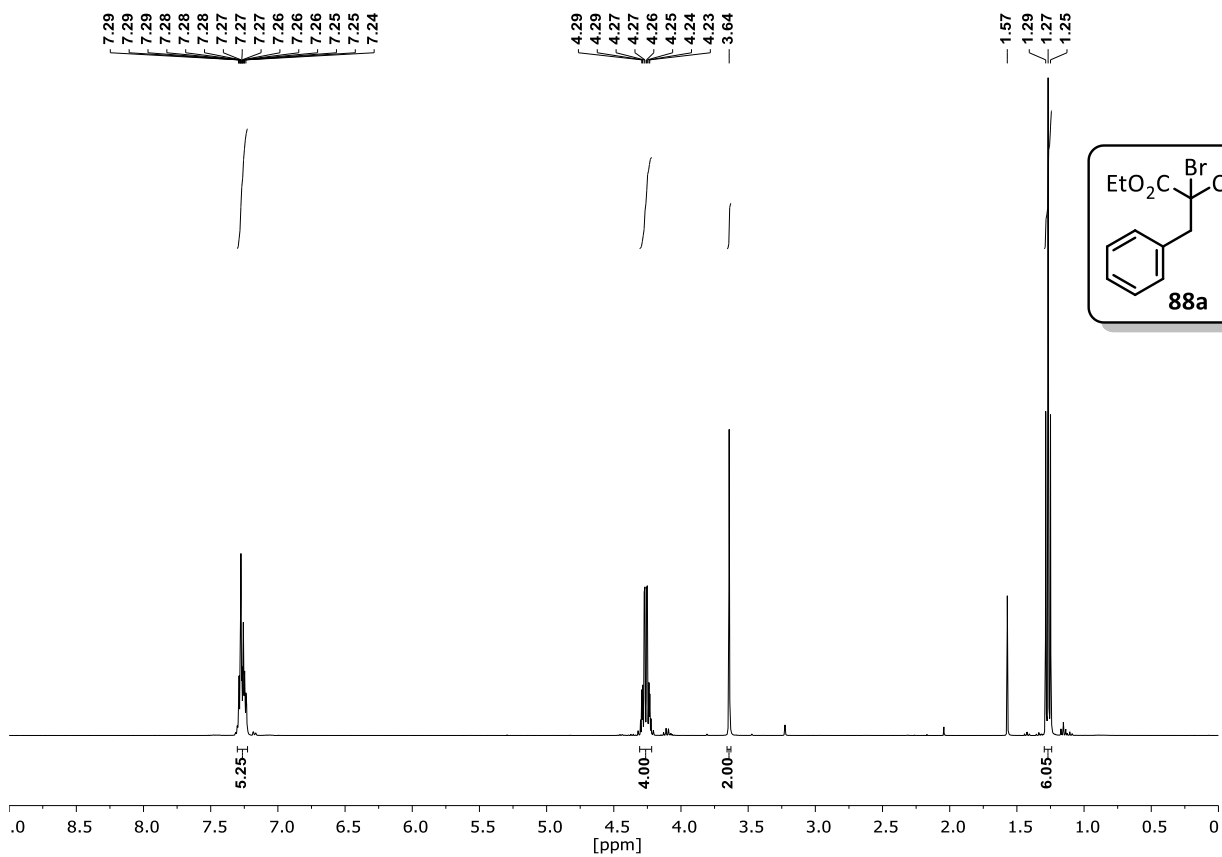
^{13}C-NMR (101 MHz, CDCl$_3$):
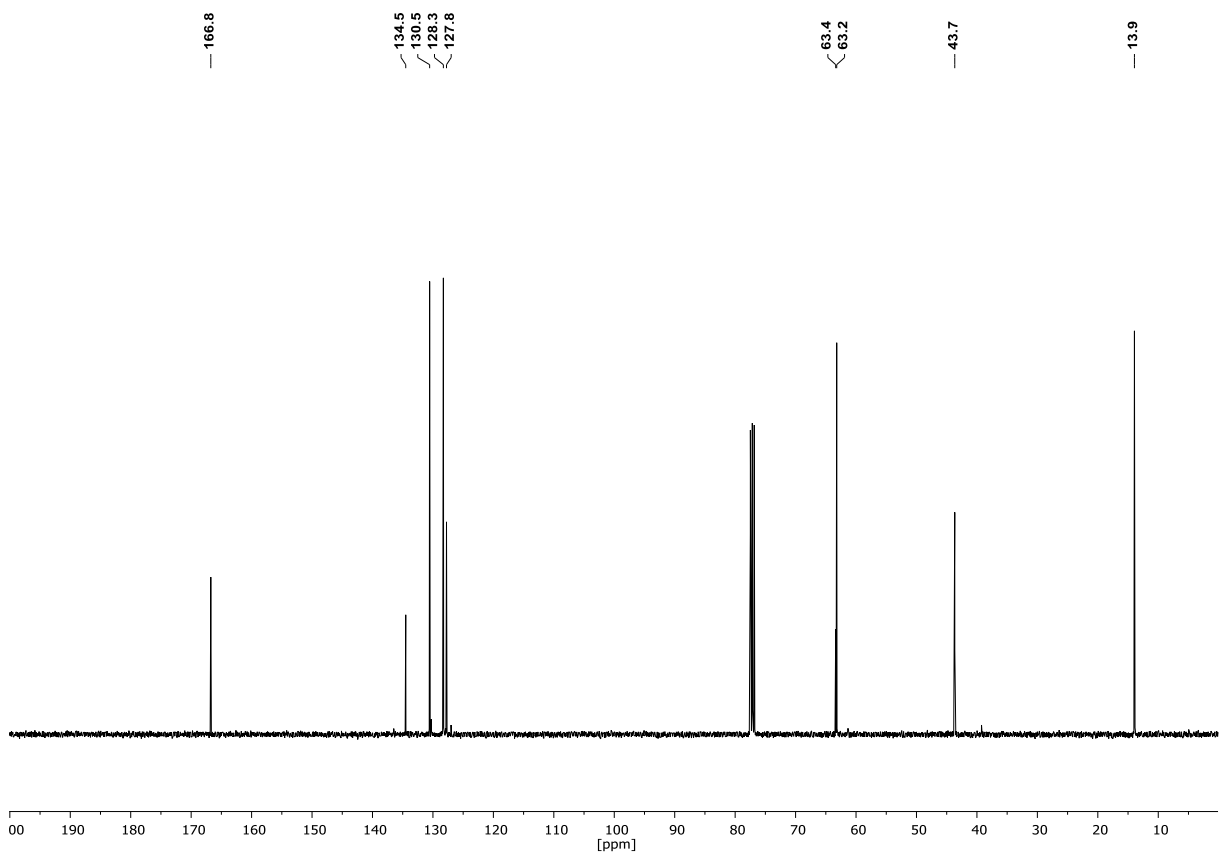
Diethyl 2-bromo-2-(2-methylbenzyl)malonate (88b)

^{1}H-NMR (300 MHz, CDCl$_3$):
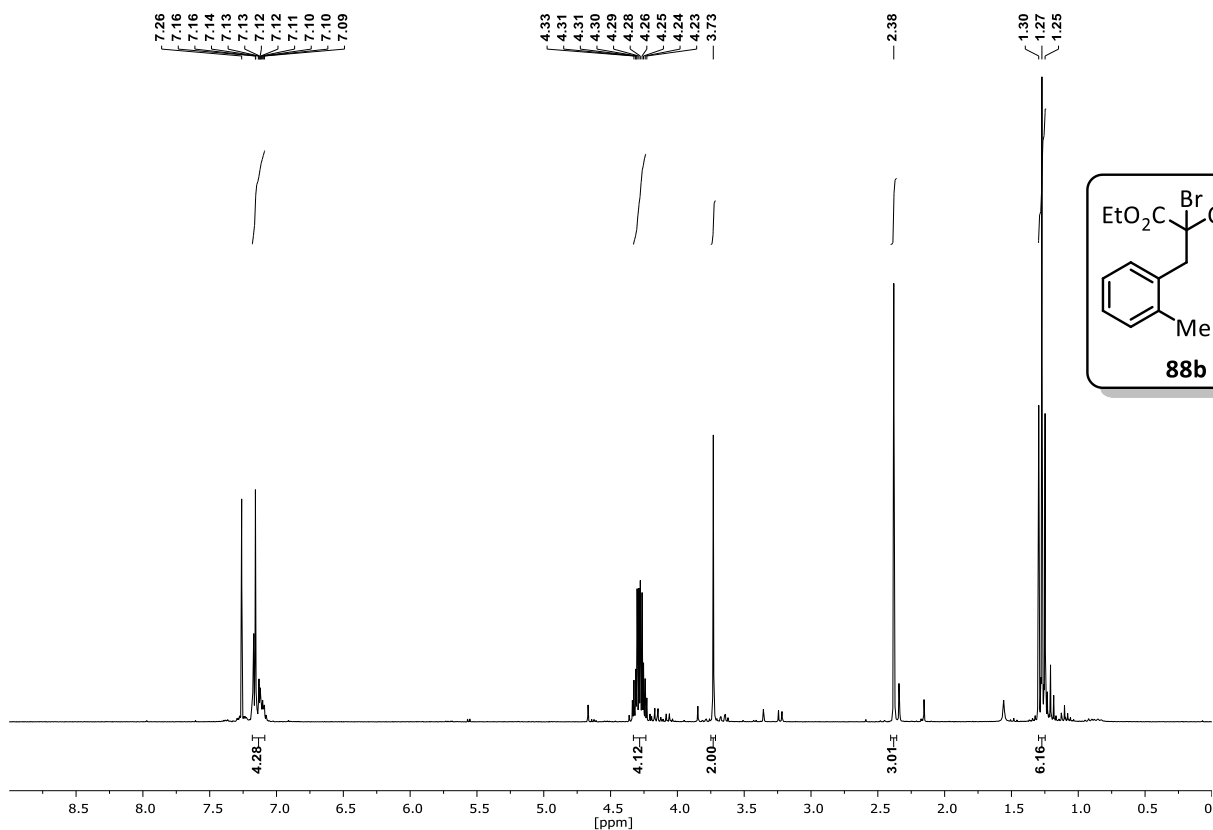
Diethyl 2-bromo-2-(4-methylbenzyl)malonate (88c)

^{1}H-NMR (400 MHz, CDCl$_3$):
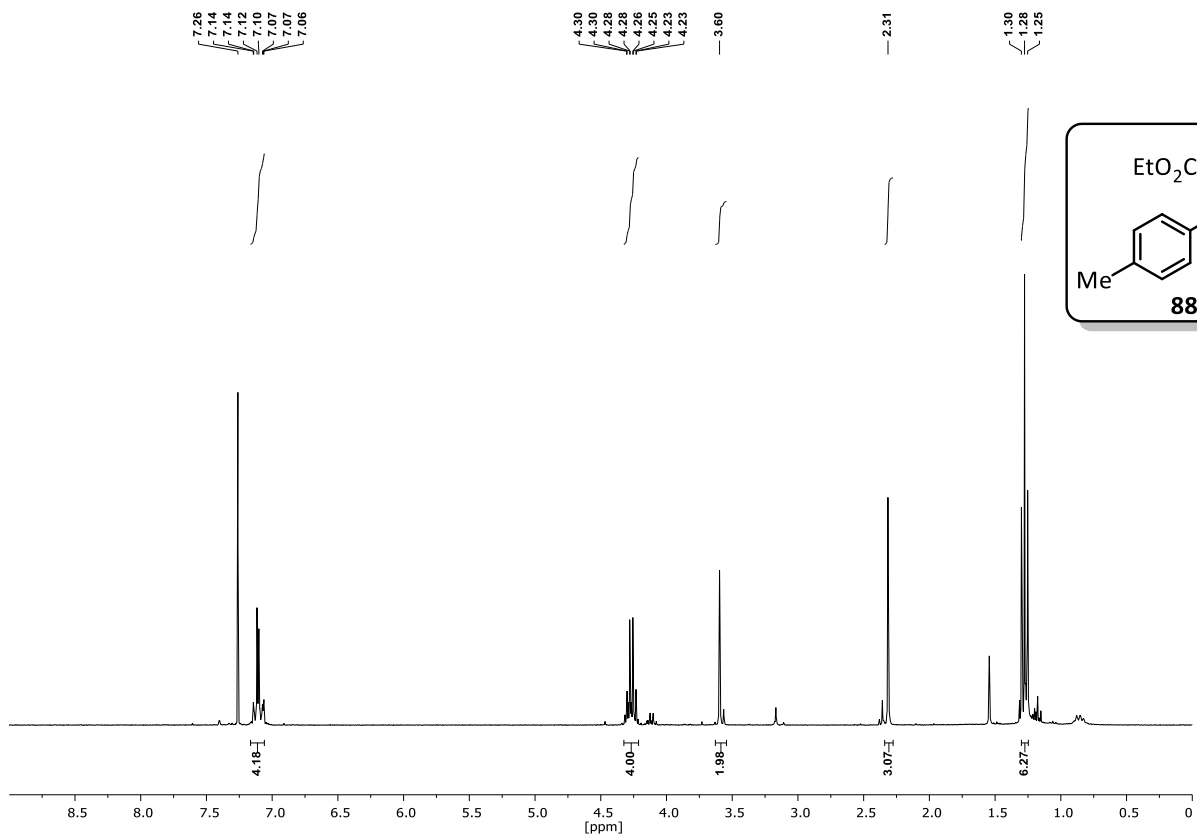
Diethyl 2-bromo-2-(4-bromobenzyl)malonate (88d)

^{1}H-NMR (400 MHz, CDCl$_3$):
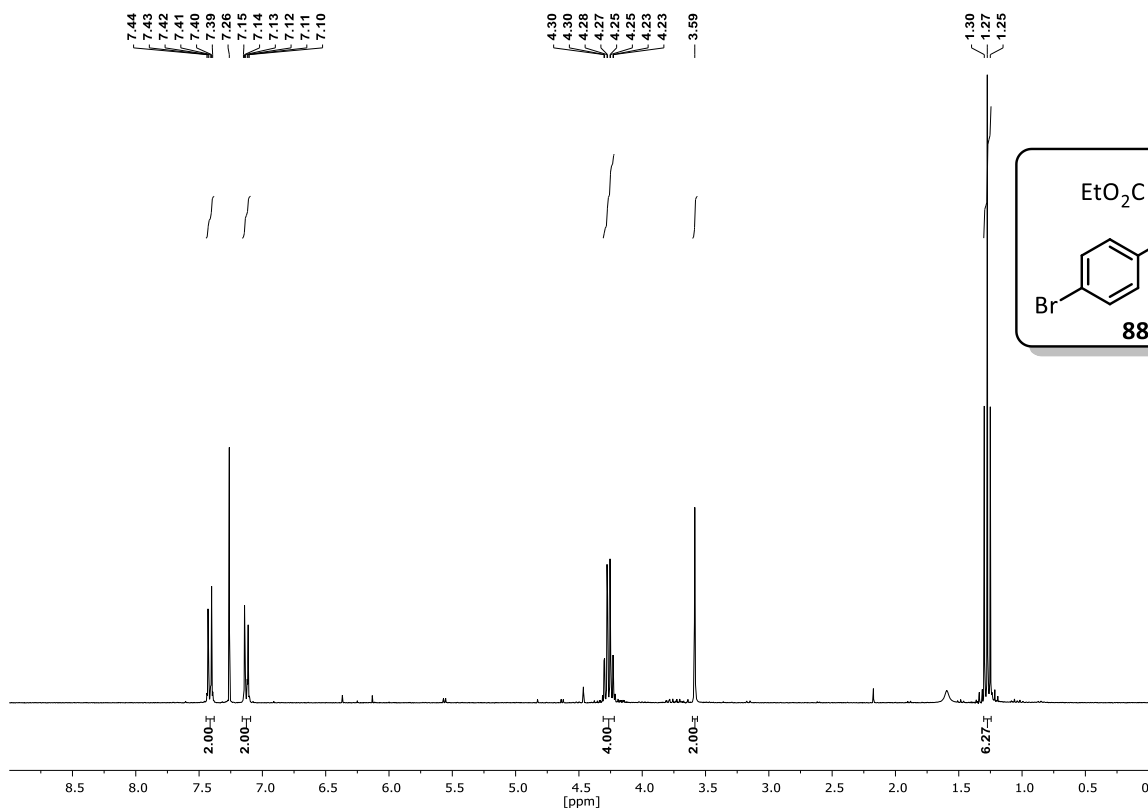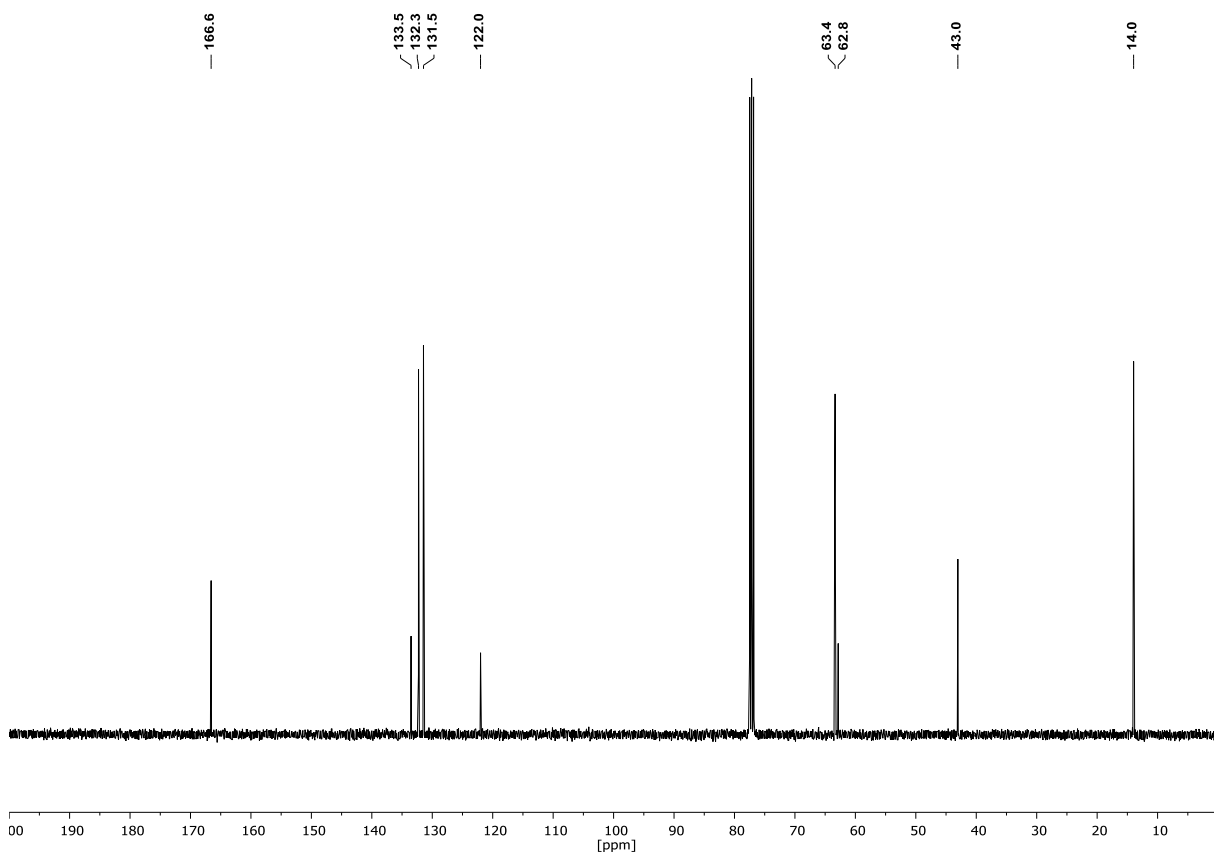
^{13}C-NMR (101 MHz, CDCl$_3$):

Diethyl 2-bromo-2-(4-nitrobenzyl)malonate (88e)

¹H-NMR (400 MHz, CDCl₃):

8.17
8.16
8.16
8.15
8.14
8.14
7.46
7.45
7.44
7.43
7.43
7.42
7.26
4.31
4.31
4.29
4.29
4.27
4.27
4.26
4.25
3.73
1.30
1.28
1.26

2.00
2.00
4.00
2.00
6.01

8.5 8.0 7.5 7.0 6.5 6.0 5.5 5.0 4.5 4.0 3.5 3.0 2.5 2.0 1.5 1.0 0.5 0
[ppm]

¹³C-NMR (101 MHz, CDCl₃):

166.3
147.7
142.1
131.6
123.4
63.6
62.0
43.2
14.0

00 190 180 170 160 150 140 130 120 110 100 90 80 70 60 50 40 30 20 10
[ppm]
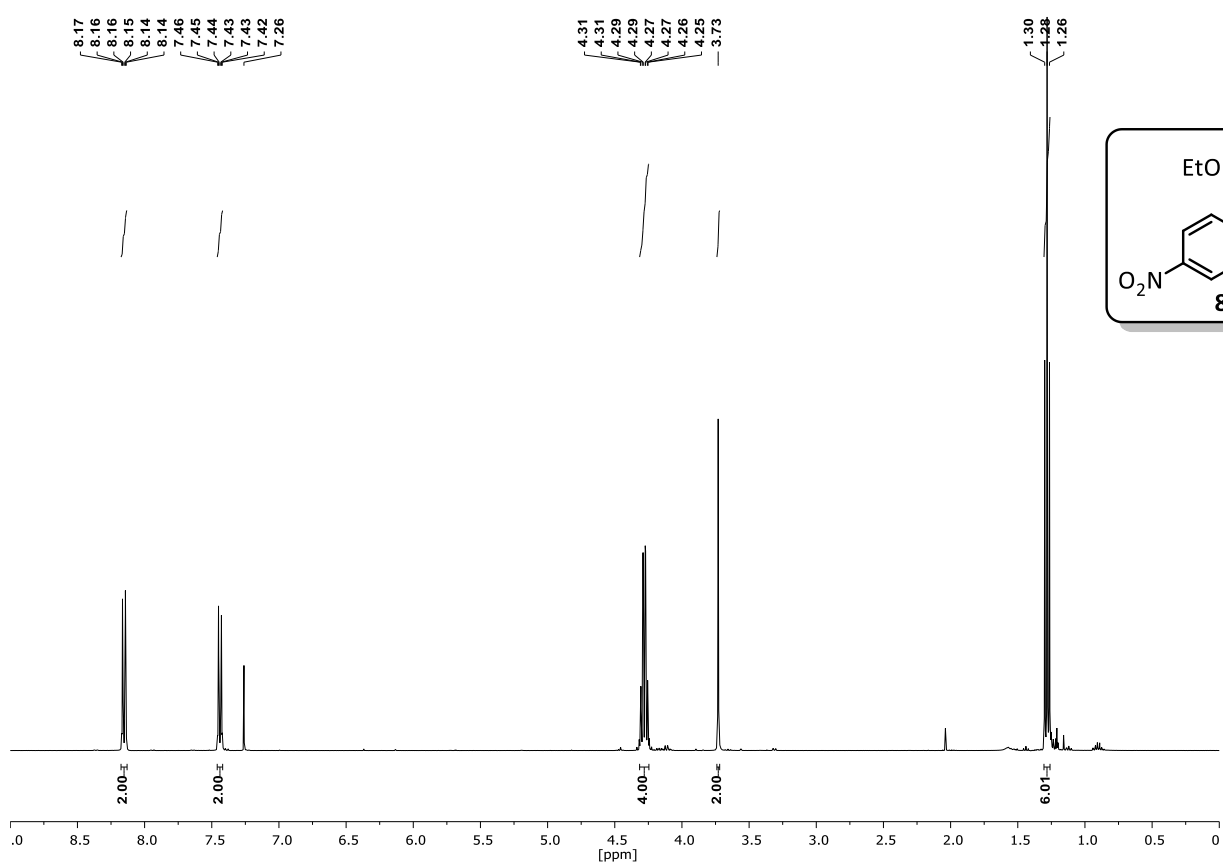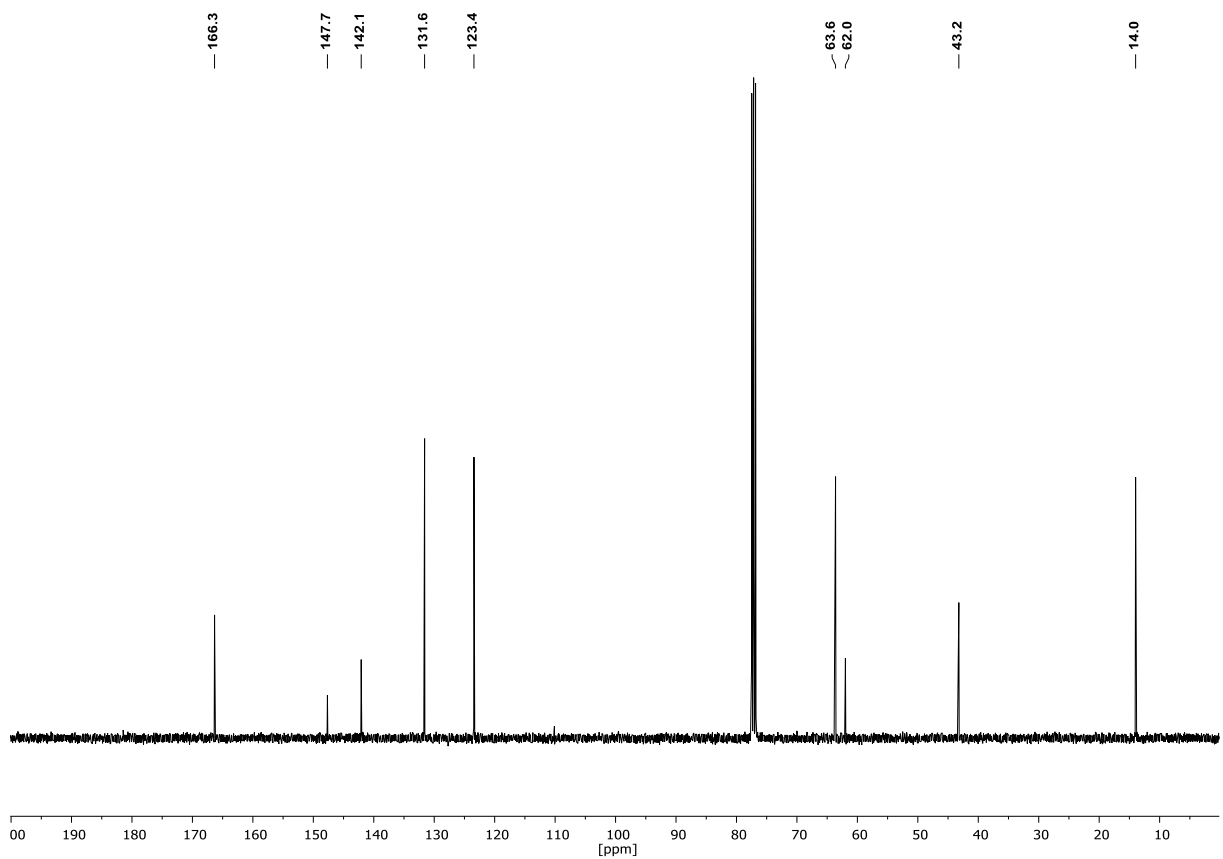
Diethyl 2-bromo-2-isopropylmalonate (88f)

¹H-NMR (300 MHz, CDCl₃):
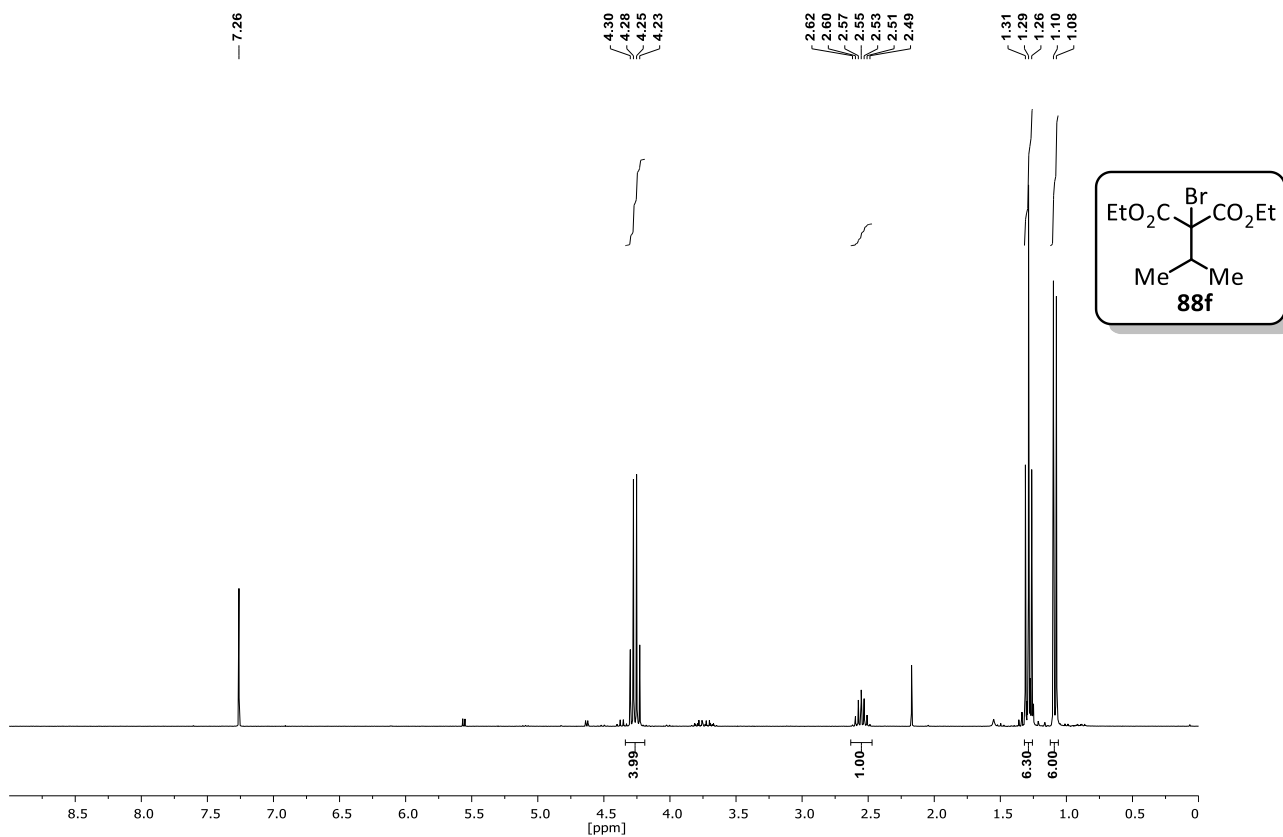
Diethyl 2-bromo-2-ethylmalonate (88h)

¹H-NMR (300 MHz, CDCl₃):
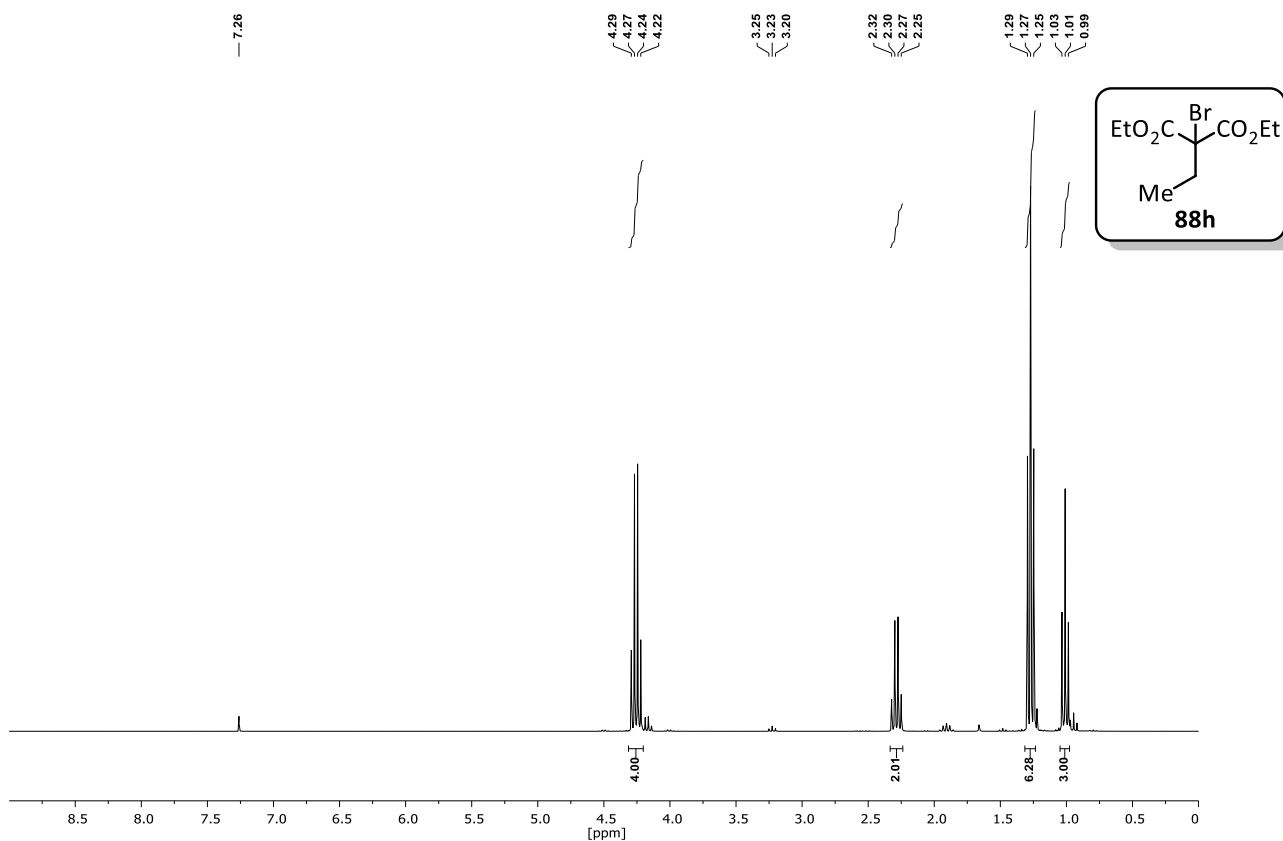
Diethyl 2-bromo-2-(2-nitro-1-phenylethyl)malonate (88i)

¹H-NMR (400 MHz, CDCl₃):
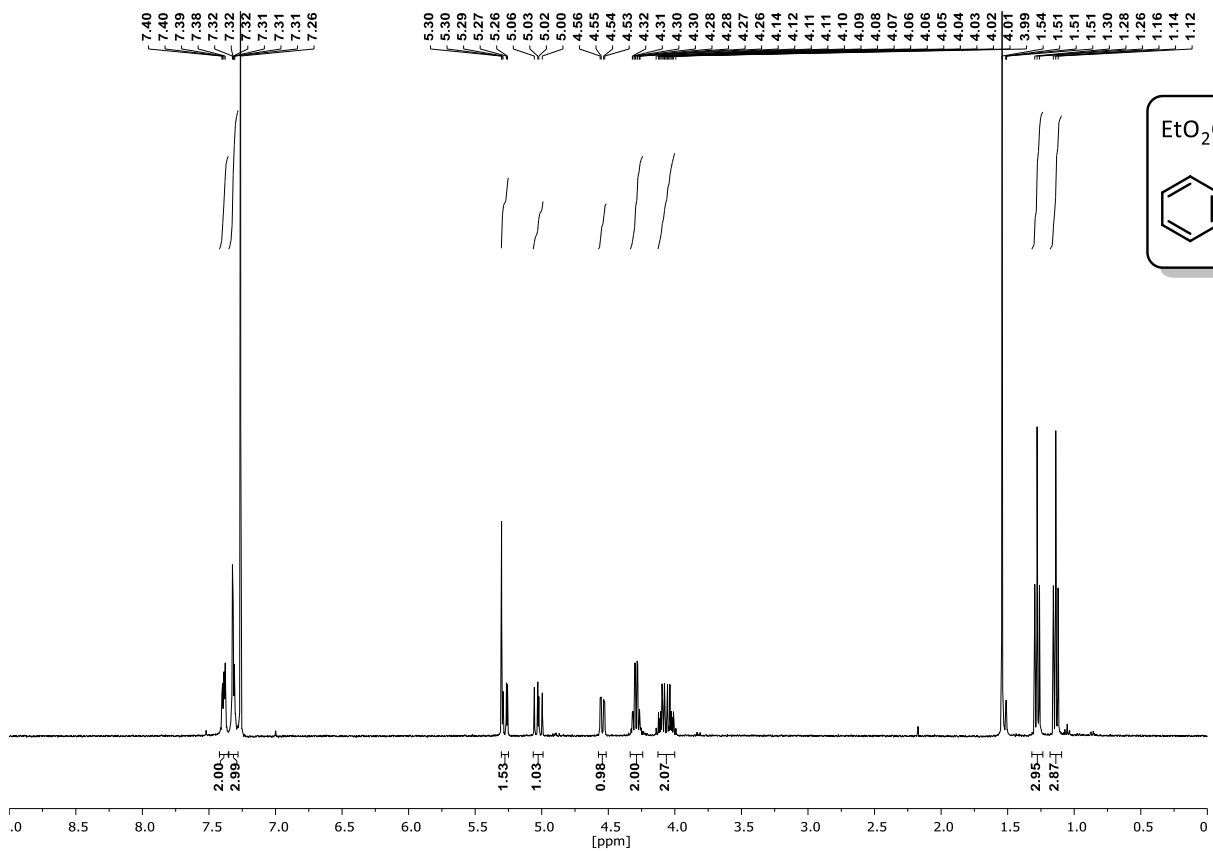
Ethyl 2-bromo-3-methylbutanoate (103)

¹H-NMR (400 MHz, CDCl₃):
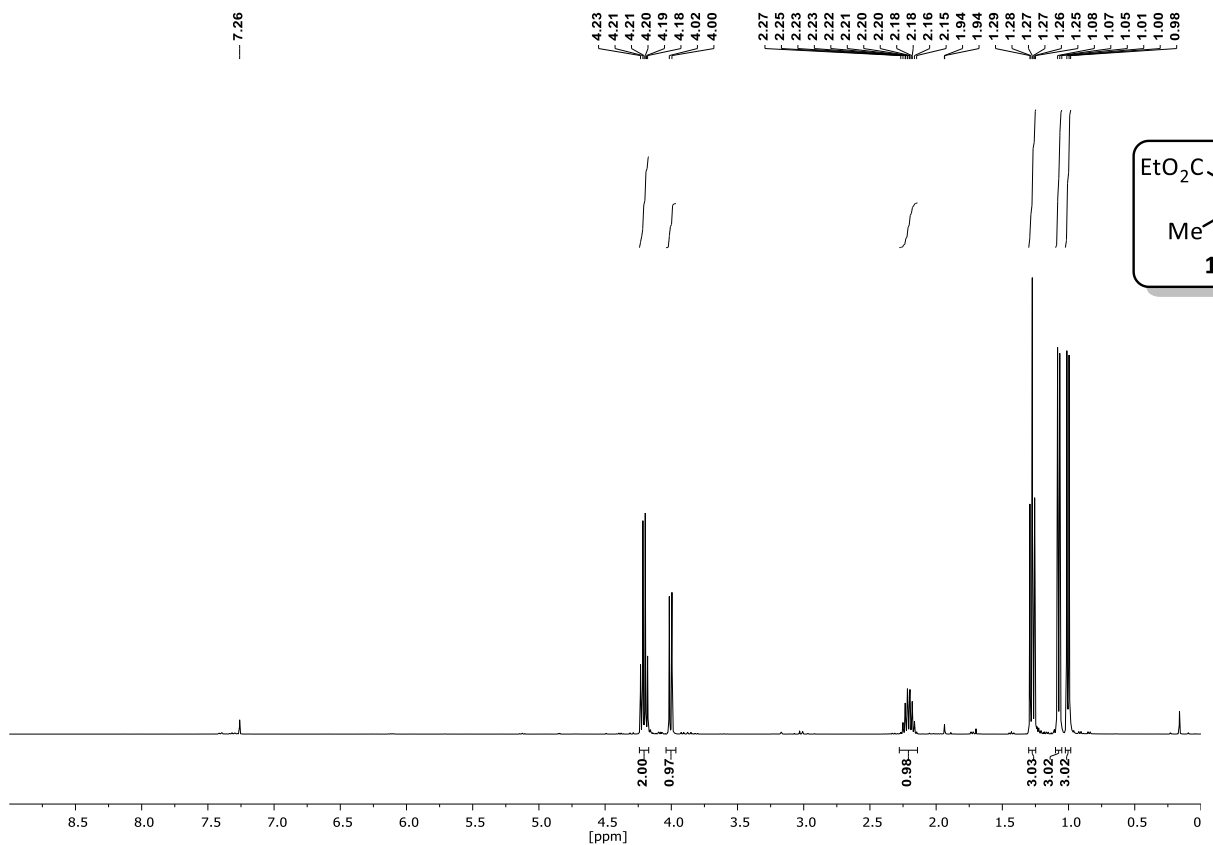
^{13}C-NMR (101 MHz, CDCl$_3$):
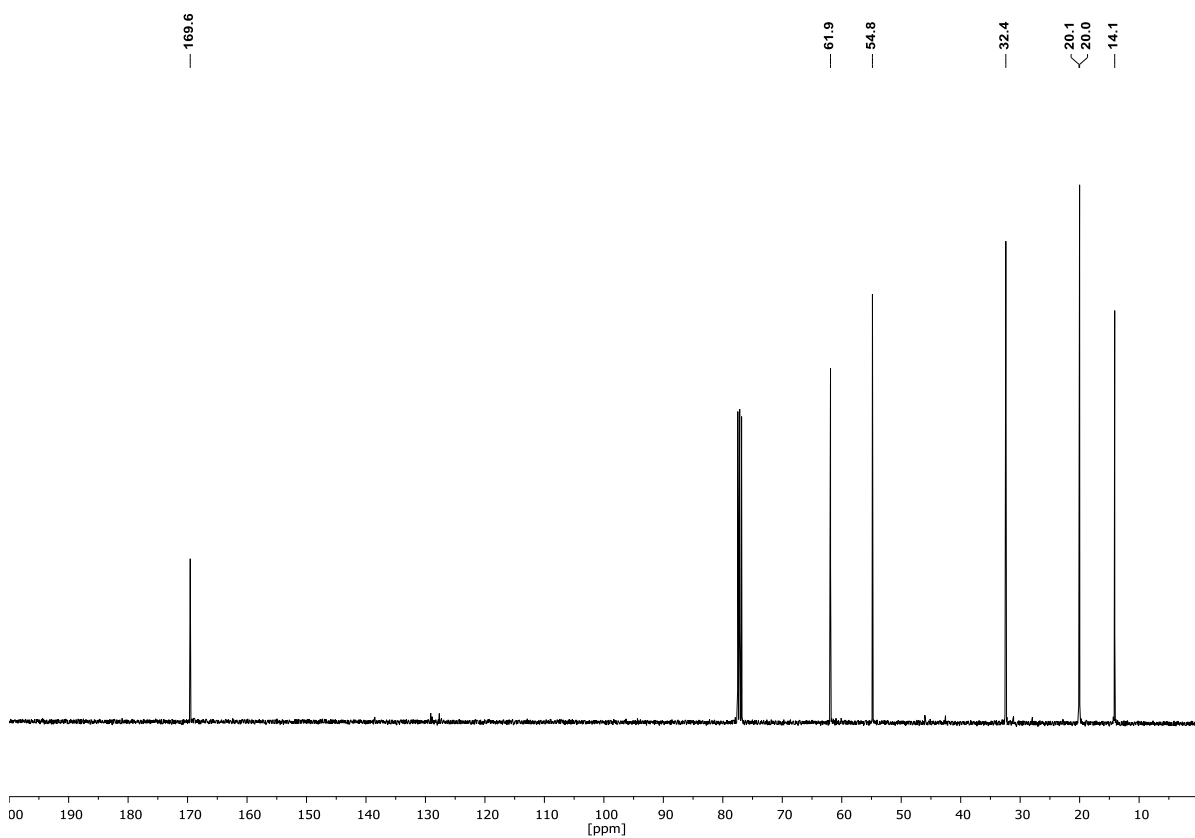
Ethyl 2-bromo-3-phenylpropanoate (105)

^{1}H-NMR (300 MHz, CDCl$_3$):
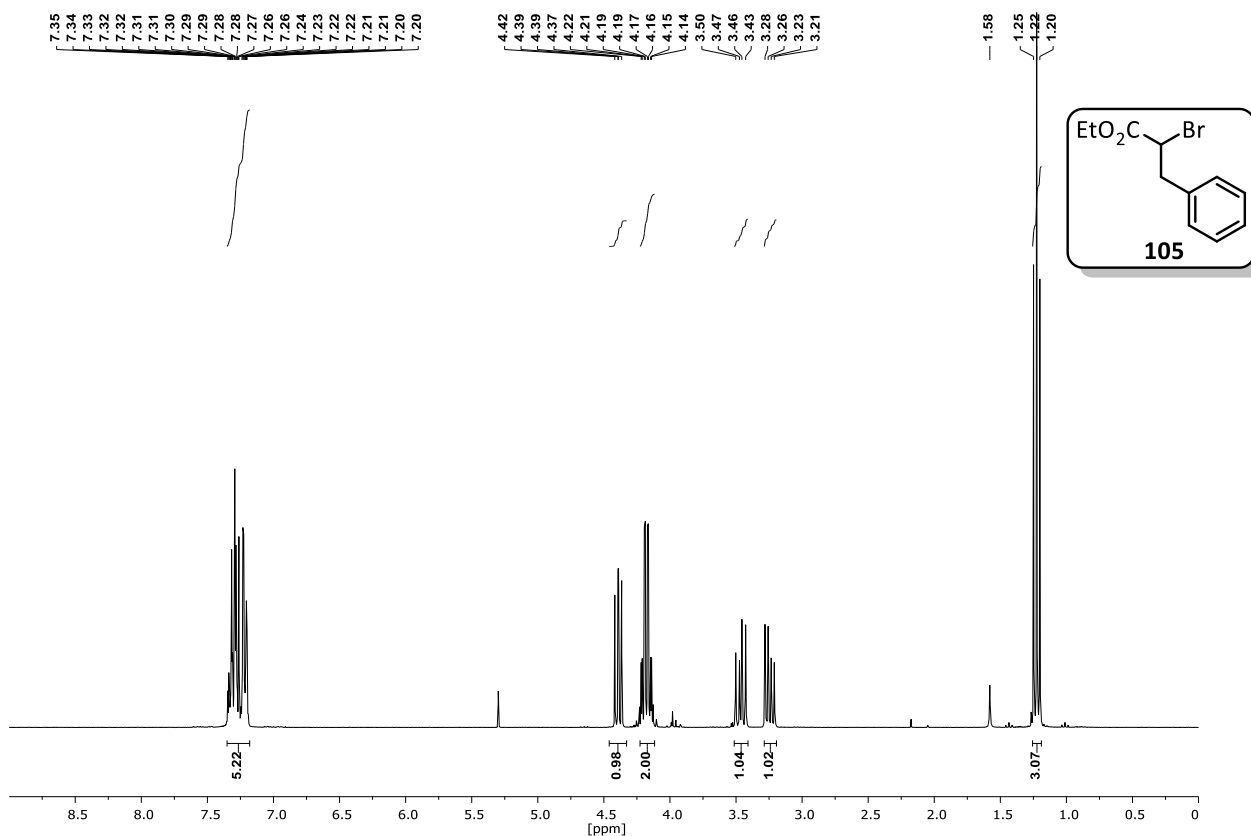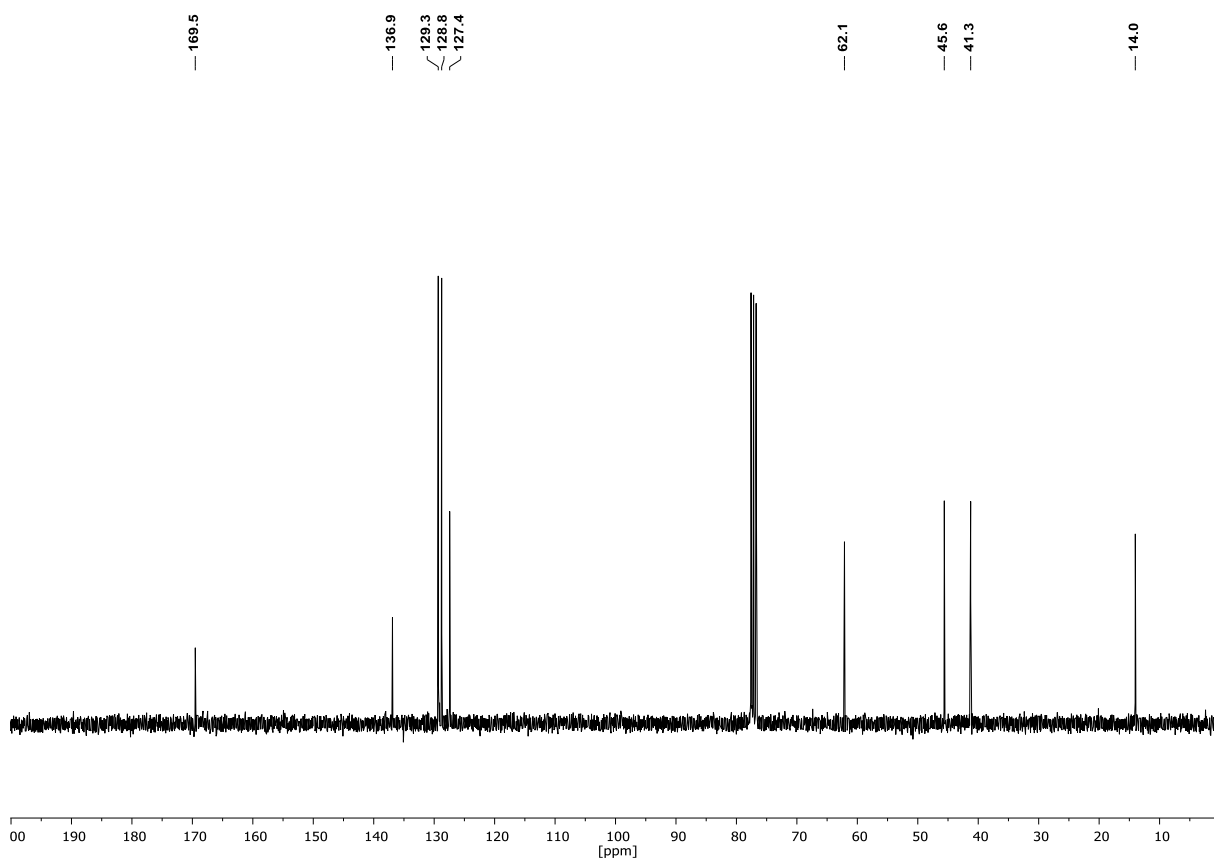
^{13}C-NMR (75 MHz, CDCl$_3$):

Ethyl 1-bromocyclohexane-1-carboxylate (107)

¹H-NMR (400 MHz, CDCl₃):
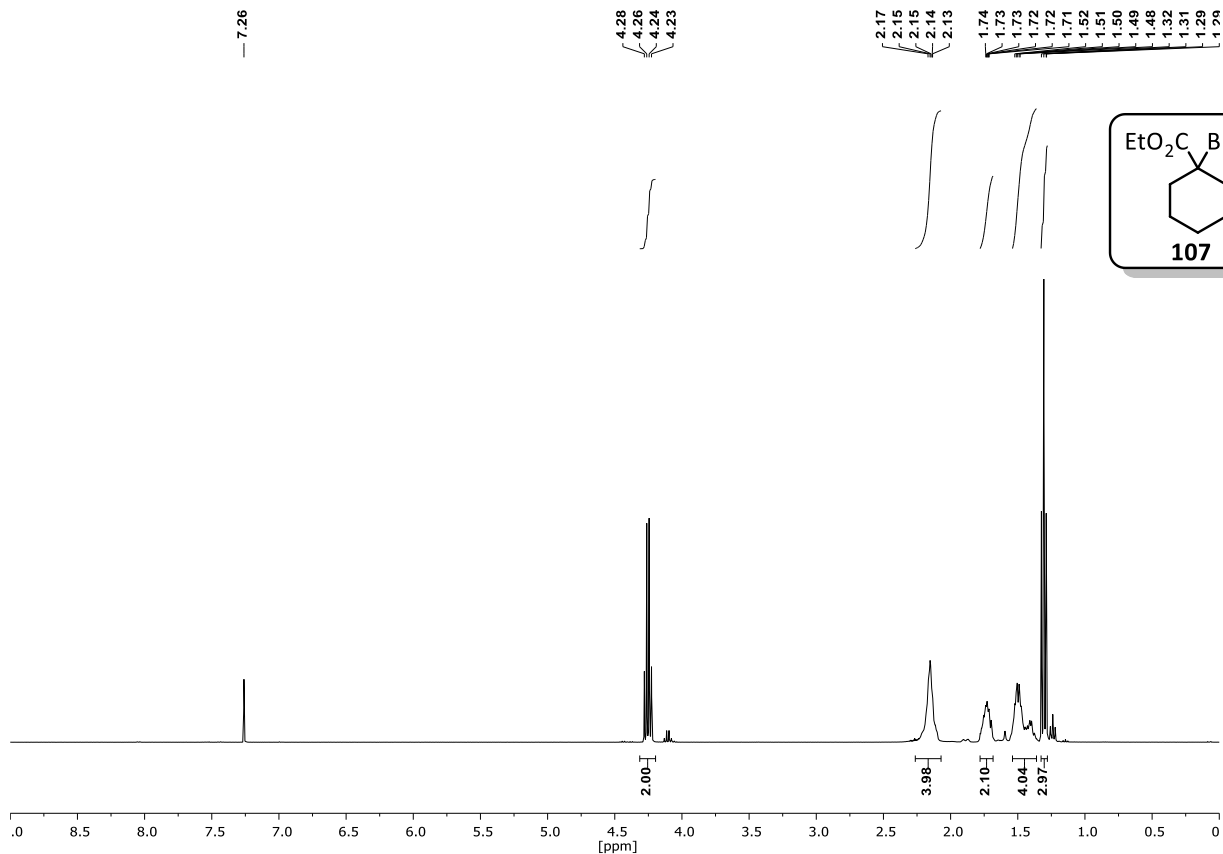
1,3-dioxoisoindolin-2-yl 1-methylcyclohexane-1-carboxylate (110)

¹H-NMR (300 MHz, CDCl₃):

7.91
7.90
7.89
7.88
7.87
7.86
7.85
7.85
7.81
7.80
7.79
7.78
7.78
7.77
7.76
7.76
7.75
7.75
7.26

2.04
1.70
1.69
1.68
1.65
1.64
1.63
1.59
1.58
1.57
1.55
1.54
1.52
1.51
1.43
1.41
1.38
1.36
1.34
1.33
1.31
1.28
1.25
1.23
1.21
1.11

110

1.98
2.01

2.04

5.50
3.49
3.03

[ppm]

8.5 8.0 7.5 7.0 6.5 6.0 5.5 5.0 4.5 4.0 3.5 3.0 2.5 2.0 1.5 1.0 0.5 0

¹³C-NMR (101 MHz, CDCl₃):

173.8
162.4
134.8
129.2
124.0
43.3
35.8
26.9
25.6
23.2

[ppm]

00 190 180 170 160 150 140 130 120 110 100 90 80 70 60 50 40 30 20 10

1,3-dioxoisoindolin-2-yl 3-phenylpropanoate (136)

¹H-NMR (400 MHz, CDCl₃):

7.93
7.93
7.92
7.91
7.83
7.82
7.81
7.39
7.38
7.37
7.37
7.36
7.35
7.35
7.34
7.30
7.29
7.28
7.28
7.26

3.16
3.16
3.14
3.13
3.12
3.04
3.04
3.02
3.02
3.01
3.00
3.00

136

2.00
2.05
2.04
3.51
2.03
2.02

.0   8.5   8.0   7.5   7.0   6.5   6.0   5.5   5.0   4.5   4.0   3.5   3.0   2.5   2.0   1.5   1.0   0.5   0
[ppm]

¹³C-NMR (75 MHz, CDCl₃):

169.0
162.0
139.3
134.9
129.1
128.9
128.5
126.9
124.1
32.9
30.7

00 190 180 170 160 150 140 130 120 110 100 90 80 70 60 50 40 30 20 10
[ppm]
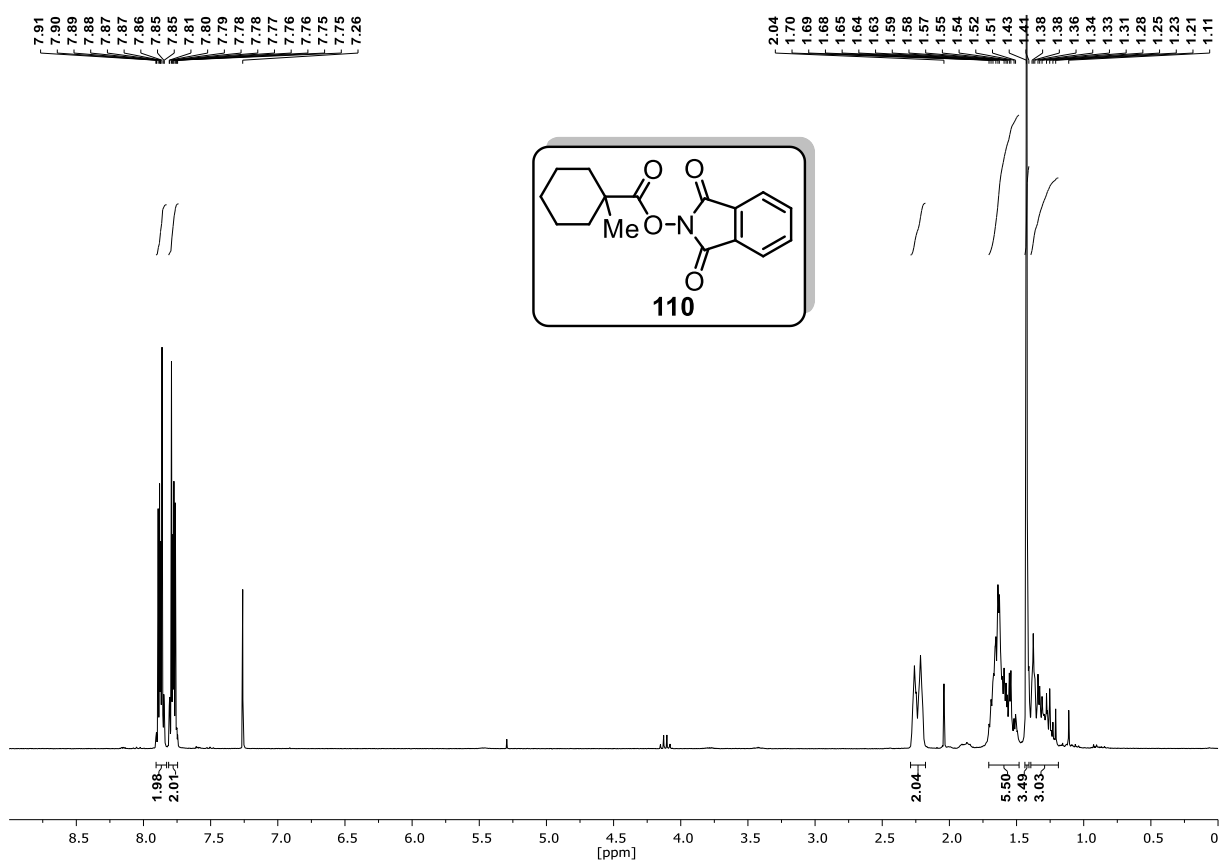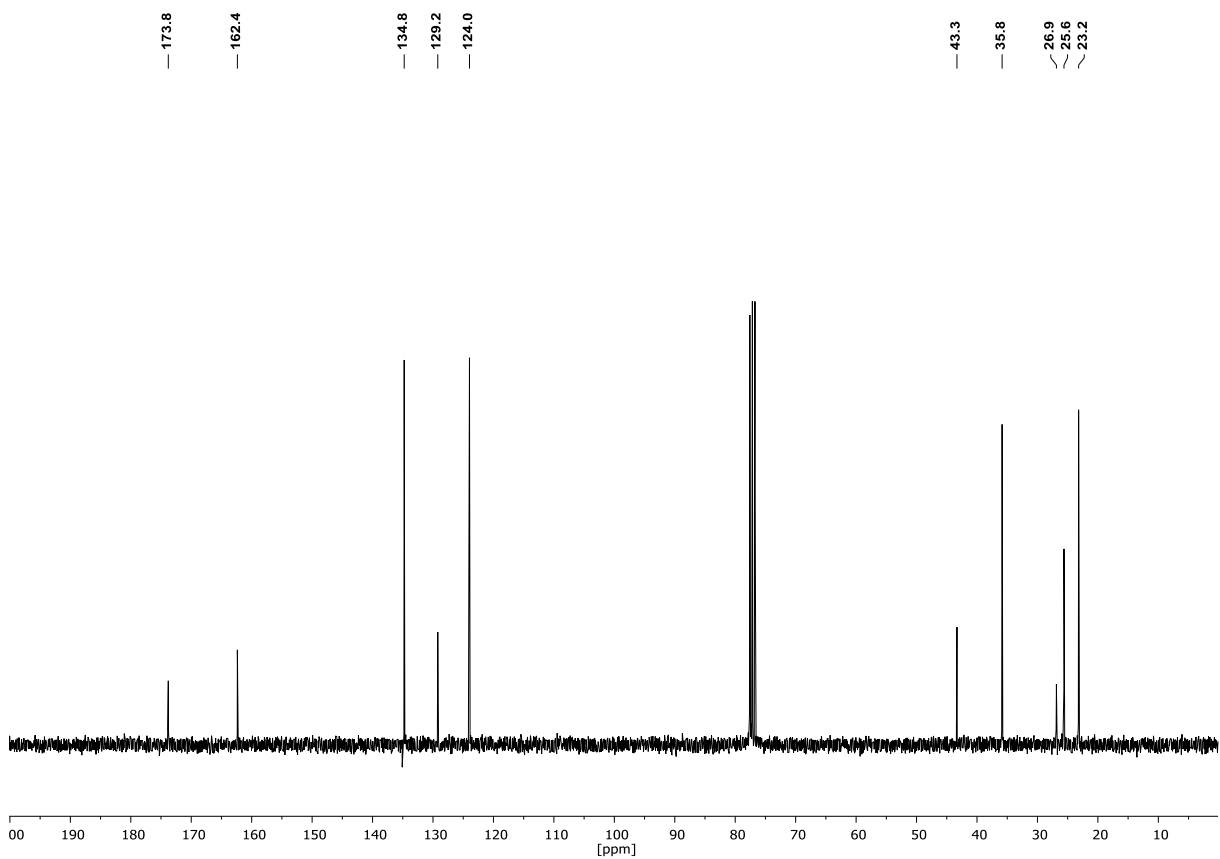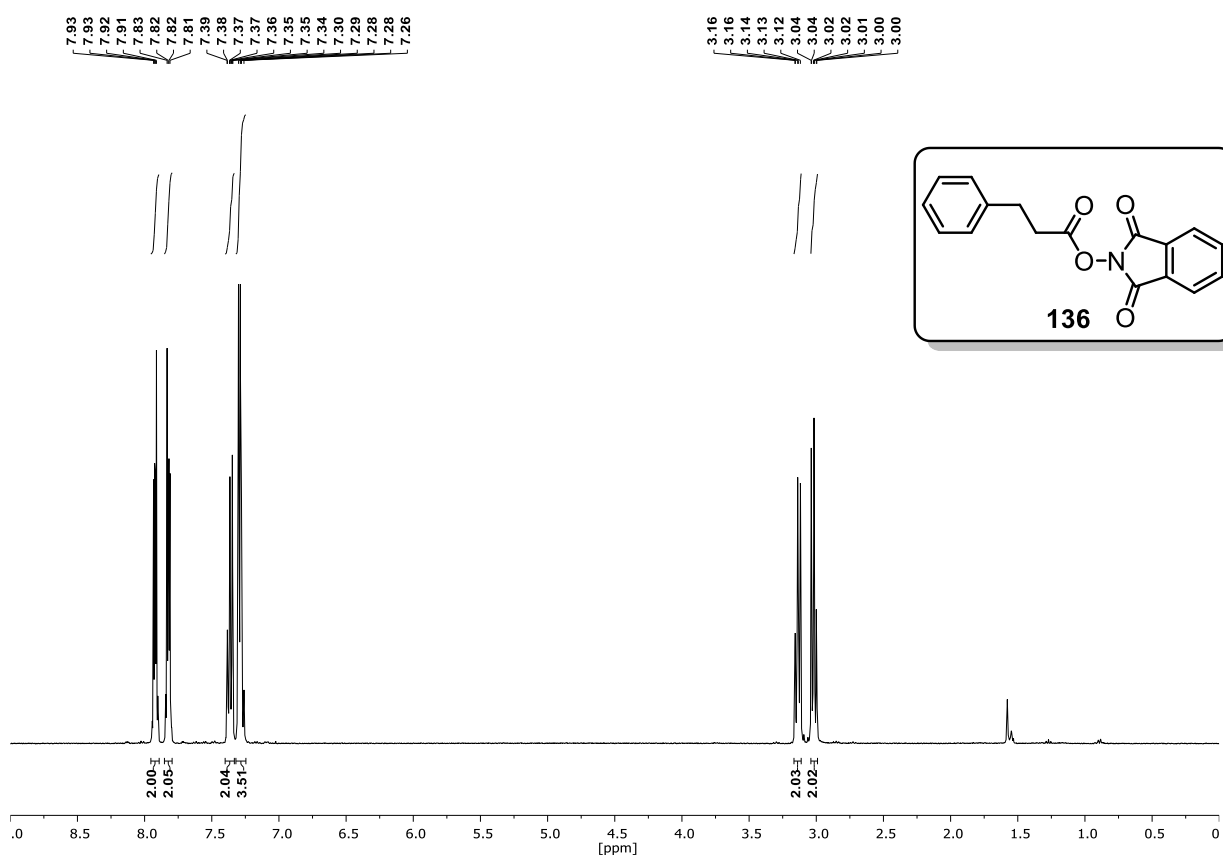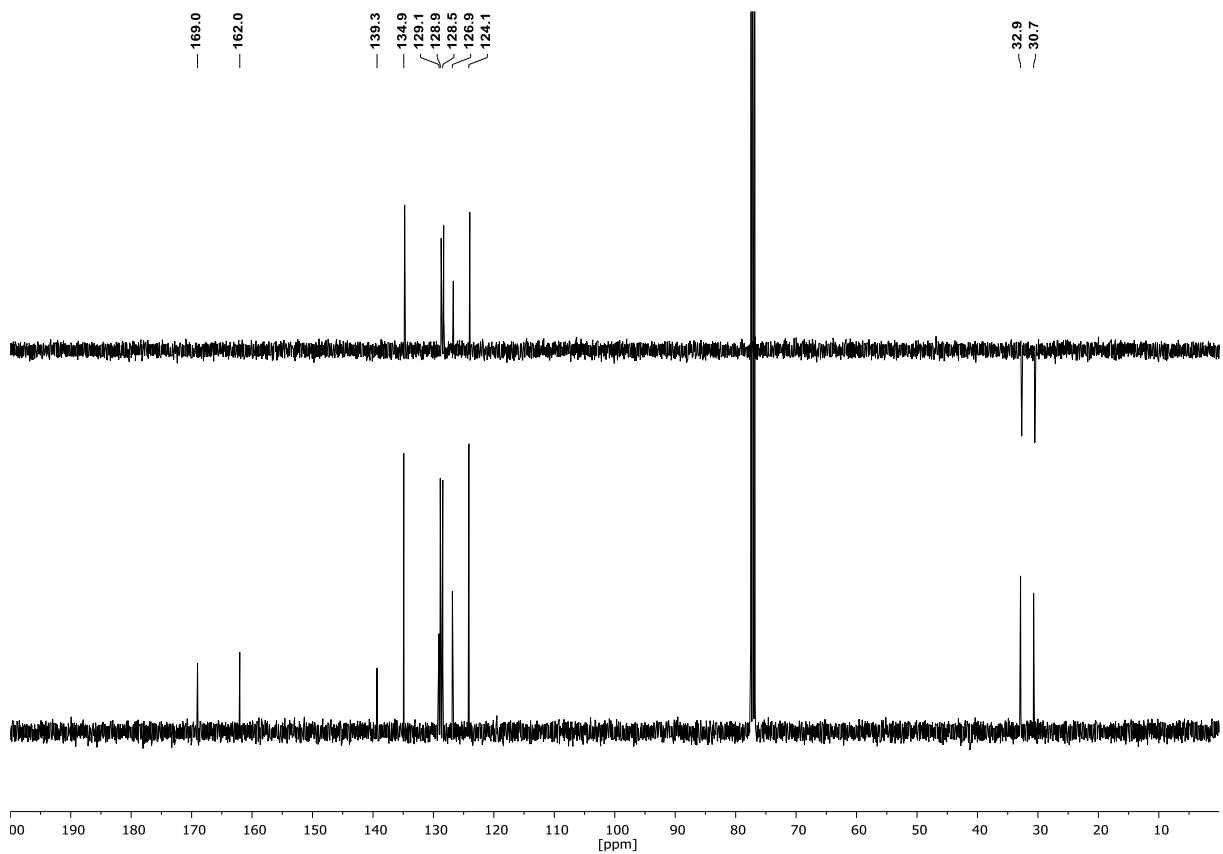
1,3-dioxoisoindolin-2-yl (tert-butoxycarbonyl)phenylalaninate (138)
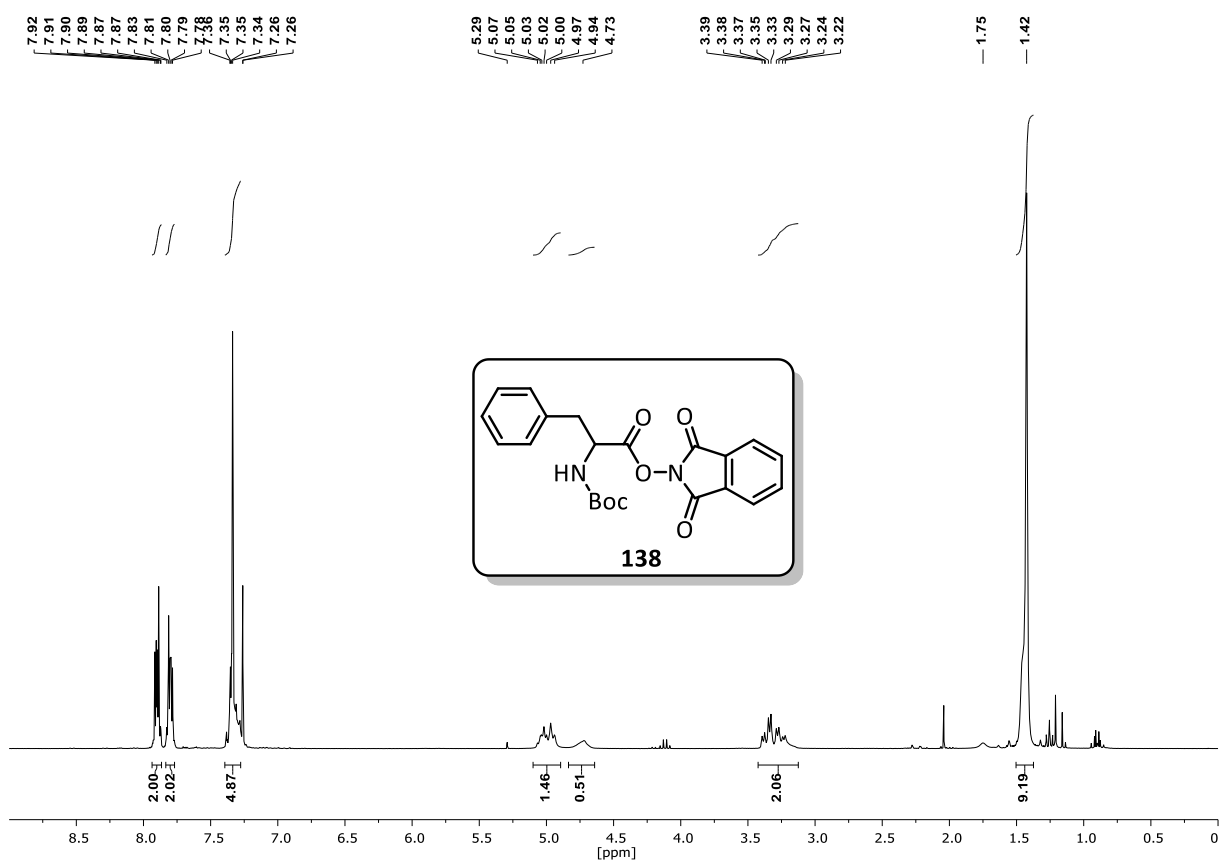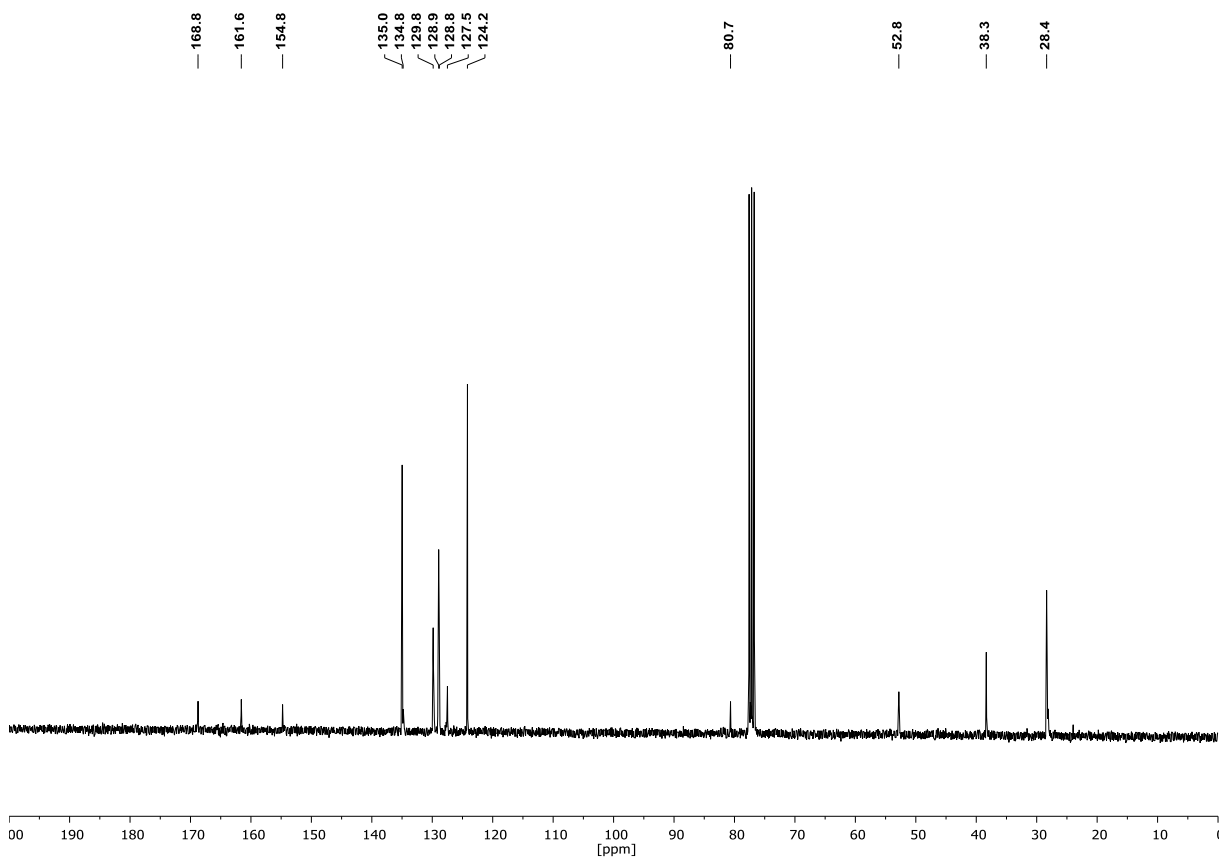
¹H-NMR (300 MHz, CDCl₃):

¹³C-NMR (75 MHz, CDCl₃):

3-phenylcyclobutan-1-one (128)

¹H-NMR (400 MHz, CDCl₃):

7.40
7.38
7.37
7.34
7.33
7.32
7.31
7.30
7.28
7.26

3.71
3.69
3.66
3.64
3.62
3.51
3.49
3.47
3.46
3.44
3.27
3.25
3.22
3.20

1.98
3.01

0.99
2.00
2.00

¹³C-NMR (101 MHz, CDCl₃):

206.2

143.5

128.5
126.4
126.3

54.4

28.2

3-phenylcyclobutan-1-one oxime

¹H-NMR (400 MHz, CDCl₃):

9.76

7.42
7.40
7.38
7.34
7.32
7.30
7.28
7.26

3.70
3.68
3.66
3.64
3.62
3.58
3.57
3.57
3.56
3.55
3.54
3.54
3.53
3.52
3.52
3.51
3.50
3.47
3.46
3.46
3.45
3.44
3.43
3.42
3.41
3.41
3.40
3.39
3.39
3.16
3.15
3.15
3.14
3.13
3.12
3.11
3.10
3.09
3.09

0.89

2.00
3.00

1.00
1.00
1.00
1.00

2.00

| 1.0 | 10.5 | 10.0 | 9.5 | 9.0 | 8.5 | 8.0 | 7.5 | 7.0 | 6.5 | 6.0 | 5.5 | 5.0 | 4.5 | 4.0 | 3.5 | 3.0 | 2.5 | 2.0 | 1.5 | 1.0 | 0.5 | 0 |

[ppm]

¹³C-NMR (101 MHz, CDCl₃):

156.5

144.0

128.6
126.5
126.4

39.2
38.3
32.8

| 190 | 180 | 170 | 160 | 150 | 140 | 130 | 120 | 110 | 100 | 90 | 80 | 70 | 60 | 50 | 40 | 30 | 20 | 10 | |

[ppm]

3-phenylcyclobutan-1-one O-(4-(trifluoromethyl)benzoyl) oxime (129)

¹H-NMR (400 MHz, CDCl₃):
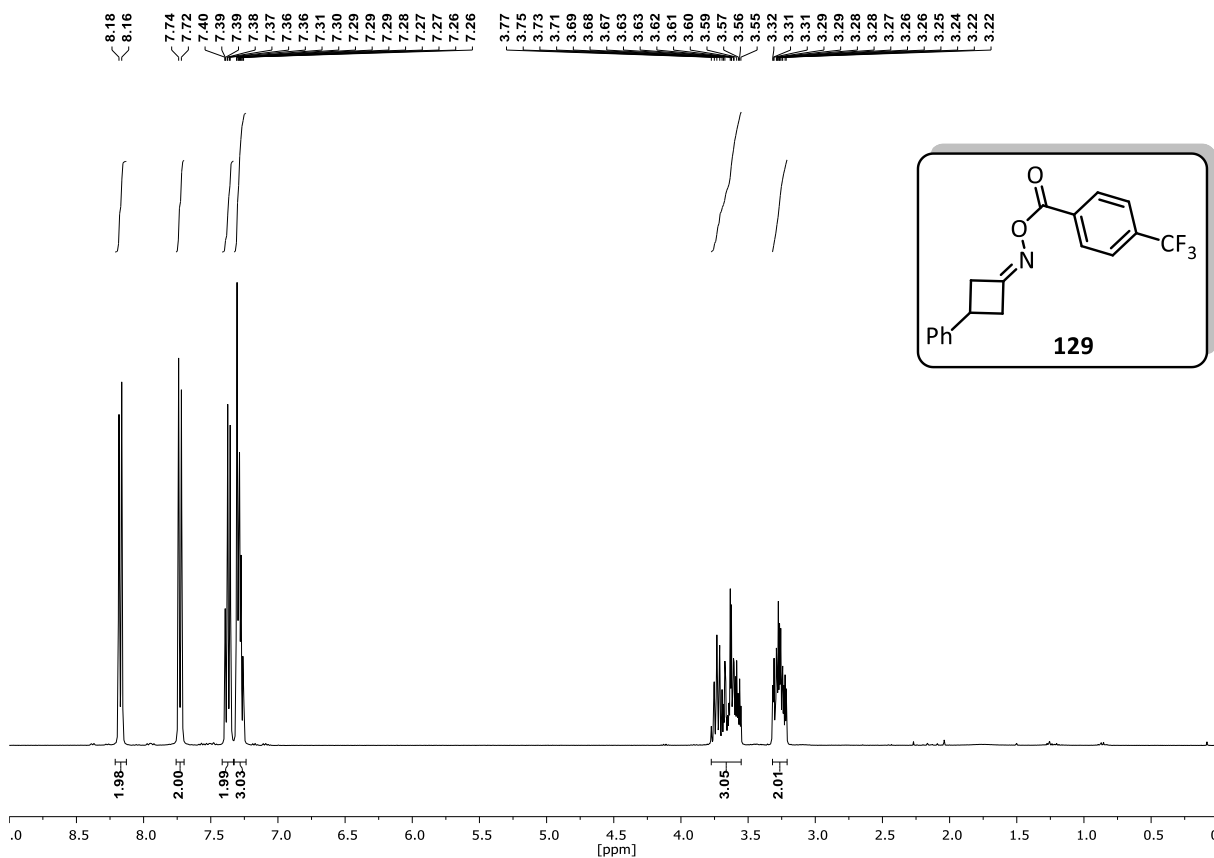
¹³C-NMR (101 MHz, CDCl₃) & **DEPT135** (101 MHz, CDCl₃):

¹⁹F-NMR (377 MHz, CDCl₃):

-63.7
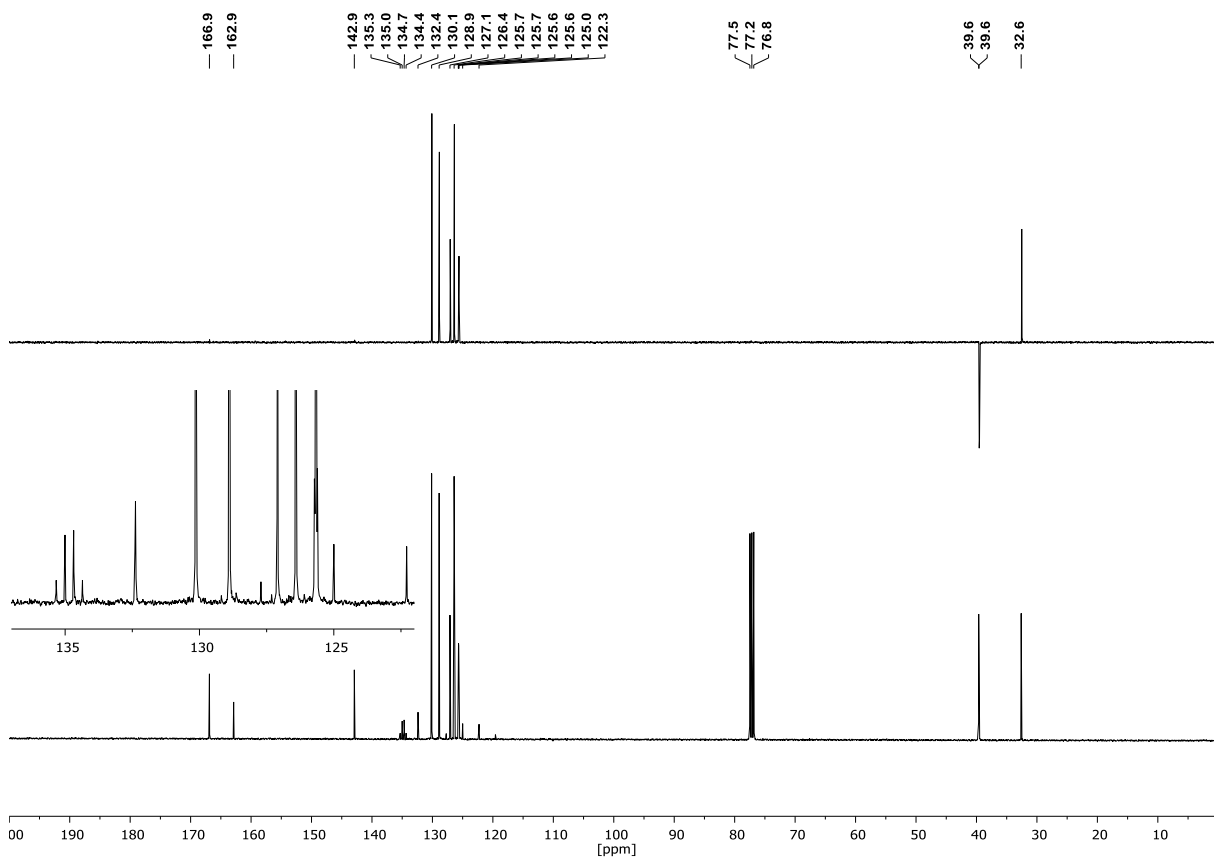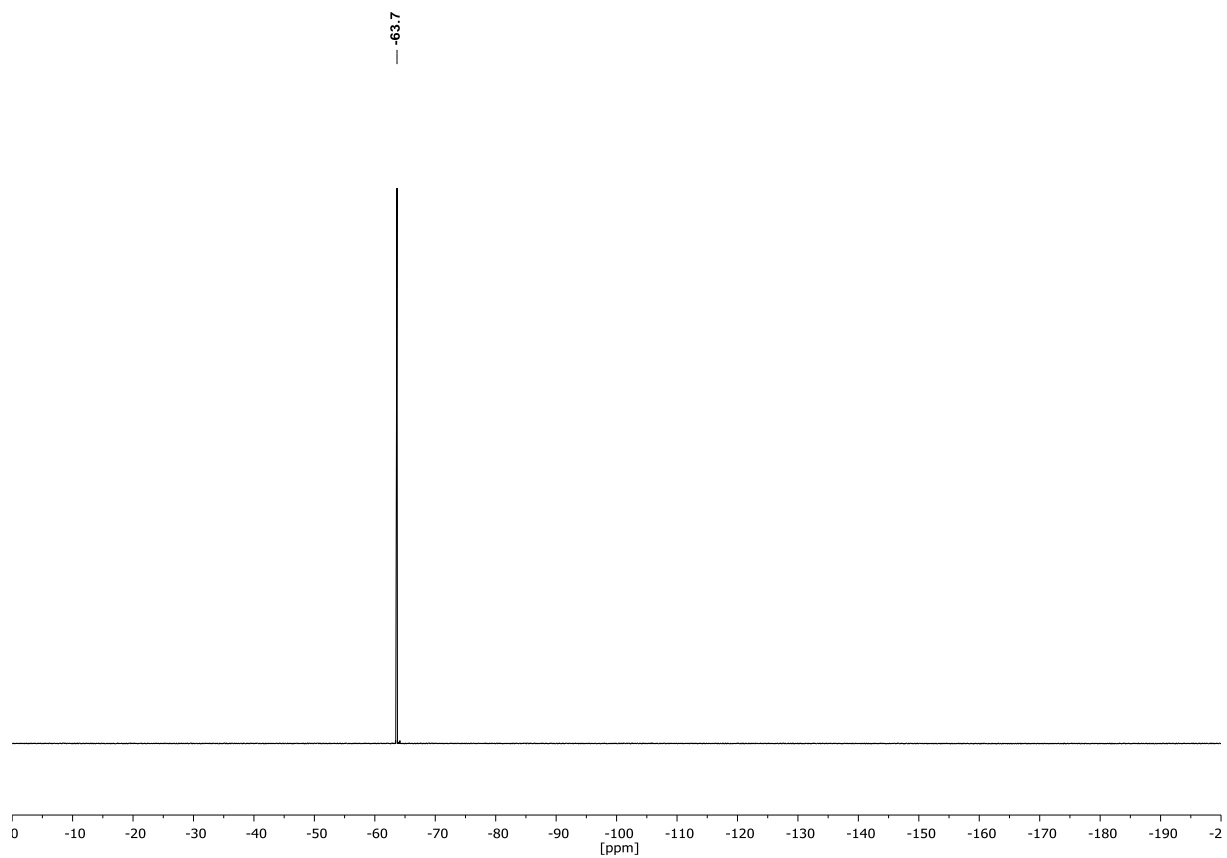
4-(1,2-dibromoethyl)benzonitrile (83b)

^{1}H-NMR (400 MHz, CDCl$_3$):
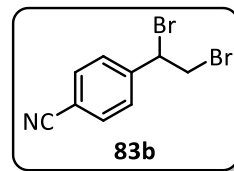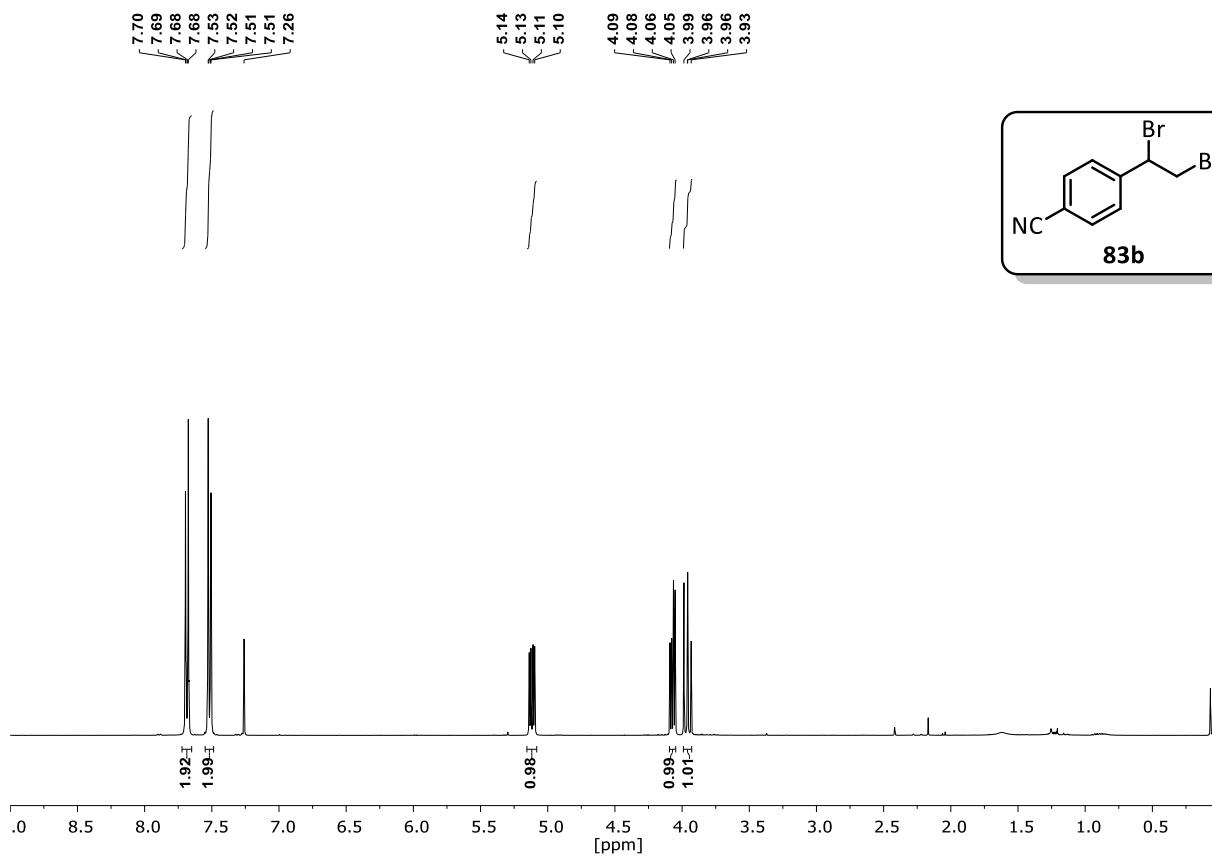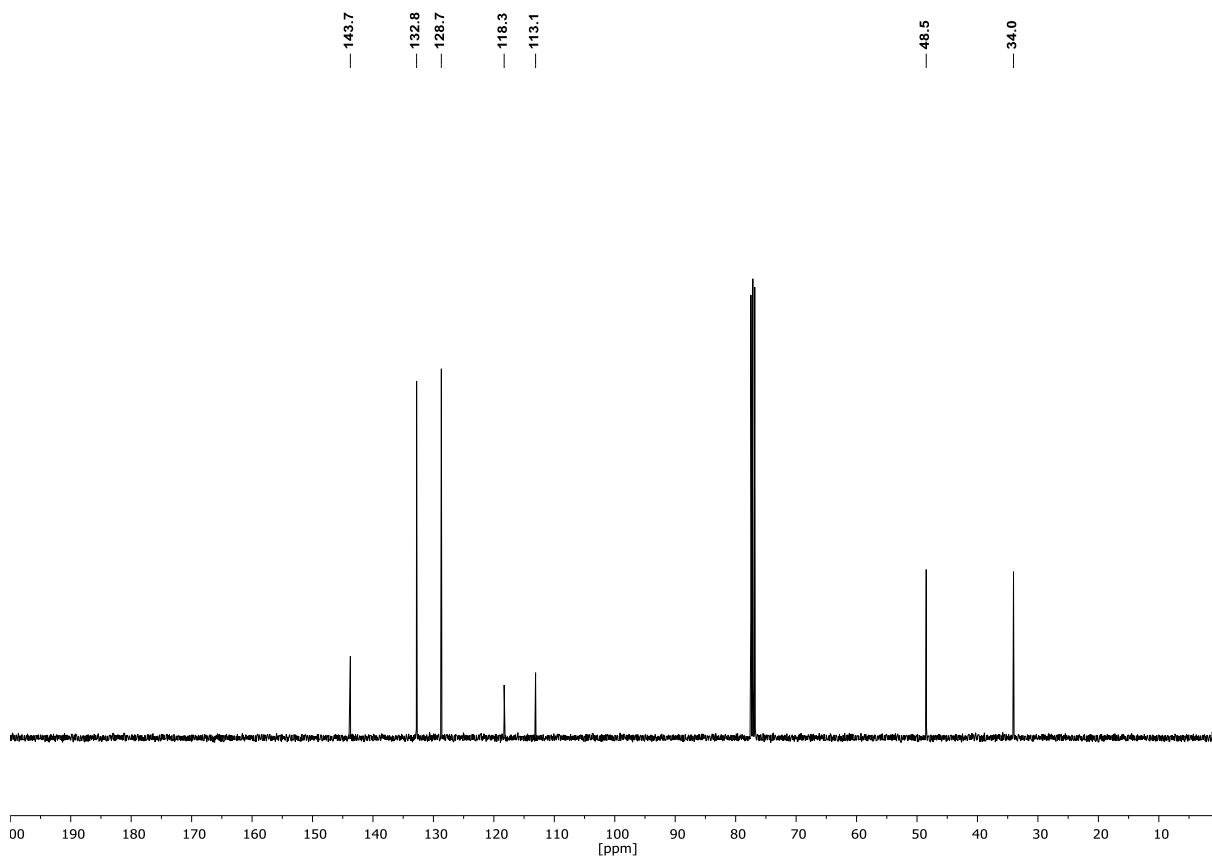
^{13}C-NMR (101 MHz, CDCl$_3$):

Methyl 4-(1,2-dibromoethyl)benzoate (123c)

^{1}H-NMR (400 MHz, CDCl$_3$):
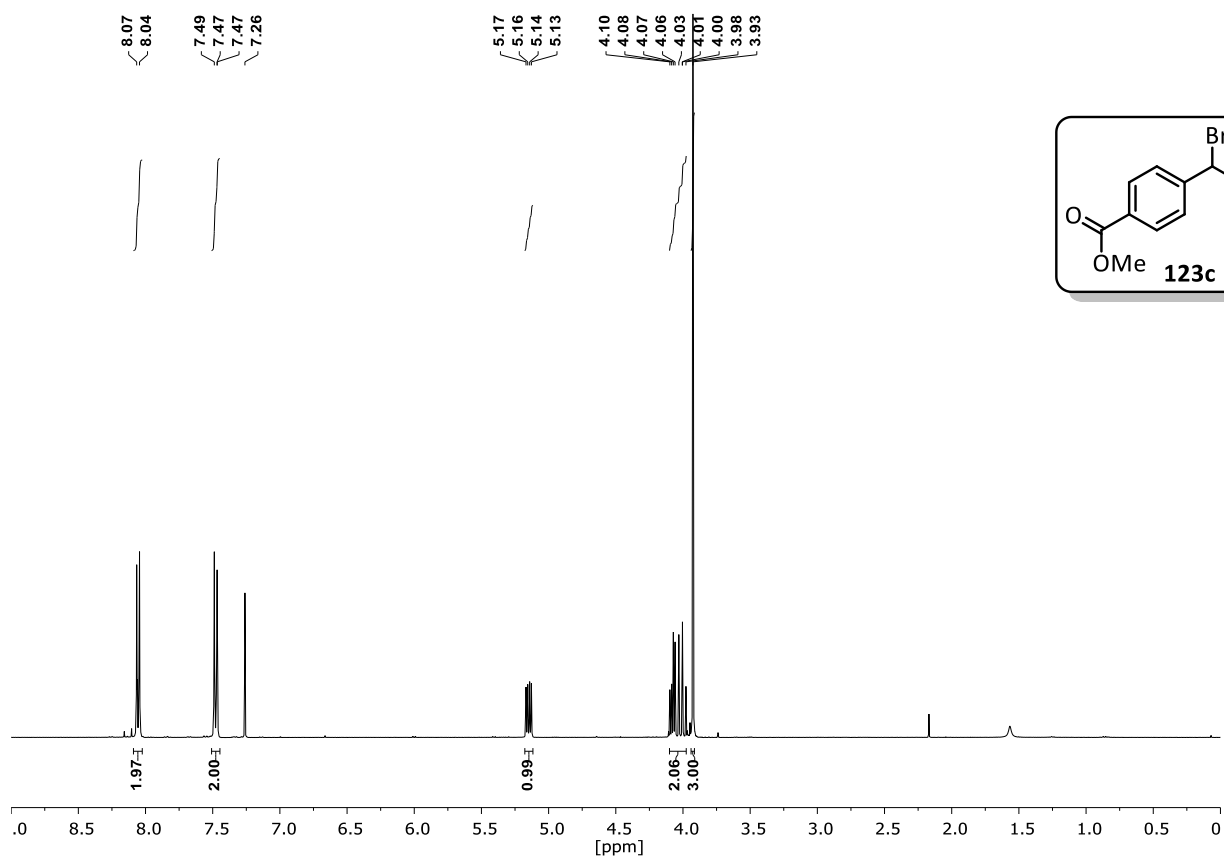
^{13}C-NMR (101 MHz, CDCl$_3$):
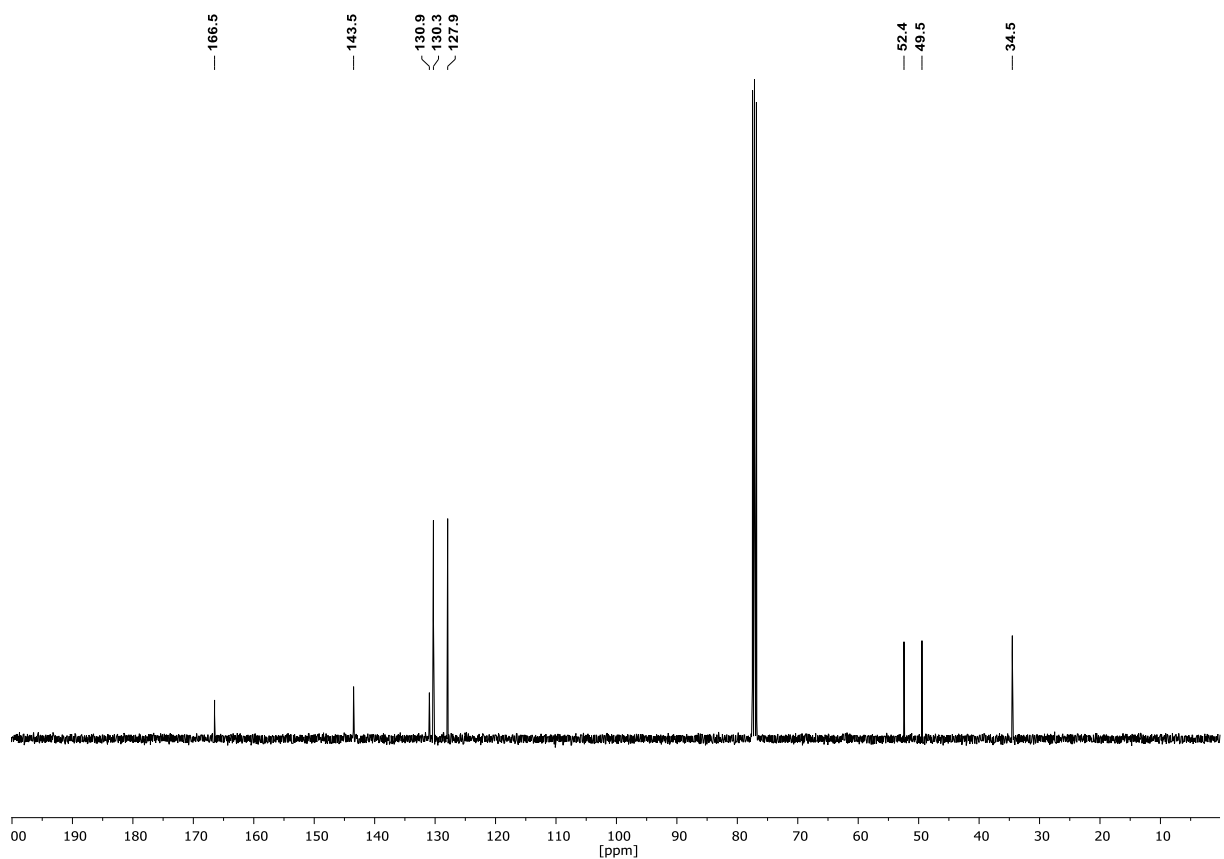
1-chloro-3-(1,2-dibromoethyl)benzene (123d)

¹H-NMR (400 MHz, CDCl₃):

7.35
7.34
7.27
7.27
7.26
7.26
7.24
7.23
7.20

5.04
5.02
5.01
4.99

4.02
4.00
3.99
3.98
3.93
3.91
3.88

0.96
3.10

0.98

1.03
1.03

.0 8.5 8.0 7.5 7.0 6.5 6.0 5.5 5.0 4.5 4.0 3.5 3.0 2.5 2.0 1.5 1.0 0.5 0
[ppm]

¹³C-NMR (101 MHz, CDCl₃):

140.7
134.8
130.2
129.5
128.0
126.0

49.4

34.7

00 190 180 170 160 150 140 130 120 110 100 90 80 70 60 50 40 30 20 10 0
[ppm]
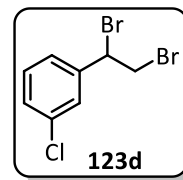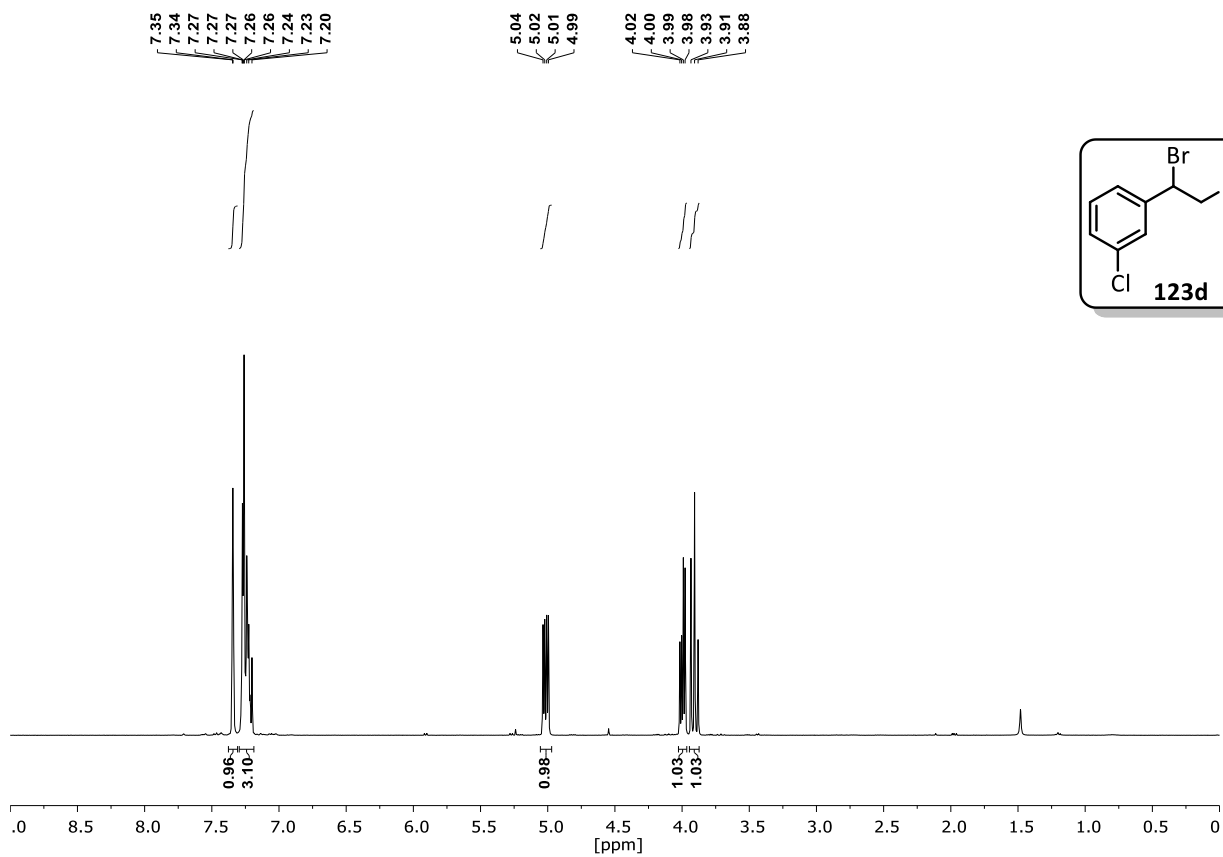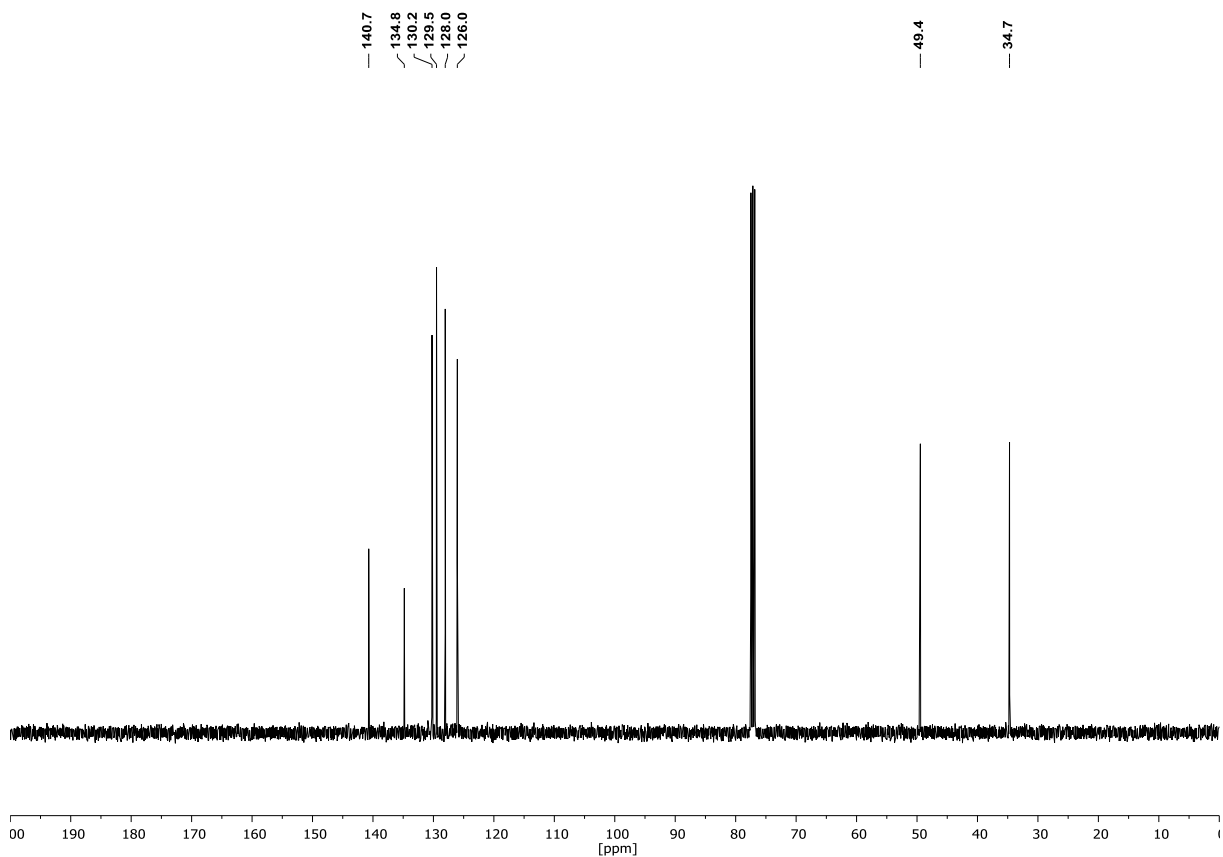
2-(1,2-dibromoethyl)naphthalene (123e)

^{1}H-NMR (400 MHz, CDCl$_3$):

7.91
7.88
7.87
7.87
7.86
7.86
7.86
7.85
7.85
7.84
7.83
7.83
7.82
7.81
7.81
7.80
7.55
7.54
7.54
7.53
7.52
7.52
7.51
7.51
7.26
5.36
5.34
5.34
5.32
4.17
4.16
4.15
4.12

4.27
3.00
1.00
2.12

[ppm]

^{13}C-NMR (101 MHz, CDCl$_3$):

135.8
133.6
133.0
129.2
128.3
127.9
127.6
127.1
126.8
124.5

77.5
77.2
76.8

51.5

34.9

[ppm]
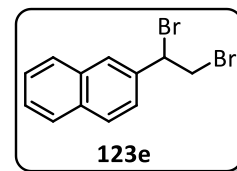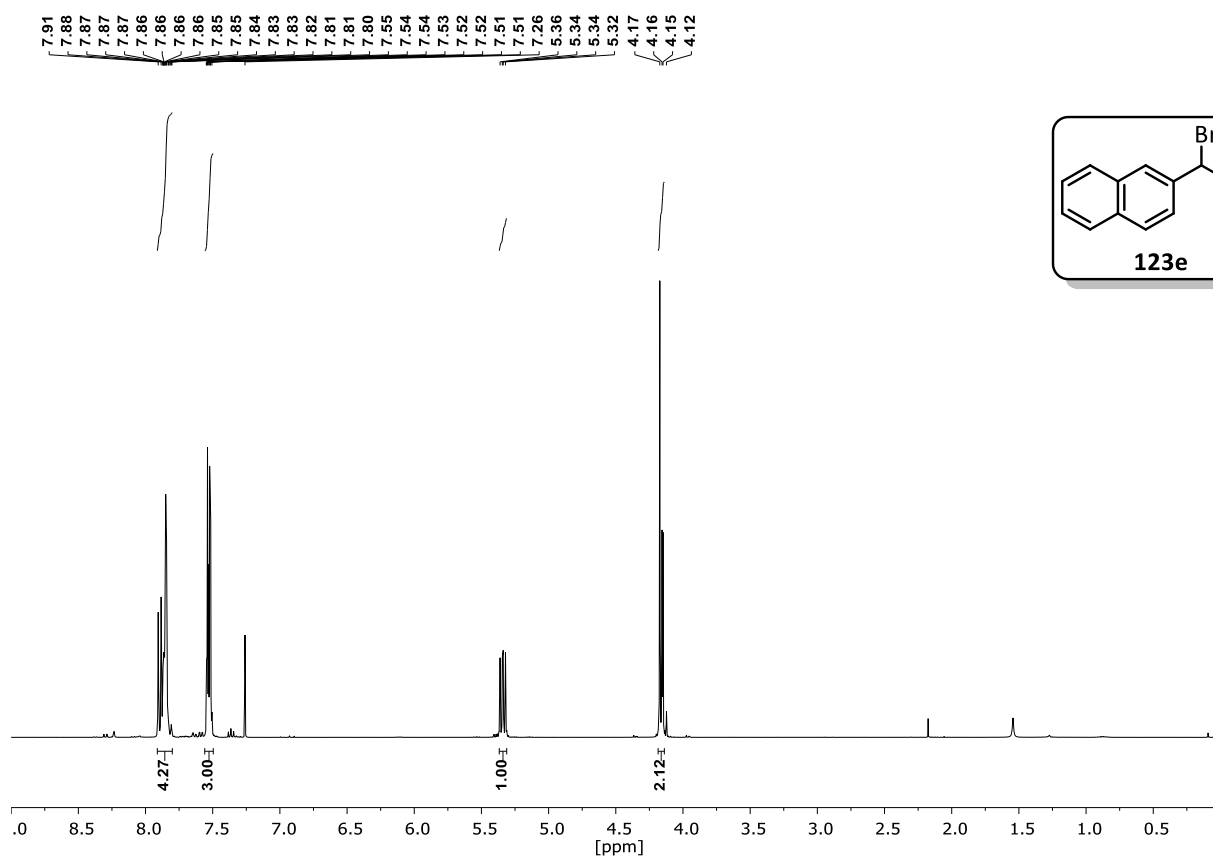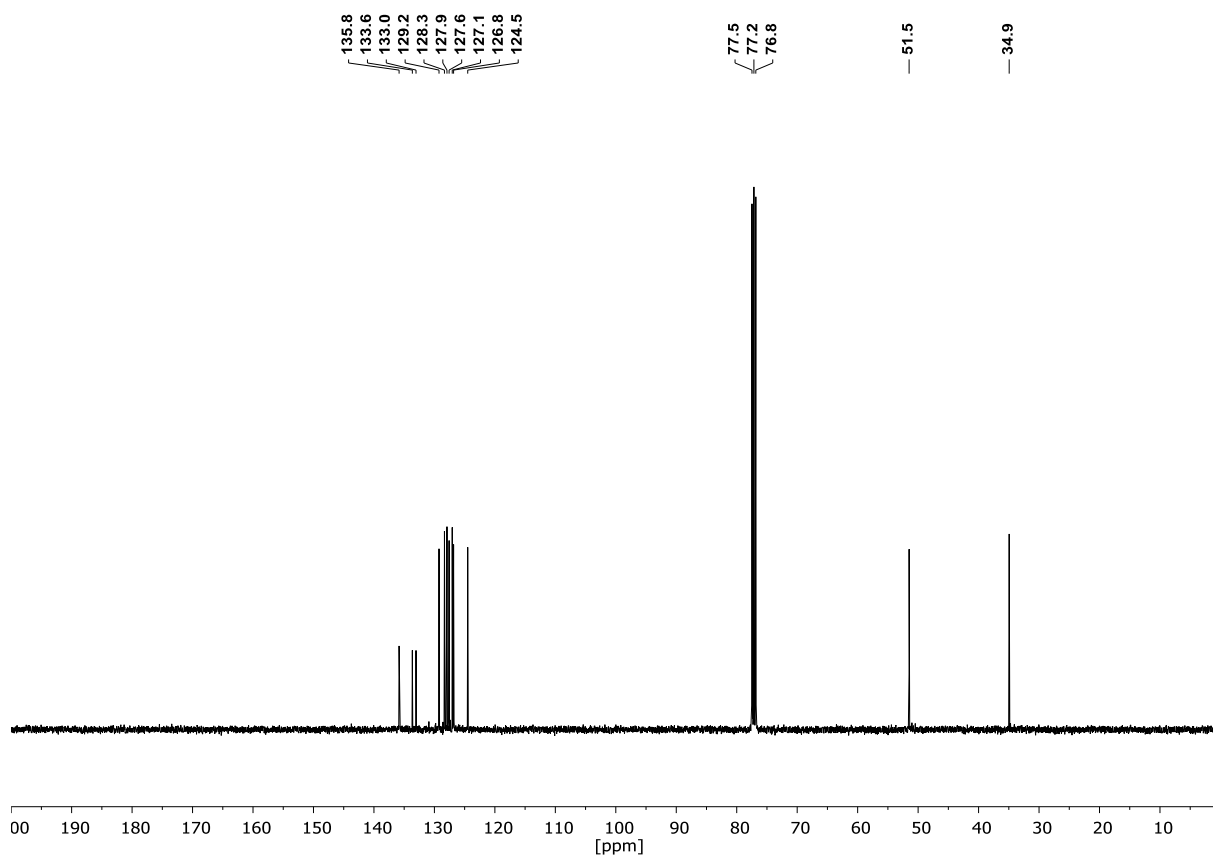
Methyl 2,3-dibromopropanoate (123f)

¹H-NMR (300 MHz, CDCl₃):
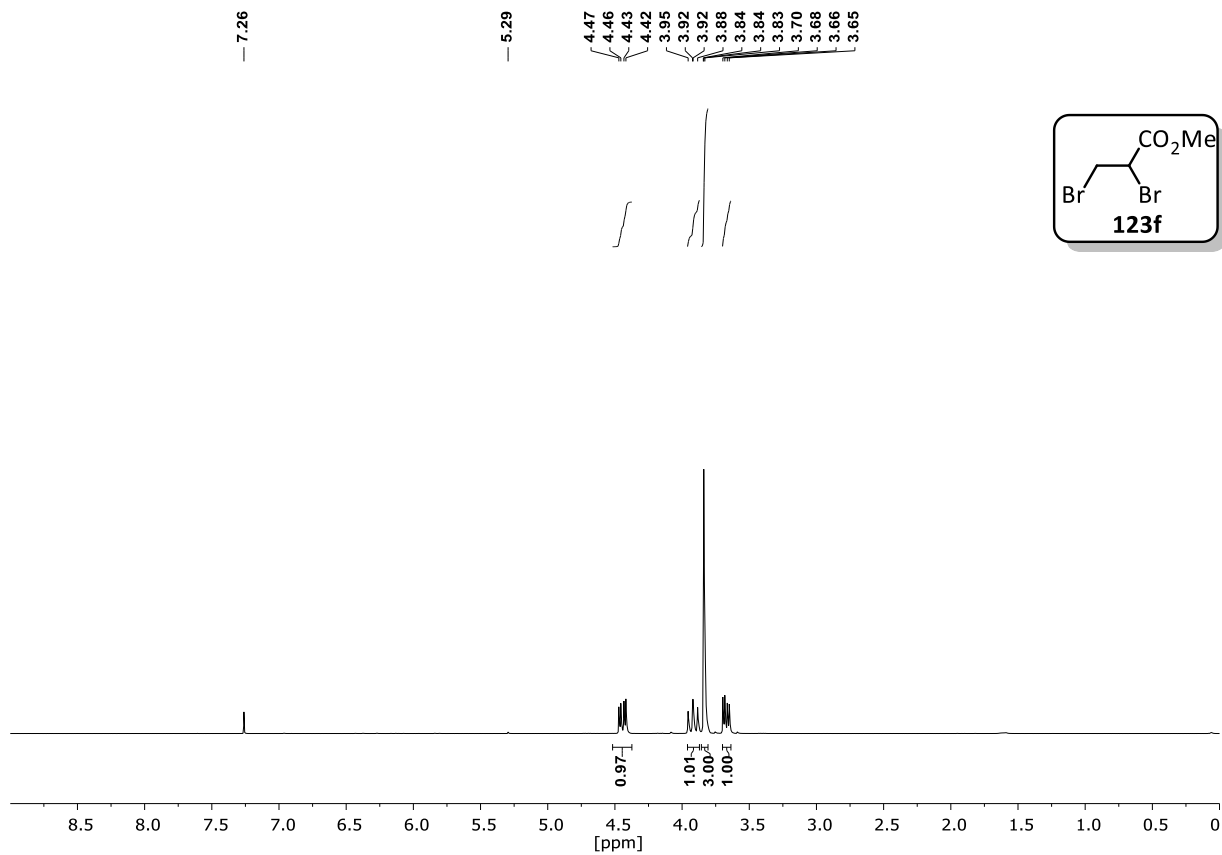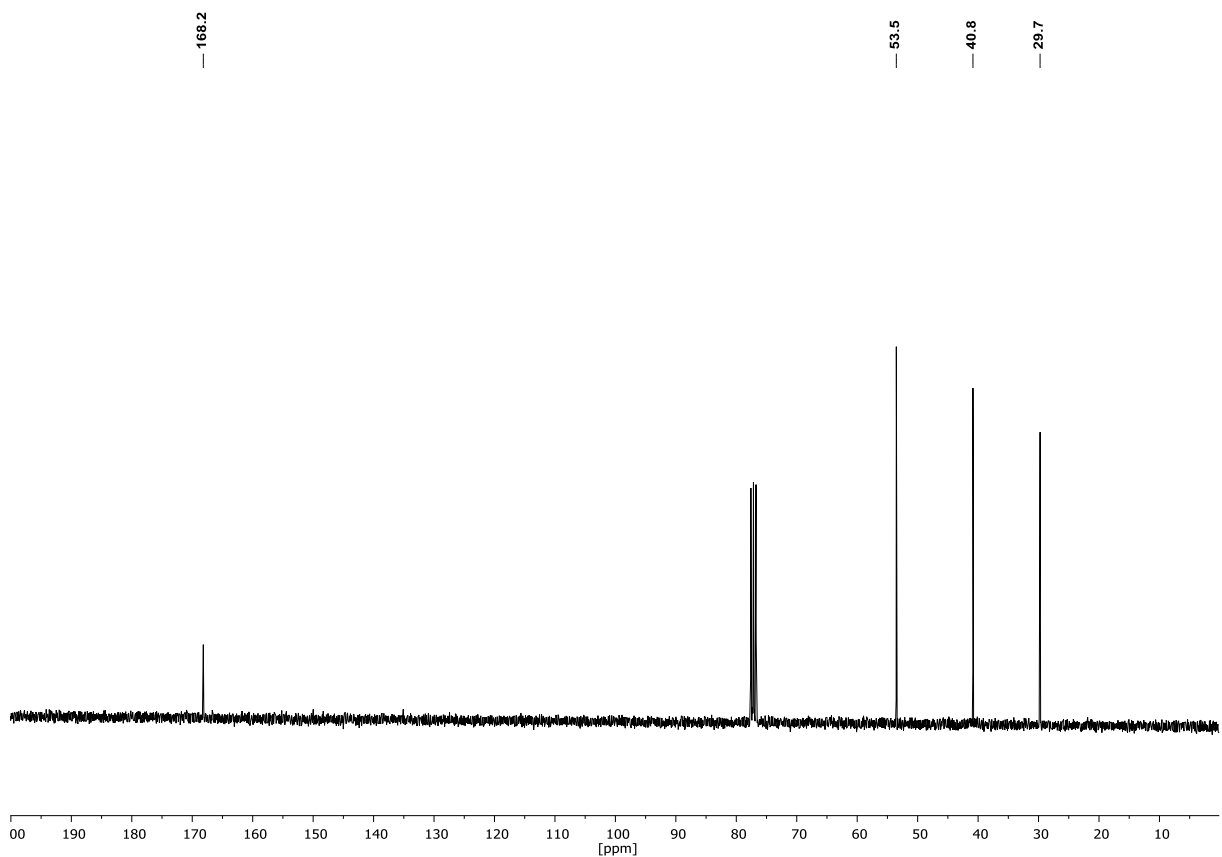
¹³C-NMR (75 MHz, CDCl₃):

(1-azidovinyl)benzene (83a)

^{1}H-NMR (400 MHz, CDCl$_3$):

7.59
7.58
7.58
7.57
7.41
7.40
7.39
7.38
7.38
7.37
7.37
7.26

5.45
5.45

4.98
4.98

1.55

2.00
3.00

1.00

1.00

[ppm]

^{13}C-NMR (101 MHz, CDCl$_3$):

145.1

134.3
129.1
128.5
125.6

98.0

[ppm]
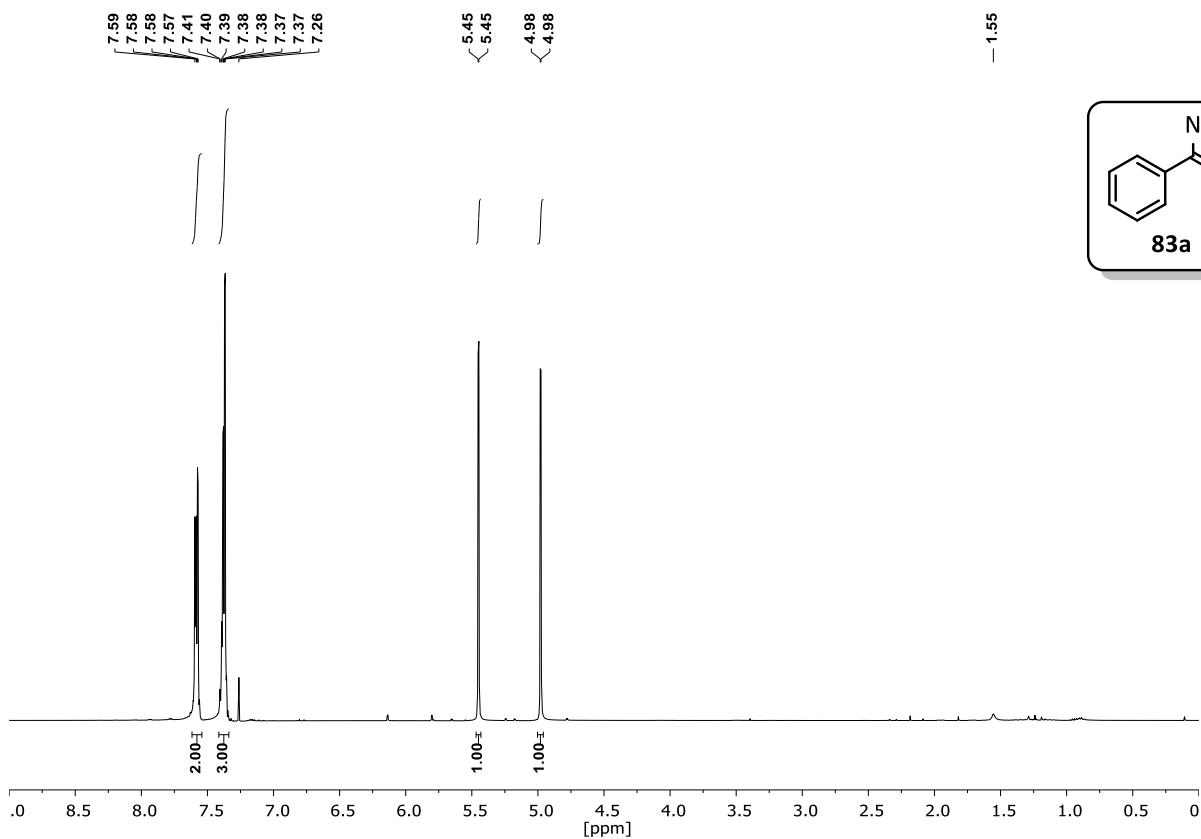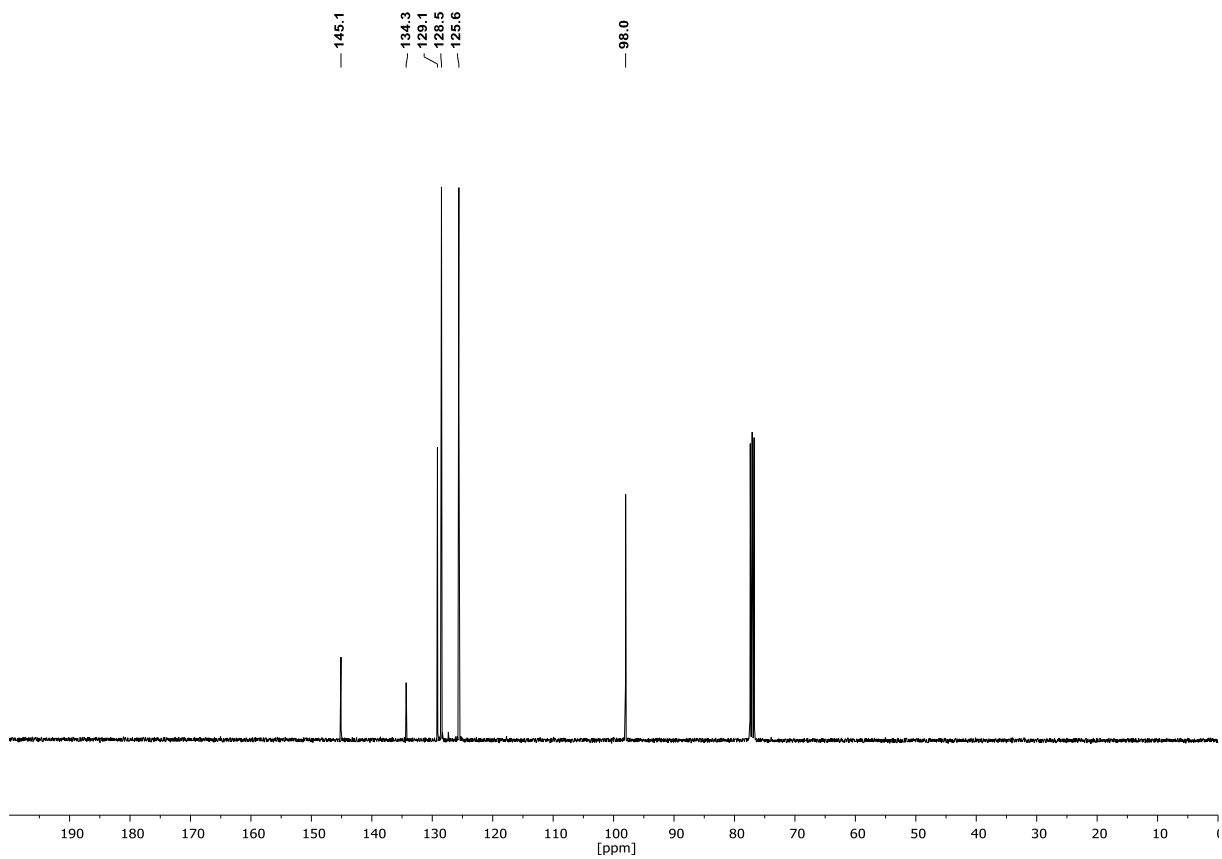
4-(1-azidovinyl)benzonitrile (83b, 1.17:1 mixture of regioisomers)

¹H-NMR (300 MHz, CDCl₃):

4-(2-azidovinyl)benzonitrile

4-(1-azidovinyl)benzonitrile
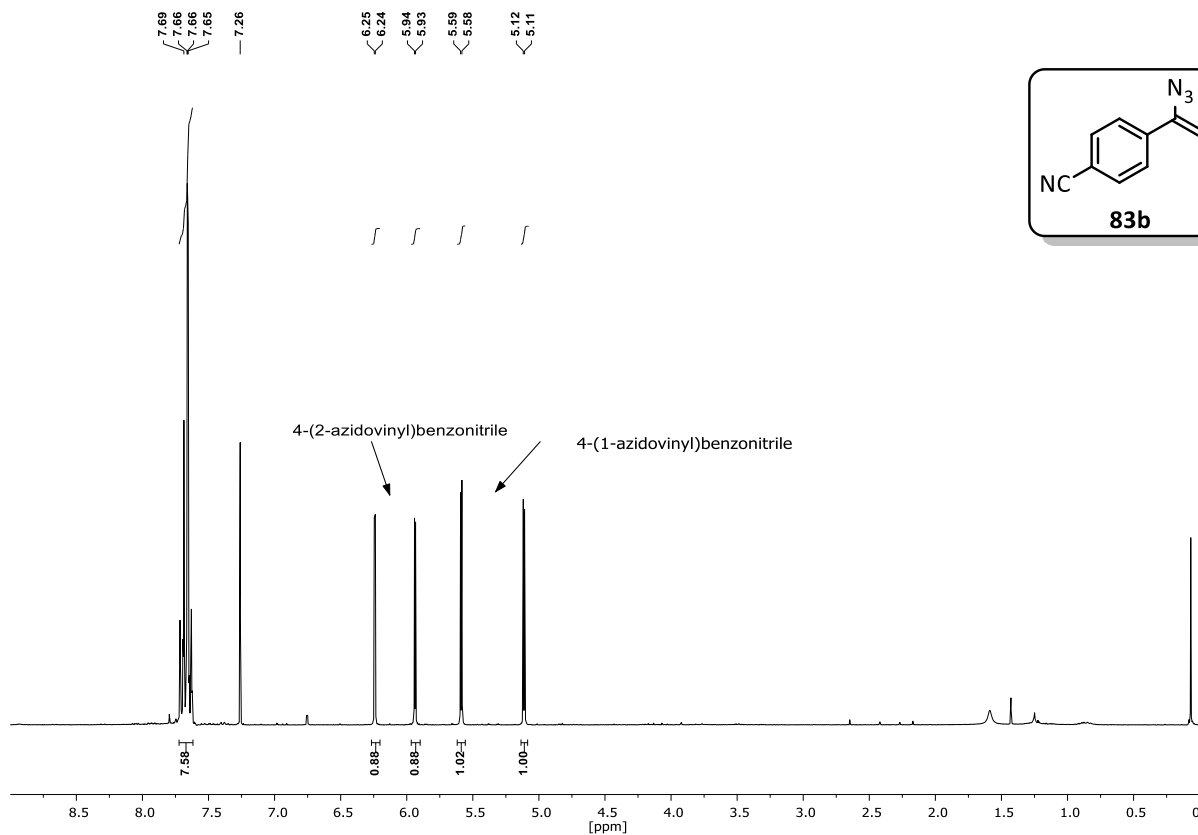
Methyl 4-(1-azidovinyl)benzoate (83c, 3.23:1 mixture of regioisomers)

¹H-NMR (300 MHz, CDCl₃):

methyl 4-(1-azidovinyl)benzoate

methyl 4-(2-azidovinyl)benzoate
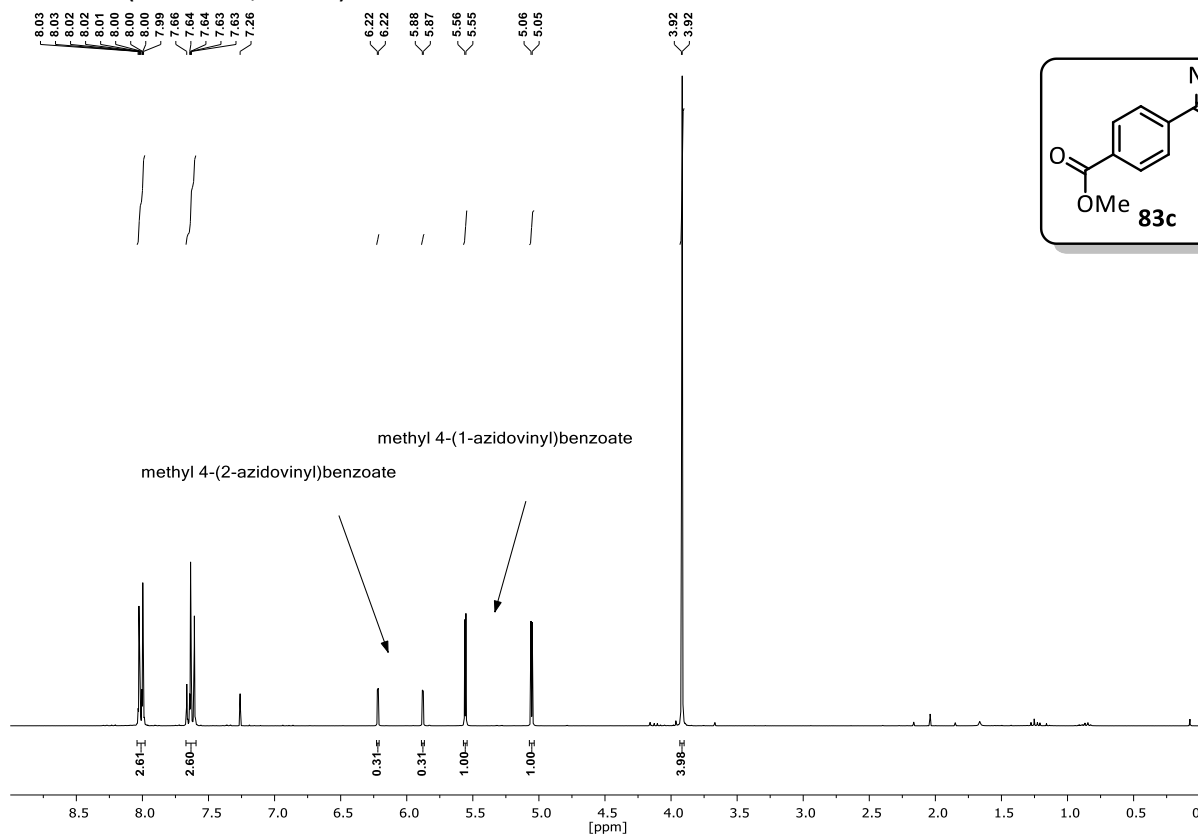
1-(1-azidovinyl)-3-chlorobenzene (83d, 10:1 mixture of regioisomers)

¹H-NMR (300 MHz, CDCl₃):

1-(1-azidovinyl)-3-chlorobenzene

1-(2-azidovinyl)-3-chlorobenzene
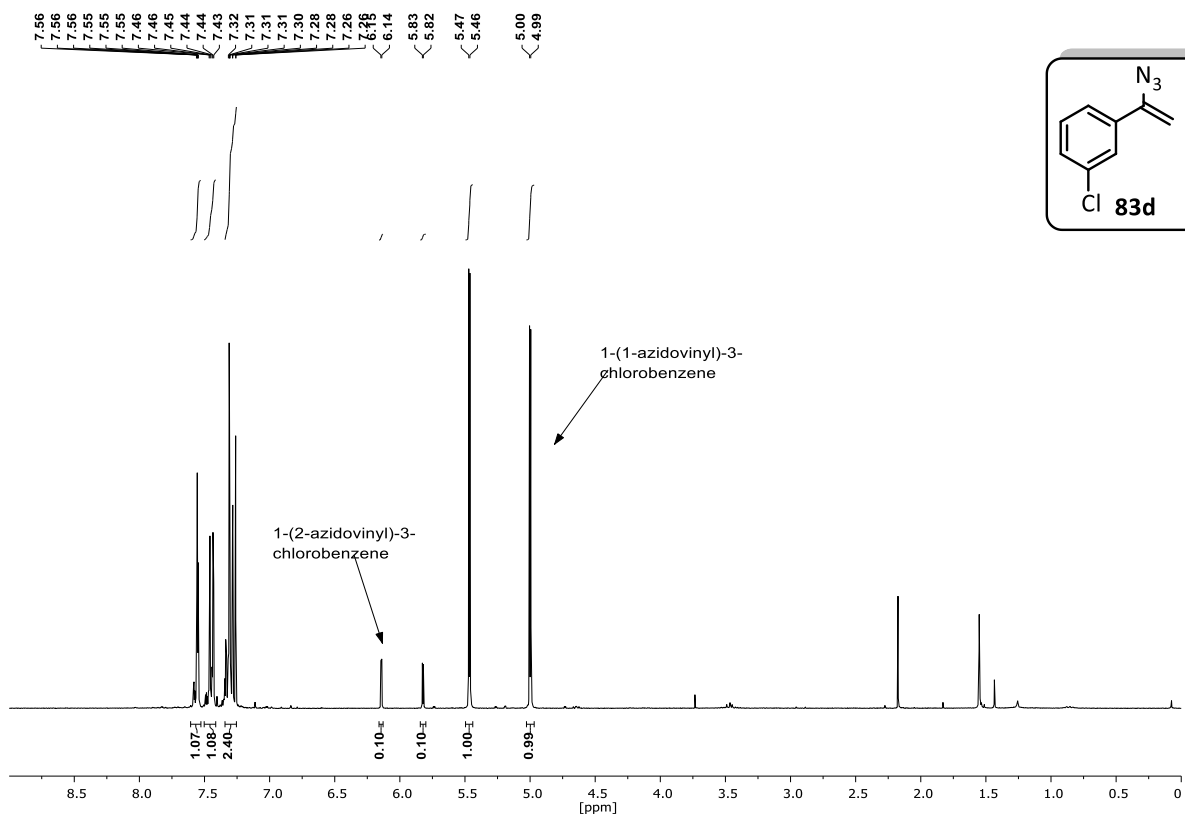
2-(1-azidovinyl)naphthalene (83e, 20:1 mixture of regioisomers)
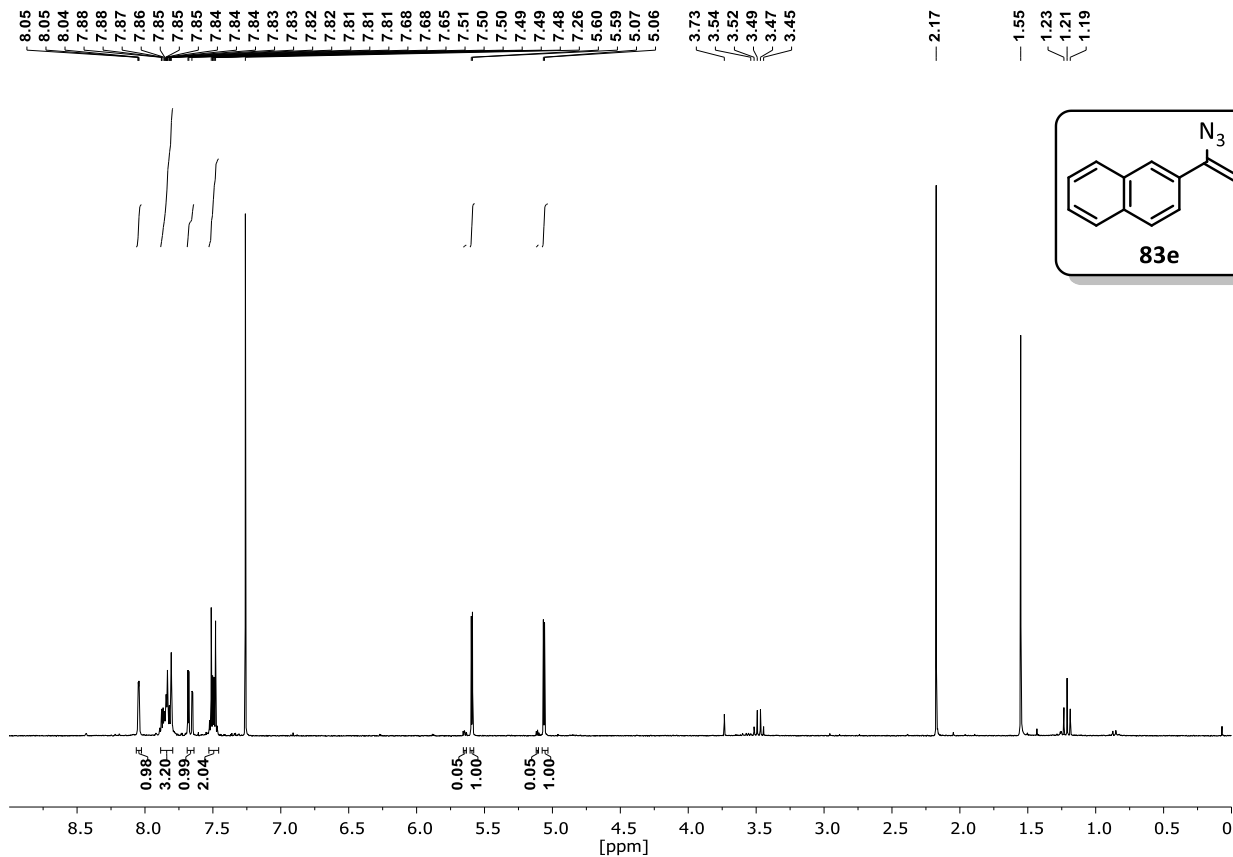
¹H-NMR (300 MHz, CDCl₃):

Methyl 2-azidoacrylate (83f)

^{1}H-NMR (300 MHz, CDCl$_3$):
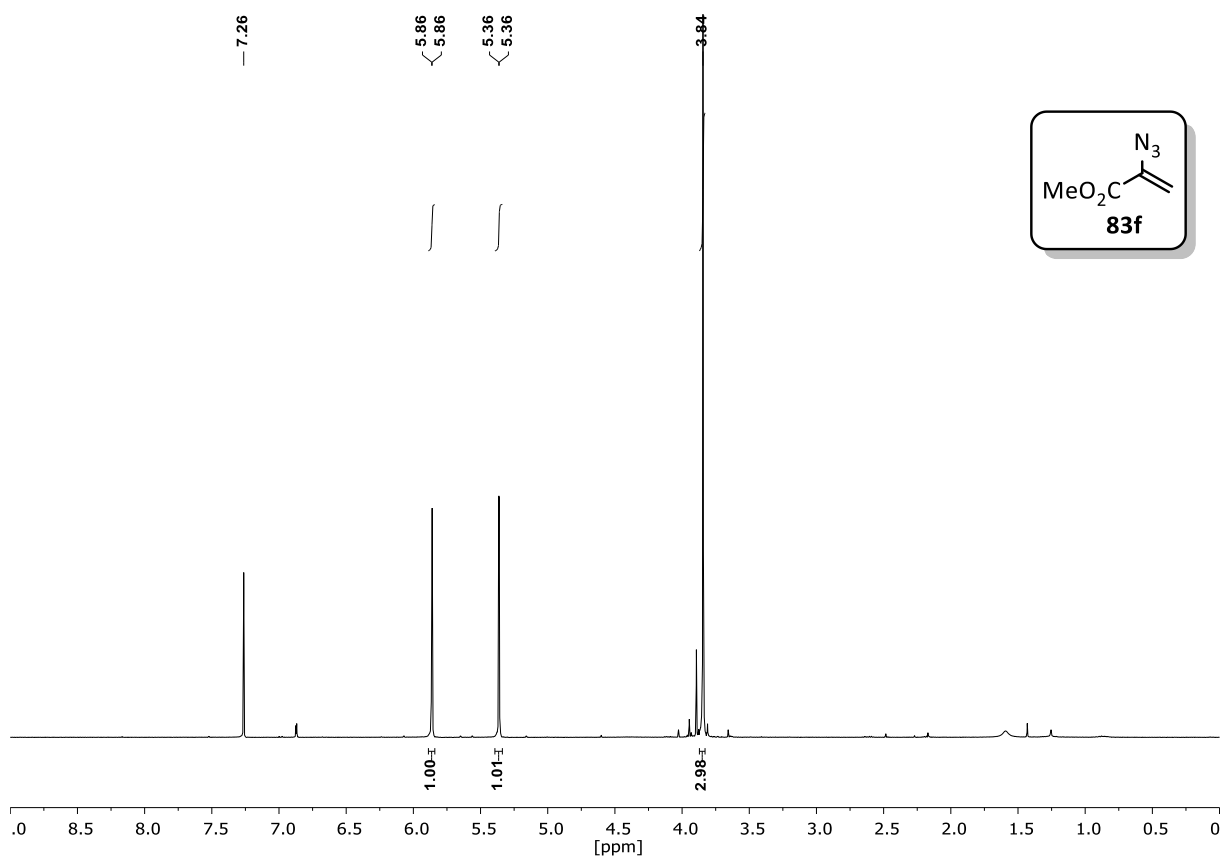
^{13}C-NMR (75 MHz, CDCl$_3$):
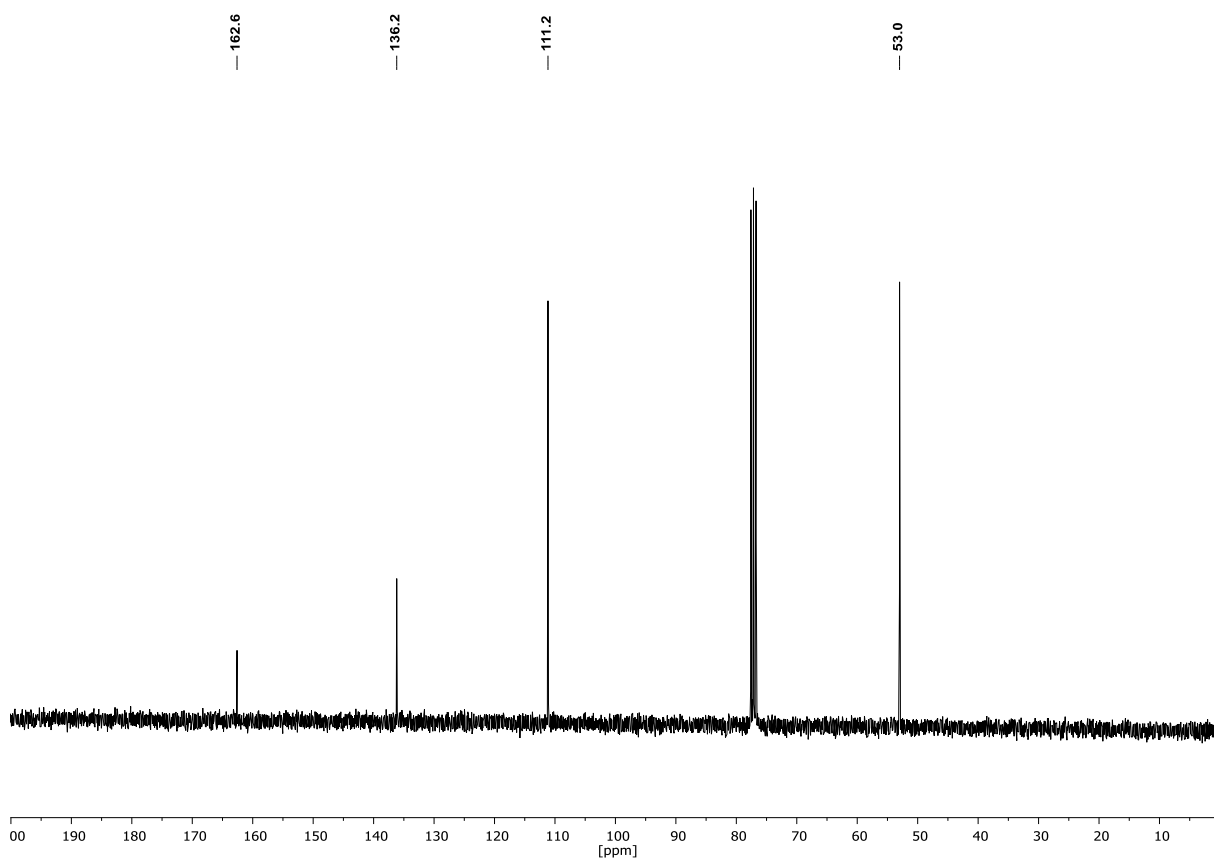
1-(1-azidovinyl)-2-methoxybenzene (83g)

^{1}H-NMR (400 MHz, CDCl$_3$):
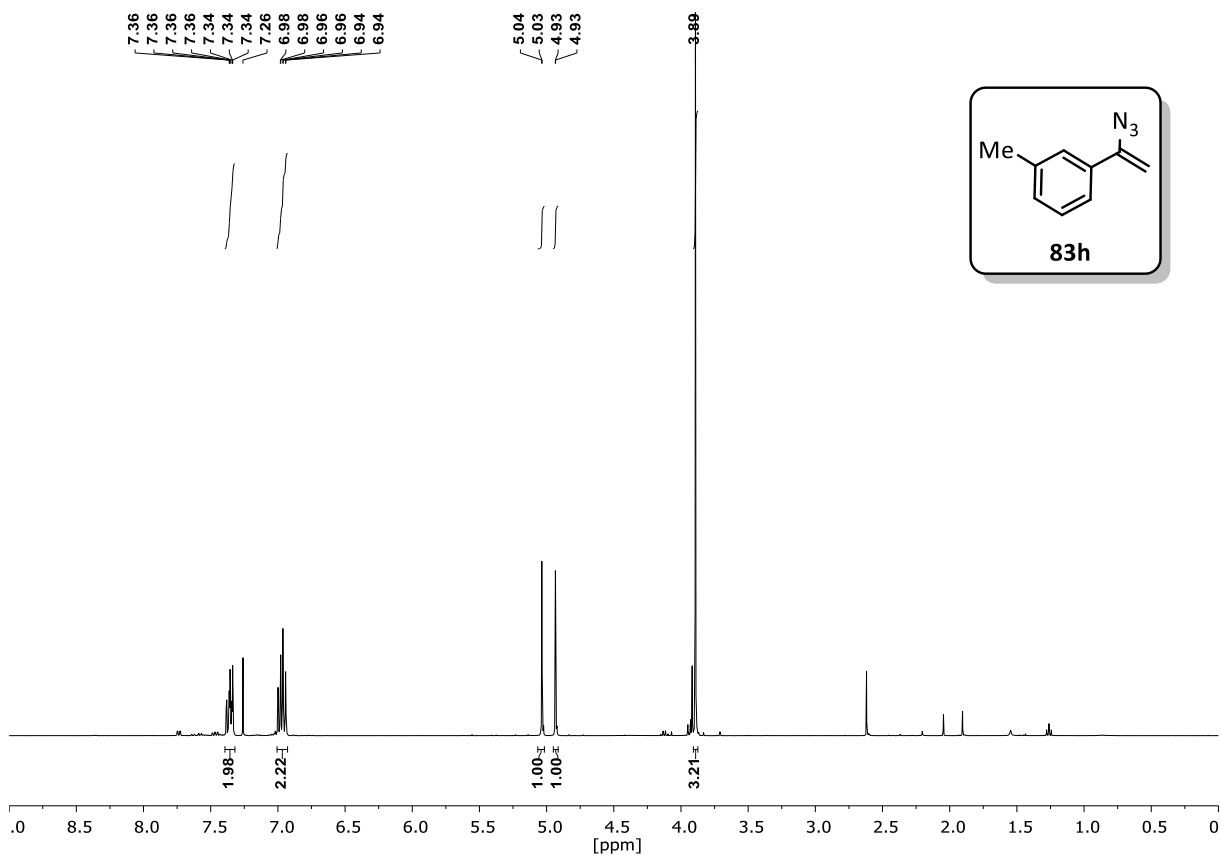
1-(1-azidovinyl)-3-methylbenzene (83h):

^{1}H-NMR (300 MHz, CDCl$_3$):
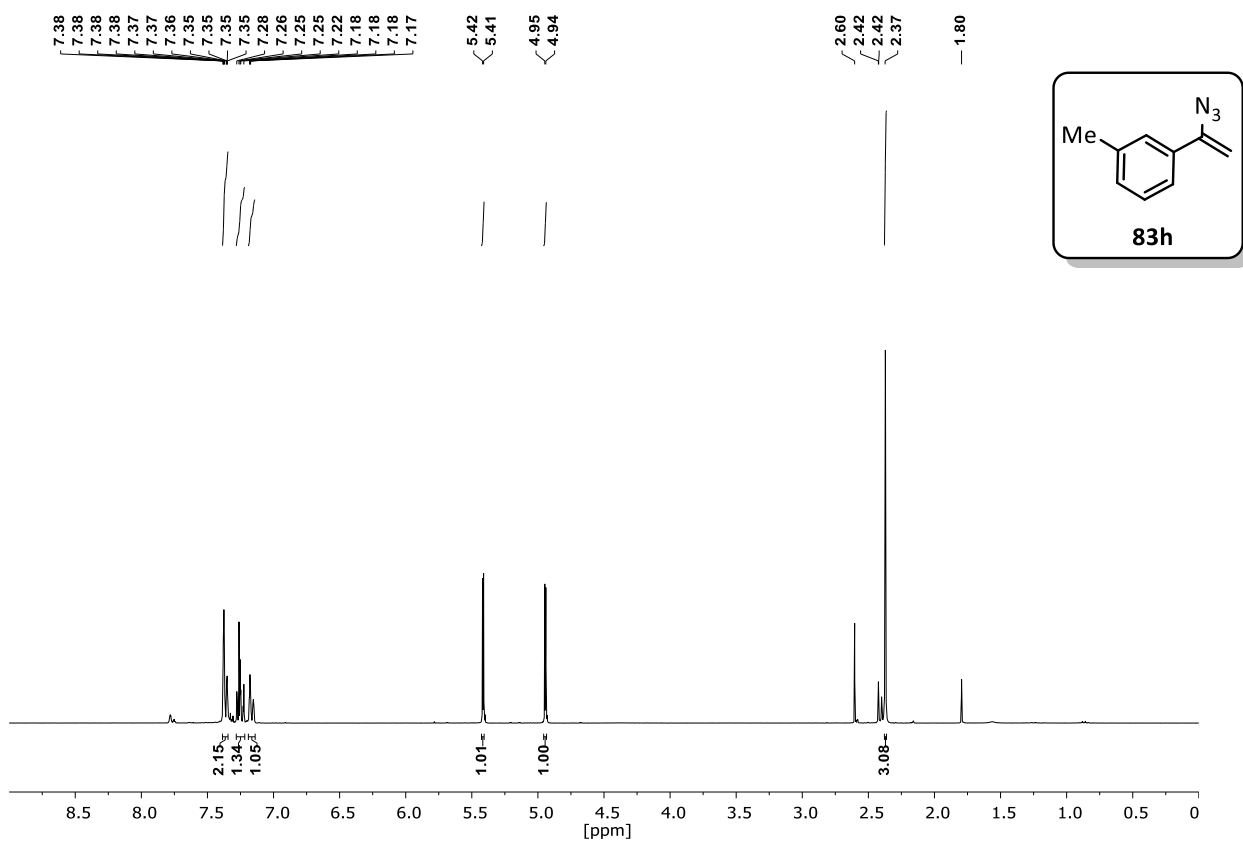
1-(1-azidovinyl)-4-fluorobenzene (83i):

^{1}H-NMR (400 MHz, CDCl$_3$) :

7.78, 7.76, 7.76, 7.74, 7.48, 7.28, 7.26, 7.24
5.60, 5.59, 5.16, 5.16, 5.15
—2.81
—1.77

1.96, 1.94, 1.01, 1.01

.0 8.5 8.0 7.5 7.0 6.5 6.0 5.5 5.0 4.5 4.0 3.5 3.0 2.5 2.0 1.5 1.0 0.5 0
[ppm]
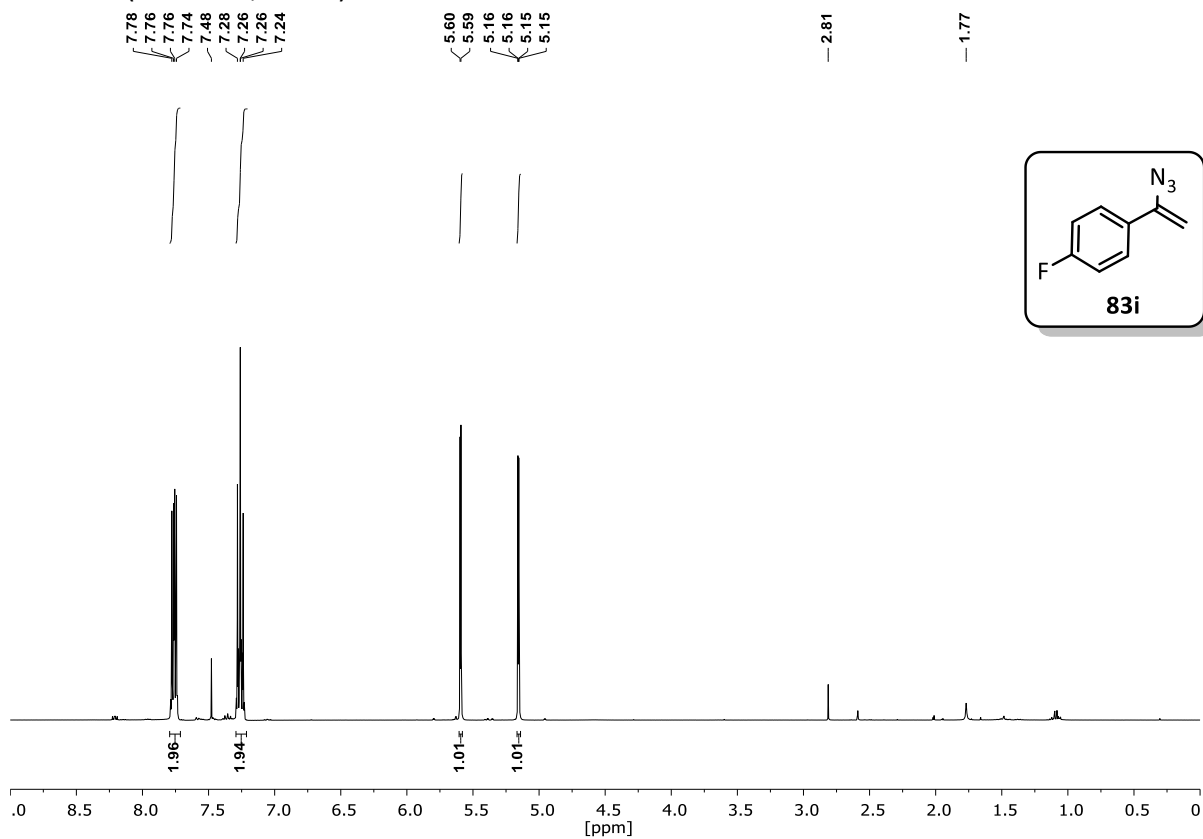
3-(1-azidovinyl)pyridine (83j)

^{1}H-NMR (400 MHz, CDCl$_3$):

8.83, 8.83, 8.83, 8.82, 8.59, 8.58, 8.57, 7.86, 7.86, 7.85, 7.85, 7.84, 7.84, 7.83, 7.83, 7.82, 7.82, 7.82, 7.32, 7.31, 7.30, 7.30, 7.29, 7.27, 7.26, 5.53, 5.52, 5.06, 5.05

1.00, 0.96, 0.96, 1.00, 1.00, 1.00

8.5 8.0 7.5 7.0 6.5 6.0 5.5 5.0 4.5 4.0 3.5 3.0 2.5 2.0 1.5 1.0 0.5 0
[ppm]
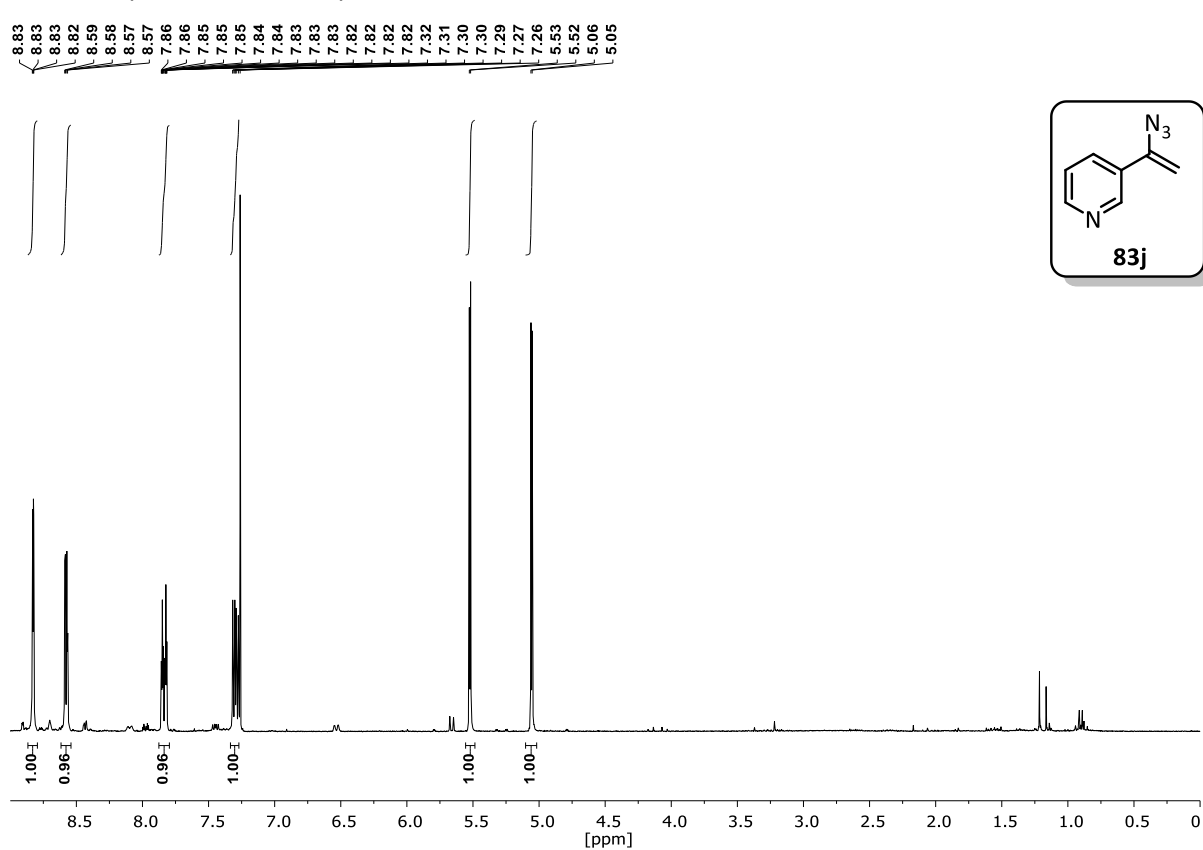
Diethyl 2,5-diphenyl-2,4-dihydro-2*H*-pyrrole-3,3-dicarboxylate (90a)

¹H-NMR (400 MHz, CDCl₃):
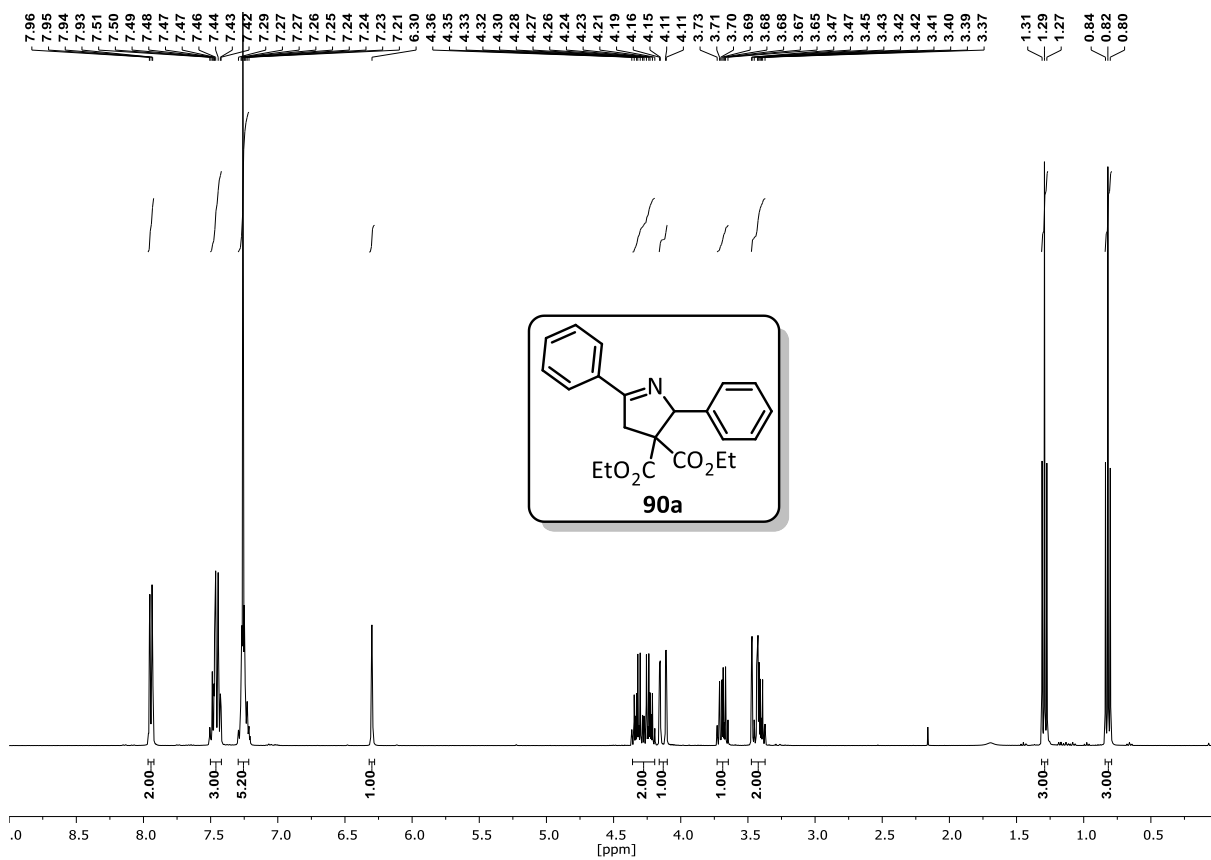
¹³C-NMR (101 MHz, CDCl₃) & **DEPT135** (101 MHz, CDCl₃):
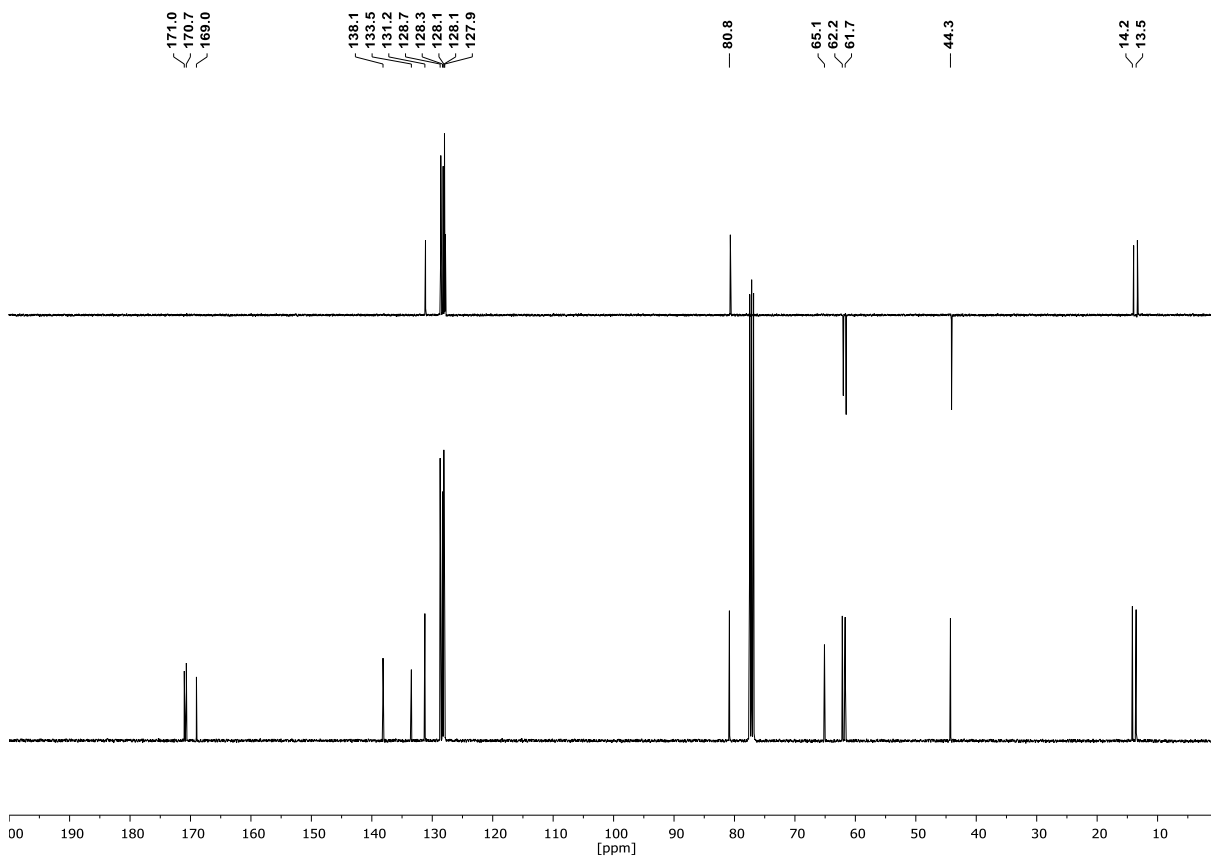
Diethyl 5-phenyl-2-(o-tolyl)-2,4-dihydro-2H-pyrrole-3,3-dicarboxylate (90b)

¹H-NMR (400 MHz, CDCl₃):
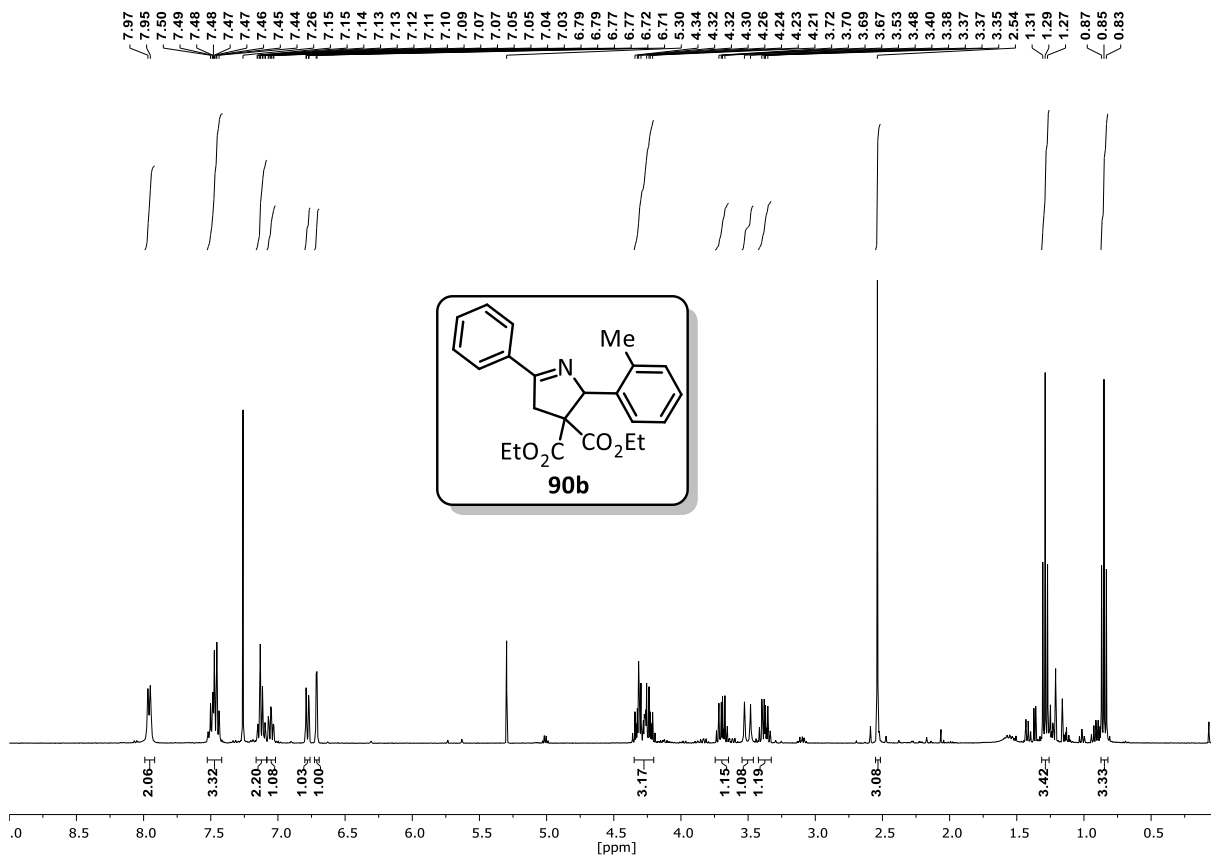
¹³C-NMR (101 MHz, CDCl₃) & **DEPT135** (101 MHz, CDCl₃):
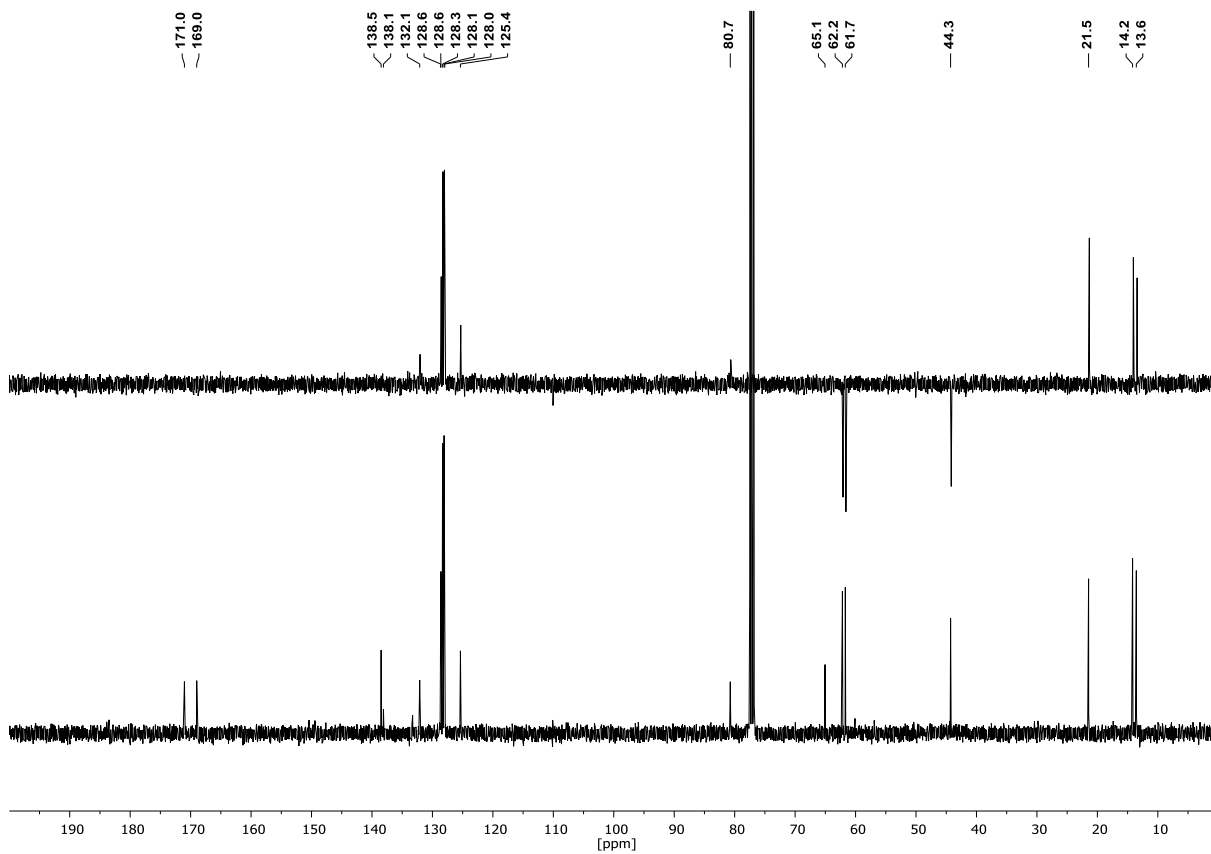
Diethyl 2-phenyl-5-(m-tolyl)-2,4-dihydro-2*H*-pyrrole-3,3-dicarboxylate (90a) & Diethyl 6-methyl-4-oxo-1-phenyl-3,4-dihydronaphthalene-2,2(1*H*)-dicarboxylate (99c)

¹H-NMR (400 MHz, CDCl₃):
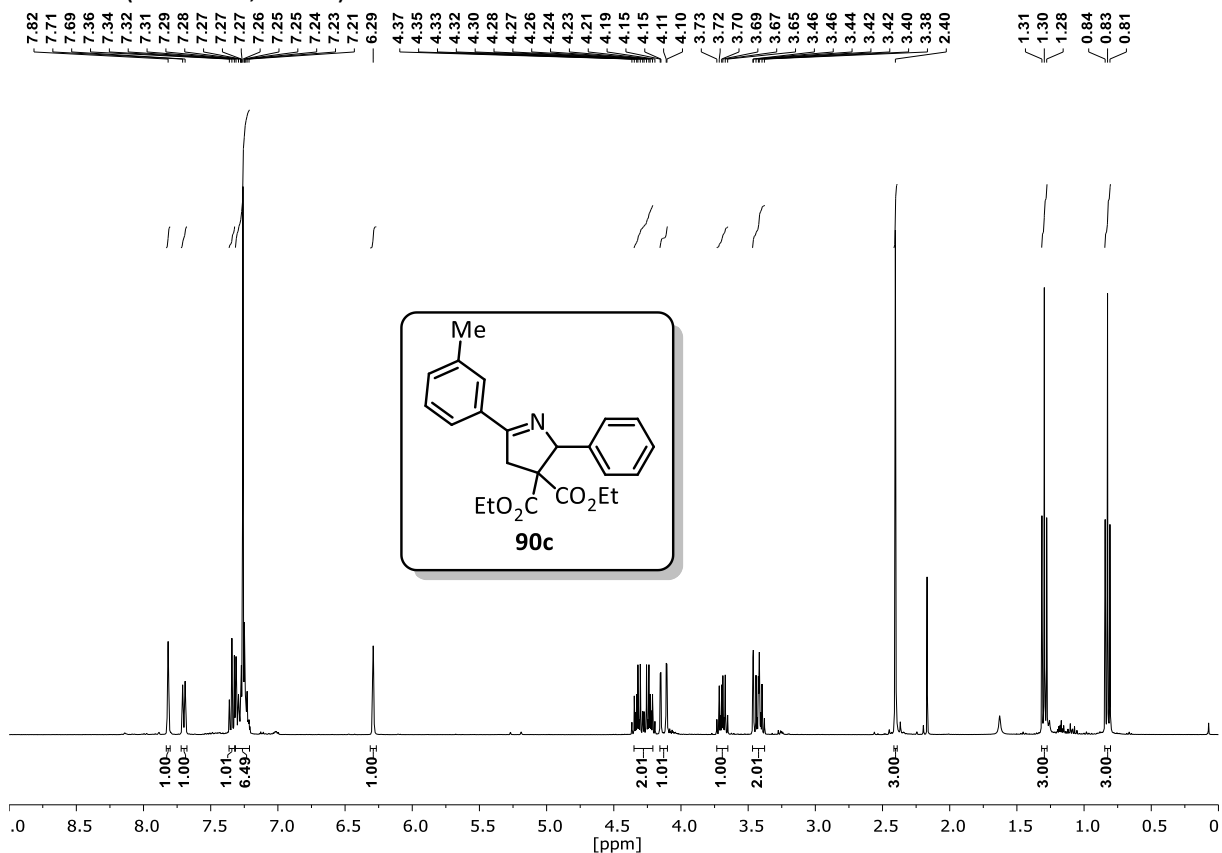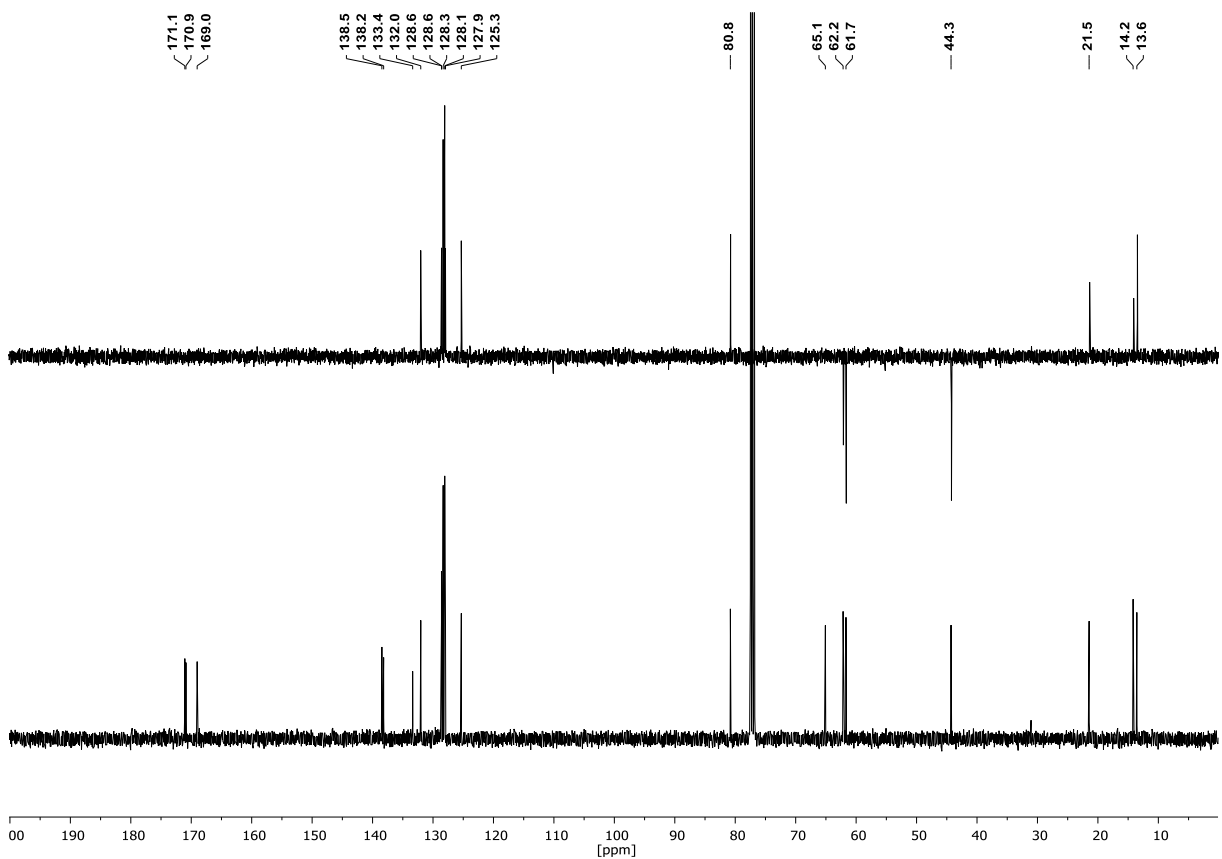
¹³C-NMR (101 MHz, CDCl₃) & **DEPT135** (101 MHz, CDCl₃):
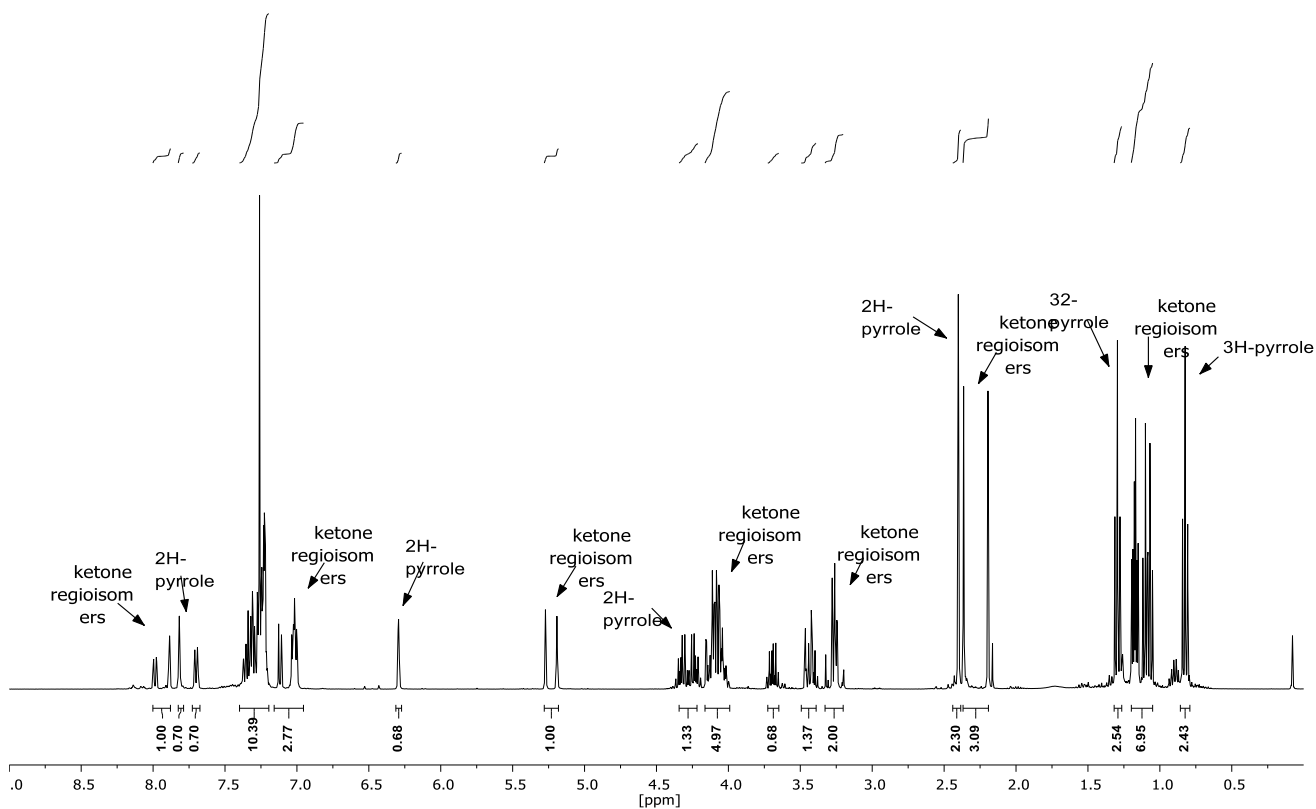
^{1}**H-NMR** (400 MHz, CDCl$_3$):

Diethyl 5-(2-methoxyphenyl)-2-phenyl-2,4-dihydro-2*H*-pyrrole-3,3-dicarboxylate (90d)

¹H-NMR (400 MHz, CDCl₃):
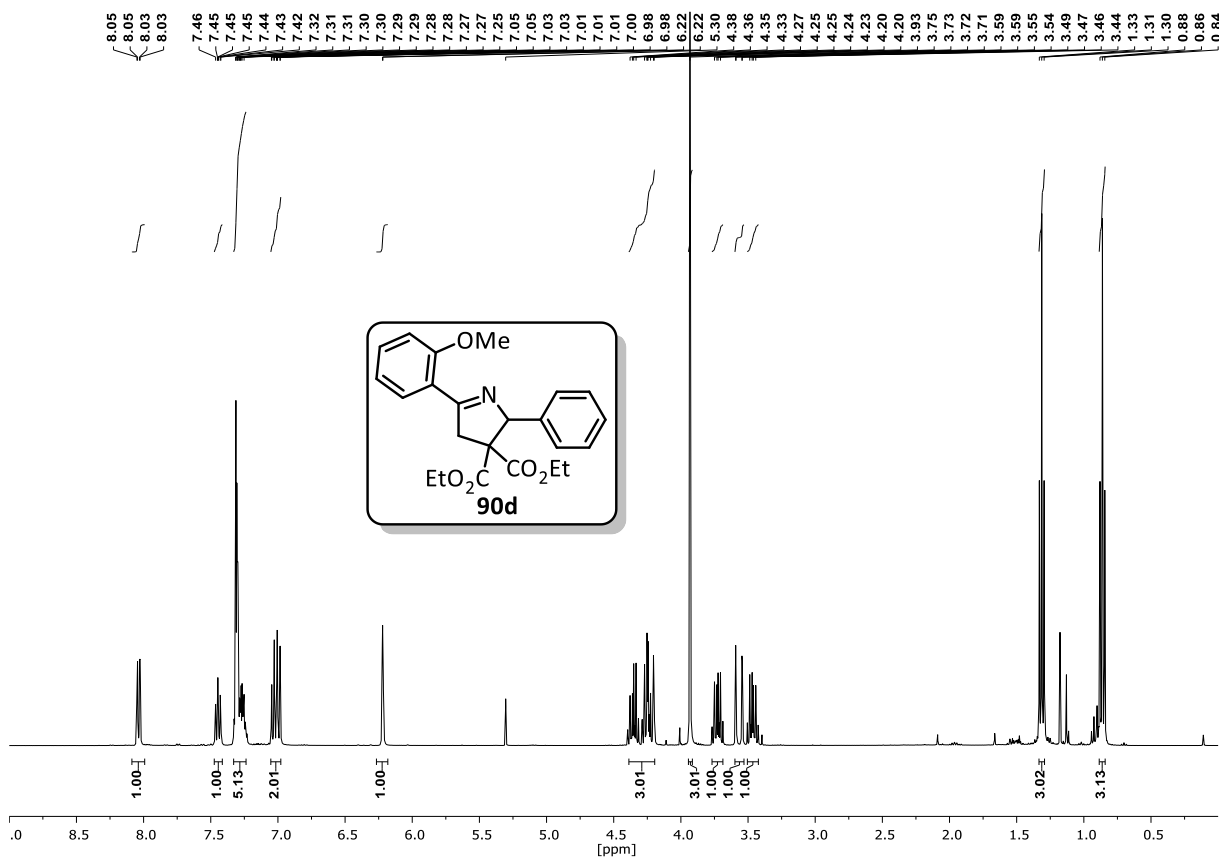
¹³C-NMR (101 MHz, CDCl₃) & **DEPT135** (101 MHz, CDCl₃):
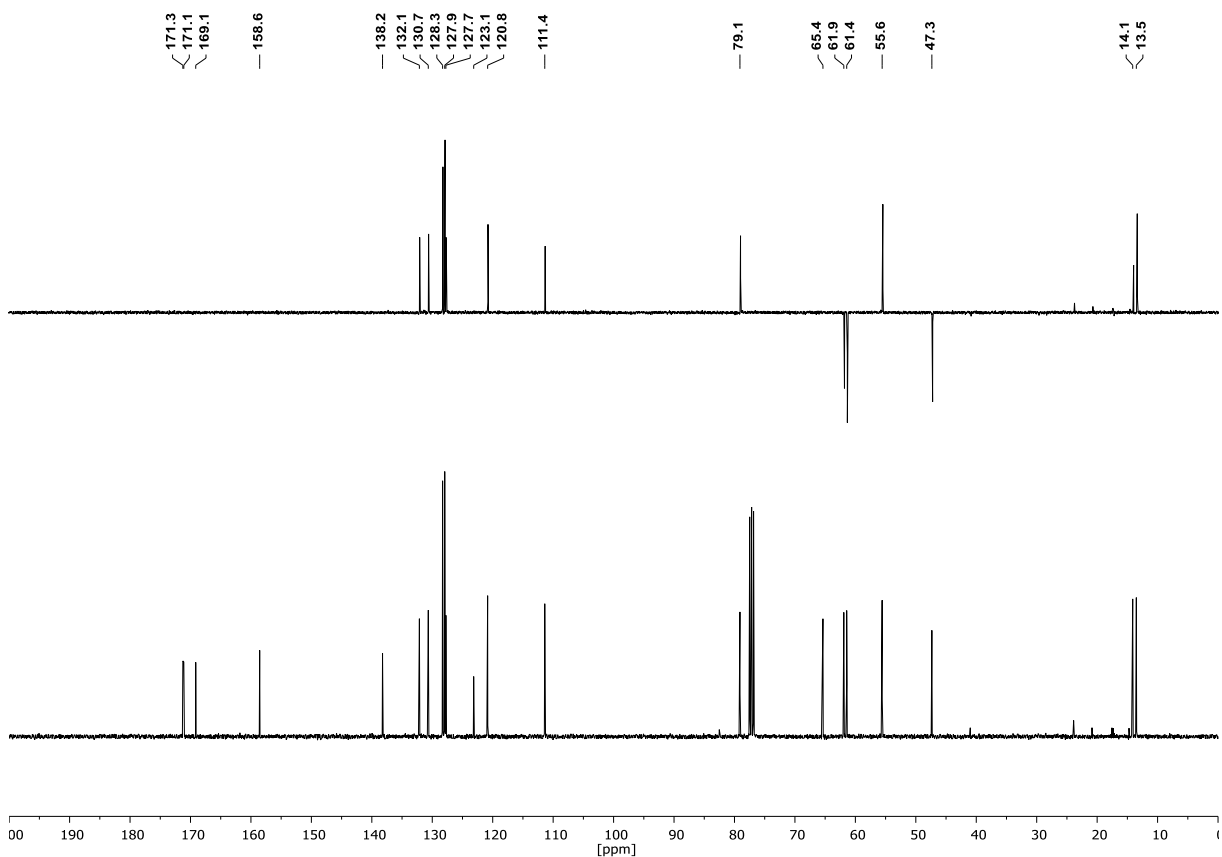
Diethyl 5-(3-chlorophenyl)-2-phenyl-2,4-dihydro-2*H*-pyrrole-3,3-dicarboxylate (90e)

¹H-NMR (400 MHz, CDCl₃):
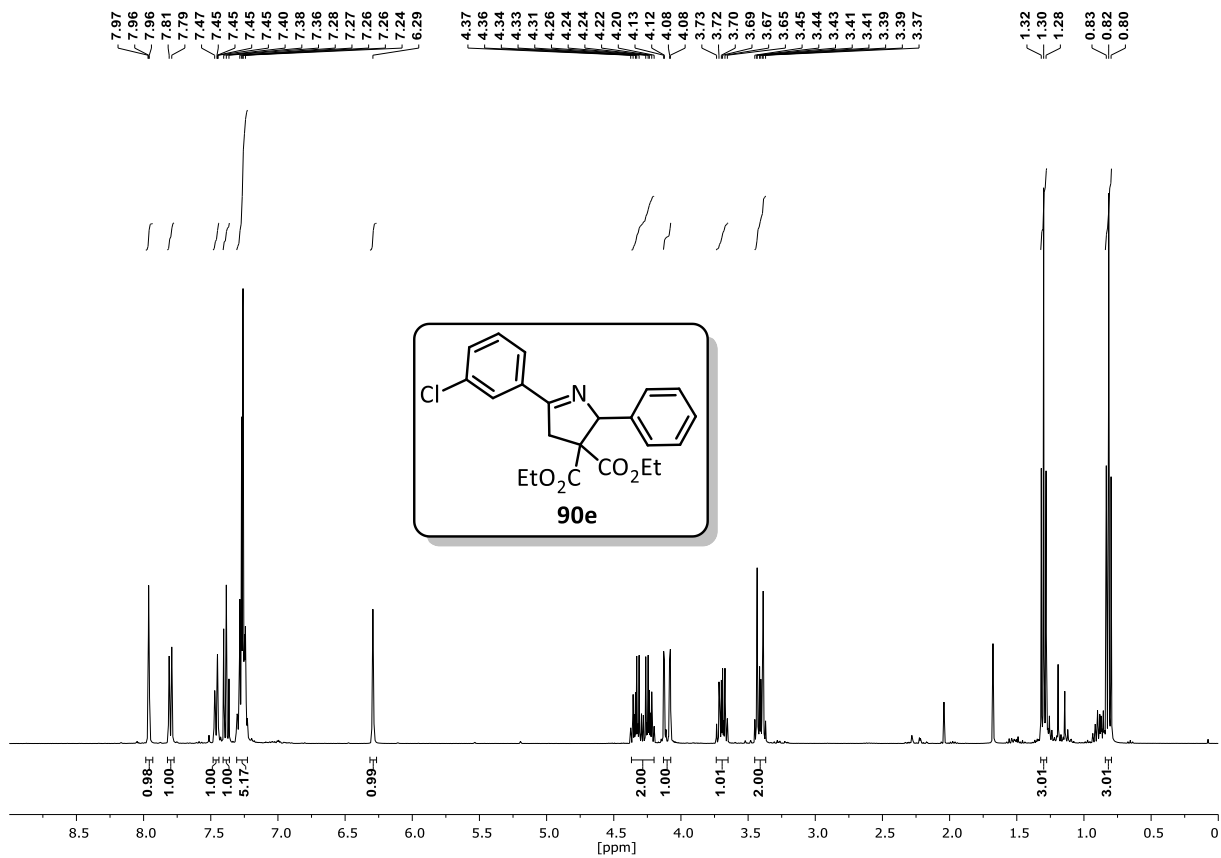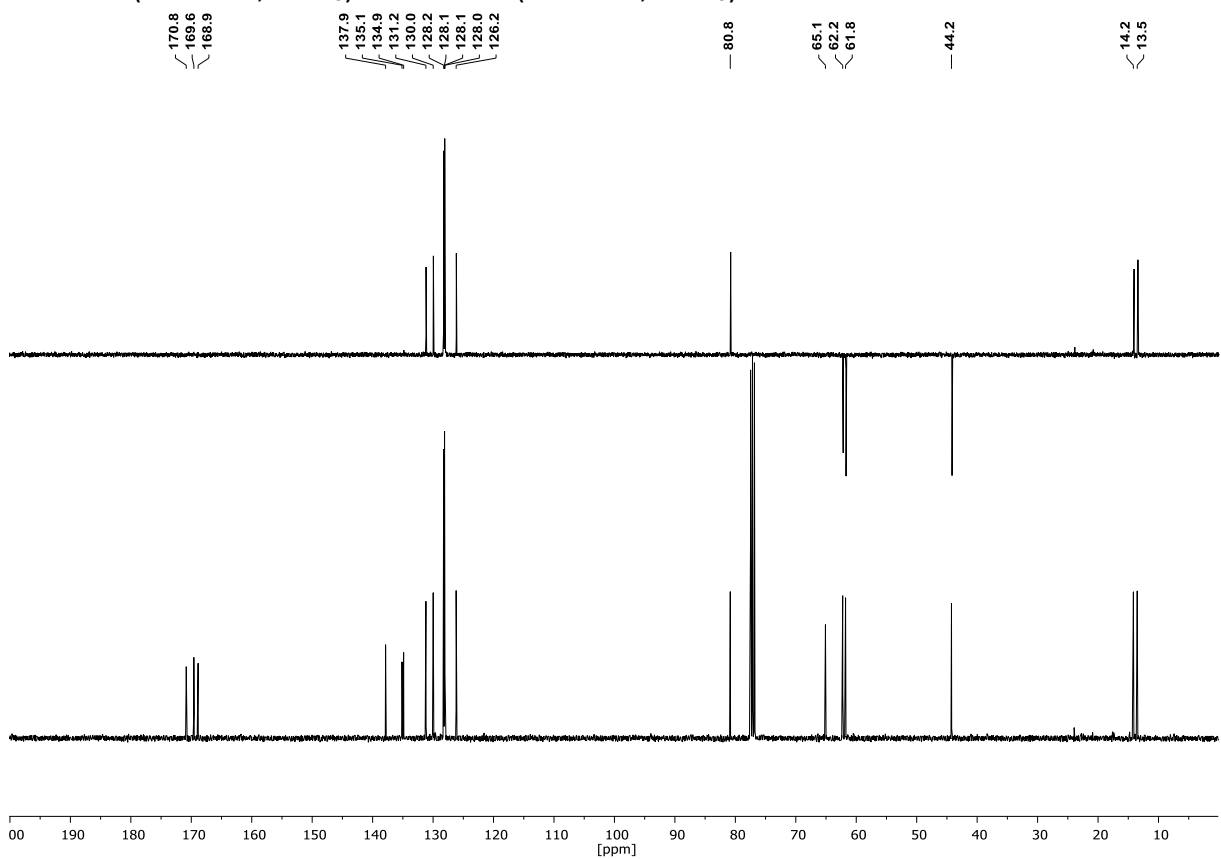
¹³C-NMR (101 MHz, CDCl₃) & **DEPT135** (101 MHz, CDCl₃):

Diethyl 5-(4-fluorophenyl)-2-phenyl-2,4-dihydro-2H-pyrrole-3,3-dicarboxylate (90f) & diethyl 7-fluoro-4-oxo-1-phenyl-3,4-dihydronaphthalene-2,2(1H)-dicarboxylate (99f)

1H-NMR (400 MHz, CDCl₃):
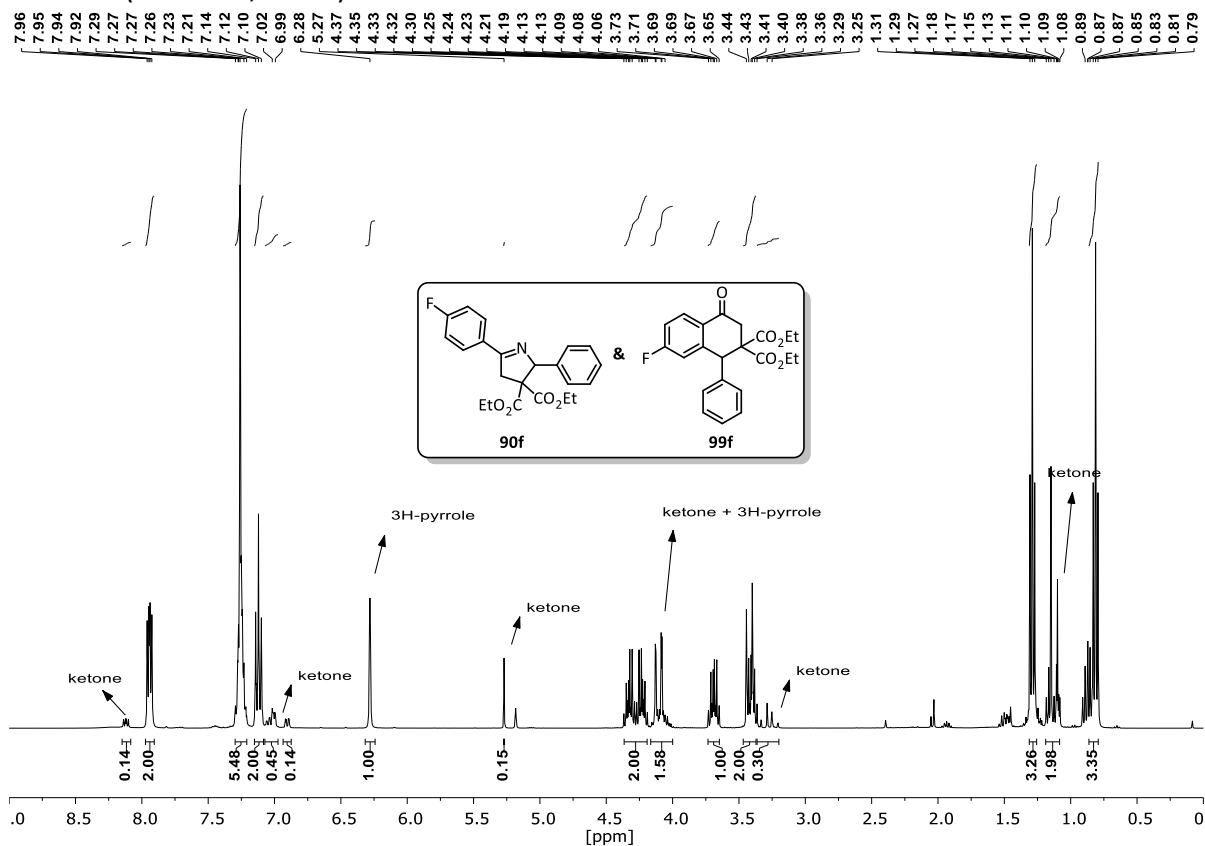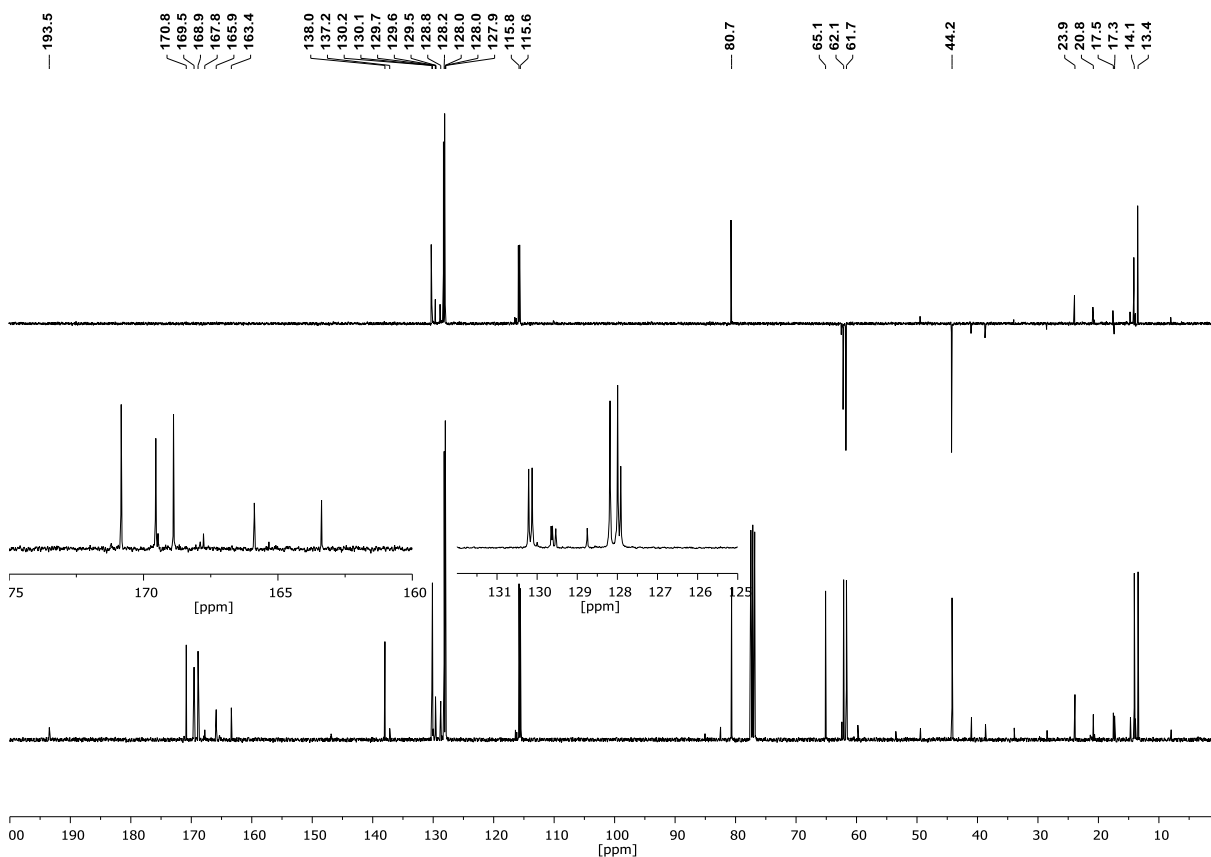
13C-NMR (101 MHz, CDCl₃) & **DEPT135** (101 MHz, CDCl₃):

¹⁹F-NMR (377 MHz, CDCl₃):
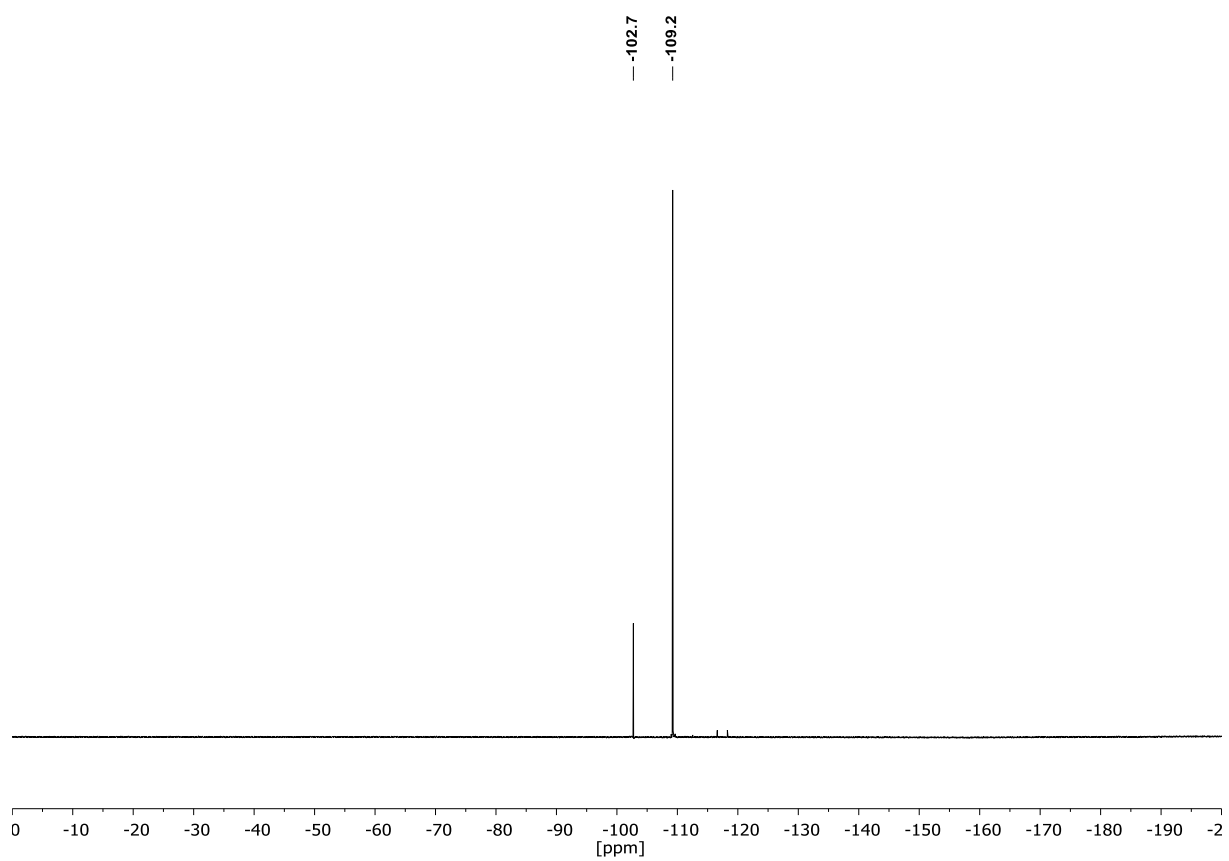
Diethyl 2-(4-bromophenyl)-5-phenyl-2,4-dihydro-2*H*-pyrrole-3,3-dicarboxylate (90g)

¹H-NMR (400 MHz, CDCl₃):
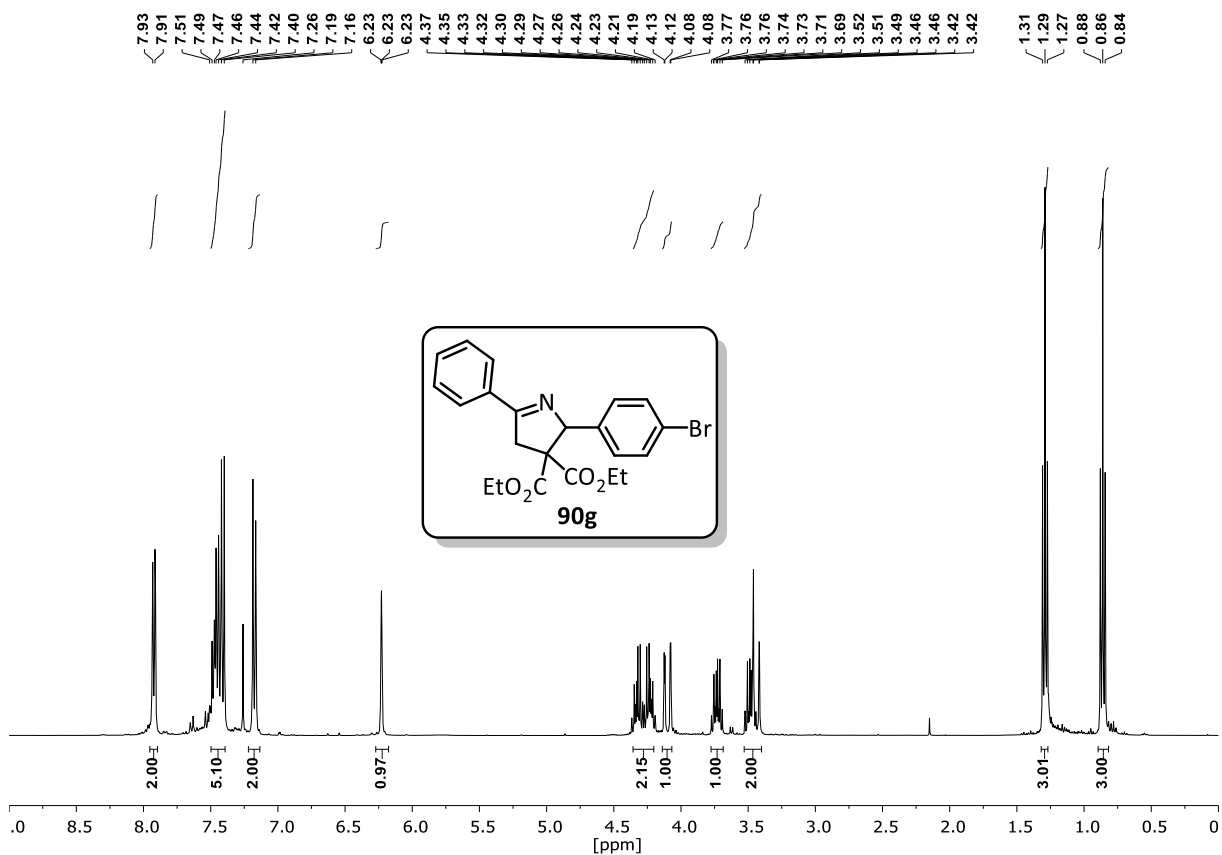
¹³C-NMR (101 MHz, CDCl₃) & **DEPT135** (101 MHz, CDCl₃):
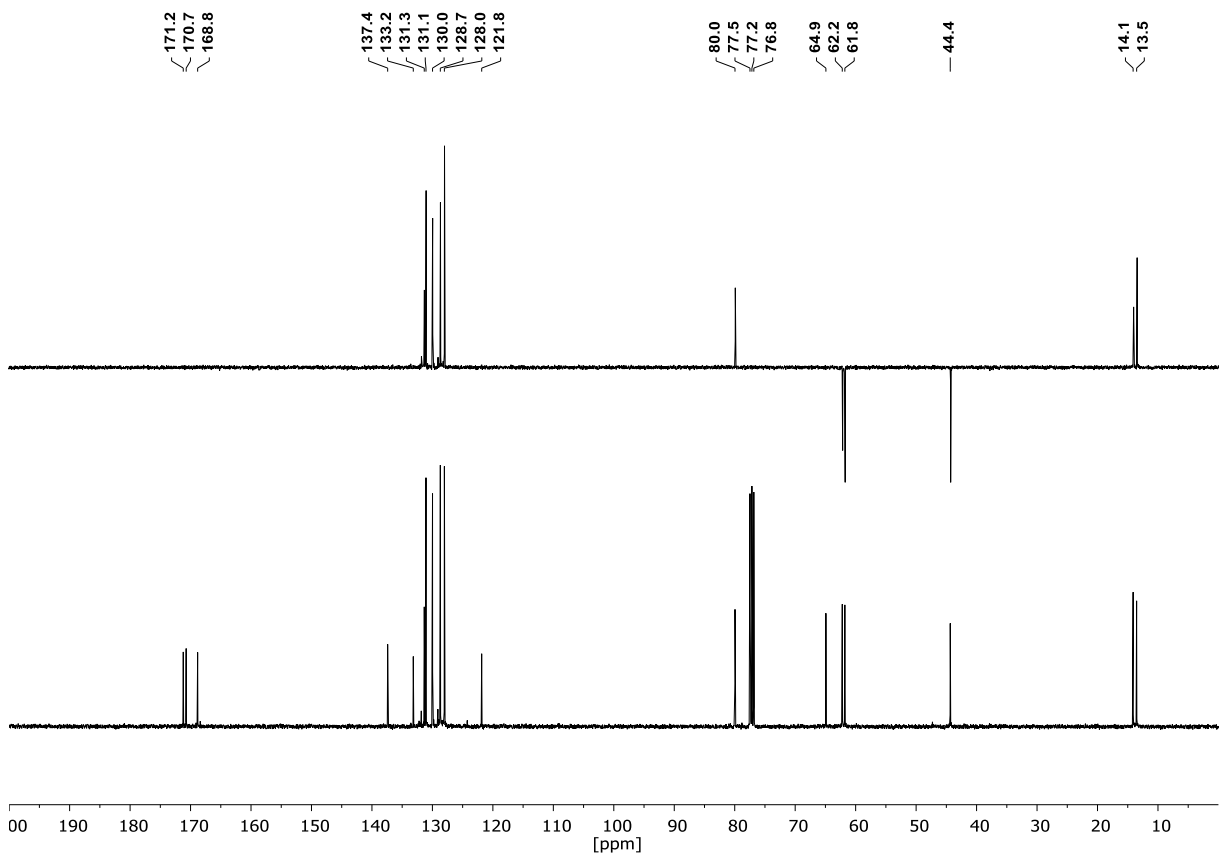
Diethyl 2-phenyl-5-(pyridin-3-yl)-2,4-dihydro-2*H*-pyrrole-3,3-dicarboxylate (90h)

¹H-NMR (400 MHz, CDCl₃):
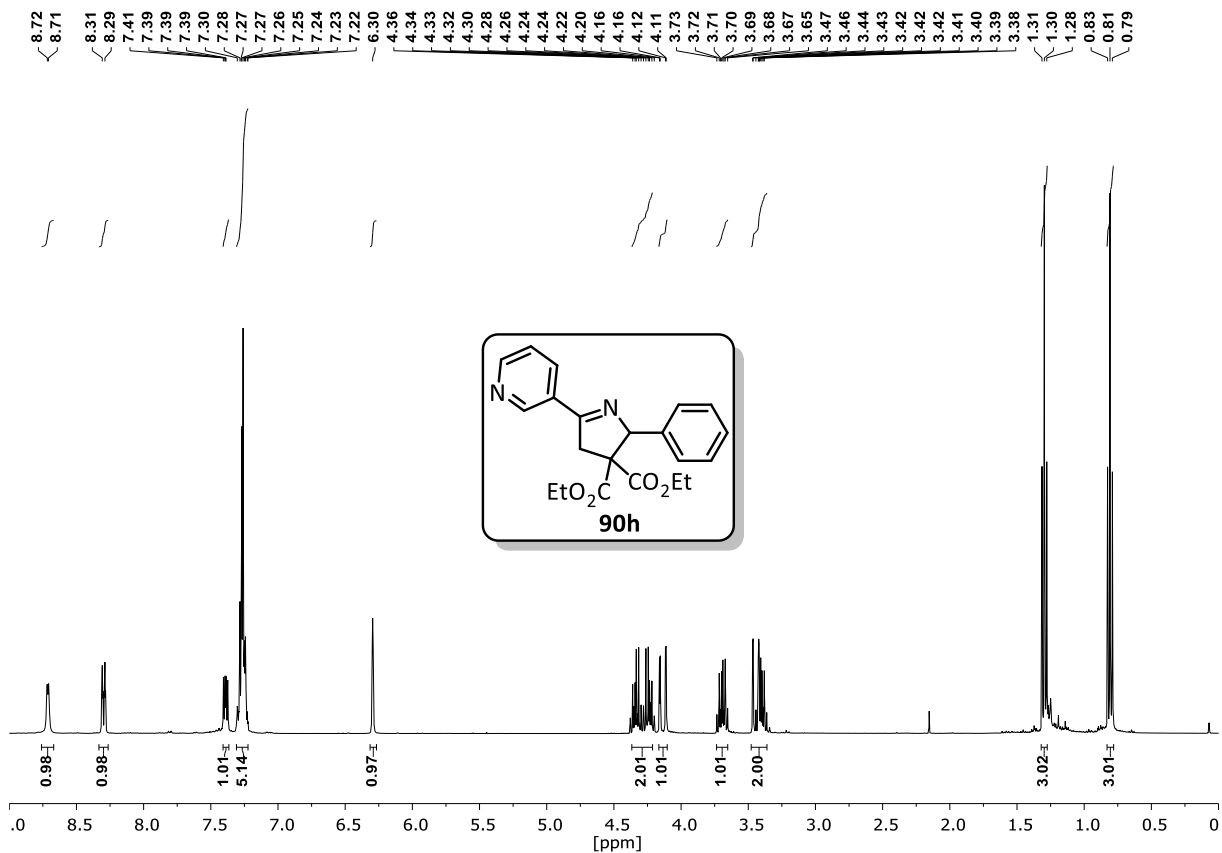
¹³C-NMR (101 MHz, CDCl₃) & **DEPT135** (101 MHz, CDCl₃):
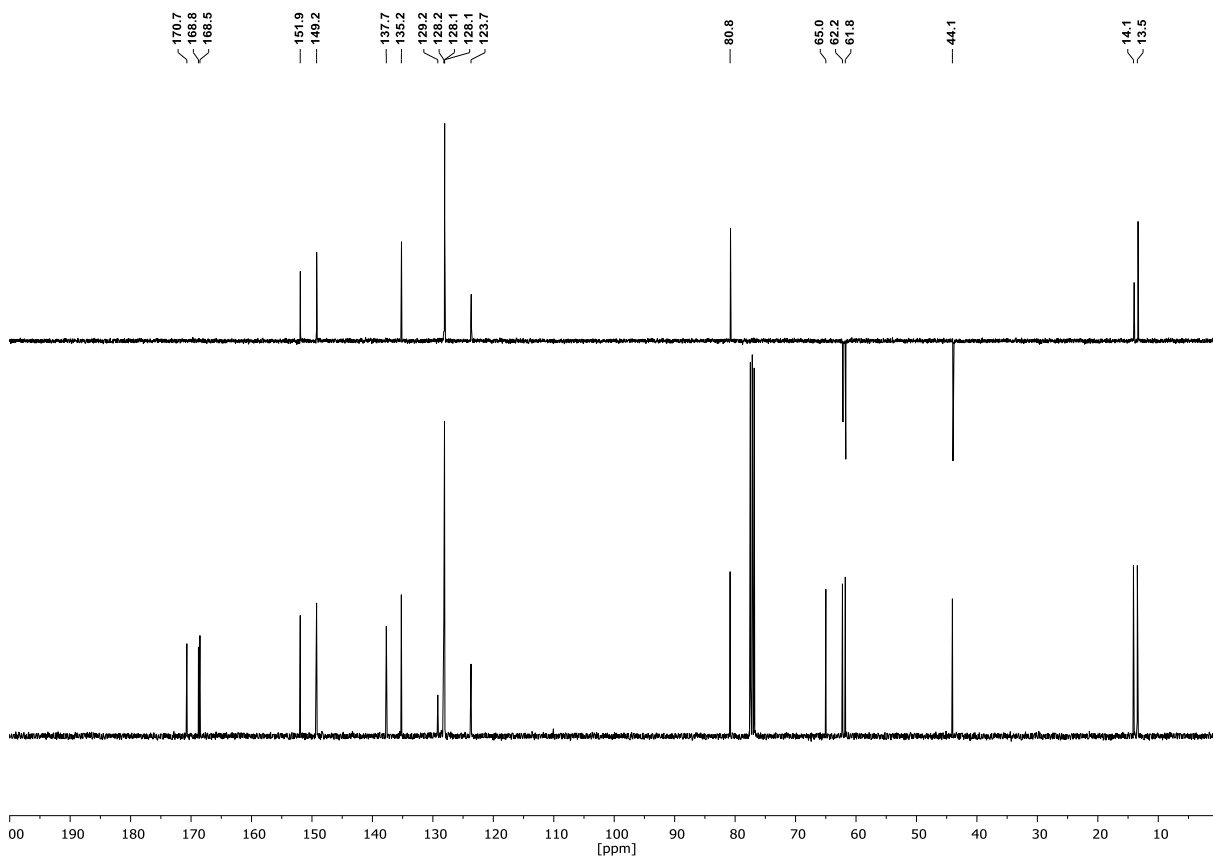
Diethyl 5-(naphthalen-2-yl)-2-phenyl-2,4-dihydro-3*H*-pyrrole-3,3-dicarboxylate (90i)

¹H-NMR (400 MHz, CDCl₃):
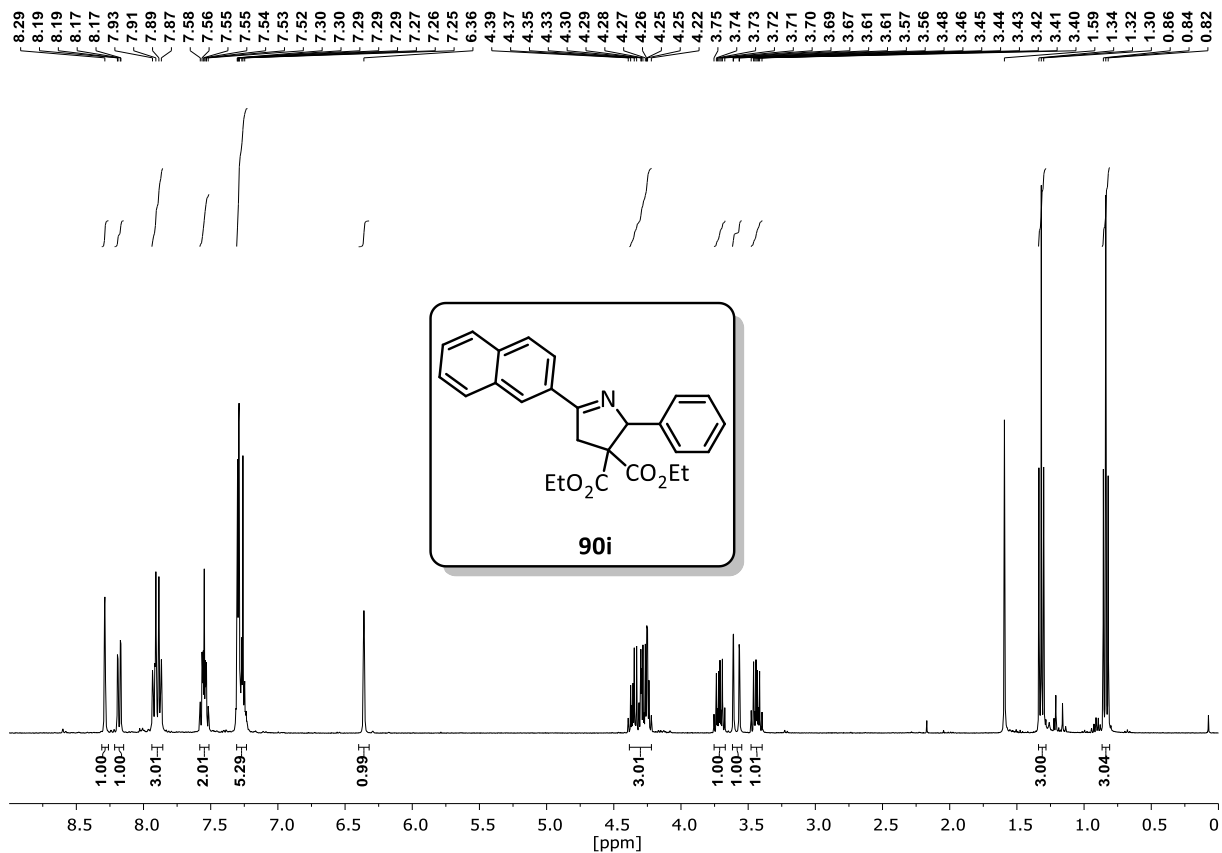
¹³C-NMR (101 MHz, CDCl₃) & **DEPT135** (101 MHz, CDCl₃):
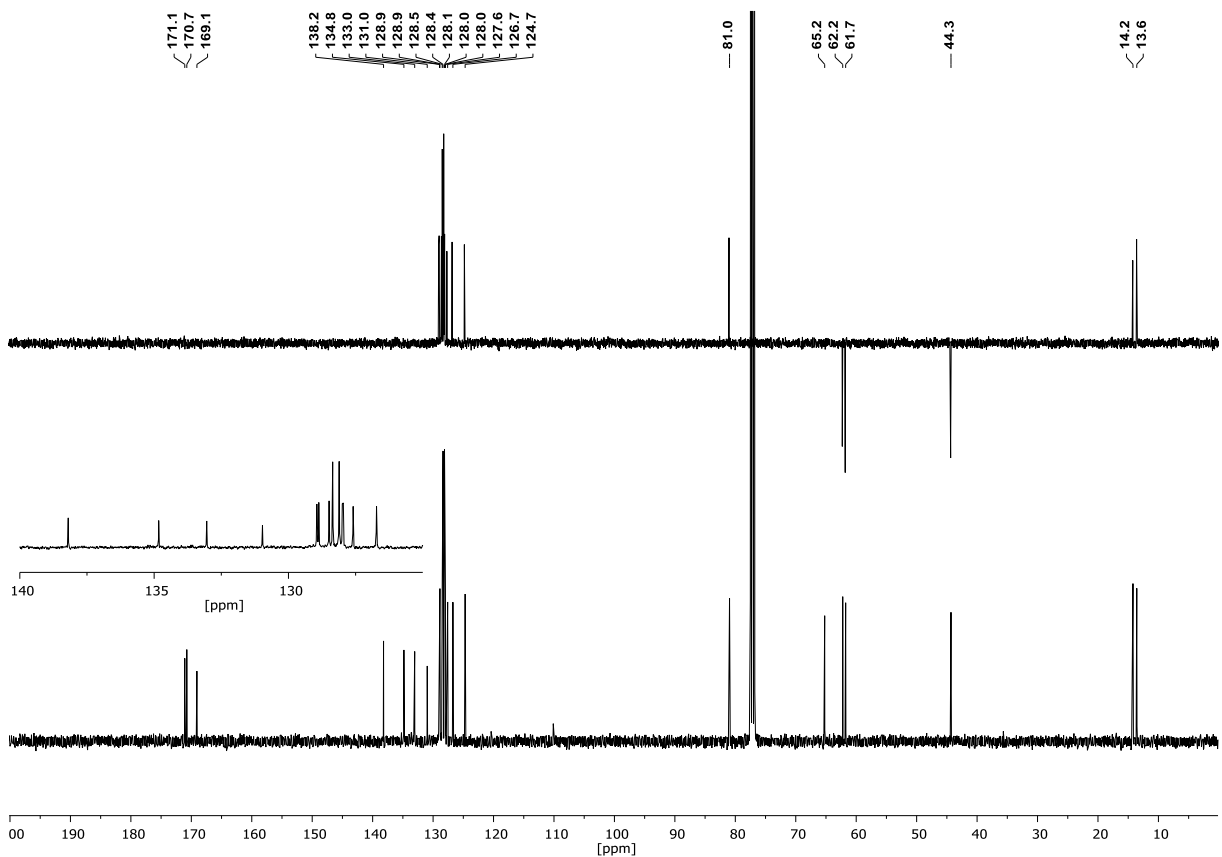
Diethyl 4-oxo-1-phenyl-3,4-dihydroanthracene-2,2(1*H*)-dicarboxylate (99i)

¹H-NMR (400 MHz, CDCl₃):
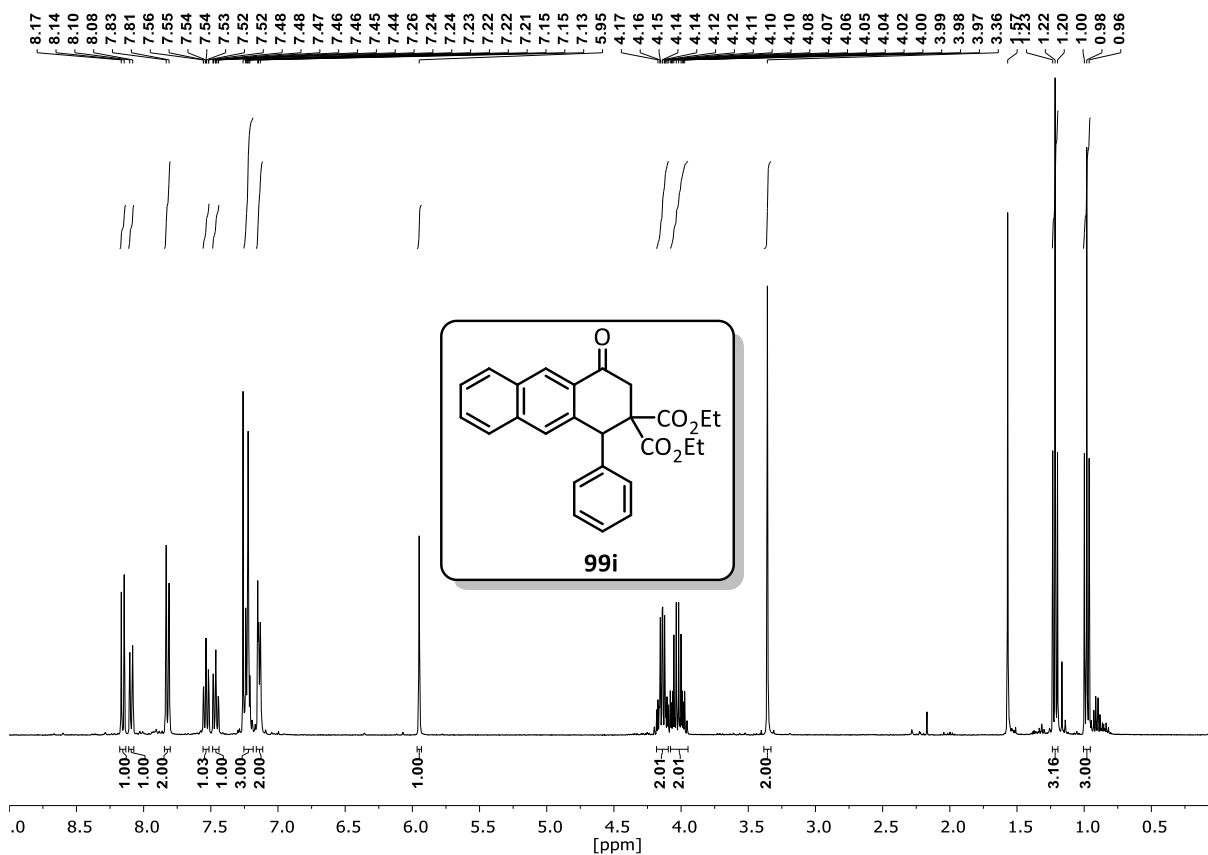
¹³C-NMR (101 MHz, CDCl₃) & **DEPT135** (101 MHz, CDCl₃):
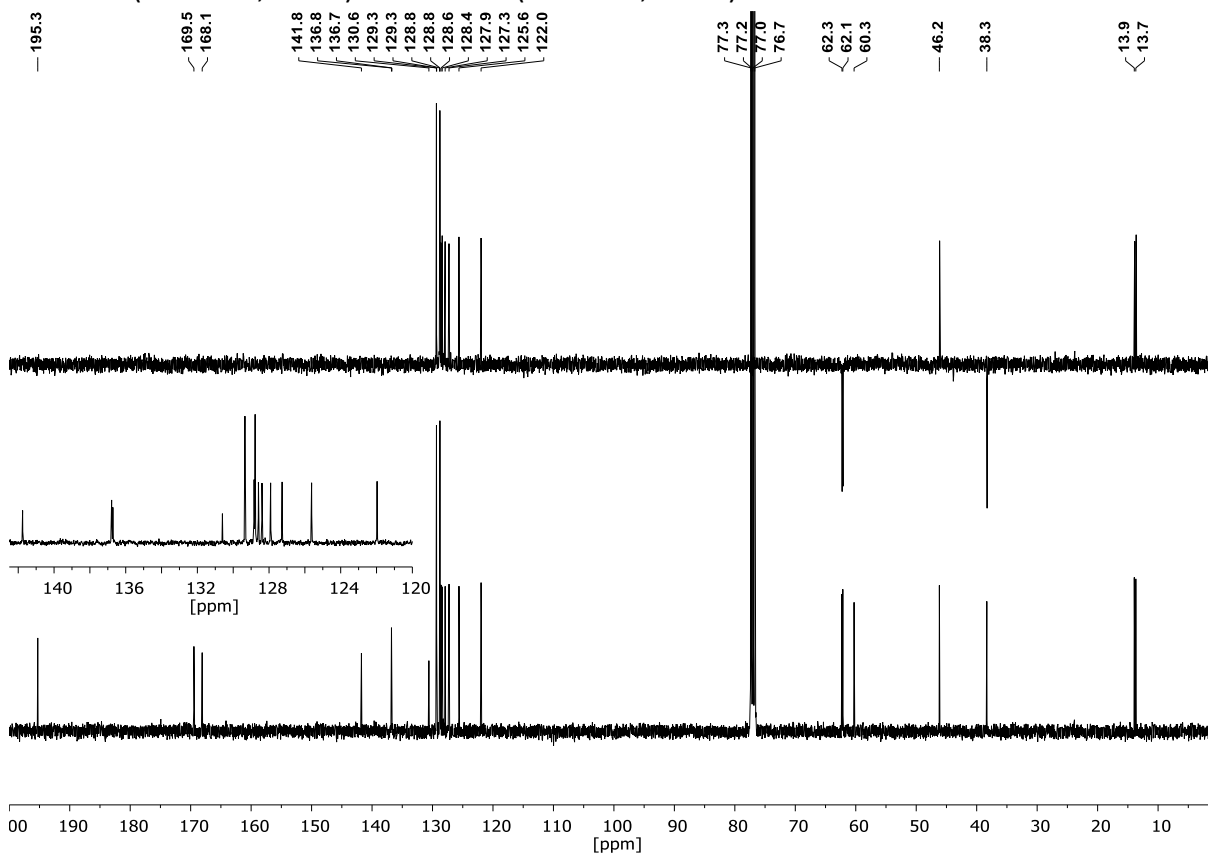
Diethyl 2,2-dimethyl-5-phenyl-2,4-dihydro-2*H*-pyrrole-3,3-dicarboxylate (90f)

¹H-NMR (400 MHz, CDCl₃):
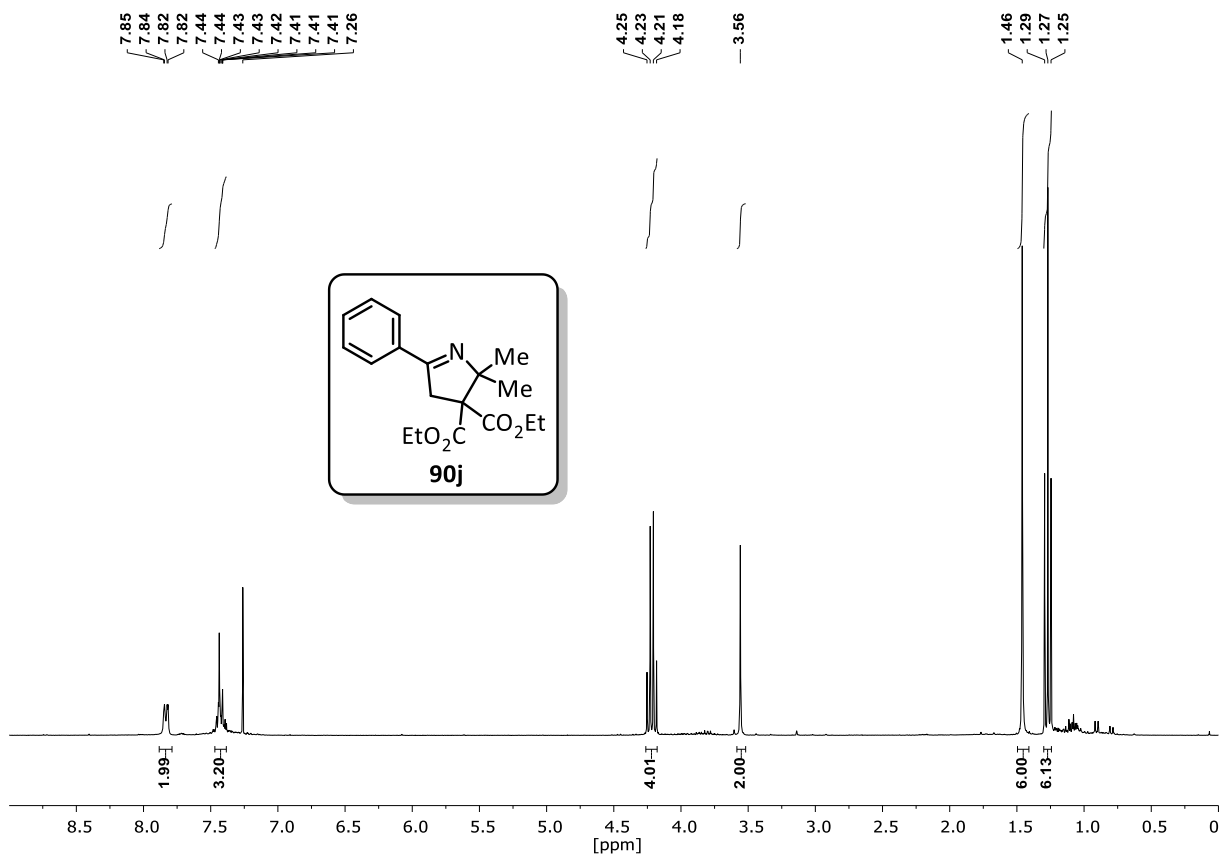
¹³C-NMR (101 MHz, CDCl₃) & **DEPT135** (101 MHz, CDCl₃):
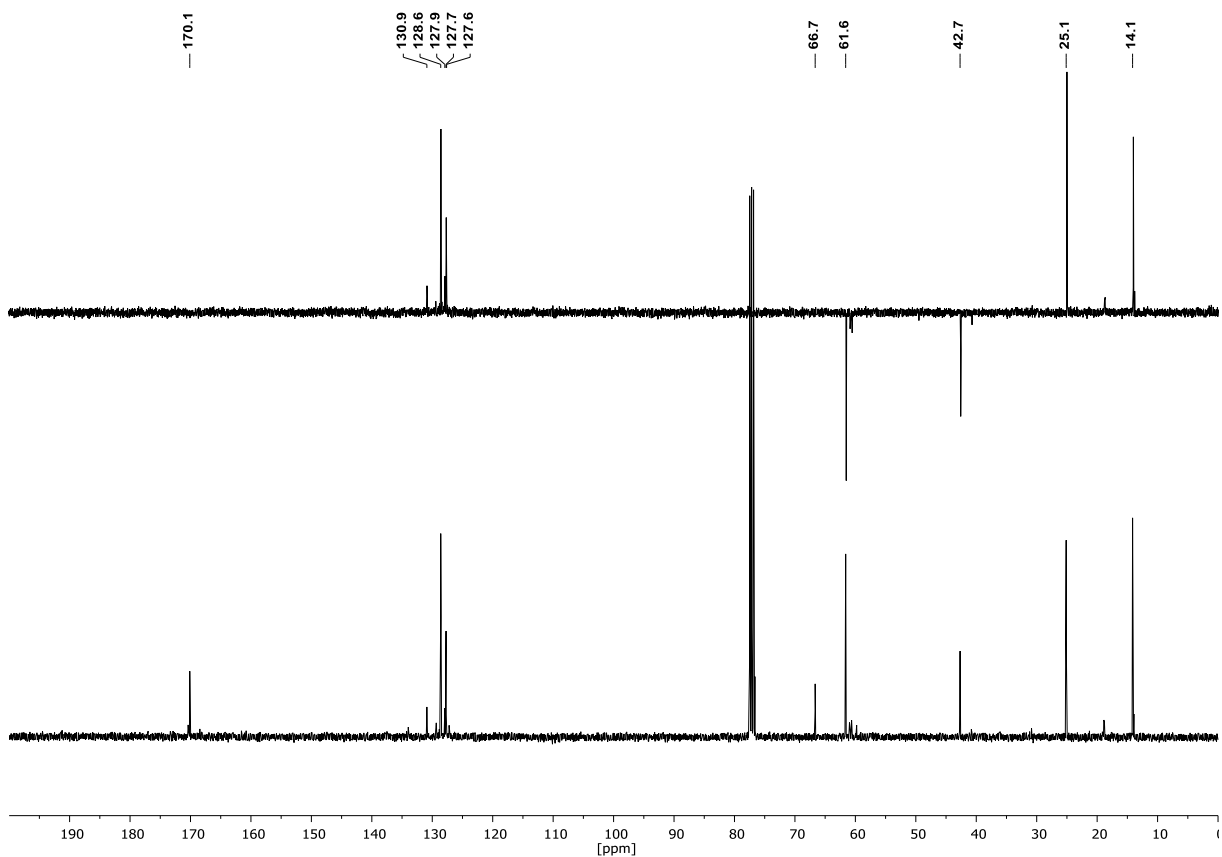
Ethyl (2Z,4Z)-4-(formylimino)-2-isopropyl-4-phenylbut-2-enoate (139):

¹H-NMR (400 MHz, CDCl₃):
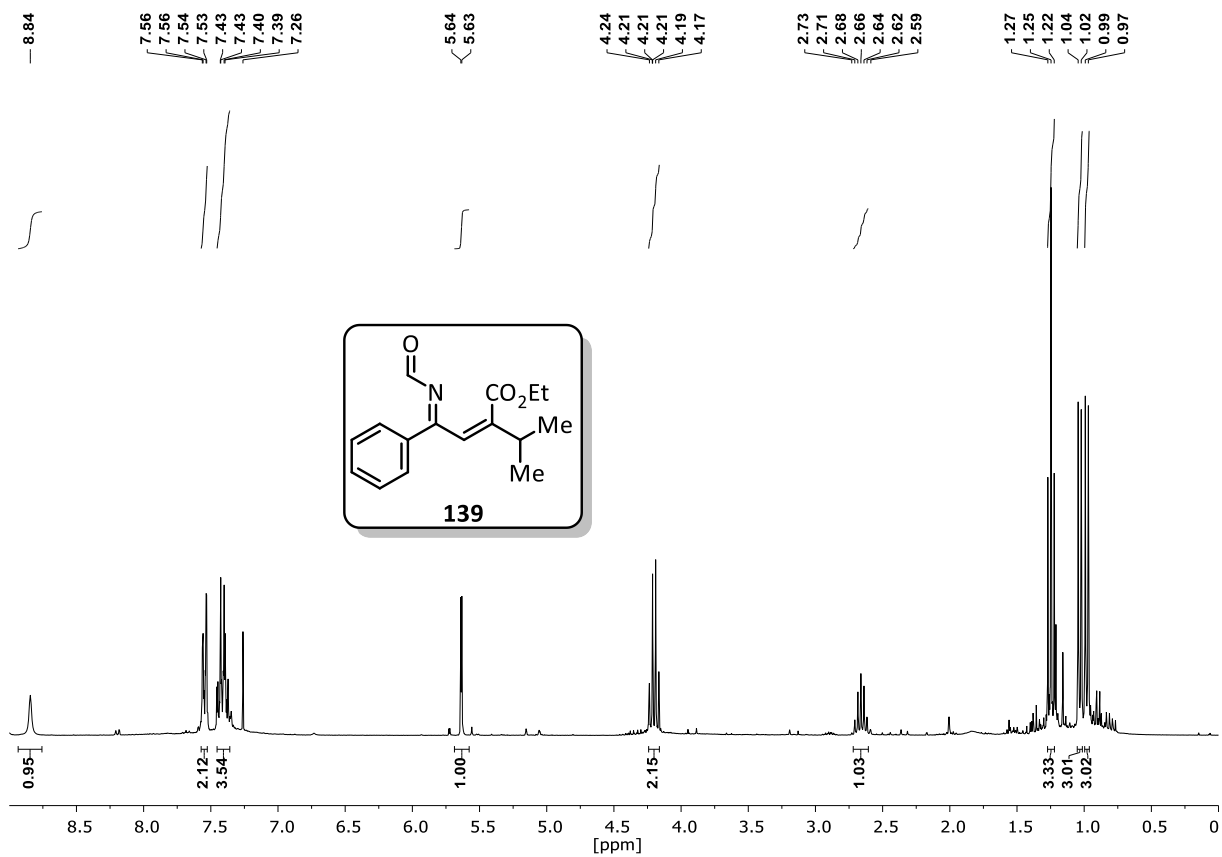
¹³C-NMR (101 MHz, CDCl₃) & **DEPT135** (101 MHz, CDCl₃):
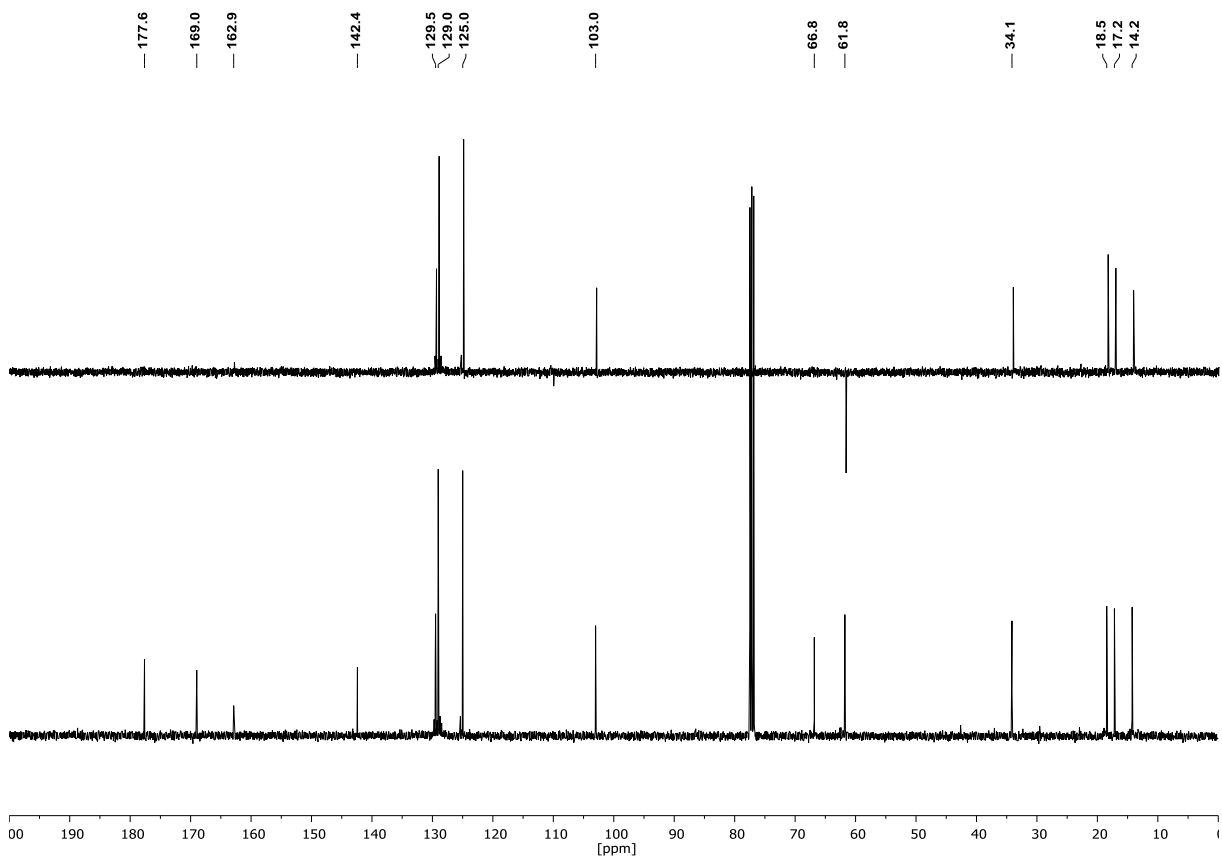
2-(2,5-Diphenyl-3,4-dihydro-2*H*-pyrrol-2-yl)acetonitrile (130a)

¹H-NMR (400 MHz, CDCl₃):
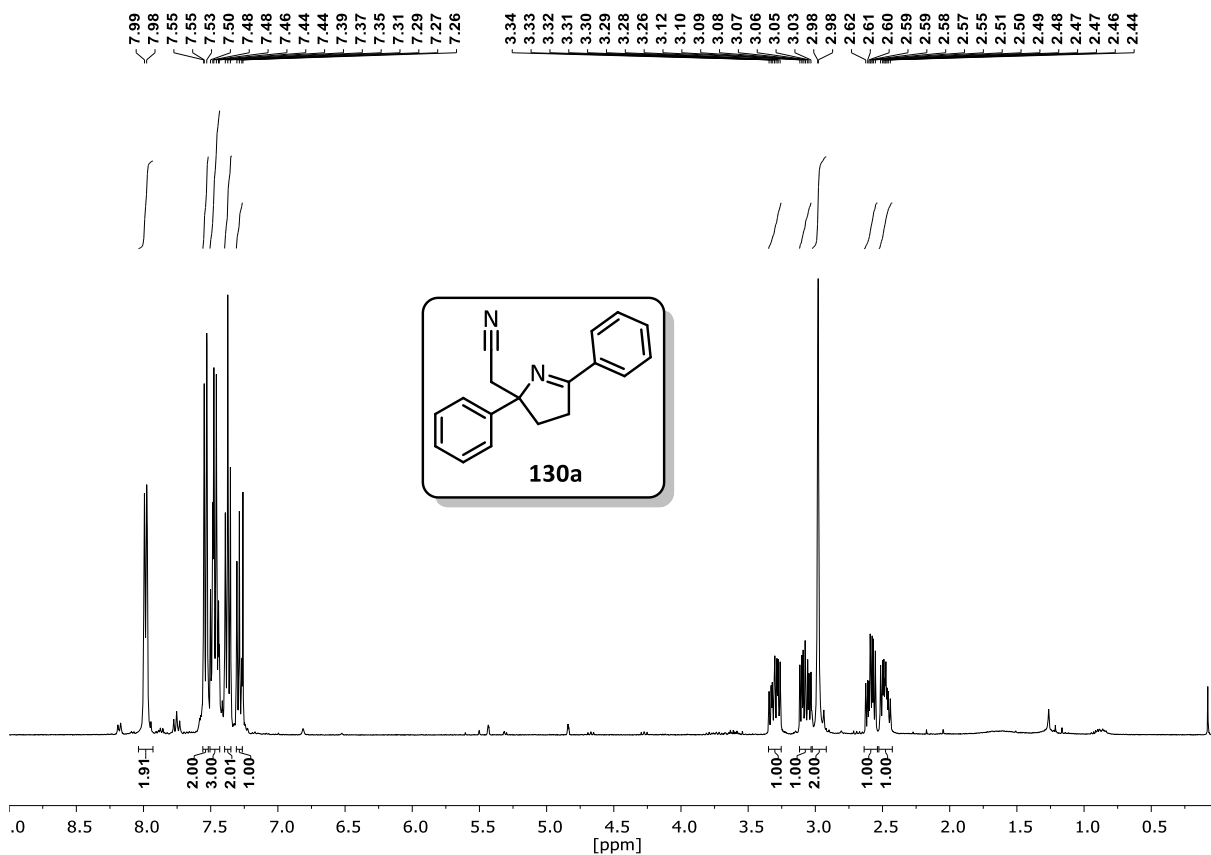
¹³C-NMR (101 MHz, CDCl₃) & **DEPT135** (101 MHz, CDCl₃):
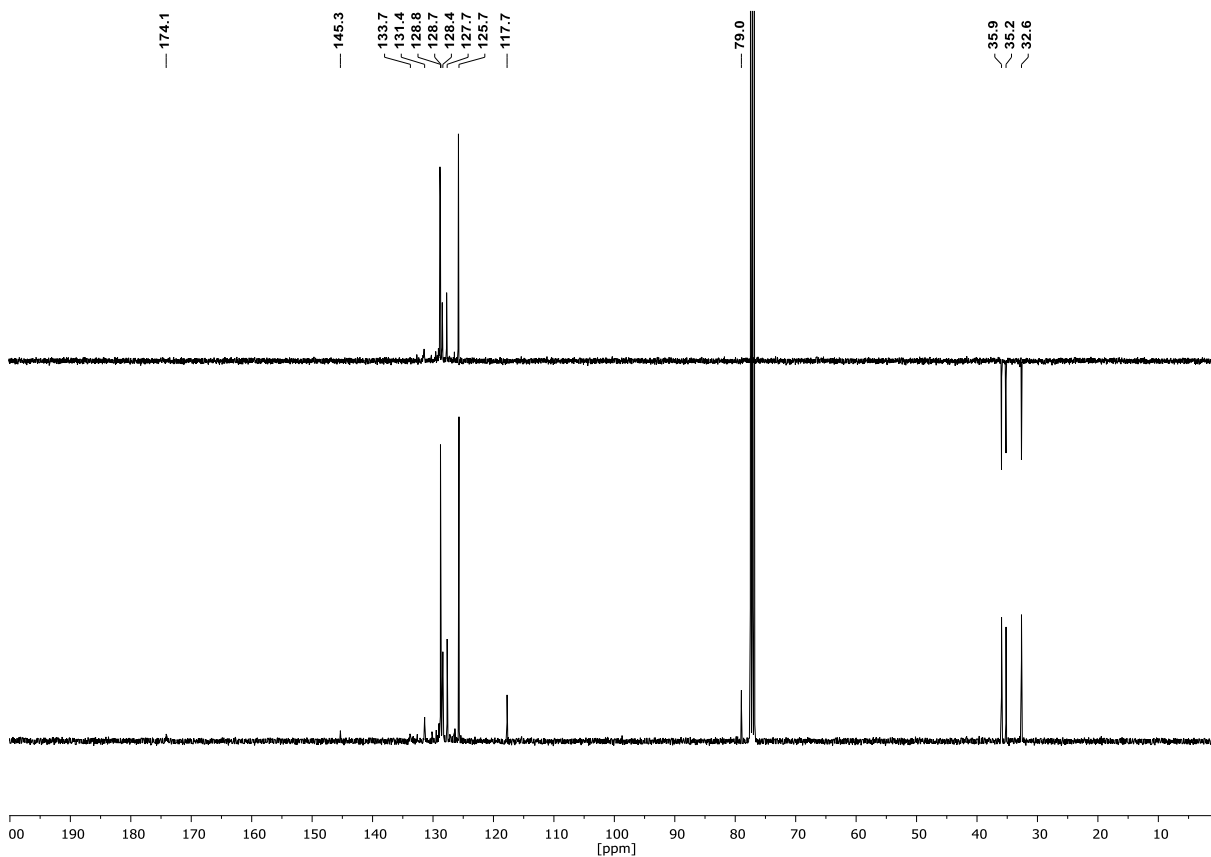
2-(2-(4-fluorophenyl)-5-phenyl-3,4-dihydro-2*H*-pyrrol-2-yl)acetonitrile (130b)

¹H-NMR (400 MHz, CDCl₃):
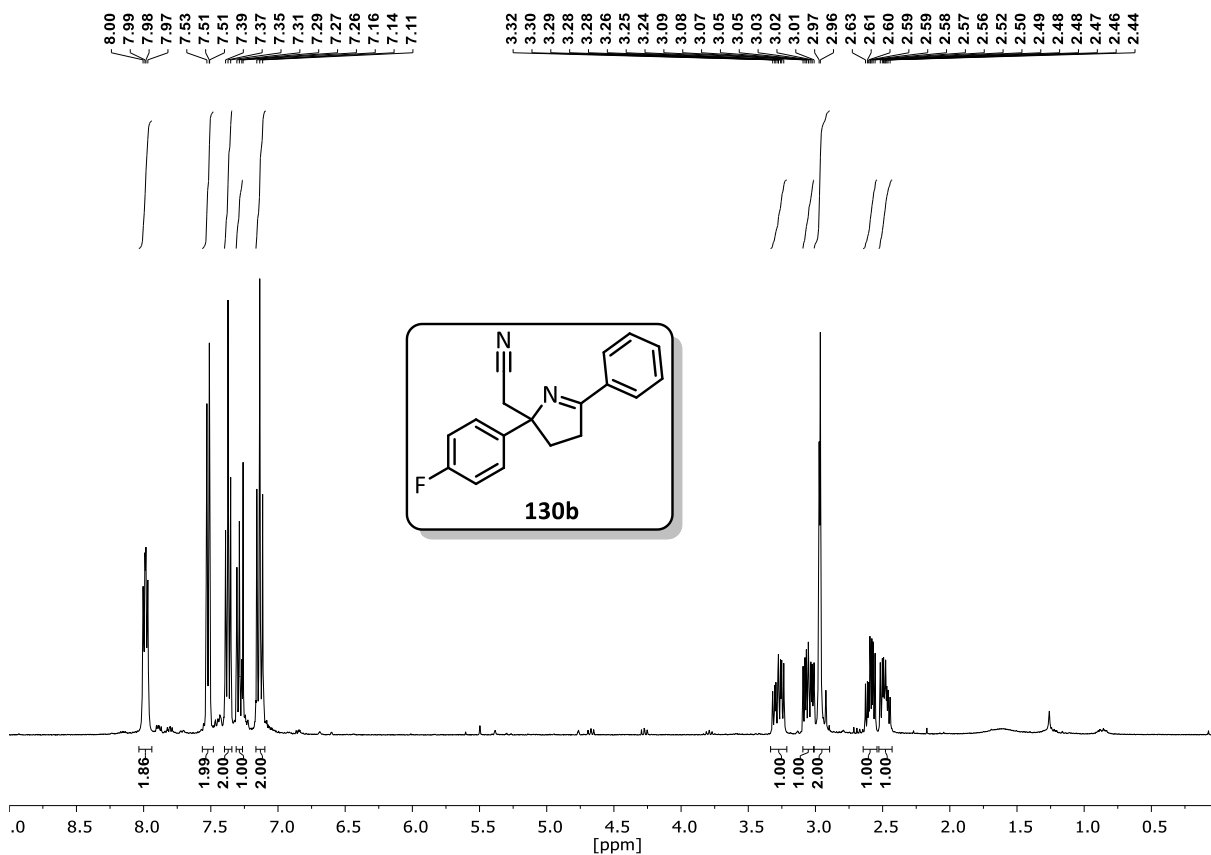
¹³C-NMR (101 MHz, CDCl₃) & **DEPT135** (101 MHz, CDCl₃):
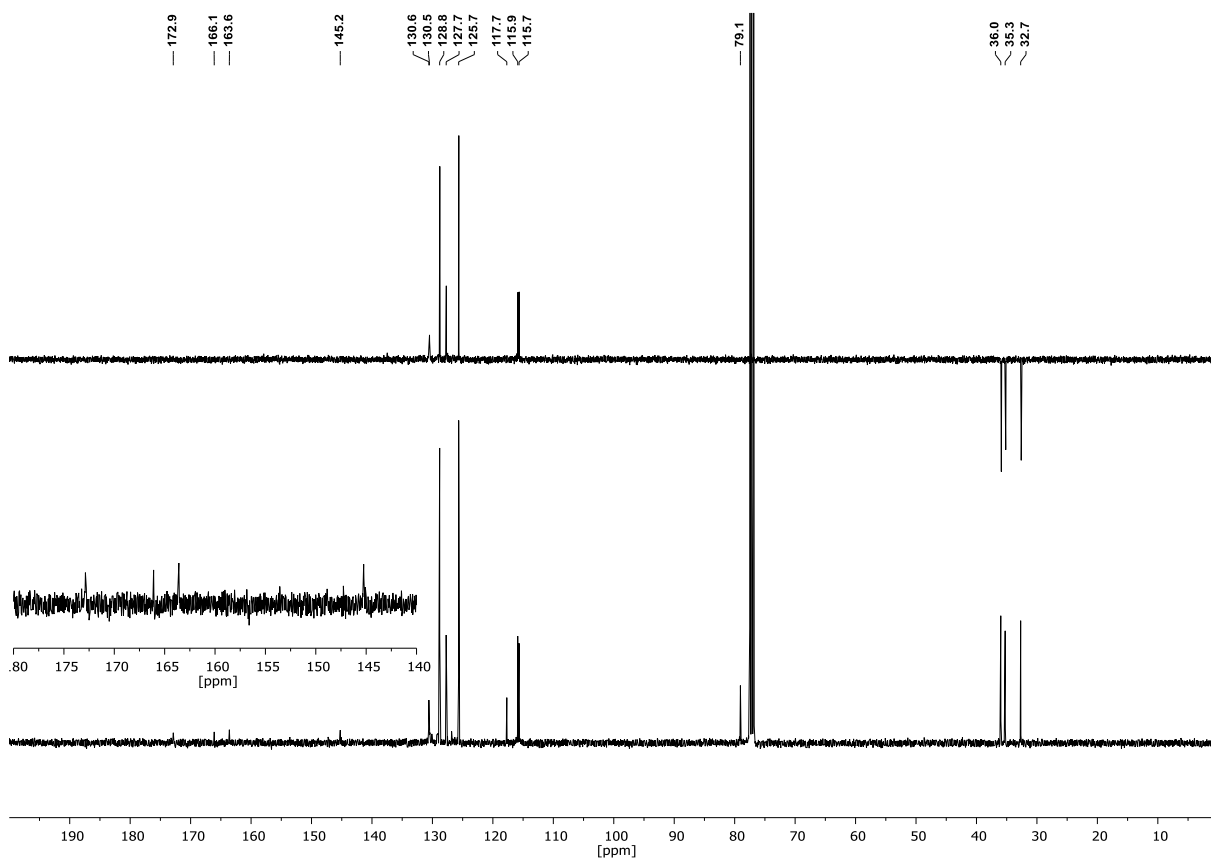
2-(5-phenyl-2-(m-tolyl)-3,4-dihydro-2H-pyrrol-2-yl)acetonitrile (130c)

¹H-NMR (400 MHz, CDCl₃):
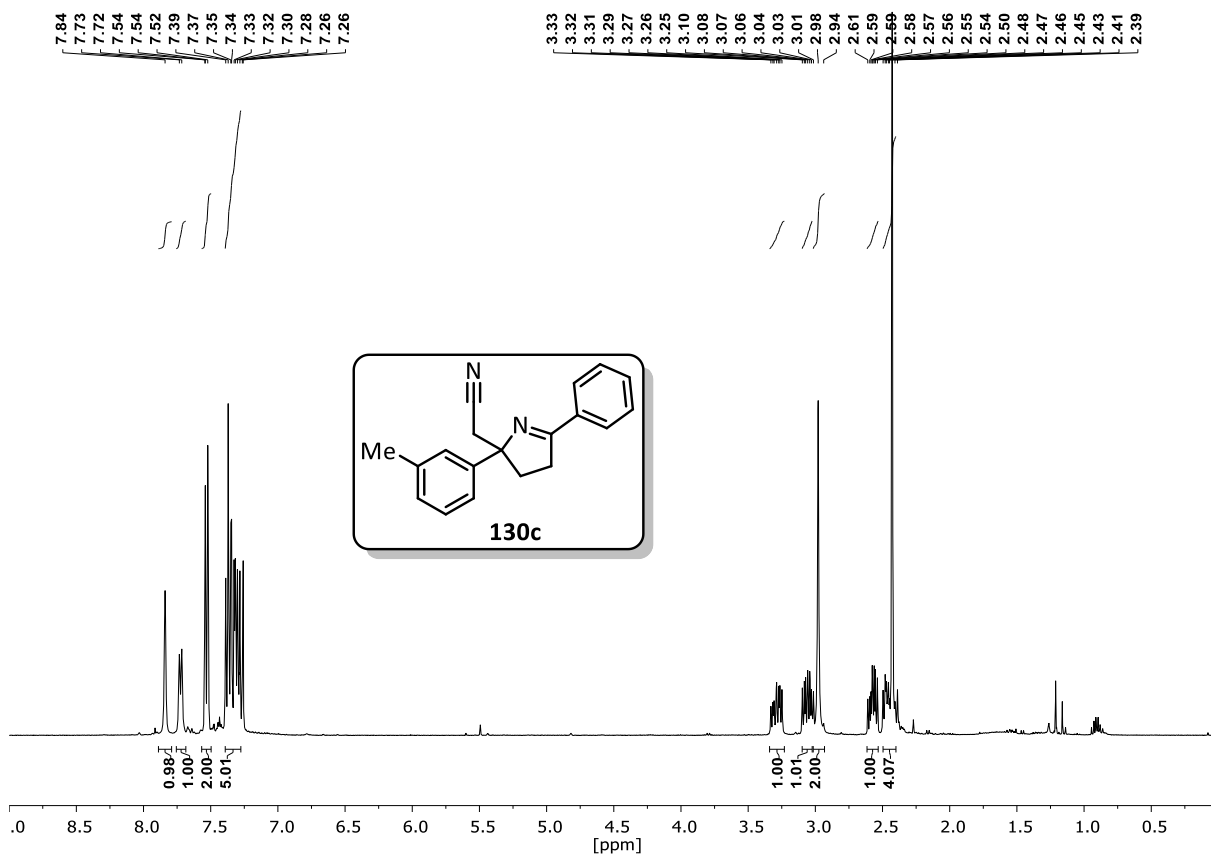
¹³C-NMR (101 MHz, CDCl₃) & **DEPT135** (101 MHz, CDCl₃):
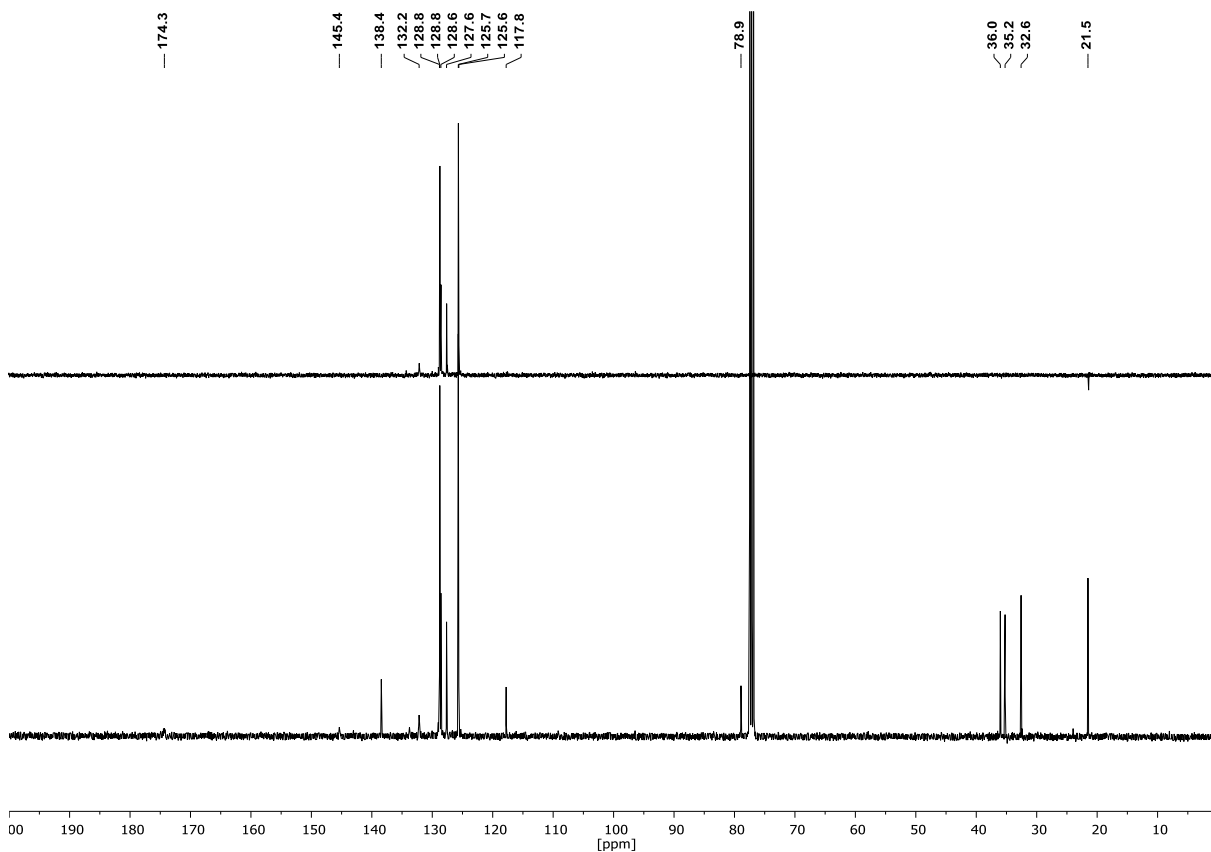
Diethyl 2,5-diphenylpyrrolidine-3,3-dicarboxylate (156, 3.57:1 d.r.)

¹H-NMR (400 MHz, CDCl₃):
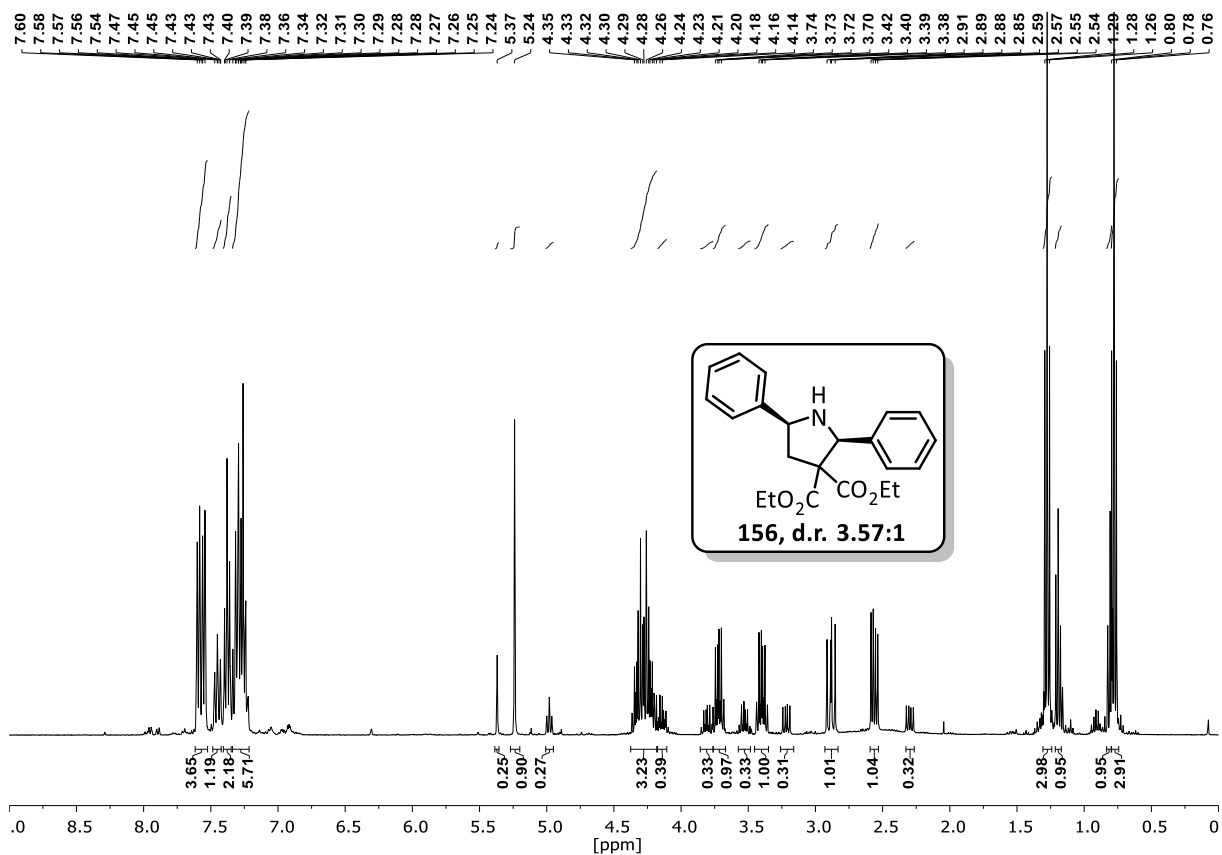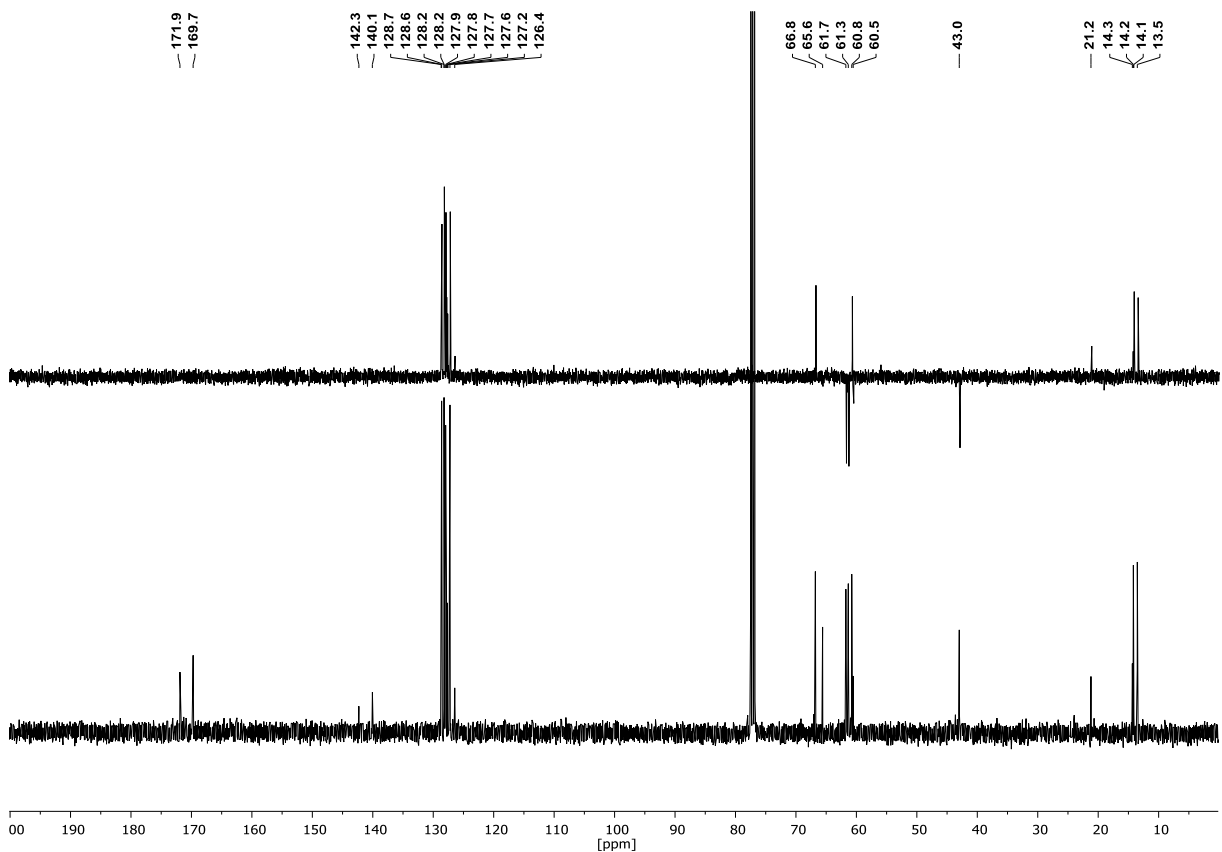
¹³C-NMR (101 MHz, CDCl₃) & **DEPT135** (101 MHz, CDCl₃):
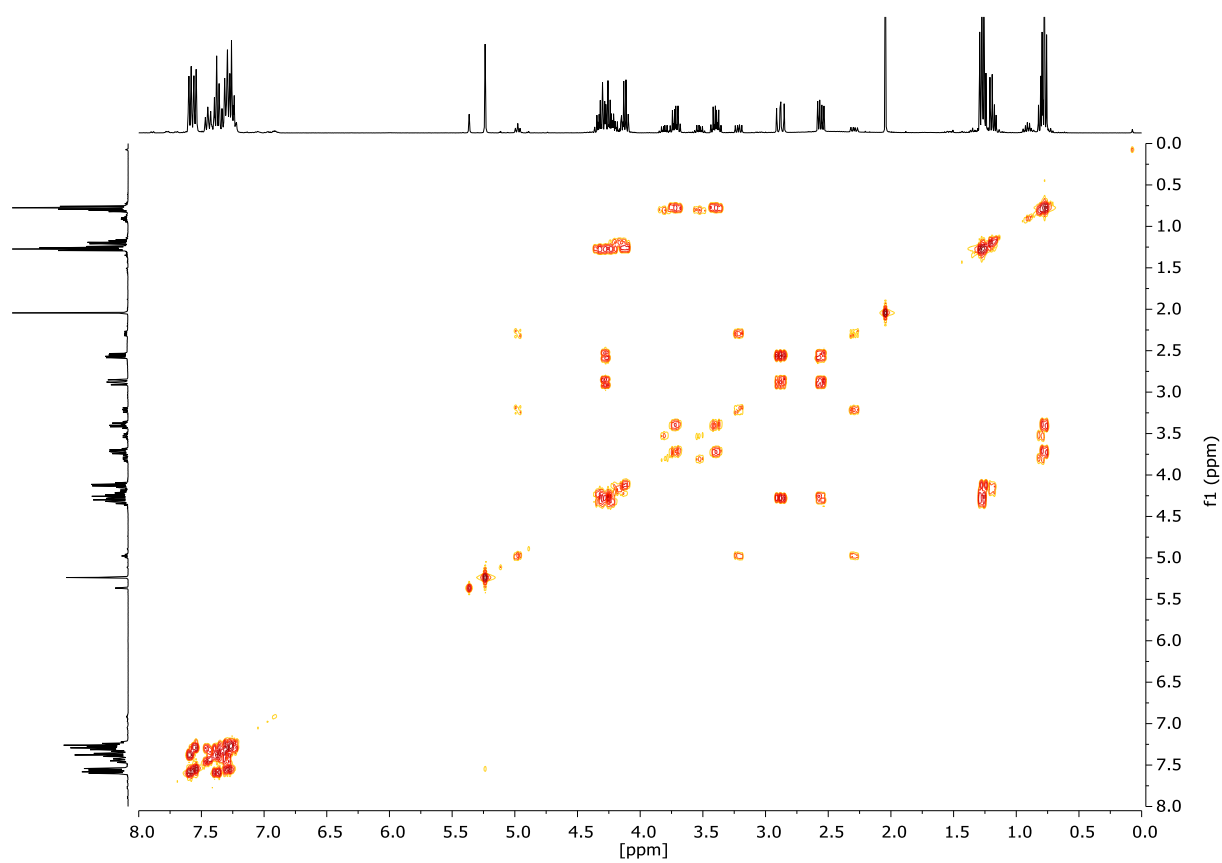
COSY (400 MHz, CDCl$_3$):
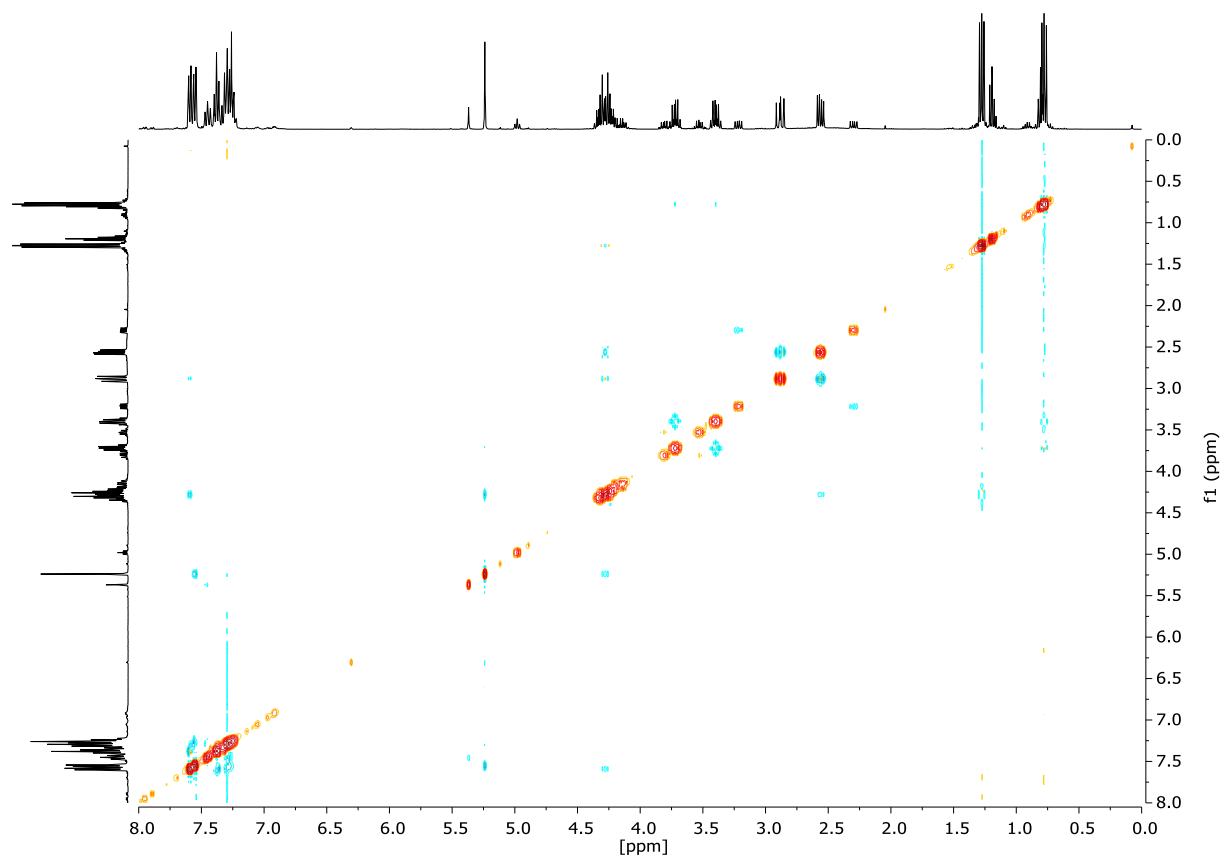
NOESY (400 MHz, CDCl$_3$):

Ethyl 2,5-diphenyl-3,4-dihydro-2H-pyrrole-3-carboxylate (157)

¹H-NMR (400 MHz, CDCl₃):
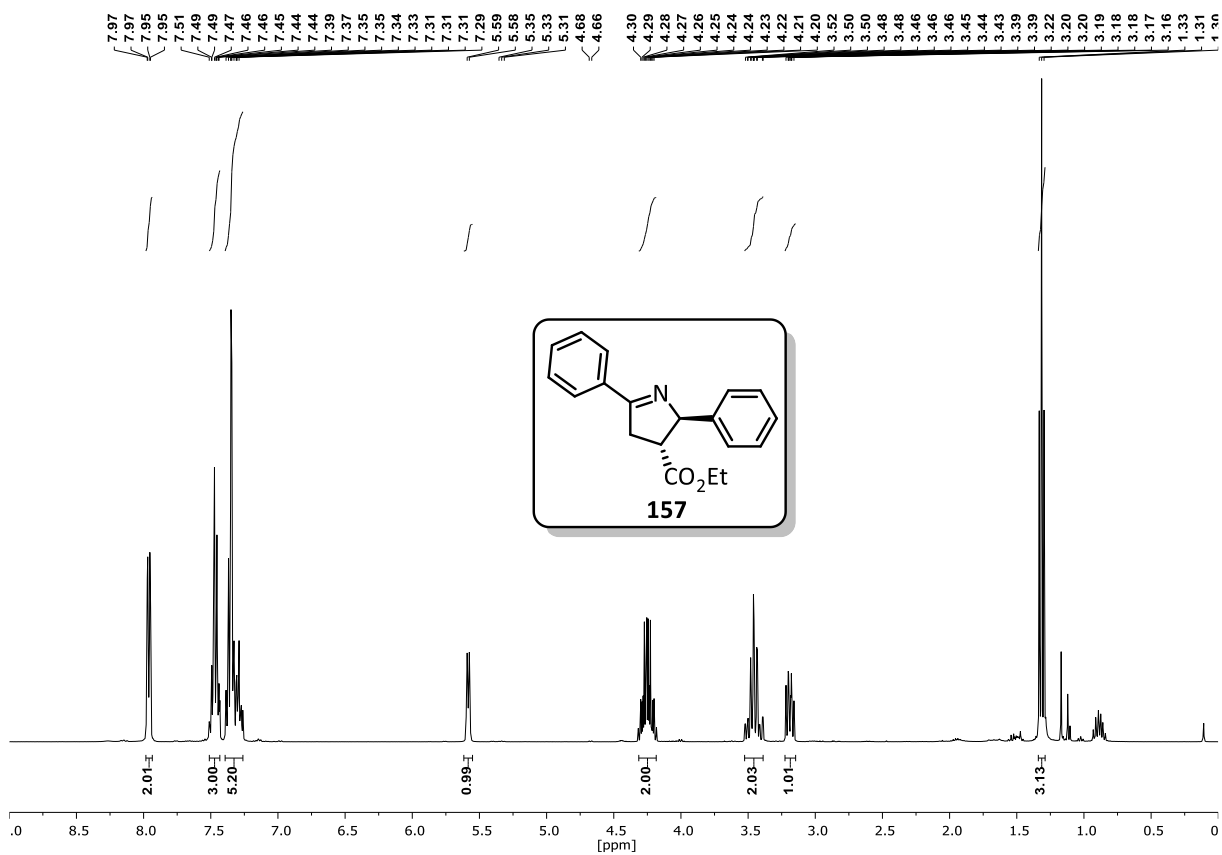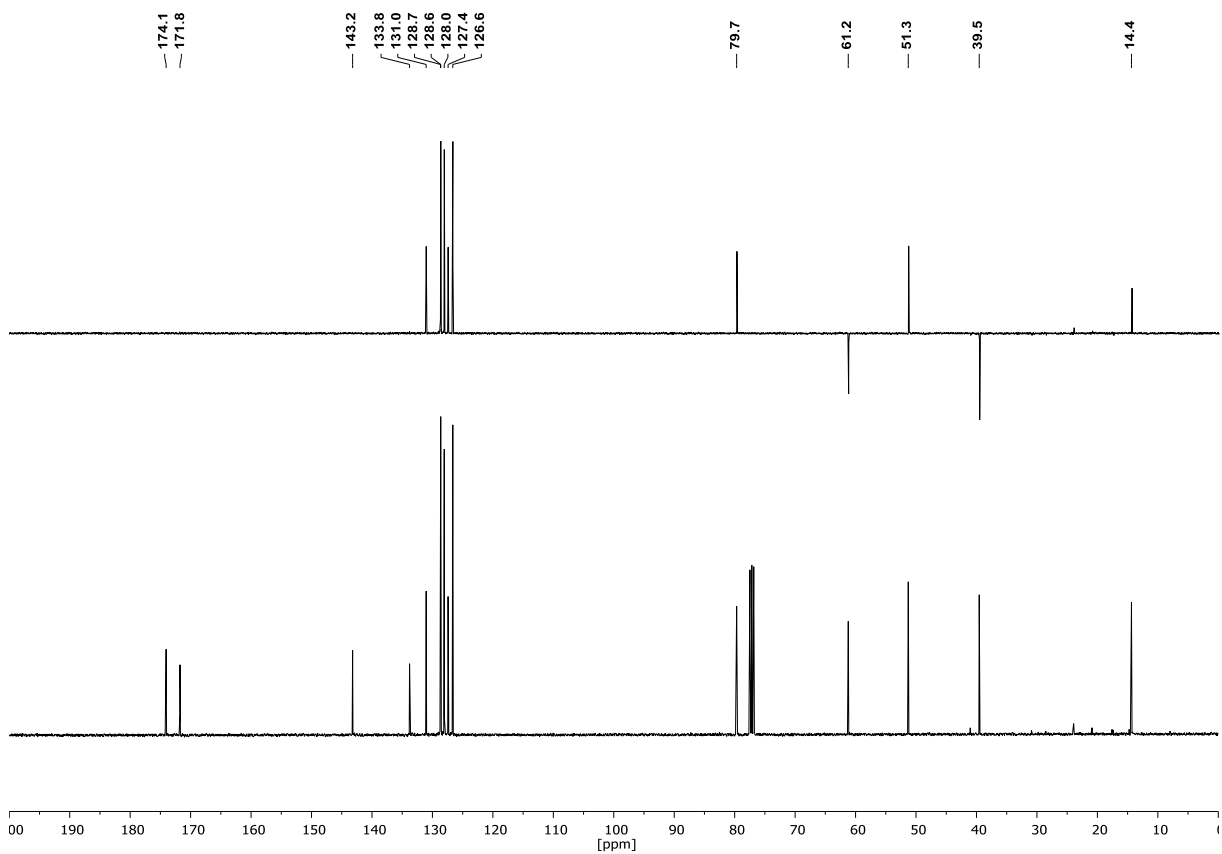
¹³C-NMR (101 MHz, CDCl₃) & **DEPT135** (101 MHz, CDCl₃):
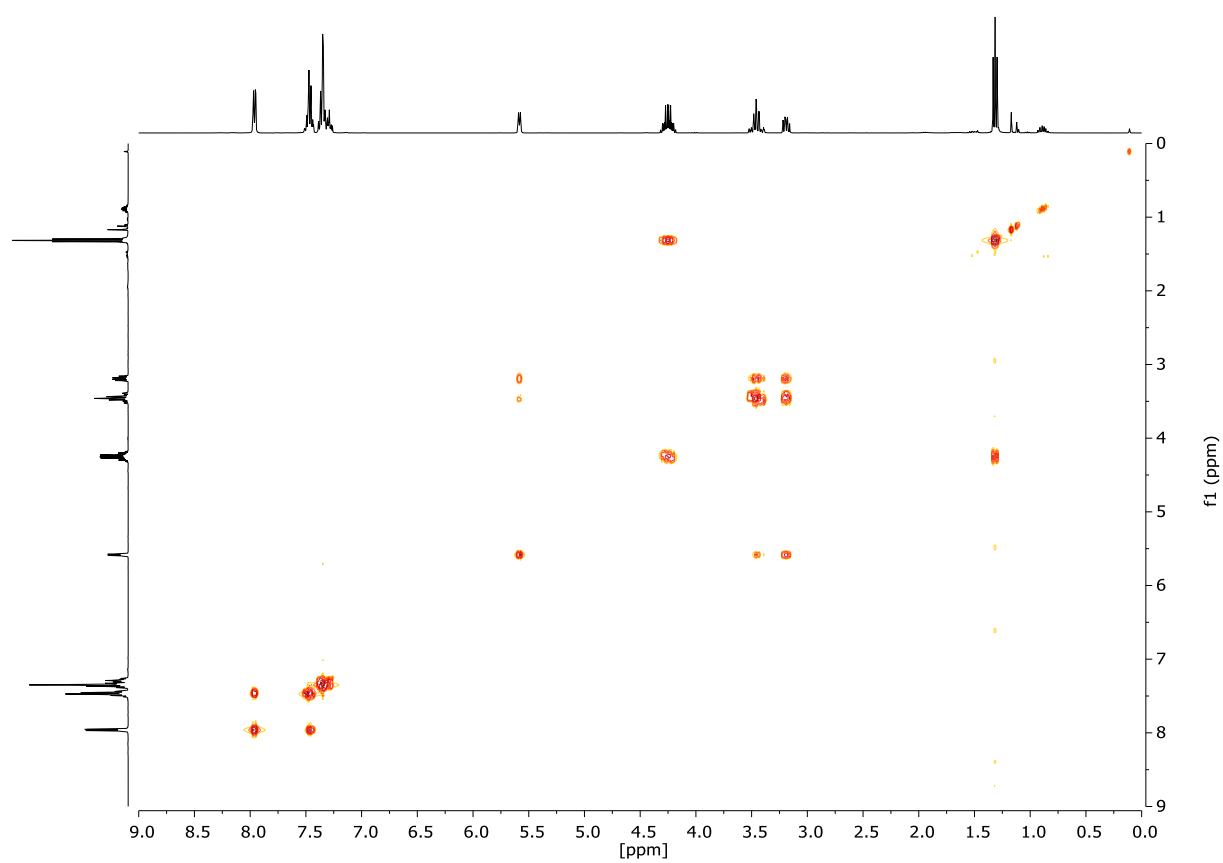
COSY (400 MHz, CDCl$_3$):
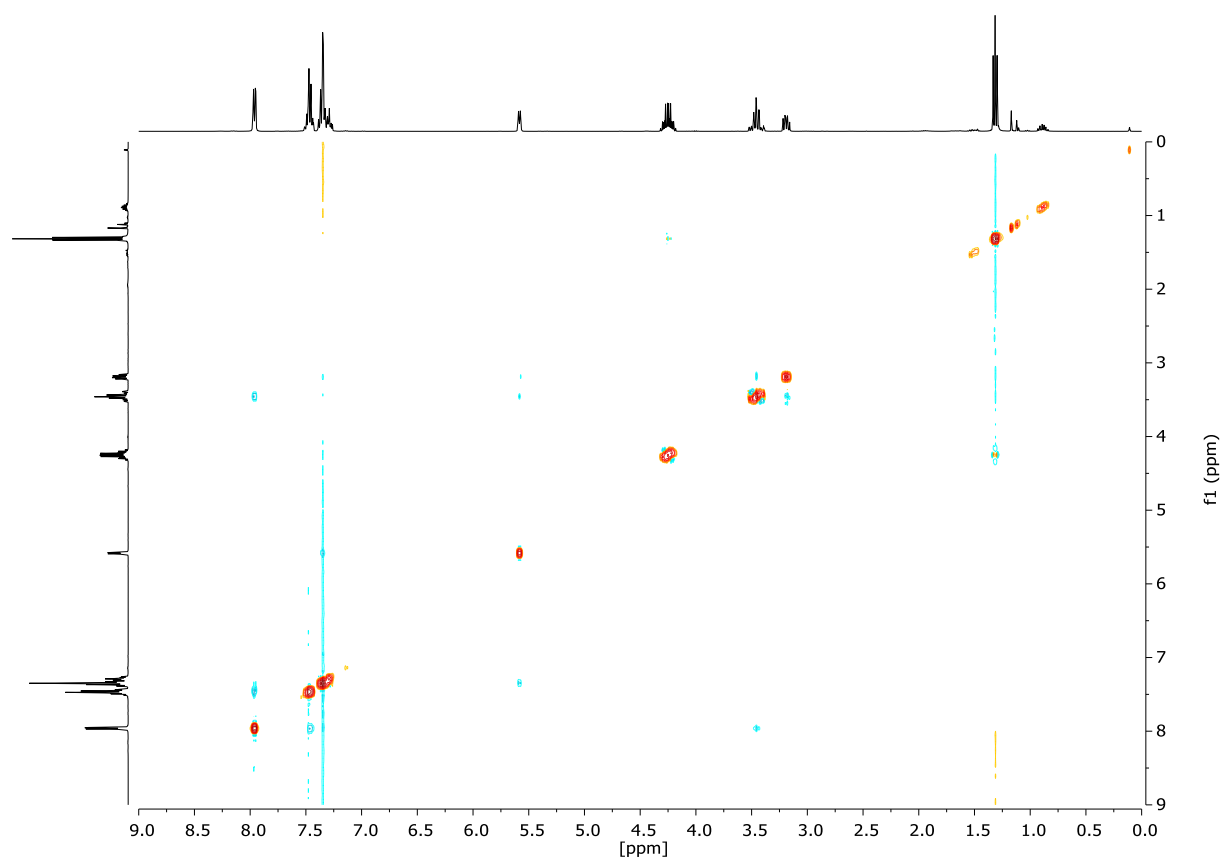
NOESY (400 MHz, CDCl$_3$):

Ethyl 2,5-diphenylpyrrolidine-3-carboxylate (*syn*-158)

¹H-NMR (400 MHz, CDCl₃):
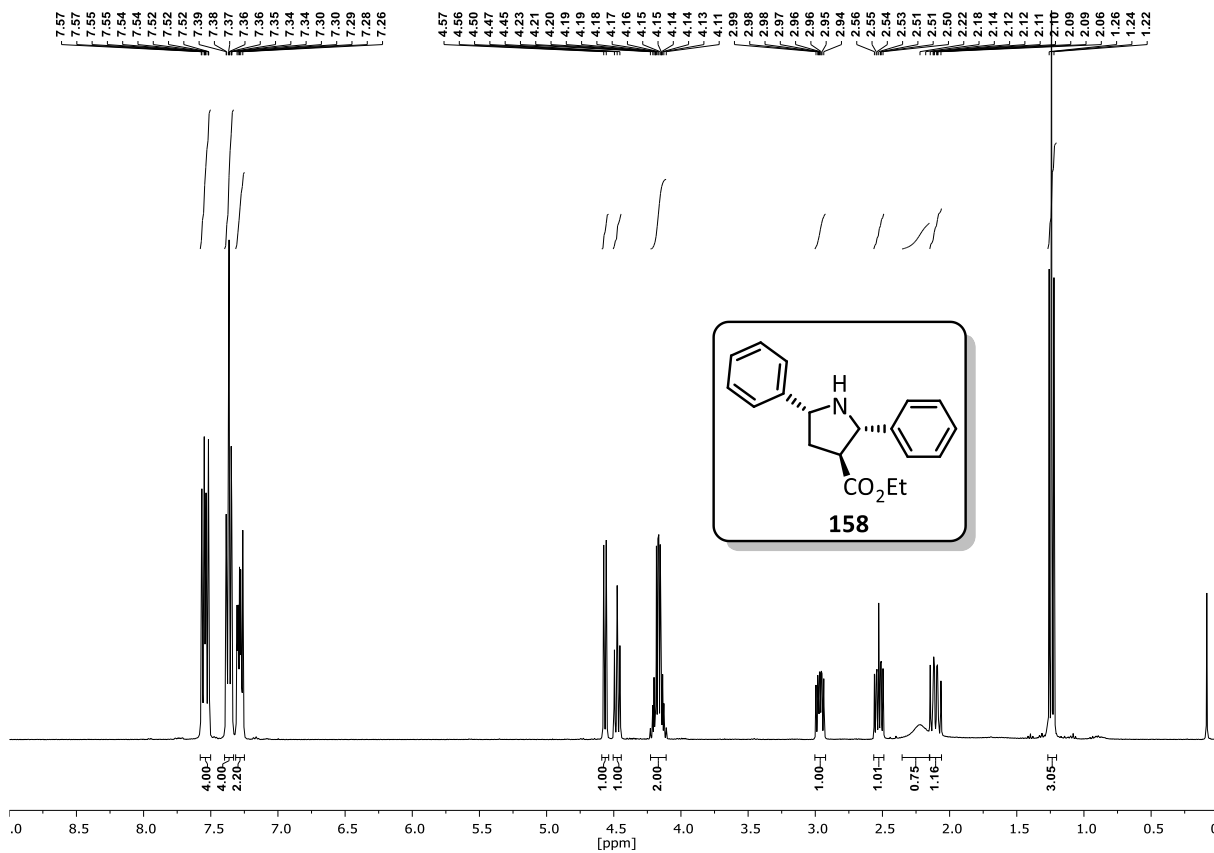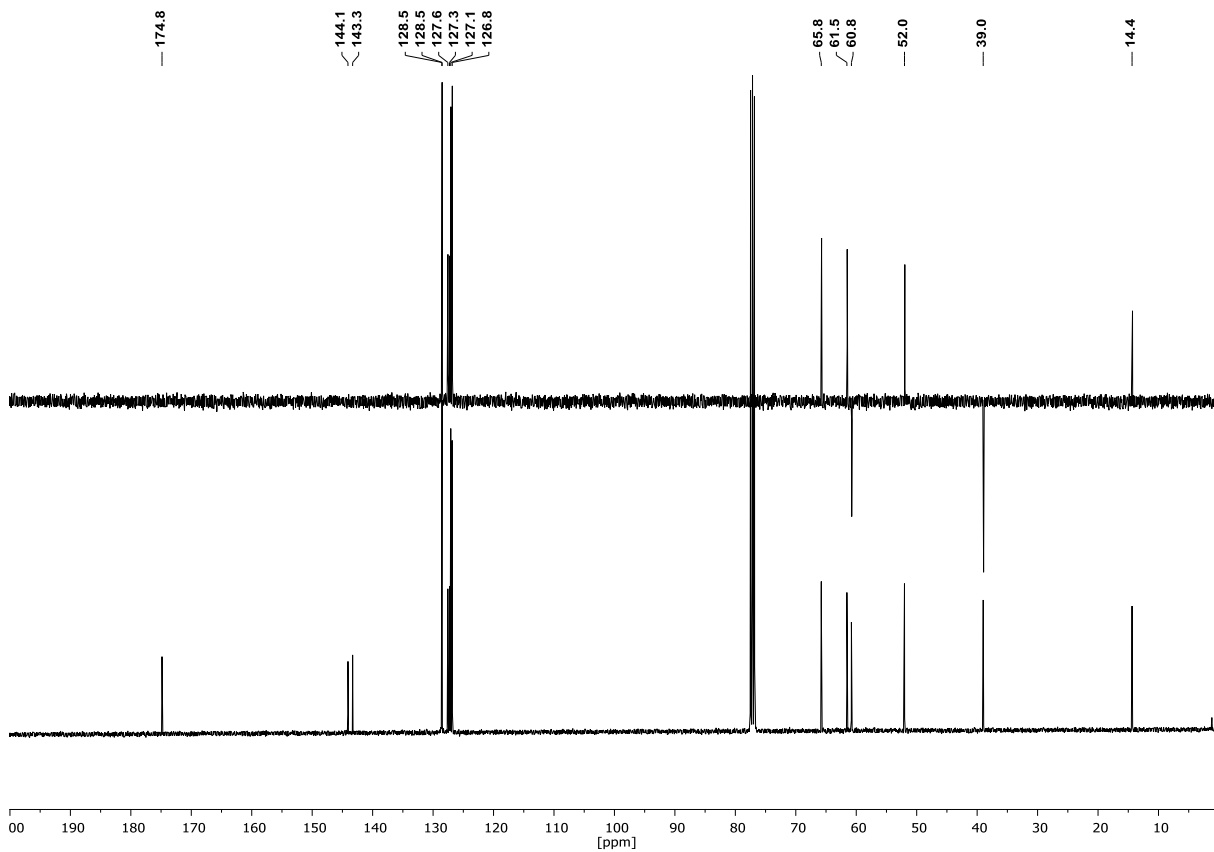
¹³C-NMR (101 MHz, CDCl₃) & **DEPT135** (101 MHz, CDCl₃):
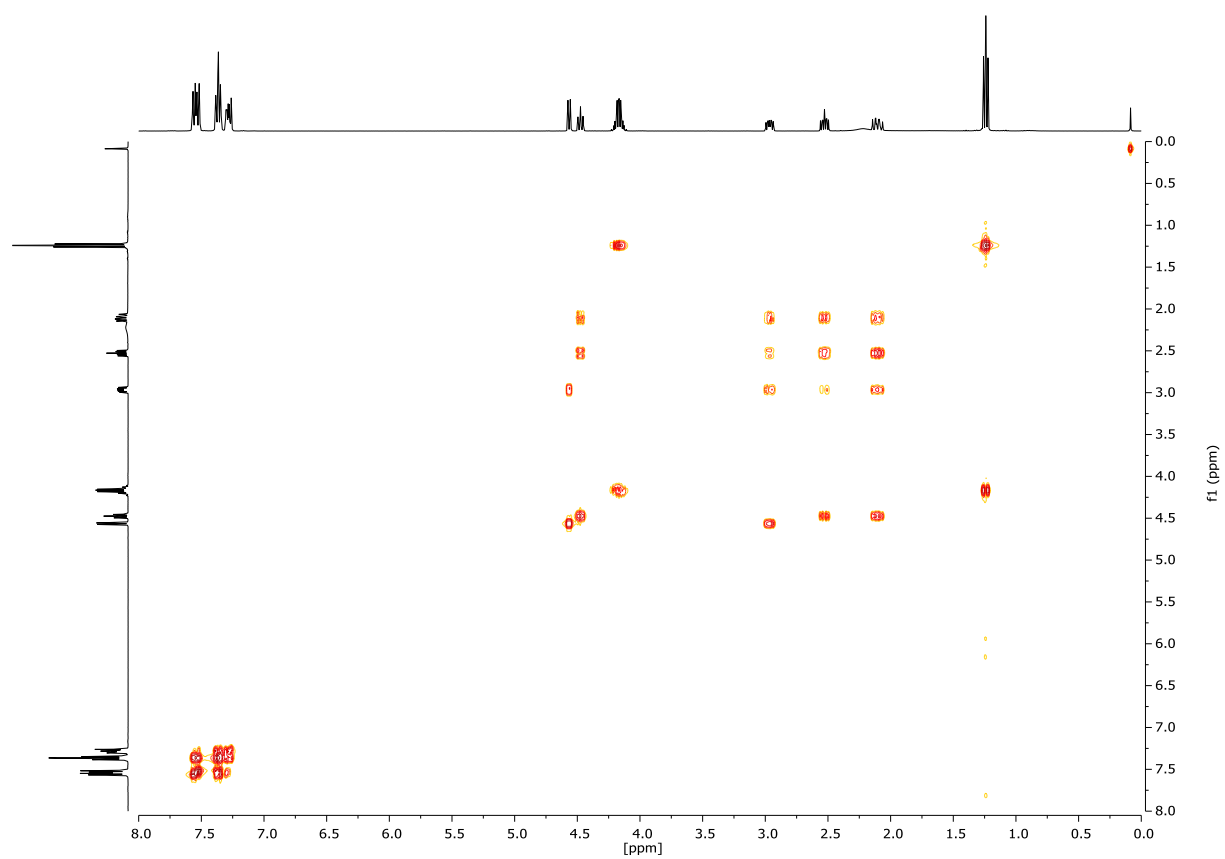
COSY (400 MHz, CDCl$_3$):
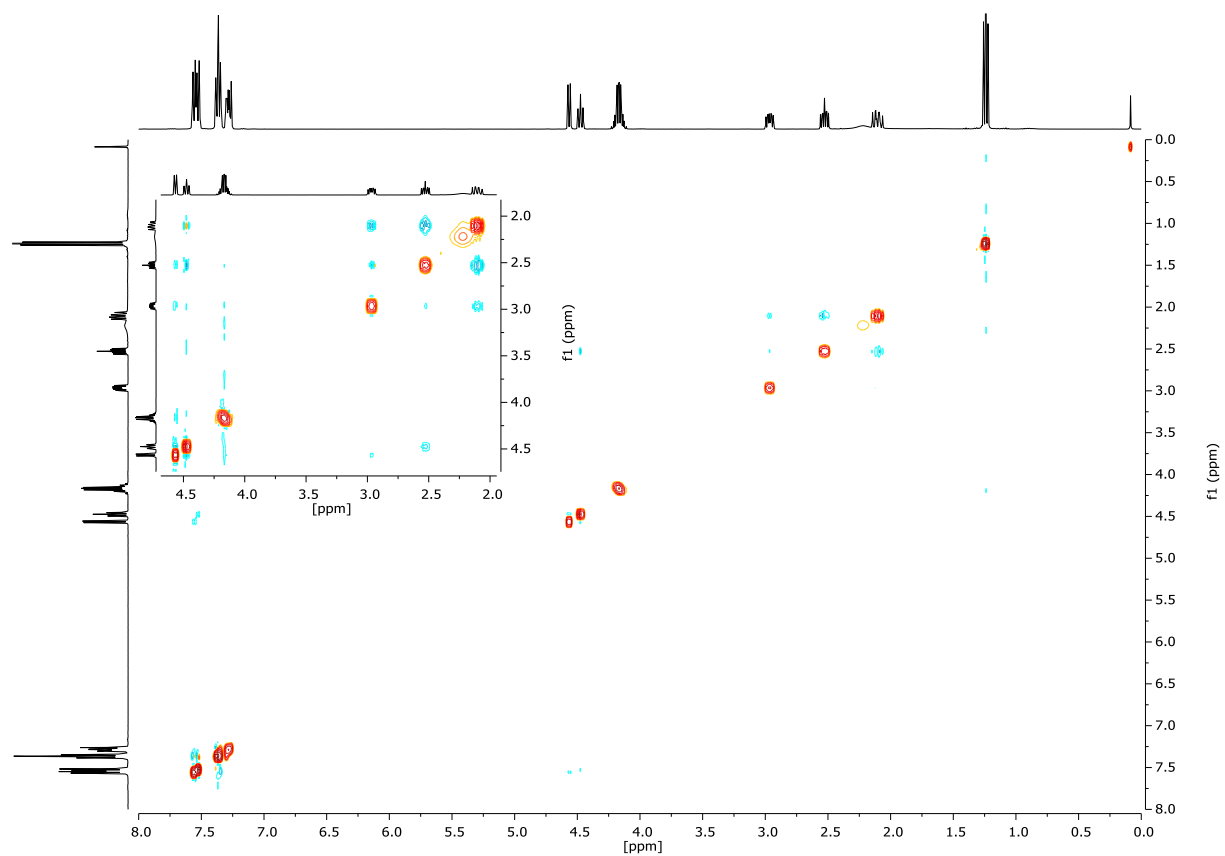
NOESY (400 MHz, CDCl$_3$):

Ethyl 2,5-diphenylpyrrolidine-3-carboxylate (*anti*-158)

¹H-NMR (400 MHz, CDCl₃):
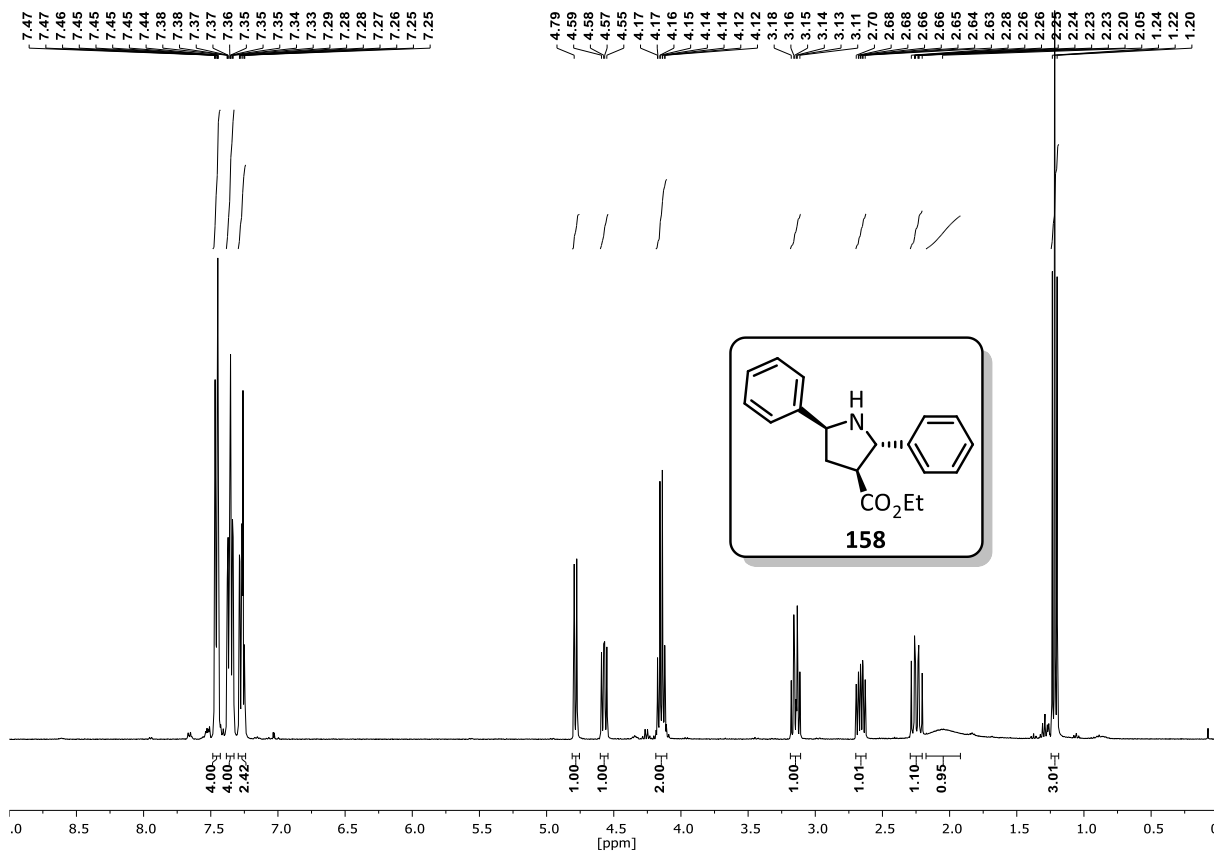
¹³C-NMR (101 MHz, CDCl₃) & **DEPT135** (101 MHz, CDCl₃):
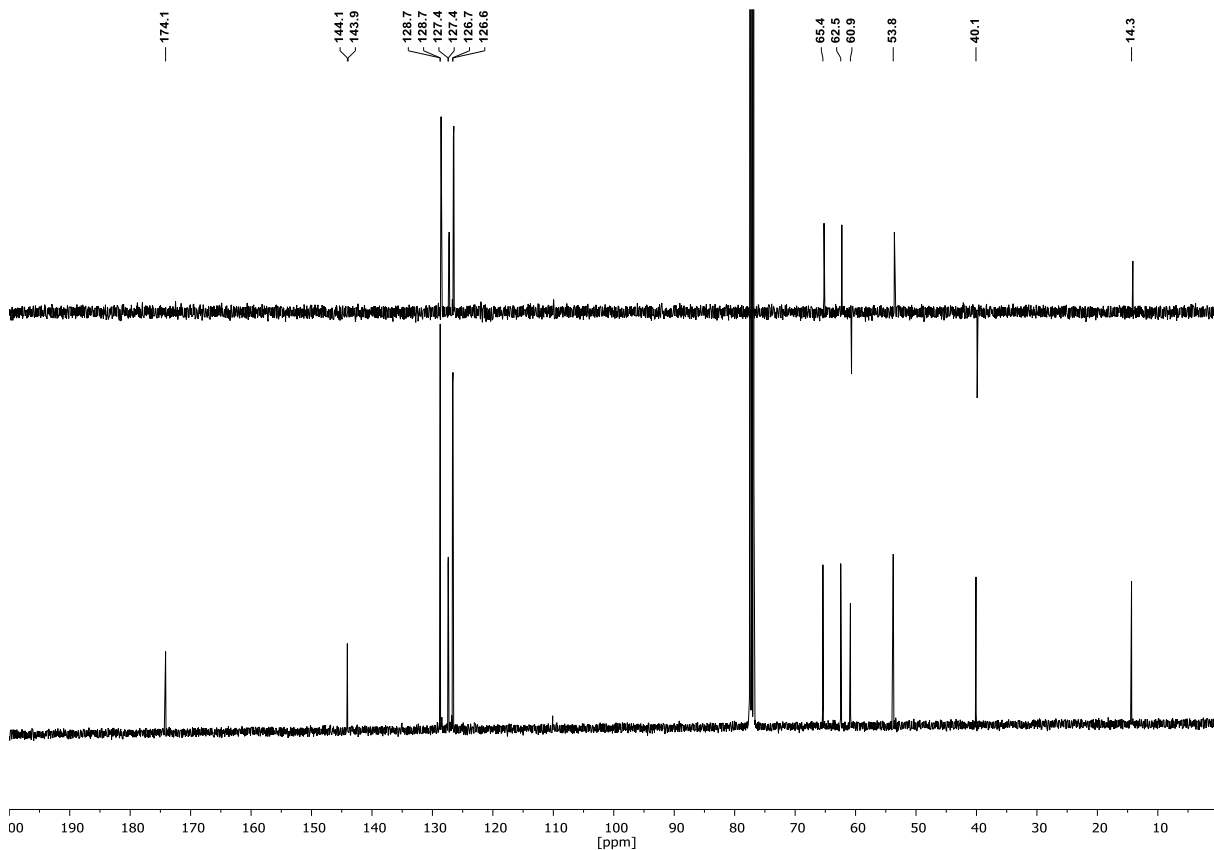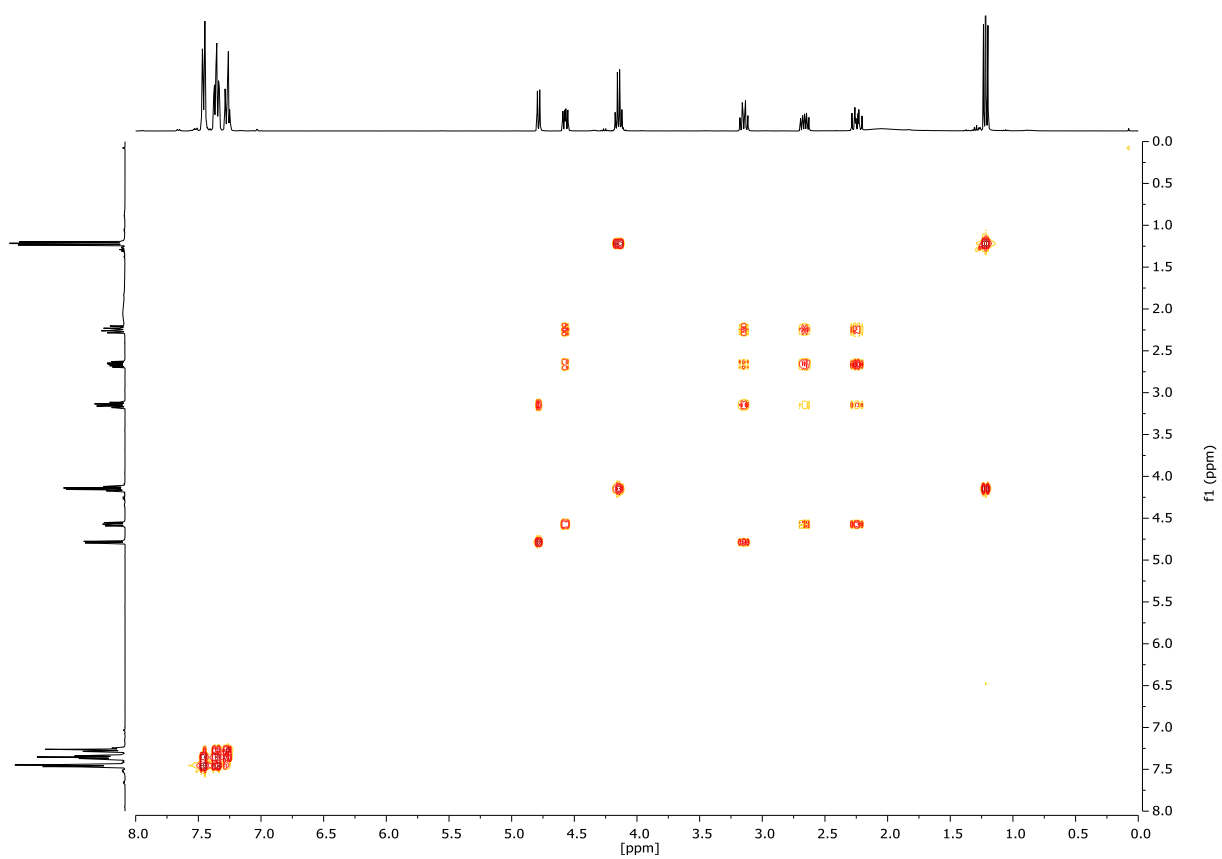
COSY (400 MHz, CDCl$_3$):
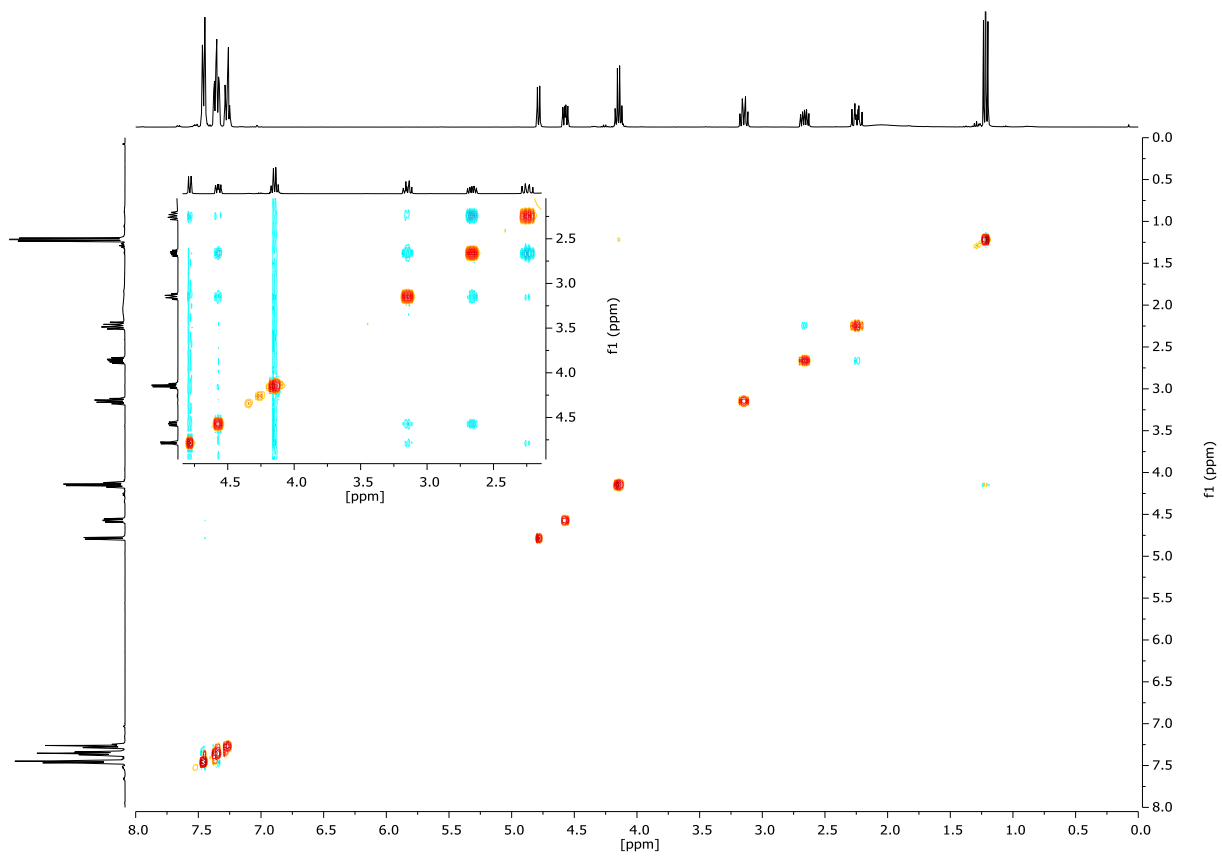
NOESY (400 MHz, CDCl$_3$):

Diethyl 3,4-bis(4-methoxyphenyl)cyclobutane-1,2-dicarboxylate (185e/186e)

¹H-NMR (400 MHz, CDCl₃, *trans* diastereomer):
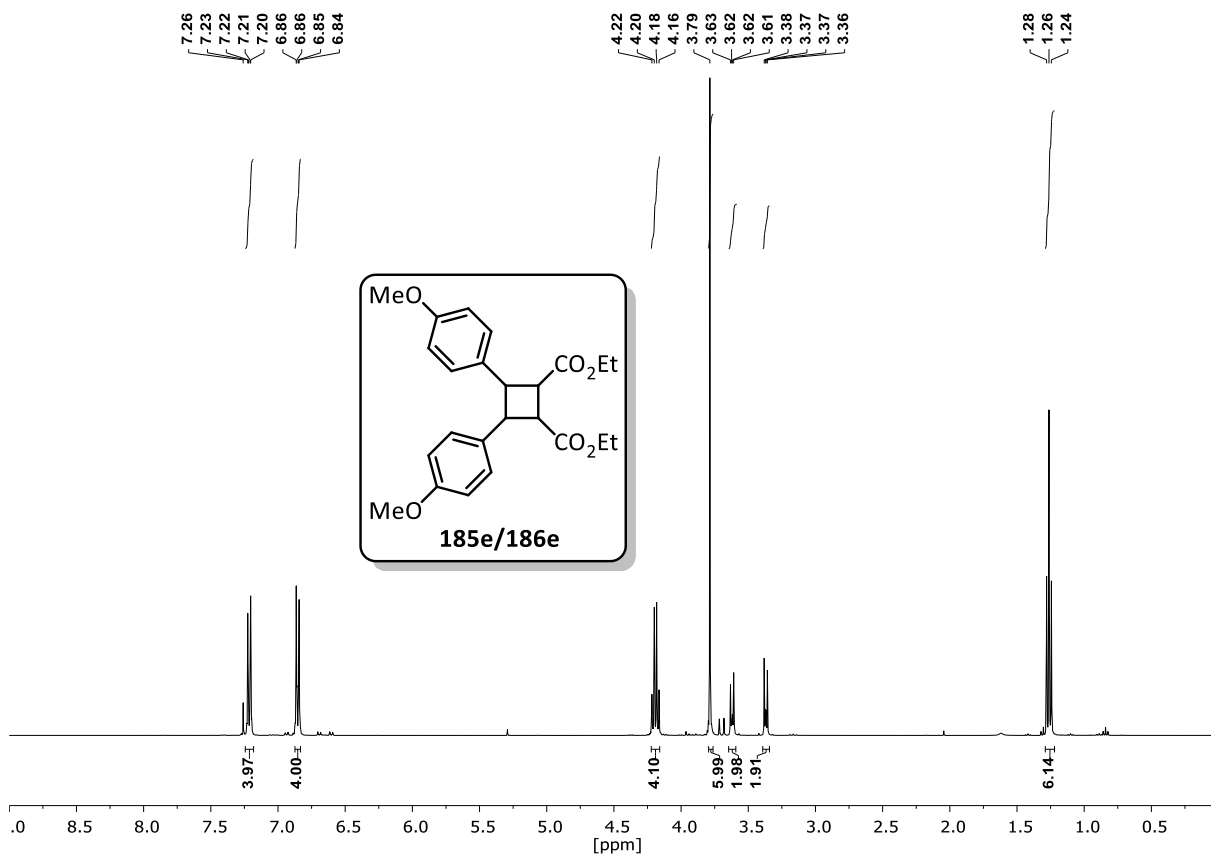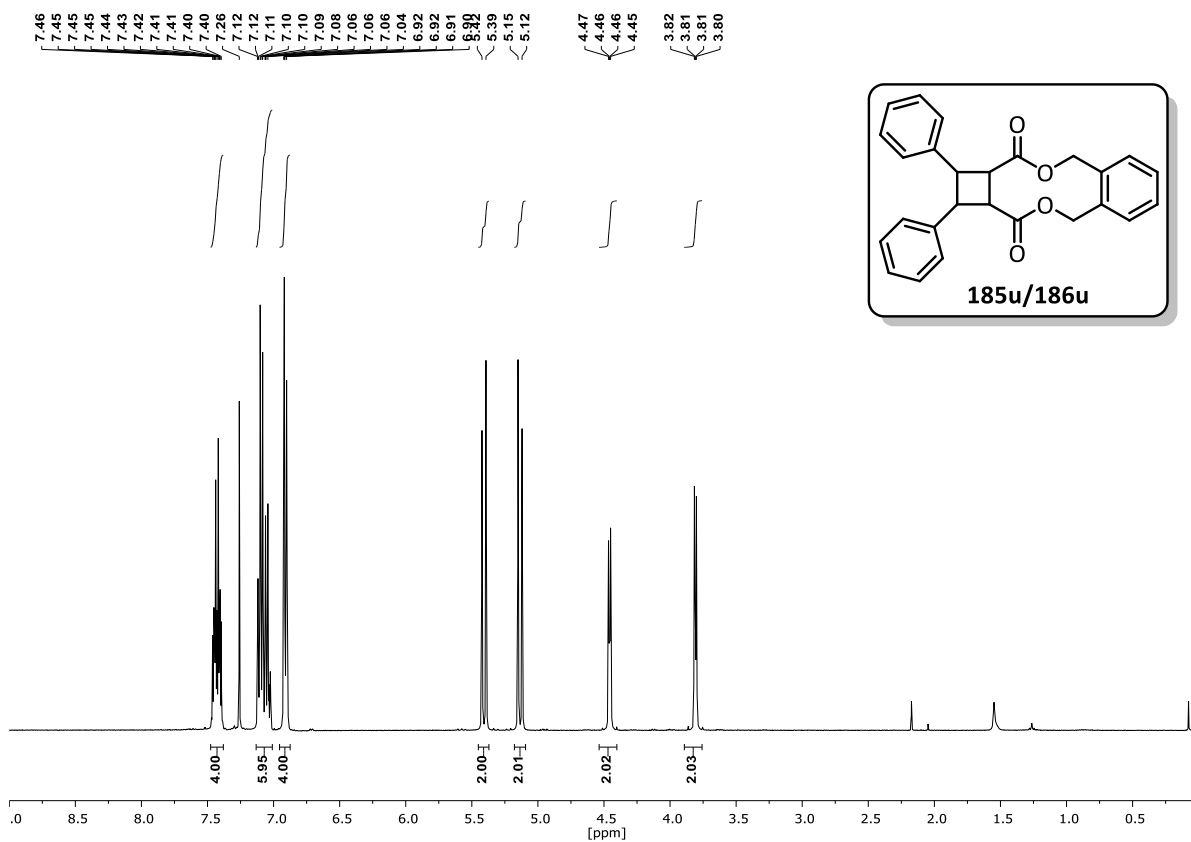

¹H-NMR (400 MHz, CDCl₃, mixture of diastereomers):
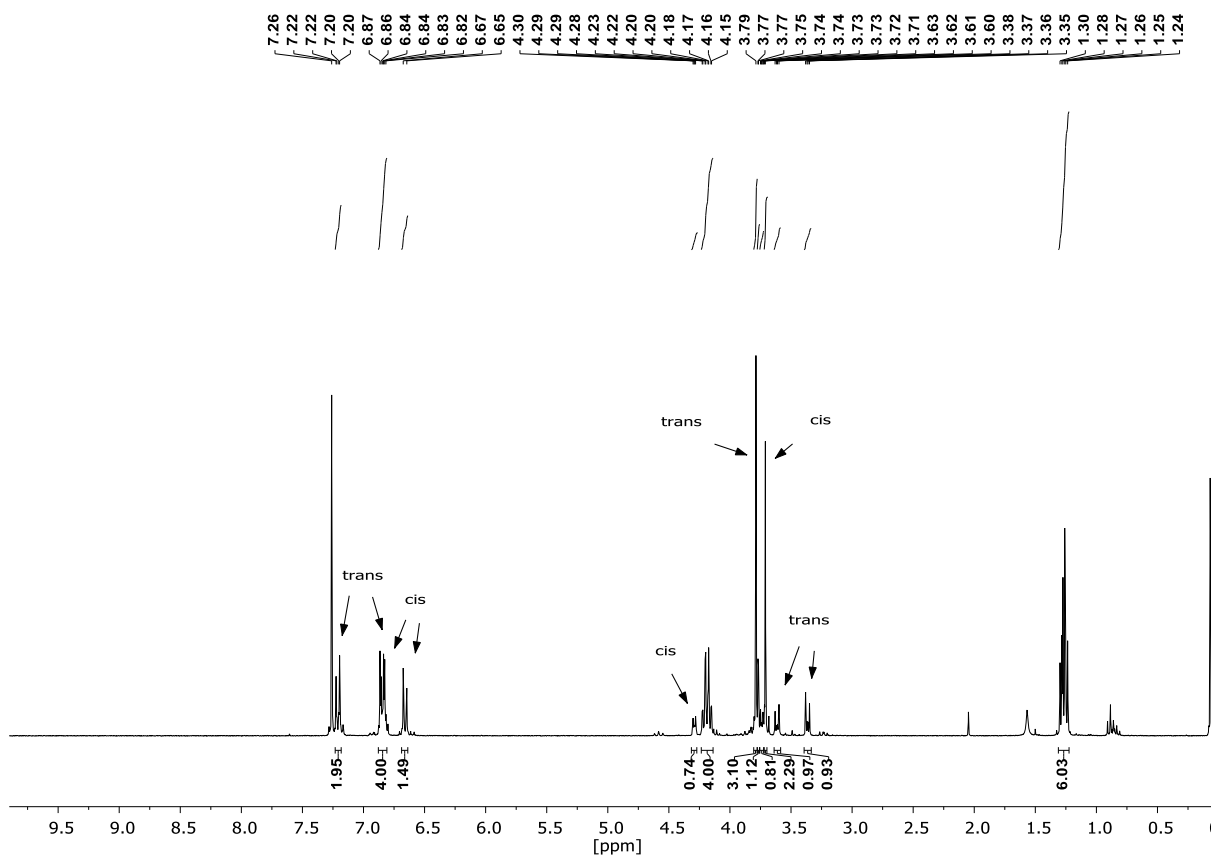
13C-NMR (101 MHz, CDCl₃) & **DEPT135** (101 MHz, CDCl₃):
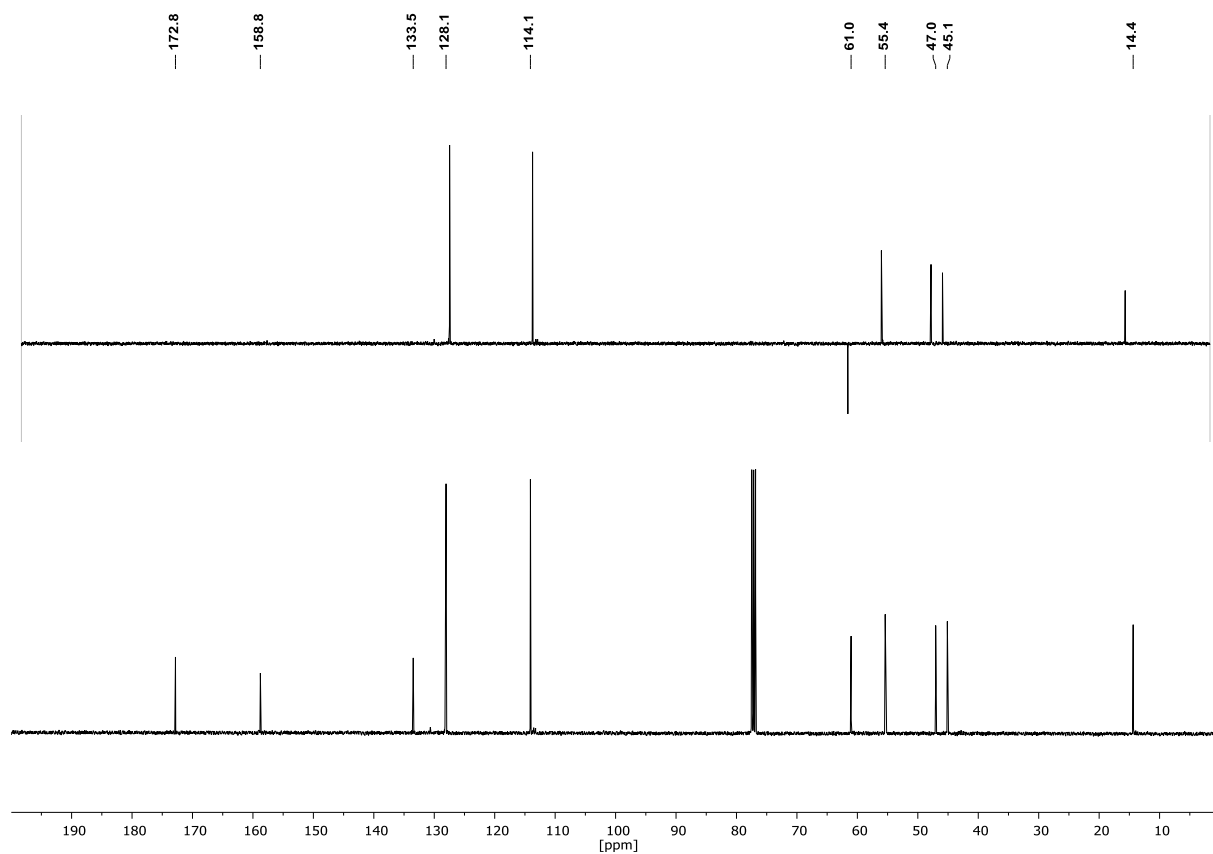
Diethyl 3,4-bis(4-cyanophenyl)cyclobutane-1,2-dicarboxylate (185h/186h)

1H-NMR (400 MHz, CDCl₃, *trans* diastereomer):
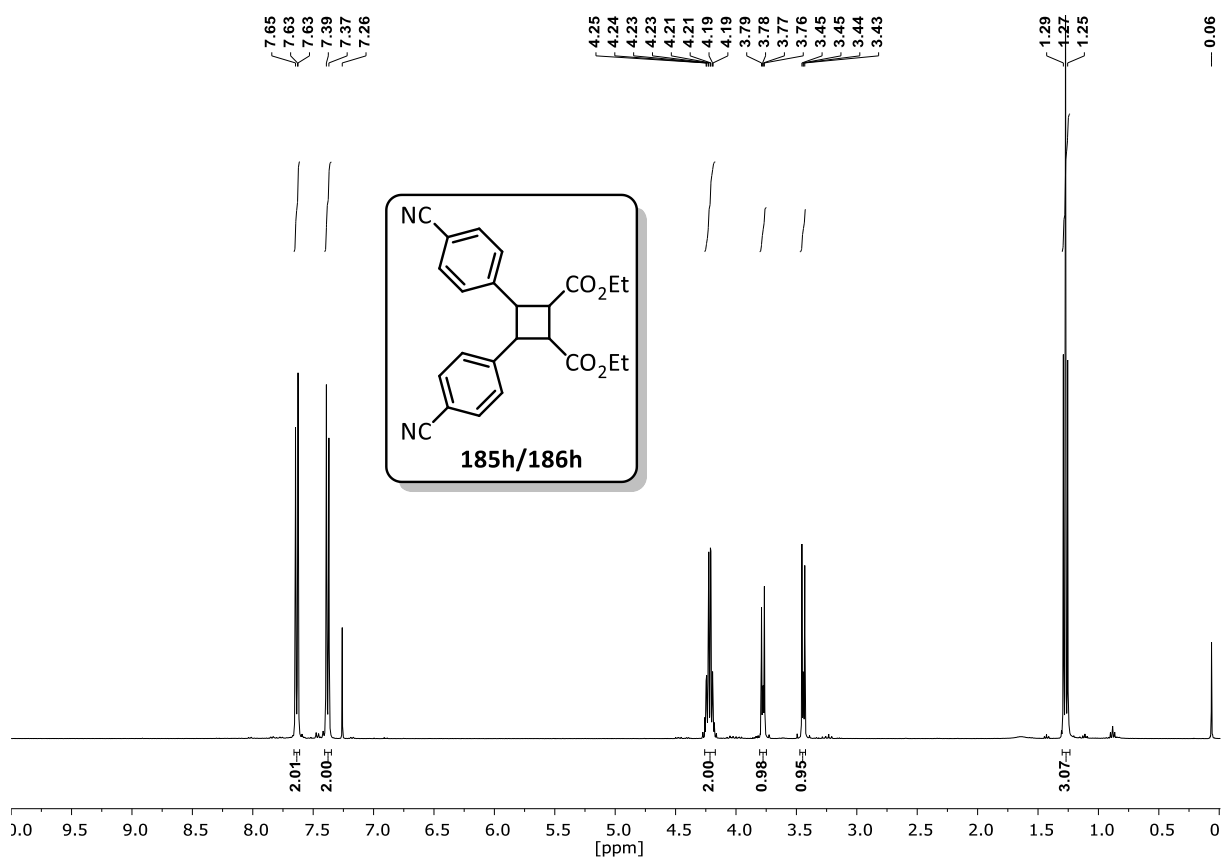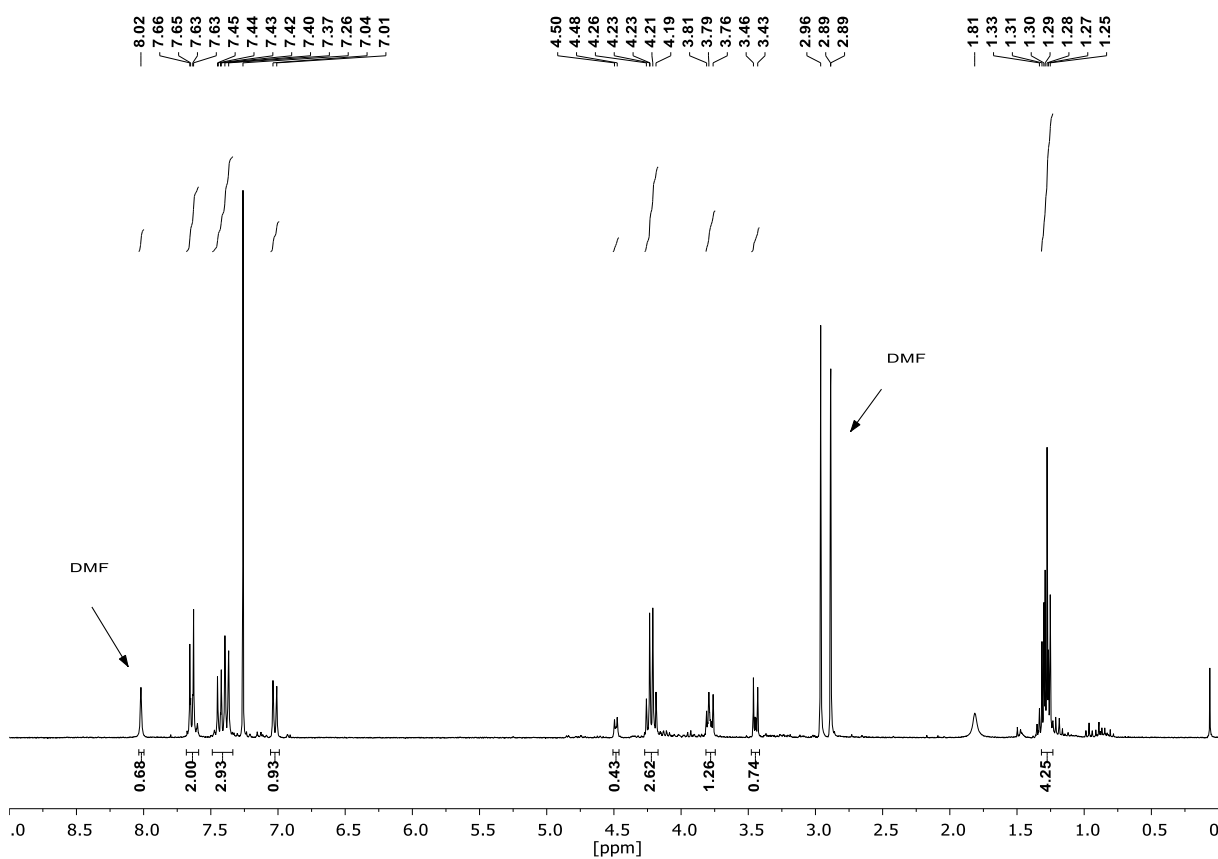
¹H-NMR (400 MHz, CDCl₃, mixture of diastereomers):

¹³C-NMR (101 MHz, CDCl₃) & **DEPT135** (101 MHz, CDCl₃):
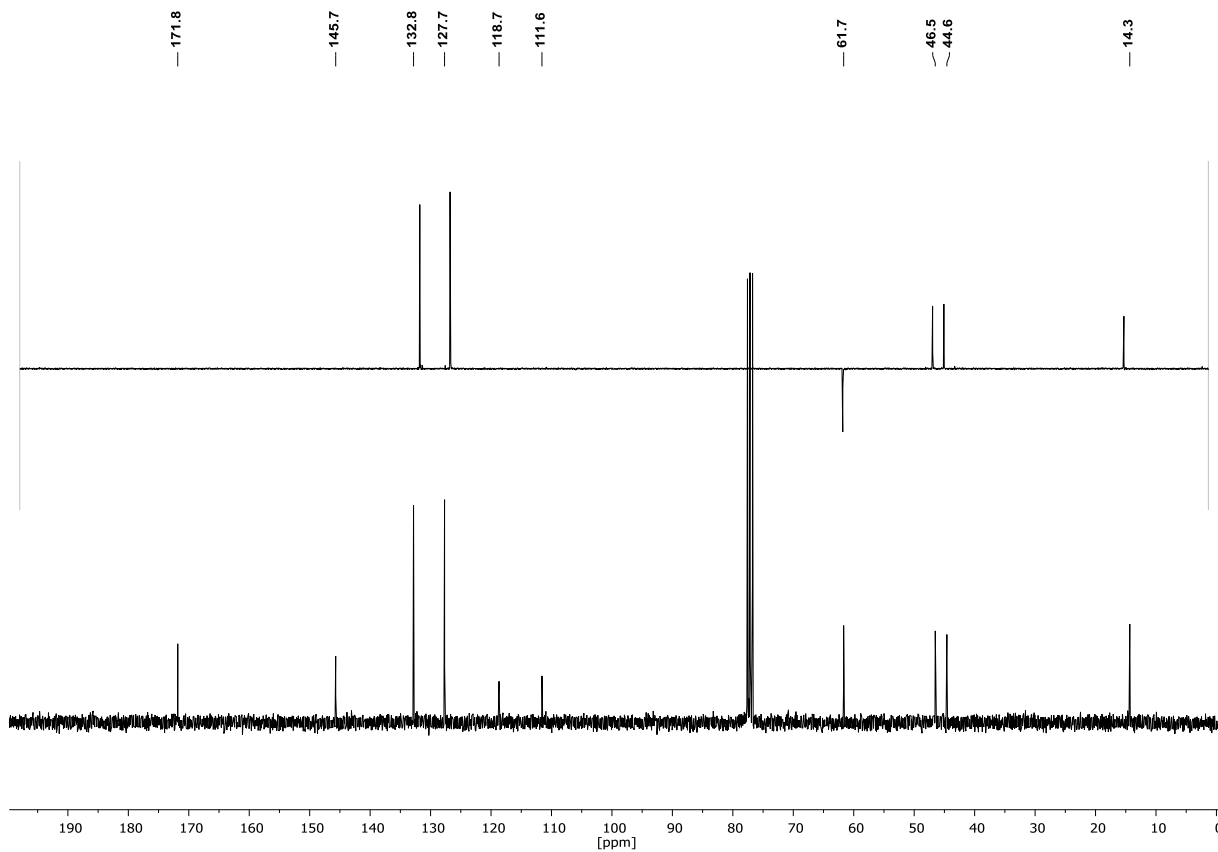
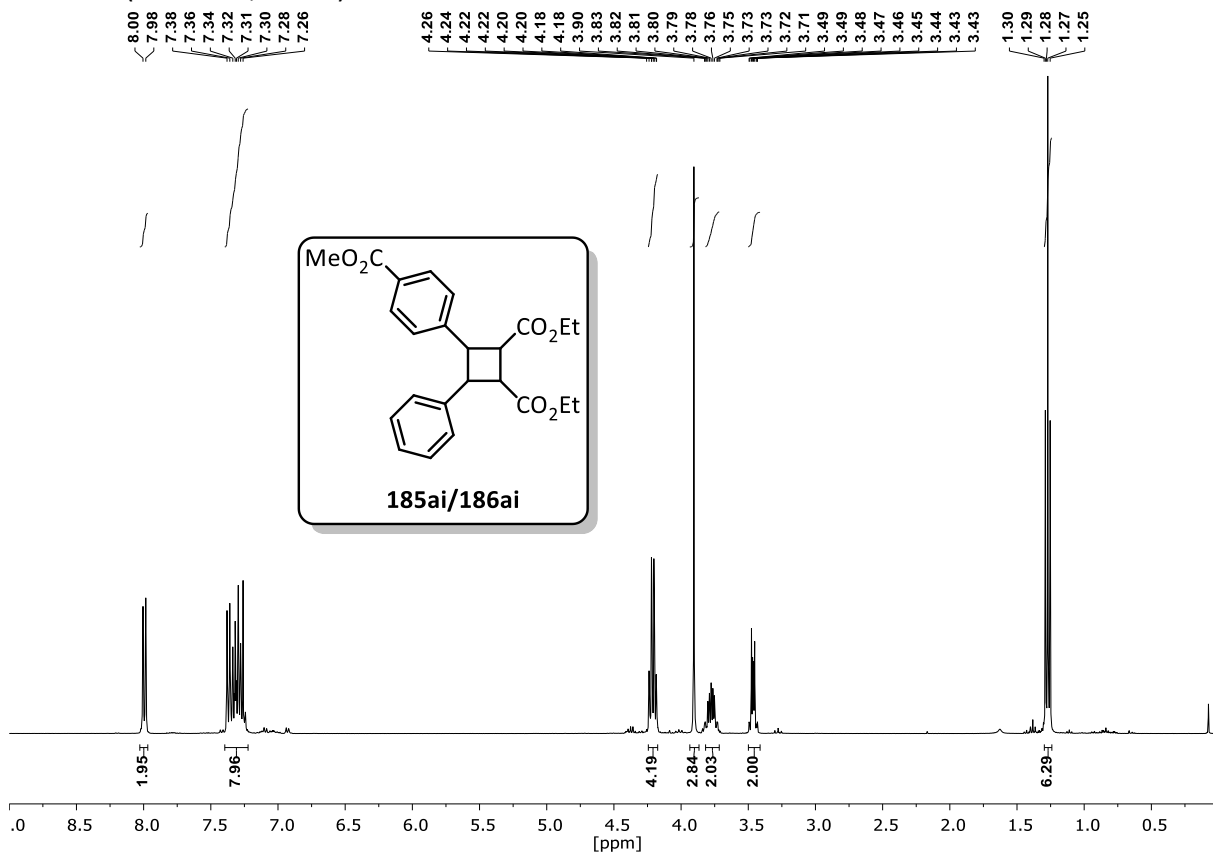## Diethyl 3,4-bis(4-(methoxycarbonyl)phenyl)cyclobutane-1,2-dicarboxylate (185i/186i)

^{1}H-NMR (300 MHz, CDCl$_3$, *trans* diastereomer):
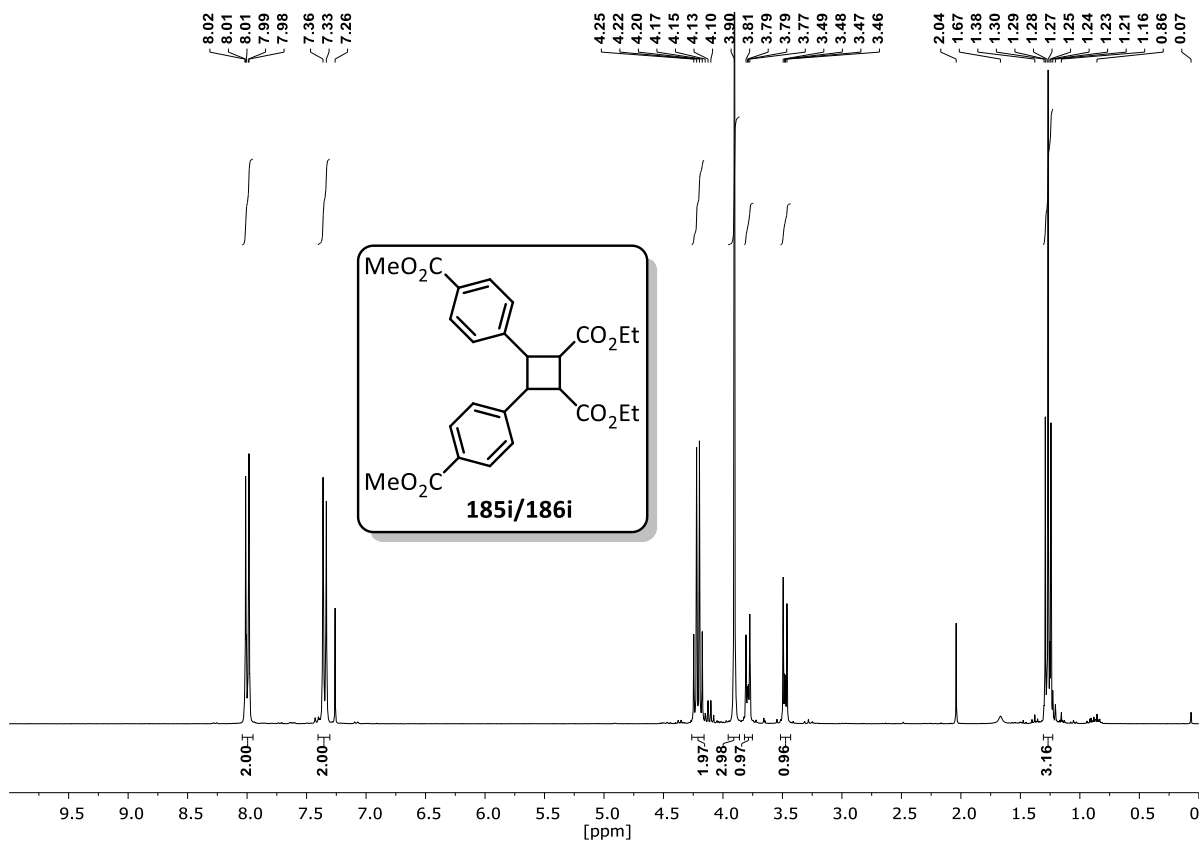
^{1}H-NMR (300 MHz, CDCl$_3$, *cis* diastereomer):
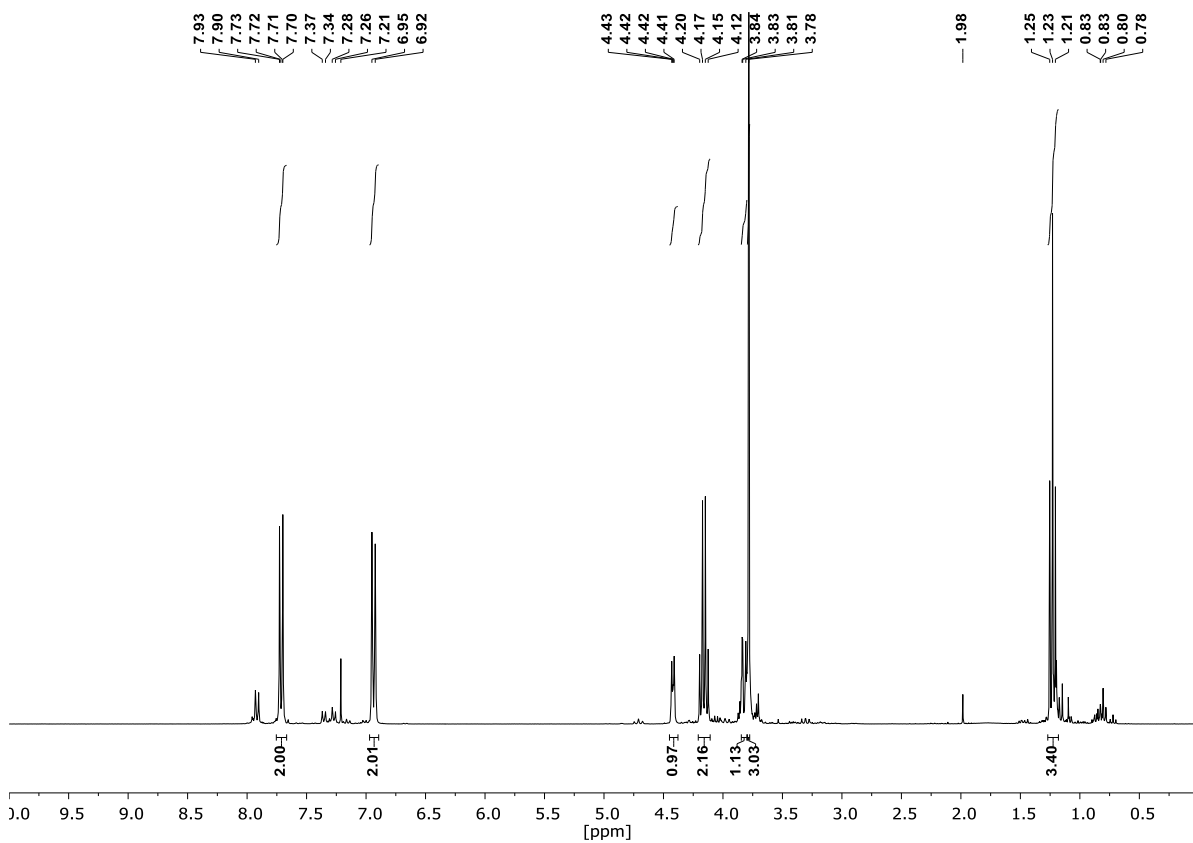
13C-NMR (75 MHz, CDCl₃) & **DEPT135** (75 MHz, CDCl₃):
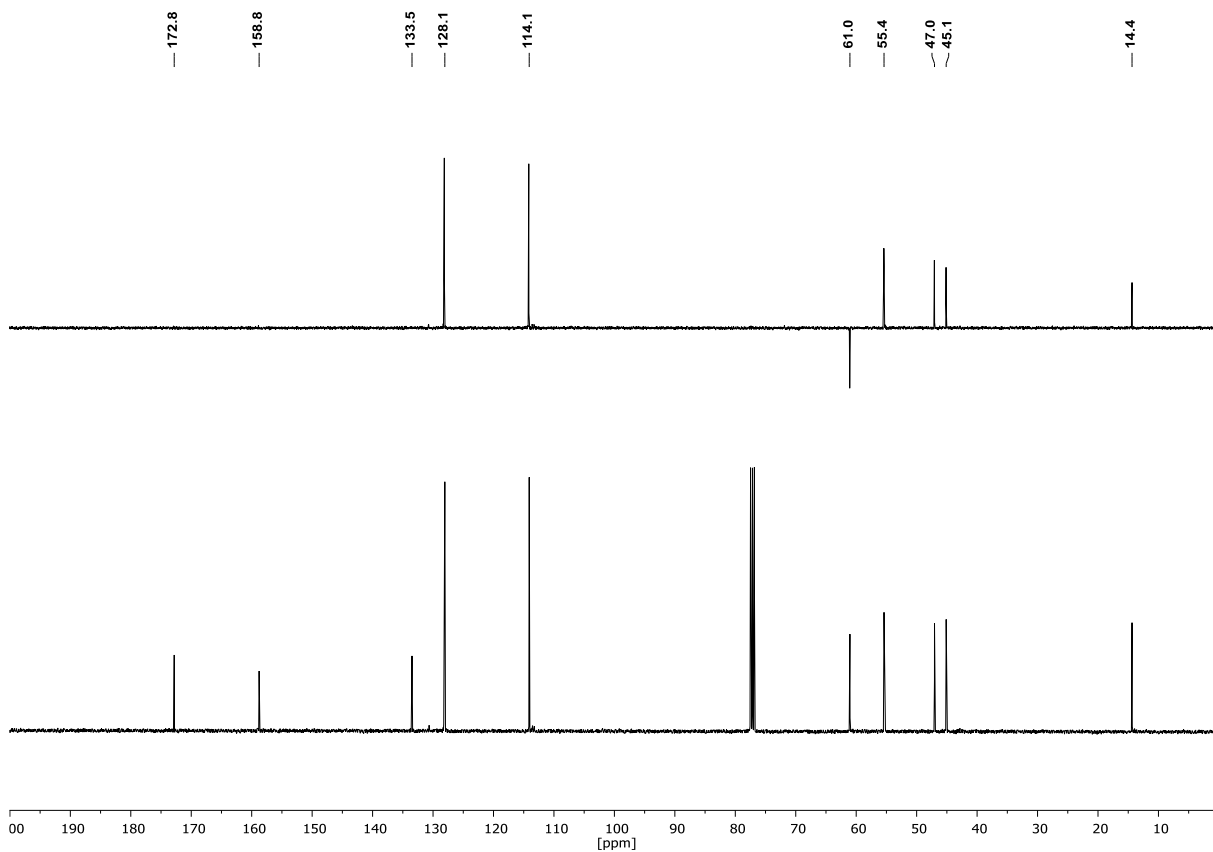
Diethyl 3,4-bis(4-nitrophenyl)cyclobutane-1,2-dicarboxylate (185j/186j)

¹H-NMR (400 MHz, CDCl₃, *trans* diastereomer):
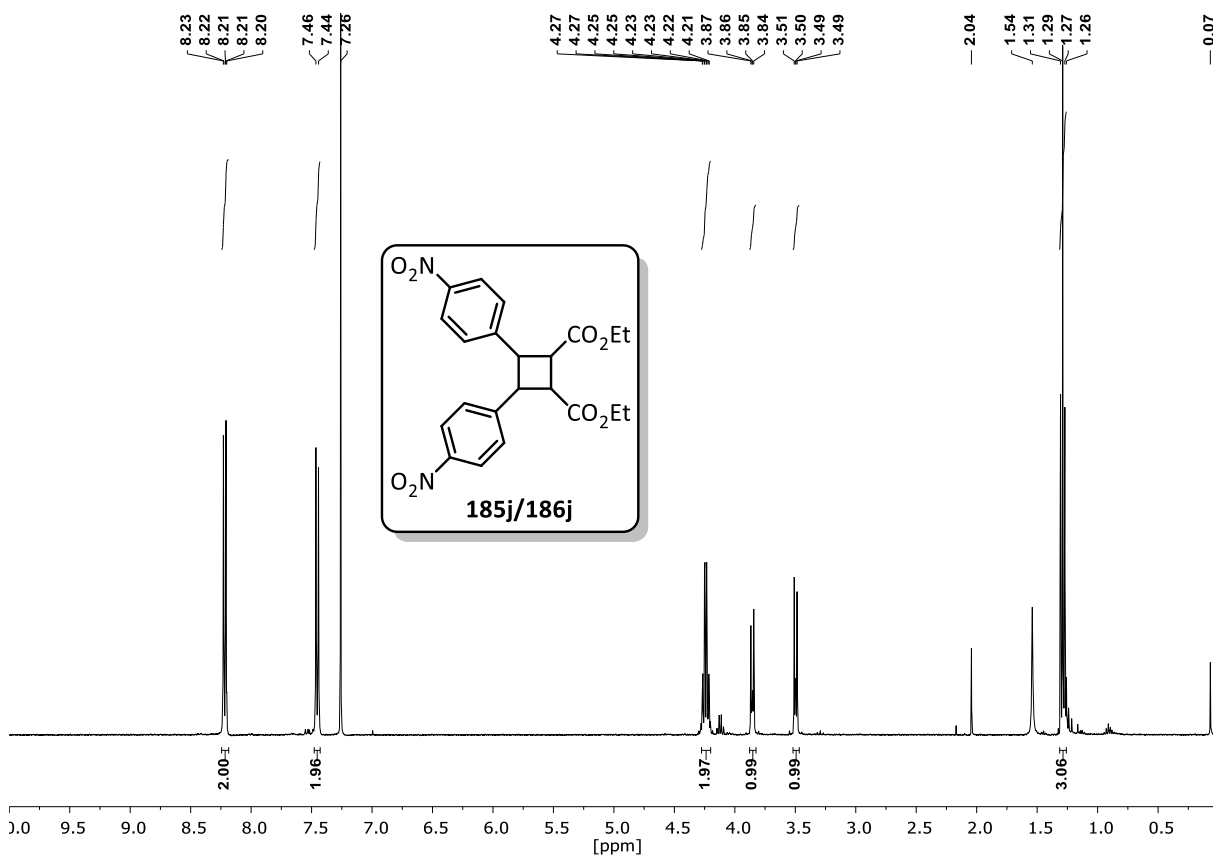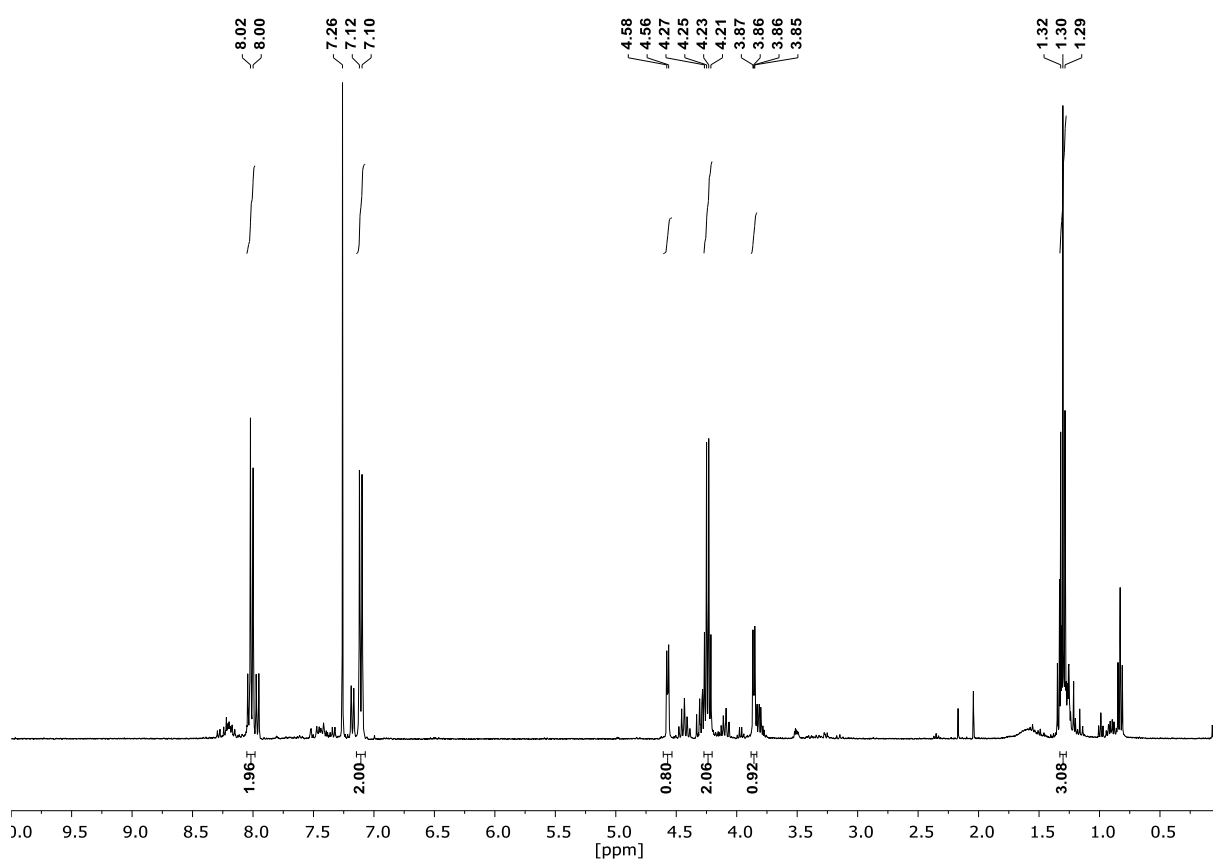
¹H-NMR (400 MHz, CDCl₃, *cis* diastereomer):

8.02
8.00
7.26
7.12
7.10
4.58
4.56
4.27
4.25
4.23
4.21
3.87
3.86
3.85
1.32
1.30
1.29

1.96
2.00
0.80
2.06
0.92
3.08

).0 9.5 9.0 8.5 8.0 7.5 7.0 6.5 6.0 5.5 5.0 4.5 4.0 3.5 3.0 2.5 2.0 1.5 1.0 0.5
[ppm]

¹³C-NMR (101 MHz, CDCl₃) & **DEPT135** (101 MHz, CDCl₃):

171.7
147.6
147.4
127.8
124.3
61.7
46.5
44.7
14.3

00 190 180 170 160 150 140 130 120 110 100 90 80 70 60 50 40 30 20 10
[ppm]
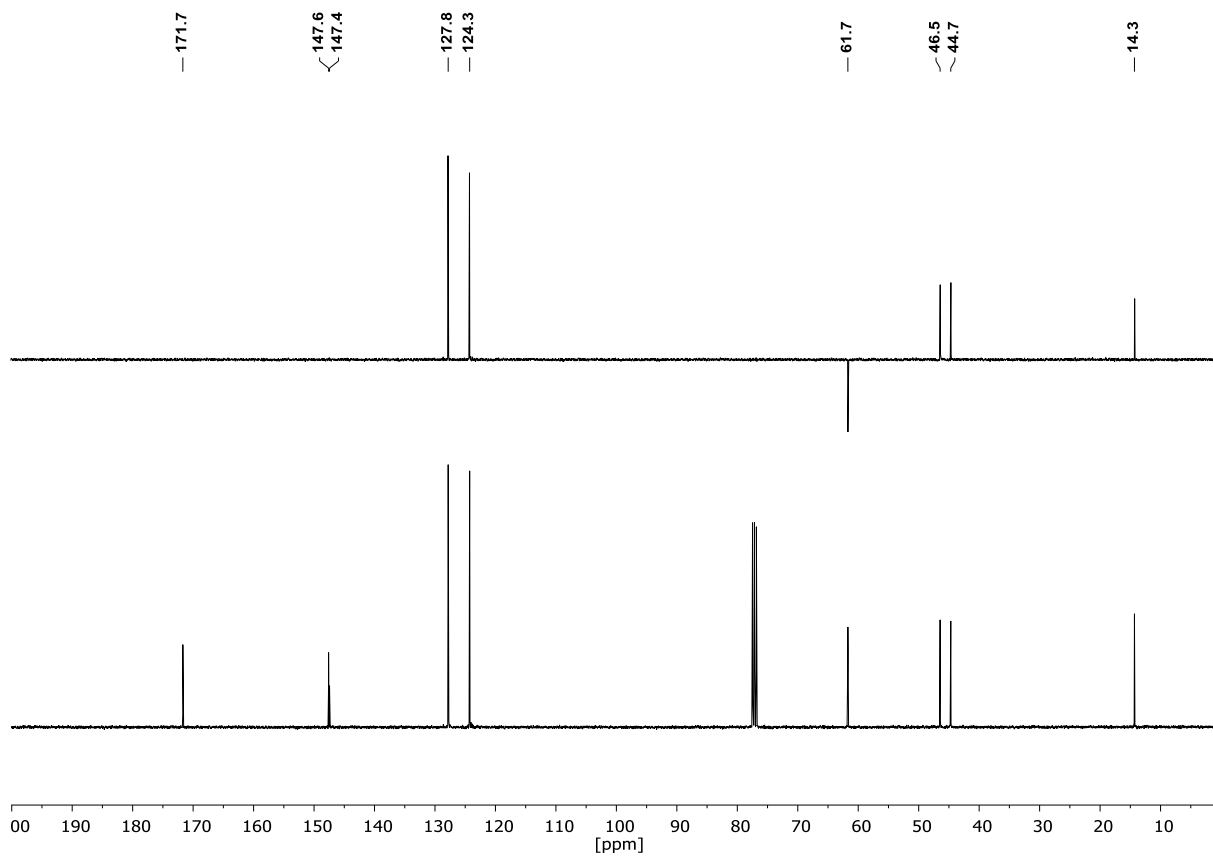
Diethyl 3,4-di(furan-2-yl)cyclobutane-1,2-dicarboxylate (185q/186q)

^{1}H-NMR (400 MHz, CDCl$_3$, *trans* diastereomer):
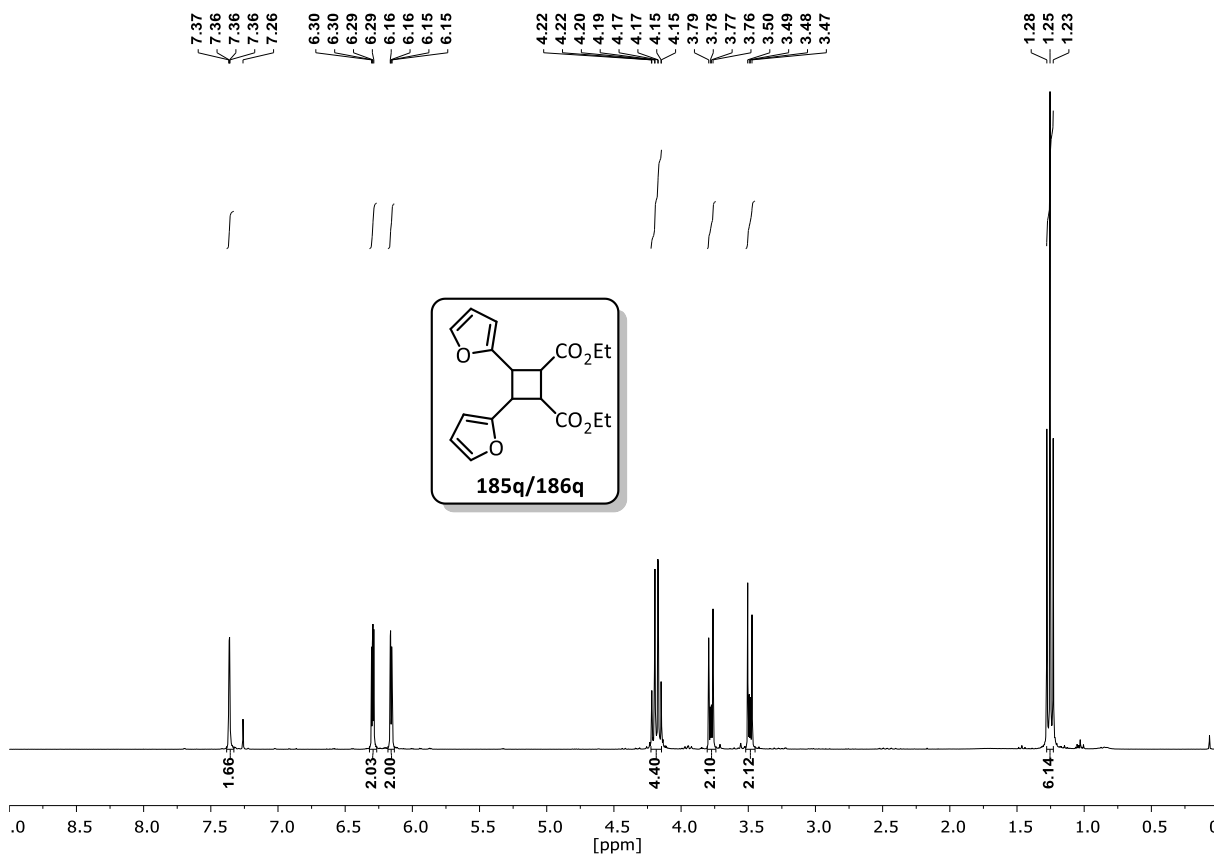
^{1}H-NMR (400 MHz, CDCl$_3$, mixture of diastereomers):
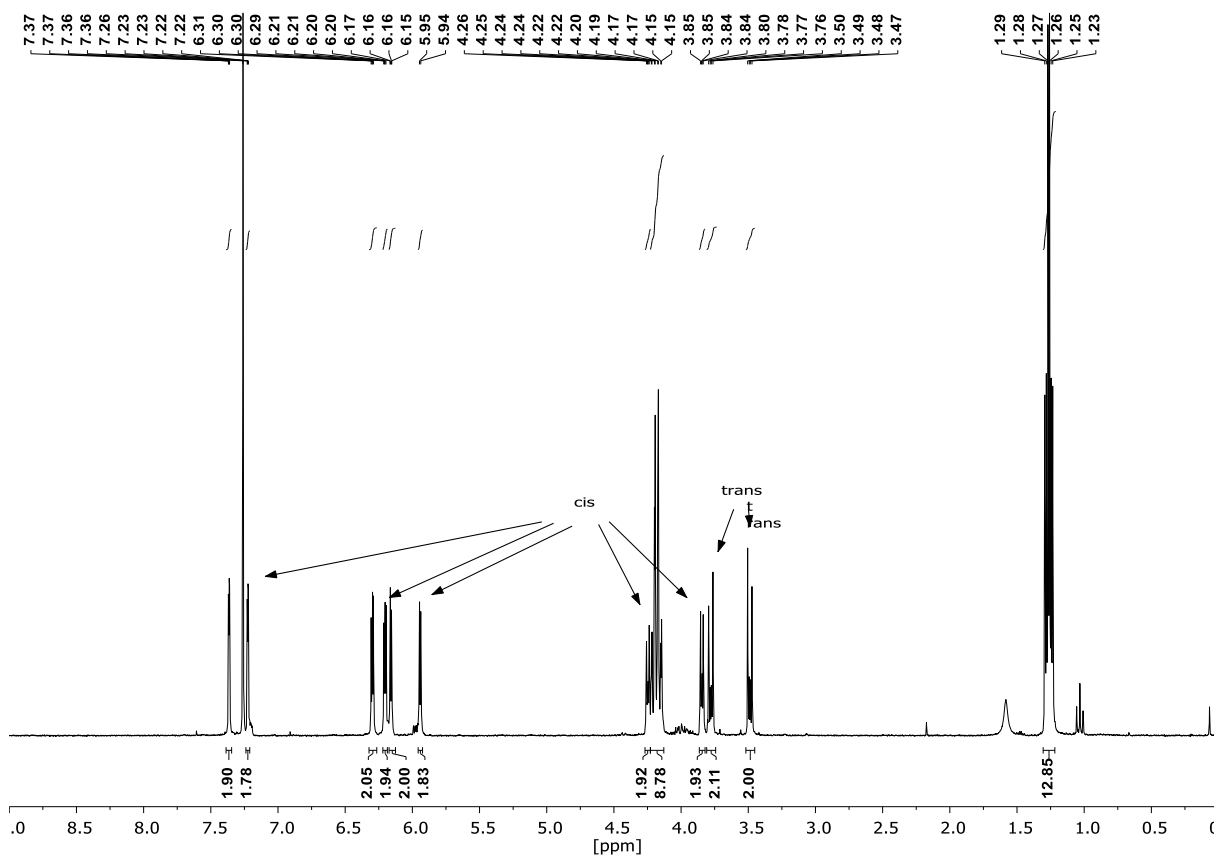
¹H-NMR (400 MHz, CDCl₃, head-to-tail conformer):
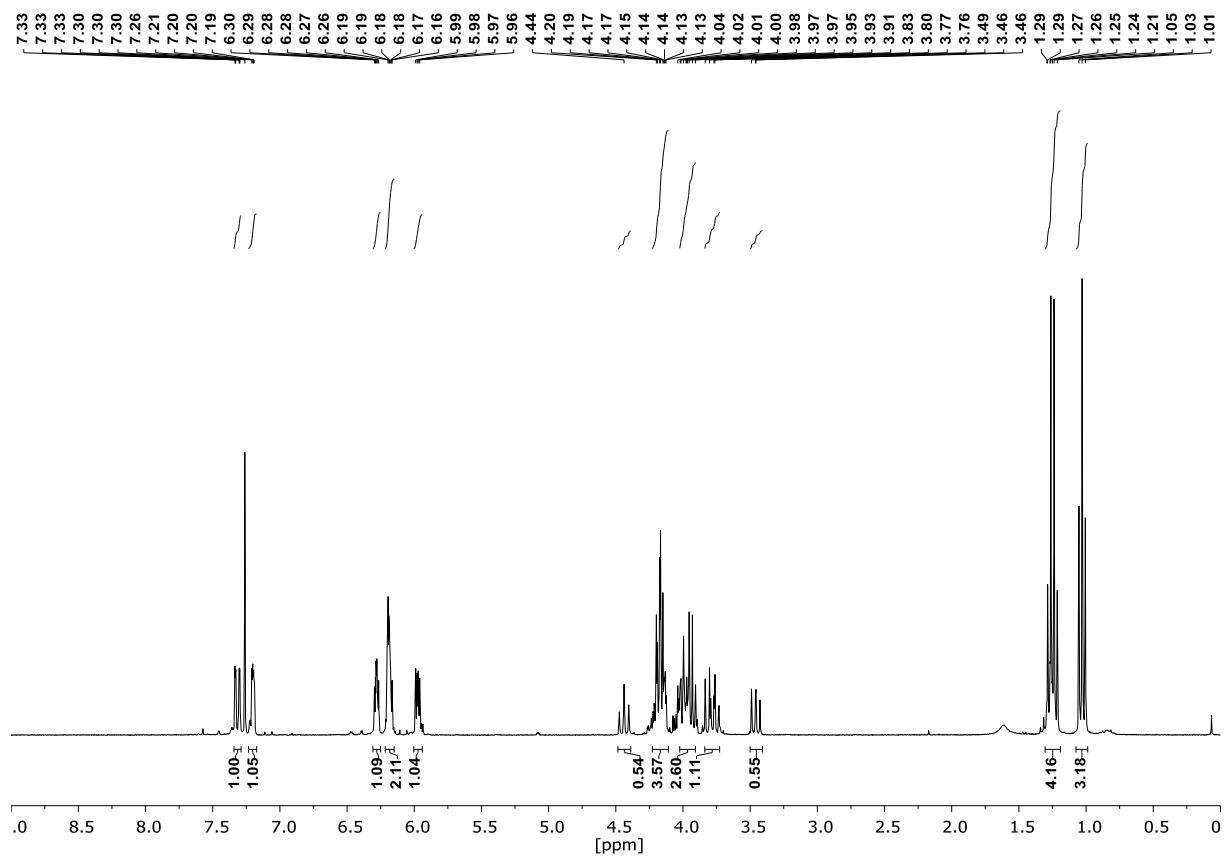
¹³C-NMR (101 MHz, CDCl₃) & **DEPT135** (101 MHz, CDCl₃):
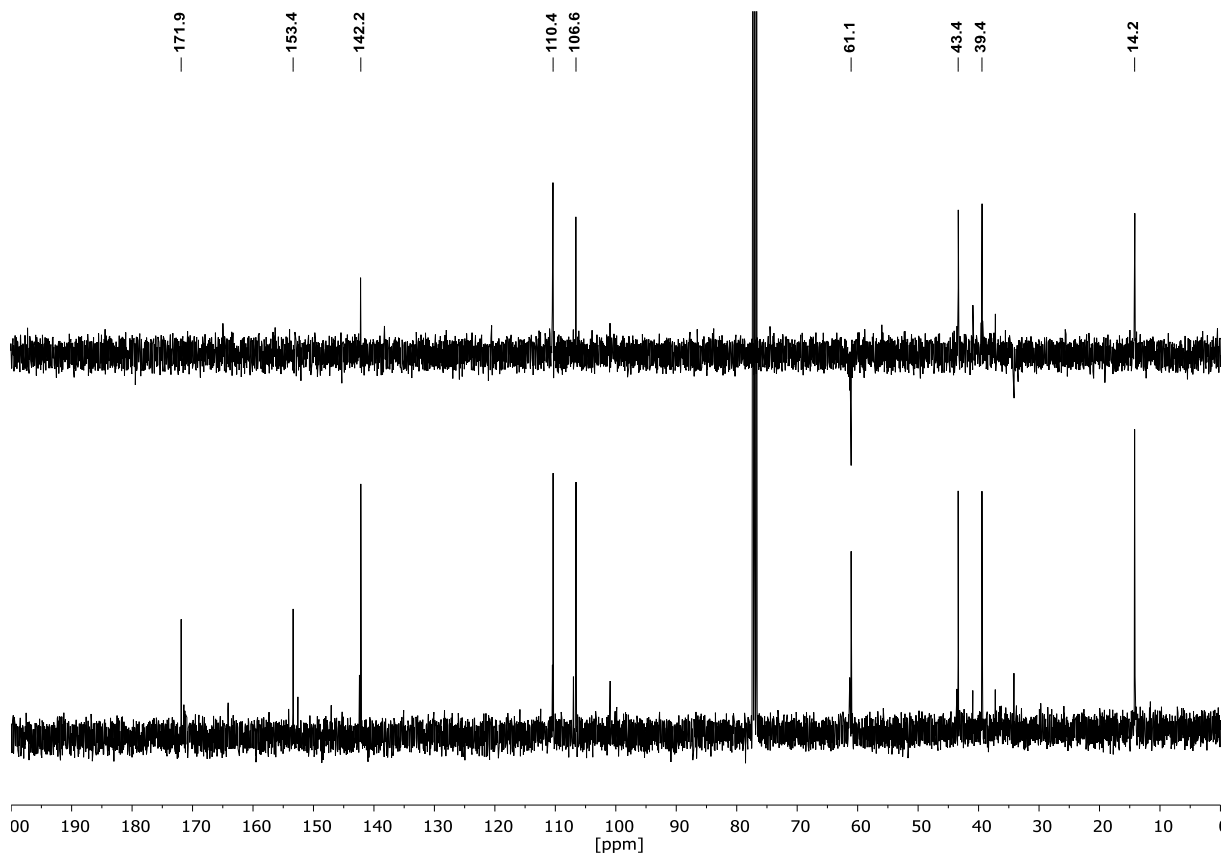
1,2-diphenyl-1,2,2a,5,10,12a-hexahydrobenzo[c]cyclobuta[h][1,6]dioxecine-3,12-dione (185u/186u)

¹H-NMR (400 MHz, CDCl₃, major diastereomer):

¹H-NMR (400 MHz, CDCl₃, mixture of diastereomers):
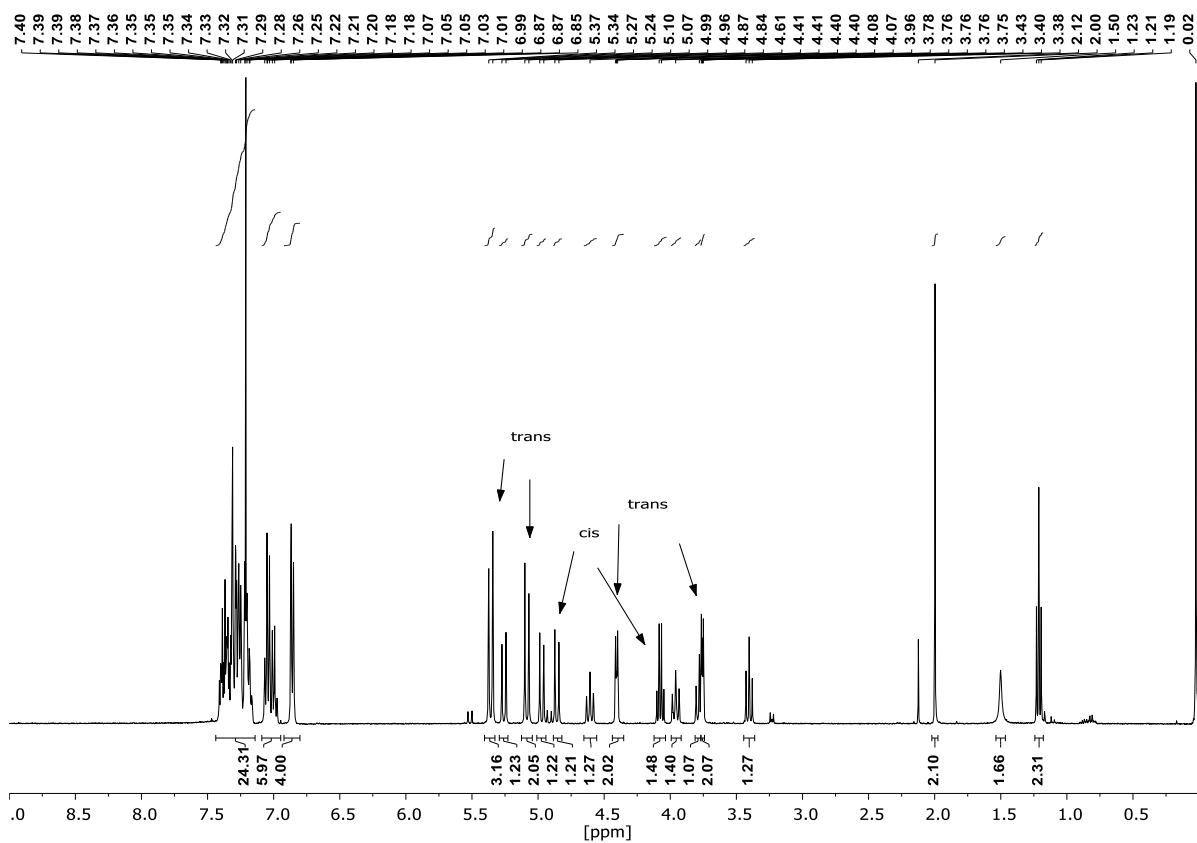
^{13}C-NMR (101 MHz, CDCl$_3$, major diastereomer) & **DEPT135** (101 MHz, CDCl$_3$):
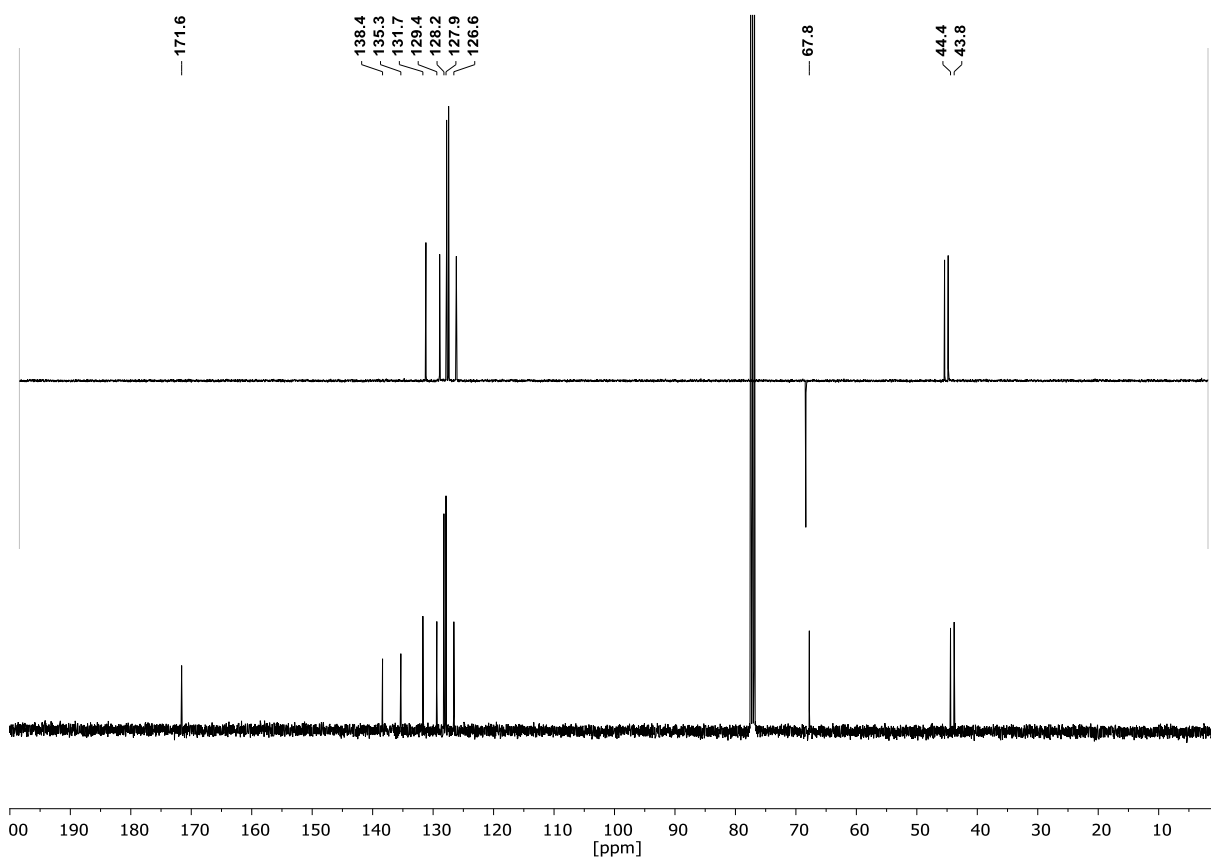
Diethyl 3-(4-methoxyphenyl)-4-phenylcyclobutane-1,2-dicarboxylate (185ae/186ae)

^{1}H-NMR (400 MHz, CDCl$_3$):
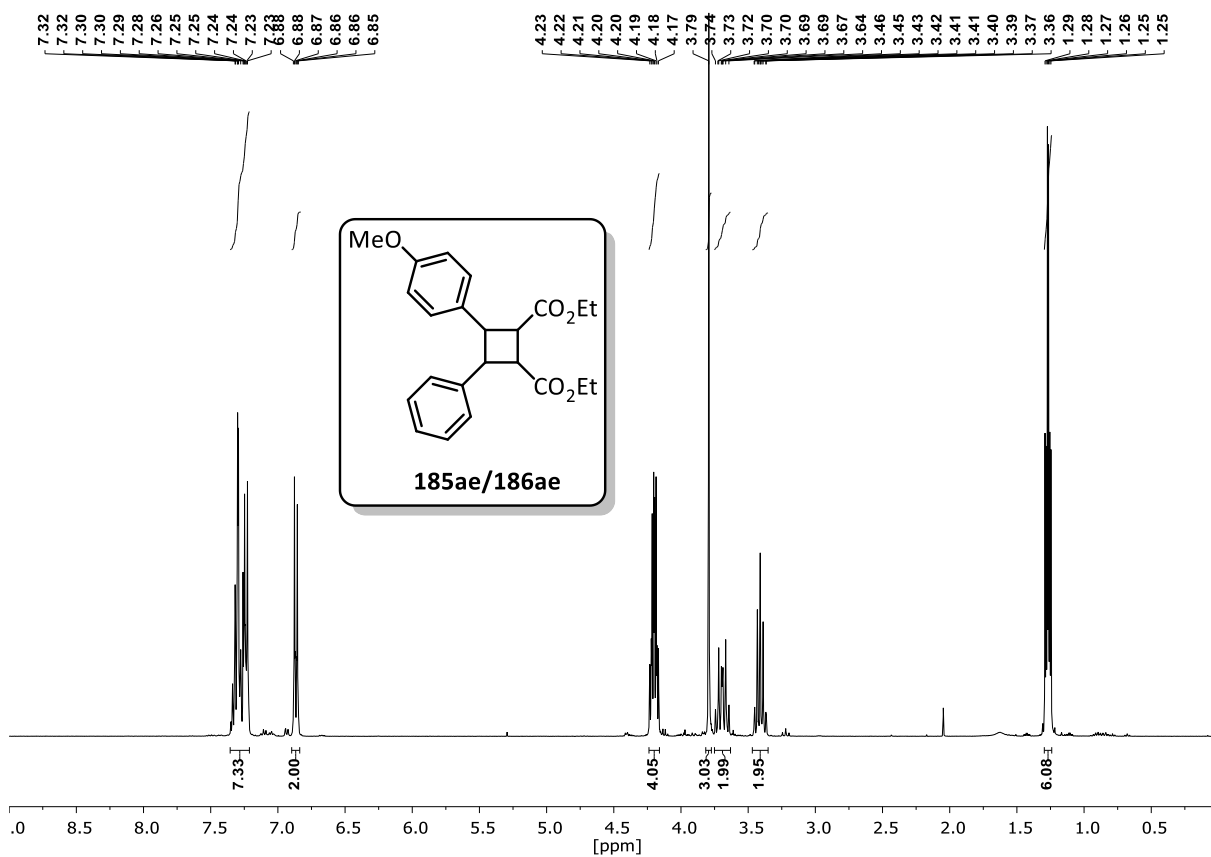
¹³C-NMR (101 MHz, CDCl₃) & **DEPT135** (101 MHz, CDCl₃):
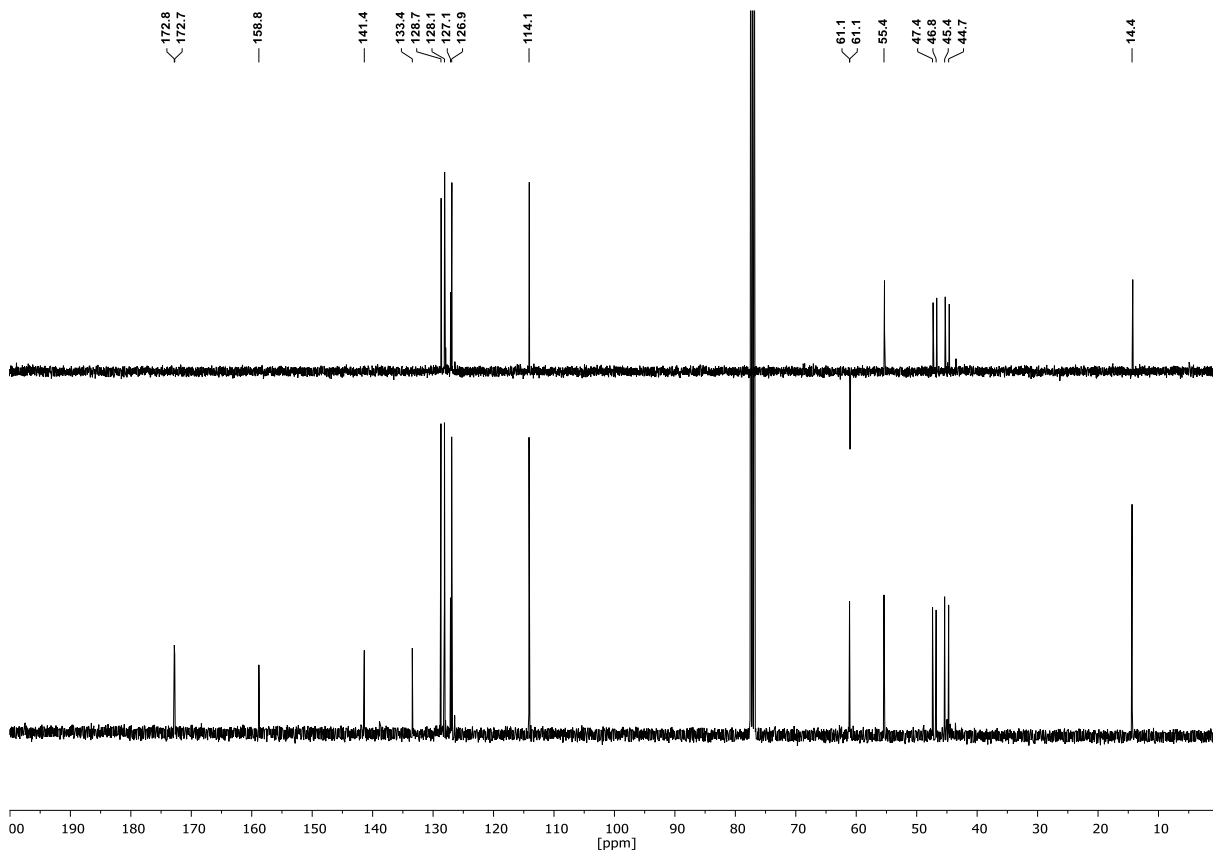
Diethyl 3-(4-(methoxycarbonyl)phenyl)-4-phenylcyclobutane-1,2-dicarboxylate (185ai/186ai)

¹H-NMR (400 MHz, CDCl₃):
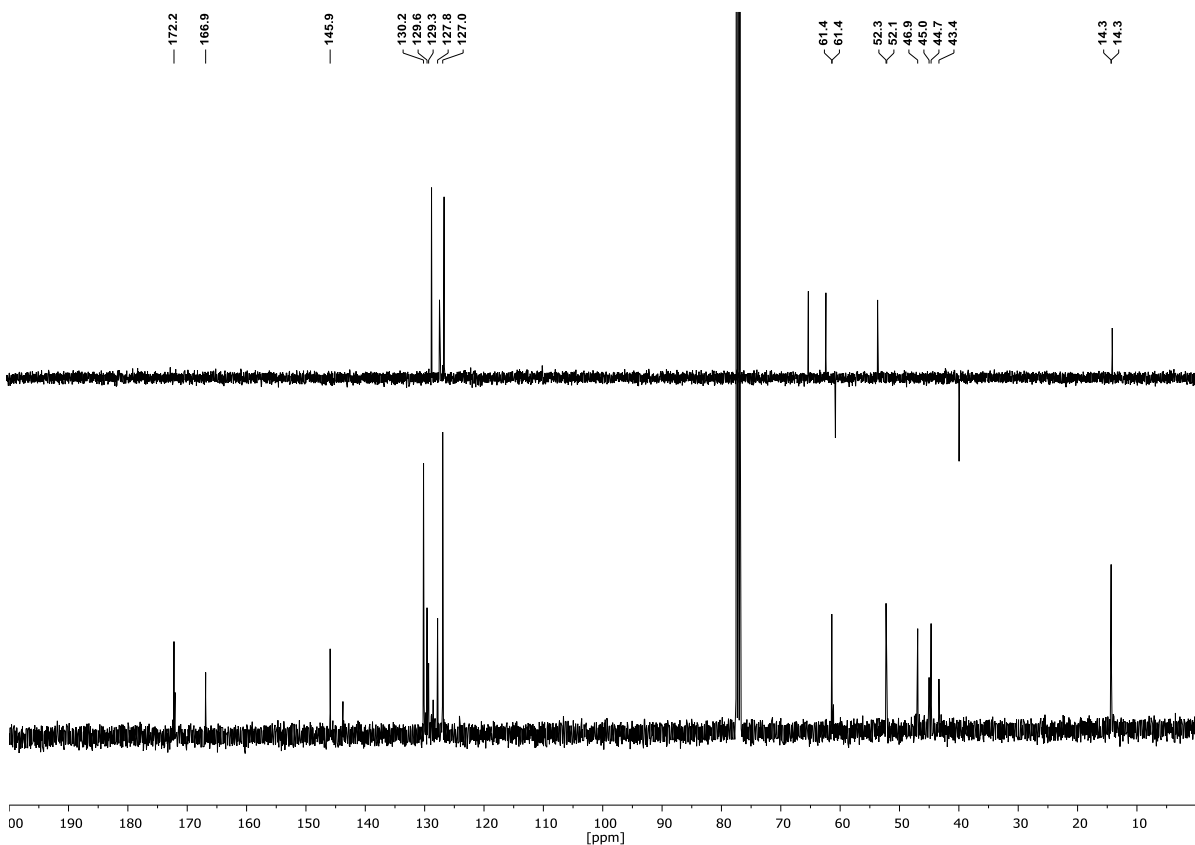
¹³C-NMR (101 MHz, CDCl₃) & **DEPT135** (101 MHz, CDCl₃):

Diethyl 3-(4-cyanophenyl)-4-(4-(methoxycarbonyl)phenyl)cyclobutane-1,2-dicarboxylate (185eh/186eh)

¹H-NMR (400 MHz, CDCl₃):
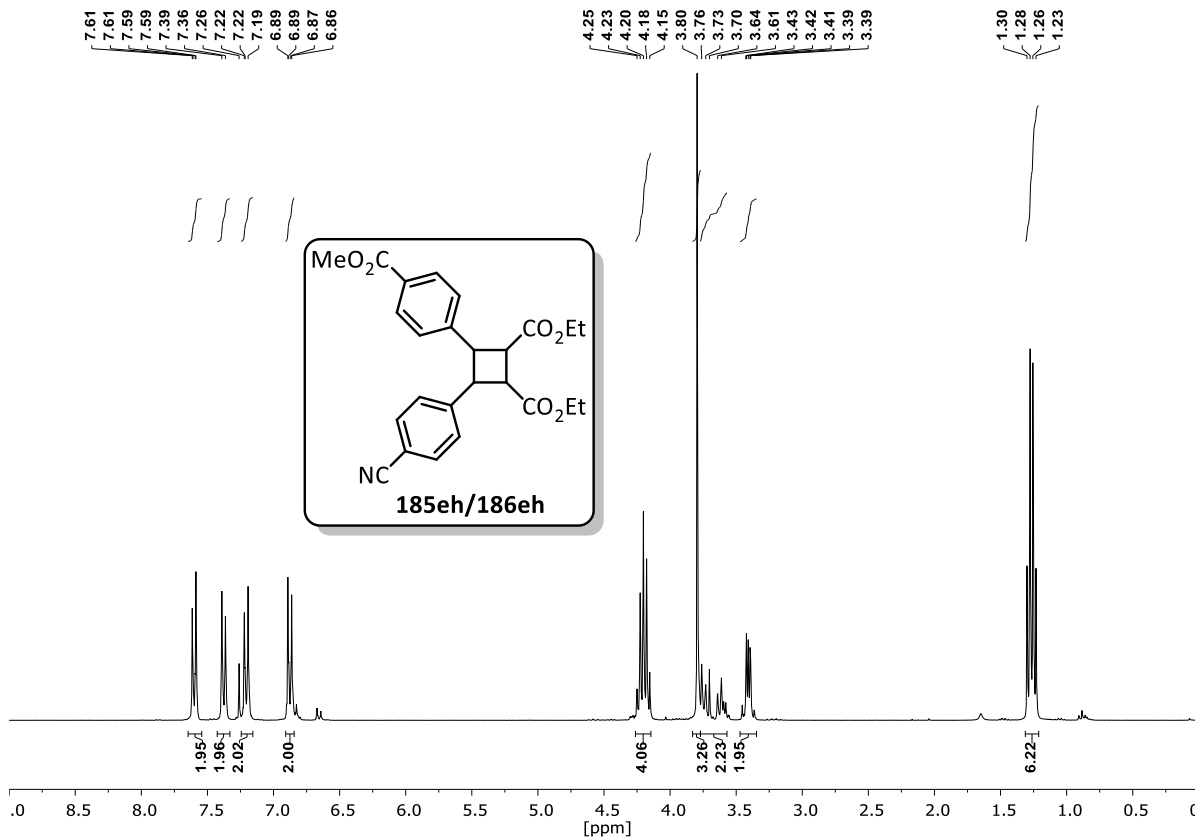
¹³C-NMR (101 MHz, CDCl₃) & **DEPT135** (101 MHz, CDCl₃):
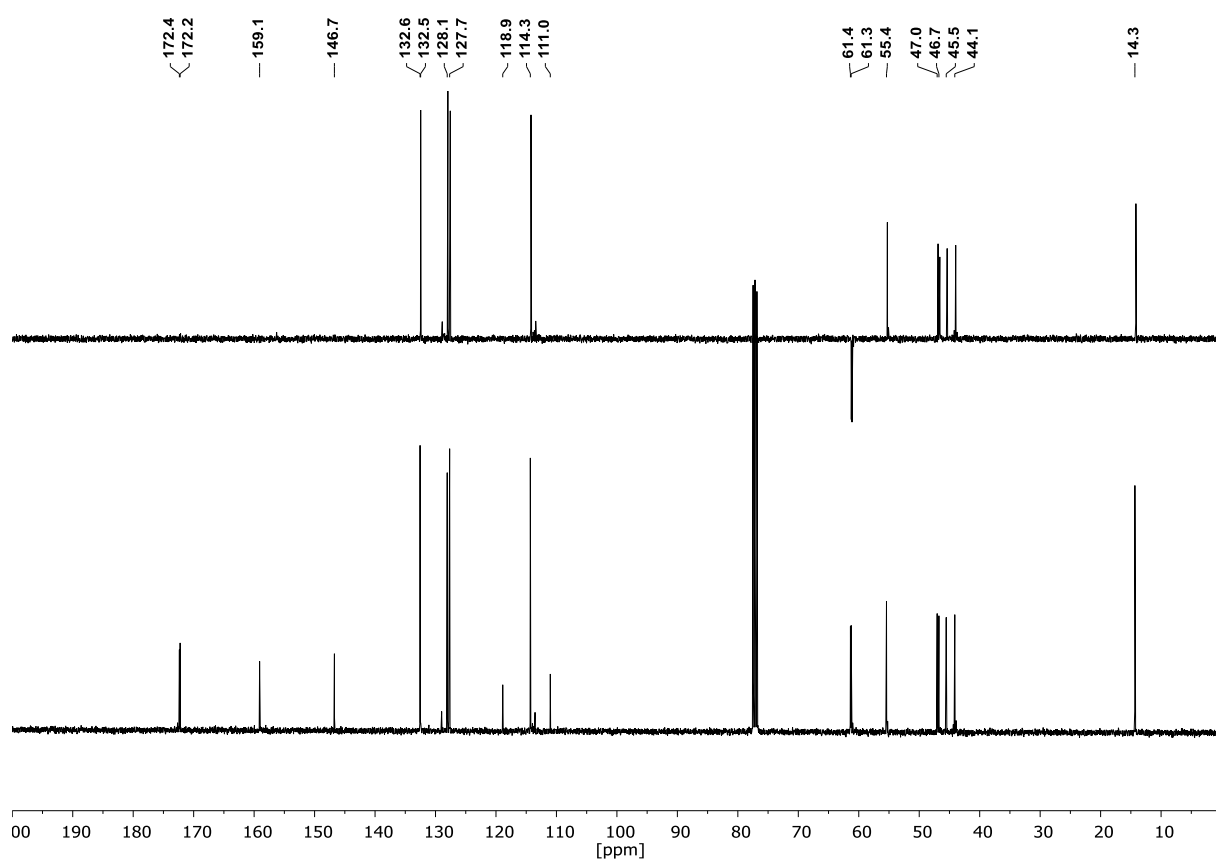
8.2 X-Ray crystallographic data

Diethyl 2,5-diphenyl-2,4-dihydro-3H-pyrrole-3,3-dicarboxylate 90a

90a
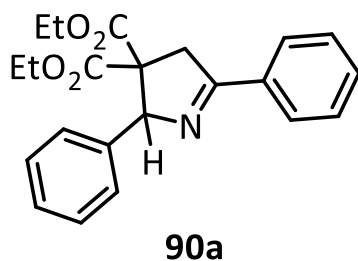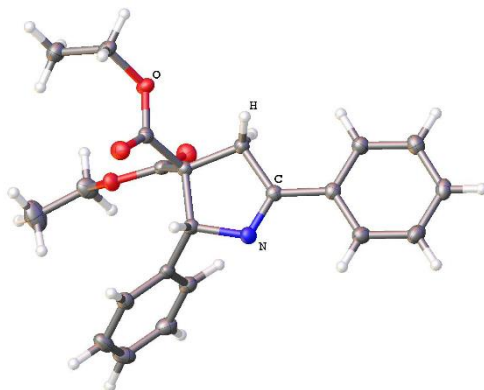
Crystal Data. $C_{22}H_{23}NO_4$, M_r = 365.41, triclinic, P-1 (No. 2), a = 7.5079(2) Å, b = 10.5930(2) Å, c = 11.9272(3) Å, α = 80.561(2)°, β = 86.625(2)°, γ = 89.174(2)°, V = 934.11(4) Å³, T = 123.00(10) K, Z = 2, Z' = 1, μ(Cu Kα) = 0.724, 27437 reflections measured, 3880 unique (R_{int} = 0.0272) which were used in all calculations. The final wR_2 was 0.0819 (all data) and R_1 was 0.0317 (I > 2(I)).

|	
Formula	$C_{22}H_{23}NO_4$
$D_{calc.}$/ g cm⁻³	1.299
μ/mm⁻¹	0.724
Formula Weight	365.41
Colour	clear colourless
Shape	prism
Size/mm³	0.18×0.15×0.13
T/K	123.00(10)
Crystal System	triclinic
Space Group	P-1
a/Å	7.5079(2)
b/Å	10.5930(2)
c/Å	11.9272(3)
α/°	80.561(2)
β/°	86.625(2)
γ/°	89.174(2)
V/Å³	934.11(4)
Z	2
Z'	1
Wavelength/Å	1.54184
Radiation type	Cu Kα
Θ_{min}/°	3.763
Θ_{max}/°	76.103
Measured Refl's.	27437
Ind't Refl's	3880
Refl's with I > 2(I)	3617
R_{int}	0.0272
Parameters	336
Restraints	0
Largest Peak	0.270
Deepest Hole	-0.230
GooF	1.031
wR_2 (all data)	0.0819
wR_2	0.0800
R_1 (all data)	0.0340
R_1	0.0317

Diethyl 4-oxo-1-phenyl-3,4-dihydroanthracene-2,2(1*H*)-dicarboxylate 99i
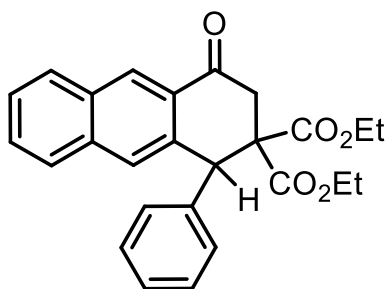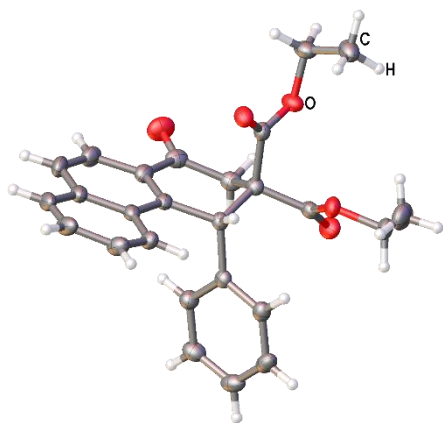
99i

Crystal Data. $C_{26}H_{24}O_5$, M_r = 416.45, monoclinic, $P2_1/c$ (No. 14), a = 17.6278(3) Å, b = 8.42279(12) Å, c = 14.7422(2) Å, β = 104.1659(15)°, $\alpha = \gamma = 90$°, V = 2122.29(6) Å^3, T = 123.00(10) K, Z = 4, Z' = 1, μ(Cu K) = 0.530, 23375 reflections measured, 4227 unique (R_{int} = 0.0211) which were used in all calculations. The final wR_2 was 0.0897 (all data) and R_1 was 0.0343 (I > 2(I)).

Formula	$C_{26}H_{24}O_5$
$D_{calc.}$/ g cm^{-3}	1.303
μ/mm^{-1}	0.530
Formula Weight	416.45
Colour	clear light yellow
Shape	prism
Size/mm^3	0.62×0.43×0.36
T/K	123.00(10)
Crystal System	monoclinic
Space Group	$P2_1/c$
a/Å	17.6278(3)
b/Å	8.42279(12)
c/Å	14.7422(2)
α/°	90
β/°	104.1659(15)
γ/°	90
V/Å^3	2122.29(6)
Z	4
Z'	1
Wavelength/Å	1.39222
Radiation type	Cu K
Θ_{min}/°	2.334
Θ_{max}/°	59.959
Measured Refl's.	23375
Ind't Refl's	4227
Refl's with I > 2(I)	3923
R_{int}	0.0211
Parameters	282
Restraints	0
Largest Peak	0.236
Deepest Hole	-0.183
GooF	1.041
wR_2 (all data)	0.0897
wR_2	0.0881
R_1 (all data)	0.0364
R_1	0.0343

N-(3-oxo-3-phenylpropyl)benzamide 149
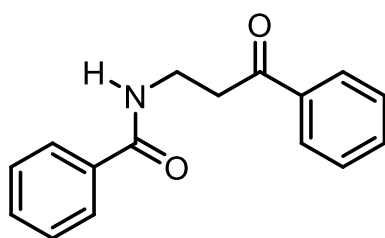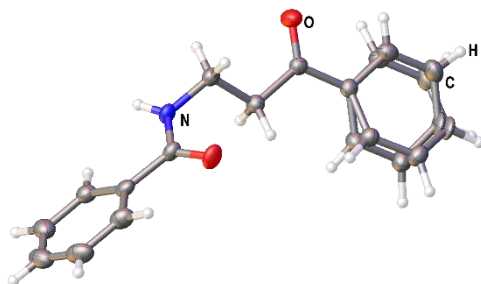
149

Crystal Data. C$_{16}$H$_{15}$NO$_2$, M_r = 253.29, monoclinic, *Pc* (No. 7), a = 4.7540(2) Å, b = 14.1568(5) Å, c = 9.6853(4) Å, β = 94.335(4)°, $\alpha = \gamma$ = 90°, V = 649.97(4) Å^3, T = 123.00(10) K, Z = 2, *Z'* = 1, μ(Cu K) = 0.498, 6715 reflections measured, 2673 unique (R_{int} = 0.0307) which were used in all calculations. The final wR_2 was 0.0935 (all data) and R_1 was 0.0355 (I > 2(I)).

Formula	C$_{16}$H$_{15}$NO$_2$
$D_{calc.}$/ g cm^{-3}	1.294
μ/mm^{-1}	0.498
Formula Weight	253.29
Colour	clear colourless
Shape	prism
Size/mm^3	0.23×0.18×0.11
T/K	123.00(10)
Crystal System	monoclinic
Flack Parameter	0.1(3)
Hooft Parameter	0.2(3)
Space Group	*Pc*
a/Å	4.7540(2)
b/Å	14.1568(5)
c/Å	9.6853(4)
α/°	90
β/°	94.335(4)
γ/°	90
V/Å^3	649.97(4)
Z	2
Z'	1
Wavelength/Å	1.39222
Radiation type	Cu K
Θ_{min}/°	2.818
Θ_{max}/°	74.223
Measured Refl's.	6715
Ind't Refl's	2673
Refl's with I > 2(I)	2506
R_{int}	0.0307
Parameters	289
Restraints	8
Largest Peak	0.261
Deepest Hole	-0.150
GooF	1.053
wR_2 (all data)	0.0935
wR_2	0.0911
R_1 (all data)	0.0386
R_1	0.0355

8.3 List of abbreviations

A	acceptor	calc.	calculated
Å	Ångström (10^{-10} m)	cat.	catalyst
Abbr.	abbreviated	*cf.*	confer (Latin: compare)
abs.	absoluted	CI	chemical ionization
Ac	acetyl	CN	cyano
AcOH	acetic acid	^{13}C-NMR	carbon NMR
AIBN	2,2'-azobis(2-methyl propionitrile)	cm	centrimeter
alk	alkyl	cm^{-1}	wavernumber(s)
Approx..	approximately	COSY	correlation spectroscopy
Ar	aryl	conv.	conversion
atm.	atmosphere	CT	charge-transfer
ATRA	atom transfer radical addition	CV	cyclic voltammetry
binc	bis(2-isocyanophenyl) phenyl phosphonate	Cy	cyclohexyl
Bn	benzyl	δ	chemical shift
Boc	tert-butyloxycarbonyl	D	donor
BOX	bis(oxazoline)	dap	2,9-bis(para-anisyl)-1,10-phenanthroline
b.p.	boiling point	DBU	1,8-Diazabicyclo[5.4.0]undec-7-ene
br	broad (spectral peak)	DBN2PO	3,7-di([1,1'-biphenyl]-4-yl)-10-(naphthalen-2-yl)-10H-phenoxazine
bpy	2,2'-bipyridine	DCC	N,N'-Dicyclohexylcarbodiimide
Bu	butyl	DCE	1,1,2,2-dichloroethane
*t*Bu	*tert*-butyl	DCM	dichloromethane
*n*Bu	*n*-butyl	deg.	degree

°C	degree celsius	DDQ	2,3-dichlor-5,6-dicyano-1,4-benzochinon
de facto	existing in fact	eq.	equivalents
DEPT	distortionless enhancement by polarization transfer	ESI	electrospray ionization
dF(CF3)ppy	2-(2,4-difluorophenyl)-5-(trifluoromethyl) pyridine	ET	energy transfer
DIPEA	*N,N*-diisopropylethylamine	Et	ethyl
DMA	*N,N*-dimethylacetamide	*et al.*	et alia (Latin: and others)
DMAP	4-(dimethylamino)-pyridine	etc.	and so forth
DMF	*N,N*-dimethylformamide	Et_2O	diethylether
DN1PA	2-naphtyl-5,10-di(naphthalen-1-yl)-5,10-dihydrophenazine	eV	electronvolt
DN2PA	2-naphtyl-5,10-di(naphthalen-2-yl)-5,10-dihydrophenazine	EWG	electron withdrawing group
d.r.	diastereomeric ratio	Φ	quantum yield
dtbbpy	4,4'-di-tert-butyl-2,2'-bipyridine	Φ_{PL}	photoluminescence quantum yield
ε	molar extinction coefficient	F	Faraday
e.g.	exempli gratia (Latin: for example)	*fac*	facial
E/Z	Entgegen/Zusammen	FC	ferrocene
$E_{1/2}$	standard reduction potential	FID	flame ionization detector
EDG	electron donating group	FTIR	fourier transform infrared spectroscopy
EI	electron ionization	g	gram(s)
EPR	electron paramagnetic resonance	GC	gas chromatography
EA	ethyl acetate	glyme	1,2-dimethoxyethane
ed.	edition	h	hour(s)
Ed.	editor	*h*	Planck's constant

ee	enantiomeric excess	HAT	hydrogen atom transfer
EI	electron ionization	HH	head-to-head
hν	light	M	molar [mol/L]
^{1}H-NMR	proton NMR	Me	methyl
HOMO	highest occupied molecular orbital	MeCN	acetonitile
HPLC	high pressure liquid chromatography	MLCT	metal to ligand charge transfer
HRMS	high resolution mass spectrometry	m.p.	melting point
HT	head-to-tail	MS	mass spectrometry
Hz	hertz	m/z	mass to charge ratio (in MS)
I		ν	frequency
i.e.	id est (Latin: in other words)	NBS	*N*-bromosuccinimide
in vacuo	under reduced pressure	NCS	*N*-chlorosuccinimide
IR	infrared spectroscopy	NMR	nuclear magnetic resonance
ISC	inter system crossing	NOESY	nuclear Overhauser effect spectroscopy
J	Joule [Nm]	nosyl	*N*-chloro-*N*-methyl-4-nitrobenzenesulfonamide
J	coupling constant	n.r.	no reaction
K		Nu	nucleophile
L	ligand	o	ortho
l	liter	ox.	oxidation
λ	wavelength [nm]	P	
λ$_{max}$	wavelength at maximum [nm]	p	para
λ$_{abs}$	wavelength of absorption	P$_{abs}$	absorbed radiant power
LED	light emitting diode	PC	photocatalyst
LMCT	ligand to metal charge transfer	PE	petrol ether
LRMS	low resolution mass spectrometry	PET	photo electron transfer

LUMO	lowest unoccupied molecular orbital	Ph	phenyl
ppm	parts per million	X	arbitrary reagent, halogen
ppy	2-phenylpyridine		
*i*Pr	isopropyl		
Q	quencher		
R	arbitrary residue		
rac.	racemic		
red.	reduction		
redox	reduction oxidation		
ref	reference		
R_f	retention factor		
rt	room temperature		
rxn.	reaction		
SCE	saturated calomel electrode		
SET	single electron transfer		
SM	starting material		
SOMO	singly occupied molecular orbital		
τ	lifetime		
TFA	trifluoroacetic acid		
THF	tetrahydrofuran		
TLC	thin layer chromatography		
TMS	trimethylsilyl		
Ts	tosyl, 4-toluenesulfony		
UV	ultraviolet		
VIS	visible light		
vol	volume		
vs.	versus (Latin: against)		
wt%	weight percent		

8.4 List of publications

S. K. Pagire, A. Hossain, **L. Traub,** S. Kerres und O. Reiser: Photosensitized regioselective [2+2]-cycloadditon of cinnamates and related alkenes. Chem. Commun., **2017**, 53, 12072 - 12075. DOI: 10.1039/C7CC06710K

L. Traub und O. Reiser: Homogenous visible light mediated transition metal catalysis other than Ruthenium and Iridium. In: B. König, (Ed.): *Chemical Photocatalysis,* 2nd Edition, DeGruyter, **2019**. DOI: 10.1515/psr-2017-0172

L. Traub und O. Reiser: A holistic picture of three distinct ATRA mechanisms exemplified at the haloamination of styrenes. **2020**. *Manuscript in preparation.*

L. Traub und O. Reiser: The diverse reactivity of nitrogen-centered radicals. Review. **2020**. *Manuscript in preparation.*

8.5 Congresses and scientific meetings

26th lecture conference on photochemistry
09/2018 Munich

EuCHeMS2018
06/2018 Marseille
Conference on Organic Free Radicals
Posterpräsentation zum Thema:
„Accessing nitrogen centred radicals through visible light photocatalysis"

26th ISHC Congress
09/2017 Regensburg
International Society of Heterocyclic Chemistry
Aktive Teilnahme am Organisationsteam
Posterpräsentation zum Thema:
„Visible light catalyzed [2+2] cycloadditons of α,β-unsaturated esters by energy transfer"

8.6 Curriculum vitae

Promotion „Organische Chemie"

11/2016 – 06/2020 Universität Regensburg

Abschlussarbeit: „Expanding the Scope of Visible Light Chemistry – Research and Development into *N*-centered radical reactions"

Note: Magna cum laude

Master of Science „Organische Chemie"

01/2015 – 10/2016

Universität Regensburg

Notendurchschnitt: 1,4

Schwerpunkte: Organische Chemie

Anorganische Chemie

Bioanalytik

Biochemie

Abschlussarbeit: „Synthesis of tetradentate 1,10-phenanthroline-2,9-bisoxazoline ligands" (Note: 1,7)

Bachelor of Science „Chemie"

10/2012 – 12/2014

Universität Regensburg

Notendurchschnitt: 2,6

Abschlussarbeit: „Photokatalysierte Ringöffnung von vinylischen Cyclopropanderivaten" (Note: 1,0)

Abitur

09/2002 – 07/2011

Bertha-von-Suttner Gymnasium Neu-Ulm (Notendurchschnitt: 2,0)

Facharbeit: „Analyse und Synthese von Pflanzenfarbstoffen" (Note: 15 Punkte)

9 Acknowledgements

Acknowledgements

Vielen Dank!

10 Declaration

Herewith I declare that this present thesis is a presentation of my original work prepared single-handed. Wherever contributions from others are involved, all of them are marked clearly, with reference to the literature, license and acknowledgement of collaborative research

X
_____
Lukas Traub
Regensburg, der 25.05.2020